Università degli Studi di Ferrara

DOTTORATO DI RICERCA
in
Scienze Umane

IDQP

Erasmus Mundus Joint Doctorate in Quaternary and Prehistory

CICLO XXXIII

COORDINATORE Prof. Paolo TROVATO

Reconstructing past climate and environment using rodent assemblages from the Middle to Late Pleistocene in western Asia

Settore Scientifico Disciplinare L-ANT / 01

Dottorando/a
Dott.Iván Rey-Rodríguez

Tutore
Prof. Marta Arzarello

Tutore
Prof. Juan Manuel López-García

MUSÉUM NAL HIST NATURELLE

UNIVERSITAT ROVIRA i VIRGILI

ipt Instituto Politécnico de Tomar

A miña nai, miña irmá e a miña sobriña

Abstract

Western Asia is the westernmost subregion of Asia and constitute an important enclave of passage between Africa, Asia and Europe. In this region, during the last decade, the small vertebrate studies are increasing, mainly for their interest as a useful tool for palaeoenvironmental and palaeoclimatic reconstructions, however most of them propose preliminary taxa list, due to the lack of osteological referential and the limited knowledge of molar characters.

Taking into account this background, the main objective of this PhD thesis is to reconstruct the past environmental and climatic conditions using rodents assemblages in western Asia, focusing in the archaeological sites of Azokh 1 Cave and Kaldar Cave. In parallel to this work, barn owl pellets from Birecik region have been analyzed in order to obtain a better knowledge of rodent species. The correct identification of rodents was the main aim of this work, for that we used the literature and references collection. However, for some genus, as *Ellobius*, it was not enough that is the reason because we applied the Geometric Morphometric method analyzing the morphological and morphometric characters.

Then, a preliminary taphonomic study and also the Habitat weighting and the Bioclimatic model have been applied to the fossil rodent assemblage. Last both, in order to test the potential of these methods for the environmental and climatic reconstructions. Showing that our results validated both methodologies for further archaeological studies in this region.

Besides, the palaeoclimatic and paleoenvironmental results obtained from Azokh 1 Middle to Late Pleistocene layers, indicate that climate was relatively warm-temperate and an environment mainly composed of shrubland and steppe. No major changes have been observed between the studied layers, indicating favourable conditions for human populations.

Moreover, palaeoecological analysis performed in Kaldar Cave revealed lower temperatures and lower precipitation than present-day conditions for the Late Pleistocene, indicating that hominin population lived in an environment mainly composed of dry steppes with patches of forested areas.

Summarizing, the different methodologies used allow us to improve the taxonomic identifications, identify the predators at the origins of the assemblages and to recover important paleoenvironmental and palaeoclimatic information in western Asia, especially in the Zagros mountains of Iran and the Caucasus region. Also, regarding the paleobiogeography of our rodent identified species, which are mainly composed by taxa of Asiatic origin, indicating that probably the Zagros and Caucasus mountains acted as a barrier for small mammals coming from Africa.

Keywords : Rodentia, Birds of prey pellets, Habitat weighting, Bioclimatic model, Geometric Morphometric, Marine Isotope Stage 9-2.

Résumé

L'Asie occidentale est la sous-région la plus occidentale de l'Asie et constitue une importante enclave de passage entre l'Afrique, l'Asie et l'Europe. Dans cette région, au cours de la dernière décennie, les études sur les petits vertébrés se sont multipliées, principalement en raison de leur intérêt comme outil utile pour les reconstructions paléoenvironnementales et paléoclimatiques. Cependant, la plupart d'entre elles proposent une liste préliminaire de taxons, en raison du manque de référentiel ostéologique et de la connaissance limitée des caractères molaires.

En tenant compte de ce contexte, l'objectif principal de cette thèse de doctorat est de reconstruire les conditions environnementales et climatiques passées en utilisant des assemblages de rongeurs en Asie occidentale, en se concentrant sur les sites archéologiques de la grotte d'Azokh 1 et de la grotte de Kaldar. Parallèlement à ce travail, des pelotes de chouettes effraies de la région de Birecik ont été analysés afin d'obtenir une meilleure connaissance des espèces de rongeurs. L'identification correcte des rongeurs était le but principal de ce travail, pour cela nous avons utilisé la littérature et les collections de référence. Cependant, pour certains genres, comme *Ellobius*, cela n'a pas suffi et nous avons appliqué la méthode de la Géométrie morphométrique en analysant les caractères morphologiques et morphométriques.

Ensuite, une étude taphonomique préliminaire ainsi que les méthodes de la pondération de l'habitat et du modèle bioclimatique ont été appliqués aux assemblages de rongeurs fossiles. Enfin, ces deux méthodes ont été utilisées pour tester leur potentiel pour les reconstructions environnementales et climatiques. Nos résultats ont validé ces deux méthodologies pour de futures études archéologiques dans cette région.

En outre, les résultats paléoclimatiques et paléoenvironnementaux obtenus dans les couches du Pléistocène moyen au Pléistocène supérieur du site d'Azokh 1, indiquent que le climat était relativement chaud-tempéré et un environnement principalement composé d'arbustes et de steppes. Aucun changement majeur n'a été observé entre les couches étudiées, ce qui indique des conditions favorables pour les populations humaines.

En outre, l'analyse paléoécologique effectuée dans la grotte de Kaldar a révélé des températures et des précipitations plus faibles que les conditions actuelles pour le Pléistocène supérieur, ce qui indique que la population humaine vivait dans un environnement principalement composé de steppes sèches avec des parcelles de zones boisées.

En résumé, les différentes méthodologies utilisées permettent d'améliorer les identifications taxonomiques, d'identifier les prédateurs à l'origine des assemblages et de récupérer d'importantes informations paléoenvironnementales et paléoclimatiques en Asie occidentale, notamment dans les montagnes du Zagros en Iran et dans la région du Caucase. De plus, concernant la paléobiogéographie de nos espèces de rongeurs identifiées, qui sont principalement composées de taxons d'origine asiatique, indiquant que les montagnes du Zagros et du Caucase ont probablement servi de barrière pour les petits mammifères provenant d'Afrique.

Mots-clés : Rodentia, Pelotes de réjection, Pondération de l'habitat, Modèle bioclimatique, Morphométrie géométrique, Stade Isotopique Marin 9-2.

Riassunto

L'Asia Occidentale è la regione dell'Asia più occidentale e costituisce un importante sito di passaggio tra Africa, Asia ed Europa. In questa regione, durante l'ultimo decennio, gli studi riguardanti i piccoli vertebrati sono aumentati, soprattutto per via del loro interesse come utile strumento per le ricostruzioni paleo-ambientali e paleo-climatiche, tuttavia la maggior parte propone un elenco preliminare di *taxa*, dovuto alla mancanza di materiale osteologico di riferimento e limitata conoscenza delle caratteristiche dei molari.

Prendendo in considerazione questo contesto, il principale obiettivo di questa tesi di dottorato è ricostruire le condizioni ambientali e climatiche del passato analizzando insiemi faunistici di micro-mammiferi dell'Asia occidentale, con particolare interesse ai siti archeologici Azokh 1 Cave e Kaldar Cave. Parallelamente a questo lavoro, sono stati analizzati boli di barbagianni provenienti dalla regione Birecik al fine di ottenere maggiori informazioni circa le specie di micro-mammiferi. Il principale scopo di questo lavoro è stato quello di identificare correttamente i micro-mammiferi e per questo abbiamo usato letteratura e collezione di riferimento. Tuttavia, per alcuni generi, come *Ellobius*, non è stato abbastanza per cui abbiamo applicato come metodologia la Morfometria Geometrica per analizzare caratteri sia morfologici che morfometrici.

Una preliminare analisi tafonomica e inoltre l'influenza dell'ambiente ed il modello bioclimatico sono stati applicati all'insieme fossile di micro-mammiferi. Questi ultimi, con l'obiettivo di testare la potenzialità di questi metodi per le ricostruzioni ambientali e climatiche, mostrano che i nostri risultano hanno validato entrambe le metodologie per ulteriori studi archeologici nella regione.

Inoltre, i risultati paleo-climatici e paleo-ambientali ottenuti per gli strati dal medio al tardo Pleistoicene da Azokh 1 indicano un clima relativamente caldo-temperato ed un ambiente principalmente costituito da boscaglia e steppa. Non sono stati osservati importanti cambiamenti tra gli strati analizzati, indicando condizioni favorevoli per le popolazioni umane.

Inoltre, analisi paleo-ecologiche effettuate a Kaldar Cave hanno evidenziato per il tardo Pleistocene più basse temperature e minori precipitazioni rispetto alle condizioni attuali, indicando che popolazioni umane hanno vissuto in un ambiente costituito principalmente da steppe aride con macchie di aree forestali.

Nel complesso, le diverse metodologie utilizzate ci permettono di migliorare le identificazioni tassonomiche, identificare i predatori all'origine degli insiemi di micro-mammiferi ed ottenere importanti informazioni paleo-ambientali e paleo-climatiche in Asia occidentale, specialmente nella regione montuosa di Zagros in Iran e nella regione del Caucaso. Inoltre, con riguardo alla paleobiogeografia delle nostre specie di micro-mammiferi identificate, che sono principalmente composte da taxa di origine asiatica, indica che probabilmente le aree montuose di Zagros e del Caucaso hanno fatto da barriera per i piccoli mammiferi provenienti dall'Africa.

Keywords: Rodentia, boli di rapaci, influenza dell'habitat, modello bioclimatico, Morfometria Geometrica, MIS 9-2

Acknowledgements

This PhD thesis was funded by the Erasmus Mundus- International Doctorate in Quaternary and Prehistory (IDQP) fellowship that gave me the opportunity to work out with the best specialist in my research area, I am really grateful to the organizers for this opportunity.

Firstly I would like to thank Dr. Juan Manuel López-García, we know and we have worked since 2014, you have always helped me in each step, advising me, encouraging me and sharing your knowledge, infinite thanks it has been a pleasure to have you as director and I hope to continue working with you. I would like to thank also my French directors Christiane Denys and Emmanuelle Stoetzel, thank you for you help and also because you have taught me the taphonomic world, the support for the visits to the reference collections, your comments and suggestions on the manuscripts and also the beginnings of this PhD thesis, thanks for all your time. Also, a really special thank to Prof. Marta Arzarello, you were always available (the best IDQP coordinator that I could have had) answering all my mails and you made simple all the procedures, thank you again Marta.

In this PhD I include material from different sites (Birecik , Azokh and Kaldar Cave) and I would like to thank for trusting me to study the material: Dr. Chistiane Denys (Birecik), Tania King (Azokh Cave) and Behrouz Bazgir (Kaldar Cave). And also to I would like to thank R. Portela Miguez, Senior Curator in Charge of Mammals, for his help with the reference collection in the Natural History Museum of London; L. Heaney, A. Ferguson and L. Smith of Chicago Field Museum; and M. Surovy, J. Galkin and C. Mehling of the American Museum of Natural History of New York.

I would like to express my gratitude to all the Azokh team excavation group, Tania King, Jan van der Made, Jong Murray Maribel Maestre, Anna, Arpiné, Lilit, Masis, Philip, Vardhuhi, Elham, Saman, Sara, Faramaz, Nemat, and all the guys that worked with his during this years. Muchísimas gracias a mis compañeras y amigas Amaya y Cristina, desde que os conocí en el 2018 habéis sido un pilar más en mi vida, gracias de verdad por teneros siempre disponibles y preocupándoos por mí, os deseo de corazón lo mejor y Gracias infinitas.Thank you to Behrouz Bazgir and Laxmi Tumung for my stay in Iran, and also to Ali, for his help.

The first place where officially started my PhD was in Paris, I would like to thank Chafika Falgueres for her availability and support, David Pleurdeau, François Semah and Houria Kaci (for you patient). Thanks to my colleagues in Museé de l´Homme, Lou, Jeremy, Wanda, Delphine and Helene (for you visits in french-spanish) and specially to Janani, Hanna, Madhavi and Alez and my colleague and flatmate Pamela, it was really funny to share our small apartment thank you Pam for everything Paris with you was much easier. My gratitude to Emmanuelle Stoetzel and Christiane Denys for helping me with all the administrative stuff with the museum and help me to contact with other specialist as Raphaël Cornette (thank for you GMM advise). Muchas gracias también a mis compis del curso de francés (Liliana, José Luis, Karen, Raúl, Miguel, Laura, Dulce, Giulia y Paola) por aprender a que soy capaz de hablar con todos vosotros en la clase de francés en diferentes idiomas, sin utilizar el francés.

Grazie ai miei amici di Ferrara, dal giorno in cui sono arrivato mi sono sentito a casa, tanto col master come con la tese. Ferrara per me è molto importante per me e lo è per voi, Marta, Jiulie, Sara, Gabbro, Claudio, Marco, Alison (tutti due),Giulia, Sandro, Maite, Ricardo, Roberto, Madda, Marija (grazie mille per farmi fare di modello) e come no Rosa. Mi manchi tanto. Marta

grazie mille per avere sempre la parola giusta e tirarmi su la morale (anche quando fai il corvo per terra), Julie grazie per tutto il tuo aiuto sempre e per scoprimi il mundo della salsa (e la Biofamily), Sara e Gabbro grazie mille per farmi da mangiare tante volte e le conversazioni. Rosa, tu sei stata a Parigi con me, doppo a Ferrara, grazie tanto, per tutte le videochiamatte e quelle chi mancano, per tradurre tutto ciò di cui avevo bisogno per avermi accompagnato a negozi, mercati ... abbiamo ancora una gita a Venezia da fare (grazie anche a le tue conquiline Diana e Vanessa per il Apperitivo). Grazie, Grazie e ancora Grazie a tutto voi congiunti per avermi fatto stare così a Ferrara (anche col covid), per portarmi a gli escavi, a cena, a fare apperitivo e ricordartevi che dobbiamo andare a vedere Giorgio il piccolo principe a Maggio. Volevo ringraziare anche al migliore paleontologo del mondo Professore Benedetto Sala per essere sempre gentille con me.

Muchísimas gracias al equipo de micro de Tarragona: Hugo, Juanma, Iván, Mónica, Sandra, Elisa, Ángel, Almudena y Ana. Hugo, gracias por acompañarme a Irán y por todos los consejos durante todos estos años. Almudena, por tener siempre esa buena energía y esa "sensibilidad" que te caracteriza, ya son años desde que te conocí con el gorrito. Elisa, por estar siempre pendiente de que me sintiera a gusto tanto en Tarragona como en Ferrara, gracias. Sandra, al principio te tenía miedo, pero luego Ferrara y conocerte me ha demostrado que no, gracias por todos los consejo y que conste que no te guardo rencor por no querer ser mi directora! Por muchos años trabajando juntos, así sea en nuestro propio IPHES cuando nos toque la lotería. Ana (o ser de luz), eres una persona increíble y siempre estás ahí. Juanma, no tengo nada más que decirte que gracias, gracias y gracias.

Muchas gracias también a mis compis de mesa, Sandra, Vanessa, Miguel, Patri e Irene, somos la mejor isla, también a Félix, que ya es parte de nuestra isla también . No puedo olvidarme de todas aquellas personas que he conocido en el IPHES gracias de verdad, sobre todo a Lena, Leo, Toni, Esther, Joana, Patri y Montse. Lena, gracias por tu apoyo cuando he ido a Azokh, por preocuparte y estar siempre pendiente, te deseo lo mejor en Liege. Esther y Patri, gracias por ser cencerros como yo y las conversaciones, a pesar de la distancia durante muchos años nunca os he sentido lejos, GRACIAS. Potra, porque volver retomar a relación contigo foi una das mellores cousas da pandemia, Vaca e Potra, por moitos anos máis (paloma´s Friends, pa´revolver). El IPHES también me dio la oportunidad de conocer al equipo de Cova Eirós, muchas gracias Arturo, Xosé, María, Mikel, Cirstian, Xes, Alicia, Noelia, Miguel, Olalla e todos os demáis; así como a Blanca, muchas gracias por tus visitas a Ferrara y París y espero que nos veamos pronto.

No puedo olvidarme de mi grupo burbuja, Sandra, Ana, Juanma, Antonia y Chiara, gracias por todos los cafés, conversaciones y espero futuros paseos ahora que espero estar más libre.

As miñas amigas Emma, Noa, Paula, Raquel, Lulu, Natalia e Uxía, moitas gracias por todo sodes as mellores. Emma, sabes que somos iguais e que nos entendemos perfectamente, para min es unha irmá e es unha parte fundamental e imprescindible da miña vida, non me faltes nunca.

También agradecer a mis compañeras del máster de Turismo, Nerea, Encarni, Laura y Carmen, por la paciencia y compresión. Muchas gracias OurekApp.

Doro, por tu paciencia infinita, por aguantarme los cambios de humor estos últimos meses, GRACIAS, por ser cada día mejor el uno para el otro, Ivan[2], por muchos años más.

Por último a miña familia, miña nai, miña irmá e a miña sobriña. Estou infinitamente orgulloso

e agradecido por contar sempre con vos, fostes as que verdadeiramente me apoiastes todos estes anos, incluso cando eu non tiña forzas vos sempre me axudastes. Uxía, a ver se aprendes a leer e así xa non cho ten que contar a mamá, aínda que sempre estamos peleando quérote un mundo es a persoíña máis especial que teño na miña vida, cáeme a baba cada vez que me chamas padriño; sempre terás o meu apoio para o que precises.

Espero non olvidarme de ninguén, únicamente engardir, moitísimas gracias, thank you, grazie mille, merci e grazallas por todo a tod@s.

Index

Structure of the PhD thesis 23

Chapter 1. Introduction 27

1.Introduction 29

1.1. Small mammal studies and their importance for the palaeoenvironmental and palaeoclimatic reconstructions 29

1.2. General context 29

1.3. Archaeological, environmental and climatic context of the study sites 32

1.4. General research questions 34

1.5. Objectives of the research study 35

Chapter 2. Material and methods 37

2.1. Field work 39

2.2. Reference collections 40

2.3. Taxonomical nomenclature and measurement 44

2.4. Methods applied for the identifications, environmental and climatic reconstruction 48

Chapter 3. Implications of modern Barn owls pellets analysis for archaeological studies in the Middle East 51

1. Introduction 55

2. Material and Methods 55

2.1. Sampling of the studied material 55

2.2. Taxonomy 55

2.3. Taphonomy 56

2.3.1. Skeletal element proportions 56

2.3.2. Breakage 57

2.3.3. Digestion 57

2.4. Statistical analysis 57

2.5. Climatic reconstruction 57

2.6. Environmental reconstruction 58

3. Results and discussion 58

3.1. Taxonomic study 58

3.2. Taphonomic study 62

3.2.1. Taphonomic implications 65

3.3. Environmental and climatic remarks 68

3.3.1. Climatic data 68
3.3.2. Environmental data 69
4. Conclusions 70
References 71
Chapter 4. Distinguishing between three modern *Ellobius* species (Rodentia, Mammalia) and identification of fossil *Ellobius* from Kaldar Cave (Iran) using geometric morphometric analyses of the first lower molar 75
1.Introduction 79
2.The genus *ELLOBIUS* Fischer, 1814 79
2.1. Distribution and Ecological Remarks of the Extant *Ellobius* Species 79
2.2. Fossil Record of *Ellobius* 80
2.3. Description of Tooth Morphology 81
3.Material and methods 8 2
3.1. Modern and Fossil Material Studied 82
3.2. Data Acquisition 85
3.3. Shape Analyses 86
4.Results 87
5.Discussion 89
5.1. Sliding Semi-Landmarks and Anatomical Landmarks Compared with Previous Systematic Methods of *Ellobius* Identification 89
6.Conclusions 91
References 92
Chapter 5. New palaeoecological inferences using rodent's assemblages for the Middle to the Late Pleistocene site of Azokh 1 Cave (Southern Caucasus) 99
1. Introduction 103
1.1.Azokh 1 103
1.1.1.Chronology and previous studies carried out in Azokh 1 cave 104
1.1.1.1. Unit V 106
1.1.1.2. Unit IV 107
1.1.1.3. Unit III 107
1.1.1.4. Unit II 107
1.1.1.5. Unit I 108
2. Material and methods 108
2.1. Taxonomy 109
2.2. Taphonomy 110
2.3. Palaeoenvironmental and palaeoclimatic reconstructions 110

2.3.1. Habitat weighting method 110
2.3.2. Bioclimatic Model 110
3. Results and discussion 111
3.1. Systematics, current distribution and ecology 111
3.2. Preliminary taphonomic study 122
3.3. Palaeoecological reconstruction of the Azokh 1 Cave sequence 2 124
3.4. Comparisons with other palaeoenvironmental proxies from Azokh 1 Cave 126
3.5. Azokh 1 Cave and the Southern Caucasus context 128
4.Conclusions 131
References 131

Chapter 6. Exploring the landscape and climatic conditions of Neanderthals and anatomically modern humans in the Middle East : the rodent assemblage from the Late Pleistocene of Kaldar Cave (Khorramabad Valley, Iran) 141
1. Introduction 145
2. Kaldar Cave 145
3. Material and methods 146
3.1. Taxonomy 147
3.2. Taphonomic remarks 147
3.3. Palaeoenvironmental and palaeoclimatic reconstructions 147
3.3.1. Habitat weighting method 147
3.3.2. Bioclimatic Model 148
4. Results and discussion 149
4.1. Taxonomic identifications 149
4.2. Past landscape and climate at Kaldar Cave 158
4.3. Kaldar Cave in the Middle Eastern context 159
5. Conclusions 162
References 164

Chapter 7. General discussion 171
7.1. Rodent assemblages 173
7.2. Synthesis of Taphonomic inferences 189
7.3. Integration of our data in a broader climatic context 191

7.3.1. MIS 9 – MIS 7 (ca. 334-185 ka) 192
7.3.2. MIS 6 - MIS 4 (ca. 185-60 ka) 194
7.3.3. MIS 3 - MIS 2 (60-11.6 ka) 196

Chapter 8. General conclusions and perspectives 199

8.1. General conclusions 201
8.1.1. Barn owls pellets analysis 201
8.1.2. Identification of modern and fossil *Ellobius* species using geometric morphometric (GM) methods on molars 201
8.1.3. Azokh 1 Cave 201
8.1.4. Kaldar Cave 202
8.2. Perspectives 203

References 205

List of tables and figures 223

Appendix 1 233

Appendix 2 237

Structure of the PhD thesis



This PhD is divided in 8 main chapters, combining published and unpublished data, references and 2 appendixes.

In the first chapter, *Introduction*, is presented the importance of small mammals for the archaeological and palaeontological studies, the archaeological and climatic context of the study area, and the main objectives of the research study.

Then second chapter, *Material and methods*, we give a brief description of the study methodology and the modern specimens used for comparison.

The third chapter is composed of the paper, *Implications of modern Barn owls pellets analysis for archaeological studies in the Middle East,* published in 2019 in *Journal of Archaeological Science*. This is a case of study of 40 owl pellets, on which we applied palaeoclimatic and palaeoenvironmental methods in order to test the Habitat weighting and the Bioclimatic model in this region.

The fourth chapter is entitled *Distinguishing between three modern Ellobius species (Rodentia, Mammalia) and identification of fossil Ellobius from Kaldar Cave (Iran) using geometric morphometric analyses of the first lower molar.* This work was published in *Palaeontologia Electronica* in 2021. Using Geometric Morphometrics, we were able to discriminate between the different *Ellobius* species occurring today in the southeastern Europe, western and central Asia, and to effectively identify fossils from Kaldar Cave.

The fifth chapter focuses on *Azokh Cave*, and include the rodents study and the palaeoenvironmental and palaeoclimatic inferences for the Middle to Late Pleistocene site of Azokh 1. This part has not been submitted for publication yet, but a submission to an international journal is planned for 2021.

The sixth chapter is composed of the paper *Exploring the landscape and climatic conditions of Neanderthals and anatomically modern humans in the Middle East: the rodent assemblage from the Late Pleistocene of Kaldar Cave (Khorramabad Valley, Iran),* published in *Quaternary Science Reviews* in 2020. It focuses on the study of the rodent assemblage of the Late Pleistocene levels from Kaldar Cave, with palaeoenvironmental and palaeoclimatic reconstructions.

The seventh chapter, *General discussion*, is divided in two main parts: the first one analyzes the rodent assemblage composition of all the studied samples, and the second one presents a comparison and a discussion of the palaeoenvironmental and palaeoclimatic results obtained in this work with the global climatic changes registered in the Marine Isotope Stages (from MIS 9 to MIS 2).

In the eighth chapter, *General conclusions and perspectives*, we indicate the most important conclusions obtained in this PhD and we propose the unsolved problems of this PhD thesis and also the posibily future collaborations to expand these studies.

Finally, we include a list of bibliographic references. In the appendix 1 we include a regression that allows us to calculate climatic parameters related to the Bioclimatic Model and in the appendix 2 the three scientific papers in their published format.

Chapter 1.

Introduction



1.Introduction

1.1.Small mammal studies and their importance for the palaeoenvironmental and palaeoclimatic reconstructions

The application of small vertebrates (including birds, bats, insectivores, rodents, amphibians and reptiles) studies in archaeology is essential and a very useful tool for palaeoenvironmental and palaeoclimatic reconstructions (e.g., Bañuls-Cardona et al., 2014; Blain et al., 2019; Lopez-Garcia et al., 2013; López-García et al., 2018, among others). Among the small vertebrate taxa, Rodentia is the most studied order in the Quaternary because of its abundance and good preservation in archaeological and palaeontological sites; and also for their palaeoenvironmental, palaeoclimatic and biostratigraphic value. Indeed, they are sensitive to weather conditions, present a great adaptability to specific biotopes, and climatic changes may force them to migrate to other areas (Belmaker and Hovers, 2011; Maul and Markova, 2007, among others).

These studies have a large path in European countries along the Pleistocene (e.g. Berto et al., 2021; Blain et al., 2008; López-García et al., 2015; Luzi et al., 2019, among others). Studies of small vertebrates from archaeological sites in the western Asia are increasing during the last decade (Behrouz Bazgir et al., 2017; Belmaker et al., 2016; Belmaker and Hovers, 2011; Blain, 2016; Demirel et al., 2011; Kandel et al., 2017; Maul et al., 2020, 2015; Parfitt, 2016; Smith et al., 2015; Weissbrod and Weinstein-Evron, 2020; Weissbrod and Zaidner, 2014) but, most of them only propose preliminary lists of taxa often limited to the genus level, due to a lack of osteological referential and the limited knowledge of the molar morphology of some species in this region (Table 1.1).

On the other hand, some studies of extant owl pellet assemblages have been performed in the Middle East (Abi-said et al., 2014; Haddadian Shad et al., 2014; Obuch and Khaleghizadeh, 2012; Shehab et al., 2013), providing taxonomic and some taphonomic reference data in Iran, Lebanon and Syria (Table 1.2). Analysing pellets composition and their taphonomic implications, produced by barn owl allows us to have a reference for the taphonomic studies.

1.2. General context

Modern and Archaeological rodent´s assemblages from western Asia, particularly from the mountainous regions of the Caucasus (Azokh 1) and the Zagros (Kaldar Cave) are still poorly known while rodents are the most diversified and abundant small mammals of the faunas. Rodents are important constituents of the archaeological assemblages because they may be accumulated in great quantities via predation in fossil sites. Because they generally have small territories they can be good indicators of paleoclimate and paleoenvironmental conditions (e.g. Belmaker and Hovers, 2011) so they constitute a reference material for using and testing paleoenvironmental methods of reconstruction.

The Caucasus is a mountainous area between the Black Sea, to the West, and the Caspian Sea, to the East (Asryan, 2015). It covers several countries the south-western part of Russia, the northern part of Georgia, Azerbaijan and Armenia. The Zagros Mountains extend to Iran, Iraq and Turkey, with an approximately total length of 1500km.

Both areas are located at the crossroads between Africa, Europe and Asia and have yielded evidences of *H. heidelbergensis*, *H. neanderthalensis* and anatomically modern

Species	Kaldar Cave (Bazgir et al. 2017)	Dzuadzuana Cave (Belmaker et al, 2016)	Amud Cave (Belmaker and Hovers, 2011)	Karain Cave (Demirel et al. 2011)	Aghitu-3 (Kandel et al., 2017)	Qesem Cave (Maul et al. 2015a)	Azokh 1 (Parfitt, 2016)	Misliya Cave (Weisbrood and Weinstein-Evron, 2020)		Nesher Ramla (Weisbrrod and Zaidner, 2014)	
Allocricetus sp.							X				
Cricetulus sp.								X			
Cricetulus migratorius	X	X	X	X	X	X	X				
Cricetus cricetus		X									
Mesocricetus sp.							X	X			
Mesocricetus brandti	X	X		X	X						
Mesocricetus auratus				X							
Apodemus cf. *flavicollis*	X					X					
Apodemus sp.		X		X			X			X	
Apodemus flavicollis								X			
Apodemus mystacinus			X					X			
Rattus sp.						X	X				
Mus sp.		X						X			
Mus abboti				X							
Mus macedonicus			X				X				
Mus musculus	X					X					
Gerbillus dasyurus						X					
Meriones sp.	X						X				
Meriones tristami			X	X		X			X		X
Calomyscus sp.	X										
Spalax sp.								X			
Spalax ehrembergi						X				X	
Sciurus sp.								X			
Allactaga sp.	X	X			X		X				
Dryomys nitedula	X						X				
Myomimus sp.	X					X		X			
Myomimus roachi			X	X							
Ellobius sp.	X						X	X			
Ellobius talpinus	X										
Ellobius lutescens	X	X			X						
Clethrionomys glareolus		X					X				
Arvicola terrestris/amphibius		X		X	X						
Chionomys sp.		X			X			X			
Chionomys gud							X				
Chionomys nivalis	X			X			X				
Microtus sp.					X						
Microtus guentheri			X	X		X			X		X
Microtus gud				X							
Microtus arvalis		X		X							
Microtus gr. *arvalis-socialis*							X				
Microtus (*Terricola*) spp							X				
Microtus (Microtus) socialis	X										
Mastomys sp.								X			
Arvicanthis sp.								X			

Table 1.1. Rodent species previously identified in the Middle Eastern archaeo-paleontological studied sites and comparative sites used in this work.

	Lebanon (Abi-said et al. 2014)	Iran (Haddadian Shad et al., 2014)	Syria (Shehab et al., 2013)	Iran (Obuch and Khaleghizadeg, 2012)
Prey Species	**Barn owl**	**Owl**	**Owl**	**Barn Owl**
Nesokia indica		x	x	x
Cricetulus migratorius	x	x	x	x
Mesocricetus auratus			x	
Apodemus sp.		x		
Apodemus mystacinus	x			
Rattus sp.		x		
Rattus norvegicus				x
Rattus rattus			x	x
Mus domesticus /mace-donicus	x		x	
Mus sp.		x		x
Mus musculus			x	
Gerbillus nanus				x
Gerbillus mesopotamiae			x	x
Gerbillus nanus		x		
Jaculus sp.				x
Meriones tristami	x		x	x
Meriones libycus			x	x
Meriones persicus				x
Meriones crassus			x	x
Meriones sp.		x		x
Jaculus jaculus			x	
Calomyscus sp.		x		
Calomyscus bailwardi				x
Allactaga sp.		x		
Allactaga euphratica			x	
Sylvaemus (Sylvaemus) iconicus			x	
Tatera indica				x
Spalax ehrembergi	x			
Acomys tridens				x
Eliomys melanurus			x	
Myomimus sp.				x
Rhombomys opimus		x		
Dipodillus dasyurus	x			
Ellobius sp.		x		
Ellobius talpinus		x		
Ellobius lutescens		x		x
Ellobius fuscocapilus		x		
Chionomys nivalis				x
Arvicola terrestris				x
Microtus sp.		x		
Microtus (Microtus) socialis			x	x
Microtus (Microtus) philistinus			x	
Myomimus rachi				
Microtus guentheri	x			
Nannospalax ehrenbergi			x	

Table 1.2. Rodent species composition of the main taphonomic studies based on modern owl pellets.

human (AMH) occupations (Belmaker et al., 2016; Bermúdez de Castro and Martinón-Torres, 2013), making this region a prime location to study past human occupations over the Quaternary. This geographical area plays an important role to understand the biological history of human lineages and their techno-cultural complexes during the Pleistocene, as well as large and small mammals migrations. It was a natural corridor and refuge between Africa and Eurasia during the Pleistocene, and it was a very attractive area for humans as evidenced by the high number of sites located in this region, such as Dmanisi, Qesem Cave, Misliya Cave, Agithu-3, Dzudzuana Cave, among others (Belmaker et al., 2016; Coil et al., 2020; Kandel et al., 2017; Maul et al., 2015; Weissbrod and Weinstein-Evron, 2020).

The taxonomy and systematics of the modern rodent faunas of west Asia still need to be precised and the literature is lacking of skull and dental characters to identify properly fossil taxa. A first synthetic work is available for Turkey and some others for Iran. The recent increase of molecular taxonomies is not always accompanied by morphological ones. Consequently the observation of modern reference collections and molar morphology of properly moleculary defined taxa would be useful to improve their identification in the fossil assemblages (Stroetzel et al. 2019). Moreover, the development of Geometric Morphometric methods allow us to study separately size and shape and separate allometries on dental and skeletal elements and this represents new tools available to study western Asia rodents.

1.3. Archaeological, environmental and climatic context of the study sites

The chronology covered by our study sites comprises the Middle Pleistocene, the Late Pleistocene and the Holocene.

The Middle and Late Pleistocene were characterised by climatic fluctuations from cold to warm temperate conditions (Figure 1.1), which had an impact on flora, fauna

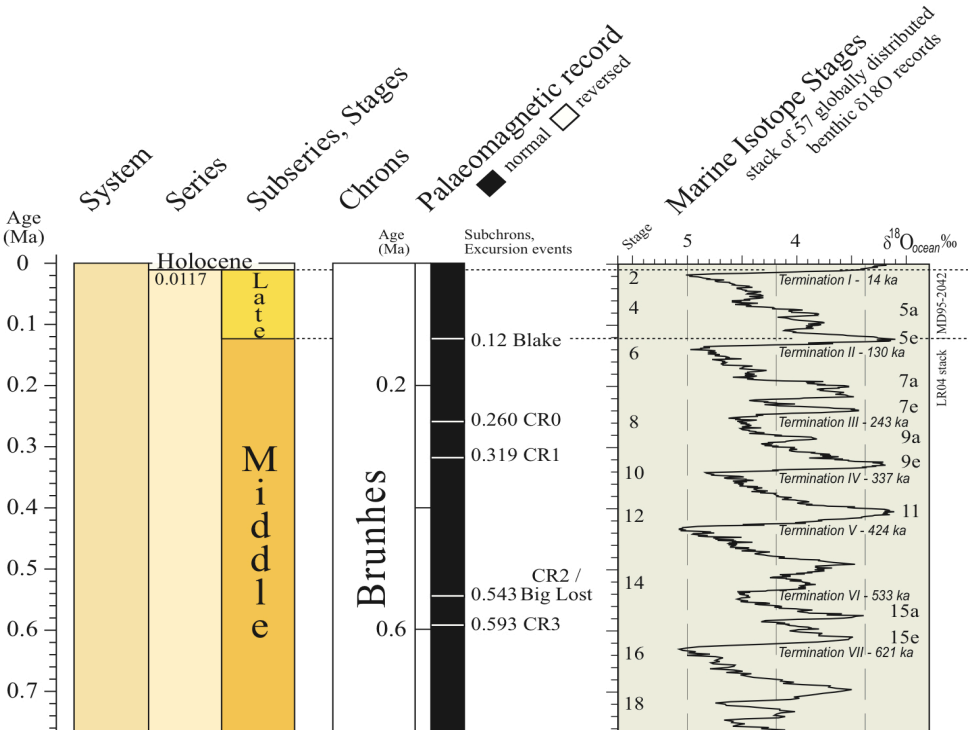


Figure 1.1. Oxygen Isotope (δ18O) data related from the Middle to the Late Pleistocene with the chronology and the palaeomagnetism record. Image modified from http://quaternary.stratigraphy.org/charts/



Figure 1.2: Location of the Caucasus, Zagros Mountains, Mediterranean Sea, Black Sea, Caspian Sea and the sites studied in this PhD thesis (map elaborated by Dr. Ana Fagoaga Moreno).

and human populations. The details of the climatic fluctuations having occurred during this period will be presented in the Discussion section.

In order to study these paleoclimatic fluctuations and observe whether rodent can be good climatic proxies we choose three different caves situated in both sides of the Caucasus and Zagros mountains. Because it is well known that rodent are mainly accumulated by owls in various fossil sites, we first tested the methodology upon and owl pellet assemblage of Middle East after a taphonomic analysis to verify the homogeneity of the assemblage and the modifications brought by the predator.

Azokh Cave (Figure 1.2) takes its name from the village situated near the cave. It is located in the Ishkhanaget River valley, Southern Caucasus (39º 37.15´ N; 46º 59.32´E) at 929 meters a.s.l (Asryan et al., 2020). It is an important site for the understanding of human evolution in its archaeological, paleontological, environmental and ecological context (Fernández-Jalvo, 2016). The main chamber is Azokh 1, which provided evidence for human occupations from the Middle Pleistocene to the present. This is a well stratified, well dated and well-studied site through a multidisciplinary approach including the study of lithic assemblages (Asryan, 2015; Asryan et al., 2020, 2017) as well as geology, geomorphology, taphonomy, zooarchaeology, palaeontology and anthracology (Allué, 2016; Asryan, 2015; Blain, 2016; Fernández-Jalvo, 2016; Fernández-Jalvo et al., 2010; Murray et al., 2016; Parfitt, 2016; Sevilla, 2016; Van Der Made et al., 2016). Azokh is today with a warm-temperate climate with continental conditions, where the annual mean temperature is 10.1°C, the maximum mean temperature is 22.9°C and the minimum mean temperature is -3°C. Annual rainfall is about 665 mm (https://en.climate-data.org/).

The current vegetation map of shows the presence of a broad belt of semi-xerophyllous woodland on the lowlands 4–6 km to the east of Azokh (Manuk 2010). Further to the east are belts of sagebrush steppe and sagebrush desert, and both would have constituted parts of the ranges of larger mammals and birds of prey (Andrews et al., 2016).

Kaldar Cave (Figure 1.2) is located in the northern part of the Khorramabad valley, Lorestan Province, western Iran (48º17'35" E, 33º33'25" N) at 1290 m a.s.l. The Khorramabad Valley is a narrow passage connecting the northern highlands with the southern lowlands of Khuzistan and constitutes one of the most important passage-ways for both humans and animals to cross the Zagros mountain range (Bazgir et al., 2014; 2017) ranging from 23,100 ± 3300 to 29,400 ± 2300 BP, and three AMS radiocarbon dates from charcoal samples belonging to the lower part of the same layer, yielding ages of 38,650–36,750 cal BP, 44,200–42,350 cal BP, and 54,400–46,050 cal BP (all at the 95.4% confidence level. This site provides evidence for the Middle to Upper Palaeolithic transition in the Middle East (Bazgir et al., 2017). Moreover, Kaldar Cave has yielded the oldest evidence of *Prunus* spp. in the area, through the study of charcoal remains (Allué et al., 2018), evidencing a wooded vegetation. The present climate in Khorramabad Valley is warm and temperate. The average mean annual temperature is 16.90ºC, the maximum mean temperature occurs in July with 29.60ºC and the minimum mean temperature is in January with 5ºC, with a mean annual precipitation of 488 mm (https://en.climate-data.org/asia/iran/lorestan/khorramabad-764550/).

These sites cover a chronological range from the Middle Pleistocene to the Late Pleistocene, and belong today to different bioclimatic regions. They allow to perform palaeoenvironmental and palaeoclimatic reconstructions with a high resolution throughout the study period. They will be presented and discussed more in detail in the following papers and in the discussion section (Chapter 8), establishing a relation between the obtained climatic data through the study of rodents, and the global climatic and isotopic chronology.

In parallel to the study of the archaeological material from Azokh and Kaldar, we also studied modern owl pellets coming from the Birecik region (37°1´N, 37°58´E) in Turkey (Figure 1.2). The area is located at the west of Euphrates River, in the Southern Anatolia, close to Syria and Iraq border. The sample is composed of forty pellets collected in a *Tyto alba* nest by Jean Francois Noblet in 2003. The study of this assemblage allows us to better characterize the taphonomic impact of such predator on the Middle Eastern prey species, which is still few documented. We also studied modern owl pellet samples from Turkey. Birecik is located in the Sanliurfa province, the centre of the South-eastern Anatolia. The altitude of the region is between 300-600 meters above the sea level and has a semiarid Mediterranean climate. Annual mean temperature is 18.5°C; the maximum mean temperature is 39°C and the minimum mean temperature is 2.7°C. Annual rainfall is about 458.1 mm and the precipitation regime is winter, spring, autumn, and summer. Birecik is characterised by a steppe vegetation (Vagif Atamov, 2007).

1.4. General research questions

The PhD thesis has the aim to answer the following questions:

- What was the origin of the accumulation for rodent remains in Azokh and Kaldar Cave?

-Are the Habitat Weighting and the Bioclimatic model a suitable methods for the palaeoenvironmental and palaeoclimatic

reconstructions in western Asia?

-Is it possible to obtain good classifications for western Asia rodents through the Geometric Morphometric Method (GMM)?

-Was the climate and the landscape favourable for human occupations during the Middle and Late Pleistocene in Azokh 1 and Kaldar Cave?

-Are mountains zones of Caucasus and Zagros uninterrupted geographic barriers for small mammals dispersal during the late Pleistocene?

-Are the rodent faunas affected by the climatic fluctuations? Are rodents an effective climatic proxy for the region?

1.5. Objectives of the research study

In order to answer these questions we developed a multi-disciplinary approach combining different methods of taxonomy, taphonomy and paleoecology. The main objectives are:

-Identify the rodent species and display dental morphological criteria, including a revision of the genus *Ellobius* using Geometric Morphometric methods because of its abundance in the archaeological sites. And also contribute to a better knowledge of modern and fossil rodent composition in western Asia.

-Identify the origin of the rodent accumulations. Usually small vertebrate accumulations are produced by predator(s), and taphonomic studies would help to determine them through bone representation, fragmentation and digestion and verify the ecological requirement of the predator responsible of the accumulations. This also allow to determine the homogeneity of the fossil assemblage (single or multi predator origin).

-Adapt and test the Habitat Weighting and the Bioclimatic Model methods to Middle Eastern species, on both modern and archaeological assemblages.

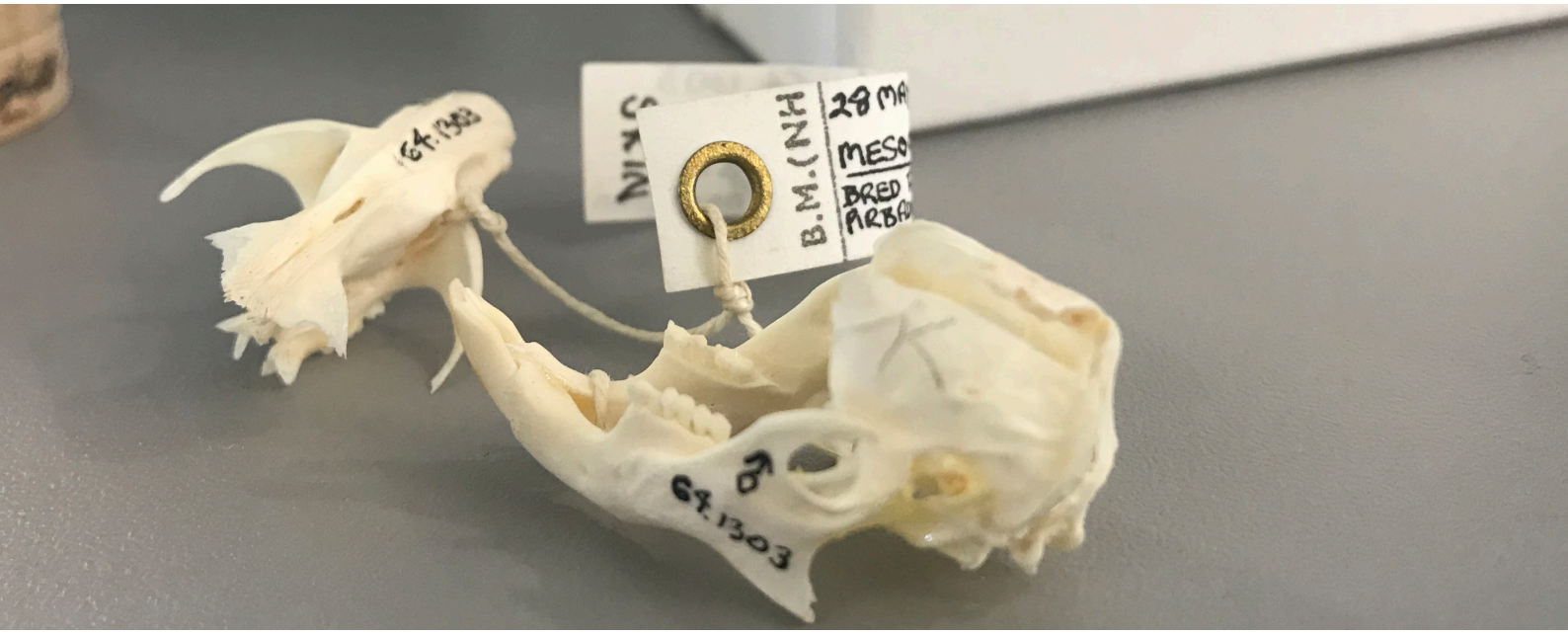
-Propose reconstructions of the past environment and climate of the studied archaeological sites during the Middle and Later Pleistocene in western Asia.

-Quantify the effects of past climatic and landscape changes which affected different hominin populations that inhabited in the studied sites in order to investigate if it was favourable for hominin occupations.

-Discuss the biogeographic origin of the rodent species found in the studied sites, and correlate the palaeoenvironmental and palaeoclimatic results with the Middle to Late Pleistocene general climatic context and try to see differences between the archaeological sites in western Asia.

Chapter 2.

Material and methods



The detailed archaeological material and study methods are given in the published manuscripts (Chapter 3, 4 and 6) and also on the unpublished one (Chapter 5). However, we considered that it was necessary to include a general methodological section explaining the main techniques used on the field and at the laboratory, as well as the detail of the reference specimens used in this work. Including the nomenclature, the measurements, a synthesis of the methods applied for the identification, environmental and climatic reconstruction; these methods would be explained in length in the manuscript chapters.

2.1. Field work

The rodent remains studied in this PhD thesis were recovered from the sediment samples extracted during the excavation campaigns at Azokh and Kaldar Caves. I personally participated in the field excavations of both sites: in Azokh in 2018 and 2019; also I picked up the sediments for Kaldar Cave 2014, 2015 in 2018 with Dr. Blain. This allowed me to better understand the sites occupations and stratigraphy, and to participate in the sediment sampling, sieving and sorting in order to recover small vertebrate remains.

In both sites, the sediment was collected in buckets during the excavation process. Then, it was transported in bags to the washing area, closed to the river where they were washed and dry. The sediments were sieved on two superimposed meshes of 5 mm and 1mm. After that the sediment was picked up by hand and under a binocular microscope when it was necessary (Figure 2.1).

Once the sediments were picked up, the fossil remains were stored in a minigrip bag with a label which includes the name of the site, the year, the date, the level, the square and the depth (z).

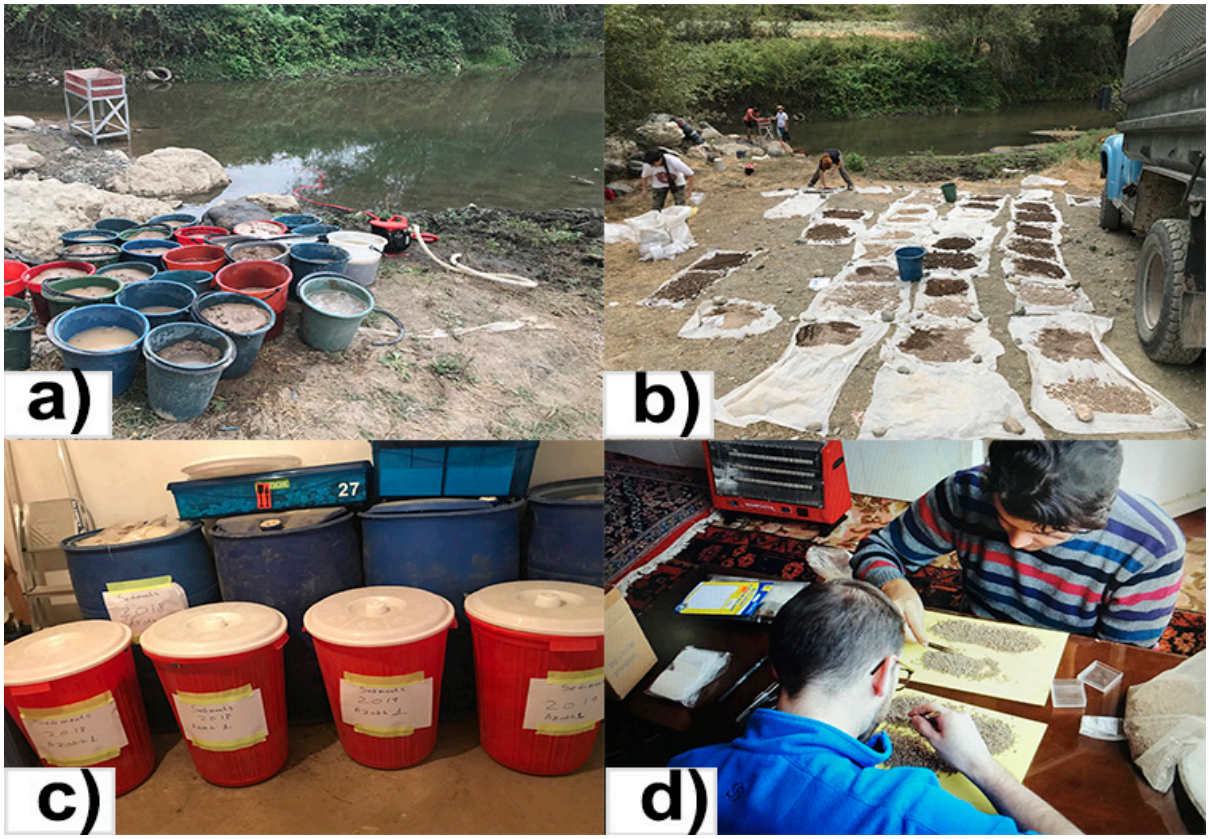


Figure 2.1. Sampling on the field. a) buckets with water and sediments from Azokh 1, b) sediments drying from Azokh 1, c) sediments from Azokh 1 prepared for sorting, and d) picking up the sediments at Kaldar Cave

2.2. Reference collections

The identification of fossil material was not elaborated satisfactory in this region, limiting most of identifications to the genus level. Species identification of the fossil material was our main priority, and few osteological discriminant characters were available in the literature. For correct identifications, we thus needed to compare our recovered fossil remains to modern osteological collections in order to assign the assemblage skeletal and dental remains to family, genus and/or species level when possible. We thus visited the modern reference collections of the Natural History Museum of London, the Field Museum of Chicago and the American Museum of Natural History of New York in order to observe modern specimens, detect dental characters and take pictures in order to better identify the archaeological material (Table 2.1) and perform further geometric morphometrics analyses.

I visited the Natural History Museum of London from 2/07/2018 to 27/07/2018, the American Museum of Natural History of New York from 4/09/2018 to 14/09/2018 and finally the Field Museum of Chicago 16/09/2018 to 30/09/2018. We chose to come to this museums because they hold a large amount of specimens from our concerned geographical areas, including the western and Central Asia, and also southeastern Europe, mainly from Iran, Russia, Armenia, Azerbaijan, Turkey and Afghanistan (Figure 2.2). Unfortunately, the rodent collections from the Muséum national d'Histoire naturelle from Paris were closed and we could not observe F. Petter Iranian collections.

	NHM	AMNH	FM	
Species	**Nº of Individuals**	**Nº of Individuals**	**Nº of Individuals**	**Total**
Cricetulus migratorius	33	8	11	**52**
Mesocricetus auratus			3	**3**
Mesocricetus brandti	9		1	**10**
Mesocricetus raddei	2			**2**
Apodemus witherbyi		6		**6**
Apodemus sylvaticus	5			**5**
Mus musculus	30	10		**40**
Tatera indica	8	5	43	**56**
Meriones crassus	22	32	51	**105**
Meriones hurrianae	20	7		**27**
Meriones libycus	30	33	86	**149**
Meriones meridianus	10	5		**15**
Meriones persicus	25	5	152	**182**
Meriones rex bunyi			12	**12**
Meriones tristrami	17		35	**52**
Jaculus jaculus		1		**1**
Jaculus blandfordi	3	4		**7**
Calomyscus mystax	1	5		**6**
Calomyscus bailwardi	13	5		**18**
Calomyscus hotsoni	1			**1**
Allactaga elater	7	12		**19**
Allactaga euphatica	4			**4**
Allactaga williamsi	4			**4**
Dryomys nitedula	5	5		**10**
Myomimus personatus	3			**3**
Ellobius fuscocapillus	7		37	**44**
Ellobius lutescens	7			**7**
Ellobius larvatus		16		**16**
Ellobius talpinus	9	14	20	**43**
Microtus majori	15			**15**
Microtus arvalis	16			**16**
Microtus irani	2			**2**
Microtus paradoxus/socialis	5	13		**18**
Microtus schelkovniko	2			**2**
Microtus socialis	33			**33**
Chionomys gud	6			**6**
Chionomys nivalis	9			**9**
Chionomys roberti	8			**8**
Clethrionomys glareolus	7			**7**
Total	**378**	**186**	**451**	**1015**

Table 2.1. Modern reference collections that I had the opportunity to consult in different museums: Natural History Museum of London (NHM), American Museum of Natural History of New York (AMNH) and Field Museum of Chicago (FM).



Figure 2.2. Pictures from the visited museums during this PhD thesis.

During these visits, the first step was to observe the osteological and molar characters with a binocular microscope, studying isolated tooth, mandibles and skulls, and taking some measurements in order to differentiate the species. After that, molars were all photographed in occlusal view with a digital camera (Canon EOS 700D) coupled with a binocular microscope (Leica M125) (Figure 2.3a), with a re-flex camera (Nikon D300 with and objective of 40mm) (Figure 2.3b) and also with a Dino-Lite microscope (model AM7915MZTL) when it was necessary and also for some videos (Figure 2.3c). As a support, we used plasticine and a small container filled with sand or pearls to put the skulls and mandibles in an adequate and totally motionless position. This is a non-invasive methodology that did not cause any damage on bones or teeth.

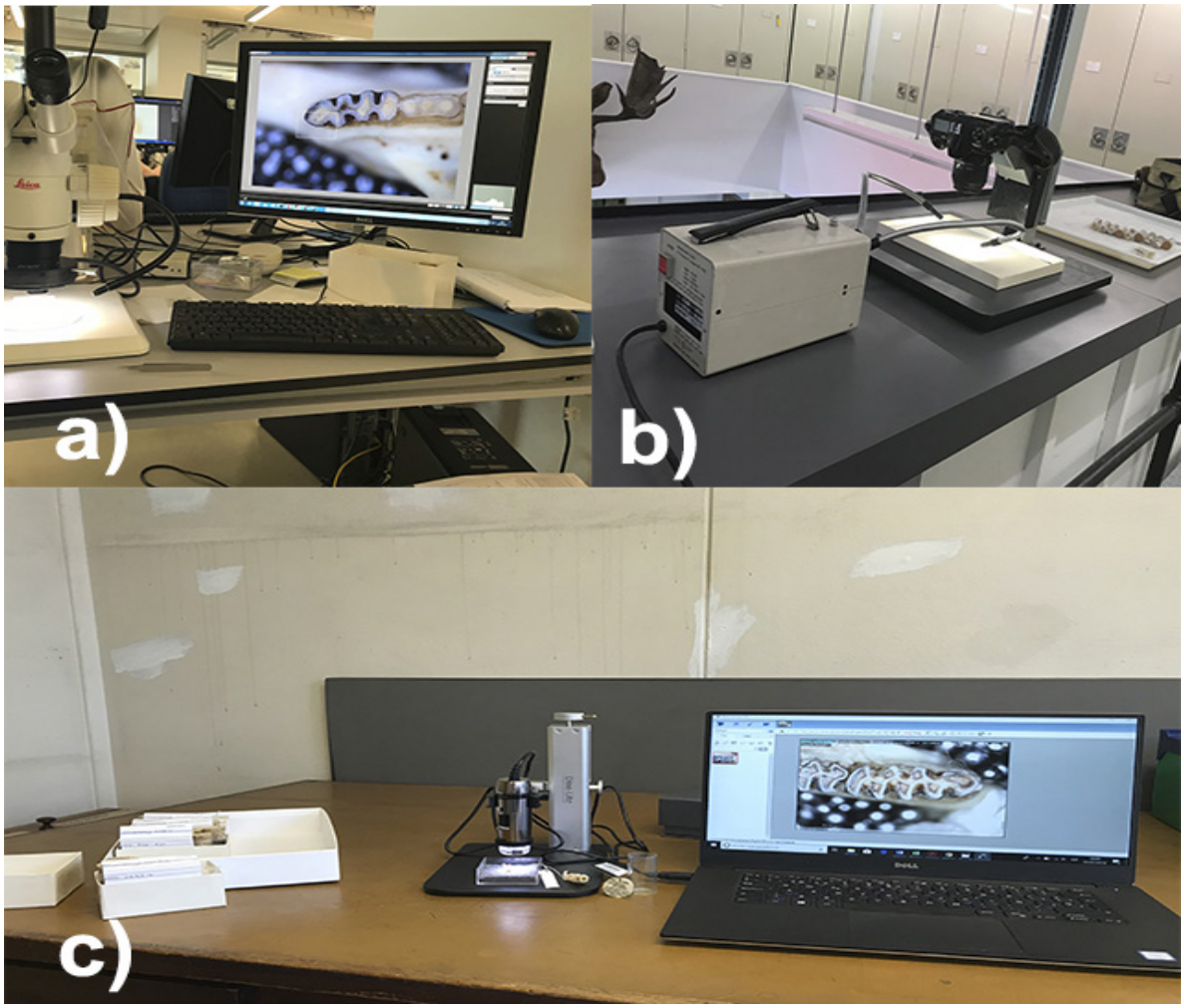


Figure 2.3. Photograph equipments used during the museums visits. a) digital camera coupled with a binocular microscope, from the NHM; b) reflex camera (Nikon D300 with and objective of 40mm) in ANHM and c) Dino-Lite microscope (model AM7915MZTL) in the NHM

2.3. Taxonomical nomenclature and measurements

In this part we expose the nomenclature and measurements used in the rodents study.

Family Cricetidae Fischer, 1817

For the Cricetidae molars which show a combination of cusps and lophs, we used the dental nomenclature defined by Mein & Freundenthal and modified by López-Guerrero et al., 2013. For each molar after examination under the binocular (or dinolite) of its integrity we realized general measurements of the maximal length (L) and width (W) in millimetres (Figure 2.4)

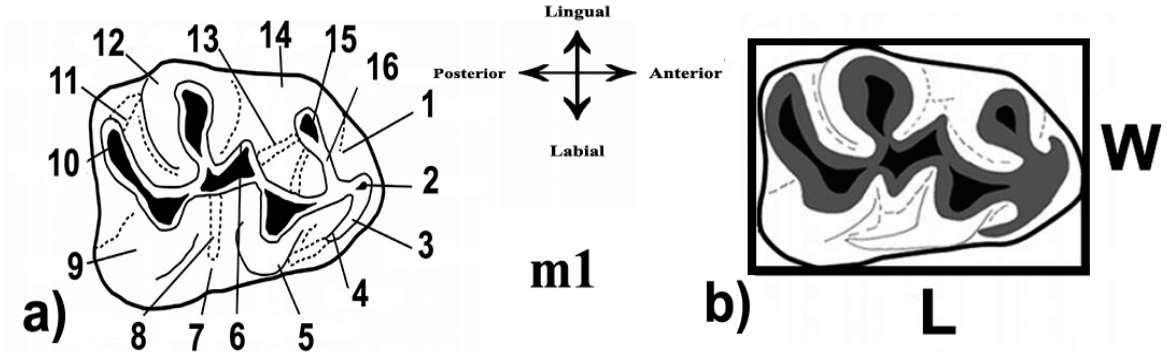


Figure 2.4. Cricetidae nomenclature. *Cricetodon* right first lower molar, m1. a) 1-Anteriosinusid, 2-Anteroconid, 3-Labial anterolophid, 4-Protosinusid, 5-Protoconid, 6- Mesolophid, 7-Sinusid, 8-Ectomesolophid, 9-Hypoconid, 10-Posterolophid, 11-Posterosinusid, 12-Entoconid, 13-Metalophulid II, 14-Mesosinusid, 15-Metaconid and 16-Metalophulid I ; b) L- total length and W- total width (modified after Mein and Freudenthal, 1963 and López-Guerrero et al., 2013).

Subfamily Arvicolinae Gray, 1821

For Arvicolinae molars, composed by triangles (T), the posterior lobe (PL) and the anterior cap (AC), we followed the dental nomenclature of Van der Meulen, modified by Rey-Rodríguez (2015). For *Arvicola* we applied the SDQ developed by Heinrich and modified by Lozano-Fernández (2013); we also took into consideration general measurements as the total length (L) and total width (W) in milimeters (Figure 2.5)

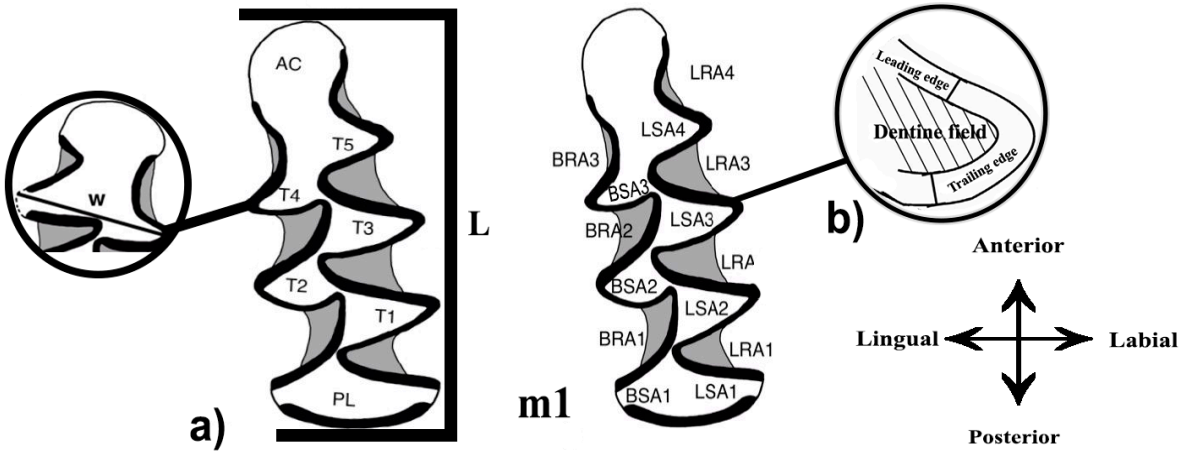


Figure 2. 5. Arvicolinae nomenclature. a) Occlusal surface of *Arvicola* right first lower molar m1. T- triangle, BRA- buccal re-entrant angle, LRA- lingual re-entrant angle, AC- anterior cap and PL- posterior lobe, L- total length and W- total width ; b) elements used for the SDQ calculation (According to Van der Meulen, 1972 and modified from Rey-Rodríguez, 2015 and Lozano-Fernández et al., 2013).

Subfamily Gerbillinae Gray, 1825

For the Gerbillinae skull measurements have been done, taking into account the condylo-basal length, zygomatic breadth, maxillary tooth row and the tympanic bullae length following Kryštufek and Vohralík (2009) (Figure 2.6a). For molars we followed the dental nomenclature of Kryštufek and Vohralík (2009) and we took into consideration the morphology of the anterolophulide, the neolophide and the lobes; we also made general measurements as the total length (L) and total width (W) in milimeters (Figure 2.6).

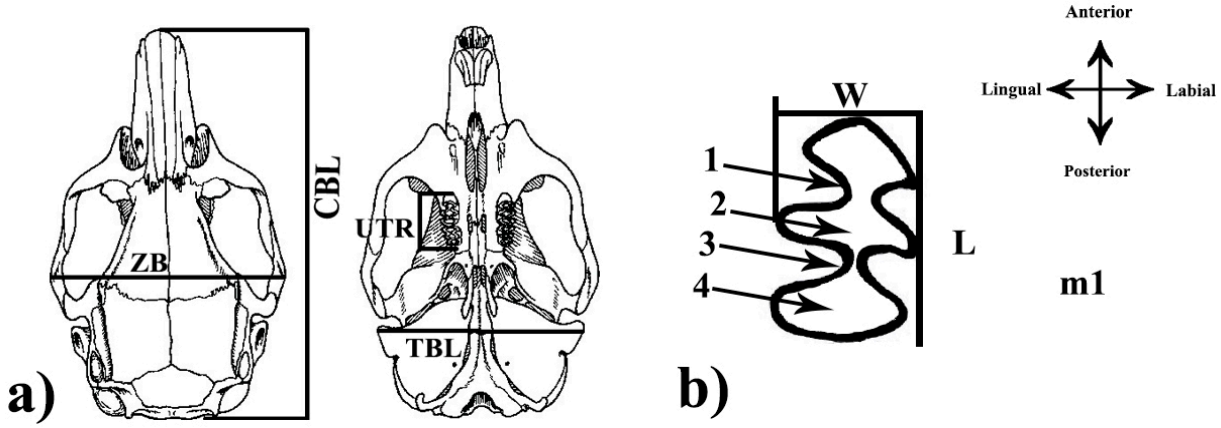


Figure 2.6. Gerbilinae nomenclature. a) Skull measurements abbreviations. CBL- Condylo-basal length, ZB- Bizygomatic breadth, UTR- Upper tooth row and TBL- tympanic bullae length of Meriones skull; b) L- total length and W- total width, 1- anterolophulide, 2- first lobe, 3- neolophide and 4- second lobe of first right lower molar (m1) of *Meriones*, picture modified from Kryštufek and Vohralík (2009).

Family Muridae Illiger, 1811

For the Muridae molar that shows cusps, protocone, paracone, hypocone we followed Michaux 1971 modified by López-García 2008 (Figure 2.7)

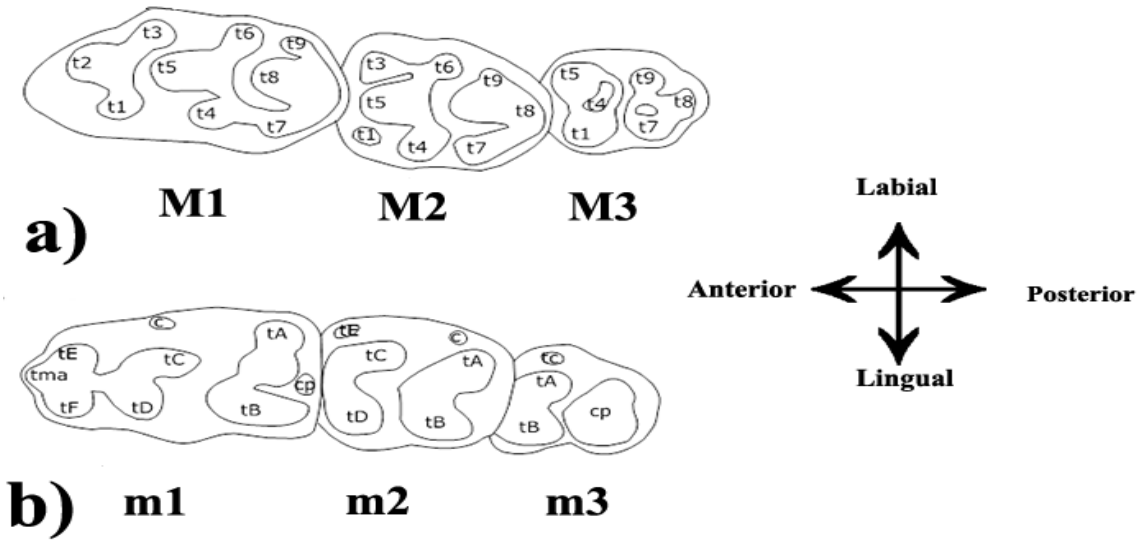


Figure 2.7. Murinae nomenclature. Upper and lower molars of Apodemus. a) right upper molars. T (1-9)- cusp, t5- protocone, t6- paracone, t8- hypocone, t9- metacone ; b) right lower molars. C- labial accessory cusp, cp- posterior accessory cusp, tma- medium anterior cusp, tF- principal antero-lingual cusp, tE- principal antero-labial cusp, tD- metaconid, tC- protoconid, tB- entoconid, tA- Hipoconid (according to Michaux 1971 and López-García 2008).

Family Dipodidae Fischer, 1817

For the Dipodidae molars we followed the nomenclature of Nesin and Kovalchuk (2017), however the dental characters of these species are not well studied in western Asia representatives (Figure 2.8)

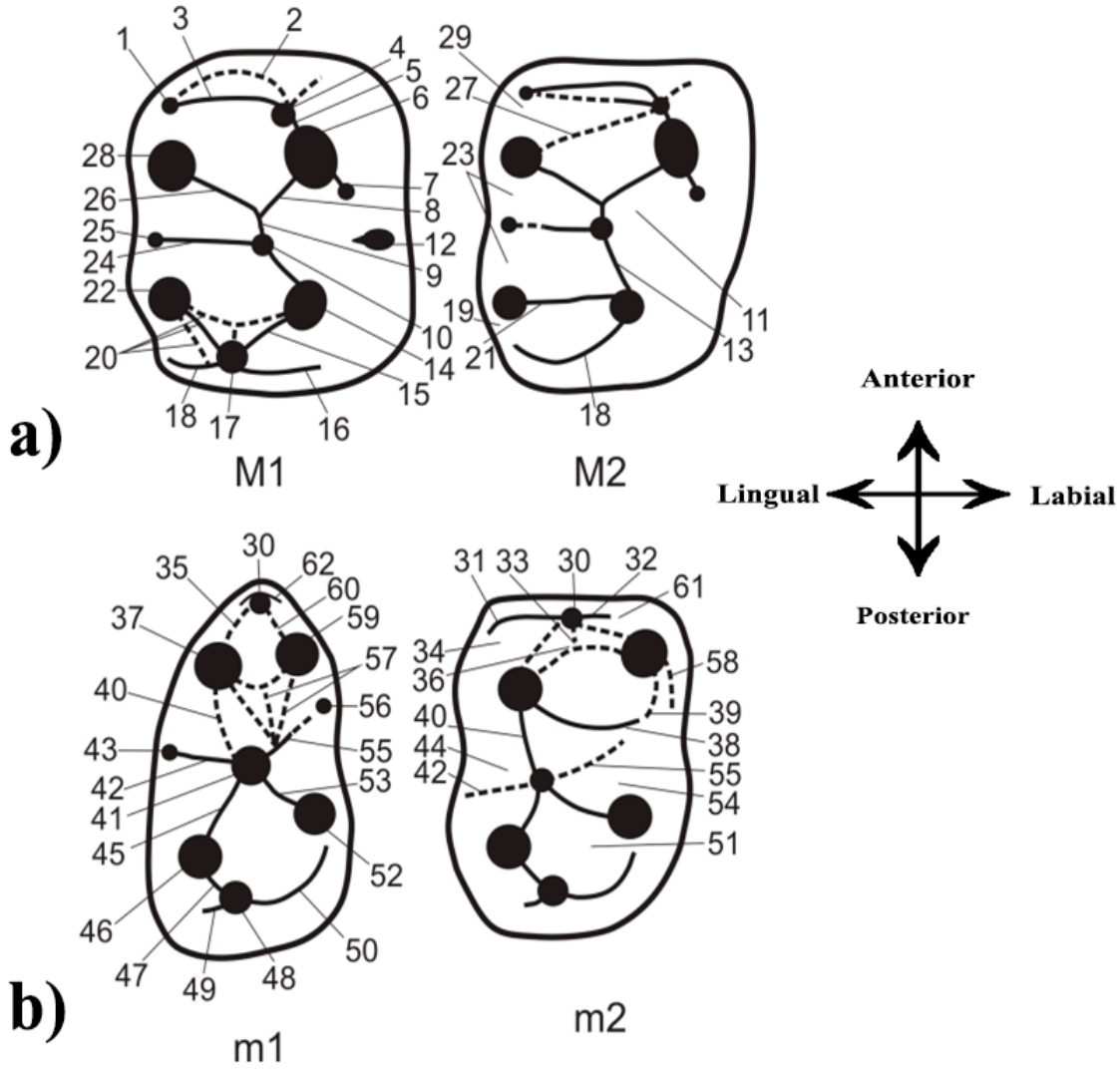


Figure 2.8 . Dipodida nomenclature. *Allactaga* upper and lower teeth. a) Upper dentition: 1, anterostyle; 2, anteroloph I; 3, anteroloph II; 4, anterocone; 5, anterior arm of the protocone; 6, protocone; 7, protostyle; 8, posterior arm of the protocone; 9, anterior endoloph; 10, mesocone; 11, endosinus; 12, endostyle; 13, posterior endoloph; 14, hypocone; 15, posterior arm of the hypocone; 16, lingual arm of the posteroloph; 17, the metaconule; 18, labial arm of the posteroloph; 19, posterofossette; 20, metaloph II; 21, metaloph I; 22, metacone; 23, mesofossette; 24, mesoloph; 25, mesostyle; 26, protoloph II; 27, protoloph I; 28, paracone; 29, anterofossette; b) Lower dentition: 30, anteroconid; 31, labial arm of the anterolophid; 32, lingual arm of the anterolophid; 33, anterolophulid; 34, anterosinusid; 35, anterior arm of the protoconid; 36, metalophid I; 37, protoconid; 38, posterior arm of the protoconid; 39, metalophid II; 40, ectolophid; 41, mesoconid; 42, ectomesolophid; 43, ectostylid; 44, ectosinusid; 45, anterior arm of the hypoconid; 46, hypoconid; 47, posterior arm of the hypoconid; 48, hypoconulid; 49, labial arm of the posterolophid; 50, posterolophid; 51, posterofossettid; 52, entoconid; 53, anterior arm of the entoconid; 54, mesofossettid; 55, mesolophid; 56, mesostylid; 57, endolophid; 58, metastylid crest; 59, metaconid; 60, anterior arm of the metaconid; 61,anterofossettid; 62, cingulid. Modified from Nesin and Kovalchuk (2017).

Family Gliridae Thomas, 1897

For the Gliridae molars we followed Kaya and Kaymakçı, (2018), however the dental characters of this genus are not well detailed for western Asia species (Figure 2.9)

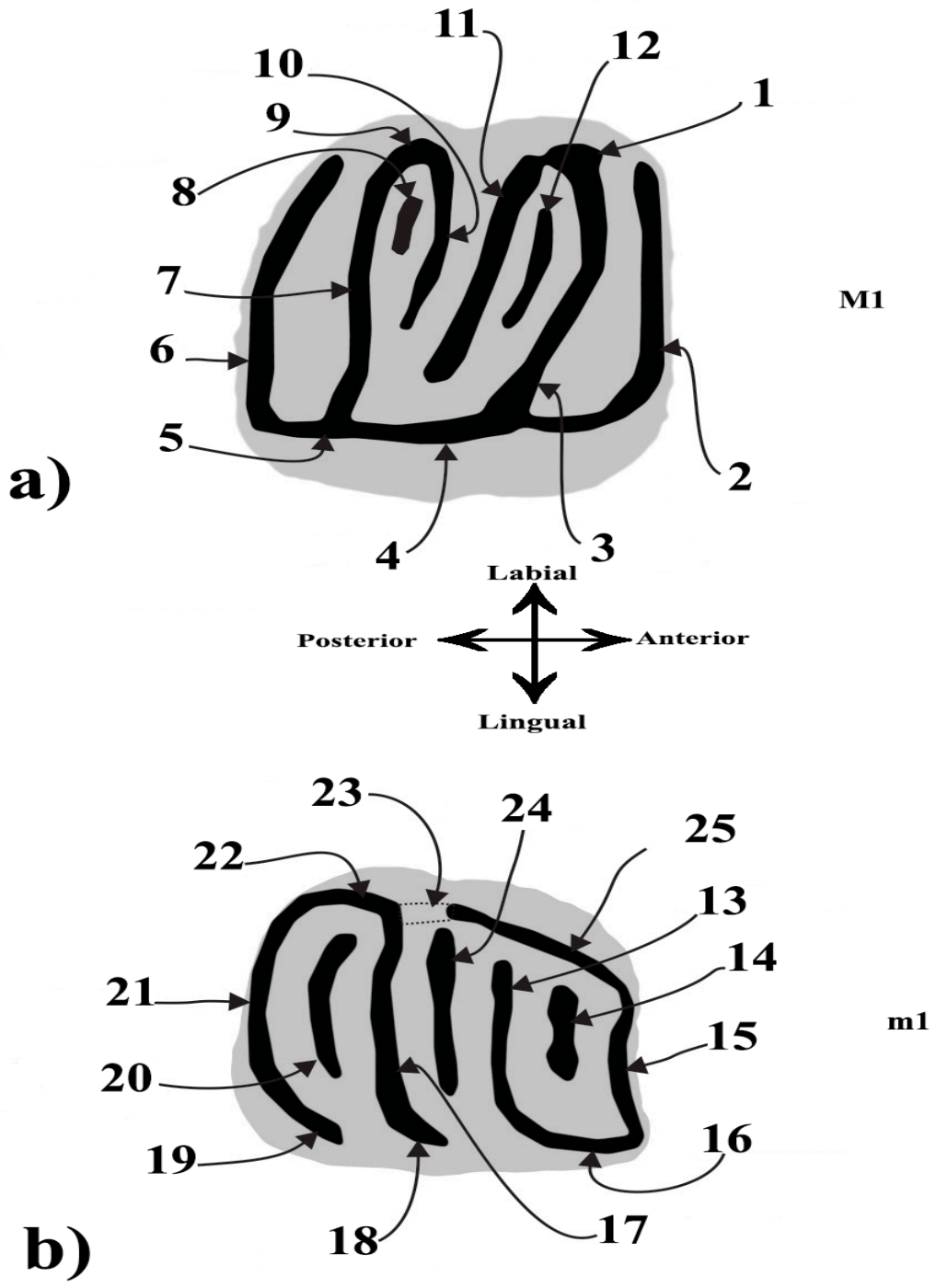


Figure 2.9. Gliridae nomenclature. *Myomimus* upper and lower teeth. a) Right first upper molar, M1. 1-paracone, 2-anteroloph, 3-protoloph, 4-endoloph, 5-protocone, 6-posterioloph, 7-metaloph, 8-posterior extra ridge, 9-metcanoce, 10-posterior centralloph, 11-anterior centraloph, 12-anterior extra ridge ; b) right first lower molar, m1; 13-metalophid, 14-anterior extra ridge, 15-anterolophid, 16-protoconid, 17-mesolophid, 18-mesoconid, 19-hypoconid, 20-posterior extra ridge, 21-posterolophid, 22-entoconid, 23-endolophid ,24-centrolophid and 25-metaconid. Modified from Kaya and Kaymakçı, (2018).

2.4. Methods applied for the identifications, environmental and climatic reconstruction

During the elaboration of this PhD thesis several methods has been applied.

For the taxonomical identification on rodents we mainly used molars of reference specimens that were identified at a specific level, when it was possible, thought the comparative morphological analysis. We also used the basic morphometric data available from the literature, combined with those obtained in the reference collections (Chapter 1).

In some cases it was necessary to take measurement with the Mitutoyo caliper, on the most complete elements of the skull and mandibles, and also with the Image J software on molars. With the objective to elaborate comparative tables and also Principal Component Analysis (PCA).

More information about the detailed identification of the species is available on Chapter 3, 5 and 6. The limitation of classical morphometric data that prevented us to reach specific identifications in the case of some genera (eg: *Ellobius*) lead us to applied some of the Geometric Morphometric (GM) approach. These were performed on the lower m1 in the genus *Ellobius*, it would be necessary to combine GM with systematics avaliable date and use all the criteria together; complete explanation of the method is found in Chapter 4.

A complete taphonomic study was also developed on the Birecik sample, Chapter 3, and also some preliminary taphonomic studies in Azokh 1 and Kaldar Cave are available on Chapter 5 and 6. The main objective of these works is to better identify the nature and the origin of the acumulation, and esential proxy for the palaeoecological interpretations based on small mammals.

In order to reconstruc the enviroment we apply the Habitat weighting (Evans et al., 1981; Andrews, 2006; modified by Blain et al., 2008; López-García et al., 2011), which is based on the current distribution of each taxon in the habitat(s) where it can be found nowadays, adapting this method to our studied area (Rey-Rodríguez et al., 2020).

For the paleoclimatic reconstruction we used the Bioclimatic Model, tha was developed by Hernández-Fernández (2001) and updated by Royer et al. (2020). This methods is based on the faunal spectrum, assuming that small- and large-mammal species can be ascribed to ten different climates (Hernández-Fernández, 2001; Hernández-Fernández & Peláez-Campomanes, 2003; Hernández-Fernández et al., 2007).

Specific details about both methods are present in the methodological section of Chapter 3, 5 and 6.

Chapter 3.

Implications of modern Barn owls pellets analysis for archaeological studies in the Middle East



Abstract

Situated at the crossroad between Africa, Asia and Europe, the Middle East is an important region for the knowledge of human and mammal migrations. Among mammals, fossil small mammals are good proxies for palaeoenvironmental reconstructions, and can also play the role of markers of prehistoric movements. In the aim to better characterize the origins and the palaeoecological signal delivered by the small vertebrate assemblages in Middle East archaeological sites, we performed a taxonomic and taphonomic study of the small mammal remains found in pellets from Barn owl (*Tyto alba*) from a poorly known region of South of Turkey at the Syrian border, east of Euphrates River. This will constitute the first available taphonomic referential for this region.

The studied sample constituted by more than 40 disintegrated pellets provided 2503 rodent skeletal elements. The most common preys are *Meriones tristami*, followed by *Mus musculus*. The taphonomic study showed that our assemblage fits well with a predator category of light modification. Regarding the preservation, our mean bone relative abundance reached 82% and the bone fragmentation showed that more than 77% of our sample is intact. The digested elements represented 22% and the low to moderate grades were dominant (83.5%). Implications for environmental and climatic reconstructions based on small mammal communities were also explored using Bioclimatic model and Habitat Weighting methods.

Keywords: Regurgitation Pellets, *Tyto alba*, Southern Anatolia, Bone modification, Environmental reconstruction



Rey-Rodríguez, I., Stoetzel, E., López-García, J.M., Denys, C., 2019. Implications of modern Barn owls pellets analysis for archaeological studies in the Middle East. Journal of Archaeological Science 111, 105029. https://doi.org/10.1016/j.jas.2019.105029

1.Introduction

Birds of prey predate small mammals that they usually swallow in the whole and regurgitate bones, teeth and fur as compact pellets (Shad and Kakhki, 2014). The studies of the pellets are really useful because they provide information about small mammal species occurrences in some regions, as well as the extent of bone modifications after the regurgitation process.

Our current understanding of small mammal distribution is based on the specimens found in zoological collections of the museums and most of them result of trapping surveys, scavenging of road killed individuals. More rarely museums host owl pellets assemblages while they can also provide useful information about the predatory birds diet, as well as rare prey-species abundance or distribution, habitat preferences, cyclic population dynamics, or seasonal changes (Boitani and Molur, 2016; Kryštufek and Vohralík, 2009; Haddadian Shad et al., 2014). Consequently, pellet assemblages are often used as supplementary data for faunistic surveys, and a some studies have been performed in the Middle East (Abi-said, Shehab and Amr, 2014; Darvish et al., 2000; Kopij and Livenschulman, 2013; Obuch and Khaleghizadeh, 2012; Haddadian Shad et al., 2014; Shehab et al., 2013).

For the archaeologists and palaeontologists, owl pellets assemblages are considered as the major source of fossilised accumulations (Andrews 1990). A taxonomic study of such fossil small mammal assemblages resulting from owl pellets represent an efficient tool for palaeoenvironmental reconstructions, but needs a preliminary taphonomic analysis to ensure that no major bias has altered the palaeoecological signal (e.g., Fernández-Jalvo et al., 2016; Stoetzel et al., 2011). In order to refine theses taphonomic analyses and to better identify the origin of the accumulations, we need an exhaustive referential of modern avian predation for the study area (Eurasia, and more precisely Middle East). Indeed, each area has particular characteristics in term of predator and prey species, which may lead to different taphonomic signals.

The Barn owl is one of the major contributors to the fossil bone accumulations, being opportunistic and taking a wide range of preys, including mostly rodents and insectivores (Andrews, 1990). Here we present the first combined taxonomic and taphonomic study of small mammals remains from *Tyto alba* pellets from South Turkey, in order to contribute to a better knowledge of the Middle East small vertebrate predators and their taphonomic impact on prey bones.

2.Material and Methods

2.1.Sampling of the studied material

The studied pellets come from the region called Birecik (37°1´N, 37°58´E) in Turkey (Figure. 3.1). The area is located at the west of Euphrates River, in the Southern Anatolia, close to Syria and Iraq border. Forty pellets have been collected by Jean Francois Noblet in June 2003, in a *Tyto alba* nest behind the breeding station of Northen bald Ibises (*Geronticus seremita)* installed in a valley near the Euphrates riverside, 3 km north of Birecik Şanlıurfa.

The pellets were disintegrated during handling and their contents were sorted by hand under microscope in order to identify and count the skeletal elements.

2.2.Taxonomy

Bones were recovered manually and



Figure 3.1. Geographic location of the studied area, Birecik (Southern Anatolia, Turkey).

identified at a specific level when it was possible, following the established available identification keys (Boitani and Molur, 2016; Coşkun, 1999; Darvish et al., 2006; Darvish, 2011; Pavlinov, 2008; Kryštufek and Vohralík, 2009; Mamkhair et al., 2007; Momtazi et al., 2008; Musser and Carleton, 2005; Yicit and Çolak, 1996; Siahsarvie and Darvish, 2008; Tez, 2000). Some measurements were done using Mitutoyo caliper (precision 0.01 mm) on the most complete elements of the skull and mandibles. Regarding the nomenclature and identification keys, for Soricidae we followed Kryštufek and Vohralík (2001), for Gerbillinae we followed Pavlinov (2008) and for Murinae Darvish et al. (2006).

The Minimal Number of Individuals (MNI) has been estimated using the most abundant skeletal element present in the assemblage, including cranial and postcranial elements.

2.3.Taphonomy

The taphonomic study focused upon bone representation, fragmentation and digestion of small mammal elements recovered from the pellets. For this we followed the methodology developed by Andrews (1990), Denys et al. (1996) and Fernández-Jalvo et al. (2016).

2.3.1.Skeletal element proportions

The differing proportions by which the various elements of the prey skeletons are represented in a predator assemblage are frequently used to distinguish different types of predators. The numbers of the skeletal elements are usually expressed to be present for a given number of prey individuals, which is usually the minimum number of individuals (MNI). This proportion is called the relative abundance (Andrews 19 90).

$$R_i = N_i / (MNI \times E_i)$$

Where:

R_i= the relative abundance of the element i

N_i= the number of element i in the sample

MNI= the Minimum Number of Individuals

E_i= the number of element i in the prey skeleton

For example, the number of bones found in the skeleton of an individual of a rodent like a mouse is: 1 skull, 2 maxillaries, 2 mandibles, 12 molars, 4 incisors, 2 femora, 2 humeri, 2 radii, 2 ulnae, 2 tibiae, 2 scapulae, 2 pelves, 2 astragali, 2 calcanei, 1 sacrum, 20 metapodials, 54 phalangias, 54 vertebrae, 24 ribs (Denys & Patou-Mathis, 2014; Stoetzel

et al., 2011).

The calculation is based on the notion that the predator consumes most or all of the body of the prey and modern samples indicate that predators have characteristic patterns for the proportional abundances of prey elements. As a result, the MNI should approximate to the number of preys eaten.

Three indices have been used to compare the preservation of postcranial and cranial elements. The first compares femora and humeri with the number of mandibles and maxillae ((F+H)/ (Md+Max)*100). The second compares the number of all long bones with the major cranial elements and isolated molars ([femora + tibiae+ humeri + radii + ulnae]*16/([mandibles + maxillae + molars] *10)*100) and the third is the comparison between tibia and radii between femora and humeri [(tibia+radii) / (femora+humeri)] (Andrews 1990; Stoetzel et al., 2011).

2.3.2.Breakage

Breakage can also help to differentiate major groups of predators (Andrews 1990), notably the breakage of long bones, skulls and mandibles. But in our sample, most of the postcranial material cannot be identified at the species level, so we didn't analyse the breakage by taxa.

We also have to keep in mind that if in modern assemblages bone breakage can help identify the predator, in archaeological or palaeontological context many post-depositional processes may lead to an over-breakage of the material, and hide the "*predator signal*". Consequently, other taphonomic parameters (notably digestion) have to be taken into account for more reliable interpretations.

2.3.3.Digestion

The corrosive effects of digestion on bones and teeth in the predator´s stomach are well distinguishable from other alteration processes (e.g. Fernandez Jalvo et al., 2014). Digestion is the most reliable parameter used to identify the predator type at the origin of a small mammal accumulation. It is based on both the degree of digestion and on the proportion of teeth and bones affected, considering that each type of predator has a different effect of digestion (Andrews 1990). In our study we have considered light, moderate and strong digestion grades following Andrews (1990) and Fernandez-Jalvo et al. (2016) on molars, incisors, femora and humeri. We precise that we have not found any postpredation modification in our sample.

Patterns of digestion, if they are well visible to the naked eye, are best distinguished using the Scanning Electron Microscope (SEM) (Andrews 1990; Demirel et al., 2011). In our study we used the SEM Hitachi SU 3500 from the *Service Commun de Microscopie Electronique du Museum National d'Histoire Naturelle* (MNHN-Paris), using secondary electron emission mode at an accelerating voltage of 15 kV.

2.4.Statistical analysis

Size differences have been investigated using Principal Component Analysis (PCA) between our sample and the references provided by the literature using the statistical software XLSTAT 10.0. Skull measurements have been done, taking into account the condylo basal length, zygomatic breadth, maxillary tooth row and the tympanic bullae length (Figure 3. 2).

2.5.Climatic reconstruction

Finally, we tried to evaluate the potential of small mammal associations accumulated by Barn owl to infer environmental and climatic parameters in using methods previously developed for fossil mammal assemblages. The Bioclimatic Model

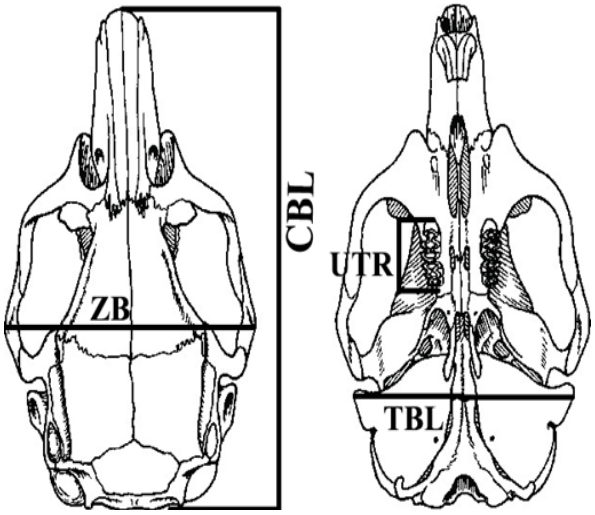


Figure 3.2. Skull measurements abbreviations. CBL: Condylo-basal length; ZB: Bizygomatic breadth; UTR: Upper tooth row; TBL: tympanic bullae length. *Meriones* skull picture modified from Kryštufek and Vohralík (2009)

(BM) was developed by Hernández-Fernández (2001) in order to reconstruct palaeoclimatic conditions based on faunal spectrum, in assuming that small- and large-mammal species can be ascribed to ten different climates (Hernández-Fernández, 2001; Hernández-Fernández & Peláez-Campomanes, 2003; Hernández-Fernández et al., 2007). We applied this method for the first time on an assemblage from South Anatolia. It was first necessary to calculate the Climatic Restriction Index (CRIi=1/n, where i is the climatic zone where the species appear and n is the number of zones where the species is present) and the Bioclimatic Component (BCi = (Σ CRIi) 100/S, where i is the climatic zone; S is the number of species). From the BC a mathematical model has been developed as a regression that allows us to calculate climatic parameters (see Appendix 1).

The different climatic groups defined by Hernández-Fernández (2001) and Hernández-Fernández et al. (2007) are: I Equatorial; II Tropical with summer rains; II/III Transition tropical semiarid; IV, Subtropical with winter rains and summer droughts; V, Warm temperate with not very severe winters but high humidity; VI, Typical temperate with winters that are cold but not very long, but summers that are cool; VII, Arid-temperate with large temperature contrasts between winter and summer and VIII, Cold-temperate with cool summers and long cold winters (boreal).

By means of the BM we are able to estimate the mean annual temperature (MAT), the mean temperature of the coldest month (MTC), the mean temperature of the warmest month (MTW) and the mean annual precipitation (MAP).

2.6. Environmental reconstruction

The method used for the palaeoenvironmental reconstruction is the Habitat Weighting method (Evans et al., 1981; Andrews, 2006; modified by Blain et al., 2008; López-García et al., 2011), which is based on the current distribution of each taxon, in the habitat or habitats where it is possible to find each taxon nowadays. We adapted the method to our studied area, including the following types: Forest (Fo) a long area covered with trees, Shrubland (Sh) where the vegetation is dominated by shrubs; Grassland (Gr) an open area covered with grass, Desert (De) area with little precipitation and no vegetation cover and Wetlands (We) are normally use in agriculture (cereal fields).

3.Results and discussion

3.1.Taxonomic study

In total, 2503 identifiable skeletal elements were recovered from the studied pellets, belonging to only four small mammal taxa (Table 3.1). Rodents constituted the bulk of *T. alba* Birecik preys with 38 individuals and three genera (*Meriones*, *Nesokia* and *Mus*) followed by Eulipotyphla represented by one species (*Suncus etruscus*)

Species	MNI	%
Suncus etruscus	1	2.56
Nesokia indica	1	2.56
Mus musculus	5	12.82
Meriones tristami	32	82.05
Total	**39**	**100**

Table 3.1. MNI: Minimal Number of Individual; %: percentage of relative abundance.

and one individual. We present here some of the cranio-dental characters that allowed taxonomic identifications.

Order Eulipotyphla , Waddell et al. 1999

Family Soricidae, G. Fishcher, 1814

Genus *Suncus*, Ehrenberg, 1832

***Suncus etruscus* (Savi, 1822)**

Material: 2; one right **mandible** and one left **mandible** (Fig. 3.3.1).

Description and discussion: In Turkey four species of white-toothed shrews are documented (Kryštufek and Vohralík, 2001; Tez, 2000): *Crocidura leucodon*, *Crocidura suaveolens*, *Crocidura arispa* and *Suncus etruscus*. *Suncus* differs from *Crocidura* in having four upper unicuspids instead of three. In our material, the absence of maxillary prevents precise identification on this criterion. However, regarding mandibules, we can attribute our samples

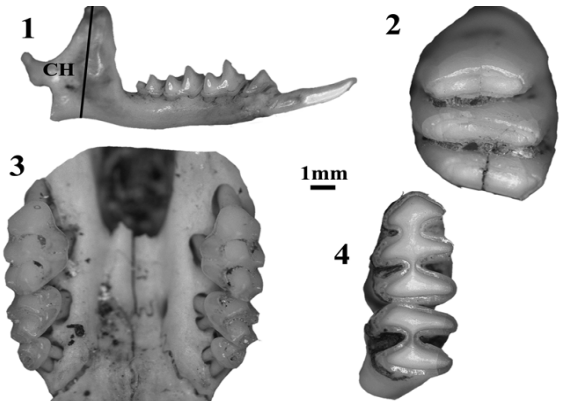


Figure 3.3. 1-Right mandible *Suncus etruscus*, CH (Coronoid height); 2-Right Left Upper M1 molar *Nesokia indica*; 3-*Mus musculus* maxilla; 4-Left lower molar row with m1 and m2 of *Meriones tristami*.

to *Suncus etruscus*, because of their smaller height of the coronoid process (Table 3.2).

Habitat and distribution: found in the Mediterranean region *Suncus etruscus* prefers abandoned olive groves, vineyards, and other cultivated areas overrun by Mediterranean shrubs, but occurs also in gardens, low maquis, scrub, and open forest of Mediterranean oaks and pines. This species avoids sand dunes, dense forest and intensively cultivated land. It is more active during night than day. *Suncus etruscus* is distributed from Southern Europe, North Africa, parts of the Near East, Arabian Peninsula, Central Asia, South Asia and

Specimen	Coronoid Height	Number of specimens	Min-max	Mean
Birecik sample	3.13- 3.25	2	3.13-3.25	3.19
Crocidura leucodon	4.3-5.9	63	4.3-5-9	4.92
Crocidura suaveolens	4.0-5.0	230	4.0-5.0	4.52
Crocidura arispa	4.1	2	4.1	4.1
Suncus etruscus	2.8-3.3	43	2.8-3.3	3.06

Table 3.2. Measurements of the coronoid height of the mandible in mm from Krystufek and Vorhalik (2001).

mainland Southeast Asia, to the island of Borneo in the east. It occurs from sea level to altitudes of 3000 meters above sea level (Aulagnier et al., 2017). In Turkey it was found mainly in the western and South Anatolia, especially in anthropogenic habitats up to 1200m (Kryštufek and Vorhalik, 2001).

Order Rodentia Bowdich, 1821

Family Muridae Illiger, 1811

Genus *Nesokia*, Gray 1842

***Nesokia indica* (Gray, 1830)**

Material: 2; one right **maxillary** fragment with M1 and one **isolated** Upper right M2.

Description and discussion: In our sample (Figure 3.3.2) the M1 and the M2 are high-crowned, broad and transversely laminated. There are three simple and isolated laminae on the M1, and only two on the M2. The first laminae of the M1 of Birecik pellets is wide and convex, while in Gerbillinae the first lamina (or prelobe) is small and much narrower; this allows us to distinguish it from *Tatera* and attribute this material to *Nesokia indica*. The relative size of the 2 M also is typical of *Nesokia*, the first molar being the longest and the most complex, and the last molar being the shortest and the most simplified (Kryštufek et al., 2017).

Habitat and distribution: This specie has a predominantly Palearctic distribution. It requires firm damp soil to dig in and succulent grass roots or underground bulbs to feed upon. It is found in humid areas in dry steppes, semi-deserts and deserts, but occurs mainly around permanent water bodies (Kryštufek and Vohralík, 2009). *Nesokia indica* is very widespread in south-western and Central Asia (Boitani and Molur, 2016). In South Anatolia, *Nesokia indica* is mainly distributed near cultivated field and it is strictly limited to agricultural activities (Kryštufek and Vohralík, 2009).

Genus *Mus* ,Linnée 1758

***Mus musculus* (Linaeus, 1758)**

Material: **Skull**: one fragmented skull; **Mandibles**: 10; five complete right mandibles, five complete left mandibles; Maxillae: 4; one complete right maxilla, three complete left maxilla; **Isolated Teeth**: 4, one right lower m1, one left lower m1; two right Upper M2.

Description and discussion: Like in other Murinae, the first upper molar (M1) has three rows of tubercles: the first (t1, t2, t3) and second (t4, t5 and t6) groups situated in the anterior part has three tubercles and the last group has two tubercles (t7 and t9) (Darvish et al., 2006). In South Turkey (Kryštufek and Vohralík, 2009) both *Mus musculus* and *Mus macedonicus* may be found.

Our specimens from Birecik *T. alba* pellets fit well with *M. musculus* (Figure 3.3.3) in the upper M1 morphology: the lingual row of cusps (t1 and t4) is shifted posteriorly; cusp t7 is reduced to an enamel ridge; distal cusps t8 and t9 leave no space for posterior cingulum or postero-labial cusp t12. The second upper molar lacks cusp t3; t7 is suppressed to a mere enamel ridge; t9 is small. The anterior half of m1 has a symmetrical X pattern formed at the anterior portion of the tooth (Siahsarvie and Darvish, 2008). Dental elds of mesial and central cusps on 1st lower molars fuse early; mesiolabial cusp is small. Upper molar normally have three roots each, one lingual and two labial , lower molars are two rooted, each with anterior and posterior root (Kryštufek and Vohralík, 2009). We reported also an incisor with the notch that characterize *Mus musculus* (Kryštufek and Vohralík, 2009).

Habitat and distribution: This species is well distributed around all over the world, it is present over all continents, except

Antarctica. It is found in a wide range of habitats but it not tends to be found in forest and deserts. *Mus musculus* is ecologically highly opportunistic but a weak competitor, it can cope with aridity and its expanding also in the desert (Kryštufek and Vohralík, 2009). It is found also on arid habitats along the border with Syria and Iraq, in desert landscape and also near the Euphrates river (Kryštufek and Vohralík, 2009 and Musser et al., 2016).

Genus *Meriones*, Illiger 1811

***Meriones tristami* (Thomas, 1892)**

Material: Skull: 33 fragments; **Mandibles**: 75; 28 complete right mandibles, 29 complete left mandibles; **Maxillae**: 57; 27 complete right maxilla, 30 complete left maxilla; **Isolated Teeth**: 96; nine right lower m1, six left lower m1; 14 right Upper M1; 15 Left Upper M1, thirty two M2; twenty M3.

Description and discussion: The genus *Meriones* is one of the most diversified representative of the Gerbillini tribe in the Palaearctic region, particularly in arid regions of Asia (Darvish et al., 2011; Denys et al., 2017). The current Meriones species reported in Turkey according to Kryštufek and Vohralík (2009) are: *Meriones tristami, Meriones vinogradovi*, *Meriones persicus*, *Meriones crassus*, *Meriones dahli* and *Meriones lybicus*. Although regarding their distribution the only one that is today present in Southern Anatolia is *Meriones tristami* (Kryštufek & Vohralík, 2009 and Sozen et al., 2017).

The Birecik molars attributed to *Meriones* are semi-hypsodont and display the typical morphology of the genus with prismatic triangles of enamel related by a longitudinal crest and no trace of cusps. In our sample we have identified first upper molars (M1) with three roots, so we could infer that it does not belong to *Meriones dalhi*, *Meriones lybicus* or *Meriones vinogradovi,* which present four roots on their M1 (Kryštufek & Vohralík, 2009). Moreover, the dental morphology of *Meriones persicus* and *Meriones tristami* is similar. A PCA was performed on skull measurements, taking into account the condylo-basal length, zygomatic breadth, maxillary tooth row and tympanic bullae length from our specimens compared with the data from Kryštufek & Vohralík (2009) (Figure 3.4 and Table 3.3). The result shows that size is not the main criteria to distinguish between both species.

Axis 1 and 2 explain respectively 81.64% and 8.3% of the total variance. Variables best correlated with Axis 1 are CBL (Condylo basal lenght), UTR (Upper tooth row) and ZB

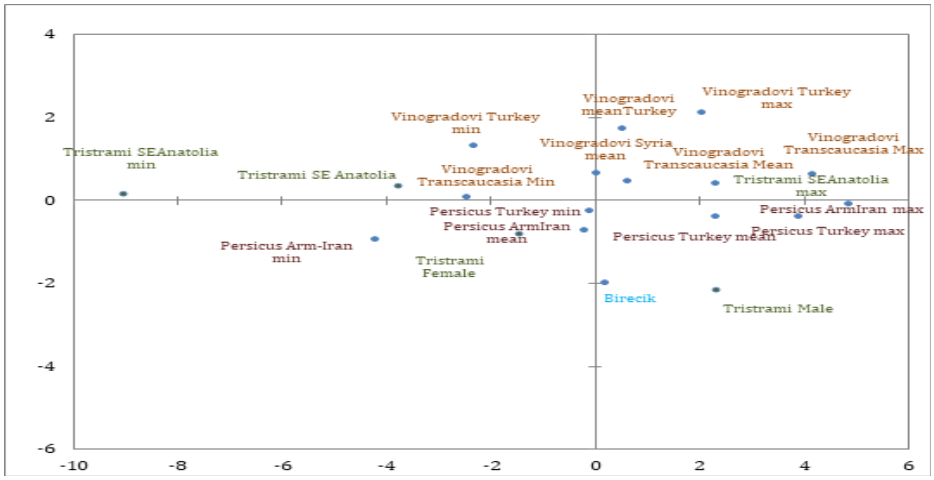


Figure 3.4. PCA graph on skull measurements of *Meriones* spp (Axis 1, horizontal x Axis 2, vertical). Colours indicate the species. Green: *Meriones tristami*; brown: *Meriones vinogradovi*, Red: *Meriones persicus*, Blue: Birecik sample.

(Zygomatic Breadth), while TBL (Tympanic bullae length) is correlated with Axis 2. The Birecik samples fit well with *Meriones tristrami* specimens but are also close to *Meriones persicus* ones. *Meriones tristrami* has a wide size variability but comparing with Syrian specimens, these latter have relatively long tympanic bullae compared to a small CBL.

We provisionally attribute our specimens to *Meriones tristrami* (Figure 3.3.4) pending a revision of the Middle East species of the genus.

Habitat and distribution: the genus *Meriones* is distributed in North Africa, Central Asia, Transcaucasia, Turkey and Pakistan (Darvish, et al., 2014, Wilson et al. ,2017). They mostly live in dry steppes of short or tall grass, open hillside, among rocky outcrops in desolate steppes, or open dry meadows. *Meriones tristrami* habitat is limited to 100 mm of rainfall annually and need well drained soil although it avoids rocky situations. In Turkey it has been mainly found in dry steppe and short or tall grass (Kryštufek and Vohralík, 2009).

3.2.Taphonomic study

-Bone representation

On the 2503 skeletal elements recovered in the Birecik *Tyto alba* pellets, a total of 39 individuals (MNI) were counted, following the number of maxillae which were the most abundant elements. We found that all bones are present but in variable proportions. The most represented are maxillae (89%) and mandibles (87%) followed by tibiae (82%). On the other hand, the less represented elements (excluding the isolated molars) are the ribs (33%) and the calcanei (34%) (Table 3. 4).

Species	CBL	ZB	UTR	TBL
Birecik sample				
N=5				
Mean	38.5	20.5	5.33	11.68
Max-Min	38.5	20.5	5.4-5.26	11.55-11.82
Meriones tristrami				
N=22-34				
Male	40.3	21	5.5	13.2
Female	36.3	20.2	5.2	13.2
Meriones persicus				
Turkey N= 4				
Mean	39.5	22.5	6.5	12.7
Max-Min	37.4 – 40.8	21.7 – 23.0	6.1 – 6.8	11.8 – 13.6
Armenia, Iran N=50				
Mean	37.6	21.2	6.3	11.5
Max-Min	34.4 – 41.4	6.1 – 6.8	5.9-6.9	10.0-14.4

Table 3.3. Comparison between the measurements in the different *Meriones* species found in Syria, Armenia, Iran and Birecik pellets (after this work and Krsytufek & Vorhalik 2009). All measurements are given in millimetres. CBL: Condylo-basal length; ZB: Bizygomatic breadth; UTR: Upper tooth row; TBL: tympanic bullae length.

The mean representation percentage is 45.21% for all the taxa present in our assemblage, that is very close to the one proposed by Andrews (1990) for Barn owl from Africa (48.91%).

Some rodent bones are anatomically connected: nine femora connected with a tibiae (tibia+fibula) and also with the phalanges and three humeri linked with radii.

Regarding the taphonomic representation pattern, we can say that all elements are well represented, with small elements like foot bones, teeth and vertebrae lost during collecting.

Most skeletal elements are well preserved and unbroken, as expected from a barn owl assemblage (Figure 3.5). There is a preferential loss of some elements, among which the distal parts or the limbs. The average relative abundances (the mean relative abundance for all skeletal elements, except the isolated teeth) vary from 33.01%

Prey species	***Suncus etruscus***			***Nesokia indica***			***Mus musculus***			***Meriones tristami***		
	MNI=1			**MNI=1**			**MNI=5**			**MNI=32**		
Anatomical elements	**Ni**	**Ei**	**Ri%**	**Ni**	**Ei**	**Ri%**	**NI**	**Ei**	**Ri%**	**Ni**	**Ei**	**Ri%**
Maxillae				2	2	100	6	10	60	57	64	89.06
Mandibles	2	2	100				10	10	100	56	64	87.5
Isolated Incisors				1	4	25	1	20	5	39	156	25
Isolated Molars				1	12	8.3	4			96	486	19.75
Femora										63	78	80.77
Tibiae (Tibia+ fibula)										64	78	82.05
Pelves										61	78	78.21
Calcanei (calcaneum)										26	78	33.33
Tali (astragalus)										30	78	38.46
Humeri										60	78	76.92
Radii										48	78	61.54
Ulnae										59	78	75.64
Scapulae										53	78	67.95
Ribs										309	936	33.01
Vertebrae										817	2106	38.79
Metaphods										340	780	43.59
Phalanges										284	780	36.41
Sacrum										14	39	35.9
Skull						1						
Total:	2			4			21			2476	6113	**Mean**: 45.21
MNI	1			1			5			32		

Table 3.4. Anatomical representation of small mammal remains from the Birecik Tyto alba pellets (Ni: Number of elements in our sample; Ei: number of expected element i in the assemblage, Ri: Relative abundance in Percentage).

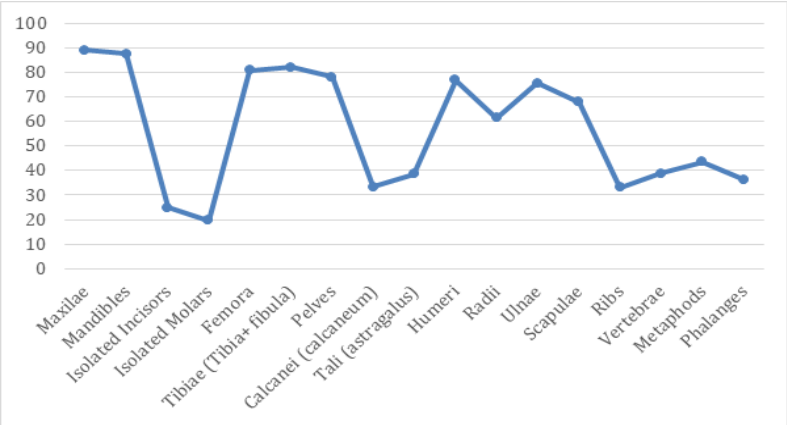


Figure 3.5. Profiles of representation percentage of the small mammal skeletal elements for Barn owl pellets from the sample from Birecik.

to 89.06%, which means that between one or two thirds of the prey has been lost from the sample during ingestion and digestion (Andrews, 1990).

The table 3.5 presents the proportions of postcranial *versus* cranial elements. The ratios (f+h)/(m+max)*100 reaches 108.85%, and 91.06%for the (t+r)/(f+h)+100 ratio. There is a slight long bone over-representation compared with mandibles and maxillae.

Ratios	%
(femora+humeri) /(mandible + maxillae) *100	108.85
(tibia+radii) /(femora+humeri)	91.06
([femora + tibiae+ humeri + radii + ulnae]*16/([mandibles + maxillae + molars] *10)*100)	225.08

Table 3.5. Proportions of postcrania to crania elements (calculated according Andrews 1990).

-Fragmentation

Our post-cranial sample presents a low percentage of fragmentation, with more than 77% of complete elements (Table 3.6). The preservation does not vary too much between the post-cranial bones, but the most broken ones in Birecik pellets are the pelvis (67.8%) and the scapulae (48.8%). The best preserved are the femora (98.3%).

In the case of *Suncus etruscus* we only

Element	Complete			Broken	Total
		Proximal	Distal	Shafts	
Femora	58	1			59
Humeri	61	5			66
Tibiae (Tibia+Fibula)	59	1		3	63
Ulnae	48	9	1	1	59
Radius	47			1	48
Pelvis	13	48			61
Scapula	22	21			43
Total (NR)	**308**	**85**	**1**	**5**	**399**
Percentage of fragmentation	**77.19**	**21.30**	**0.25**	**1.25**	**100.00**

Table 3.6. Number of remains (NR) and percentage of broken postcranial elements of Birecik sample.

			Suncus etruscus		*Mus musculus*		*Meriones tristami*	
			N	%	N	%	N	%
Skull	Complete				2	12.5	8	6.96
	Broken	Isolated Maxilla with zygomatic				0	1	0.87
		Isolated Maxilla without zygomatic				0		0
		Maxilla molars loss			1	6.25	28	24.35
		Maxilla incisors loss			3	18.75	22	19.13
Mandible	Complete		2	100	6	37.5	28	24.35
	Broken	Broken ascendant ramous			1	6.25	3	2.61
		Ascendant ramous missing				0	6	5.22
		Missing and inferior border broken				0	4	3.48
		Fragment				0		0
		Mandible molar loss				0	11	9.57
		Mandible incisors loss			3	18.75	4	3.48
Total			**2**	**100**	**16**	**100**	**115**	**100**

Table 3.7. Representation (N) and percentage of fragmentation (%) of the cranial elements.

have two complete mandibles. For *Mus musculus* and *Meriones tristami,* most of the maxillae and mandibles are broken. Only 12% of the *Mus* skulls are partially complete, and almost 7% for *Meriones* almost 7%. For the mandibles, 37% are intact for *Mus* and 24% for *Meriones* (Table 3.7).

-Digestion

In total 22.51% of the studied elements (femur, humerus, molars and incisors) are digested (Table 3.8 and Figure 3.6) and the dominant grade of digestion is the light one (86.6%). The moderate grade was observed on one femur and one humerus, and strong digestion is only present in one femur. We observed also that the isolated molars are more digested than *in situ* ones, because of the exposition. This value is quite high for *T. alba* but the pellets came from a nest, where digestion by young individuals is slightly higher than for adults (Denys et al.,2018).

For the elements in connexion we could find three femora harbouring light digestion upon free epiphysis.

3.2.1.Taphonomic implications

Tyto alba is an active hunter, especially at night, consequently nocturnal prey-species are taken more commonly than diurnal ones, which corresponds to what we found in the Birecik pellet assemblage. Moreover, the preferred hunting areas of the owl may be over-represented, notably the wetter and more open habitats (Mikola, 1983). Compared to previous studies performed in the same region, our sample is poorly diversified: we only have four species, mainly rodents (three species) and just one shrew. In the others studies, a higher species diversity was found. Shehad et al. (2013) identified 23 species, including chiroptera

Elements	Total	Total digested		No digestion		Low digestion		Moderate digestion		Strong digestion		In connexion Not digested		In connexion light digestion	
		N	%	N	%	N	%	N	%	N	%	N	%	N	%
Isolated incisor	39	18	46.15	21	53.85	15	37.46	3	7.69						
In situ incisor	90	34	37.78	56	62.33	34	37.78								
Isolated molars	96	4	4.17	92	95.83	4	4.17								
In situ molars	84	3	3.57	81	96.43	3	3.57								
Femora	62	22	35.48	40	64.52	13	20.97	1	1.61	1	1.61	4	6.45	3	4.84
Humerii	60	16	26.67	44	73.33	12	20	1	1.67			3	5		
Total	**431**	**97**	**22.51**	**334**	**74.49**	**81**		**5**	**0**	**1**	**0**	**7**	**0**	**3**	**0**

Table 3.8. Representation (N) and Percentages of digestion (%) on cranial and post-cranial elements from the Birecik pellets

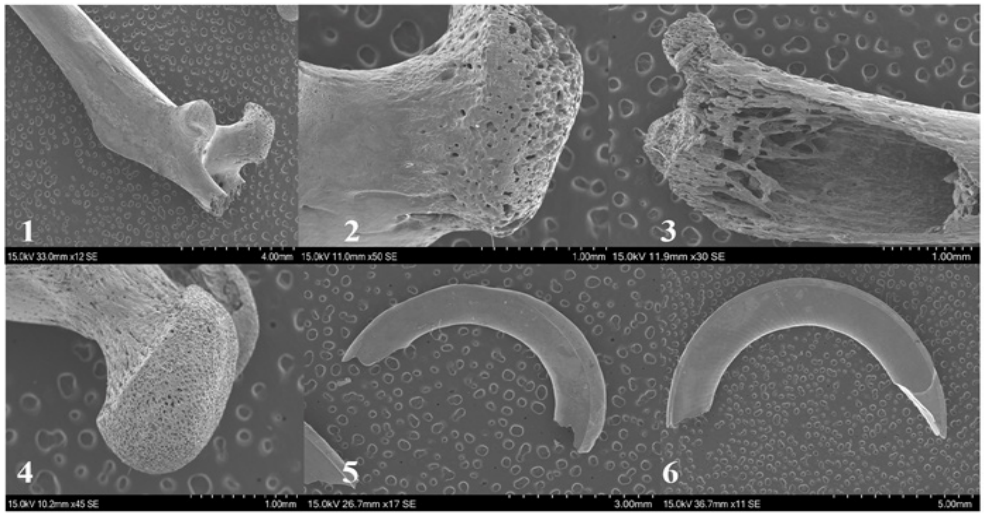


Figure 3.6. SEM pictures of digested rodent elementsfrom the Birecik pellets. 1- Moderate digestion is observable on the trochanter and on the basis of the femoral head and 2- detail of the same femur; 3- Rodent distal femur with strong digestion, 4- Femur head with moderate digestion; 5- Rodent upper incisor with moderate digestion; 6- Incisor with light digestion at the tip

(five species) and rodents (18 species).

In Lebanon, Abi Said et al. (2014) identified six rodents and two shrews. In some assemblages, bats or birds were also identified as preys (Shehab at al., 2013, Maul et al., 2015) but we didn't recover any of these taxa in our assemblage. *Meriones* may be very abundant locally and represent a high biomass for the owl (Shehab et al., 2013). Considering the opportunistic diet of *Tyto alba* (Andrews, 1990), this may explain why *Meriones* are the most represented species in our material and why the owl did not need to diversify its diet spectrum. Also the predominance of *Meriones* can be explained as a hunting preference of barn owl (Andrews, 2018). Another explanation may result from the low number of pellets analyzed here, or from the season of capture, which both may favor a higher diversity. Indeed, prey composition and digestion can differ from a month to another, but the highest differences occur generally between summer and winter (Andrews, 2018). Our pellets were collected in June 2003, and our values are similar to the ones displayed by the owls during summer (Andrews, 2018).

The diet of *Tyto alba* from our collected pellets fits well with the other studies in Europe and Asia. The Barn owls' preys are small vertebrates, including a wide range of rodents and insectivores (Andrews, 1990).

Tyto alba is well known because it is widespread around the word and it was identified as one of the major accumulator of small mammal remains in several archaeological sites. Few studies were devoted to taphonomy in Pleistocene archaeological contexts in the Middle East, notably in Iran, Israel and Syria (Bazgir et al., 2017; Demirel et al., 2011; Maul et al., 2015; Smith et al., 2015). Most of the studies concluded that the origin of the accumulation was predation activity, mainly owls, but generally without any study of ana-

tomical representation, bone breakage or digestion.

Regarding the postcranial fragmentation, most of our sample is intact, only 22.8% is fragmented mainly in the proximal part.. The best-preserved bone in our Birecik is the Femora. These values fit well with other *T. alba* assemblages, where around 80% is intact (Andrews, 1990).

Following the criteria established by Andrews (1990), our sample displays a good proportion of complete elements, corresponding to a Category 1 predator, including *Tyto alba*.

Few studies (Dauphin and Denys, 1992; Denys et al., 1996, 1992) have analyzed the differences in the fragmentation in different prey taxa. We were able to analyse it using skulls and mandibles, because most of the post-cranial bones cannot be specifically identified here. Most of the skulls from *Mus musculus* and *Meriones tristami* are complete with a few skulls fragmented. This corresponds well with the data from Denys et al. (1996) which showed a better skull preservation in favor of more robust rodents like *Meriones* spp. and some Dipodidae. The comparison between both species is not well correlated because we only have 16 *Mus* against 115 *Meriones* remains. *Meriones* are medium size rodents, which bones are generally more resistant compared to those of smaller species such as *Mus*. There is no correlation between the size and the preservation, but we have personally seen that *Meriones* skulls are more resistant, as suggested by previous studies (Dauphin and Denys, 1992; Denys et al., 1996, 1992). On the contrary, the fact that we also found small species such as *Suncus etruscus*, indicates that shrews may also display a good resistance to fragmentation.

3.3. Environmental and climatic remarks

3.3.1. Climatic data

Redding (1978) pointed out that small vertebrates are more sensitive to the climatic changes than larger ones and are sources of more detailed and precise paleoenvironmental interpretations. Because predation can bias the faunistic composition of assemblages, it needs to be recognized before any paleoecological study of the taxonomic list (Fernandez-Jalvo et al., 2016). So in the archaeological assemblages the predator responsible for the accumulation should be identified as far as possible in order to identify potential bias of faunal and anatomical representation, and get a better picture of past environments and taphonomic history of the site (Demirel et al., 2011).

Barn owls have a restricted hunting area and are opportunistic predators, so their pellets represent a good picture of the relative availability of prey species and their contents are good indicator for knowing the environment if applied to archeological assemblages (Demirel et al. 2011).

Birecik is located in the Sanliurfa province, the centre of the South-eastern Anatolia. The altitude of the region is between 300-600 meters above the sea level and has a semiarid Mediterranean climate. Annual mean temperature is 18.5°C; the maximum mean temperature is 39°C and the minimum mean temperature is 2.7°C. Annual rainfall is about 458.1 mm and the precipitation regime is winter, spring, autumn, and summer. Birecik is characterised by a steppe vegetation (Vagif Atamov and Gulsefile, 2007).

For the climatic reconstruction we applied the Bioclimatic model (Table 3. 10) directly based on the faunal list, in order to know if we could obtain the same results as

Species	I	II	II/III	III	IV	V	VI	VII	VIII	IX
Suncus etruscus	0.333	0.333	0	0	0.333	0	0	0	0	0
Nesokia indica	0	0	0.25	0.25	0.25	0	0	0.25	0	0
Mus musculus	0.111	0.111	0.111	0.111	0.111	0.111	0.111	0.111	0.111	0
Meriones tristami	0	0	0	0	1	0	0	0	0	0

Table 3.9. Distribution of species scores for the Bioclimatic Model of the Birecik assemblage (according to Hernández-Fernández, 2001; Hernández-Fernández et al., 2007).

the ones provided by the Vagif Atamov et al. (2007) and validate the methodology for South Anatolia.

Concerning the Birecik rodent assemblage, nine of the different climatic groups defined by Hernández-Fernández (2001) and Hernández-Fernández et al. (2007) are represented (Table 3.9).

We can observe that there is a relatively good correspondence between the estimated means values of the Bioclimatic model and the current temperatures and precipitation taking into account the Standard Deviation. We obtain a mean annual temperature of 20.86°+/- 3.39 with the model against 18.5°C according to meteorological surveys. Similarly, for the mean annual precipitation we found 432 mm in average against 458 mm (Table 3.10).

We could see that there is a correspondence between the values obtained with the Bioclimatic model and the current ones.

3.3.2.Environmental data

The Habitat Weighting method, based on the habitat frequentation of represented species in the assemblage, where the value of 1 is divided between the habitats where it is possible to find the species at present (Table 3.11), indicates a steppe-like environment characterised by a vegetation dominated by shrubs and grass with low precipitation, which corresponds well to the environment found in Birecik today.

Mus musculus is highly adaptable and found in all environments but *Meriones*

		SD	Current values
Annual Mean temperature	20.86 °C	3.39	18.5ºC
Maximum mean temperature	27.61°C	4.77	39ºC
Minimum mean temperature	11.45°C	4.66	2.7ºC
Mean anual precipitation	431.98 mm	533.24	458.1mm

Table 3. 10. Birecik sample Bioclimatic model results. SD (Standard Deviation)

	Fo	Sh	Gr	De	We
Meriones tristami		0.5		0.5	
Mus musculus		0.33	0.33		0.33
Nesokia indica	0.33	0.33	0.33		
Suncus etruscus	0.25	0.25	0.25	0.25	
Total	**0.6**	**1.4**	**0.9**	**0.8**	**0.3**

Table 3.11. Percentage of the palaeoenvironmental reconstruction for the Birecik sample, Fo (Forest), (Sh) Shrubland, (Gr) Grassland, (De) Desert and (We) Wetlands (Habitat Weighting model).

tristrami is restricted only to habitat IV. *Nesokia indica* is also found in three different zones (II/III, III, IV, VII). Both taxa may be good palaeoenvironmental indicators in archaeological sites.

Nesokia indica and *Suncus etruscus* represent only 5% of the fauna, while *Mus musculus* represents 12,82% and *Meriones tristami* 82%, these two species making up 95% of the preys. Habitat weighting does not consider the proportion of the species, just their presence/absence. Following the percentages obtained with the Habitat weighting model, the most represented environment is the Shrubland (vegetation dominated by shrubs) and Grassland (open area covered with grass), followed by desert. On the basis of this result, we can said that the Habitat weighting gives a good overview of the landscape in the region today (according to Vagif Atamov et al., 2007).

We have to keep in mind that *Meriones* are the major preys in this faunal assemblage, which indicates a favourable dry open environmental condition for gerbils (steppes). Following the Bioclimatic model the results combined with the Habitat weighting, support an steppe environment.

We can thus conclude that *Tyto alba* pellets from the region represent good proxies for reconstructing environments and then it becomes possible to apply these inferences to the archaeological record in the Middle east.

4.Conclusions

This work presents the first combined taxonomic and taphonomic study of *Tyto alba* pellets in the Middle East. Our objective was to increase the modern referential for this predator in that region, to contribute to a better understanding of small vertebrate accumulations in archaeological sites in the Middle East and to test the use of owl pellets faunal lists as proxies for paleoenvironmental reconstructions.

We have identified *Suncus etruscus*, *Nesokia indica*, *Mus musculus* and *Meriones tristami* in our sample. Their current ecology, combined with the Bioclimatic model and the Habitat weighting, confirmed that the values obtained for the climate (temperatures and precipitations) and landscape reconstructions based on owl pellet assemblages are valid and applicable in archaeological context.

Such studies will serve as reference to better identify the origin of some fossil accumulation, before deposition and fossilization. The taphonomic study showed that our assemblage fits well with a predator category of light modification. Most skeletal elements are well preserved and unbroken, our mean bone relative abundance reached 82% and the more than 77% of our sample is intact. Around 22% of the total elements are digested, and the light moderate grade is dominant (83.5%). *Tyto alba* represents a

major cause of small mammal accumulation in archaeological sites, especially in caves. However, it is not the only predator that can produce such accumulations.

The emphasis of this article has remained on the nature of the modifications, and geographic variation (or lack of it) from one part of the world to another, as we could see, the modifications in this region are the same as we can find in other parts of the world produced by *T. alba*. Further studies will allow to define the role and importance of avian predators and mammalian carnivores in the accumulations of small mammals in archeological sites of the Middle East.

Acknowledgments: I. Rey-Rodriguez is beneficiary of PhD scholarship funded by the Erasmus Mundus Program (IDQP). J.M. López-García was supported by a Ramón y Cajal contract (RYC-2016-19386) with financial sponsor of the Spanish Ministry of Science, Innovation and Universities. SEM pictures have been taken on the *Plateforme de Microscopie Electronique du Muséum national d'Histoire naturelle*, thanks to Geraldine Toutirais for her help. J.F. Noblet must be thanked for providing us the owl pellets material. We also want to thank to the Editor Prof. Marcos Martinón-Torres and the anonymous reviewers for their comments and suggestions that improve the final version of the manuscript.

References

Abi-said, M.R., Shehab, A.H., Amr, Z.S., 2014. Diet of the Barn Owl, pp. 109–112, 7.

Andrews, P., 2018. Seasonal Variation in Prey Composition and Digestion in Small Mammal Predator Assemblages 1–14. https://doi.org/10.1002/oa.2656.

Andrews, P., 2006. Taphonomic effects of faunal impoverishment and faunal mixing. Palaeogeogr. Palaeoclimatol. Palaeoecol. 241, 572–589. https://doi.org/10.1016/j. palaeo.2006.04.012.

Andrews, P., 1990. Owls, Caves and Fossils. https://doi.org/10. 2307/3889096.

Aulagnier, S., Hutterer, R., Jenkins, P., Bukhnikashvili, A., Kryštufek, B., Kock, D., 2017. *Suncus etruscus*. The IUCN Red List of Threatened Species 2017: e. T90389138A22288134. (Accessed 6 November 2018).

Bazgir, B., Ollé, A., Tumung, L., Becerra-Valdivia, L., Douka, K., Higham, T., Van Der Made, J., Picin, A., Saladié, P., López-García, J.M., Blain, H.A., Allué, E., Fernández- García, M., Rey-Rodríguez, I., Arceredillo, D., Bahrololoumi, F., Azimi, M., Otte, M., Carbonell, E., 2017. Understanding the emergence of modern humans and the disappearance of Neanderthals: insights from Kaldar Cave (Khorramabad Valley, western Iran). Sci. Rep. 7, 1–16. https://doi.org/10.1038/srep43460.

Blain, H.-A., Bailon, S., Cuenca-Bescós, G., 2008. The Early–Middle Pleistocene palaeoenvironmental change based on the squamate reptile and amphibian proxies at the Gran Dolina site, Atapuerca, Spain. Palaeogeogr. Palaeoclimatol. Palaeoecol. 261, 177–192. https://doi.org/10.1016/j.palaeo.2008.01.015.

Boitani, L., Molur, S., 2016. *Nesokia Indica* (Errata Version Published in 2017). The IUCN Red List of Threatened Species 2016: e.T14661A115123428. https://doi.org/10.2 305/IUCN.UK.2016-3.RLTS. T14661A22410105.en. Downloaded on 23 April 2018.

Coşkun, Y., 1999. Morphological characteristics of *Meriones tristrami* Thomas, 1892 (rodentia: gerbillinae) from Diyarbakır, Turkey. Turk. J. Zool. 23, 345–355.

Darvish, J., 2011. Morphological comparison of fourteen species of the genus *Meriones Illiger* , 1811 (Rodentia : Gerbillinae) from Asia and North Africa. Iranian Journal of Animal Biosystematics 7, 49–74.

Darvish, J., Mohammadi, Z, Mahmoudi, A., Siahsarvie, R., 2014. Faunistic and taxonomic study of Rodents from northwestern Iran. Iranian Journal of Animal Biosystematics (IJAB) 10, 119–136.

Darvish, D., Orth, A., Michaux, J., 2006. *Mus spretus* et *M. musculus* (Rodentia, Mammalia) en zone méditerranéenne: Différenciation biométrique et morphologique: Application à des fossiles marocains pléis-

tocènes. Mammalia 70, 90–97. https://doi.org/10.1515/MAMM.2006.010

Darvish, J., Ghiyasi, R., Khosravi, M., 2000. Recognition of rodents of Robat Sharaf pellets owl by morphological and neontological studies. Journal of Sciences 12.

Dauphin, Y., Denys, C., 1992. Diagenèse différentielle chez les rongeurs fossiles — validité des paramètres géochimiques pour les reconstitutions des régimes alimentaires. Palaeogeography, Palaeoclimatology, Palaeoecology 99, 213–223. https://doi.org/10.1016/0031-0182(92)90016-X

Demirel, A., Andrews, P., Yalçinkaya, I., Ersoy, A., 2011. The taphonomy and palaeoenvironmental implications of the small mammals from Karain Cave, Turkey. Journal of Archaeological Science 38, 3048–3059. https://doi.org/10.1016/j.jas.2011.07.003

Denys, C., Stoetzel, E., Andrews, P., Bailon, S., Rihane, A., Huchet, J.B., Fernandez- Jalvo, Y., Laroulandie, V., 2018. Taphonomy of Small Predators multi-taxa accumulations: palaeoecological implications. Hist. Biol. 30 (6), 868–881. https://doi.org/10.1080/08912963.2017.1347647.

Denys, C., Patou-Mathis, M., 2014. Manuel de Taphonomie, Collection. ed.

Denys, C., Dauphin, Y., Rzebik-Kowalska, B., Kowalski, K., 1996. Taphonomic study of Algerian owl pellet assemblages and differential preservation of some rodents: palaeontological implications. Acta Zoologica Cracoviensia 39, 103–116.

Denys, C., Kowalski, K., Dauphin, Y., 1992. Mechanical and chemical alterations of skeletal tissues in a recent Saharian accumulation of faeces from *Vulpes rueppell*i (Carnivora, Mammalia). Acta Zoologica Cracoviensia 35, 265–283.

Evans, E.M.N., Van Couvering, J.A.H., Andrews, P., 1981. Palaeoecology of Miocenesites in western Kenya. J. Hum. Evol. 10, 99–116.

Fernández-Jalvo, Y., Andrews, P., Denys, C., Sesé, C., Stoetzel, E., Marin-Monfort, D., Pesquero, D., 2016. Taphonomy for taxonomists: Implications of predation in small mammal studies. Quaternary Science Reviews 139, 138–157. https://doi.org/10.1016/j.quascirev.2016.03.016.

Fernández-Jalvo, Y., Andrews, P., Sevilla, P., Requejo, V., 2014. Digestion versus abrasion features in rodent bones. Lethaia 47, 323–336. https://doi.org/10.1111/ let.12061.

Haddadian Shad, H., Darvish, J., Mohammadian, T., Mahmoudi, A., Alaie Kakhki, N., Ghanbarifardi, M., Molavi, F., Barani-Beiranvand, H., 2014. Preliminary study of rodents using pellets of predatory birds in Iran. Iranian Journal of Animal Biosystematics 10, 36–50.

Hernández Fernández, M., Álvarez Sierra, M.Á., Peláez-Campomanes, P., 2007. Bioclimatic analysis of rodent palaeofaunas reveals severe climatic changes in Southwestern Europe during the Plio-Pleistocene. Palaeogeography, Palaeoclimatology, Palaeoecology 251, 500–526. https://doi.org/10.1016/j.palaeo.2007.04.015

Hernandez Fernández, M., Peláez-Campomanes, P., 2003. The bioclimatic model: A method of palaeoclimatic qualitative inference based on mammal associations. Glob. Ecol. Biogeogr. 12, 507–517. https://doi.org/10.1046/j.1466-822X.2003.00057.x.

Hernández Fernández, M., 2001. Bioclimatic discriminant capacity of terrestrial mammal faunas. Global Ecology and Biogeography 10, 189–204. https://doi.org/10.1046/j.1466-822x.2001.00218.x

Kopij, G., Liven-schulman, I., 2013. Zoology in the Middle East Diet of the Lesser Kestrel , *Falco naumanni* , in Israel 7140. https://doi.org/10.1080/09397140.2012.10648914

Kryštufek, B., Bukhnikashvili, A., Sozen, M., Isfendiyaroglu, S., 2017. *Cricetulus migratorius*. The IUCN Red List of Threatened Species 2016: e.T5528A1150733908235.

Kryštufek, B., Vohralík, V., 2009. Mammals of Tur-

key and Cyprus, Rodentia II: Cricetinae, Muridae, Spalacidae, Calomyscidae, Capromyidae, Hystricidae, Castoridae. https://doi.org/10.1644/10-MAMM-R-221.1

Kryštufek, B., Vohralík, V., 2001. Mammals of Turkey and Cyprus, Introduction, Check-List, Insectivora. Koper

López-García, J.M., Blain, H.-A., Cuenca-Bescós, G., Alonso, C., Alonso, S., Vaquero, M., 2011. Small vertebrates (Amphibia, Squamata, Mammalia) from the late Pleistocene-Holocene of the Valdavara-1 cave (Galicia, northwestern Spain). Geobios 44, 253–269. https://doi.org/10.1016/j.geobios.2010.10.001

Mamkhair, I.H., Samara, F.F., Shehab, A.H., 2007. Morphological characteristics of the libyan jird, *Meriones libycu*s lichtenstein, 1823 (rodentia: gerbillinae), in syria. Zoology in the Middle East 42, 37–46. https://doi.org/10.1080/09397140.2007.10638244

Maul, L.C., Smith, K.T., Shenbrot, G., Bruch, A.A., Wegmüller, F., Le Tensorer, J.M., 2015. Microvertebrates from unit G/layer 17 of the archaeological site of Hummal (El Kowm, Central Syria): Preliminary results. Anthropologie (France) 119, 676–686. https://doi.org/10.1016/j.anthro.2015.10.010

Mikkola, H., 1983. Owls of Europe. T. &; A. D. Poyser, Carlton.

Musser, G., Hutterer, R., Kryštufek, B., Yigit, N., Mitsain, G., 2016. *Mus musculus* (errata version published in 2017). The IUCN Red List of Threatened Species 2016: e. T13972A115117618.

Momtazi, F., Darvish, J., Ghassemzadeh, F., Moghimi, A., 2008. Elliptic Fourier analysis on the tympanic bullae in three *Meriones* species (Rodentia, Mammalia): its application in biosystematics. Acta zoologica cracoviensia 51A, 49–58. https://doi.org/10.3409/azc.51a

Musser, G.C., Carleton, M.D., 2005. Superfamily Muroidae, in: Wilson, D.E., Reeder, D.M. (Eds.), Mammal Species of the World. A Taxonomic and Geographic Reference. Baltimore, pp. 894–1531.

Obuch, J., Khaleghizadeh, A., 2012. Spatial Variation in the Diet of the Barn Owl Tyto alba in Iran 6, 103–116.

Pavlinov, Igor Ya., 2008. A Review of Phylogeny and Classification of Gerbillinae (Mammalia:rodentia), Moscow Uni (Moscow).

Redding, W.R., 1978. Rodents and the archaeological palaeoenvironment: Considerations, problems and future. Approaches to faunal analysis in the Middle East. In: Meadow, R.H., Zeder, M.A. (Eds.), Harvard, Peabody Museum of Archaeology and Ethnology, 2. Peabody Museum Bulletin, pp. 63–68.

Shad, H., Kakhki, A., 2014. Preliminary study of rodents using pellets of predatory birds in Iran. Iranian Journal of Animal Biosystematics 10, 36–50.

Shehab, A., Daoud, A., Kock, D., Amr, Z., 2013. Zoology in the Middle East Small mammals recovered from owl pellets from 7140. https://doi.org/10.1080/09397140.2004.10638061

Siahsarvie, R., Darvish, J., 2008. Geometric morphometric analysis of Iranian wood mice of the genus *Apodemus* (Rodentia, Muridae). Mammalia 72, 109–115. https://doi.org/10.1515/MAMM.2008.020

Smith, K.T., Christian, L., Flemming, F., Barkai, R., Gopher, A., 2015. The microvertebrates of Qesem Cave : A comparison of the two concentrations. Quaternary International 1–13. https://doi.org/10.1016/j.quaint.2015.04.047

Sozen, M., Bukhnikashvili, A., Shenbrot, G., Scott, D., Amori, G., Kryštufek, B., Yigit, N., Mitsain, G., 2016. *Meriones tristrami* (errata version published in 2017). The IUCN Red List of Threatened Species 2016: e.T13170A115110701.

Stoetzel, E., Sime, W.B., Pleurdeau, D., Asrat, A., Assefa, Z., Desclaux, E., Denys, C., 2017. Preliminary study of the rodent assemblages of Goda Buticha: new insights on Late Quaternary environmental and cultural changes in southeastern Ethiopia. Quat. Int.https://doi.

org/10.1016/j.quaint.2017.08.050.

Stoetzel, E., Marion, L., Nespoulet, R., El Hajraoui, M.A., Denys, C., 2011. Taphonomy and palaeoecology of the late Pleistocene to middle Holocene small mammal succession of El Harhoura 2 cave (Rabat-Témara, Morocco). Journal of Human Evolution 60, 1–33. https://doi.org/10.1016/j.jhevol.2010.07.016

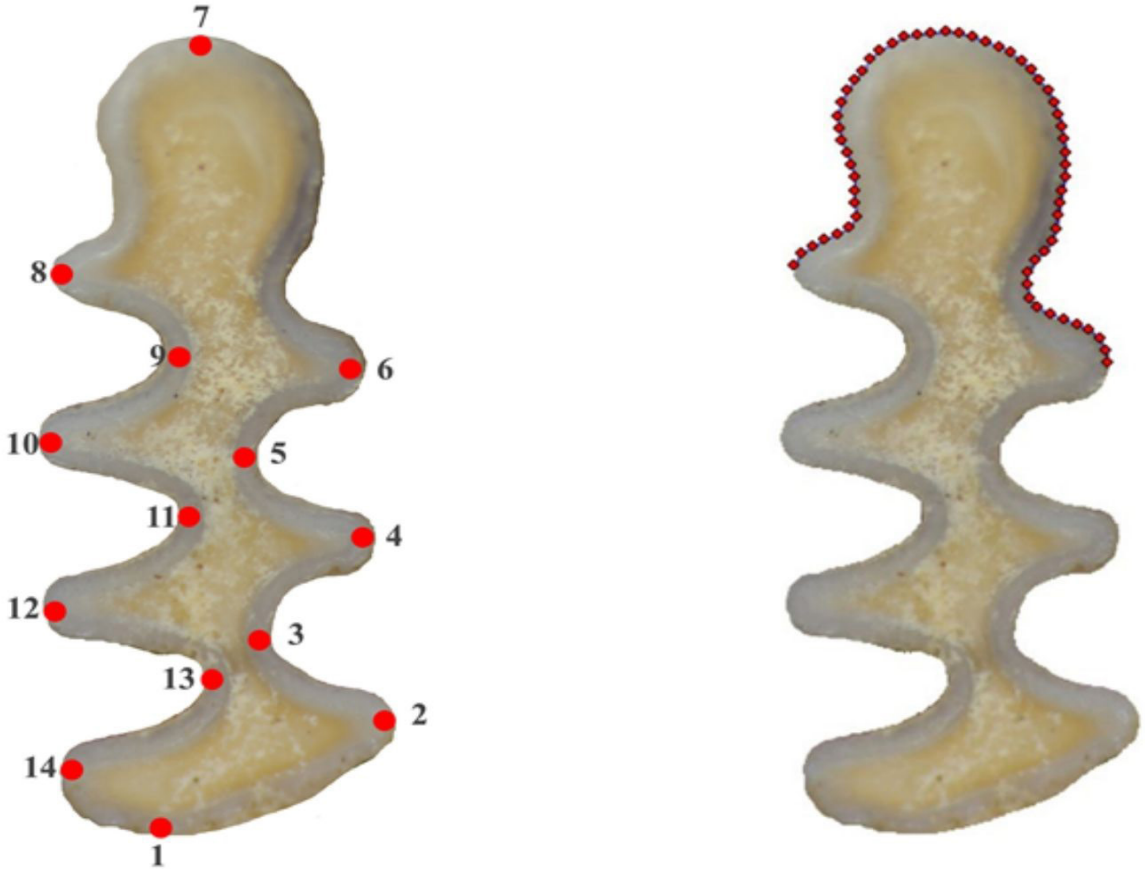
Tez, C., 2000. Taxonomy and distribution of the white-toothed shrews (*Crocidura*) (Soricidae: Insectivora: Mammalia) of Turkey. Turkish Journal of Zoology 24, 365–374.

Vagif Atamov, M, A., Gulsefile, A., 2007.Flora of Mezra City (Birecik, SanliurfaTurkey). Asian Journal of Plant Sciences 6 (2), 225-238.

Yicit, N., Colak, M.S., 1996. Investigations on biology of *Meriones crassus* Sundevall, 1842 (Mammalia: Rodentia) in Turkey. Turk. J. Zool. 20, 211–215.

Chapter 4.

Distinguishing between three modern *Ellobius* species (Rodentia, Mammalia) and identification of fossil *Ellobius* from Kaldar Cave (Iran) using geometric morphometric analyses of the first lower molar



Abstract

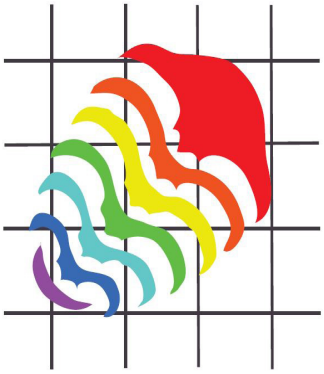
Ellobius remains are common and often abundant in southeastern Europe, western and central Asia archaeological sites. A correct identification of species is crucial for our understanding of the evolution of species and communities through time, including biostratigraphic sequences to be established.

This study applies geometric morphometric methods (GMM) to *Ellobius* first lower molars, with the objectives: 1) to discriminate modern species and explore morphological and size differences in reference samples; and 2) to identify fossil specimens recovered in archaeological sites, based on the aforementioned analysis. The reference dataset used in this paper includes specimens belonging to the three species that today occur in the southeastern Europe, western and central Asia: *Ellobius fuscocapillus*, *E. lutescens* and *E. talpinus*. The archaeological material comes from Late Pleistocene Iranian site of Kaldar Cave (Khorramabad valley, Lorestan Province, western Iran).

Our study shows that the shape of the anterior cap and the arrangement of the following triangles allow discriminating the three studied extant *Ellobius* species. The shapes of *E. fuscocapillus* and *E. lutescens* m1 appear rather similar, whereas *E. talpinus* is well separated from these two species. The total length and the anterior cap of m1 in E. fuscocapillus is greater than in Ellobius lutescens.

The GMM analyses performed on the modern reference dataset allowed us to identify fossil specimens from Kaldar Cave as *E. lutescens* and some as *E. fuscocapillus*, and excluding *E. talpinus*.

Keywords: Rodentia; Arvicolinae; m1 shape; multivariate analysis; Pleistocene





Rey-Rodríguez, I., Arnaud, J., López-García, J.M., Stoetzel, E., Denys, C., Cornette, R., Bazgir, B., 2021. Distinguishing between three modern *Ellobius* species (Rodentia, Mammalia) and identification of fossil *Ellobius* from Kaldar Cave (Iran) using geometric morphometric analyses of the first lower molar. Palaeontologia Electronica 24 (1):a01, 1–18. https://doi.org/10.26879/1122

1. Introduction

This study focuses on three species of the vole genus *Ellobius* (Rodentia, Cricetidae, Arvicolinae) nowadays occurring in Iran, and on fossil material from Late Pleistocene Kaldar Cave site in the Zagros mountains. This region is a key area for human evolution and lies at the conjunction of potential migration routes between Africa, Europe and eastern Asia. A well-based characterization of the palaeoenvironmental context is crucial for a good understanding of human occupations (subsistence, cultural adaptations, site occupations, territory, and resource management, dispersal events, etc.). Small mammals may serve as good palaeoenvironmental and palaeoclimatic indicators of the surroundings of an archaeological site. Moreover, voles (arvicolines) in particular are commonly used in Quaternary biostratigraphy because of their rapid evolution and their abundance in the fossil record.

Ellobius is an interesting vole genus since its Pleistocene distribution reached North Africa (Stoetzel, 2013) and the southern Levant (Weissbrod and Weinstein-Evron, 2020), where it is absent now. Nowadays it occurs in southeastern Europe, western and central Asia (e.g., Rey-Rodríguez et al., 2020). It is often abundant in Middle Eastern archaeological sites, and has biostratigraphic potential for this region.

However, the identification of fossil *Ellobius* material is not yet elaborated satisfactory. The identification of most *Ellobius* specimens in museums collections is based on criteria which is usually not applicable to fragmented fossil material. Previous studies on *Ellobius* have mainly focused on chromosomes (Romanenko et al., 2007, 2018, 2020; Coşkun, 2016) and species discrimination based on external characters, not applicable to fossils (Gharkheloo,M.M., 2003; Kryštufek and Vohralík, 2009; Tesakov, 2016). In the archaeological literature, taxonomic attributions are often restricted to *Ellobius* sp. (e.g., Maul et al., 2015a; Weissbrod and Weinstein-Evron, 2020).

The most common and diagnostic element in fossil vole samples are the teeth, in particular the first lower molars (m1). However, in *Ellobius* m1s morphological differences are hard to find, and there are apparently broad overlaps between the species (Maul et al., 2015a; Kandel et al., 2017; Weissbrod et al., 2017).

With the Geometric morphometrics method (GMM), fine morphological differences can be detected and variations in shape and size can be quantified, which would have been undetectable by conventional approaches, such as linear measurements or morphotype scores (Adams et al., 2009; Kaya et al., 2018). Previous GMM analyses of various fossil rodent groups (e.g., *Microtus* spp. Cucchi et al., 2014; Luzi et al., 2019; *Meriones* spp. Stoetzel et al., 2017a; and *Rattus* spp. Hulme-Beaman et al., 2018) provided more comprehensive identifications compared to conventional investigations.

The purpose of this study is to investigate morphological and size differences between three species of the genus *Ellobius* from Iran and to apply the results to specimens of the archaeological site of Kaldar Cave. With this article we hope to demonstrate the potential of the GMM approach to the *Ellobius* genus and discuss its use in combination with other morphological criteria.

2. The genus *ELLOBIUS* Fischer, 1814

2.1. Distribution and Ecological Remarks of the Extant *Ellobius* Species

Nowadays, the genus *Ellobius* Fischer, 1814, occurs in southeast Europe, western and central Asia with five species (Coşkun, 2001, 2016; Wilson et al., 2017, Kaya et al., 2018): *E. talpinus* (Pallas, 1770), *E. tancrei* Blasius, 1884, *E. alaicus* Vorontsov et al., 1969, *E. fuscocapillus* (Blyth, 1843) and *E. lutescens* Thomas, 1897. These fossorial species inhabit steppes, grasslands and semi-deserts, and are highly adapted to subterranean life (Kryštufek and Vohralík, 2009; Coşkun, 2016).

In Iran, where Kaldar Cave (where the fossil material under study come from) is located, *Ellobius* is currently represented by *E. lutescens*, *E. fuscocapillus* and *E. talpinus* (Gharkheloo, M.M., 2003; Firouz, 2005; Kryštufek and Vohralík, 2009; Kryštufek and Shenbrot, 2016; Rusin, 2017).

Ellobius lutescens (western mole vole) is distributed in northwestern Iran, Iraq, Azerbaijan, Armenia and eastern Anatolia (Thomas, 1905; Ellerman and Morrison-Scott, 1951; Darlington, 1957; Osborn, 1962; Walker, 1964; Lay, 1967; Hassinger, 1973; Roberts, 1977; Corbet, 1978; Corbet and Hill, 1991; Coşkun, 1997; Nowak, 1999; Wilson and Reeder, 2005; Kryštufek and Shenbrot, 2016; Wilson et al., 2017). In Iran, this species is found in mountain grasslands, sandy semi-deserts and steppe areas (Kryštufek and Shenbrot, 2016; Tesakov, 2016).

Ellobius fuscocapillus (southern mole vole) shows a range across northeastern Iran, Turkmenistan, Afghanistan and Pakistan. In Iran it is found in open steppes with loose soil (Gharkheloo, M.M., 2003; Shenbrot et al., 2016).

Ellobius talpinus (northern mole vole) is distributed in southeastern Ukraine and Russia, Kazakhstan, Uzbekistan, Turkmenistan and in the small part of northern Iran. Its habitat requirements are similar to that of *Ellobius lutescens* (Rusin, 2017).

The geographical areas occupied by the three species show differences in mean annual temperatures and precipitations (Table 4.1). *E. talpinus* is found in regions with drier conditions and lower maximum annual temperature than that of the other two species. The geographic ranges of *E. fuscocapillus* and *E. lutescens* display similar temperatures, but *E. fuscocapillus* occurs in wetter environments. All the temperatures and precipitation levels are estimations, consistent with the above-described type of habitat. However, since their subterranean life makes them relatively insensitive to high variations in surface temperatures and precipitations, we can consider that all three species have essentially the same habitat requirements. What can make differences is the resulting vegetation cover, which is of course important for the survival of the animals. But all what we can assume in the current state of knowledge is that the *Ellobius* species provide significant information as indicators for steppe environments. Further studies are needed to evaluate more precisely the potential of the different *Ellobius* species as palaeoenvironmental and palaeoclimatic indicators.

2.2. Fossil Record of *Ellobius*.

Arvicolines are commonly used in Quaternary biostratigraphy because of their rapid evolution and their abundance in the fossil record. The genus *Ellobius* may

	Temperature (Max/ Min)	**Precipitation (mm per month)**
E. fuscocapillus	11.62/ 0.1°C	36.01
E. lutescens	10.79/ 0.1°C	28.17
E. talpinus	4.75 /0.1°C	24.94

Table 4.1. Ranges of month precipitations and mean annual temperatures within the geographic distribution area of various Ellobius species (https://eol.org/).

represent a crucial biostratigraphic yardstick in the Zagros mountain range, which marks the western limits of its extant distribution range in the western Asia (Weissbrod and Weinstein-Evron, 2020). However, the palaeobiogeographic and stratigraphic range of the genus in this region is still debated.

Remains of cf. *Ellobius* have been reported in Early Pliocene (Ruscinian) sites in Kotovka, Odessa in the Ukraine (Nesin and Nadachowski, 2001), and in two late Pliocene (Late Villanyian) sites, in the west of Ukraine and in Rivoli Veronese, northeastern Italy (Sala et al., 1994). However, Tesakov (1998) believes that the *Ellobius* record from Italy belongs to *Ungaromys dehmi*.

According to several authors (compiled in Topachevsky and Rekovets, 1982; Maul and Markova, 2007; Tesakov, 2016), there was a succession of several *Ellobius* species during the early Pleistocene in Eastern Europe: *E. paleotalpinus*, *E. melitopoliensis*, *E. primigenis*, *E. lakhutensis, E. tauricus E. kujalnikensis* and *E. tarchancutensis*. The morphology of *E. tarchancutensis* suggests that it could be the ancestor of *E. lutescens* (Topachevsky and Rekovets, 1982; Tesakov, 2016).

In western Asia, *Ellobius* has been recognized in several Middle Pleistocene archaeological sites in Sel'-Ungur in Kyrgyzstan (*Ellobius* ex gr. *tancrei*; Markova, 1992), in Hummal layer G in Syria (*Ellobius* sp.; Maul et al., 2015), Azokh-1 units Vm, Vu, III, II/III, II (*Ellobius* sp.; Fernández-Jalvo, 2016a) in Nagorno Karabakh and Krasarin (*Ellobius* (*Bramus*) *pomeli*; Tesakov (2016).

During the Middle Pleistocene, *Ellobius* extended its range westwards to Israel, Tabun C and D (Bate, 1937; Frumkin and Comay, *in press*), Misliya Cave (Weissbrod and Weinstein-Evron, 2020) and North Africa as far as to the Moroccan Atlantic coast (Jaeger, 1988; Stoetzel, 2013). It probably arrived there from western Asia via the Libyco-Egyptian route during a cooling and aridification of North Africa favouring the development of steppes at the beginning of the Middle Pleistocene (Stoetzel, 2013). The North African species then evolved independently from the Asian ones, through the succession of *E. africanus*, *E. atlanticus*, *E. barbarus* and *E. zimae* (Jaeger, 1988). In most studies, it is concluded that *Ellobius*, outside its current range, disappeared at the end of the Middle Pleistocene at the latest (Stoetzel, 2013; Maul et al., 2015; Weissbrod and Weinstein-Evron, 2020).

In the Late Pleistocene, *E. trancrei* has been described from the Mousterian site of Ogzy-Kichik, Tadzhikistan (Markova, 1992). The modern species *E. lutescens* was found in Iraq (Bate, 1930) in the layers of Hazar Merd, dated to 25,000 years ago (Coşkun, 2016). Hashemi et al. (2006) noted that remains of *E. lutescens* have been found in several Late Pleistocene and early Holocene sites in western and northwestern Iran: Kani Mikaeil (Kordestan), Qalaloun near Kouhdasht, Yafteh Gar, and Arjeneh near Khoramabad (Lorestan). *Ellobius lutescens* has also been documented in Upper Palaeolithic and Neolithic units of Dzudzuana Cave (Georgia, 34.4-6 ka cal BP; Belmaker et al., 2016), and also in Aghitu-3 level VII (Armenia, Upper Palaeolithic, 39-36 ka cal BP; Kandel et al., 2017). *Ellobius* sp. has been described in Azokh 1 unit I (157 ± 26 ka BP) and in the Holocene site Azokh 5 (Nagorno Karabakh, Parfitt, 2016).

2.3. Description of Tooth Morphology

We restrict our analysis to the first lower molar, the most diagnostic tooth in arvicolines. The *Ellobius* lower m1 is composed of the anterior cap (AC), five triangles (T) with three buccal (BRA) and

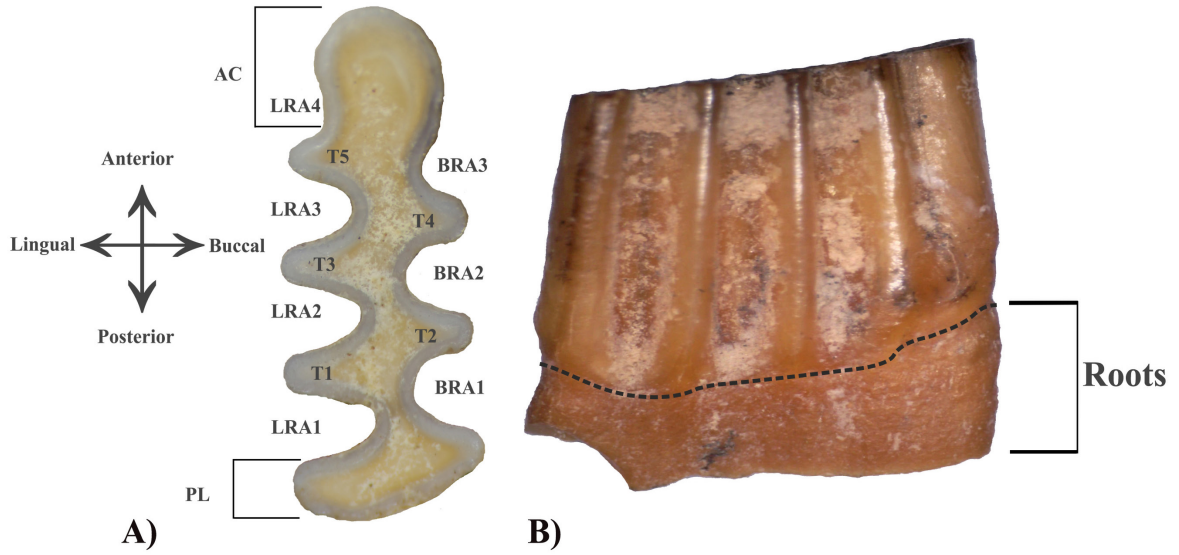


Figure 4.1. A) Occlusal surface of *Ellobius* right lower m1: triangle (T); buccal re-entrant angle (BRA); lingual re-entrant angle (LRA), anterior cap (AC); posterior lobe (PL); B) Lingual view of left lower m1.

four lingual (LRA) re-entrant angles, and one posterior lobe (PL) (Figure 4.1A). *Ellobius* molars are notably characterized by broadly confluent triangles, and the presence of roots that are visible in adult and old individuals (Figure 4.1B). Moreover, *Ellobius* molars lack cement in the re-entrant angles (Coşkun, 2016).

For modern representatives, the skull morphology (Kaya et al., 2018) we examined a total of 43 samples belonging to three Ellobius lutescens populations from Turkey, Iran and Nakhchivan, which are geographically separated by the Zagros, Tendürek and Alborz mountain ranges. We applied geometric morphometric methods (GMMs and external characters (Kryštufek and Vohralík, 2009) contain the main diagnostic features, whereas fossil samples mostly consist of isolated molars or broken jaws. The occlusal morphology of the lower m1 is rather similar in the various *Ellobius* species (especially the three Iranian species *E. fuscocapillus*, *E.lutescens* and *E. talpinus*). However, some specific morphological characters have been pointed out in previous studies: the AC is broad in *Ellobius lutescens*, narrow in *Ellobius talpinus* and elongated in *Ellobius fuscocapillus* (Maul et al., 2015b) Gekkota indet., Lacertidae indet. (2-3 taxa; the distance between T4 and T5 (W) and the total length (L) differ between the species, *Ellobius fuscocapillus* showing the largest teeth and *Ellobius talpinus* the smallest (Rey-Rodríguez et al., 2020). However, these varying morphological and biometric characters are not always clear nor reliable distinction is possible.

3. Material and methods

3.1. Modern and Fossil Material Studied

For this study we compared modern reference collections and fossil material of *Ellobius* using dental morphometric markers, because teeth represent the most abundant and diagnostic elements in fossil assemblages (Stoetzel et al., 2017). A total of 111 first lower molars (m1s) were measured. In our analysis, we took into account the individual age of the specimens using the classification of Coşkun (2016). We observed a striking difference in the occlusal pattern

between young and old individuals, so we only use adult individuals, in order to avoid any bias (Stoetzel et al., 2017a). Damaged and/or digested molars were not considered. In the reference collections, both males and females were used because no significant sexual dimorphism is known for *Ellobius* (Gharkheloo, 2003). Figure 4.2 shows all the frequent morphotypes of the three extant and fossil analysed species.

We used specimens from the modern reference collections of the Natural History Museum of London (NHM), the Field Museum of Chicago (FM) and the American Museum of Natural History of New York (AMNH) (Table 4.2); all the specimens were captured in the field, not bred in captivity.

The archaeological samples come from the Iranian site of Kaldar Cave (Table 4.2), located in the Zagros Mountains, in the northern part of Khorramabad Valley, Lorestan Province, western Iran (Becerra-Valdivia et al., 2017) the concomitant replacement of Neanderthals across Eurasia, and the emergence of new technological traditions. The Zagros Mountains region assumes importance in discussions concerning this period as its geographic location is central to all pertinent hominin migration areas, pointing to both east and west. As such, establishing a reliable chronology in the Zagros Mountains is crucial to our understanding of these biological and cultural developments. Political circumstance, coupled with the poor preservation of organic material, has meant that a clear chronological definition of the Middle to Upper Paleolithic transition for the Zagros Mountains region has not yet been achieved. To improve this situation, we have obtained new archaeological samples for AMS radiocarbon dating from three sites: Kobeh Cave, Kaldar Cave, and Ghār-e Boof (Iran (Figure 4.3). The material is hosted at the Institut Català de Paleoecologia Humana i Evolució Social (IPHES, Tarragona, Spain). More information on the archaeological context and the discoveries from this site can be found in Bazgir et al (2014, 2017) and Rey-Rodríguez et al. (2020).

The study material comes from Layer 5 (attributed to the Middle Palaeolithic) and Layer 4 (attributed to the Upper Palaeolithic) (Bazgir et al., 2014, 2017; Rey-Rodríguez et al., 2020) ranging from 23,100 ± 3300 to 29,400 ± 2300 BP, and three AMS radiocarbon dates from charcoal samples belonging to the lower part of the same layer, yielding ages of 38,650-36,750 cal BP, 44,200-42,350 cal BP, and 54,400-46,050 cal BP (all at the 95.4% confidence level. A total of 264 minimum number of individuals were identified from the small-mammal assemblages of Kaldar Cave. Layers 4 and 5 are dominated by *Microtus* spp. (60 individuals in Layer 4 and 79 in Layer 5), followed by *Ellobius* spp. (18 individuals in Layer 4 and 17 in Layer 5) and *Meriones* cf. *persicus* (17 individuals in Layer 4 and 18 in Layer 5). Other species were found in lesser proportions: *Chionomys nivalis*, *Cricetulus migratorius*, *Mesocricetus brandti*, *Allactaga* sp., *Myomimus* sp. These species indicate that the environment in the area was mainly composed of open dry and steppe areas. However, we also found *Apodemus* sp.which are related rather to a dense vegetation cover (including trees/ bush), as well as few remains of *Mus* cf. *musculus* in both Layers 4 and 5. In this cave, there are also other levels, as Layers 1-3, that do not yield enough material to draw palaeoclimatic inferences (MNI < 30). All the species identified at Kaldar Cave still occur in the area today (Rey-Rodríguez et al., 2020).

Small-mammal remains were collected in the field by water screening, using superimposed 5 and 0.5-mm mesh screens. In subsequent years (2018, 2019), the sediment was sorted by hand and under microscope in order to identify and count

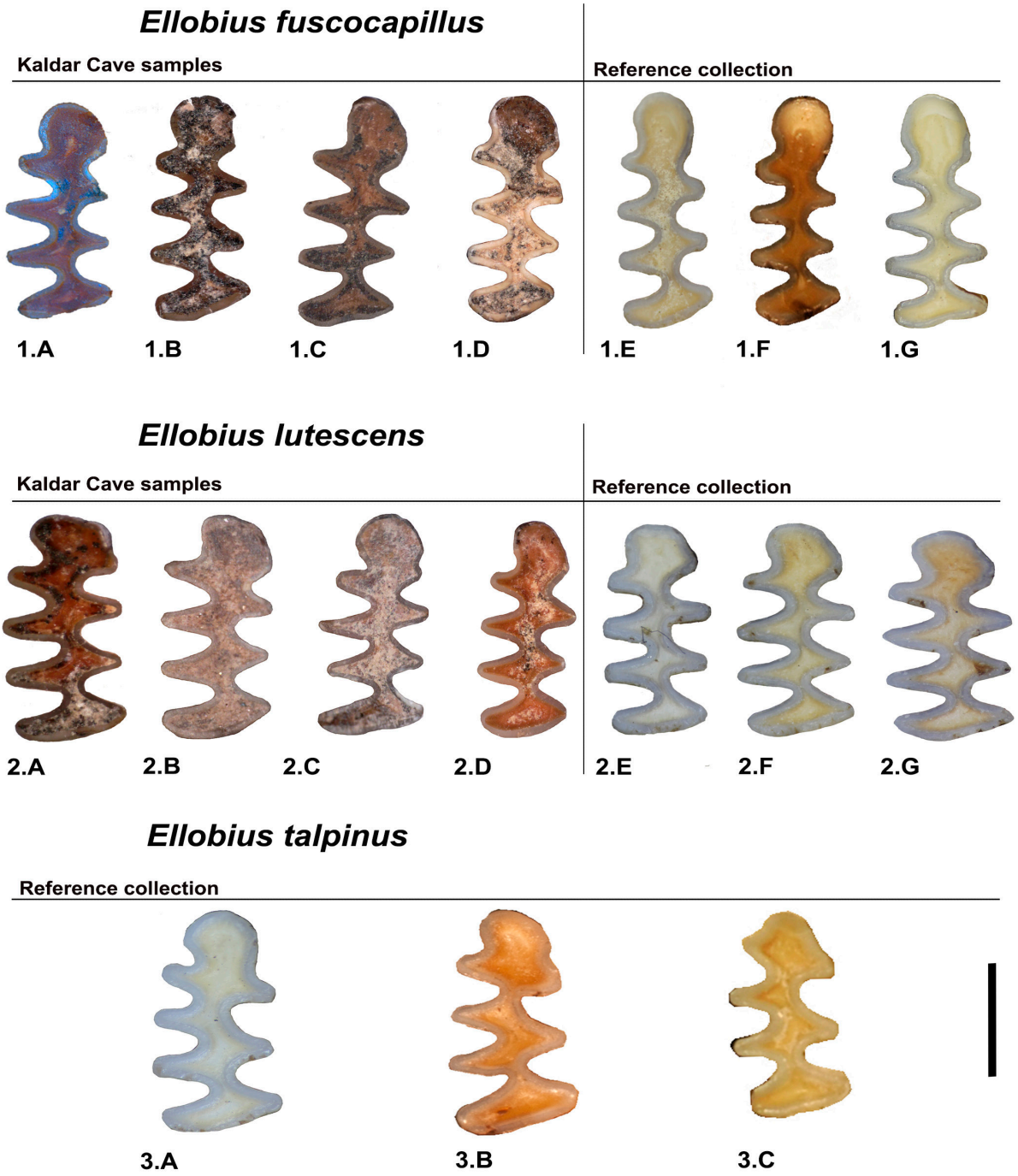


Figure 4.2. *Ellobius* lower m1 (all figured as right ones) from the extant reference collections and Kaldar Cave. 1) *Ellobius fuscocapillus*: 1.A-Kaldar Cave, 2014/4/SL5II/E6/125-130, right lower m1, number 157. 1.B-Kaldar Cave, 2014/4/SL5/E5/109-111, right lower m1, number 520. 1.C-Kaldar Cave, 2014/5/SL7II/E7/170-180, right lower m1, number 104. 1.D- Kaldar Cave, 2014/5/SL7II/F6/135-145, right lower m1, number 547.1.E-modern, NHM86101513, Afghanistan, right lower m1. 1.F-modern, FM111846, Iran, right lower m1. 1.G-modern, NHM86101512, Afghanistan, right lower m1; 2) *Ellobius lutescens***:** 2.A-Kaldar Cave, 2014/5/SL7II/F6/130-140, right lower m1, number 319. 2.B- Kaldar Cave, 2014/4/SL5II/F7/115-118, right lower m1, number 90. 2.C- Kaldar Cave, 2014/4/SL5II/F7/115-118, right lower m1, number 91. 2.D- Kaldar Cave, 2014/5/SL7II/E7/145-150, right lower m1, number 436.2.E-modern, NMH916416, Turkey, right lower m1. 2.F-modern, NMH916414, Turkey, right lower m1. 2.G-modern, NMH916412, Turkey, right lower m1; 3) *Ellobius talpinus***:** 3.A-modern, NHM3421126, Russia, right lower m1. 3.B-modern, FM103163, Afghanistan, right lower m1. 3.C-modern, AMNH59797, Mongolia, right lower m1. Scale equals 1 mm.

Reference collection				
Right lower m1	**NHM**	**AMNH**	**FM**	**Total**
Ellobius fuscocapillus	6	-	34	40
Ellobius lutescens	6	-	-	6
Ellobius talpinus	7	11	20	38
Total	**19**	**11**	**54**	**84**
Kaldar Cave				
Right lower m1	**Level 5(MP)**		**Level 4(UP)**	**Total**
Ellobius fuscocapillus	1		1	2
Ellobius lutescens	6		2	8
Total	**7**		**3**	**10**
Left lower m1	**Level 5(MP)**		**Level 4(UP)**	**Total**
Ellobius fuscocapillus	4		2	6
Ellobius lutescens	4		7	11
Total	**8**		**9**	**17**

Table 4.2. Modern reference collection for each museum specimen. Natural History Museum of London (NHM), Field Museum of Chicago (FM) and American Museum of Natural History of New York (AMNH). Archaeological specimens from Kaldar Cave, MP = Middle Palaeolithic, UP = Upper Palaeolithic.

the small-mammal elements and extract *Ellobius* remains for the present study.

3.2. Data Acquisition

The *Ellobius* lower molars were all photographed under constant conditions with a digital camera (Canon EOS 700D) coupled with a binocular microscope (Leica M125). All the pictures of the first lower molars were taken in occlusal view, and right molars were used; when they were not available (only in the fossil molars), the left lower molars were used and successively mirrored before the positioning of the landmarks and semi-landmarks. A scale bar was included in all the photographs in order to facilitate the extraction of a scaling factor, which can be used to estimate the centroid

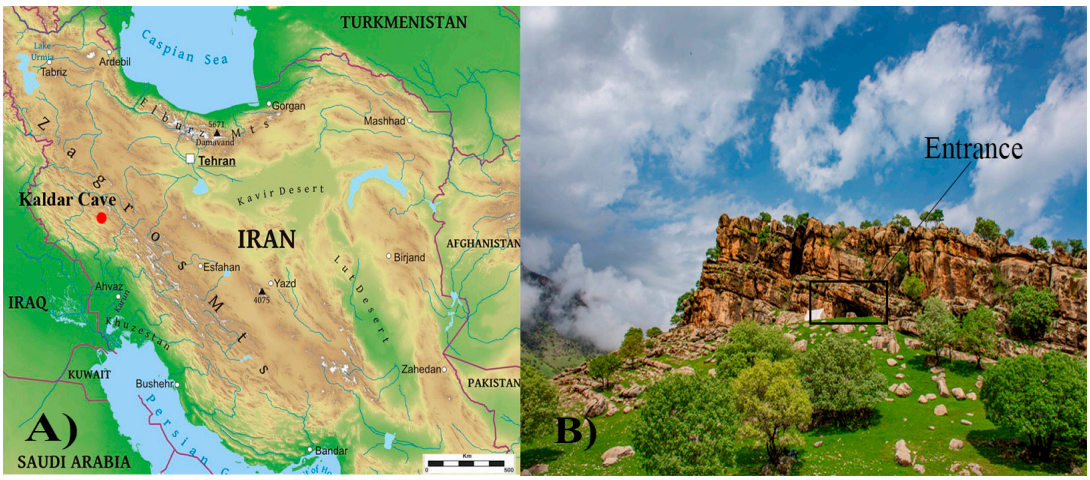


Figure 4.3. A) Kaldar Cave location. B) Entrance from the south of Kaldar Cave.

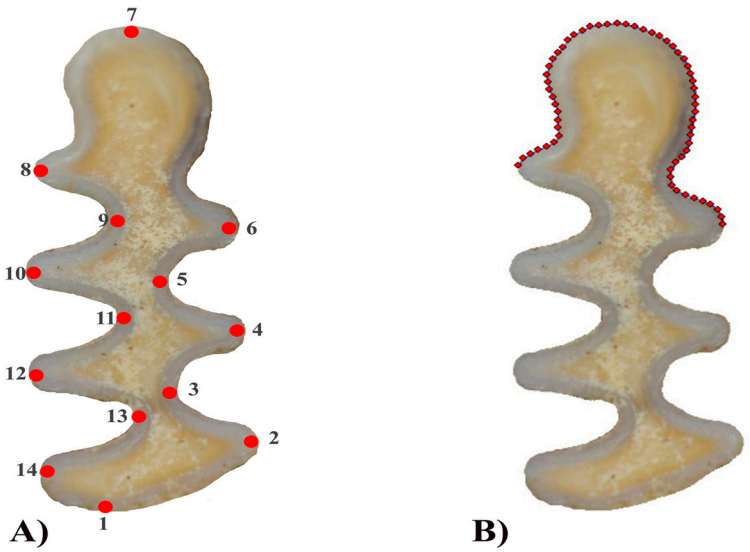


Figure 4.4 *Ellobius* right lower m1. A) 14 landmarks: Landmarks on the outermost turning point of buccal (2, 4, 6) and lingual (8, 10, 12, 14) salient angles, and on the innermost turning point of buccal (3, 5) and lingual (9, 11, 13) re-entrant angle. B) 60 semi-landmarks on the anterior cap.

size (Tabatabaei Yazdi and Alhajeri, 2018). We took in account the lateral side for the age classification.

To investigate the first lower molar size and shape we combined two-dimensional (2D) landmarks (LM) and semi-landmarks (SLM) on the photographs using TPSdig2 v.2.32 software package (Rohlf, 2016) for 2D geometric morphometric analyses (we include our data on a TPS file, Appendix 2). The methodology was adapted from the previous studies of Klenovšek and Kryštufek (2013), Cucchi et al. (2014, 2017), Cornette et al. (2015), Maul et al. (2015b), Kryštufek et al.(2016), Stoetzel et al. (2017a) and Dianat et al. (2017, 2020)introduced onto the Orkney archipelago (Scotland.

Fourteen landmarks were placed at the maximum curvature on the salient and re-entrant lingual and buccal angles, on the posterior lobe and the anterior cap, where the landmarks were positioned on the outline (Figure 4.4A).

In order to characterize the size and shape of the anterior cap, 60 equidistant semi-landmarks were automatically positioned along the curve corresponding to the external outline of the tooth enamel from buccal salient angle 3 to lingual salient angle 4 (Figure 4.4B).

To test the repeatability of the procedure, we re-digitized the set of landmarks and semi-landmarks 10 times on three randomly selected teeth. We estimate the measurement error on this new set of variables from the Procrustes ANOVA mean squares following the method proposed by Fruciano (2016). The procedure has been retained highly repeatable (R=0.97).

3.3. Shape Analyses

All the following analyses were performed with R (R Core Team, 2020) using the Geomorph (Adams et al., 2020) and Morpho (Schlager, 2017) packages.

Before undertaking the statistical analysis, the 2D landmark and semi-landmark coordinates were scaled through a general Procrustes analysis (GPA), allowing the semi-landmarks to slide along the outline (Gunz and Mitteroecker, 2013). A

principal component analysis (PCA) was then performed on the new normalized landmark and semi-landmark coordinates of the reference collection. Archaeological specimens were added a posteriori as supplementary individuals in the PCA shape space. A canonical variate analysis (CVA) was then performed on the PC scores, keeping 90 % of the overall shape variation (Baylac and Frieß, 2006). To assess the classification accuracy, a cross-validation test was performed on the CVA scores. Finally, the allometric effect was investigated through univariate and multivariate linear regression of the PC scores on the log centroid size.

4. Results

The PCA (Table 4.3) performed on the normalized landmarks and sliding semi-landmarks of the first lower molar reveals significant differences between the analysed species, the first two principal components (PCs) account for 52.7% of the total variance (Figure 4.5). Component 3 was also analysed but the variance was too low, and there was no differentiation between the species. We included the complete table with all statistical data in Appendix 2.

The main variation along the PC1 (38.2%) regards the morphology of the Anterior Cap, which is more flattened for the positive values and more rounded for the negatives ones. *Ellobius talpinus* occur on the positive part of the PC1 axis while *E. fuscopapillus* and *E. lutescens* are located on the negatives ones reflecting a broader and more rounded AC. Along the PC2 (14.5%) scores, the positive values show an AC elongated and

PC	PC1	PC2	PC3	PC4	PC5	PC6	PC7	PC8	PC9	PC10
%	38.2	14.5	8.1	6.9	4.2	2.8	2.6	2.2	1.6	1.5

Table 4.3. Contribution of the first 10th PCs to the total variance (%). PCA: principal component analysis

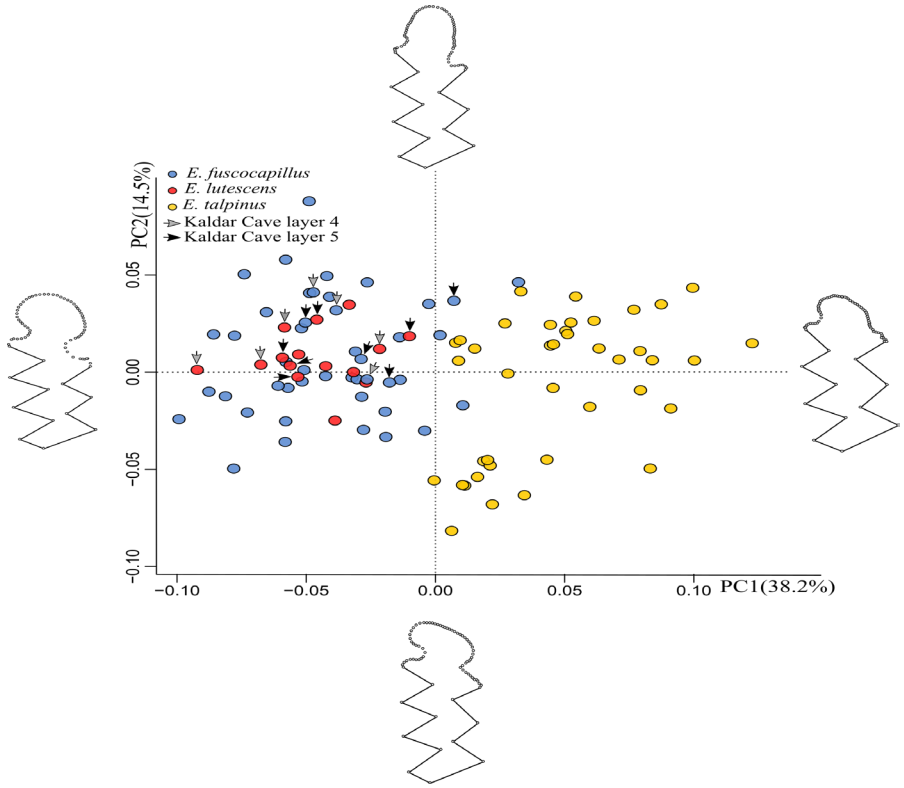


Figure 4. 5. Principal component analysis on the normalized landmarks and sliding semilandmarks and shape configuration at the extreme ends of the PCs.

pronounced on the buccal side, negative values display a more rounded AC with a clear constriction between BRA3 and LRA4. On PC2 there is not a clear differentiation between the three species. However, *E. lutescens* specimens are located principally in the upper half of the *E. fuscocapillus* and *lutescens* cloud, with positive PC2 values.

The shape of *E. talpinus* with narrower AC (Figure 4.5) is significantly different from that of *E. fuscocapillus* and *lutescens,* which appear morphologically very close one to another. The Kaldar Cave specimens are well distributed in the cloud of *E. lutescens* and E. *fuscocapillus,* with all of them having negative PC1 values. We can conclude that *Ellobius talpinus* is not present in the archaeological sample.

Estimating possible allometric effects on the samples, we performed a linear regression of the PCs onto the log of the centroid size (following the approach of Mitteroecker et al., 2015). Only PC1 shows a significant correlation with size (R^2 = 0.02956, p=0.04783). In this graph (Figure 4. 6A), it is possible to discriminate *E. lutescens* from *E. fuscocapillus*, the latter showing larger dimensions. *E. talpinus* presents a wide size range overlapping the ranges of the two latter (Figure 4.6). The archaeological remains are placed again in the cloud of *E. lutescens* and *E. fuscocapillus* but with some ambiguous identifications. We have also evidenced this confusion in the reference dataset with three *E. fuscocapillus* individuals from the Field Museum that were replaced among *E. lutescens* in our analysis, indicating a possible misidentification of the museum specimens. On Figure 4.6B, Kaldar Cave fossil specimens appear in general smaller that the reference specimens, but inside the standard deviation.

The canonical variate analysis of 90% of the total variation (PCs1 to 16) in the sample

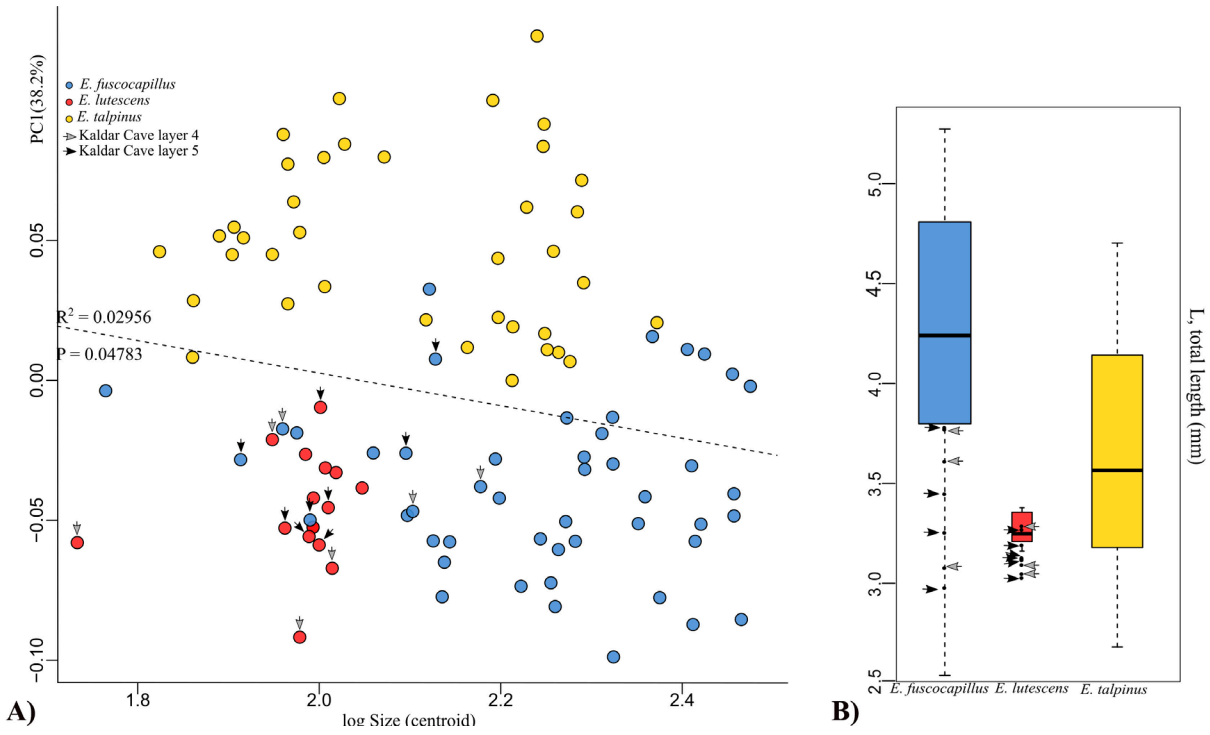


Figure 4.6. A) First two principal components of size and shape including the reference collection and Kaldar Cave material. B) Boxplot of the total length of *Ellobius* from the extant reference collections and Kaldar Cave.

	E. fuscocapillus		*E. lutescens*		*E. talpinus*		None	
Taxon	**N**	**%**	**N**	**%**	**N**	**%**	**N**	**%**
E. fuscocapillus	37	78.72	10	21.27	0	-	0	-
E. lutescens	2	13,33	13	86.66	0	-	0	-
E. talpinus	0	-	0	-	36	94.73	2	5.26

Table 4. 4. Cross-validated classification results in frequencies and %.

and the relative cross-validation procedure give an overall classification accuracy of 86 % (with almost 100% correct classification for *E. talpinus*) (Table 4.4).

5. Discussion

Our results indicate that it is possible to accurately identify *Ellobius* species by applying GMM to m1 shape and size. The main differences between species concern the AC shape, the size and the general disposition of the triangles.

One result of the performed GMM is that the shape of *E. fuscocapillus* and *E. lutescens* clusters in one cloud, and *E. talpinus* in another. This is in agreement with the distinction of two clades among the genus *Ellobius*: the subgenus (*Bramus*) Pomel, 1892 (with *E. fuscocapillus* Blyth, 1843, and *E. lutescens* Thomas, 1897) and the subgenus *Ellobius* Fischer, 1814 (with *E. talpinus* Pallas, 1770; *E. tancrei* Blasius, 1884; and *E. alaicus* Vorontsov et al. 1969) (Carleton and Musser, 2005).

The shape differences between *E. fuscocapillus* and *E. lutescens* is grossly in agreement with some earlier considerations based on conventional methods. Previously, Maul et al. (2015b) considered that the AC shape is a discriminant criteria, being broad in *Ellobius lutescens*, narrow in *Ellobius talpinus* and elongated in *Ellobius fuscocapillus*. Tesakov (2016) found that the size of *E. lutescens* is slightly smaller than in *E. fuscocapillus*. Rey-Rodríguez et al. (2020) reported that the confluence between T4 and T5 differs among the species, with T1-T2 and T3-T4 being slightly less pairwise opposed in *E. lutescens*.

Our GMM analyses allowed these previously examined criteria to be assessed all together, in taking into account the size, the morphology of the AC and the general disposition of the triangles. In our fossil samples many teeth are fragmented, and could not have been included in our GMM. However, it could be possible to consider fragments of *Ellobius* m1 in further analyses, for example by focusing only on the shape of the anterior cap.

5.1. Sliding Semi-Landmarks and Anatomical Landmarks Compared with Previous Systematic Methods of *Ellobius* Identification

Despite classic methods enable to distinguish between many m1s of some of the species, a throughout discrimination remains unclear. According to Maul et al. (2015b), morphological features of the AC (without performing GMM analyses) would be enough to permit species identification, and especially to differentiate *Ellobius talpinus* from *Ellobius lutescens* and *fuscocapillus*, because *Ellobius talpinus* has a less developed and narrower AC than in the other two species.

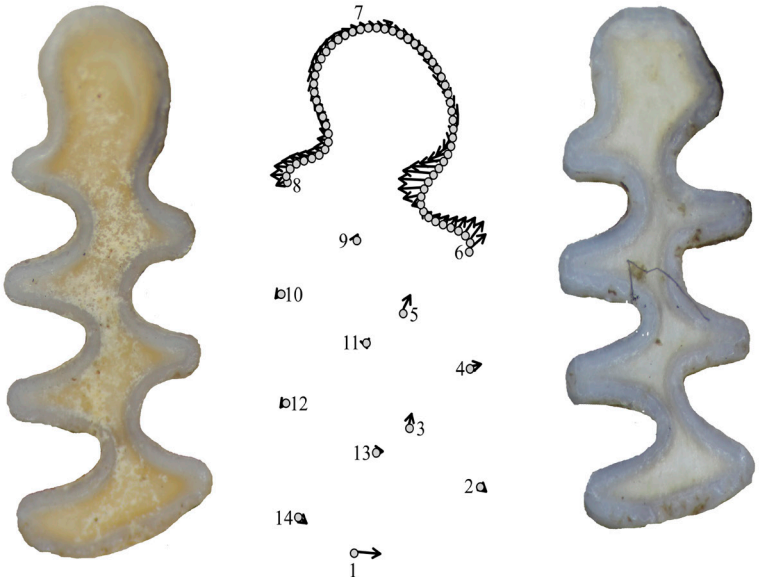


Figure 4.7. Morphological differences between *Ellobius fuscocapillus* (left) and *Ellobius lutescens* (right). Arrows depict the displacements between corresponding landmarks in the reference (dots) and E*llobius lutescens* as target specimens.

But in the present study, we have seen that there is a morphological overlap between *E. lutescens* and *E. fuscocapillus*. So, while "*classic*" morphological criteria often result in unclear features or overlaps between species, our GMM analysis of *Ellobius* m1 allowed two groups to be accurately differentiated, *Ellobius talpinus* on the one hand and *Ellobius lutescens* and *fuscocapillus* on the other. The distinction between these two latter species is more complex, and indeed no straightforward grouping was observed with the PCA (Figure 4.5). However, morphological differences between them could have been detected by comparing the mean shapes of their m1 (Figure 4.7) and by including the size parameter (Figure 4.6).

Figure 4.7 shows the means (dots) and variations (arrows) of the different landmark and semi-landmarks between *E. fuscocapillus* and *E. lutescens*. Major morphological differences are seen in point 1 (posterior lobe), 3, 4, 5 and 6 (BRAs and BSAs). This means that T1-T2 and T3-T4 are less parallel in *E. lutescens* than in *E. fuscocapillus*, as observed in the buccal part. Rey- Rodríguez et al. (2020) proposed that the width between T4 and T5 (W) and the total length (L) of the two species are different. The configuration of the AC shows that the transition between T4-T5 is narrower in *E. lutescens* than in *E. fuscocapillus*, which generates a smaller and more closed AC in *E. lutescens* than in *E. fuscocapillus*, in accordance with the observations of Maul et al. (2015b). Finally, also the previous observation of Tesakov (2016) is confirmed that size is a valid criterion for distinguishing *Ellobius fuscocapillus* (larger) and *Ellobius lutescens* (smaller).

Combining shape and size allowed us identifying the fossil *Ellobius* m1s from Kaldar Cave. The morphology of the AC, the size and the W (width between T4 and T5) are valid criteria in most of the cases, but we have seen that GMM analyses allowed them all to be combined and a number of previous identifications to be re-analysed (Bazgir et al., 2014, 2017; Rey-Rodríguez et al., 2020). The results of the present analysis allowed some *E. lutescens* from the archaeological material to be re-assigned to *E. fuscocapillus* (five *E. fuscocapillus*, three from Layer 4 and two from Layer 5 were re- assigned). These misclassifications were due to the fact that *E.*

fuscocapillus and *E. lutescens* are quite similar from a morphological point of view, and because the previous identifications were based on the W, L and the AC, subjected to overlapping problems, which have subsequently been clarified with the GMM.

In this study we have not seen morphological differences between specimens from Layer 4 and 5. As we are working in an archaeological site, the fact that we have two species in the same levels does not mean that they were deposited at the same time. Layer 4 as a chronological date on the bottom of 54,400–46,050 cal BP and the top is 23,100 ± 3 300 to 29,400 ± 2 300 BP, so we have a gap were one species could be replaced by the other one. The same observation can be made for Layer 5, whose chronology is still under review. Moreover, the fact that we have two species in the same levels does not mean that they lived in the exact same place, because the small mammal assemblages from Kaldar Cave were accumulated by nocturnal raptors (Rey-Rodríguez et al., 2020), which could hunt in different habitats on a territory of several (tens of) km^2.

E. fuscocapillus is not present in the area nowadays, but it may have lived there in the past. Indeed, at Kaldar Cave, the palaeoenvironmental data (obtained with the habitat weighting method) have shown that the landscape was mainly composed of steppes in both levels, which are favorable habitats for the *Ellobius* species (Rey-Rodríguez et al., 2020). The absence of *E. talpinus* in our archaeological sample could be linked to the climatic requirements of the species, but this hypothesis remains to be deepened.

6. Conclusions

In the present study, based on modern and fossil specimens of *Ellobius* species, we found potential size and shape differences within the examined material thanks to GMM analyses. On the basis of the m1 shape alone, we were able to differentiate two groups: *E. talpinus* on the one hand, and *E. fuscocapillus* and *E. lutescens* on the other. Taking size into account, moreover, it is possible to distinguish *E. fuscocapillus* from *E. lutescens*. However, we agree that it would be necessary to increase the reference dataset, particularly for *E. lutescens*, which may help us find further discriminative patterns between these three species in future studies.

GMM enabled us to obtain good results in fossil species attributions. Here, only complete teeth were used, i.e. not the whole fossil *Ellobius* sample from Kaldar Cave. We obtained better results in the classifications in including all the teeth landmarks instead of the AC alone. It would thus be really useful to improve the results in order to be able to identify broken or digested molars, albeit with the caveat that when only the anterior cap of the molar is preserved we cannot discriminate between *E. fuscocapillus and E. lutescens*. Accordingly, it would be necessary to combine this method with other techniques and use all the criteria together.

It would be interesting to extend this GMM study to other modern and fossil *Ellobius* species, especially from Middle Pleistocene sites, in order to obtain a more complex overview of their morphological differences and their evolution throughout their current and past geographic range, and to explore the potential and usefulness of this tool in the archaeological sites of southeastern Europe, western and central Asia.

Acknowledgments: I. Rey-Rodriguez is the beneficiary of a PhD scholarship funded by the Erasmus Mundus Program (IDQP). J.M. López-García was supported by a Ramón y Cajal contract (RYC-2016-19386) with financial sponsorship from the Spanish Ministry of Science, Innovation and Universities. This

work was developed within the framework of projects 2017SGR859, 2017SGR840 and 2017SGR1040 (AGAUR, Generalitat de Catalunya), and 2018PFRURVB291 (Univ. Rovira i Virigli). We thank the head of the Research Institute of Cultural Heritage and Tourism (RICHT) (Dr. B. Omrani) and the head of the Iranian Center for Archaeological Research (ICAR) (Dr. R. Shirazi) for providing us with the necessary support and permissions in studying the materials. We thank the head of the Lorestan Cultural Heritage, Handicraft and Tourism Organization (Mr. A. Ghasemi) for all his support. We also thank the head of International Collaboration and Ties of the RICHT (Mrs. M. Kholghi) for all her cooperation and help. B. Bazgir received his PhD scholarship from the Fundación Atapuerca, for which he is grateful. We would like to thank R. Portela Miguez, Senior Curator in Charge of Mammals, for his help with the reference collection in the Natural History Museum of London; L. Heaney, A. Ferguson and L. Smith of Chicago Field Museum; and M. Surovy, J. Galkin and C. Mehling of the American Museum of Natural History of New York. We thank A. Profico for his precious help.

We would like to thank R. Glasgow for reviewing the English language of the manuscript. We also want to thank to the Editors Dr. D. Nowakowski, Dr. D. Hembree and Dr. C. Haug, as well as the three anonymous reviewers for their comments and suggestions that strongly improved the final version of the manuscript.

References

Adams, D.C., Collyer, M.L., and Kaliontzopoulou, A. 2020. Geomorph: Software for geometric morphometric analyses. R package version 3.2.1.

Adams, D.C., Rohlf, F.J.,and Slice, D.E. 2009. Geometric morphometrics: Ten years of progress following the revolution. Italian Journal of Zoology, 71 (1): 5-16, https://doi.org/10.1080/11250000409356545

Bate, D.M.A. 1937. Palaeontoogy: the fossil fauna of the Wady El-Mughara caves. In Garrod, D.A.E. and Bate, D.M.A. (eds.), Excavations at the Wady El-Mughara. Clarendon Press, Oxford.

Bate, D.M.A. 1930. Animal remains from the Dark Cave, Hazar Merd. American School of Prehistoric Research Bulletins, 6: 38-41.

Baylac, M. and Frieß, M. 2006. Fourier Descriptors, Procrustes Superimposition, and Data Dimensionality: An Example of Cranial Shape Analysis in Modern Human Populations, p.145-165. In Slice, D.E. (ed.), Modern Morphometrics in Physical Anthropology. Kluwer Academic Publishers-Plenum Publishers, New York. https://doi.org/10.1007/0-387-27614-9_6

Bazgir, B., Ollé, A., Tumung, L., Becerra-Valdivia, L., Douka, K., Higham, T., Van Der Made, J., Picin, A., Saladié, P., López-Garciá, J.M., Blain, H.-A., Allué, E., Fernández-Garciá, M., Rey-Rodríguez, I., Arceredillo, D., Bahrololoumi, F., Azimi, M., Otte, M., and Carbonell, E. 2017. Understanding the emergence of modern humans and the disappearance of Neanderthals: Insights from Kaldar Cave (Khorramabad Valley, Western Iran). Scientific Reports 7. Article number: 43460 https://doi.org/10.1038/srep43460

Bazgir, B., Otte, M., Tumung, L., Ollé, A., Deo, S.G., Joglekar, P., López-García, J.M., Picin, A., Davoudi, D., and van der Made, J. 2014. Test excavations and initial results at the middle and upper paleolithic sites of Gilvaran, Kaldar, Ghamari caves and Gar Arjene Rockshelter, Khorramabad Valley, western Iran. Comptes Rendus-Palevol, 13: 511-525. https://doi.org/10.1016/j.crpv.2014.01.005

Becerra-Valdivia, L., Douka, K., Comeskey, D., Bazgir, B., Conard, N.J., Marean, C.W., Ollé, A., Otte, M., Tumung, L., Zeidi, M., and Higham, T.F.G. 2017. Chronometric investigations of the Middle to Upper Paleolithic transition in the Zagros Mountains using AMS radiocarbon dating and Bayesian age modelling. Journal of Human Evolution, 109: 57-69. https://doi.org/10.1016/j.jhevol.2017.05.011

Belmaker, M., Bar-Yosef, O., Belfer-Cohen, A., Meshveliani, T., and Jakeli, N. 2016. The environment in the Caucasus in the Upper Paleolithic (Late Pleistocene): Evidence from the small mammals from Dzudzuana cave, Georgia. Quaternary International, 425:4-15. https://doi.org/10.1016/j.quaint.2016.06.022

Blasius, W. 1884. Comptes rendus des séances de l´Académie des Sciences. Tome XCVIII. Nos 1 et 2. Paris.

Blyth, E. 1843. The Journal of the Asiatic Society of Bengal. Calcutta: Bishop's College Press,1832-1936

Carleton, M.D. and Musser, G.G. 2005. Order Rodentia, p. 745-752. In Wilson, D.E. and Reeder, D.M. (eds.), Mammal Species of the World, Third Edition. The Johns Hopkins University Press, Baltimore.

Corbet, G.B. and Hill, J.E. 1991. A World List of Mammalian Species. 3rd ed. London, UK: British Museum (Natural History).

Corbet, G.B. 1978. The Mammals of the Palearctic Region: A Taxonomic Review. London, Brit. Mus. (Nat. Hist.). Cornell Univ. Press. 117-118.

Cornette, R., Stoetzel, E., Baylac, M., Moulin, S., Hutterer, R., Nespoulet, R., El Hajraoui, M.A., Denys, C., and Herrel, A. 2015. Shrews of the genus *Crocidura* from El Harhoura 2 (Témara, Morocco): The contribution of broken specimens to the understanding of Late Pleistocene-Holocene palaeoenvironments in North Africa. Palaeogeography, Palaeoclimatology, Palaeoecology, 436:1-8. https://doi.org/10.1016/j.palaeo.2015.06.020

Coşkun, Y. 2016. Review of unique odd chromosome-numbered underground rodent species of the Palearctic region: *Ellobius Lutescens* Thomas 1897 (Rodentia: Cricetidae). Turkish Journal of Zoology, 40:831-841. https://doi.org/10.3906/zoo-1509-53

Coşkun, Y. 2001. On distribution, morphology and biology of the mole vole*, Ellobius lutescens* Thomas, 1897 (Mammalia: Rodentia) in eastern Turkey. Zoology in the Middle East, 23:5-12. https://doi.org/10.1080/09397140.2001.10637861

Coşkun, Y. 1997. *Ellobius lutescens* Thomas, 1897 (Rodentia: Cricetidae) Turk. Journal of Zoology. 21, 349-354.

Cucchi, T., Barnett, R., Martínková, N., Renaud, S., Renvoisé, E., Evin, A., Sheridan, A., Mainland, I., Wickham-Jones, C., Tougard, C., Quéré, J.P., Pascal, Michel, Pascal, Marine, Heckel, G., O'Higgins, P., Searle, J.B., and Dobney, K.M. 2014. The changing pace of insular life: 5000 years of microevolution in the Orkney vole (*Microtus arvalis orcadensis*). Evolution, 68: 2804–2820. https://doi.org/10.1111/evo.12476

Cucchi, T., Mohaseb, A., Peigné, S., Debue, K., Orlando, L., and Mashkour, M. 2017. Detecting taxonomic and phylogenetic signals in equid cheek teeth: Towards new palaeontological and archaeological proxies. Royal Society Open Science 4. https://doi.org/10.1098/rsos.160997

Darlington, P.J. 1957. Zoogeography: The Geographical Distribution of Animals. New York, NY, USA, John Wiley and

Sons.

Dianat, M., Darvish, J., Aliabadian, M., Siahsarvie, R., Krystufek, B., and Nicolas, V. 2020. Systematics and evolution of the libyan jird based on molecular and morphometric data. Journal of Zoological Systematics and Evolutionary Research, 58:439-458. https://doi.org/10.1111/jzs.12335

Dianat, M., Darvish, J., Cornette, R., Aliabadian, M., and Nicolas, V. 2017. Evolutionary history of the Persian Jird, M*eriones persicus*, based on genetics, species distribution modelling and morphometric data. Journal of Zoological Systematics and Evolutionary Research, 55:29-45. https://doi.org/10.1111/jzs.12145

Ellerman, J.R., and Morrison-Scott, T.C.S. 1951. Checklist of Palearctic and Indian Mammals, 1780 to 1946. Brit. Mus. Nat. Hist. London, 1-810.

Fischer von Waldheim, G. 1814. Zoognosia tabulis synopticis illustrata: in usum praelectionum Academiae imperialis medico-chirugicae mosquensis edita. Mosquae: Typis Nicolai S. Vsevolozsky

Fruciano, C. 2016. Measurement error in geometric morphometrics. Development Genes and Evolution, 226:139-158. https://doi.org/10.1007/s00427-016-0537-4

Frumkin, A. and Comay, O. In press. The last glacial cycle of the southern Levant: Paleoenvironment and chronology of modern humans. Journal of Human Evolution 2019, 102609. https://doi.org/10.1016/j.jhevol.2019.04.007

Gharkheloo, M.M. 2003. A Study on the Morphology, Karyology and Distribution of *Ellobius* Fischer, 1814 (Mammalia: Rodentia) in Iran. Turkish Journal of Zoology, 27:281-292.

Gunz, P. and Mitteroecker, P. 2013. Semilandmarks: A method for quantifying curves and surfaces. Hystrix, 24:103-109.

Hassinger, J.D. 1973. A survey of the mammals of Afghanistan: Resulting from the 1965 Street Expedition (Excluding Bats). Fieldiana Zoology, Vol. 60. Chicago, IL, USA, Field Museum of Natural History.

Hashemi, N., Darvish, J., Mashkour, M., and Biglari, F. 2006. Rodents and Lagomorphs remains from late Pleistocene and early Holocene Caves and Rochshelter sites in the Zagros region, Iran. Iranian Journal of Animal Biosystematics, 2:25-33.

Hulme-Beaman, A., Cucchi, T., Evin, A., Searle, J.B., and Dobney, K. 2018. Exploring *Rattus praetor* (Rodentia, Muridae) as a possible species complex using geometric morphometrics on dental morphology. Mammalian Biology, 92:62-67. https://doi.org/10.1016/j.mambio.2018.04.002

Jaeger, J.J. 1988. Origine et evolution du genre *Ellobius* (Mammalia, Rodentia) en Afrique Nord-Occidentale. Folia Quaternaria 57:3-50.

Kandel, A.W., Gasparyan, B., Allué, E., Bigga, G., Bruch, A.A., Cullen, V.L., Frahm, E., Ghukasyan, R., Gruwier, B., Jabbour, F., Miller, C.E., Taller, A., Vardazaryan, V., Vasilyan, D., and Weissbrod, L. 2017. The earliest evidence for Upper Paleolithic occupation in the Armenian Highlands at Aghitu-3 Cave. Journal of Human Evolution, 110:37-68. morhttps://doi.org/10.1016/j.jhevol.2017.05.010

Kaya, A., Gharkheloo, M.M., and Coşkun, Y. 2018. Geographic variation in the skull morphology of *Ellobius lutescens* Thomas, 1897 (Mammalia: Rodentia) by geometric morphometric analyses. Vertebrate Zoology, 68:157-164.

Klenovšek, T. and Kryštufek, B. 2013. An ontogenetic perspective on the study of sexual dimorphism, phylogenetic variability, and allometry of the skull of European ground squirrel, *Spermophilus citellus* (Linnaeus, 1766). Zoomorphology, 132:433-445. https://doi.org/10.1007/s00435-013-0196-1

Kryštufek, B. and Shenbrot, G. 2016. *Ellobius lutescens*. The IUCN Red List of Threatened Species 2016: e. T7655A22340006. https://dx.doi.org/10.2305/IUCN.UK.2016-2.RLTS.T7655A22340006.en.

Kryštufek, B., Janžekovič, F., Hutterer, R., and Klenovšek, T. 2016. Morphological evolution of the skull in closely related bandicoot rats: A comparative study using geometric morphometrics. Hystrix, 27:1-7. https://doi.org/10.4404/hystrix-27.2-11639

Kryštufek, B. and Vohralík, V. 2009. Mammals of Turkey and Cyprus, Rodentia II: Cricetinae, Muridae, Spalacidae, Calomyscidae, Capromyidae, Hystricidae, Castoridae. https://doi.org/10.1644/10-MAMM-R-221.1

Lay, D.M. 1967. A Study of the Mammals of Iran, Resulting from the Street Expedition of 1962-63. Fieldiana Zool., 54:168-171.

Luzi, E., Pazonyi, P., and López-García, J.M. 2019. The influence of climate on morphometric traits of fossil populations of *Microtus arvalis* and *M. agrestis* from the Carpathian Basin, northern Hungary. Lethaia, 52:123132. https://doi.org/10.1111/let.12294

Markova, A. 1992. Fossil rodents (Rodentia, Mammalia) from the Sel'-Ungur Acheulian cave site (Kirghizstan). Acta Zoologica Cracoviensia, 35 (2): 217-239.

Maul, L.C. and Markova, A.K. 2007. Similarity and regional differences in Quaternary arvicolid evolution in Central and Eastern Europe. Quaternary International, 160:81-99. https://doi.org/10.1016/j.quaint.2006.09.010

Maul, L.C., Smith, K.T., Shenbrot, G., Bruch, A.A., Wegmüller, F., and Le Tensorer, J.M. 2015. Microvertebrates from unit G/layer 17 of the archaeological site of Hummal (El Kowm, Central Syria): Preliminary results. Anthropologie, 119:676-686. https://doi.org/10.1016/j.anthro.2015.10.010

Michaux, J., Reyes, A., and Catzeflis, F. 2001. Evolutionary history of the most speciose mammals: Molecular phylogeny of muroid rodents. Molecular Biology and Evolution, 18:2017-2031. https://doi.org/10.1093/oxfordjournals.molbev.a003743

Mitteroecker, P., Windhager, S., Müller, G.B., and Schaefer, K. 2015. The morphometrics of "masculinity" in human faces. PLoS ONE, 10. https://doi.org/10.1371/journal.pone.0118374

Nesin, V. and Nadachowski, A. 2001. Late Miocene and Pliocene small mammal faunas (Insectivora, Lagomorpha, Rodentia) of Southeastern Europe. Acta Zoologica Cracoviensia, 44:107-135.

Nowak, R.M. 1999. Walker's Mammals of the World. 6th ed. Baltimore, MD, USA, The Johns Hopkins University Press.

Osborn, D.J. 1962. Rodents of subfamily Microtinae from Turkey. Journal of Mammology, 43 (4):515-529. https://doi.org/10.2307/1376914

Pallas, P. S. 1770. Spicilegia zoologica quibus novae imprimis et obscurae animalium species iconibus, descriptionibus atque commentariis illustrantur. Fasciculus octavus

Parfitt, S. A. 2016. Chapter 7: Rodents, Lagomorphs and Insectivores from Azokh

Cave,p.163-177. In Fernández-Jalvo,Y., King,T., Yepiskoposyan,L. & Andrews,P. (eds.), Azokh Cave and the Transcaucasian Corridor (Vertebrate paleobiology and paleoanthropology book series). Dordrecht: Springer. https://doi.org/10.1007/978-3-319-24924-7.

R Core Team, 2020. R: A language and environment for statistical computing. R Foundation for Statistical Computing. http://www.r-project.org/index.html

Rey-Rodríguez, I., Lopez-Garcia, J.M., Blain, H.-A., Stoetzel, E., Denys, C., Bazgir, B., and Ollé, A. 2020. Exploring the landscape and climatic conditions of Neanderthals and anatomically modern humans in the Middle East: the rodent assemblage from the late Pleistocene of Kaldar Cave (Khorramabad Valley, Iran). Quaternary Science Reviews, 236. https://doi.org/10.1016/j.quascirev.2020.106278

Roberts, T.J. 1977. The Mammals of Pakistan. London, UK, Ernst Benn Ltd.

Rohlf, F.J. 2016. tpsDig, Digitize Landmarks and Outlines, Version 2.32. Department of Ecology and Evolution, State University of New York at Stony Brook, New York. http://life.bio.sunysb.edu/morph

Romanenko, S.A., Fedorova, Y.E., Serdyukova, N.A., Zaccaroni, M., Stanyon, R., Graphodatsky, A.S. 2020. Evolutionary rearrangements of X chromosomes in voles (Arvicolinae, Rodentia). Scientific Reports 1–11. https://doi.org/10.1038/s41598-020-70226-4

Romanenko, S.A., Sitnikova, N.A., Serdukova, N.A., Perelman, P.L., Rubtsova, N. V., Bakloushinskaya, I.Y., Lyapunova, E.A., Just, W., Ferguson-Smith, M.A., Yang, F., and Graphodatsky, A.S. 2007. Chromosomal evolution of Arvicolinae (Cricetidae, Rodentia). II. The genome homology of two mole voles (genus *Ellobius*), the field vole and golden hamster revealed by comparative chromosome painting. Chromosome Research, 15:891897. https://doi.org/10.1007/s10577-007-1171-9

Romanenko, S.A., Serdyukova, N.A., Perelman, P.L., Trifonov, V.A., Golenishchev, F.N., Bulatova, N.S., Stanyon, R., and Graphodatsky, A.S. 2018. Multiple intrasyntenic rearrangements and rapid speciation in voles. Scientific Reports 2-10. https://doi.org/10.1038/s41598-018-33300-6

Rusin, M. 2017. *Ellobius talpinus*, Northern Mole Vole. The IUCN Red List of Threatened Species 2016: e. T7656A115085720. https://doi.org/10.2305/IUCN.UK.2016-3.RLTS.T7656A22339917.en

Sala, B., Masini, F., Torre, D. 1994. Villanyian arvicolids from Veronese, a karst fissure in the Adige valley, Northeastern Italy. Bolletino Societa Paleontologica Italina, 33:3-11.

Schlager, S. 2017. Morpho and Rvcg Shape Analysis, p. 217–256. In Guoyan Zheng, Shuo Li, and Gabor Szekely (ed.), Statistical Shape and Deformation Analysis. Academic Press.

Shenbrot, G., Kryštufek, B., and Molur, S. 2016. *Ellobius fuscocapillus,* Southern Mole Vole. The IUCN Red List of Threatened Species 2016: e.T7654A22339730. https://dx.doi.org/10.2305/IUCN.UK.2016-2.RLTS.T7654A22339730.en.

Stoetzel, E. 2013. Late cenozoic micromammal biochronology of northwestern Africa. Palaeogeography, Palaeoclimatology, Palaeoecology, 392:359-381. https://doi.org/10.1016/j.palaeo.2013.09.026

Stoetzel, E., Cornette, R., Lalis, A., Nicolas, V., Cucchi, T., and Denys, C. 2017. Systematics and evolution of the *Meriones shawii/grandis* complex (Rodentia,

Gerbillinae) during the Late Quaternary in northwestern Africa: Exploring the role of environmental and anthropogenic changes. Quaternary Science Reviews, 164:199-216. https://doi.org/10.1016/j.quascirev.2017.04.002

Tabatabaei Yazdi, F. and Alhajeri, H. 2018. Sexual dimorphism, allometry, and interspecific variation in the cranial morphology of seven *Meriones* species (Gerbillinae, Rodentia). Hystrix, Italian Journal of Mammalogy, 29(2):162-167. https://doi.org/10.4404/hystrix

Tesakov, A.S. 2016. Early Middle Pleistocene *Ellobius* (Rodentia, Cricetidae, Arvicolinae) from Armenia. Russian Journal of Theriology, 15(2):151-158.

Tesakov, A. S. 1998. Voles of the Tegelen fauna. Mededelingen Nederlands Instituut voor Toegepaste Geowetenschappen TNO, 60, p. 71-134.

Thomas, O. 1905. *Ellobius woosnami*. Abstr. Proc. Zool. Soc. 23; Proceeding of the Zoological Society. 526 London.

Thomas, O.1897.*Ellobius lutescens*. The Annals and Magazine of Natural History, 20: 308. London

Topachevsky, V.A. and Rekovets, L.I. 1982. New material to the systematics and evolution of mole voles of the nominative subgenus of the genus *Ellobius* (Rodentia, Cricetidae). Vestnik Zoologii, 5:47-74 (in Russian).

Vorontsov, N.N., Lyapunova, E.A., Zakaryan, G.G., and Ivanov, V.G. 1969. The karyology and taxonomy of the genus *Ellobius* (Microtinae, Rodentia). In: The Mammals, Evolution, Karyology, Taxonomy, Fauna. 2nd All-Union Mammalogy Conference, Moscow.

Walker, E.P. 1964. Mammals of the World. Vol. 2. Baltimore, MD, USA, The Johns Hopkins Press.

Weissbrod, L., Marshall, F.B., Valla, F.R., Khalaily, H., Bar-Oz, G., Auffray, J.-C., Vigne, J.-D. and Cucchi, T. 2017. Origins of house mice in ecological niches created by settled hunter-gatherers in the Levant 15,000 y ago. Proceedings of the National Academy of Sciences, 114:4099-4104. https://doi.org/10.1073/pnas.1619137114

Weissbrod, L. and Weinstein-Evron, M. 2020. Climate variability in early expansions of *Homo sapiens* in light of the new record of micromammals in Misliya Cave, Israel. Journal of Human Evolution, 139:102741. https://doi.org/10.1016/j.jhevol.2020.102741

Wilson, D.E. and Reeder, D.M. 2005. Mammal Species of the World. Washington, DC, USA: Smithsonian Institution Scholarly Press.

Wilson, D.E., Mittermeier, R.A., and Lacher, T.E. 2017. Handbook of the Mammals of the World. Volume 7.Rodents II. Lynx Edictiones.

Chapter 5.

New palaeoecological inferences using rodent's assemblages for the Middle to the Late Pleistocene site of Azokh 1 Cave (Southern Caucasus)



Abstract

Southern Caucasus is a prime location to study human populations, as a crossroads between Africa, Europe and Asia. With this work, the main objective is to infer the climatic and environmental conditions during the formation of the Azokh 1 site. Rodent remains come from the archaeological excavation campaigns carried out in 2003, 2005, 2014, 2015 and 2018, in particular from: Unit V (293 ± 23 ka), Unit III-IV (no date available) and Unit II (184 ± 13 ka - 100 ± 7 ka). The studied sample is composed of at least 13 taxa: seven arvicoline, two cricetine, two gerbilline, one dipodid and one murine species.

Unit III-IV did not yield enough material for palaeoclimatic inferences. Paleoclimatic conditions for units V and II were obtained with the Bioclimatic model method, and the paleoenvironmental reconstruction through the habitat weighting method. The interpretation differs with large mammals and charcoals data, which indicate a woodland environment, while small vertebrates (including also herpetofauna) indicate mainly arid environments, such as steppe and desert. These differences could be explained by the origin of the accumulation (i.e. humans for large mammals and wood, non-human predator such as Barn owl for small vertebrates).

Taking into account our data, hominin populations from Azokh 1 lived between the end of the Middle Pleistocene and the beginning of the Late Pleistocene surrounded by warm-temperate climate conditions with a landscape mainly composed of desert and steppe, also with grassland and forest in lesser proportions. No major palaeoenvironmental or palaeoclimatic change was highlighted between both periods, indicating favorable conditions for their activities throughout the studied period.

Keywords: Rodentia, taxonomy, taphonomy, paleoenvironment, paleoclimate.



Azokh Cave entrance in 2018

1. Introduction

Southern Caucasus, located at the crossroads between Africa, Europe and Asia, is a prime location to study *H. heidelbergensis*, *H. neanderthalensis* and anatomically modern human (AMH) occupations (Belmaker et al., 2016; Bermúdez de Castro and Martinón-Torres, 2013). It plays an important role to understand the biological history of human lineages, as well as their techno-cultural complexes during the Pleistocene. This area was a natural corridor and refuge between Africa and Eurasia during the Pleistocene, as evidenced by the high number of sites located in this region, such as Dmanisi, Qesem Cave, Misliya Cave or Agithu-3 (Fernández-Jalvo, 2016a; Fernández-Jalvo et al., 2010).

Studies of small vertebrates from archaeological sites in the Middle East are increasing during the last decade (Belmaker et al., 2016; Belmaker and Hovers, 2011; Demirel et al., 2011; Fernández-Jalvo, 2016a; Kandel et al., 2017; Maul et al., 2020, 2015a, 2015b; Rey-Rodríguez et al., 2020; Smith et al., 2015; Weissbrod and Weinstein-Evron, 2020; Weissbrod and Zaidner, 2014). We analysed here Azokh 1 site which is one of the most complete and, to date, one of the oldest archaeological sites in the Southern Caucasus.

The main objective of our work, using rodents, is to infer the climatic and environmental conditions during the formation of the site. We compare our result with the previous studies carried out in Azokh 1 Cave and also with other sites of the region where rodents were analysed, in order to obtain a framework to discuss the palaeoecological conditions where humans developed their activities in the southern Caucasus.

Azokh Cave takes its name from the village situated near the cave. It is located in the Ishkhanaget River valley in, Southern Caucasus (39º 37.15´ N; 46º 59.32´E) (Asryan et al., 2020). It is an important site for the understanding of human evolution in its archaeological, paleontological, environmental and ecological context (Fernández-Jalvo, 2016a).

The cave system is karstic and is developed on thickly bedded Mesozoic carbonates. This system is composed by a cave series of NNW to SSE trending interconnected and sub-rounded chambers that extend for almost 130 m. Several entrances passageways connect the inner parts of the cave to the exterior, but geo-archaeological sediments were found only at Azokh 1, Azokh 2 and Azokh 5 (Figure 5.1). Our research focused on Azokh 1, because it is the only entrance to date filled with Pleistocene-Holocene sediments.

1.1.Azokh 1

Azokh 1 is a broadly linear chamber of 40 m long and 11.5 m high with a WSW-ENE alignment. The cave has provided evidence of occupation by hominins from the Middle Pleistocene to the Holocene, and it is the only well stratified and dated sequence of this period in the Nagorno Karabagh region (Asryan, 2015).

It was discovered by M. Huseinov at the end of 1950´s and the first excavation started in 1960. Excavations of Azokh 1 carried out from 1960`s to 1980`s, yielded abundant archaeological remains. During this period, the volume of the sediments excavated was about 70% of the cave. Unfortunately, the information and descriptions of the excavation procedures and finds before 1975 have been lost or were too schematic, causing difficulties in interpretating the site (Asryan, 2015; Fernández-Jalvo, 2016a). The current excavations began in 2002, after an initial survey of the site in 1999 and 2001. The new excavation project re-started at Azokh Cave through

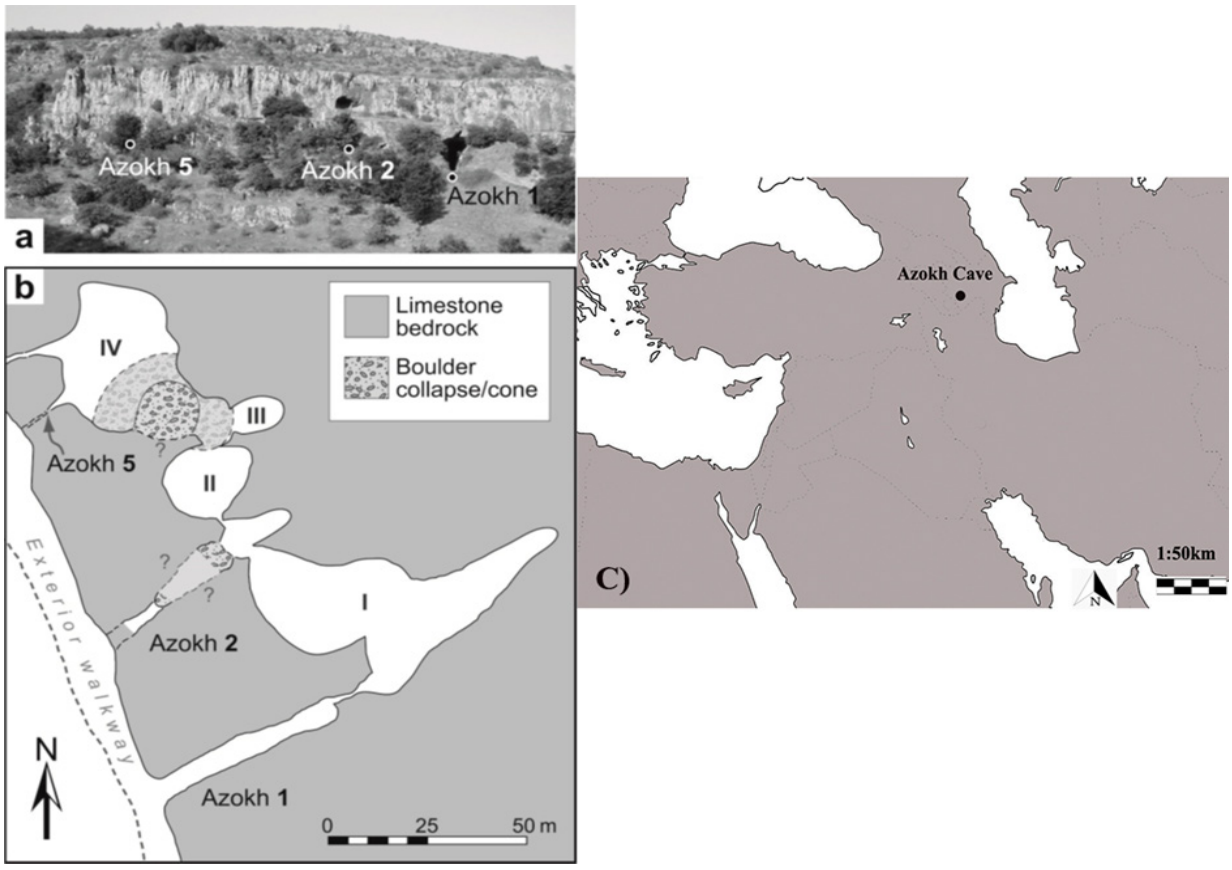


Figure 5.1. Azokh Cave system: a) View of exterior of cave system, showing three main entrance passages (Azokh 1, 2 and 5); b) Plan of Azokh Cave showing the main entrances and internal galleries (Murray et al., 2010); c) Location of Azokh Cave

the collaboration of an interdisciplinary research team. The work focused primarily on the undisturbed, complete sequence of deposits in upper levels (I-V) at the back of the cave. Systematic recovery and detailed recording of the material, with application of new methodologies, provide a high quality information regarding the site formation, human behaviour and evolution (Asryan, 2015).

1.1.1. Chronology and previous studies carried out in Azokh 1 cave.

In Azokh 1, nine stratigraphic units have been identified, actually separated in two sediment sequences, which can no longer be readily correlated due to removal of all of the intervening stratigraphy (Figure 5.2) (Murray et al., 2010):

- Sediment sequence 1: contains Units IX to VI. The test-trench excavation carried out has shown that this sequence has not recorded, so far, archaeological material. The exact age of Sediment sequence 1 still remains unclear, however, previous paleomagnetic results suggest that it is probably older than the upper units and may be of Early Pleistocene age.
- Sediment sequence 2: contains Units V to I. The new excavations are focused in this units; all of them present archaeological record with an age range from the Middle (MIS 9-8) to the Late Pleistocene (MIS 5) (Unit V to II) with some Holocene sediments at the top (Unit I) (Asryan, 2015;

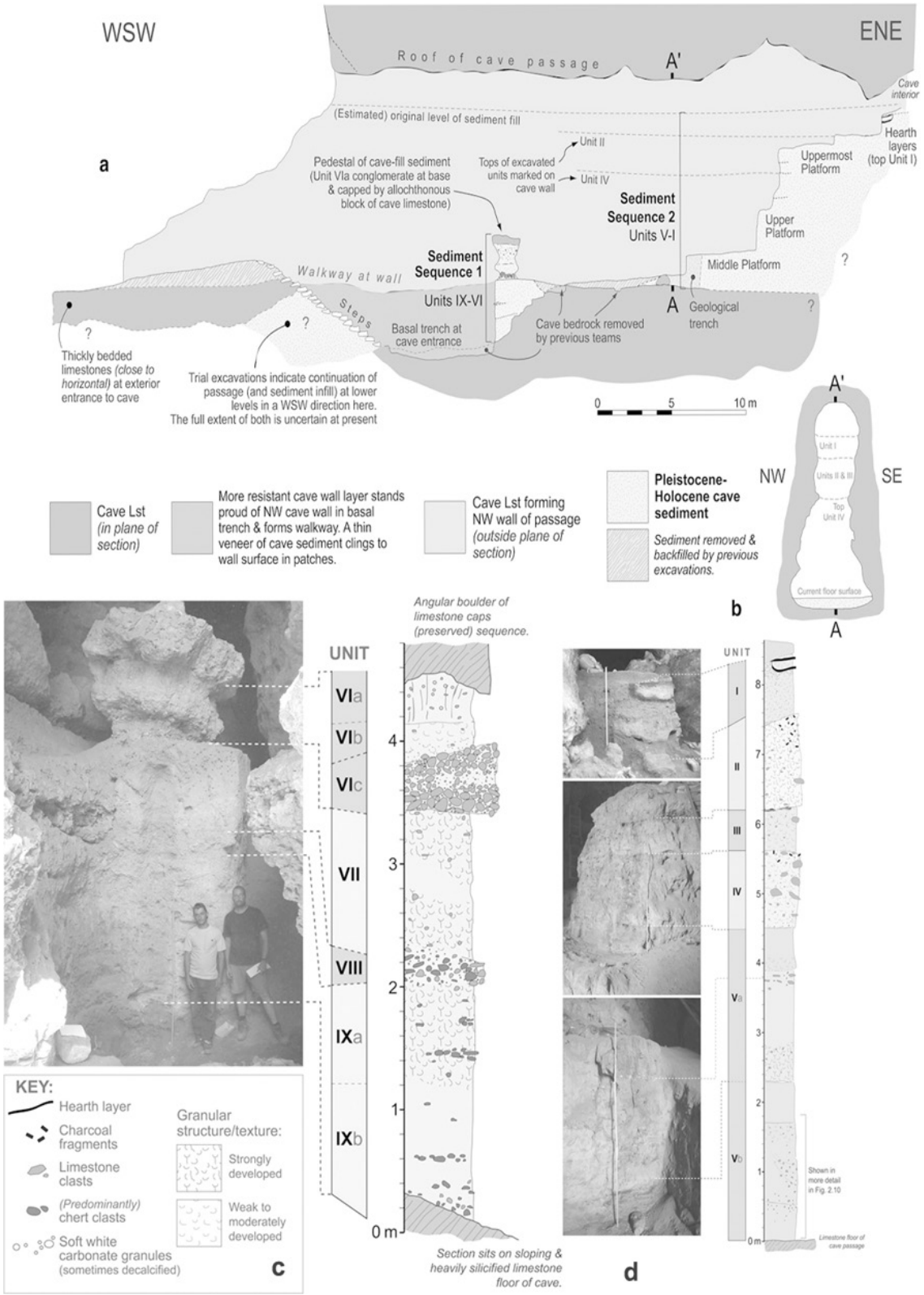


Figure 5.2. Stratigraphy of Azokh 1: a) Cross section through the entrance passage (facing NW) showing the extent of the cave sediments remaining in the chamber. These are physically separated and are labelled Sediment Sequence 1 and 2. The undated Sequence 1 includes Units VI to IX. The archaeological Sequence w (inside the rectangle) includes Units I to V; b) Cross section (orthogonal to the section shown in (a)) of Azokh 1 showing the keyhole shape of the passage; c) Stratigraphy of Sediment Sequence 1; d) Stratigraphy of Sediment Sequence 2 with dating results of archaeological units (photos modified from Murray et al., 2016)

Asryan et al., 2020, 2017; Fernández-Jalvo, 2016a; Fernández-Jalvo et al., 2010; Murray et al., 2010).

1.1.1.1.Unit V.

Unit V is located at the base of the sequence and it is the largest unit, having a thickness of approximately 4.5 m. It is divided into two subunits: Vb (located at the base) and Va (above Vb). Uranium series dating indicated an age of ca. 200 ka, racemisation (D/LAsp) indicated an age closer to ca. 300 ka and ESR dating suggested an age of 293 ± 23 ka (Murray et al., 2016). For the present study, we decided to simply refer as Unit V without considering the subdivisions, notably because these latter may be subject to further revision (Murray et al., 2016).

According to Asryan et al. (2020) lithic artefacts from this unit include a relative high presence of retouched flakes and flak fragments, as well as a few cores. There are no unknapped cobbles/pebbles or large tools (bifaces, choppers, chopping tools). Characteristics of Unit V lithic assemblage indicate that most artefacts on all raw materials were introduced as ready-made tools; however, the presence of a refit set may point to some isolated *in situ* knapping. The techno-typological characteristics and chronology (~300 ka) of Unit V shares similarities with the *Acheulo-Yabrudian* techno-culture of the Levant and the *Kudaro-Acheulean* techno-culture of the Caucasus. From a broader perspective, this assemblage is Late Acheulean or pre-Mousterian without large cutting tools.

In 1968, a fragment of hominin mandible was discovered in Unit V (King et al., 2016). It is a right mandible consisting of the posterior portion of the body and inferior part of the ramus. The study carried out by Kasimova (2001) suggests that the mandible belong to a female aged 20-25 years. This specimen has been assigned to *Homo heidelbergensis*, based on the primitive features (relief of the mylohyoid line) present on it (King et al. 2016).

Following Van der Made (2016), Unit V is mainly composed of the following large mammals: carnivores (*Canis aureus, Crocuta crocuta, Lynx sp. Felis chaus, Panthera pardus, Ursus spelaeus*), artiodactyla (*Cervus elaphus, Capra aegagrus*) and perissodactyla (*Stephanorhinus hemitoechus, Stephanorhinus kirchbergensis, Equus hydruntinus, Equus ferus*). The faunal spectrum, mainly composed of "interglacial" species; however, during glacial times, the altitude of Azokh Cave (926 m above sea level) would result depicts a harsh environment surrounding the cave (Van Der Made et al., 2016) .

Taking into account the herpetofauna of Azokh 1 published by Blain (2016), the Unit V is composed of amphibians (*Pseudepidalea viridis sensu lato*, Ranidae/Hylidae indet. and *Pelobates* cf. *syriacus*) and squamates (*Pseudopus apodus, Lacerta* sp., *Eryx jaculus,* cf. *Coronella austriaca,* cf. *Elaphe* sp., cf. *Coluber* sp. and "Colubrinae" indet.). The herpetofauna seems to be more consistent with a meadow-steppe environment, indicated by species such as *Pelobates syriacus* and the small vipers.

Bats study carried out by Sevilla (2016), shows an assemblage characteristic of an open-ground landscape with steppe vegetation in Unit V, mainly by the presence of *Myotis blythii* and the genus *Rhinolophus* spp. Rodents remains were studied by Parfitt (2016) and the results will be compared with the new study in the discussion (see discussion section 3.3 for more details).

Allué (2016) identified a low number of charcoal remains in this Unit V, attributed to three taxa only: *Prunus*, *Maloideae*, and deciduous *Quercus* sp. These taxa reflect mild

and humid environmental conditions.

1.1.1.2 Unit IV

The contact between the top of the Unit V and the overlying Unit IV is of 100-130 cm thick but diffuse and irregular. No systematic excavations were carried out in this unit, although bone and charcoals were recovered from the test-trench. ESR dating indicates an age of 205 ± 16 ka for the contact between units IV and V (Fernández-Jalvo, 2016a).

1.1.1.3. Unit III

The transition between Unit IV and III is marked by a change in the colour of the matrix. This unit is approximately 60 cm thick and contains charcoals, fossil bones and a few stone tools. No date is available for the Unit III.

The faunal list identified by Van der Made (2016) from Unit III is composed of carnivores (*Panthera pardus, Ursus spelaeus*), artiodactyla (*Cervus elaphus*, *Capra aegagrus*, *Stephanorhinus hemitoechus* and *Sus scrofa)* and perissodactyla *(Equus hydruntinus*). Unit III can be considered practically sterile in bat fossils (Sevilla, 2016). Blain (2016) recognized several squamates: *Lacerta* sp., *Eryx jaculus, Coluber* sp. and *Vipera* sp. Rodents remains were studied by Parfitt (2016), and his results will be commented in the discussion (section 3.3)

The material of this unit it is not abundant enough to perform climatic inferences.

1.1.1.4. Unit II

Unit II is 100–200 cm thick and includes fossil fauna and stone tools. Sediment diagenesis most likely caused by bat guano has strongly affected the preservation of fossil bones and some stone artefacts in this Unit. ESR dating indicates an age of 184 ± 13 ka for the bottom of the Unit II and 100 ± 7 ka for the contact between Units I and II (Fernández-Jalvo, 2016a).

Lithic artifacts were studied by Asryan et al. (2015, 2020), showing that the operative chain of different raw materials is based primarily on knapping products, including flakes, flake fragments and broken flakes. Levallois technology clearly dominates the core assemblage and knapping products. The small size of most cores and further retouch of some indicate maximum exploitation and use of good-quality, non-local raw materials. These characteristics imply almost all artefacts entered this area of Unit II as ready-made tools, with most presenting a clearly predetermined character. There may have been some *in situ* knapping and retouching activities, as suggested by the presence of knapping wastes.

In August 2010, during the excavations, an isolated hominin tooth was discovered in this Unit and studied by King et al. (2016). It was identified as an upper left first permanent molar that showed typical features of *Homo neanderthalensis*, on the basis of morphology (swollen hypocone and skewed shape) and taurodontism, as well as crown dimensions and root robusticity.

The large mammals list (Van der Made, 2016) is composed of carnivores (*Panthera pardus, Ursus spelaeus, Ursus* sp., *Vulpes vulpes* and *Canis lupus*), artiodactyla (*Cervus elaphus*, *Capra aegagrus*, *Saiga tatarica*, *Dama* sp. and *Sus scrofa)* and perissodactyla (*Stephanorhinus kirchbergensis*). The faunal spectrum suggests that this unit was characterized by a typical "interglacial" temperate environment.

Unit II has slightly more bat fossils remains than Unit III (Sevilla, 2016). Bat representation in Unit II shows a low diversity and hints at change towards colder conditions compared to Unit V, indicated notably by the presence of *Myotis mystacinus* and the absence of *Rinolophus meheyi* (Sevilla, 2016).

According to Blain (2016), the fossil

herpetofauna from Unit II is composed of amphibians (*Pseudepidalea viridis sensu lato*, *Pelobates* cf. *syriacus*) and squamates (*Pseudopus apodus, Lacerta* sp., *Ophisops elegans, Eryx jaculus,* cf. *Coronella austriaca,* cf. *Elaphe* sp., cf. *Coluber* sp., *Vipera berus* complex and *Vipera* sp. This assemblage would represent a drier period, with the presence of a representative of the *V. berus* complex (probably *V. ursinii*) and the small colubrine *Coronella austriaca*. Rodents study was carried out by Parfitt (2016), see discussion (section 3.3).

Taking into account the study carried out by Allué (2016), charcoal´s remains from Unit II show a wide diversity of taxa with: *Prunus*, *Acer*, *Quercus* sp., Maloideae, *Lonicera*, *Paliurus/Ziziphus*, *Celtis/Zelkova*, *Euonymus* and Ulmaceae. This assemblage composition indicates mild and humid environmental conditions.

1.1.1.5. Unit I

Unit I is 80–135 cm thick. This unit present a considerable disturbance and reworking of the sediments by recent mammal burrowing activity. Palaeolithic faunal and lithic remains were recovered from these burrows together with modern artefacts. Unit I has evidenced the presence of domestic animals (*Sus scrofa, Equus asinus, Equus caballus, Capra hircus*) and is considered to be of Holocene age (Van der Made, 2016). The amphibians (*Pseudepidalea viridis sensu lato*) and squamates (Agamidae indet., *Pseudopus apodus, Lacerta* sp., *Ophisops elegans,* Lacertidae indet., *Eryx jaculus,* cf. *Coronella austriaca,* cf. *Elaphe* sp., cf. *Coluber* sp., *Vipera* sp.) present in this unit indicate an environment corresponding to an arid mountain steppe (Blain, 2016).

The large-scale bioturbation has greatly complicated the internal stratigraphic details. Charcoal from the fumier in Unit I provided a radiocarbon age of 157 ± 26 years BP (OxAC^{14}19424). A Russian coin, from around the mid-1960´s, was also found in 2006, arguing in favour of high bioturbation in this level (Fernández-Jalvo, 2016a). Consequently, palaeoenvironmental interpretations have to be considered with caution.

In summary, Azokh Cave is an important site for several reasons: 1) it is located on the way of the migration route through the Caucasus used by hominins and fauna at the crossroads between Africa, Europe and Asia; 2) the site was occupied by three hominin species (documented by human remains and lithic artifacts): *H. heidelbergensis* (Azokh 1 Unit V) (Fernández-Jalvo et al., 2010), *H. neanderthalensis* (Azokh-1 Unit II) and *H. sapiens* (Azokh 2 and 5) (Fernández-Jalvo, 2016a), 3) it is a well-studied site through a multidisciplinary approach including the study of lithic assemblages (Asryan, 2015; Asryan et al., 2020, 2017,20) as well as geology, geomorphology, taphonomy, zooarchaeology, palaeontology and anthracology (Fernández-Jalvo, 2016a).

The aim of this study is to investigate the palaeoenvironmental and the paleoclimatic conditions during the formation of Azokh 1 Cave, and compare our results with the sites located near our region. No taphonomic analysis was yet performed on rodent assemblages. So before any palaeoecological study we had to identify the origin of the accumulation and its potential influence on palaeoecological results.

2. Material and methods

Rodent´s remains used in this study come from the archaeological excavation campaigns carried out in Azokh 1 in 2003, 2005, 2014, 2015 and 2018. It comes from the Sediment sequence 2: Unit V, Unit III-IV and Unit II.

The samples comprise disarticulated bones and isolated teeth that were collected in the field by water screening using

superimposed 5 and 0.5 -mm mesh screens. Most of the samples were sieved in the field by the excavation team and the resulting residues were air-dried and sorted in the site laboratory. In subsequent years, the small vertebrate bones were picked by hand and under microscope. The material was identified with a binocular microscope and photos were taken with a Dino-Lite (model AM7915MZTL). In total, 855 samples were analysed: 251 from Unit V, 10 from Unit III-IV and 594 from Unit II. The material is hosted at Azokh Village, in the project house.

2.1.Taxonomy

We focused on rodents, because they can be considered as one of the most useful tools for palaeoenvironmental and palaeoclimatic reconstructions in archaeological sites (e.g. López-García et al., 2010; Maul et al., 2015a). The taxonomic identification of the rodent remains is based mainly on molar morphology and measurements (Rey-Rodríguez et al., 2020). We focused especially on lower m1 (the most discriminant) for Arvicolinae; mandibles and maxillae were used for taxonomic identifications of Cricetidae, Gerbillinae and Murinae.

The remains were identified at a specific level whenever possible. We used specimens from the modern reference collections of the Natural History Museum of London, the Field Museum of Chicago and the American Museum of Natural History of New York. We also used comparative morphological and biometric data from the literature, notably for *Microtus* (Coşkun, 2016; Kryštufek & Shenbrot, 2016; Kryštufek and Vohralík, 2009; López-García, 2008; Rusin, 2017; Shenbrot, Kryštufek & Molur, 2016; Tesakov, 2016), *Clethrionomy*s (Kryštufek et al., 2009; 2020), *Chionomys* (Krystufek, 2017; Kryštufek and Vohralík, 2009; López-García, 2011), *Cricetulus* (Bogicevic et al., 2011; Kryštufek et al., 2017; Sándor, 2018), *Mesocricetus* (Kryštufek and Vohralík, 2009), *Meriones* (Coşkun, 1999; Darvish, 2011; Dianat et al., 2017; Kryštufek and Vohralík, 2009; Souttou and Denys, 2012; Stoetzel et al., 2017a), *Allactaga* (Karami et al., 2008; Shenbrot, 2009) and *Apodemus* (Amori et al., 2016; Bogicevic et al., 2011; Knitlová and Horáček, 2017; Kryštufek and Vohralík, 2009; López-García, 2008).

For the genus *Ellobius,* we based our identifications on data from the literature (Gharkheloo, 2003; Kryštufek and Vohralík, 2009; Tesakov, 2016), and also we applied geometric morphometric methods (GMM) in order to detect morphological differences and variations in shape and size, following Rey-Rodríguez et al. (2021). The *Ellobius* first lower molars were all photographed under constant conditions with a digital camera in occlusal view. To investigate the first lower molar size and shape we combined 2D landmarks (LM) and semi-landmarks (SLM) on the photographs using TPSdig2 v.2.32 software package (Rolf, 2016) for two-dimensional geometric morphometric analyses. All the analyses were performed with R (R Core Team, 2020) using the geomorph (Adams et al., 2020) and Morpho (Schlager, 2017) packages.

For the genus *Arvicola,* we used the molar morphology (Maul et al., 2020) as well as the enamel differentiation thickness index, also named SDQ (Schmelzband-Differenzierung-Quotient) developed by Heinrich (1978). The enamel differentiation index was calculated following the formula:

$$SDQ = [\Sigma(teet \times 100/leet)]/N$$

teet: Posterior part of the triangle

leet: distal part of the triangle

N: number of triangles

where N refers to the number of dentine fields of the studied tooth, teet (trailing edge enamel thickness) refers to the maximum thickness of the posterior enamel band, and

leet (leading edge enamel thickness) refers to the maximum thickness of the anterior enamel band of each dentine field (Heinrich, 1978; Lozano-Fernândez et al., 2013).

We also used the standard measurements of the total length (L) and total width (w) of the molars in order to identify some species, particularly among the *Cricetulus* and *Mesocricetus* genera.

Quantification of taxonomic frequencies was based on standard indices used in zooarchaeological analyses, including the number of identified specimens (NISP) and minimum number of individuals (MNI) (Weissbrod and Zaidner, 2014). This latter was estimated using the most abundant skeletal element present in the assemblage (molars in our case).

2.2. Taphonomy

A preliminary study was performed on the Azokh 1 Cave rodent remains. It was based on the systematic descriptive method that examines the modifications of prey bones induced by predation, focusing on the degree of digestion observed in teeth during the identification (Andrews, 1990; Fernández-Jalvo et al., 2016c). Predation is closely related to ecology for two main reasons that are the density dependence of prey according to population fluctuations and the trophic preferences of the predator. So, the identification of the predator(s) helps to better identify the nature and origin of the assemblage. It is necessary to take into account these factors for the palaeoecological interpretations based on small mammals accumulations (Fernandez-Jalvo and Andrews, 2016c).

We performed a preliminary study focusing on a subsample composed of 100 incisors and 90 molars per unit, for Unit V and Unit II only, to look at the digestion intensity and broadly define the predator's category of modification.

2.3. Palaeoenvironmental and palaeoclimatic reconstructions

2.3.1. Habitat weighting method

Palaeoecological interpretations derived from faunal data are based on analyses of community composition (Belmaker and Hovers, 2011). The method used for the palaeoenvironmental reconstruction is the habitat weighting method (Evans et al., 1981; Andrews, 2006; modified by Blain et al., 2008; López-García et al., 2011), which is based on the current distribution of each taxon in the habitat(s) where it can be found nowadays. We adapted the method to our studied area (Rey-Rodríguez et al., 2020), in assuming that the Azokh 1 Cave species had equivalent ecological requirements to their present-day relatives.

We consider the following types of habitats: Forest (Fo), a large area covered with trees; Shrubland (Sh), vegetation dominated by shrubs; Grassland (Gr), an open area covered with grass; Desert (De), an area with little precipitation and no vegetation cover; Wetland (We), an area where water covers the soil; Steppe (St), a dry grassy plain; and Rocky (Ro), a rocky or stony substrate. Each species has a score of 1.00, which is divided between the habitats where the species can be found at present (Table 5.1).

2.3.2. Bioclimatic Model

In order to reconstruct the past climate at Azokh 1 Cave, we applied the bioclimatic model (BM), which was developed by Hernández-Fernández (2001) and updated by Royer et al. (2020). This method is based on the faunal spectrum, assuming that small- and large-mammal species can be ascribed to ten different climates (Hernández-Fernández, 2001; Hernández-Fernández & Peláez-Campomanes, 2003; Hernández-Fernández et al., 2007). It was first necessary to calculate

Species	Fo	Sh	Gr	De	We	St	Ro
Clethrionomys glareolus	0.5	0.5					
Ellobius lutescens			0.33	0.33		0.33	
Microtus arvalis/socialis		0.33	0.33			0.33	
Arvicola persicus					1		1
Chionomys gud							1
Chionomys nivalis			0.33	0.33		0.33	
Cricetulus migratorius						1	
Mesocricetus brandti		0.33		0.33		0.33	
Meriones dahli		0.33		0.33		0.33	
Meriones tristrami		0.5		0.5			
Meriones libycus		0.33	0.33			0.33	
Meriones persicus			0.5			0.5	
Allactaga willamsi	0.5					0.5	
Apodemus spp.	0.5	0.5					

Table 5.1. Scores attributed to each rodent species found at Azokh 1 Cave according to its ecological requirements, used for the habitat weighting method: Forest (Fo), Shrubland (Sh), Grassland (Gr), Desert (De), Wetland (We), Steppe (St) and Rocky (Ro).

the climatic restriction index (CRIi=1/n, where i is the climatic zone where the species appear and n is the number of zones where the species is present) and the bioclimatic component (BCi = (Σ CRIi) 100/S, where i is the climatic zone and S is the number of species). All statistical analyses were performed using the R software package (R Core Team, 2020) using the script PalBER developed by Royer et al. (2020) in order to calculate the bioclimatic spectra and to infer the climatic zone.

The different climatic groups defined by Hernández-Fernández (2001) and Hernández-Fernández et al. (2007) present in this work are: II/III transition tropical semiarid; III subtropical arid; IV, subtropical with winter rains and summer droughts; VI, typical temperate with winters that are cold but not very long, but summers that are cool; VII, arid-temperate with large temperature contrasts between winter and summer; VIII, cold-temperate with cool summers and long cold winters (boreal) and IX, artic (Table 5.2).

By means of the BM we were able to estimate different climatic parameter, such as the mean annual temperature (MAT), the mean temperature of the coldest month (MTC), the mean temperature of the warmest month (MTW) and the mean annual precipitation (MAP). This method allowed us to infer the palaeoclimatic conditions during the Middle and Late Pleistocene at Azokh 1 Cave.

3. Results and discussion

3.1. Systematics, current distribution and ecology

A total of 434 molars were identified following the keys of systematic identifications, representing a minimum number of 237 individuals (MNI) (Table 5.3). This sample comprises the new remains coming from the 2003, 2005, 2014, 2015 and 2018 excavation campaigns, the previous material have being analysed by Parfitt (2016).

Species	II/III	III	IV	VI	VII	VIII	IX
Clethrionomys glareolus	0	0	0	0.333	0	0.333	0.333
Ellobius lutescens	0	0	0.5	0	0.5	0	0
Arvicola persicus	0	0	0.25	0.25	0.25	0.25	0
Microtus arvalis	0	0	0	0.5	0	0.5	0
Microtus socialis	0	0	0.5	0	0.5	0	0
Chionomys gud	0	0	0.333	0.333	0	0.333	0
Chionomys nivalis	0	0	0.333	0.333	0	0.333	0
Cricetulus migratorius	0	0	0.333	0.333	0.333	0	0
Mesocricetus brandti	0	0	1	0	0	0	0
Meriones libycus	0	0.5	0.5	0	0	0	0
Meriones tristrami	0	0	0.333	0.333	0	0.333	0
Meriones persicus	0	0.5	0.5	0	0	0	0
Allactaga williamsi	0.333	0	0.333	0	0.333	0	0
Apodemus spp.	0	0	0.333	0.333	0	0.333	0

Table 5.2. Scores attributed to each rodent species found at Azokh 1 Cave for the bioclimatic model (in accordance with Hernández-Fernández, 2001; Hernández-Fernández et al., 2007, updated by Royer et al., 2020). See text for the significance of the Roman numerals corresponding to the climatic groups.

Order Rodentia Bowdich, 1821

Family Cricetidae Fischer, 1817

Genus *Cricetulus* Milne-Edwards, 1867

***Cricetulus migratorius* Pallas. 1773**

Material: 10 isolated teeth. **Unit II**: eight isolated teeth, one Left lower m1, two right lower m1, one right upper M1, one left upper M1, one right upper M2 and two left upper M2. **Unit V:** two isolated teeth, one Left lower m1 and one right maxillae with and M1 and M2.

Description and discussion: the first molars (m1 and M1) are brachyodont and cuspidate, with two longitudinal series of cusps. Each series of cusps consists of three pairs. The m1 and M1 are the largest and the m3/M3 the smallest. The lower m3 only has two pairs of cusps (Kryštufek and Vohralík, 2009). We identify *Cricetulus migratorius* (Figure 5.3.1) in Unit II and Unit V of Azokh 1 Cave in accordance with the measurements (Table 5.4) and identification keys for molars based on the morphology and arrangement of the tubercles and cusps provided by Kryštufek and Vohralík (2009). We also draw comparisons with the reference collection from Iran, Afghanistan and Azerbaijan housed in the Natural History Museum of London regarding the morphology of the teeth. The grey hamster, or migratory hamster, is the smallest hamster species (Bogicevic et al., 2011; Sándor, 2018), we measure the teeth and the obtained results indicate that our specimens has the same size as the ones from the reference collection, excluding the posibility of being *Allocricetus* (Parfitt, 2016).

Habitat and distribution: *Cricetulus migratorius* extends from eastern Europe

Cricetulus migratorius			
		Azokh 1, NISP:4	**NHM, NISP:16**
L	**Min-Max**	1.4-1.81	1.41-176
	Mean	1.56	1.57
W	**Min-Max**	0.58-0.77	0.74-0.95
	Mean	0.68	0.85

Table 5. 4. Measurements of *Cricetulus migratorius* first lower molar, m1, (in mm): L, total length; W, width. NHM: Natural History Museum of London. NISP: number of identified specimens

Taxa	Unit V			Unit III-IV			Unit II		
	NISP	MNI	%	NISP	MNI	%	NISP	MNI	%
Cricetulus sp.	4	4	3.48				6	2	1.74
Cricetulus migratorius	2	1	0.87				8	2	1.74
Mesocricetus brandti	6	3	2.61				5	3	2.61
Clethrionomys glareolus	-	-	-	-	-	-	4	3	2.61
Arvicola ex. gr. *persicus*	-	-	-				1	1	0.87
Chionomys gud	3	2	1.74						
Chionomys nivalis	-	-	-				4	3	2.61
Microtus gr. *arvalis-socialis*	154	77	66.96	7	5	71.43	135	75	65.22
Microtus (Terricola) spp.	13	7	6.09	1	1	14.29	7	4	3.48
Ellobius lutescens	13	7	6.09	1	1	14.29	22	12	10.43
Meriones spp.	5	3	2.61				4	2	1.74
Meriones gr. *dahli-libycus*	4	3	2.61				1	1	0.87
Meriones gr. *persicus-tristrami*	6	3	2.61				2	2	1.74
Apodemus sp.	3	2	1.74				7	4	3.48
Allactaga sp.	2	2	1.74						
Allactaga cf. *williamsi*	2	1	0.87				2	1	0.87
Total	**217**	**115**	**100**	**9**	**7**	**100**	**208**	**115**	**100**

Table 5.3. Representation of the Azokh 1 Cave rodent species in terms of number of identified specimens (NISP), minimum number of individuals (MNI) and percentage of the MNI (%).

through Russia and central Asia to Mongolia and western China (Kryštufek et al., 2017; Kryštufek and Vohralík, 2009). The habitats of this species are mostly dry grasslands, steppes and semi-deserts. Arid areas with relatively sparse vegetation are preferred (Kryštufek et al., 2017; Maul et al., 2015a).

***Cricetulus* sp.**

Material: 10 isolated teeth. **Unit II:** six isolated teeth, two left lower m1, two right lower m2 and two left lower m2. **Unit V:** four isolated teeth, two left lower m1, one right lower m1 and one left lower m2.

In our record we recognized as *Cricetulus* sp. broken teeth that could not be identified at the species level.

Genus *Mesocricetus* Nehring, 1898

***Mesocricetus* cf. *brandti* Nehring, 1898**

Material: 11 isolated teeth. **Unit II:** five isolated teeth, one left lower mandible with and m1 and m2, one left lower m1, three left upper M2 and one left upper M3. **Unit V:** six isolated teeth, one right lower m1, one left upper M1, three left upper M2 and one right upper maxillae with and M1 and M2.

Description and discussion: the specimens from Azokh 1 Cave are attributed to *Mesocricetus brandti* (Figure 5.3.2) on the basis of the morphology of the teeth, the disposition of the cusps and the size. The molars present a similar morphological pattern to *Cricetulus migratorius*, but are significantly larger in size. On the other hand, they are smaller than representatives of the *Cricetus* genus. The first molars have six tubercles, the second and third molars only four. The largest molars are m1 and M1, whereas m2/M2 and m3/M3 are reduced (Kryštufek and Vohralík, 2009). In Azokh region we also find *Mesocricetus raddei*, which

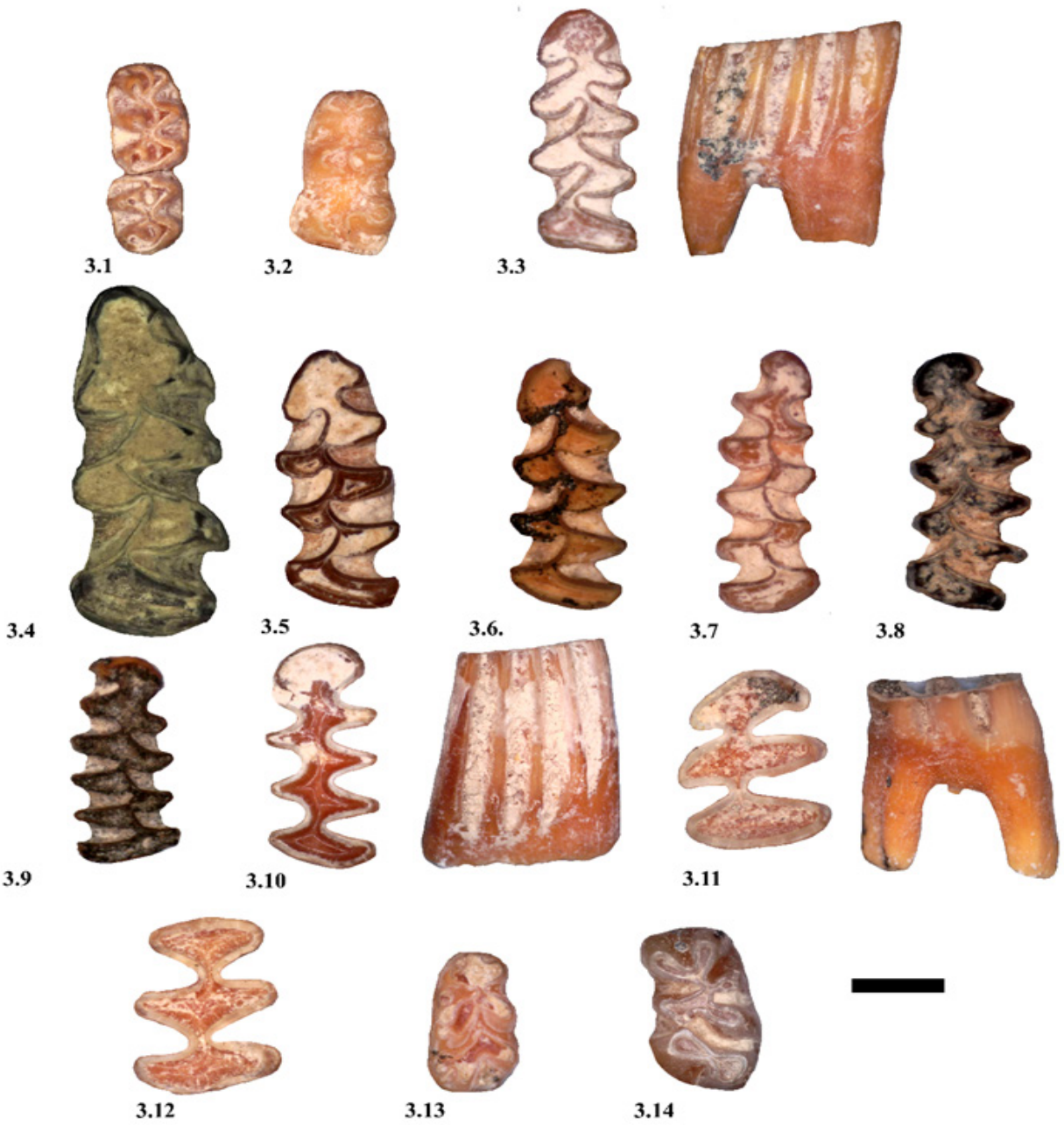


Figure 5.3. Some rodents identified at Azokh 1 Cave. 3.1- *Cricetulus migratorius*, Azokh 1 Cave, 2003, Unit V, D45, Z: 224, right M1 and M2, number 221. 3.2- *Mesocricetus brandti*, Azokh 1 Cave, 2014, Unit II, E49, Z: 320-330, left m1 and m2, number 74. 3.3- *Clethrionomys glareolus*, Azokh 1 Cave, 2018, Unit II, G56, Z: 46.48, left m1 occlusal and lingual view, number 703. 3.4- *Arvicola* ex. gr. *persicus*, Azokh 1 Cave, 2014, Unit II, G51, Z: 330-340, left m1, number 536. 3.5-*Chionomys gud*, Azokh 1 Cave, 2003, Unit V, D46, Z: 111, left m1, number 349. 3.6- *Chionomys nivalis*, Azokh 1 Cave, 2014, Unit II, F48, Z: 330-340, left m1,number 529. 3.7- *Microtus* gr. *arvalis-socialis*, Azokh 1 Cave, 2014, Unit II, G53,Z: 330-340, right m1, number 5. 3.8- *Microtus (Terricola)* spp., Azokh 1 Cave, 2005, Unit V, E40, Z: 136, left m1, number 43. 3.9- *Microtus (Terricola)* spp., Azokh 1 Cave, 2005, Unit V, D45, right m1, number 170. 3.10-*Ellobius lutescens*, Azokh 1 Cave, 2015, Unit II, F51, Z: 320-330, left m1 occlusal and lingual view, number 226. 3.11- *Meriones* gr. *persicus- tristrami*, Azokh 1 Cave,2003, Unit V, D45, right m1 occlusal and lingual view, number 169. 3.12- *Meriones* gr. *dahli-libycus*, Azokh 1 Cave,2003, Unit V, D45, Z: 224, left M1, number 222. 3.13- *Apodemus (sylvaemus)* sp., Azokh 1 Cave, 2014, F52, Z: 330-340, left m1, number 80. 3.14- *Allactaga* cf. *williamsi*, Azokh 1 Cave, 2018, H49, G50, right m1, number 635. Scale 1mm.

presents a similar morphology of the teeth to *Mesocricetus brandti*, but compared with the NHM reference collection of the latter, *Mesocricetus raddei* is bigger (Table 5.5).

Habitat and distribution: *Mesocricetus brandti* has the largest distributional area of the species belonging to the genus *Mesocricetus*, ranging from Anatolia, Transcaucasia, and southeast Dagestan to northwest Iran (Qazvin in the east, Lorestan in the south; Lay, 1967). This species is found at altitudes from sea level up to 2.600 m. However, the primary range is from 1.000-2.200 m. *Mesocricetus brandti* is found in arid and semi-arid steppe habitats in lowlands and in mountainous areas (Kryštufek et al., 2015; Kryštufek and Vohralík, 2009; Neumann et al. , 2017).

Subfamily Arvicolinae Gray, 1821

Genus *Clethrionomys* Tilesius, 1850

***Clethrionomys glareolus* Schreber, 1780**

Material: four isolated teeth. **Unit II**: one right lower m1 and three left lower m1.

Description and discussion: In our sample we identified *Clethrionomys glareolus* (Figure 5.3.3) (Kryštufek et al., 2020). In our study region there are only two genera of Arvicolinae with rooted molars: *Clethrionomys* and *Ellobius*, and they can be easily differentiated from their molar morphology. In *Clethrionomys* the m1 displays two roots; five triangles with a highly variable anteroconid complex, however T4-T5 does not variate. T5 is integrated into the anterior cap or more rarely entirely isolated from it; the anterior cap is rarely simple and oval but mostly broadly confluent with T5. There are three or four re-entrant angles on the inner side and three on the outer one (Kryštufek & Vohralík, 2005).

Habitat and distribution: The bank vole (*Clethrionomys glareolus*) is widely distributed in the Palaearctic area which stretches from the British Isles through continental Europe and Russia to Lake Baikal. It was present at Azokh 1 Cave in the past, however this species does not exist anymore in the study region today.

Regarding its habitat, it is present in all kinds of woodland, preferring densely-vegetated clearings, woodland edge and river and stream banks in forest. We can also found it in scrub, parkland and hedges (Bergl et al., 2017).

***Arvicola* ex. gr. *persicus* de Filippi , 1865**

Material: one isolated tooth. **Unit II**: one left lower m1.

Description and discussion: recent works have shown that the Iranian phylogroup of water voles can be considered

		Mesocricetus brandti		***Mesocricetus raddei***
		Azokh 1, NISP:3	**NHM, NISP:7**	**NHM, NISP:4**
L	**Min-Max**	2.14-2.19	2-2.28	2.39-2.58
	Mean	2.17	2.14	2.52
W	**Min-Max**	1-1.07	1.02-1.2	1.3-1.11
	Mean	1.03	1.1	1.23

Table 5.5. Measurements of *Mesocricetus brandti* and *Mesocricetus raddei* first lower molar, m1, (in mm): L, total length; W, width. NHM: Natural History Museum of London. NISP: number of identified specimens.

as a valid species, named *Arvicola persicus* (Figure 5.3.4) (Chevret et al., 2020; Mahmoudi et al., 2020). We chose to follow Maul et al. (2020) and to use the name *Arvicola* ex. gr. *persicus* according to the describe characters. In our material, only one m1 could have been attributed to the genus *Arvicola* based on its size and morphology.

The m1 is rootless with a clear *Mimomys*-type enamel differentiation and crown cementum filling the re-entrant angle. The m1 consist of an anterior cap (AC), five triangles (T) and a posterior lobe (PL). Enamel thickness (SDQ) is a parameter used on lower molar for the identification of *Arvicola* species. In our material, we could only use SDQ5 on the triangles, because the AC and the PL were digested. We obtained a value of 124, which assigns our sample to *Arvicola* ex. gr. *persicus* according to Maul et al. (2020). Also the shape of the anteroconid complex corresponds to this species, with a BRA3 not as deep as *A. nahalensis*. The *Mimomys*-type enamel differentiation exclude the possibility that it could be *A. amphibius*, the other current representative of the genus in the region (Mahmoudi et al., 2020). The SDQ values show that there is a close relation between *A. persicus* from Iran and Turkey, *A. italicus* from Italy and *A. sapidus* from Spain, because all display a SDQ value >100 (Maul et al., 2020). In our sample, *Arvicola* ex. gr *persicus* is the only possibility, considering the geographic distribution of the other taxa.

Habitat and distribution: the precise ecology and distribution of *Arvicola persicus* remain to be clarified (Mahmoudi et al., 2020). However, the group of water voles, in which our species is included, is always rather scarce in dry areas, most probably because these animals require suitable aquatic habitats, i.e., the vicinity of permanent water bodies such as rivers, streams, and marshes. We assumed that *A. persicus* has a semi-aquatic lifestyle, indicating the existence of water habitats (Harrison and Bates 1991; Maul et al., 2020; Mahmoudi et al., 2020). Nowadays there is a river named Ishkhanaget near the site at the bottom of the mountain, which may very well have existed in the past and favoured the presence of *Arvicola* around the site.

Genus *Chionomys* Miller, 1908

In our sample eight isolated teeth show the typical traits of the genus *Chionomys*. The enamel is of *Microtus* type with cement in the re-entrant angles (Krystufek, 2017; Kryštufek and Vohralík, 2005; López-García, 2011). These specimens differ from *Microtus* in that they only have five triangles, and an AC with a typical rounded morphology.

***Chionomys gud* Satunin, 1909**

Material: three isolated teeth. **Unit V**: one isolated right lower m1 and two isolated left lower m1.

Description and discussion: in Unit V we observed three m1, that mainly show four closed triangle, and the wear facets of triangles T5 and T6 are confluent with the anterior cap; typical of the Caucasian snow vole, *Chionomys gud* (Figure 5.3.5) (Kryštufek B. & Vohralík V., 2005; Sözen et al., 2009).

Habitat and distribution: *Chionomys gud* is closely associated with rocky habitats. It occurs in alpine meadows, in sparse fir and spruce forests and in valleys of brooks and small rivers. It prefers more mesic habitats than *Chionomys nivalis* (Kryštufek and Vohralík, 2005).

Chionomys gud is endemic to the Caucasus and the easternmost part of the Pontic mountains of Turkey, and is not represented today in Southern Caucasus (Kryštufek, 1999).

***Chionomys nivalis* Martins, 1842**

Material: 4 isolated teeth. **Unit II**: one right lower m1 and three left lower m1.

Description and discussion: in Unit II, four first lower molars display five closed

triangles and an anteroconid complex (AC) with a morphology characteristic of the *nivalis* morphotype (Figure 5.3.6), where triangles T6 and T7 are reduced and tightened at their base, and the anterior cap is of an arrowhead or oval shape, inclined towards the labial part (Kryštufek B. & Vohralík V., 2005; Nadachowski, 1991).

Habitat and distribution: *Chionomys nivalis* has a global distribution extending from southwestern Europe through southeastern Europe to the Caucasus. Turkey, Israel, Lebanon, Syria and Iran (Kryštufek, 1999).

Regarding the *Chionomys nivalis* habitat, it is present in open rocky areas, typically above the tree line and with scarce vegetation cover (Amori, 1999).

***Chionomys* sp.**

Material: one isolated tooth. **Unit II**: one isolated left lower m1.

We kept *Chionomys* sp. because of the lack of discriminant characters on the broken tooth.

Genus *Microtus* Schrank, 1798

The molars identified in the genus *Microtus* are hypsodont and arhizodont with crown cementum in the re-entrant angles and a *Microtus*-like enamel differentiation. Eight species of *Microtus* are currently recognized in southern Caucasus: *Microtus arvalis*, *Microtus daghestanicus*, *Microtus levis*, *Microtus majori*, *Microtus nasarovi*, *Microtus schelkovnikovi*, *Microtus schildlovskii* and *Microtus socialis* (Aşan Baydemir and Duman, 2009; Golenishchev et al., 2019; Firouz, 2005). *Microtus* m1s are characterized by four outer and five inner re-entrant angles, with a posterior lobe (PL), seven closed triangles (T) and an anterior cap (AC). In our material the triangles T4 and T5 are closed, which allow us to exclude the subgenus *Terricola*.

Microtus is the most abundant taxa in all the sequence, but species identification was difficult because we lack good reference collections and comparative data from the literature. However, we were able to differentiate two groups, based on the morphology of the lower m1.

Microtus* gr. *arvalis-socialis

Material: 296 isolated teeth. **Unit II:** 135 isolated teeth; 75 right lower m1, 60 left lower m1. **Unit II-IV:** seven isolated teeth; five left lower m1 and two right lower m1. **Unit V:** 154 isolated teeth; 77 right lower m1 and 77 left lower m1.

Description and discussion: the species (Figure 5.3.7) included in this group are: *Microtus arvalis*, *Microtus socialis* and *Microtus guentheri*. The triangles from T1 to T5 are closed and opposed between them. T6-T7 are confluent and parallel to BRA4 and LRA5 (Kryštufek and Vohralík, 2005).

Habitat and distribution: *Microtus* species belonging to the group *arvalis-socialis* mostly occur in steppe, shrubland or semi-desert habitats (Fernandez-Jalvo et al., 2016a). According to the IUCN Red List, all of them are present in the southern Caucasus nowadays.

***Microtus (Terricola)* spp.**

Material: 21 isolated teeth. **Unit II:** seven isolated teeth; three right lower m1 and four left lower m1. **Unit II-IV:** one isolated tooth; one left lower m1. **Unit V:** 13 isolated teeth; seven right lower m1 and six left lower m1.

Description and discussion: The second group is *Microtus* (*Terricola*) spp., (Figure 5.3.8 and 5.3.9) characterized by broadly confluent T4 and T5, forming the pitymian rhombus (Kryštufek and Vohralík, 2005). In our sample we identified at least two species, based on the size and the morphology of the AC. There are several *Terricola* species in the region: *Microtus daghestanicus*, *Microtus nasavori*, *Microtus majori* and *Microtus schidlovskii*. All of them are very close from their molar

morphology, and without a good reference collection it is not possible to identify them at the species level.

Habitat and distribution: Caucasian Pine voles, that belong to *Microtus (Terricola)* spp. group, are found in a quite variable range of habitats: *Microtus daghestanicus* and *Microtus nasarovi* prefer pastures, alpine meadows and steppe; *Microtus majori* favours clearings in forests and shrubland, as well as alpine pastures and *Microtus schidlovskii* is more closely associated with xerophytic steppes and meadow-steppes. All of them are present in the southern Caucasus nowadays, according to IUCN Red List.

Genus *Ellobius* Fischer, 1814

***Ellobius* cf. *lutescens* Thomas,1897**

Material: 36 isolated teeth. **Unit II:** 22 isolated teeth; 10 right lower m1 and 12 left lower m1. **Unit II-IV:** one isolated tooth; one left lower m1. **Unit V:** 13 isolated teeth; seven right lower m1 and six left lower m1.

Description and discussion: 36 isolated teeth show the typical traits of the genus *Ellobius* (Coşkun, 2016; Kryštufek & Shenbrot, 2016; Kryštufek and Vohralík, 2005; Rusin, 2017; Kryštufek & Molur, 2016; Tesakov, 2016).

The *Ellobius* lower m1 is composed of the anterior cap (AC), five triangles (T) with three buccal and four labial re-entrant angles, and one posterior lobe (PL). *Ellobius* molars are notably characterized by the presence of roots that are clearly visible in adults and old individuals. Moreover, *Ellobius* molars lack cement in the re-entrant angles (Coşkun, 2016).

For modern representatives, most of the discriminant characters are based on skull morphology (Kaya et al., 2018) we examined a total of 43 samples belonging to three *Ellobius lutescens* populations from Turkey, Iran and Nakhchivan, which are geographically separated by the Zagros, Tendürek and Alborz mountain ranges. We applied geometric morphometric methods (GMMs) and external characters (Kryštufek and Vohralík, 2005), whereas in an archaeological context we mostly rely on isolated molars or broken maxillae and mandibles. The lower m1 is quite similar among the different current *Ellobius* species (*Ellobius fuscocapillus*, *Ellobius lutescens* and *Ellobius talpinus*), but some specific morphological characters have been pointed out in previous studies: the AC is broad in *Ellobius lutescens*, narrow in *Ellobius talpinus* and elongated in *Ellobius fuscocapillus* (Maul et al., 2015b); the distance between T4 and T5 (W) and the total length (L) differ among the species, *Ellobius fuscocapillus* showing the largest teeth and *Ellobius talpinus* the smallest (Rey-Rodríguez et al., 2020). However, these morphological and biometric characters are not always clear or reliable, and the use of more powerful methods is necessary to obtain reliable identifications. For that we applied geometrics morphometric analyses on m1 molars following the methodology stablished by Rey-Rodríguez et al. (2021) for *Ellobius*. We used specimens from the modern reference collections of the Natural History Museum of London, the Field Museum of Chicago and the American Museum of Natural History of New York and the archaeological samples comes from Azokh 1 Cave (Unit II and Unit V).

The PCA performed on the normalized landmarks and sliding semi-landmarks of the right lower molar reveals significant differences among the analysed species, the first two principal components (PCs) accounting for 51.3% of the total variance (Figure 5.4a).

The main variation along the PC1 (37.7%) regards the morphology of the Anterior Cap which is more flattened for the positive values and more rounded for the negatives ones. *Ellobius talpinus* occur on the positive part of the PC1 axis while *Ellobius fuscocapillus* and

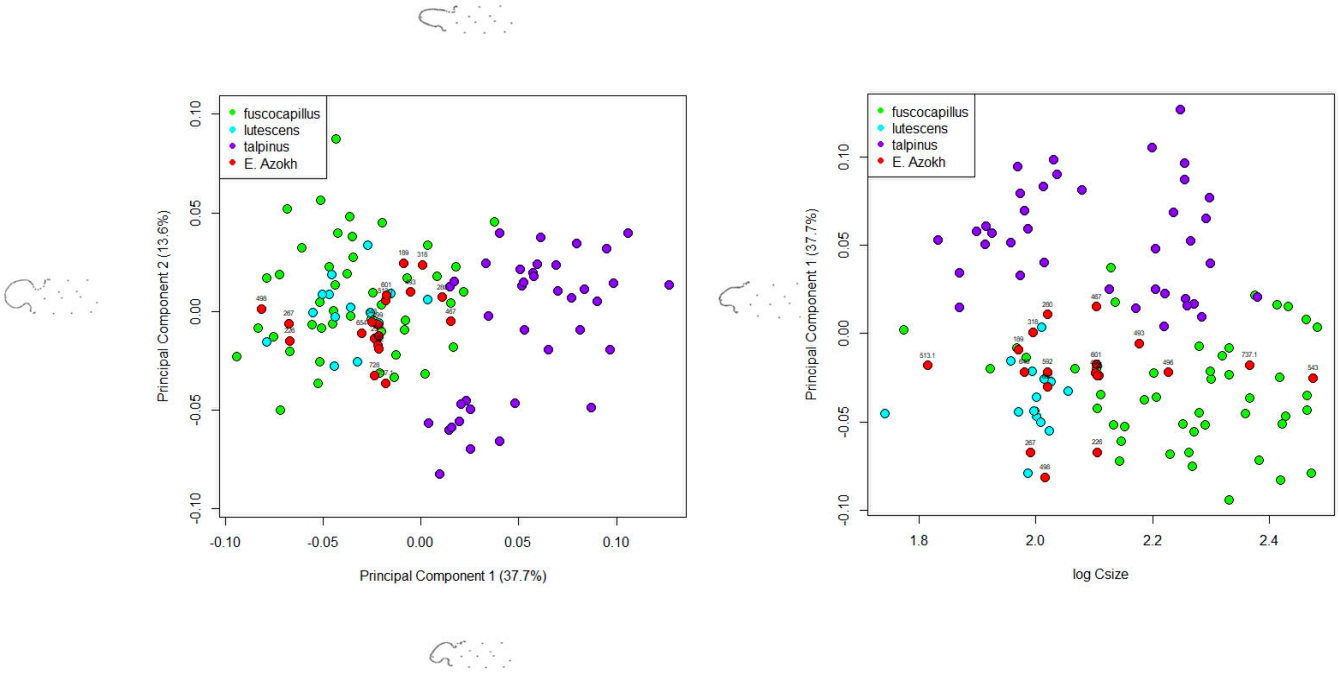


Figure 5.4. a) Principal component analysis on the normalized landmarks and sliding semilandmarks and shape configuration at the extreme ends of the PCs. b) First two principal components of size and shape including the reference collection and Azokh 1 Cave material.

Ellobius lutescens are located on the negatives ones, reflecting a broader and more rounded AC. Along the PC2 (13.6%) scores, the positive values show an elongated AC turned to the buccal side, while negative values reflect a rounded and less developed AC turned to the labial part. On PC2 there is no clear differentiation between the three species. However, it is worth noticing that *Ellobius lutescens* specimens are located principally in the upper half of the graphs, showing positive values on PC2. We can then confirm the species identifications and that *Ellobius talpinus* is not present on the archeological samples.

Looking at possible allometric effect on the samples, we performed a linear regression of the PCs onto the log of the centroid size (Mitteroecker et al., 2014). Including size allows to discriminate *E. lutescens* from *E. fuscocapillus*, the latter showing greater dimensions (Figure 5.4b). *E. talpinus* presents a wide size range overlapping the two latter, and is only discriminated by the molar conformation (PC1). The archaeological remains from Azokh 1 Cave are distributed in *E. lutescens* and *E. fuscocapillus* (Figure 5.4b).

Other criteria can allow species identifications, such as the configuration of the anterior cap (Maul et al., 2015b), with a transition between T4-T5 being narrower in *E. lutescens* than in *E. fuscocapillus*, leading to a smaller and more closed AC in *E. lutescens*. In combining GMM and PCA analyses with morphological criteria (AC and distribution of the triangles), we were able to attribute the material from Azokh 1 to the species *Ellobius lutescens* (Figure 5.3.10).

Habitat and distribution: *Ellobius* species frequent steppes, grasslands and semi-deserts in eastern Europe and central Asia; these fossorial species are specialised in subterranean life (Coşkun, 2016; Kryštufek and Vohralík, 2005). *Ellobius lutescens* (western mole vole) is distributed in northwestern Iran, Iraq, Azerbaijan,

Armenia and eastern Anatolia (Thomas, 1905; Ellerman and Morrison-Scott, 1951; Darlington, 1957; Osborn, 1962; Walker, 1964; Lay, 1967; Hassinger, 1973; Roberts, 1977; Corbet, 1978; Corbet and Hill, 1991; Coşkun, 1997; Nowak, 1999; Wilson and Reeder, 2005; 2017 Kryštufek and Shenbrot, 2016).

Subfamily Gerbillinae Gray, 1825

Genus *Meriones* Illiger, 1811

Genus *Meriones* is one of the most diverse among the tribe Gerbillini in the Palearctic region, particularly in arid regions of Asia (Darvish et al., 2011; Denys, 2017). The *Meriones* species reported in southern Caucasus nowadays are: *Meriones dahli, Meriones libycus, Meriones persicus, Meriones tristrami and Meriones vinogradovi* (Dianat et al., 2017; Fernández-Jalvo, 2016a; Kryštufek and Vohralík, 2009; Souttou and Denys, 2012). In our archaeological material from Azokh 1 unit V, III-IV and II we have identified at least two different groups of *Meriones* species regarding the molar size and morphology, as well as the number of roots on molars.

Meriones* gr. *persicus- tristrami

Material: nine isolated teeth. **Unit II:** two isolated teeth; two right lower m1. **Unit II-IV:** one isolated tooth; one left upper M1. **Unit V:** six isolated teeth; three right lower m1 and three left lower m1.

Description and discussion: Part of the material from Azokh 1 Cave attributed to the genus *Meriones* (Figure 5.3.11) displays the typical morphology of this group, including semi-hypsodont molars with prismatic enamel triangles linked by a longitudinal crest and with no trace of cusps. In our sample, we identify first upper molars (M1) with three roots, which is characteristic of *Meriones persicus* and *Meriones tristrami*. Unfortunately, the dental morphology of these two species is very similar; their m1 and M1 display three roots, the second molars (m2 and M2) have two transverse plates and two roots, whereas the third molars (m3 and M3) are simple and rounded with a single root (Coşkun, 2016; Kryštufek and Vohralík, 2009).

Habitat and distribution: the genus *Meriones* is distributed across North Africa, Central Asia, Turkey and Pakistan (Darvish et al., 2014; Wilson et al., 2017). It lives mostly in dry steppes of short or tall grass, on open hillside, among rocky outcrops in desolate steppes, or in open dry meadows.

The distribution of *Meriones persicus* ranges from the Caucasus (including the southeastern foothills of the Lesser Caucasus and the Talysh Plateau in Azerbaijan) in the west through northeastern Iraq and Iran to Turkmenistan, Afghanistan (Habibi, 2004) and Pakistan, where it is widely distributed. It generally occurs in arid, rocky or mountainous regions (Kryštufek and Vohralík 2009; Molur & Sozen, 2016).

Meriones tristrami habitat is limited to 100 mm of rainfall annually and need well drained soil although it avoids rocky situations. It has been found in Armenia; Azerbaijan; Georgia; Iran, Islamic Republic of Iraq; Israel; Jordan; Lebanon; Syrian Arab Republic and Turkey. Its habitat is mainly shrubland and desert (Kryštufek and Vohralík, 2009; Sozen et al., 2016).

Meriones* gr. *dahli-libycus

Material: five isolated teeth. **Unit II:** one isolated tooth; one right upper M1. **Unit V:** four isolated teeth; one right lower m1 and three left upper M1.

Description and discussion: in our sample we also identified upper first molars with two roots, which is characteristic of *Meriones dahli* or *Meriones libycus*. We provisionally attribute our specimens to this group (Figure 5.3.12) in the light of the number of roots and the morphology of M1, pending a revision of the Middle Eastern

species of the genus.

Habitat and distribution: *Meriones dahli* is known in the border area of Armenia and Turkey, and possibly Azerbaijan. It has been found only on local sandy habitats (Kefelioglu et al., 2008).

Meriones libycus has a wide global range, occurring in North Africa (from Western Sahara and Mauritania to Egypt) and in Asia (from the Arabian peninsula east to China). *M. libycus* occupies desert habitats, it becomes most abundant in unflooded river plains and it is often found close to wadis and dayas (Granjon, 2016).

***Meriones* sp.**

Material: nine isolated teeth. **Unit II:** four isolated teeth; one right lower m1, two right Upper M1 and one left lower m1. **Unit V:** five isolated teeth; three right lower m1 and two left lower m1.

Description and discussion: we identify as *Meriones* sp. broken or digested molars without clear discriminating character.

Family Muridae Illiger, 1811

Genus *Apodemus* Kaup, 1829

Seven *Apodemus* species are currently recognized in southern Caucasus: *A. hyrcanicus*, *A. flavicollis*, *A. witherbyi, A. ponticus*, *A. agrarius, A. mystacinus* and *A. uralensis*, all belonging to the *Sylvaemus* subgenus (Jangjoo et al., 2011).

***Apodemus* (*Sylvaemus*) sp.**

Material: 10 isolated teeth. **Unit II:** seven isolated teeth; two right lower m1, one left mandible with an m1, m2 and m3, one left upper M1, and three left lower m1. **Unit V:** three isolated teeth; one right upper M1, one right maxilla with an M1 and M2 and one right lower m1.

Description and discussion: the first lower molars (m1) from our material show the traits characteristic of the genus *Apodemus* (Figure 5.3.13): the occlusal surface is low with six main cusps and a small anterior mesial tubercle; the anterolabial and posterolabial cusps of m1 converge in an X-shape; the posterior cusp of m1 is low, rounded and well developed, with two or three secondary cusps in the labial part. Identifications at the species level are difficult due to a lack in good reference collection. Moreover, comparative morphological data available in the literature (Amori, G., Hutterer, R., Kryštufek, B., Yigit, N., Mitsain, G. & Palomo, 2016; Bogicevic et al., 2011; Darvish et al., 2015; Knitlová and Horáček, 2017; Kryštufek and Vohralík, 2009; López-García, 2008; Siahsarvie and Darvish, 2008) are sometimes unclear and/or display high variability, and some species are not documented.

Habitat and distribution: the genus *Apodemus* has a large distribution range extending from Great Britain across much of continental Europe to the Urals. It also extends east through Turkey to western Armenia, the Zagros Mountains of Iran and south to Syria, Lebanon and Israel. It inhabits a variety of woodland and bushy habitats (Amori et al., 2016).

Family Dipodidae Fischer, 1817

In the Caucasus, three species are currently represented: *Allactaga williamsi*, *Allactaga major* and *Allactaga elater*

Genus *Allactaga* Cuvier, 1837

Allactaga* cf. *williamsi

Material: four isolated teeth. **Unit II:** two isolated teeth; one right lower m1 and one left upper M1. **Unit V:** two isolated teeth; one right upper M3 and one left lower m2.

Description and discussion: this rodent group is poorly known in the Middle East (Dianat et al., 2013; Naderi et al., 2011; Shenbrot, 2009) and sometimes there is a size overlap between the species. In our sample,

we only found six remains attributed to *Allactaga*, the remains are not damaged and could have been compared with specimens from the Natural History Museum of London reference collection and with data from the literature. We have a M1 with four roots, a lower m1 with two roots and a M3 with three roots. All of them share the same morphological features as *Allactaga williamsi* (lower molars narrower than upper ones, third molars less reduced, first lower molar with small fold in front and two olds on either side). In comparison, *Allactaga major* and *Allactaga elater* have M1 with only three or two roots (Kryštufek and Vohralík, 2009; Markova, 1992). We thus tentatively attributed the remains from Azokh 1 to *Allactaga* cf. *williamsi,* (Figure 5.3.14) waiting further studies on the molar morphology among this genus.

Habitat and distribution: *Allactaga williamsi* is distributed in Anatolia (Turkey), the Caucasus (Armenia, Azerbaijan, Iran and Turkey), and northwestern Iran, with an isolated population in central Afghanistan. Regarding the habitat, this species occurs in steppes with sparse vegetation (Eken et al, 2016).

***Allactaga* sp.**

Material: two isolated teeth. **Unit V:** two isolated teeth; two lower m3.

Description and discussion: we left as *Allactaga* sp. the broken teeth for which it was not possible to count the roots or to see property the molar morphology.

3.2. Preliminary taphonomic study

In order to develop a preliminary taphonomic study, we considered a subsample composed of 380 incisors and rodent molars, mainly muridae and arvicolinae (100 incisors and 90 molars for each unit). This is the first approach to small mammal taphonomy on rodent assemblages in Azokh 1 Cave. We considered that it was necessary to identify the origin of the accumulation and its potential influence on the interpretations before any palaeoecological study.

A considerable part of the molars and incisors show evidence of digestion: 26.83% in Unit V and 22.22% in Unit II (Table 5.6). According to Andrews (1990) and Fernández-Jalvo (2016) the digestion intensities are in majority light (14.53% in Unit V and 17.50% in Unit II) and moderate (5.77% in Unit V and 8.37% in Unit II) in both units (Table 5.6), suggesting that they were probably accumulated by a category 1 predator, such as barn owl species (Andrews, 1990; Fernández-Jalvo et al. 2016). Such owls have opportunistic hunting habits and are sedentary, so their prey spectrum is assumed to be a good representation of the ecosystem in which they live, considering their nocturnal habits and their size.

	Unit V								Unit II							
Elements	**Total**	**No digestion**	**Total digested**		**Light digestion**		**Moderate digestion**		**Total**	**No digestion**	**Total digested**		**Light digestion**		**Moderate digestion**	
	N	N	N	%	N	%	N	%	N	N	N	%	N	%	N	%
Isolated incisor	100	73	27	27.00	21	21	6	6	100	75	25	25.00	22	70	3	7
Isolated molars	90	66	24	26.67	19	11.11	5.00	5.56	90	72	18	20.00	9	10	9	10
Total	**190**	**139**	**51**	**26.83**	**40**	**21.05**	**11**	**5.78**	**190**	**147**	**43**	**22.63**	**31**	**16.31**	**12**	**6.31**

Table 5.6. Representation (N) and Percentages of digestion (%) on Isolated incisors and Isolated molars from Azokh 1 Cave, Unit V and Unit II.

3.3. Palaeoecological reconstruction of the Azokh 1 Cave sequence 2

The small-mammals sequence of Azokh 1 Cave is quite diverse, with at least 13 taxa identified in this work (Table 5.3). Compared to the previous studies (Parfitt, 2016), we identified new taxa such as (Table 5.7): *Mesocricetus brandti*, *Arvicola* ex. gr. *persicus*, *Ellobius lutescens*, *Meriones* gr. *persicus-tristrami, Meriones* gr. *dahli-libycus* and *Allactaga* cf. *williamsi*.

There is no significant turnover between the studied units, containing similar rodents assemblage (Table 5.3). The most abundant taxa in all the units is *Microtus* gr. *arvalis-socialis* (77 individuals in Unit V, seven in Unit III-IV and 75 in Unit II), followed by *Ellobius* cf. *lutescens* (seven individuals in Unit V and 12 individuals in Unit II) and *Microtus* (*Terricola*) spp. (seven individuals in Unit V and four individuals in Unit II). Most of the species identified at Azokh 1 Cave are still present in the area today, but we have some exceptions, as for example *Chionomys gud*, *Ellobius*

	This study			Parfitt (2016)				
Taxa	**Unit V**	**Unit III-IV**	**Unit II**	**Unit V**	**Unit III**	**Unit II/III**	**Unit II**	**Unit I**
Cricetulus migratorius	X		X	X	X		X	X
Mesocricetus brandti	X		X					
Mesocricetus sp.				X	X		X	X
Allocricetus				X			X	
Clethrionomys glareolus			X	X	X			
Arvicola ex. gr. *persicus*			X					
Chionomys gud	X			X				X
Chionomys nivalis			X	X			X	X
Microtus gr. *arvalis-socialis*	X	X	X	X	X	X	X	X
Microtus (*Terricola*) spp.	X	X	X	X	X		X	X
Ellobius sp.				X	X	X	X	X
Ellobius lutescens	X	X	X					
Meriones spp.	X		X	X	X	X	X	X
Meriones gr. dahli-libycus	X		X					
Meriones gr. *persicus-tristrami*	X		X					
Apodemus sp.	X		X	X	X		X	X
Rattus sp.				X				
Mus cf. *macedonicus*				X	X			X
Dryomys nitedual				X				
Allactaga sp.				X				x
Allactaga cf. *williamsi*	X							

Table 5.7. Comparison between the new studies carried out in Azokh 1 Cave and Partiff (2016), X: indicate the presence on the sample.

	Unit V	Unit II	Current Values
MAT	11.42	10.86	10.1
MAX	18.08	17.50	
MIN	4.76	4.24	
MTW	22.50	22.44	22.9
MAX	27.81	27.71	
MIN	17.20	17.16	
MTC	1.43	0.11	-3
MAX	16.65	15.23	
MIN	-13.78	-15.02	
MAP	528.13	500.01	668
MAX	1144.00	1112.61	
MIN	-87.74	-112.60	

Table 5.8. Values of temperatures and precipitations for the Azokh 1 Unit V and Unit II, obtained by the Bioclimatic Model. MAT (mean annual temperature); MTC (mean temperature of coldest month); MTW (mean temperature of warmest month); MAP (mean annual precipitation); Max (maximum of values obtained); Min (minimum of values obtained). The current values where obtained from https://en.climate-data.org/.

lutescens and *Clethrionomys glareolus*.

Unit III-IV do not yield enough material to draw palaeoecological inferences (MNI < 30). For Units V and II the Bioclimatic Model shows similar results (Table 5.8). The BM based on the small mammals from Azokh 1 suggests mean annual temperatures and precipitations similar to the present ones (Table 5.8), being a bit colder and drier in Unit II than in Unit V. The climate seems to be relatively warm-temperate with continental conditions in both units.

The habitat weighting method (Figure 5.5) shows an environment mainly composed of steppes and shrublands, notably indicated by the presence of the *Meriones* spp. and *Mesocricetus brandti*. In Unit V, grasslands (*Allactaga* cf. *williamsi*), desert (*Cricetulus migratorius*) and rocky habitat (*Chionomys gud, C. nivalis*) are also well represented. Unit II presents a higher representation of wetlands habitat than Unit V, due to the presence of *Arvicola* ex. gr. *periscus*. Also, the proportion of forest in Unit II is bigger than in Unit V because of the presence of *Clethrionomys glareolus* and *Apodemus* (*Sylvaemus*) sp.

The current vegetation map shows the presence of a broad belt of semi-xerophyllous woodland on the lowlands 4–6 km to the east of Azokh (Manuk 2010). Further to the east are belts of sagebrush steppe and sagebrush desert, and both would have constituted parts of the ranges of larger mammals and birds of prey (Andrews et al., 2016).

In summary, through the BM we cannot observe significant paleoclimatic differences between Unit V, Unit II and the currents values. The HW shows some differences, especially in the forest and wetlands proportions. Environmental data from both Units V and II are however consistent with steppe environments with shrubland, rocky areas and arid conditions.

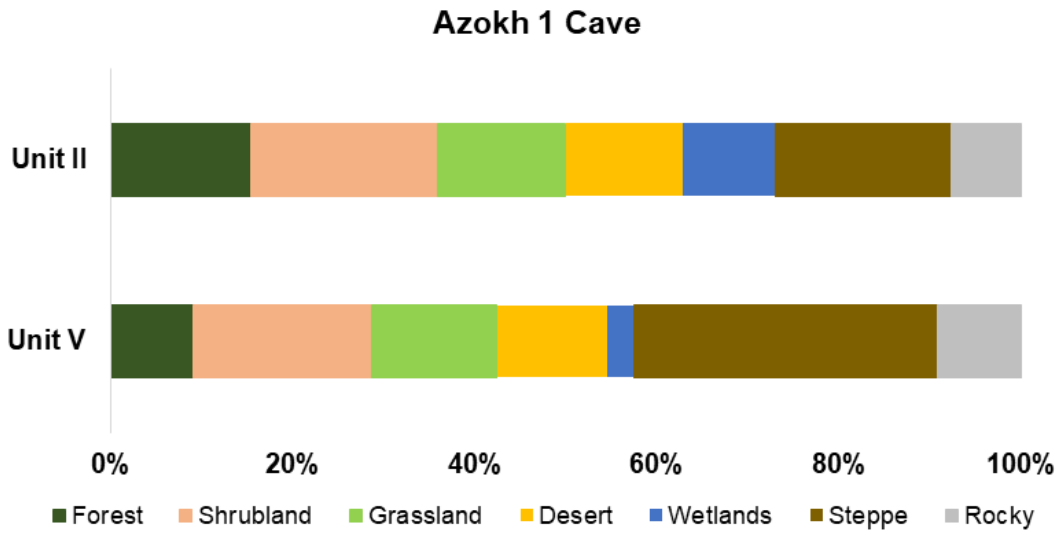


Figure 5.5. Results of the habitat weighting method for Azokh 1 Cave (Unit V and Unit II)

3.4. Comparisons with other palaeoenvironmental proxies from Azokh 1 Cave

Our results obtained with the rodent assemblages will be compared with the previous studies carried out in Azokh 1 Cave, where palaeoenvironmental proxies were estimated using large mammals, small vertebrates and archaeobotanical data (Table 5.9). We especially paid attention to the study performed by Parfitt (2016), who analysed most of the small-mammals collected between 2002 and 2009, on the sediment sequence 2 from Unit V to Unit I.

Most of the previous study on Azokh small mammals is based on Unit V, which yielded the most abundant material. Parfitt's results have shown subtle differences in faunal composition throughout the Middle (Unit V) to Late Pleistocene (Units III and II) sequence of Azokh, indicating changes in aridity and temperatures, combined with fluctuations in woodland cover and the proximity of trees to the site (Parfitt, 2016). Our study allowed to add one new species (*Arvicola persicus*) to the faunal list established by Parfitt (2016), and to specify the identifications for *Ellobius lutescens*, *Meriones* gr. *persicus- tristrami, Meriones* gr. *dahli-libycus* and *Allactaga* cf. *williamsi*, which were previously limited to the genus level. Moreover, our study allowed to provide more consequent data for the Unit II, which was the less representative unit in Parfitt (2016) sample.

According to Marin-Monfort et al. (2016), large mammals were accumulated both by carnivores and humans. Taxonomic identifications have been performed by Van der Made et al. (2016) with at least 29 species represented in all the sequence (Table 5.9). Some of the species, such as *Cervus elaphus,* are present in the whole sequence. *Ursus spelaeus* was identified in all the Pleistocene units, and a taphonomic study revealed that cave bear remains were relatively complete, with some bones in anatomical connection, suggesting that the bears were living in the cave using it as a den (Marin-Monfort et al., 2016). The remains of other mammals are, in most of the units, extremely fragmented, and mainly represented by teeth, horn/

	Large mammals (Van der made, 2016)		**Small-vertebrates** (Blain, 2016; Sevilla, 2016)		**Archeobotanical data** (Allué, 2016; Scott,2016)	
	Species	**Environmental conditions**	**Species**	**Environmental conditions**	**Species**	**Environmental conditions**
Unit V	Carnivores (*Canis aureus*, Crocuta crocuta, Lynx sp. *Felis chaus, Panthera pardus, Ursus spelaeus*), artiodactyla (*Cervus elaphus*, *Capra aegagrus*) and perissodactyla (*Stephanorhinus hemitoechus, Stephanorhinus kirchbergensis, Equus hydruntinus, Equus ferus*)	Interglaciar species. Central Asia aspect	Bat faunas: *Rhinolophus ferrumequinum, Rhinolophus mehelyi, Rhinolophus euryale, Myotis blythii, Myotis nattereri/ schaubi, Myotis mystacinus, Plecotus auritus/macrobullaris, Barbastella barbastellus, Barbastella* laucomelas, *Pipistrellus nathusii, Pipistrelus pipistrelus, Miniopterus schreibersii.* Herpetofaunal remains are composed by: amphibians: *Pseudepidalea viridis* sensu lato, *Ranidae/Hylidae* indet. and *Pelobates* cf. *syriacus*, and reptiles: *Pseudopus apodus, Lacerta* sp., *Eryx jaculus*, cf. *Coronella austriaca*, cf. *Elaphe* sp., cf.*"Coluber"* sp. and *"Colubrinae"* indet.	Bats indicate a predominance of mediterranen species. Herpetofauna indicates and environment consistent with a meadow-steppe, indicated by species such as *P. syriacus* and the small vipers	Charcoal remains indicates the presence of three taxa: *Prunus, Maloideae*, and deciduous *Quercus* sp. Phytoliths were studied from a coprolite	The data obtained with charcoal indicate that the landscape near the cave reflecting mild and humid environmental conditions. However, phytoliths that indicates a temperate steppe mosaic, with grassy conditions.
Unit II	Carnivores (*Panthera pardus, Ursus spelaeus* and *Ursus* sp. and *Vulpes vulpes*, *Canis lupus*), artiodactyla (*Cervus elaphus*, *Capra aegagrus*, *Saiga tatarica*, *Dama* sp. and *Sus scrofa)* and perissodactyla (*Stephanorhinus kirchbergensis*).	Interglaciar temperate environment	Bat faunas: *Rhinolophus ferrumequinum, Myotis blythii, Myotis dasycneme, Pipistrelus pipistrelus, Miniopterus schreibersii.* Amphibians (*Pseudepidalea viridis sensu lato, Pelobates* cf. *syriacus*) and reptiles (*Pseudopus apodus, Lacerta* sp., *Ophisops elegans, Eryx jaculus*, cf. *Coronella austriaca*, cf. *Elaphe* sp., cf. *"Coluber"* sp., *Vipera* spp.)	Bats indicate colder condition in this unit, because of the absence of *Rhinolophus mehelyi*. Accoding to the herpetofaunal remains, this assemblage would represent a drier period, with the presence of a representative of the *V. berus* complex (probably *V. ursinii*) and the small colubrine *Coronella austriaca*.	Charcoal remains: *Prunus* (plums), *Acer* (maple), *Quercus* sp. deciduous (deciduous oaks), *Maloideae* (pomes), *Lonicera* (honeysuckle), *Paliurus/Ziziphus* (Christ's thorn/ jujube), *Celtis/ Zelkova* (Hackberry/Zelkova), *Euonymus* (spindle), and *Ulmaceae* (elm family)	This assemblage composition indicates that the landscape near the cave reflecting mild and humid environmental conditions.

Table 5.9. Species and elemental interpretations carried our previously in Azokh 1 Cave with different environmental proxies.

antler and feet bones. According to Andrews (2016), using the habitat weighting method, Units V-II have the highest index value for deciduous woodland and also for Mediterranean evergreen woodland, as indicated by *Stephanorhinus kirchbergensis*, *Sus scrofa* or *Dama* sp. Unit I differs from the others by a more steppic and arid signal.

The herpetofauna of Azokh 1 is composed exclusively of extant genera and species (Table 5.9), the majority of them belonging to thermophilous and xerophilous forms (e.g., *Pelobates syriacus*, Agamidae, *Pseudopus apodus*, *Ophisops elegans*, *Eryx jaculus*, *Elaphe sauromates*, among others). The anuran *Pseudepidalea viridis* has a wide ecological tolerance. Most taxa frequent open wooded or bushy areas, such as *Pseudopus apodus* or *Ophisops elegans* (Blain, 2016). According to Blain (2016), the faunas from Units II to I would reflect a drier period, with a representative of the *Vipera berus* complex (probably *V. ursinii*) and the small colubrine *Coronella austriaca*. In Unit V, the environment seems to be more consistent with a meadow-steppe. The results obtained with the amphibians and squamates are consistent with those obtained with rodents, and indicate an environment mainly composed of desert and steppes, especially in Unit V.

Bat fauna from Azokh 1 is composed by extant genera (Table 5.9) and the main habitats that they reflect are mountains steppes, followed by mountain grassland. The Unit V is dominated by species with Mediterranean or humid affinities, indicating woodland conditions. Bat assemblage indicates colder conditions for Unit II, with a higher proportion of steppe environment. Thus we can see here some discrepancies with results obtained from rodents, which rather indicate more steppic-arid conditions in Unit V and more woody-temperate conditions in Unit II.

Archaeobotanical data (Table 5.9) obtained from charcoal studies (Allué, 2016) from Unit V and II show that wood could have been carried into the cave by humans. However, no hearth or other constructed feature were identified in the site. Also, wood could have been carried in by animals or by natural surface fires (Andrews et al., 2016). The main taxa identified from the charcoal remains are *Prunus*, *Acer* and *Quercus*, a combination of large woodland trees and small trees and shrubs. We can include the results of the phytoliths that were found in coprolites (Scott et al., 2016) for Unit II, indicating a temperate steppe mosaic, with grassy conditions, but the density of woody components cannot be determined. This interpretation agrees with our rodent´s analysis where the record shows highly variable spectra suggesting an open or semi-open landscape formed mainly by woody trees and shrubs.

In summary, large mammals and charcoal data reflect woodland environments, while small vertebrates and coprolites mainly depict arid environments, mainly steppes and shrubland. These differences could be, at least partly, explained by the origin of the accumulations. Both large mammals and wood could have been selected in specific habitats and introduced by humans in the site (Allué, 2016). On the contrary, small vertebrates and coprolithes were accumulated by non-human predators, which could have hunt over a wider diversity of habitats, especially open areas.

3.5. Azokh 1 Cave and the Southern Caucasus context

Several other Pleistocene sites have provided small mammals studies in the Middle East: Qesem Cave (Maul et al., 2015a; Smith et al., 2015), Hummal (Maul et al., 2015b), Aghitu-3 Cave (Frahm, 2019; Kandel

et al., 2017; Nishiaki and Akazawa, 2018), Nesher Ramla (Weissbrod and Zaidner, 2014), Amud Cave (Belmaker and Hovers, 2011), Misliya Cave (Weissbrod and Weinstein-Evron, 2020), Dzudzuana Cave (Belmaker et al., 2016), Kaldar Cave (Rey-Rodríguez et al., 2020) and Karain Cave (Demirel et al., 2011).

Most of these studies highlighted identification problems of rodent species in this region, especially for the Middle Pleistocene species. We especially considered Qesem Cave and Misliya Cave, both of them located in Israel (Table 5.10, Figure 5.6). We are aware that Israel is quite far from Armenia for a comparative analysis. They don't belong to the same climatic zones (Figure 5.6), and faunas may be very different. However, these sites are the only ones with well-studied rodent assemblages that could be chronologically compared with Azokh 1 Cave.

Qesem cave is an archaeological site located near Tel Aviv (32º 06´36´´ N, 34º 58´48´´E) at 90 m a.s.l. It can be chronologically compared with Azokh-Unit V (Table 5.10), regarding the chronological framework. The paleoecology of Qesem cave was explored through two methods, the first is the nearest living relatives (NRL) and the second is the coexistence approach, both of them based on the assumption that at least since the Neogene, taxa had climatic requirements similar to their NRLs, allowing inferences on past climatic conditions. The modern climatic requirements were taken from the IUCN (Maul et al., 2015a). The results obtained show a climate of Mediterranean type during the time of accumulation of the two microvertebrate concentrations. A large proportion of the annual precipitations fall in winter, whereas summers were dry. The temperatures were lower than today during the time of deposition of Concentration 2, with especially harsh winters, and winter precipitations were lower, resulting in a lower seasonality of precipitation. The landscape

Site/Author	Layer	IOS	Chronology	Environmental conditions	Rodents
Qesem Cave (Maul et al., 2015a; Smith et al., 2015)	Concentration 1	10-9	420-200 ka	Climate of Mediterranean type	*Cricetulus migratorius, Mus musculus/ macedonicus, Microtus guentheri, Spalax ehrenbergi, Gerbillus* cf. *dasyurus, Meriones* cf. *tristrami, Apodemus flavicollis* group
	Concentration 2	10-9	420-200 ka	Climate of Mediterranean type	*Myomimus judaicus/ setzeri* group, *Cricetulus migratorius, Microtus guentheri, Spalax ehrenbergi, Meriones* cf. *tristrami, Mus musculus/ macedonicus, Rattus* cf. *haasi, Apodemus flavicollis* group
Misliya Cave (Weissbrod and Weinstein-Evron, 2020)	Unit 6	7-6	250-160 ka	Heterogeneous landscape or habitat mosaics	*Microtus guenteri*, *Apodemus mystacinus*, *Apodemus flavicollis, Meriones tristrami, Mus* sp., *Mesocricetus* sp., *Myomimus* sp., *Spalax, Ellobius* sp.,*Cricetulus* sp., *Chionomys* sp., *Sciurus* sp., *Mastomys*, *Arvicanthis*

Table 5.10. Interpretation of environmental conditions and faunal lists of the comparison sites located in Israel.

was a mosaic of open habitats with sparse vegetation, shrubland, Mediterranean Forest, rocky areas and riverbanks (Maul et al., 2015a, Smith et al., 2015). Both concentrations were accumulated by the Barn Owl *Tyto alba* (Smith et al., 2015).

Misliya Cave is located on the western slope of the Mount Carmel (32º 44´29´´N, 34º 58´21´´E) facing the coastal plain and situation at an elevation of about 90 m a.s.l and it can be chronologically comparable with Azokh-Unit II (Table 5.10). The environmental conditions of Misliya Cave are characterised by a heterogeneous landscape or habitat mosaics (Weissbrod and Weinstein-Evron, 2020).

Both Israelian caves are characterized by a combination of African rodent taxa, such as *Mastomys* and *Arvicanthis*, and Euro-siberian taxa, such as *Ellobius*. This could suggest that the Transcaucasia region (as the Central Mountains in Israel and the Caucasus mountains) may have acted more as a barrier than as a migration corridor for rodents. This hypothesis, combined with the higher Mediterranean influence occurring in the Israelian sites, could explain the climatic differences observed between Qesem and Misliya Cave on one hand, and Azokh 1 Cave on the other.

Figure 5.6 shows the different main current climates in Israel according to Köppen (1936 modified by Beck et al., 2018), where Qesem and Misliya Cave are located. The

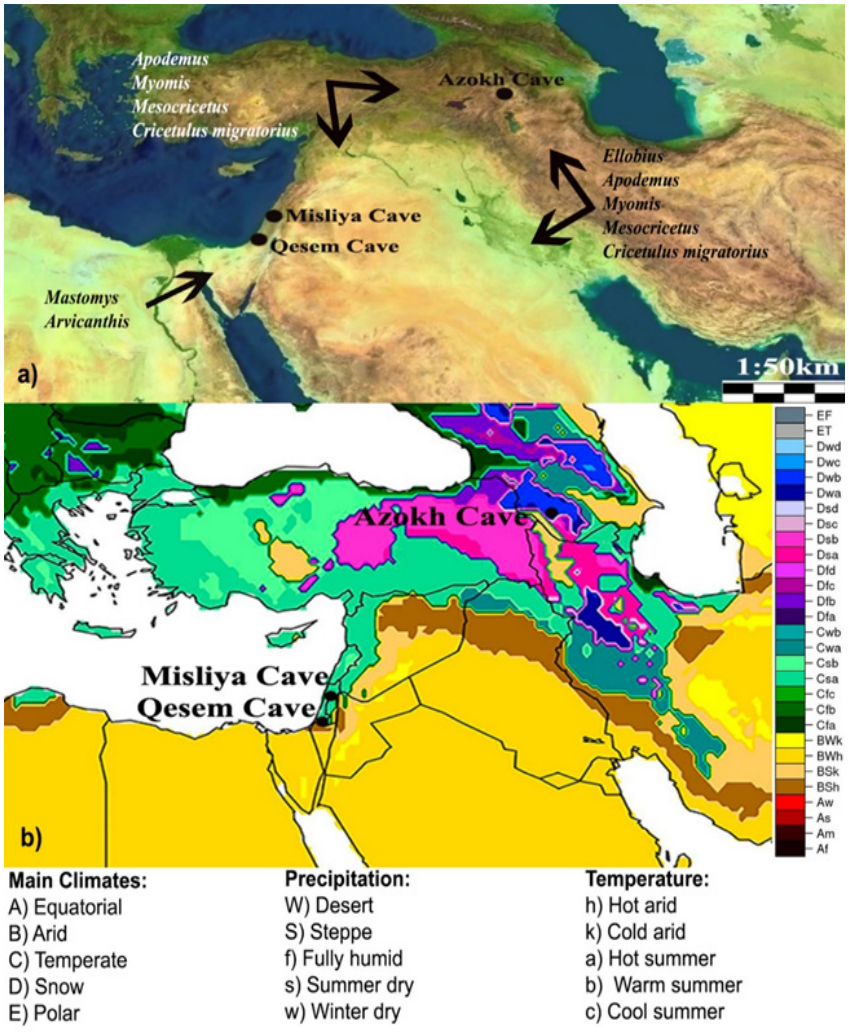


Figure 5.6. a) Location of Qesem Cave, Misliya Cave and Azokh 1. b) Climatic map of the studied region, obtained from Zittis (2015).

climate is mainly temperate (Misliya) to the arid limit (Qesem), with a hot summer and steppe environment. For Azokh 1, the climate is classified as "snow", with dry winters and warm summers.

The rodent assemblages of Azokh 1 show a strong Asiatic influence, while large mammals (Van der Made, 2016) are dominated by Western Eurasian species, also with African, Indian and central Asian elements. The rodent fauna did not record any African species, while they were found in Israel sites.

4.Conclusions

- Rodent assemblages from 2003, 2005, 2014, 2015 and 2018 excavation campaigns of Azokh 1 Cave are composed of at least 13 taxa: seven arvicoline (*Clethrionomys glareolus*, *Microtus* gr. *arvalis-socialis, Microtus* (*Terricola*) spp*., Arvicola persicus, Chionomys nivalis, Chionomys gud* and *Ellobius lutescens*), two cricetines (*Cricetulus migratorius* and *Mesocricetus brandti*), two gerbillines (*Meriones* gr. *persicus-tristrami, Meriones* gr. *dahli-libycus),* one dipodid (*Allactaga* cf. *williamsi*) and one murine species (*Apodemus* spp.).
- The palaeoclimatic parameters obtained with the Bioclimatic Model suggest similar mean annual temperatures and precipitations than today. Although climate seems to be relatively warm-temperate in both units.
- Paleoenvironmental reconstruction, is based on the habitat weighting method, that shows an environment mainly composed by shrubland and steppe, with patches of deciduous forests and desert, similar to the one found nowadays in the area.
- While large mammals and Charcoal studies indicate a woodland environment, small vertebrates and phytoliths coming from coprolithes mainly reflect arid environments, such as steppes and desert. These differences could be partly explained by the taphonomic origin of the accumulation.
- The comparison between Azokh Cave on one hand and Qesem and Misliya Caves (Israel) on the other, indicates that there is no correspondence between the rodent faunas, because the sites belong to different climatic regions and also because Israeli sites recorded African influences, which were not recorded in Azokh 1.

Acknowledgments: I. Rey-Rodriguez is the beneficiary of a PhD scholarship funded by the Erasmus Mundus Program (IDQP). J.M. López-García was supported by a Ramón y Cajal contract (RYC-2016-19386) with financial sponsorship from the Spanish Ministry of Science, Innovation and Universities. We would like to thank Roberto Portela Miguez, Senior Curator in Charge of Mammals, for his help with the reference collection in the Natural History Museum of London; Lawrence Heaney, Adam Ferguson and Lauren Smith of Chicago Field Museum; and Marisa Surovy, Judith Galkin and Carl Mehling of the American Museum of Natural History of New York.

References

Adams, D.C., Collyer, M.L., Kaliontzopoulou, A., 2020. Geomorph: Software for geometric morphometric analyses. R package version 3.2.1.

Amori, G., Hutterer, R., Kryštufek, B., Yigit, N., Mitsain, G. & Palomo, L.J., 2016. *Apodemus flavicollis*. The IUCN Red List of Threatened Species 2016: e. T1892A115058023. 8235. https://doi.org/http://dx.doi.org/10.2305/IUCN.UK.2016-3.RLTS.T1892A22423256.en

Amori, G., 1999. *Chionomys nivalis*. In: Mitchell-Jones, A.J., Amori, G., Bogdanowicz, W., Kry_stufek, B., Reijnders, P.J.H., Spitzenberger, F., Stubbe, M., Thissen, J.B.M., Vohralík, V., Zima, J. (Eds.), The Atlas of European Mammals. Academi Press, London, UK

Andrews, P., Hixson A. S., King, T., Fernández-Jalvo, Y., & Nieto-Díaz ,M., 2016. Palaeoecology of Azokh , in: Y. Fernández-Jalvo, T. King, L. Yepiskoposyan & P. Andrews (Eds.), Azokh Cave and the Transcaucasian Corridor, Vertebrate Paleobiology and Paleoanthropology. Springer International Publishing, Cham. https://doi.org/10.1007/978-3-319-24924-7

Andrews, P., 2006. Taphonomic effects of faunal impoverishment and faunal mixing. Palaeogeography, Palaeoclimatology, Palaeoecology 241, 572–589. https://doi.org/10.1016/j.palaeo.2006.04.012

Andrews, P., 1990. Owls, Caves and Fossils, https://doi.org/10.2307/3889096

Asryan, L., 2015. Azokh Cave lithic assemblages and their contextualization in the Middle and Upper Pleistocene of Southwest Asia (PhD thesis). University Rovira i Virgili, Tarragona.

Asryan, L., Oll, A., Moloney, N., King, T., 2020. Occupying Cave-Sites: A Case Study from Azokh 1 Cave (Southern Caucasus), in: Short-Term OOcupations in Paleolithic Archaeology. pp. 149–181. https://doi.org/10.1007/978-3-030-27403-0

Asryan, L., Ollé, A., Moloney, N., King, T., Murray, J., 2017. Chemical Alteration of Lithic Artefacts: an Experimental Case Study on the effect of Guano on Stone Flakes and Its Contextualization in the Archaeological Assemblage of Azokh Cave (Southern Caucasus). Archaeometry 59, 981–999. https://doi.org/10.1111/arcm.12300

Beck, H.E., Zimmermann, N.E., Mcvicar, T.R., Vergopolan, N., Berg, A., Wood, E.F., 2018. Data Descriptor : Present and future Köppen-Geiger climate classi fi cation maps at 1 -km resolution. Nature Publishing Group 1–12. https://doi.org/10.1038/sdata.2018.214

Belmaker, M., Bar-Yosef, O., Belfer-Cohen, A., Meshveliani, T., Jakeli, N., 2016. The environment in the Caucasus in the Upper Paleolithic (Late Pleistocene): Evidence from the small mammals from Dzudzuana cave, Georgia. Quaternary International 425, 4–15. https://doi.org/10.1016/j.quaint.2016.06.022

Belmaker, M., Hovers, E., 2011. Ecological change and the extinction of the Levantine Neanderthals: Implications from a diachronic study of micromammals from Amud Cave, Israel. Quaternary Science Reviews 30, 3196–3209. https://doi.org/10.1016/j.quascirev.2011.08.001

Bergl; R.A.; Dunn; A.; Fowler; A.; Imong; I.; Ndeloh; D.; Nicholas; A. & Oates; J.F., 2017. *Myodes glareolus*. The IUCN Red List of Threatened Species 2016: e. T4973A115070929 8235, 8.

Bermúdez de Castro, J.M., Martinón-Torres, M., 2013. A new model for the evolution

of the human Pleistocene populations of Europe. Quaternary International 295, 102–112. https://doi.org/10.1016/j.quaint.2012.02.036

Blain, H.-A., 2016. Chapter 9: Amphibians and Squamate Reptiles from Azokh 1, in: Fernández-Jalvo, Y., King, T., Yepiskoposyan, L., Andrews, P. (Eds.), Azokh Cave and the Transcaucasian Corridor, Vertebrate Paleobiology and Paleoanthropology. Springer International Publishing, Cham, pp. 211–249. https://doi.org/10.1007/978-3-319-24924-7

Blain, H.-A., Bailon, S., Cuenca-Bescós, G., 2008. The Early–Middle Pleistocene palaeoenvironmental change based on the squamate reptile and amphibian proxies at the Gran Dolina site, Atapuerca, Spain. Palaeogeography, Palaeoclimatology, Palaeoecology 261, 177–192. https://doi.org/10.1016/j.palaeo.2008.01.015

Bogicevic, K., Nenadic, D., Mihailovic, D., Lazarevic, Z., Milivojevic, J., 2011. Late Pleistocene rodents (Mammalia: Rodentia) from the baranica cave near Knja-evac (eastern Serbia): systematics and palaeoecology. Riv. Ital. Paleontol.Stratigr. 117 (2), 331e346.

Chevret, P., Renaud, S., Helvaci, Z., Ulrich, R.G., Quéré, J.P., Michaux, J.R., 2020. Genetic structure, ecological versatility, and skull shape differentiation in Arvicola water voles (Rodentia, Cricetidae). Journal of Zoological Systematics and Evolutionary Research 58, 1323–1334. https://doi.org/10.1111/jzs.12384

Corbet, G.B. and Hill, J.E. 1991. A World List of Mammalian Species. 3rd ed. London, UK: British Museum (Natural History).

Corbet, G.B. 1978. The Mammals of the Palearctic Region: A Taxonomic Review. London, Brit. Mus. (Nat. Hist.). Cornell Univ. Press. 117-118.

Coşkun, Y., 2016. Review of unique odd chromosome-numbered underground rodent species of the Palearctic region: *Ellobius Lutescens* Thomas 1897 (Rodentia: Cricetidae). Turkish Journal of Zoology 40, 831–841. https://doi.org/10.3906/zoo-1509-53

Coşkun, Y., 1999. Morphological characteristics of *Meriones tristrami* Thomas, 1892 (Rodentia: Gerbillinae) from Diyarbakır, Turkey. . Turk. J. Zool 23, 345–355.

Coşkun, Y. 1997. *Ellobius lutescens* Thomas, 1897 (Rodentia: Cricetidae) Turk. Journal of Zoology. 21, 349-354.

Darlington, P.J. 1957. Zoogeography: The Geographical Distribution of Animals. New York, NY, USA, John Wiley and Sons.

Darvish, J., 2011. Morphological comparison of fourteen species of the genus *Meriones* Illiger , 1811 (Rodentia : Gerbillinae) from Asia and North Africa. Iranian Journal of Animal Biosystematics 7, 49–74.

Darvish, J., Mohammadi, Z., Ghorbani, F., Mahmoudi, A., Dubey, S., 2015. Phylogenetic Relationships of *Apodemus* Kaup, 1829 (Rodentia: Muridae) Species in the Eastern Mediterranean Inferred from Mitochondrial DNA, with Emphasis on Iranian Species. Journal of Mammalian Evolution 22, 583–595. https://doi.org/10.1007/s10914-015-9294-9

Darvish, J., Mohammadi, Z., Mahmoudi, A., Siahsarvie, R., 2014. Faunistic and taxonomic study of Rodents from northwestern Iran. Iranian Journal of Animal

Biosystematics (IJAB) 10, 119–136.

Demirel, A., Andrews, P., Yalçinkaya, I., Ersoy, A., 2011. The taphonomy and palaeoenvironmental implications of the small mammals from Karain Cave, Turkey. Journal of Archaeological Science 38, 3048–3059. https://doi.org/10.1016/j.jas.2011.07.003

Dianat, M., Aliabadian, M., Darvish, J., Akbarirad, S., 2013. Molecular phylogeny of the Iranian Plateau five-toed jerboa, *Allactaga* (Dipodidea: Rodentia), inferred from mtDNA. mammalia 77. https://doi.org/10.1515/mammalia-2012-0011

Dianat, M., Darvish, J., Cornette, R., Aliabadian, M., Nicolas, V., 2017. Evolutionary history of the Persian Jird, *Meriones persicus*, based on genetics, species distribution modelling and morphometric data. Journal of Zoological Systematics and Evolutionary Research 55, 29–45. https://doi.org/10.1111/jzs.12145

Eken, G., Bozdogan, M., Molur, S., 2016. *Allactaga williamsi* (errata version published in 2017). The IUCN Red List of Threatened Species 2016: e.T136326A115205783. 8235.

Ellerman, J.R., and Morrison-Scott, T.C.S. 1951. Checklist of Palearctic and Indian Mammals, 1780 to 1946. Brit. Mus. Nat. Hist. London, 1-810.

Evans, E.M.N., Van Couvering, J.A.H., Andrews, P., 1981. Palaeoecology of Miocenesites in western Kenya. J. Hum. Evol. 10, 99–116

Fernandez-Jalvo, Y., King, T., Yepiskoposyan, L., Andrews, P., 2016a. Azokh Cave and the Transcaucasian Corridor, Vertebrate Paleobiology and Paleoanthropology. Springer International Publishing, Cham. https://doi.org/10.1007/978-3-319-24924-7

Fernandez-Jalvo, Y., Andrews, P., 2016b. Atlas of Taphonomic Identifications. https://doi.org/10.1007/978-94-017-7432-1

Fernández-Jalvo, Y., Andrews, P., Denys, C., Sesé, C., Stoetzel, E., Marin-Monfort, D., Pesquero, D., 2016c. Taphonomy for taxonomists: Implications of predation in small mammal studies. Quaternary Science Reviews 139, 138–157. https://doi.org/10.1016/j.quascirev.2016.03.016

Fernández-Jalvo, Y., King, T., Andrews, P., Yepiskoposyan, L., Moloney, N., Murray, J., Domínguez-Alonso, P., Asryan, L., Ditchfield, P., van der Made, J., Torres, T., Sevilla, P., Nieto Díaz, M., Cáceres, I., Allué, E., Marín Monfort, M.D., Sanz Martín, T., 2010. The Azokh Cave complex: Middle Pleistocene to Holocene human occupation in the Caucasus. Journal of Human Evolution 58, 103–109. https://doi.org/10.1016/j.jhevol.2009.07.005

Frahm, E., 2019. Upper Palaeolithic Settlement and Mobility in the Armenian Highlands : Agent-Based Modeling , Obsidian Sourcing , and Lithic Analysis at Aghitu-3 Cave.

Granjon, L., 2016. *Meriones libycus* (errata version published in 2017). The IUCN Red List of Threatened Species 2016: e. T13164A115110005. 8235.

Habibi, K., 2004. Mammals of Afghanistan. Zoo Outreach Organisation/USFWS, Coimbatore, India

Harrison D.L., Bates P.J.J. 1991. The Mammals of Arabia. Sevenoaks: Harrison Zoological Museum Publication.

Hassinger, J.D. 1973. A survey of the mammals of Afghanistan: Resulting from the 1965 Street Expedition (Excluding Bats). Fieldiana Zoology, Vol. 60. Chicago, IL, USA, Field Museum of Natural History.

Heinrich, W.-D. 1978. Zur biometrischen erfassung eines evolutionstrends bei Arvicola (Rodentia, Mammalia) aus dem pleistozän thüringens.Säugetierkundliche Informationen. 1 (2), 3-21.

Hernández Fernández, M., Álvarez Sierra, M.Á., Peláez-Campomanes, P., 2007. Bioclimatic analysis of rodent palaeofaunas reveals severe climatic changes in Southwestern Europe during the Plio-Pleistocene. Palaeogeography, Palaeoclimatology, Palaeoecology 251, 500–526. https://doi.org/10.1016/j.palaeo.2007.04.015

Hernández Fernández, M., Peláez-Campomanes, P., 2003. The bioclimatic model: A method of palaeoclimatic qualitative inference based on mammal associations. Glob. Ecol. Biogeogr. 12, 507–517. https://doi.org/10.1046/j.1466-822X.2003.00057.

Hernández Fernández, M., 2001. Bioclimatic discriminant capacity of terrestrial mammal faunas. Global Ecology and Biogeography 10, 189–204. https://doi.org/10.1046/j.1466-822x.2001.00218.x

Kandel, A.W., Gasparyan, B., Allué, E., Bigga, G., Bruch, A.A., Cullen, V.L., Frahm, E., Ghukasyan, R., Gruwier, B., Jabbour, F., Miller, C.E., Taller, A., Vardazaryan, V., Vasilyan, D., Weissbrod, L., 2017. The earliest evidence for Upper Paleolithic occupation in the Armenian Highlands at Aghitu-3 Cave. Journal of Human Evolution 110, 37–68. https://doi.org/10.1016/j.jhevol.2017.05.010

Karami, M., Hutterer, R., Benda, P., Siahsarvie, R., Kryštufek, B., 2008. Annotated checklist of the mammals of Iran. Lynx (Praha) 39, 63–102.

Kasimova, R. M. (2001). Anthropological research of Azykh Man osseous remains. Human Evolution, 16, 37–44

Kaya, A., Gharakhloo, M.M., Coşkun, Y., 2018. Geographic variation in the skull morphology of *Ellobius lutescens* Thomas, 1897 (Mammalia: Rodentia) by geometric morphometric analyses. Vertebrate Zoology 68, 157–164.

Kefelioglu, H., Yigit, N., Kryštufek, B., 2008. *Meriones dahli*. The IUCN Red List of Threatened Species 2008: e.T13162A3415328.8235.

King, T., Compton, T., Rosas, A., Andrews, P., Yepiskoyan, L., & Asryan, L. (2016). Azokh cave hominin remains, in: Y. Fernández- Jalvo, T. King, L. Yepiskoposyan & P. Andrews (Eds.), Azokh Cave and the Transcaucasian Corridor (pp. 103–116). Dordrecht: Springer. https://doi.org/10.1007/978-3-319-24924-7

Knitlová, M., Horáček, I., 2017. Late Pleistocene-Holocene paleobiogeography of the genus *Apodemus* in Central Europe. PLoS ONE 12, 1–23. https://doi.org/10.1371/journal.pone.0173668

Kryštufek, B., Tesakov, A.S., Lebedev, V.S., Bannikova, A.A., Abramson, N.I., Shenbrot, G., 2020. Back to the future: The proper name for red-backed voles is *Clethrionomys* Tilesius and not *Myodes* Pallas. Mammalia 84, 214–217. https://doi.org/10.1515/mammalia-2019-0067

Krystufek, B., 2017. *Chionomys nivalis*, European Snow Vole. The IUCN Red

List of Threatened Species 2016: e. T4659A115069366 8235. https://doi.org/http://dx.doi.org/10.2305/IUCN.UK.2016-3.RLTS.T4659A22379147.en

Kryštufek, B., Bukhnikashvili, A., Sozen, M. & Isfendiyaroglu, S., 2017. *Cricetulus migratorius*. The IUCN Red List of Threatened Species 2016: e.T5528A115073390 8235. https://doi.org/http://dx.doi.org/10.2305/IUCN.UK.2016-3.RLTS.T5528A22391440.en

Kryštufek, B. & Shenbrot, G., 2016. *Ellobius lutescens* , Transcaucasian Mole Vole. The IUCN Red List of Threatened Species 2016: e.T7655A22340006. 8235. https://doi.org/http://dx.doi.org/10.2305/IUCN.UK.2016- 2.RLTS.T7655A22340006.en

Kryštufek, B., Yigit, N. & Amori, G., 2015. *Mesocricetus brandti* , Brandt ' s Hamster. The IUCN Red List of Threatened Species 2008: e.T13220A3421550. 8235. https://doi.org/http://dx.doi.org/10.2305/IUCN.UK.2008.RLTS.T13220A3421550.en

Kryštufek, B., Vohralík, V., 2009. Mammals of Turkey and Cyprus, Rodentia II: Cricetinae, Muridae, Spalacidae, Calomyscidae, Capromyidae, Hystricidae, Castoridae. https://doi.org/10.1644/10-MAMM-R-221.1

Kryštufek B. & Vohralík V., 2005. Mammals of Turkey and Cyprus. Rodentia I: Sciuridae, Dipodidae, Gliridae, Arvicolinae.

Kryštufek, B., 1999. Snow voles, genus *Chionomys*, of Turkey. Mammalia 63(3), 323–339.

Lay, D.M. 1967. A Study of the Mammals of Iran, Resulting from the Street Expedition of 1962-63. Fieldiana Zool., 54:168-171.

López-García, J.M., 2008. Evolución de la diversidad taxonómica de los micromamíferos en la Península Ibérica y cambios Paleoambientales durante el Pleistoceno Superior.

López-García, J.M., Blain, H.-A., Cuenca-Bescós, G., Alonso, C., Alonso, S., Vaquero, M., 2011. Small vertebrates (Amphibia, Squamata, Mammalia) from the late Pleistocene-Holocene of the Valdavara-1 cave (Galicia, northwestern Spain). Geobios 44, 253–269. https://doi.org/10.1016/j.geobios.2010.10.001

López-García, J.M., Blain, H.A., Cuenca-Bescós, G., Ruiz-Zapata, M.B., Dorado-Valiño, M., Gil-García, M.J., Valdeolmillos, A., Ortega, A.I., Carretero, J.M., Arsuaga, J.L., de Castro, J.M.B., Carbonell, E., 2010. Palaeoenvironmental and palaeoclimatic reconstruction of the Latest Pleistocene of El Portalón Site, Sierra de Atapuerca, northwestern Spain. Palaeogeography, Palaeoclimatology, Palaeoecology 292, 453–464. https://doi.org/10.1016/j.palaeo.2010.04.006

Lozano-Fernández, I., Agusti, J., Cuenca-Bescós, G., Blain, H.A., López-Garcia, J.M., Vallverdú, J., 2013. Pleistocene evolutionary trends in dental morphology of *Mimomys savini* (rodentia, mammalia) from iberian peninsula and discussion about the origin of the genus arvicola. Quaternaire 24, 179–190.

Mahmoudi, A., Maul, L.C., Khoshyar, M., Darvish, J., Aliabadian, M., Kryštufek, B., 2020. Evolutionary history of water voles revisited: Confronting a new phylogenetic model from molecular data with the fossil record. Mammalia 1–14. https://doi.org/10.1515/mammalia-2018-0178

Manuk, V., 2010. Atlas of the Nagorno-Karabagh Republic. Stepanakert

2010.

MarÍn-Monfort, M. D., Cáceres, I., Andrews, P., Pinto, A. C. & Fernández-Jalvo, Y. (2016). Taphonomy and Site Formation of Azokh 1, in: Y. Fernández-Jalvo, T. King, L. Yepiskoposyan & P. Andrews (Eds.), Azokh Cave and the Transcaucasian Corridor (pp. 211–249). Dordrecht: Springer. https://doi.org/10.1007/978-3-319-24924-7

Markova, A., 1992. Fossil rodents (Rodentia, Mammalia) from the Sel'-Ungur Acheulian cave site (Kirghizstan). Acta Zoologica Cracoviensia 35, 217–239.

Maul, L.C., Rabinovich, R., Biton, R., Maul, L.C., 2020. At the southern fringe : extant and fossil water voles of the genus Arvicola (Rodentia , Cricetidae , Arvicolinae) from Israel , with the description of a new species Cricetidae , Arvicolinae) from Israel , with the description of a new species. Historical Biology 00, 1–21. https://doi.org/10.1080/08912963.2020.1827240

Maul, L.C., Bruch, A.A., Smith, K.T., Shenbrot, G., Barkai, R., Gopher, A., 2015a. Palaeoecological and biostratigraphical implications of the microvertebrates of Qesem Cave in Israel. Quaternary International. https://doi.org/10.1016/j.quaint.2015.04.032

Maul, L.C., Smith, K.T., Shenbrot, G., Bruch, A.A., Wegmüller, F., Le Tensorer, J.M., 2015b. Microvertebrates from unit G/layer 17 of the archaeological site of Hummal (El Kowm, Central Syria): Preliminary results. Anthropologie (France) 119, 676–686. https://doi.org/10.1016/j.anthro.2015.10.010

Molur, S. & Sozen, M., 2016. *Meriones persicus*, Persian Jird. The IUCN Red List of Threatened Species 2016: e.T13166A22433231.8235. https://doi.org/http://dx.doi.org/10.2305/IUCN.UK.2016-2.RLTS.T13166A22433231.en

Moradi Gharkheloo, M., 2003. A Study on the Morphology , Karyology and Distribution of *Ellobius* Fisher , 1814 (Mammalia : Rodentia) in Iran. Turkish Journal of Zoology 27, 281–292.

Murray, J., Lynch, E.P., Dominguez-Alonso, P., Barham, M., 2016. Chapter 2: Stratigraphy and Sedimentology of Azokh Caves, South Caucasus., in: Fernández-Jalvo, Y., King, T., Yepiskoposyan, L., Andrews, P. (Eds.), Azokh Cave and the Transcaucasian Corridor, Vertebrate Paleobiology and Paleoanthropology. Springer International Publishing, Cham, pp. 27–54. https://doi.org/10.1007/978-3-319-24924-7

Murray, J., Domínguez-alonso, P., Fernández-, Y., King, T., Lynch, E.P., Andrews, P., Yepiskoposyan, L., Moloney, N., Cacères, I., Allué, E., Asryan, L., Ditchfield, P., Williams, D.M., Murray, J., Dominguez-alonso, P., Fernandez-jalvo, Y., King, T., Lynch, E.P., Andrews, P., Yepiskoposyan, L., Moloney, N., Caceres, I., Allue, E., Asryan, L., Williams, D.M., 2010. Pleistocenen to Holocene stratigraphy of Azokh 1 Caves, lasser caucasus. Irish Journal of Earth Sciences 28, 75–91. https://doi.org/10.3318/IJES.2010.28.75

Nadachowski, A., 1991. Systematics, geographic variation, and evolution of snow voles (*Chionomys*) based on dental characters. Acta Theriologica 36, 1–45.

Naderi, G., Hemami, M.R., Mohammadi, S., 2011. Investigation of habitat preferences of Iranian jerboa (*Allactaga firouzi* Womochel 1978). mammalia 75. https://doi.org/10.1515/mamm.2011.008

Neumann, K., Yiğit, N., Fritzsche, P., Çolak, E., Feoktistova, N., Surov, A., Michaux, J., 2017. Genetic structure of the Turkish hamster (*Mesocricetus brandti*). Mammalian Biology 86, 84–91. https://doi.org/10.1016/j.mambio.2017.06.004

Nishiaki, Y., Akazawa, T., 2018. The Middle and Upper Paleolithic Archeology of the Levant and Beyond. Replacement of Neanderthals by Modern Humans Series 35–47. https://doi.org/10.1007/978-981-10-6826-3_3

Nowak, R.M. 1999. Walker's Mammals of the World. 6th ed. Baltimore, MD, USA, The Johns Hopkins University Press.

Osborn, D.J. 1962. Rodents of subfamily Microtinae from Turkey. Journal of Mammology, 43 (4):515-529. https://doi.org/10.2307/1376914

Parfitt, S.A., 2016. Chapter 7 Rodents, Lagomorphs and Insectivores from Azokh Cave, in: Fernández-Jalvo, Y., King, T., Yepiskoposyan, L., Andrews, P. (Eds.), Azokh Cave and the Transcaucasian Corridor, Vertebrate Paleobiology and Paleoanthropology. Springer International Publishing, Cham, pp. 163–176. https://doi.org/10.1007/978-3-319-24924-7

R Core Team, 2020. R: A language and environment for statistical computing. R Foundation for Statistical Computing.

Rey-Rodríguez, I., Arnaud, J., López-García, J.M., Stoetzel, E., Denys, C., Cornette, R., Bazgir, B., 2021. Distinguishing between three modern *Ellobius* species (Rodentia, Mammalia) and identification of fossil *Ellobius* from Kaldar Cave (Iran) using geometric morphometric analyses of the first lower molar. Palaeontologia Electronica 24 (1):a01, 1–18. https://doi.org/10.26879/1122

Rey-Rodríguez, I., López-García, J.-M., Blain, H.-A., Stoetzel, E., Denys, C., Fernández-García, M., Tumung, L., Ollé, A., Bazgir, B., 2020. Exploring the landscape and climatic conditions of Neanderthals and anatomically modern humans in the Middle East: the rodent assemblage from the late Pleistocene of Kaldar Cave (Khorramabad Valley, Iran). Quaternary Science Reviews 236, 106278. https://doi.org/10.1016/j.quascirev.2020.106278

Roberts, T.J. 1977. The Mammals of Pakistan. London, UK, Ernst Benn Ltd.

Rohlf, F.J. 2016. tpsDig, Digitize Landmarks and Outlines, Version 2.32. Department of Ecology and Evolution, State University of New York at Stony Brook, New York. http://life.bio.sunysb.edu/morph

Royer, A., García, B.A., Laffont, R., Hernández, M., Cnrs, U.M.R., Franche-comté, U.B., Gabriel, B., 2020. New bioclimatic models for the quaternary palaearctic based on insectivore and rodent communities 560.

Rusin, M., 2017. *Ellobius talpinus* , Northern Mole Vole. The IUCN Red List of Threatened Species 2016: e.T7656A115085720.8235. https://doi.org/http://dx.doi.org/10.2305/IUCN.UK.2016-3.RLTS.T7656A22339917.en

Sándor, A.D., 2018. Rediscovered after half a century: A new record of the grey dwarf hamster, *Cricetulus migratorius* (Mammalia: Cricetidae), in Romania. Turkish Journal of Zoology 42, 495–498. https://doi.org/10.3906/zoo-1712-15

Schlager, S., 2017. Morpho and Rvcg Shape Analysis, in: Guoyan Zheng and Shuo

Li and Gabor Szekely (Ed.), Statistical Shape and Deformation Analysis. pp. 217–256.

Shenbrot, G., Kryštufek, B. & Molur, S., 2016. *Ellobius fuscocapillus* , Southern Mole Vole. The IUCN Red List of Threatened Species 2016: e.T7654A22339730. 8235. https://doi.org/http://dx.doi.org/10.2305/IUCN.UK.2016- 2.RLTS.T7654A22339730.en

Shenbrot, G., 2009. On the conspecifity of *Allactaga hotsoni* Thomas, 1920 and *Allactaga firouzi* Womochel, 1978 (Rodentia: Dipodoidea). Mammalia 73, 231–237. https://doi.org/10.1515/MAMM.2009.043

Scott, L., Rossouw, L., Cordova, C., & Risberg, J. (2016). Palaeoenvironmental context of coprolites and plant microfossils from Unit II. Azokh 1, in: Fernández-Jalvo, Y., King, T., Yepiskoposyan, L., Andrews, P. (Eds.), Azokh Cave and the Transcaucasian Corridor, Vertebrate Paleobiology and Paleoanthropology. Springer International Publishing, Cham, pp. 177–189. https://doi.org/10.1007/978-3-319-24924-7

Siahsarvie, R., Darvish, J., 2008. Geometric morphometric analysis of Iranian wood mice of the genus *Apodemus* (Rodentia, Muridae). Mammalia 72. https://doi.org/10.1515/MAMM.2008.020

Smith, K.T., Christian, L., Flemming, F., Barkai, R., Gopher, A., 2015. The microvertebrates of Qesem Cave : A comparison of the two concentrations. Quaternary International 1–13. https://doi.org/10.1016/j.quaint.2015.04.047

Souttou K., Manaa A., Stoetzel E., Sekour M., Hamani A. , Doumandji S., Denys C. 2012 Small mammals bone modifications in Black-shouldered Kite *Elanus caeruleus* pellets from Algeria: implications for archaeological sites. J. Taphonomy 10 (1), 1-19.

Sozen, M., Bukhnikashvili, A., Shenbrot, G., Scott, D., Amori, G., Kryštufek, B., Yigit, N., Mitsani, G., 2016. *Meriones tristrami* (errata version published in 2017). The IUCN Red List of Threatened Species 2016: e.T13170A115110701. 8235.

Sözen, M., Özkurt, S.O., , Karataş, A., Çolak, E. and, Matur, F., 2009. On the karyology, morphology and biology of *Chionomys gud* (Satunin, 1909) (Mammalia: Rodentia) in Turkey. North-Western Journal of Zoology 5 (1), 121–129.

Stoetzel, E., Cornette, R., Lalis, A., Nicolas, V., Cucchi, T., Denys, C., 2017. Systematics and evolution of the *Meriones shawii/grandis* complex (Rodentia, Gerbillinae) during the Late Quaternary in northwestern Africa: Exploring the role of environmental and anthropogenic changes. Quaternary Science Reviews 164, 199–216. https://doi.org/10.1016/j.quascirev.2017.04.002

Tesakov, A.S. 2016. Early Middle Pleistocene *Ellobius* (Rodentia, Cricetidae, Arvicolinae) from Armenia. Russian Journal of Theriology, 15(2):151-158.

Thomas, O. 1905. *Ellobius woosnami*. Abstr. Proc. Zool. Soc. 23; Proceeding of the Zoological Society. 526 London

Van Der Made, J., Torres, T., Ortiz, J.E., Moreno-Pérez, L., Fernández-Jalvo, Y., 2016. Chapter 6: The new material of Large Mammals from Azokh and comments on the older collections, in: Fernández-Jalvo, Y., King, T., Yepiskoposyan, L., Andrews, P. (Eds.), Azokh Cave and the

Transcaucasian Corridor, Vertebrate Paleobiology and Paleoanthropology. Springer International Publishing, Cham. https://doi.org/10.1007/978-3-319-24924-7

Walker, E.P. 1964. Mammals of the World. Vol. 2. Baltimore, MD, USA, The Johns Hopkins Press.

Weissbrod, L., Weinstein-Evron, M., 2020. Climate variability in early expansions of Homo sapiens in light of the new record of micromammals in Misliya Cave, Israel. Journal of Human Evolution 139, 102741. https://doi.org/10.1016/j.jhevol.2020.102741

Weissbrod, L., Zaidner, Y., 2014. Taphonomy and paleoecological implications of fossorial microvertebrates at the Middle Paleolithic open-air site of Nesher Ramla, Israel. Quaternary International 331, 115–127. https://doi.org/10.1016/j.quaint.2013.05.044

Wilson, D.E., Mittermeier, R.A., and Lacher, T.E. 2017. Handbook of the Mammals of the World. Volume 7. Rodents II. Lynx Edicions, Barcelona, Spain

Wilson, D.E. and Reeder, D.M. 2005. Mammal Species of the World. Washington, DC, USA: Smithsonian Institution Scholarly Press.

Chapter 6.

Exploring the landscape and climatic conditions of Neanderthals and anatomically modern humans in the Middle East : the rodent assemblage from the Late Pleistocene of Kaldar Cave (Khorramabad Valley, Iran)



Abstract

The Middle East, specially the Zagros region, lies in a strategic position as a crossroads between Africa, Europe and eastern Asia. The landscape of this region that prevailed around the Neanderthal and anatomically modern human occupations is not well known. Only a few sites have been studied in detail in this area, often providing only a faunal list. These reveal that Neanderthals and anatomically modern humans lived in a landscape mainly composed of dry steppes.

Here we extend the data obtained from Kaldar Cave through a systematic study of the rodent assemblage. The site provided evidence of a Pleistocene occupation attested by lithic tools associated with the Middle and Upper Palaeolithic, but it was also occupied during the Holocene, as evidenced by Neolithic artefacts. First excavations have revealed small vertebrates in Layer 4 (sub-layer 5 and 5II), belonging to the Upper Palaeolithic, and Layer 5 (sub-layers 7 and 7II), belonging to the Middle Palaeolithic.

The rodent assemblage of Kaldar Cave is mainly composed of six arvicoline, two cricetine, one glirid, one dipodid, one gerbilline and two murine species.

This assemblage shows that during the Late Pleistocene the environment around the site was mainly composed of open dry steppes, as indicated by the most abundant taxa, *Microtus*, *Ellobius* and *Meriones*. However, murine species indicate the presence of a vegetation cover. The palaeoclimatic conditions are characterised by lower temperatures and also less precipitation than at present.

The results obtained with the rodent assemblages show that there is no major palaeoenvironmental or palaeoclimatic change that would explain the cultural shift between Layer 5 (Middle Palaeolithic) and Layer 4 (Upper Palaeolithic).

Keywords: Rodentia, Middle East, taxonomy, palaeoecology, human occupations



Rey-Rodríguez, I., López-García, J. M., Blain, H. A., Stoetzel, E., Denys, C., Fernández-García, M., Tumung, L., Ollé, A., Bazgir, B. (2020) Exploring the landscape and climatic conditions of Neanderthals and anatomically modern humans in the Middle East: the rodent assemblage from the late Pleistocene of Kaldar Cave (Khorramabad Valley, Iran). Quaternary Science Reviews 236, 106278. https://doi.org/10.1016/j.quascirev.2020.106278

1. Introduction

Small vertebrates are recognized to be good palaeoecological indicators due to their rapid evolution, the limited geographic range of a species and unique niche requirements, as well as their frequent preservation in archaeological and palaeontological sites. They might be excellent indicators of palaeovegetation type and provide a high-resolution proxy for palaeoenvironmental changes (e.g. Belmaker and Hovers, 2011). Studies of small vertebrates from archaeological sites in the Middle East are still scarce (Belmaker and Hovers, 2011; Belmaker et al., 2016; Demirel et al., 2011; Fernández-Jalvo, 2016a; Kandel et al., 2017; Maul et al., 2015a, 2015b; Smith et al., 2015; Weissbrod and Zaidner, 2014), and they mainly propose preliminary lists of taxa. On the other hand, some studies of extant owl pellet assemblages have been performed in the Middle East (Abi-said et al., 2014; Darvish et al., 2000; Haddadian Shad et al., 2014; Kopij and Livenschulman, 2013; Obuch and Khaleghizadeh, 2012; Rey-Rodríguez et al., 2019; Shehab et al., 2013), providing taxonomic and some taphonomic reference data in Iran, Lebanon, Israel, Turkey and Syria.

The main palaeoecological and palaeoclimatic reconstructions based on faunal assemblages relate to the unique niche requirements of a particular species. Belmaker et al. (2011) pointed out that their interpretations, in contrast, are based on analyses of community composition. Analyses of persistence versus change over time should take into account species presence-absence, rank abundance and proportional abundance (Belmaker and Hovers, 2011).

The Middle East is a prime location to study Neanderthal and anatomically modern human (AMH) interactions during the Middle to Upper Palaeolithic transition (Belmaker et al., 2016). However, sites yielding evidence of both Neanderthal and AMH occupations in the same sequence are rare, only five sites were well excavated (Bazgir et al., 2014; Bazgir et al., 2017). In this framework, Kaldar Cave is a key archaeological site for evaluating the influence of environment on cultural changes in both human species because of its location and the faunal and lithic remains. The main objective of this paper is to infer the landscape composition and the climatic conditions in which Neanderthal and AMH populations pursued their activities through the study of small mammals. We identify and describe the rodent fossils recovered from Kaldar Cave in order to establish the main criteria for further identifications in this region and provide a preliminary basis for future systematic studies.

2. Kaldar Cave

Kaldar Cave is located in the northern part of the Khorramabad Valley, Lorestan Province, western Iran (48º17'35" E, 33º33'25" N) at 1290 m a.s.l. (Fig. 6.1a,b). The cave was discovered in 2007, and the first archaeological intervention was undertaken by an Iranian-Spanish team in 2011-2012, revealing the great potential of the cave (Bazgir et al., 2014). A second excavation was performed in 2014-2015. The trench exposed an approximately 2m-thick section of sedimentary deposits, characterized by 5 main layers, themselves divided into several sub-layers (Fig. 6.1c).

Layer 5 (including sub-layers 7 and 7II) consists of an extremely cemented reddish-brown sediment with some small angular limestone blocks and Middle Palaeolithic artefacts with Levallois elements. So far, no chronometric data are available for this layer (Bazgir et al., 2017).

Layer 4 (including sub-layers 5, 5II, 6 and 6II) consists of a silty but compact dark-brown sediment with cultural remains attributed to the Upper and early Upper Palaeolithic. In the

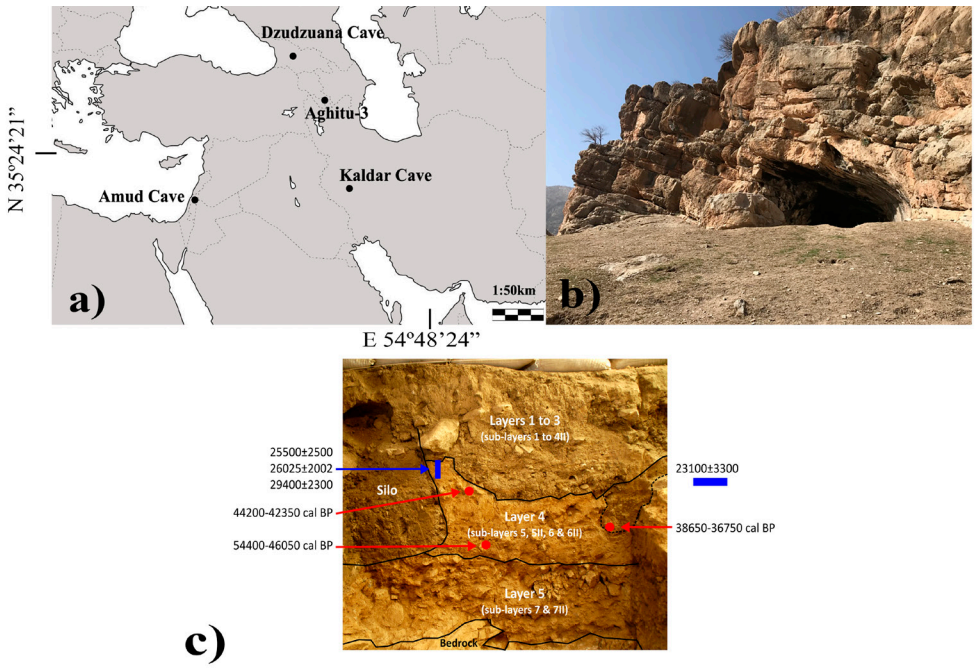


Figure 6.1. a) Locations of the Late Pleistocene sites with rodent studies in the Middle East, including Kaldar Cave. b) General view of the entrance to Kaldar Cave. c) Stratigraphy of the eastern section of Kaldar Cave, including the location and results of the dated samples, from A. Ollé and B. Bazgir (Bazgir et al., 2017).

uppermost parts of this layer, two fireplaces made of clay were recovered and dated through thermoluminescence, yielding ages that ranged from 23,100 ± 3 300 to 29,400 ± 2 300 BP (Bazgir et al., 2017). The dates obtained show that these fireplaces were made or re-used from existing older sediment from the upper part of this layer in the later stages of the Upper Palaeolithic. AMS radiocarbon dates of 38,650–36,750 cal BP, 44,200–42,350 cal BP, and 54,400–46,050 cal BP have been obtained from charcoal material located below this layer (Bazgir et al., 2017; Becerra-Valdivia et al., 2017).

Layers 1 to 3 (including sub-layers 4 and 4II) consist of ashy sediments of a blackish-green colour containing both thick and thin angular limestone clasts. These layers varied in thickness from 60 to 90 cm and contained many phases dating to the Holocene: Islamic and historical eras, Iron Age, Bronze Age, Chalcolithic and Neolithic. However, due to the presence in these layers of bioturbation mainly by burrowing animals, the phases were recognized only by a preliminary study of the potsherds, metal artefacts and some diagnostic lithic artefacts from the lower layers.

This site provides evidence for the Middle to Upper Palaeolithic transition in the Middle East (Bazgir et al., 2017). Moreover, Kaldar Cave has yielded the oldest evidence of *Prunus* spp. in the area, through the study of thirty charcoal remains (Allué et al., 2018), that helps us to reconstruct the environmental conditions, evidencing a wooded vegetation.

3. Material and methods

The rodent fossil remains used in this study, 1112 molars, come from the archaeological excavation campaigns carried out in Kaldar Cave in 2011-2012 and 2014-2015.

The samples comprise disarticulated bones and isolated teeth that were collected in the field by water screening using superimposed 5 and 0.5 -mm mesh screens.

3.1. Taxonomy

In this article we only focus on rodents, because these are one of the most useful tools for palaeoenvironmental and palaeoclimatic reconstructions of archaeological sites, and the other material, as amphibians, squamates, birds, shrews and bats, will be studied later. The taxonomic identification of the rodent remains is based mainly on molar morphology and measurements of the lower m1, the taxonomically most diagnostic tooth.

The remains were identified at a specific level whenever possible, thanks to comparisons with reference collections from the Natural History Museum of London (NHM) and comparative morphological and biometric data from the literature, notably for *Microtus* (Coşkun, 2016; Kryštufek and Shenbrot, 2016; Kryštufek and Vohralík, 2009; López-García, 2011; Rusin, 2017; Shenbrot, Kryštufek et al. 2016; Tesakov, 2016), *Cricetulus* (Bogicevic et al., 2011; Kryštufek et al., 2017; Sándor, 2018), *Mesocricetus* (Kryštufek and Vohralík, 2009), *Meriones* (Coşkun, 1999; Darvish, 2011; Dianat et al., 2017; Kryštufek and Vohralík, 2009; Souttou and Denys, 2012; Stoetzel et al., 2017) , *Allactaga* (Karami et al., 2008; Shenbrot, 2009), *Myomimus* (Gerrie and Kennerley, 2017; Karami et al., 2008; Kennerley and Kryštufek, 2019), *Apodemus* (Amori et al., 2016; Bogicevic et al., 2011; Knitlová and Horáček, 2017; Kryštufek and Vohralík, 2009; López-García, 2011)and *Mus* (Darvish et al., 2006; Kryštufek and Vohralík, 2009; Siahsarvie and Darvish, 2008).

Quantification of taxonomic frequencies was based on standard measures in zooarchaeological analyses, including the number of identified specimens (NISP) and minimum number of individuals (MNI) (Weissbrod and Zaidner, 2014). This latter was estimated using the most abundant skeletal element present in the assemblage (molars in our case).

3.2. Taphonomic remarks

A preliminary study was performed on the Kaldar Cave micromammal remains. This was based on the systematic descriptive method that examines the modifications of prey bones induced by predation, focusing on the degree of digestion observed in teeth during the identification (Andrews, 1990; Fernández-Jalvo et al., 2016b) acting as predators, produce bone accumulations similar to carnivore accumulations. Similarly, small mammal fossil sites are mainly occupation levels of predators (nests or dens. This study showed a significant number of digested teeth (Bazgir et al., 2017), indicating that predation activity was the origin of at least part of the accumulation. According to the different degrees of digestion (mostly light, moderate and, heavy in a few cases) observed in the molars, the predator responsible for this accumulation could be a category 3 predator such as the tawny owl (*Strix aluco*) or the Eurasian eagle owl (*Bubo bubo*). Both species are currently present in the area, have opportunistic hunting habits, and are sedentary, so their prey spectrum is assumed to be a good representation of the ecosystem in which they live.

3.3. Palaeoenvironmental and palaeoclimatic reconstructions

3.3.1. Habitat weighting method

Palaeoecological interpretations derived from faunal data are based on analyses of community composition (Belmaker and Hovers, 2011). The method used for the palaeoenvironmental reconstruction is the habitat weighting method, also named the taxonomic habitat index (Evans et al., 1981; Andrews, 2006; modified by Blain et al., 2008; López-García et al., 2011), which is based on the current distribution of each taxon in the habitat(s) where it can be found nowadays. We assume that the Kaldar Cave species

Species	Fo	Sh	Gr	De	We	St	Ro
Ellobius lutescens			0.33	0.33		0.33	
Ellobius fuscocapillus						1	
Microtus irani			1				
Microtus guentheri			1				
Microtus socialis		0.5				0.5	
Chionomys nivalis							1
Cricetulus migratorius			0.33	0.33		0.33	
Mesocricetus brandti						1	
Meriones persicus		0.33	0.33				0.33
Allactaga sp.				0.5		0.5	
Apodemus sp.	1						
Mus musculus		0.33	0.33		0.33		
Myomimus sp.				1			

Table 6.1. Scores attributed to each rodent species found at Kaldar Cave according to its ecological requirements, used for the habitat weighting method: Forest (Fo), Shrubland (Sh), Grassland (Gr), Desert (De), Wetland (We), Steppe (St) and Rocky (Ro).

had equivalent ecological requirements to their present-day relatives, because the Late Pleistocene species are the same as those today and no extinct fossil species are found in the assemblage. We adapt the method to our studied area, differentiating the following types of habitats: Forest (Fo), a large area covered with trees; Shrubland (Sh), vegetation dominated by shrubs; Grassland (Gr), an open area covered with grass; Desert (De), an area with little precipitation and no vegetation cover; Wetland (We), an area where water covers the soil; Steppe (St), a dry grassy plain; and Rocky (Ro), a rocky or stony substrate. Each species has a score of 1.00, which is divided between the habitats where the species can be found at present (Table 6.1), all the species ranges were taken from the IUCN Red List of Threatened Species (https://www.iucnredlist.org/resources/spatial-data-download).

3.3.2. Bioclimatic Model

In order to reconstruct the climate at Kaldar Cave, we applied the Bioclimatic Model (BM), which was developed by Hernández-Fernández (2001) on the basis of the faunal spectrum, assuming that small- and large-mammal species can be ascribed to ten different climates (Hernández-Fernández, 2001; Hernández-Fernández and Peláez-Campomanes, 2003; Hernández-Fernández et al., 2007). It was first necessary to calculate the climatic restriction index (CRIi=1/n, where i is the climatic zone where the species appear and n is the number of zones where the species is present) and the bioclimatic component (BCi = (Σ CRIi) 100/S, where i is the climatic zone and S is the number of species). To BC a mathematical model is applied as a regression that allows us to calculate climatic parameters (see Appendix 1).

The different climatic groups defined by Hernández-Fernández (2001) and Hernández-Fernández et al. (2007) are: I equatorial; II tropical with summer rains; II/III transition tropical semiarid; III sub-tropical arid; IV, subtropical with winter rains and summer droughts; V, warm temperate with not very severe winters but high humidity; VI, typical temperate with winters that are cold

Species	I	II	II/III	III	IV	V	VI	VII	VIII	IX
Ellobius lutescens								1		
Ellobius fuscocapillus				0.33	0.33			0.33		
Microtus irani					1					
Microtus socialis					0.5			0.5		
Chionomys nivalis					0.25		0.25		0.25	0.25
Cricetulus migratorius					0.33		0.33	0.33		
Mesocricetus brandti					1					
Meriones persicus				0.5	0.5					
Allactaga sp.				0.5				0.5		
Apodemus sp.							1			
Mus musculus	0.11	0.11	0.11	0.11	0.11	0.11	0.11	0.11	0.11	

Table 6.2. Scores attributed to each rodent species found at Kaldar Cave for the bioclimatic model (in accordance with Hernández-Fernández, 2001; Hernández-Fernández et al., 2007). See text for the significance of the Roman numerals corresponding to the climatic groups.

but not very long, but summers that are cool; VII, arid-temperate with large temperature contrasts between winter and summer; VIII, cold-temperate with cool summers and long cold winters (boreal) and IX, artic (Table 6.2).

By means of the BM we were able to estimate the mean annual temperature (MAT), the mean temperature of the coldest month (MTC), the mean temperature of the warmest month (MTW) and the mean annual precipitation (MAP). This method also allowed us to assess whether there were changes in the temperature and precipitation regimes during the Middle to Upper Palaeolithic transition at Kaldar Cave.

4. Results and discussion

4.1. Taxonomic identifications

In total 264 minimum number of individuals (MNI) were identified (Table 6.3 and Fig. 6.2). Some differences were found with respect to the preliminary list previously published by Bazgir et al. (2017). We notably found some new specimens and reconsidered the identifications for *Ellobius talpinus*, *Calomyscus* sp. and *Dryomys* cf. *nitedula*.

Order Rodentia Bowdich, 1821

Rodentia indet.

There are 14 teeth (11 in Layer 4 and 3 in Layer 5) that have not been identified to the family or genus level because they were broken.

Family Cricetidae Fisher, 1817

Subfamily Arvicolinae Gray, 1821

Genus *Microtus* Schrank, 1798

***Microtus* spp.**

Material: 554 isolated teeth**. Layer 1-3:** four isolated teeth; three left lower m1 and one right lower m1. **Layer 4:** 258 isolated teeth; 81 m2; 101 m3, 13 right upper M1, 31 right lower m1; four left upper M1 and 28 left lower m1. **Layer 5:** 292 isolated teeth; 119 m2; 53 m3; nine left upper M1, 51 left lower m1; 10 right upper M1; 50 right lower m1.

***Microtus socialis* Pallas, 1773**

Material: 74 isolated teeth. **Layer 1-3:** three isolated teeth, three right lower m1. **Layer 4:** 36 isolated teeth; 20 right lower m1 and 16 left lower m1. **Layer 5:** 35 isolated teeth; 20



Figure 6.2. Some rodent species identified at Kaldar Cave in comparison with equivalent (analogue) modern specimens from the NHM of London. **1) *Microtus irani***: 1.1-Kaldar Cave, 2014, Layer 5 (sub-layer 7II), E7, 150-156, right lower m1, number 447. 1.2-modern, NHM205207, Iran (Shiraz), right lower m1; **2) *Microtus guentheri***: 2.1-Kaldar Cave, 2014, Layers 1-3 (sub-layer 4II), F6, 97-107, left lower m1, number 17; **3) *Microtus socialis***: 3.1-Kaldar Cave, 2014, Layer 4 (sub-layer 5II), F7, 115-118, right lower m1, number 106. 3.2-modern, NHM631799, Turkey (Amasya); **4) *Chionomys nivalis***: 4.1-Kaldar Cave, 2014, Layer 4 (sub-layer 5), E6, 94-104, left lower m1, number 542. 4.2-modern, NHM71820, Syria, left lower m1; **5) *Ellobius fuscocapillus***: 5.1-Kaldar Cave, 2014, Layer 4 (sub-layer 5II), E6, 125-130, right lower m1, number 157. 5.2-modern, NHM86101513, Afghanistan, right lower m1; **6) *Ellobius lutescens***: 6.1-Kaldar Cave, 2014, Layer 5 (sub-layer 7II), F6, 130-140, right lower m1, number 319. 6.2-NMH916416, Turkey, right lower m1; **7) *Cricetulus migratorius***: 7.1- Kaldar Cave, 2014, Layer 4 (sub-layer 5II), E6, 135-140, left lower m1, number 259. 7.2-modern, NHM773029, Iran, right lower m1; **8) *Mesocricetus brandti***: 8.1-Kaldar Cave, 2014, Layer 5 (sub-layer 7II), F6, 135-145, left upper M1, number 549. 8.2- modern, NHM193461226, Caucasus, left upper M1; **9) *Meriones* cf. *persicus***: 9.1-Kaldar Cave, 2014, Layer 5 (sub-layer 7II), F6, 156-166, left lower m1, number 551. 9.2-modern, NHM510434, Iran, left lower m1; **10) *Allactaga* sp.**: 10.1-Kaldar Cave, 2014, Layer 5 (sub-layer 7II), E7, 141-147, right lower m3, number 203; **11) *Myomimus* sp.**: 11.1- Kaldar Cave, 2014, Layer 5 (sub-layer 7II), E7, 141-147, left lower m1 and m2. 11.2-modern, ***Myomimus personatus***, NHM67623, Turkey, left lower mandible; **12) *Apodemus* sp.**: 12.1-Kaldar Cave, 2014, Layer 4 (sub-layer 5), E6, 94-104, right m1 and m2, number 547; **13) *Mus* cf. *musculus***: 13.1-Kaldar Cave, 2014, Layer 5 (sub-layer 7II), 166-174, left lower m1, number 495. Scale 1 mm

	Layer 5			Layer 4			Layers 1-3		
Taxon	**NISP**	**MNI**	**%**	**NISP**	**MNI**	**%**	**NISP**	**MNI**	**%**
Indet.	3	-	-	11	-	-	-	-	-
Microtus spp.	292	51	52.33	258	31	48.31	4	3	20
Microtus irani	14	9	2.51	0	0	0.00	1	1	5
Microtus guentheri	0	0	0.00	16	9	3.00	1	1	5
Microtus socialis	35	20	6.27	36	20	6.74	3	3	15
Chionomys nivalis	6	3	1.08	17	12	3.18	2	1	10
Ellobius spp.	80	7	14.34	91	8	17.04	2	2	10
Ellobius fuscocapillus	5	4	0.90	5	3	0.94	1	1	5
Ellobius lutescens	10	6	1.79	10	7	1.87	-	-	-
Cricetulus migratorius	5	3	0.90	14	3	2.62	1	1	5
Mesocricetus brandti	7	4	1.25	3	1	0.56	0	0	0
Meriones cf. *persicus*	88	18	15.77	65	17	12.17	3	2	15
Allactaga sp.	1	1	0.18	1	1	0.19	0	0	0
Myomimus sp.	5	3	0.90	0	0	0.00	0	0	0
Apodemus sp.	5	2	0.90	6	3	1.12	2	1	10
Mus cf. *musculus*	2	1	0.36	1	1	0.19	0	0	0
Total	**558**	**132**	100	**534**	**116**	100	**20**	**16**	100

Table 6.3. Representation of the Kaldar Cave rodent species in terms of number of identified specimens (NISP), minimum number of individuals (MNI) and percentage of the NISP (%).

right lower m1 and 15 left lower m1.

***Microtus irani* Thomas, 1921**

Material: 15 isolated teeth. **Layer 1-3:** one isolated tooth, one right lower m1. **Layer 5:** 14 isolated teeth; nine right lower m1 and five left lower m1.

***Microtus guentheri* Danford & Alston, 1880**

Material: 17 isolated teeth. **Layer 1-3:** one isolated tooth, one left lower m1. **Layer 4:** 16 isolated teeth; nine right lower m1 and seven left lower m1.

Description and discussion: all the molars are hypsodont and arhizodont with crown cementum in the re-entrant angles. The enamel differentiation is *Microtus*-like. Six extant species of *Microtus* have been identified in Iran: *Microtus arvalis*, *Microtus irani*, *Microtus kermanensis*, *Microtus socialis*, *Microtus transcaspicus* and *Microtus guentheri* (Aşan Baydemir and Duman, 2009; Golenishchev et al., 2019; Firouz, 2005).

Microtus m1 are characterized by four buccal and five lingual re-entrant angles (Kryštufek and Vohralík, 2009; Tsytsulina et al., 2017) with a posterior lobe (PL), seven triangles (T) and an anterior cap (AC). We identified the Kaldar specimens on the basis of their measurements (Table 6.4), the arrangement and morphology of the triangles, and the AC (which may or may not be connected with the other elements).

In our sample we identified *Microtus* spp., *Microtus socialis*, *Microtus guentheri* and *Microtus irani*.

In *Microtus socialis*, the triangles from T1-T5 are closed, but T6-T7 are parallel and broadly confluent with the AC. *Microtus guentheri* is distinguishable from *Microtus socialis* by the rounded shape of the AC, which

Species	NS	L (Length)		La (Width T4)		Li (Width T5)		Total Width	
Reference collection		**Mean**	**Min-Max**	**Mean**	**Min-Max**	**Mean**	**Min-max**	**Mean**	**Max-Min**
Microtus irani	4	3.06	2.98-3.23	0.42	0.40-0.44	0.64	0.62-0.67	1.06	1.03-1.08
Microtus socialis	69	2.78	2.29-3.34	0.42	0.32-0.51	0.6	0.44-0.73	1.02	0.78-1.19
Microtus arvalis	25	2.72	2.45-2.96	0.39	0.32-0.46	0.6	0.50-0.70	1	0.83-1.13
Microtus guentheri	70	2.58	2.2-3						
Kaldar Cave									
Microtus guentheri	17	2.52	2.18-3.01	0.35	0.27-0.43	0.54	0.40-0.68	0.90	0.70-1.10
Microtus irani	15	2.89	2.52-3.39	0.41	0.37-0.50	0.62	0.54-0.70	1.05	0.92-1.18
Microtus socialis	74	2.54	2.06-3.01	0.37	0.28-0.48	0.55	0.40-0.70	0.92	0.70-1.16

Table 6.4. Measurements of *Microtus* specimens (in mm): NS, number of specimens; L, length; La, T4 width; Li, T5 width.

is of an arhombomorph type (Aşan Baydemir and Duman, 2009), and also by T6-T7, which are separated from the AC. In accordance with the measurements given in Aşan Baydemir et al. (2009), the size of *Microtus guentheri* and *Microtus socialis* is similar. In *Microtus irani*, triangles T1-T5 are closed, but T6-T7 are open and not parallel with one another; moreover, *Microtus irani* is clearly larger than the other species considered in our reference collection and also in our sample. Finally, we include in *Microtus* spp. all the elements that we cannot attribute to one species or another, in particular because of their bad state of preservation (due to digestion, breakage).

Habitat and distribution: *Microtus irani* occupies grasslands in Iran, Turkey and the Caucasus (Kryštufek and Kefelioglu, 2001).

Microtus socialis is found in Russia, Ukraine, the Caucasus, Transcaucasia, Turkestan, Iran and Afghanistan (Tsytsulina et al., 2017), although the range is fragmented. It is a highly colonial species, found in steppe habitats and also in agricultural lands, but extending also to bushy scrubs and uncultivated mountain valleys, as well as to open oak forests on dry hillsides (Tsytsulina et al., 2017).

Microtus guentheri occurs from the southeastern Balkans and Turkey through Syria, Lebanon and Israel, with an isolated range segment in northern Libya, Iran and some parts of Europe (Aşan Baydemir and Duman, 2009). This species is present in dry grasslands with sparse vegetation (Amr, 2015).

Genus *Chionomys* Miller, 1908

***Chionomys nivalis* Martins, 1842**

Material: 25 isolated teeth. **Layer 1-3:** two isolated teeth; one left lower m1 and one right lower m1. **Layer 4:** 17 isolated teeth; 12 right lower m1; five left lower m1. **Layer 5:** six isolated teeth; three left lower m1; three right lower m1.

Description and discussion: in our specimens it can be observed that the first lower molars display five triangles and that the morphology of the anteroconid complex (AC) is characteristic of the *nivalis* morphotype, where triangles T6 and T7 are absent and the anterior cap is of an arrowhead or oval shape, inclined towards the labial part. The enamel is of the *Microtus* type with cement (Krystufek, 2017; Kryštufek and Vohralík, 2009; López-García, 2011). These specimens differ from *Microtus* in that they only have five triangles, and the morphology of the AC is the other

main characteristic of this species that helps us to differentiate it from *Microtus*.

Habitat and distribution: *Chionomys nivalis* has a global distribution extending from southwestern Europe through southeastern Europe to the Caucasus, Turkey, Israel, Lebanon, Syria and Iran. In Iran it is distributed in the north and also in the west (Shenbrot and Krasnov, 2005; Krystufek, 2017). This is the only *Chionomys* species occurring today in Iran, but two other species (*C. gud, C. roberti*) are represented a little further north (northeastern Turkey, southern Georgia).

Regarding its habitat, it is present in open rocky areas, typically above the tree line and with scarce vegetation cover (Amori, 1999).

Genus *Ellobius* Fischer, 1814

***Ellobius* spp.**

Material: 173 isolated teeth. **Layer 1-3:** two isolated teeth; two left lower m1. **Layer 4:** 91 isolated teeth; seven indet.; eight right lower m1; five left lower m1; 11 upper M1; 43 m2; 17 m3. **Layer 5:** 80 isolated teeth; seven left lower m1; three upper M1; 45 m2; 25 m3.

***Ellobius fuscocapillus* Blyth, 1843**

Material: 11 isolated teeth. **Layer 1-3:** one isolated tooth; one right lower m1. **Layer 4:** five isolated teeth; two right lower m1; three left lower m1. **Layer 5:** five isolated teeth; four left lower m1 and one right lower m1.

***Ellobius lutescens* Thomas, 1897**

Material: 20 isolated teeth. **Layer 4:** 10 isolated teeth; seven right lower m1 and three left lower m1. **Layer 5:** 10 isolated teeth; four left lower m1 and six right lower m1.

Description and discussion: 204 isolated teeth show the typical traits of the genus *Ellobius* (Miller, 1896; Hinton, 1962, Kretzoi, 1969; Coşkun, 2016; Kryštufek & Shenbrot, 2016; Kryštufek and Vohralík, 2009; Rusin, 2017; Shenbrot et al., 2016; Tesakov, 2016). *Ellobius* molars are notably characterized by the presence of roots that are well visible in adults and old individuals, but not always apparent in young specimens (Coşkun, 2016). Moreover, *Ellobius* molars lack cement in the re-entrant angles. The *Ellobius* m1 is composed of the anterior cap (AC), five triangles (T) with three buccal and four lingual salient angles, and one posterior lobe (PL). Both M3 and m3 are reduced and smaller than the other molars, with three triangles on the labial side and two triangles on the lingual side. M1 has three inner and outer folds, and M2 and M3 have two inner and two outer re-entrant folds. The first and second upper molars have three triangles on the lingual and labial sides. However, the re-entrant angle between the first and the second triangles on the lingual side is more superficial (Gharkheloo and Kıvanç, 2003).

In Iran, the genus *Ellobius* is currently represented by three species: *Ellobius fuscocapillus*, *Ellobius lutescens* and *Ellobius talpinus* (Firouz, 2005; Kryštufek & Shenbrot, 2016; Kryštufek and Vohralík, 2009; Moradi Gharkheloo, 2003; Rusin, 2017; Shenbrot et al., 2016). The m1 is quite similar among these species, but there are some differences that can help us to differentiate them.

The AC is broad in *Ellobius lutescens*, narrow in *Ellobius talpinus* and elongated in *Ellobius fuscocapillus* (Maul et al., 2015b) Gekkota indet., Lacertidae indet. (2-3 taxa. The distance between T4 and T5 (W) and the total length (L) differ among the species (Table 6.5). We have observed in modern specimens from the Natural History Museum of London that *Ellobius fuscocapillus* is the largest and *Ellobius talpinus* the smallest.

In our sample we identify as *Ellobius* spp. those m1s that are too broken or digested to distinguish, as well as all the m2, m3, M1, M2 and M3 because of the lack of discriminant characters. The identification of *Ellobius*

		Ellobius fuscocapillus				*Ellobius lutescens*			*Ellobius talpinus*
		Layer 5, NISP=5	Layer 4, NISP=5	Layer 1-3, NISP=1	NHM, NISP=12	Layer 5, NISP=9	Layer 4, NISP=10	NHM, NISP=14	NHM, NISP=14
L	Min-Max	3.29-3.84	3.73-3.74	-	3.06-4.05	3.08-3.32	3.05-3.4	3.07-3.3	2.86-3.35
	Mean	3.45	3.74	-	3.53	3.28	3.29	3.21	3.12
W	Min-Max	1.32-1.51	1.40-1.54	-	1.3-1.59	1.20-1.45	1.13-1.48	1.11-1.52	1.09-1.72
	Mean	1.45	1.48	1.5	1.41	1.34	1.32	1.34	1.24

Table 6.5 Measurements of *Ellobius* specimens (in mm): L, total length; W, width. NHM: Natural History Museum of London. NISP: number of identified specimens.

lutescens and *Ellobius fuscocapillus* in the Kaldar material is based on the morphology of the AC and the measurements (L and W). We do not identify *Ellobius talpinus* in our sample, as no specimen displays morphological features characteristic of this species, such as the narrow AC, and because the measured specimens are larger than *E. talpinus*.

Habitat and distribution: *Ellobius* species frequent steppes, grasslands and semi-deserts in eastern Europe and central Asia; these fossorial species are specialised in subterranean life (Coşkun, 2016; Kryštufek and Vohralík, 2009). *Ellobius lutescens* is a Palaearctic species distributed across Iran, Iraq, Azerbaijan, Armenia, Transcaucasia and East Anatolia (Thomas, 1905; Ellerman and Morrison-Scott, 1951; Darlington, 1957; Osborn, 1962; Walker, 1964; Lay, 1967; Hassinger, 1973; Roberts, 1977; Corbet, 1978; Corbet and Hill, 1991; Wilson and Reeder, 2005; Coşkun, 1997, 2016; Nowak, 1999; Kryštufek & Shenbrot, 2016). In Iran, this species is found in mountain grasslands, sandy semi-deserts and steppe areas (Kryštufek & Shenbrot, 2016; Tesakov, 2016). *Ellobius fuscocapillus* shows a wide range across eastern Iran, Turkmenistan, Afghanistan and Pakistan. In Iran it is found in open steppes with loose soil (Shenbrot, Kryštufek & Molur, 2016).

Subfamily Cricetinae Fischer, 1817

Genus *Cricetulus* Milne-Edwards, 1867

***Cricetulus migratorius* Pallas, 1773**

Material: 19 isolated teeth. **Layer 1-3:** one isolated tooth; one right lower m3. **Layer 4:** 13 isolated teeth; three left lower m1, two left upper M2; three right lower m1, three right upper M1 and two right upper M2. **Layer 5:** five isolated teeth; three left lower m1 and two right lower m1.

Description and discussion: the first molars (m1 and M1) are brachyodont and cuspidate, with two longitudinal series of cusps. Each series of cusps consists of three pairs. The m1 and M1 are the largest and the m3/M3 the smallest. The lower m3 only has two pairs of cusps (Kryštufek and Vohralík, 2009). We identify *Cricetulus migratorius* in all the layers of Kaldar Cave in accordance with the measurements and identification keys for molars based on the morphology and arrangement of the tubercles and cusps provided by Kryštufek and Vohralík (2009). We also draw comparisons with the reference collection from Iran, Afghanistan and Azerbaijan housed in the Natural History Museum of London. The grey hamster, or migratory hamster, is the smallest hamster

species (Bogicevic et al., 2011; Sándor, 2018).

Habitat and distribution: *Cricetulus migratorius* extends from eastern Europe through Russia and central Asia to Mongolia and western China (Kryštufek et al., 2017; Kryštufek and Vohralík, 2009). In Iran, this species is found all over the country. The habitats of this species are mostly dry grasslands, steppes and semi-deserts. Arid areas with relatively sparse vegetation are preferred (Kryštufek et al., 2017; Maul et al., 2015a).

Genus *Mesocricetus* Nehring, 1898

***Mesocricetus brandti* Nehring, 1898**

Material: 10 isolated teeth. **Layer 4:** three isolated teeth; one left upper M1, one right lower m1 and one right upper M1. **Layer 5:** seven isolated teeth; four left upper M1, one right upper M2 and two right upper M1.

Description and discussion: the specimens from Kaldar Cave are attributed to *Mesocricetus brandti* on the basis of the size and morphology of the teeth. The molars present a similar morphological pattern to *Cricetulus migratorius*, but are significantly larger in size. The first molars have six tubercles, the second and third molars only four. The largest molars are m1 and M1, whereas m2/M2 and m3/M3 are reduced (Kryštufek and Vohralík, 2009). In Iran we also find *Mesocricetus raddei*, which presents a similar morphology of the teeth to *Mesocricetus brandti*, but compared with the NHM reference collection of the latter, *Mesocricetus raddei* is bigger

Habitat and distribution: *Mesocricetus brandti* has the largest distributional area of the species belonging to the genus *Mesocricetus*, ranging from Anatolia, Transcaucasia (Armenia, Georgia and Azerbaijan) and southeast Dagestan to northwest Iran (Qazvin in the east, Lorestan in the south; Lay, 1967). This species is found at altitudes from sea level up to 2,600 m. However, the primary range is from 1,000-2,200 m. *Mesocricetus brandti* is found in arid and semi-arid steppe habitats in lowlands and in mountainous areas (Kryštufek et al., 2015; Kryštufek and Vohralík, 2009; Neumann et al., 2017).

Family Muridae Illiger, 1811

Subfamily Gerbillinae Gray, 1825

Genus *Meriones*, Illiger 1811

***Meriones* cf. *persicus* Blanford, 1875**

Material: 157 isolated teeth. **Layer 1-3:** three isolated teeth; two left upper M1 and one right lower m1. **Layer 4:** 65 isolated teeth; 21 m2; four m3; 17 left lower m1; eight right upper M1, five left upper M1; 10 right lower m1. **Layer 5:** 88 isolated teeth; eight m3; 21 m2; 18 left lower m1, 10 left upper M1, 16 right upper M1 and 15 right lower m1.

Description and discussion: the genus *Meriones* is one of the most diverse among the tribe Gerbillini in the Palaearctic region, particularly in arid regions of Asia (Darvish et al., 2011; Denys, 2017). The *Meriones* species reported in Iran are: *Meriones crassus*, *Meriones hurrianae, Meriones lybicus, Meriones meridianus, Meriones persicus, Meriones tristrami, Meriones vinogradovi* and *Meriones zarudnyi* (Darvish, 2011; Dianat et al., 2017; Kryštufek and Vohralík, 2009; Souttou and Denys, 2012).

The material from Kaldar Cave attributed to the genus *Meriones* displays the typical morphology of this group, including semi-hypsodont molars with prismatic enamel triangles linked by a longitudinal crest and with no trace of cusps. In our sample, we identify first upper molars (M1) with three roots, which is characteristic of *Meriones persicus* and *Meriones tristrami*. Unfortunately, the dental morphology of *Meriones persicus* and *Meriones tristrami* is very similar; there are three roots in m1, the second molars have

two transverse plates and two roots, whereas the third molars are simple and rounded with a single root (Coşkun, 2016; Kryštufek and Vohralík, 2009).

Given its current distribution and the morphological traits observed in the reference collection from Iran, Azerbaijan and Pakistan housed in the Natural History Museum of London, we provisionally attribute our specimens to *Meriones* cf. *persicus,* especially in the light of the number of roots and the morphology of M1 and m1, pending a revision of the Middle Eastern species of the genus.

Habitat and distribution: the genus *Meriones* is distributed across North Africa, Central Asia, Transcaucasia, Turkey and Pakistan (Darvish et al., 2014; Stoetzel et al., 2017). It lives mostly in dry steppes of short or tall grass, on open hillside, among rocky outcrops in desolate steppes, or in open dry meadows. The distribution of *Meriones persicus* ranges from the Caucasus (including the southeastern foothills of the Lesser Caucasus and the Talysh Plateau in Azerbaijan) in the west, through northeastern Iraq and Iran to Turkmenistan, Afghanistan (Habibi, 2004) and Pakistan, where it is widely distributed. It generally occurs in arid, rocky or mountainous regions (Kryštufek and Vohralík, 2009; Molur & Sozen, 2016).

Family Dipodidae Fischer, 1817

Genus *Allactaga* Cuvier, 1837

***Allactaga* sp.**

Material: two isolated teeth. **Layer 4:** one indet. **Layer 5:** one right lower m3.

Description and discussion: this rodent group is poorly known in the Middle East (Shenbrot, 2009) and sometimes there is a size overlap between the species. In our sample, we only found two items attributed to *Allactaga* sp. on the basis of the complete lower m3, which presents a morphology with two inner folds and one outer fold; the other tooth is broken, which prevents any precise identification.

Habitat and distribution: in Iran four species are currently present: *Allactaga elater*, *Allactaga euphratica*, *Allactaga firouzi* and *Allactaga hotsoni* (Karami et al., 2008). The different species are morphologically very close and remain poorly studied. They are mainly found in steppe vegetation and semi-desert areas (Shenbrot, 2009).

Family Gliridae Thomas, 1897

Genus *Myomimus* Ognev, 1924

***Myomimus* sp.**

Material: five isolated teeth, **Layer 5:** five isolated teeth, one right lower m1, three right lower m2 and one left lower m2.

Description and discussion: the genus *Myomimus* is present in Iran with two species, *Myomimus personatus* and *Myomimus setzeri* (Firouz, 2005; Gerrie & Kennerley, 2017; Karami et al., 2008; Kennerley & Kryštufek, 2019). Regarding the remains found at Kaldar, the m1 is of a trapezium-like shape, and its anterior part tends to be narrower than the posterior part. The m1 has three roots, two in the anterior part and one in the posterior part. The m2 is subrectangular, and its occlusal pattern is simpler than in the m1. There are three roots in total, two in the anterior part and one in the posterior part (Kaya and Kaymakçı, 2018; Kryštufek and Vohralík, 2009). The two species are similar to one another and poorly studied. Consequently, we were unable to identify the Kaldar material precisely. Moreover, the reference collection of the Natural History Museum of London only houses *Myomimus personatus* specimens, which could therefore not be compared with *Myomimus setzeri*.

Habitat and distribution: these species are not well known as regards their distribution. They are mainly found in desert

areas (Gerrie & Kennerley, 2017; Kennerley & Kryštufek, 2019).

Family Muridae Illiger , 1811

Genus *Apodemus* Kaup, 1829

***Apodemus* sp.**

Material: 13 isolated teeth. **Layer 1-3:** two isolated teeth; one left lower m1 and one left lower m2; **Layer 4:** six isolated teeth; three left lower m1, two right lower m1 and one left upper M1. **Layer 5**: five isolated teeth; two left lower m1, one right lower m1, one right upper M1 and one m2.

Description and discussion: the first lower molar (m1) can be seen to present a low occlusal surface with six main cusps. The anterolabial and posterolabial cusps of m1 converge in an X-shape. The posterior cusp of m1 is low, rounded and well developed, with two or three secondary cusps in the labial part, and a mesial tubercle. We attribute the remains found in Kaldar Cave to *Apodemus* sp. because they present the traits characteristic of the genus *Apodemus* (Amori et al., 2016; Bogicevic et al., 2011; Knitlová and Horáček, 2017; Kryštufek and Vohralík, 2009; López-García, 2008).

Habitat and distribution: five *Apodemus* species are currently recognized in Iran: *A. hyrcanicus*, *A. flavicollis*, *A. witherbyi, A. avicennicus* and *A. uralensis*, all belonging to the *Sylvaemus* sub-genus (Jangjoo et al., 2011). *Apodemus* has a large distribution range extending from Great Britain across much of continental Europe to the Urals. It also extends east through Turkey to western Armenia, the Zagros Mountains of Iran and south to Syria, Lebanon and Israel. It inhabits a variety of woodland habitats (Amori et al., 2016).

Genus *Mus* Linnaeus, 1758

***Mus* cf. *musculus* Linnaeus, 1758**

Material: three isolated teeth. **Layer 4**: one isolated tooth; one left upper M1. **Layer 5:** two isolated teeth; one indeterminate and one left lower m1.

Description and discussion: as in other murines, the first upper molar (M1) has three rows of tubercles: the first (t1, t2, t3) and second (t4, t5 and t6) groups situated in the anterior part have three tubercles, and the third group (t7 and t9) has two tubercles (Darvish et al., 2006). In Iran (Kryštufek and Vohralík, 2009) both *Mus musculus domesticus* and *Mus macedonicus* may be found.

The specimens from Kaldar Cave fit well with *M. musculus* as regards the upper M1 morphology: the lingual row of cusps (t1 and t4) is shifted posteriorly; cusp t7 is reduced to an enamel ridge; distal cusps t8 and t9 leave no space for a posterior cingulum or posterolabial cusp t12 (Siahsarvie and Darvish, 2006). The dental ends of the mesial and central cusps on m1 fuse early; the mesiolabial cusp is small. Upper molars normally have three roots each, one lingual and two labial, whereas lower molars are two-rooted (one anterior and one posterior) (Kryštufek and Vohralík, 2009). Despite these observations, bearing in mind the high intra-specific morphological variability, the low quantity of material and the bad state of preservation of some teeth (Fig. 6.2.13), we only attribute the Kaldar material to *M.* cf. *musculus*.

Habitat and distribution: *Mus musculus* is a commensal species, well distributed throughout the world: it is present over all the continents except Antarctica. It is found in a wide range of habitats but tends not to be found in forest and deserts. *Mus musculus* is ecologically highly opportunistic but a weak competitor; it can cope with aridity and can also expand into the desert (Kryštufek and Vohralík, 2009). It is also found in arid habitats along the border with Syria and Iraq, in desert landscapes and near the Euphrates River

(Kryštufek & Vohralík, 2009; Denys, 2017).

4.2. Past landscape and climate at Kaldar Cave

The small-mammal assemblages from Layers 4 and 5 of Kaldar Cave are dominated by the genus *Microtus* (60 individuals in Layer 4 and 79 in Layer 5), followed by *Ellobius* in Layer 4 (17 individuals) and *Meriones* cf. *persicus* (17 individuals in Layer 4 and 18 in Layer 5). These species indicate that the environment in the area was mainly composed of open dry and steppe areas, although we also found *Apodemus* sp. and *Mus* cf. *musculus*, which are related rather to a dense vegetation cover (including trees/bush). All the species identified at Kaldar Cave still occur in the area today.

Layers 1-3 do not yield enough material to draw palaeoclimatic inferences (MNI < 30). For Layers 4 and 5, the Bioclimatic Model shows similar results (Table 6.6). It should be pointed out that some species are not included in the BM data matrix, such as *Myomimus* (present in Layer 4) and *Microtus guentheri* (Layer 5), because their values did not appear in the BM and could not be used in the analysis. The BM based on the small mammals from Kaldar Cave suggests lower temperatures and lower precipitation than at present in both Layers 4 and 5 (Table 6.6). The MAT is around 6ºC lower, and there is a higher temperature amplitude between maximum and minimum mean temperatures. This indicates that Layers 4 and 5 of Kaldar Cave were deposited during a colder period, which is not in agreement with the preliminary interpretations of Bazgir et al. (2017) suggesting a temperate "interstadial".

The climate in Khorramabad nowadays is warm an temperate. The average mean annual temperature is 16.90ºC, the maximum mean temperature occurs in July with 29.60ºC and the minimum mean temperature is in January with 5ºC (https://en.climate-data.org/asia/iran/lorestan/khorramabad-764550/). This contrast with the climactic conditions inferred form the BM on Kaldar Cave with lower temperatures and drier conditions.

Applying the habitat weighting method, our data show a palaeoenvironment mainly composed of steppes in both levels. In Layer 4, grasslands are also well represented, notably through the presence of *Microtus guentheri*. In Layer 5, deserts are the second most represented habitat, thanks to the considerable presence of *Myomimus* sp. The proportion of rocky areas is also significant, indicated by the presence of *Chionomys nivalis* and *Meriones* cf. *persicus* (Figure 6.3).

There thus seems to be no major palaeoenvironmental or palaeoclimatic change that can explain the cultural shift between Layer 5 (Middle Palaeolithic) and 4 (Upper Palaeolithic). However, Layer 5 appears slightly colder and drier than Layer

	Layer 5	SD	Layer 4	SD	Current values
Mean annual temperature	10.90 ºC	3.39	11.73ºC	3.39	16.90 ºC
Maximum mean temperature	23.45 ºC	4.77	23.10ºC	4.77	29.60 ºC
Minimum mean temperature	-1.69 ºC	4.66	0.25ºC	4.66	5ºC
Mean annual precipitation	258.68mm	533.24mm	104.08mm	533.24mm	488mm

Table 6.6. Bioclimatic model estimates for Kaldar Cave. SD, standard deviation. Current values obtained from: https://en.climate-data.org/asia/iran/lorestan/khorramabad-764550/.

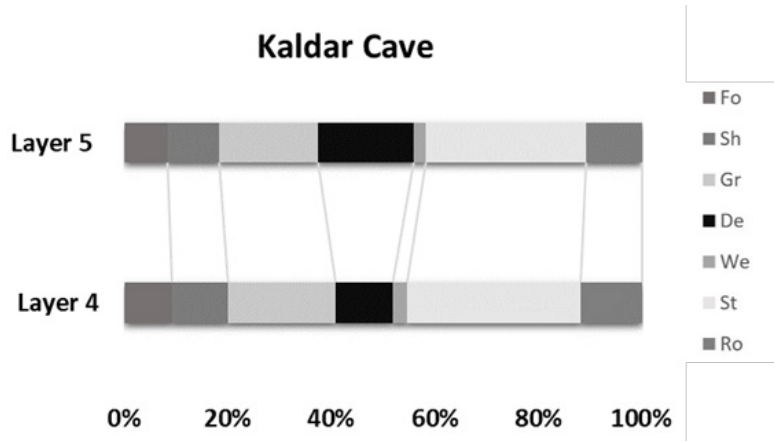


Figure 6.3. Results of the habitat weighting method for Kaldar Cave (Layer 4 and Layer 5). Forest (Fo), Shrubland (Sh), Grassland (Gr), Desert (De), Wetland (We), Steppe (St) and Rocky (Ro).

4, with a higher proportion of desert habitats.

We can compare these results with previous studies carried out in Kaldar Cave using other palaeoenvironmental proxies. Charcoal analyses (Allué et al., 2018; Bazgir et al., 2017) indicate that there were active water sources or flows, with specific plant communities characteristic of open forest growing in cool and dry conditions (Allué et al., 2018). The presence of forested areas is also supported by the large mammals, with the presence of *Sus scrofa*, *Capreolus* sp. and *Cervus elaphus* (Bazgir et al., 2017). Several amphibian and squamate species have also been found (Bazgir et al., 2017): a toad (*Bufo* sp.), an agamid lizard (Agamidae indet.), a gecko (Gekkonidae indet.), a skink (Scincidae indet.), a lacertid (Lacertidae indet.), a glass lizard (*Pseudopus* sp.), a sand boa (*Eryx* sp.), possibly six types of colubrine snakes (Colubrinae indet.), a cobra (Elapidae indet.), and a viper (Viperidae indet.). Most of these taxa (Agamidae, *Eryx* and Elapidae) live in savannahs, steppes and deserts, with a way of life always linked with warm arid areas in rocky or sandy environments. *Pseudopus* lives in dry and bushy environments, sometimes in open woodlands, but avoids dense forest areas (Bazgir et al., 2017).

Our results based on small mammals, combined with previous studies of other proxies, thus suggest a mosaic landscape alternating between dry-steppe areas and wooded patches. Nowadays, the vegetation in the Zagros is a montane grassland-woodland characterised by steppe of grassland and herbs with occasional to fairly common trees. The principal local trees are deciduous oaks and junipers, with maples, walnut, almond and ash at middle elevations, and *Pistacia* and *Olea* in drier areas (Fiacconi and Hunt, 2015). Thus, the landscape during the Middle and Upper Pleistocene at Kaldar Cave was similar to that today, despite a colder climate.

4.3. Kaldar Cave in the Middle Eastern context

Kaldar Cave is situated in the Khorramabad Valley, which played a significant role in human adaptation and dispersal during the Quaternary. Some other caves close to Kaldar, such as Gilvaran, Ghamari and Gar Arjene rock shelter, have yielded Mousterian and Aurignacian occupations (Bazgir et al., 2014). Moreover, surveys in Kermanshah have also

documented Middle and Upper Palaeolithic sites (Heydari-Guran and Ghasidian, 2020). None of them has given rise to small-mammal studies. However, Gilvaran Cave has been studied from a palaeoenvironmental point of view through charcoal analyses (Allué et al., 2018), showing a similar pattern to Kaldar, where *Prunus* is also present and indicates the presence of open forest areas. Similarly, other proxies such as pollens and charcoals have been analysed at Shanidar (Campana and Crabtree, 2019; Fiacconi and Hunt, 2015) and Gilvaran (Allué et al., 2018), indicating similar environmental conditions to Kaldar.

Other studies based on small mammals from the Middle East have been performed in Qesem Cave (Maul et al., 2015a; Smith et al., 2015), Hummal (Maul et al., 2015b), Azokh Cave (Fernández-Jalvoa, 2016), Aghitu-3 Cave (Frahm, 2019; Kandel et al., 2017; Nishiaki and Akazawa, 2018), Nesher Ramla (Weissbrod and Zaidner, 2014), Amud Cave (Belmaker and Hovers, 2011), Dzudzuana Cave (Belmaker et al., 2016) and Karain Cave (Demirel et al., 2011). These studies did not use HW or the BM for their palaeoclimatic and palaeoenvironmental reconstructions, and the sites are not always contemporary with Kaldar, except Amud Cave (Belmaker and Hovers, 2011), Aghitu-3 (Djamali et al., 2008; Kandel et al., 2017) and Dzudzuana Cave (Belmaker et al., 2016) (Table 6.7).

Most of these studies highlight problems in identifying Middle Eastern rodent species, as faced in the present work. There are some studies of present-day taxonomy and systematics in Iran, Turkey, Israel, Jordan, Lebanon and Syria (Abi-said et al., 2014; Darvish et al., 2000; Haddadian Shad et al., 2014; Kopij and Liven-schulman, 2013; Obuch and Khaleghizadeh, 2012; Shehab et al., 2013), but these are mostly based on skull morphology and thus not applicable in archaeological or palaeontological contexts where the remains are broken. Very few studies provide descriptions of molars with comparative elements, allowing for the correct identification of fossil specimens.

Site/Author	Layer	Human culture	Chronology	Environmental conditions	Rodent
Amud Cave (Belmaker and Hovers, 2011)	B4	Neanderthals	68.5 ± 3.4ka	Grassland vegetation	*Microtus guentheri*
	B2-B1	Neanderthals	56.5 ± 3.5, 57.6 ± 3.7,respectively	Woodland	*Apodemus* cf. *mystacinus* and *Mus macedonicus*
Dzudzuana Cave (Belmaker et al., 2016)	Unit C	Modern human	27-24ka cal BP	Mild and humid	*Microtus*, *Ellobius*, *Arvicola*, *Apodemus* and *Allactaga*.
Aghitu-3 (Djamali et al., 2008; Kandel et al., 2017)	Level VII-III	Modern human	The oldest layer is VII with a chronology between 39-36,000 cal BP and the most recent is layer III, between 29-24,000 cal BP	This sequence documents that the climate becomes colder	*Microtus* spp., *Chionomys* sp., *Arvicola amphibius* and *Ellobius lutescens*

Table 6.7. Comparison between Middle Eastern sites with small-mammal studies

	Kaldar Cave			Aghitu-3				Dzudzuana
Taxon	**Layers 1-3**	**Layer 4**	**Layer 5**	**VII**	**VI**	**V-IV**	**III**	**Unit C**
Microtus spp.	X	X	X	X	X	X	X	
Microtus cf. *arvalis*								X
Microtus irani	X		X					
Microtus guentheri	X	X						
Microtus socialis	X	X	X					
Chionomys nivalis	-	X	X	X	X	X	X	X
Clethrionomys glareolus								X
Ellobius spp.	X	X	X					
Ellobius fuscocapillus	X	X	X					
Ellobius lutescens	-	X	X	X				X
Cricetus cricetus								X
Cricetulus migratorius	X	X	X	X		X	X	X
Mesocricetus brandti		X	X	X	X	X	X	X
Meriones cf. *persicus*	X	X	X					
Allactaga sp.		X	X	X	X		X	X
Myomimus sp.			X					
Apodemus sp.	X	X	X					X
Mus musculus		X	X					X
Arvicola amphibius				X	X	X	X	X

Table 6.8. Comparison of the small-mammal lists from several Upper Palaeolithic sites in the Middle East.

In this context, comparison with modern specimens from museum collections of genetically typed specimens is crucial to establish a correct taxonomic reference.

Palaeoenvironmental inferences have been drawn on the basis of small-mammal studies, as well as palynological and anthracological analyses. During the Upper Pleistocene, small-mammal compositions differ from one site to another (Belmaker et al., 2016; Kandel et al., 2017) (Table 6.8), probably because the sites are not exactly contemporaneous and are likely to belong to different eco-regions. It is noteworthy that the genera *Microtus*, *Chionomys*, *Cricetulus*, *Mesocricetus*, *Ellobius* and *Allactaga* are represented in all the sites, allowing us to reconstruct the species communities of this region. Kaldar is the most diverse site in terms of small-mammal species.

We applied the habitat weighting method at other Middle Eastern sites where small-mammal studies have been performed, namely Aghitu-3 and Dzudzuana Cave, but these are located in other eco-regions (Figure 6.1a). Aghitu-3 is located in Armenia, at an elevation of 1601 m a.s.l. and the current climate is continental with considerable seasonality in temperature. Dzudzuana Cave is located in Georgia, at an elevation of 560 m a.s.l., and the current climate is warm and temperate. The estimations obtained with the habitat weighting method (Figure 6.4) show similar environmental conditions between Kaldar Cave and Aghitu-3, where the landscape is dominated by steppe

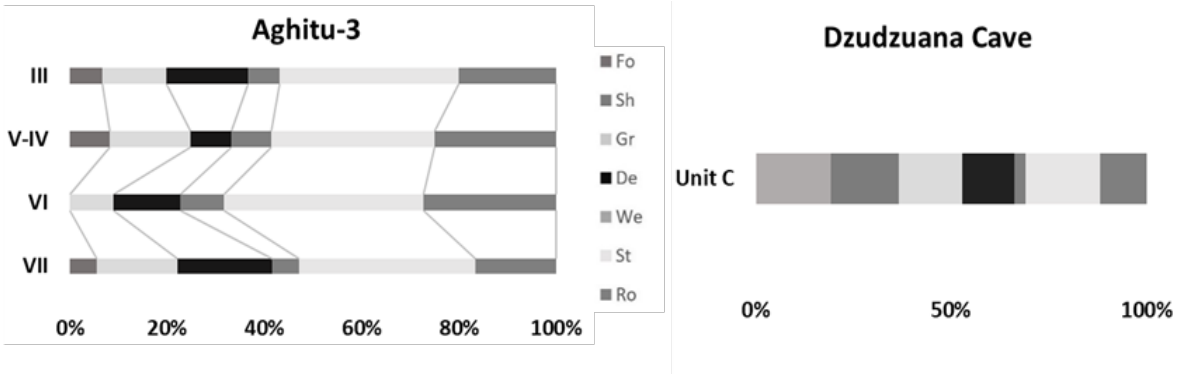


Figure 6.4. Results of the habitat weighting method for Aghitu-3 and Dzudzuana Cave. Forest (Fo), Shrubland (Sh), Grassland (Gr), Desert (De), Wetland (We), Steppe (St) and Rocky (Ro).

(indicated by the presence of *Ellobius lutescens*, *Mesocricetus brandti*, *Cricetulus migratorius* and *Allactaga*), with a relatively high percentage of grassland and forests.

To ascertain the palaeoclimatic conditions, we calculated and directly compared our results with Aghitu-3 and Dzudzuana Cave using the bioclimatic method (Table 6.9). The results obtained for Aghitu-3 show higher temperatures and precipitation than at present, whereas Dzudzuana Cave shows the same pattern as Kaldar Cave, with drier conditions and lower temperatures than today. For Amud Cave, it was not possible to calculate HW and BM, but data from the literature (Belmaker and Hovers, 2011) indicate a grassland environment similar to the one that we reconstructed at Dzudzuana Cave.

5. Conclusions

This work represents the first study of a Late Pleistocene rodent assemblage from the Middle East with palaeoenvironmental and palaeoclimatic reconstructions, using and adapting the habitat weighting method and the bioclimatic model to this area. We identified 1112 rodent remains, corresponding to a minimum number of 264 individuals. The rodent assemblage is composed of 13 taxa: six arvicoline (*Microtus socialis, Microtus irani, Microtus guentheri, Chionomys nivalis, Ellobius fuscocapillus* and *Ellobius lutescens*), two cricetine (*Cricetulus*

	Aghitu-3						Dzudzuana Cave		
	VII	VI	V-IV	III	SD	Current Values	Unit C	SD	Current Values
Mean annual Temperature	15.46 ºC	19.44 ºC	19.21 ºC	17.87 ºC	3.39	8.5 ºC	5.09 ºC	3.39	9.7 ºC
Maximum mean temperature	23.59 ºC	24.44 ºC	24.09 ºC	24 ºC	4.77	20.2 ºC	18.55 ºC	4.77	20.3 ºC
Minimum mean temperature	7.31 ºC	14.67 ºC	14.72 ºC	11.96 ºC	4.66	-3.8 ºC	-8.26 ºC	4.66	-1.6 ºC
Mean annual precipitation	1169.04 mm	1729.48 mm	1825.99 mm	1484.60 mm	533.24	532 ºC	194.98mm	533.24	868mm

Table 6.9. Estimates using the bioclimatic method for Aghitu-3 and Dzudzuana Cave. SD, standard deviation. Current values obtained from Kandel et al. (2017) for Aghitu-3 and https://es.climate-data.org/asia/georgia/imereti/jria-414325/?amp=true for Dzudzuana Cave.

migratorius and *Mesocricetus brandti*), one glirid (*Myomimus* sp.), one gerbilline (*Meriones* cf. *persicus),* one dipodid (*Allactaga* sp.) and two murine species (*Apodemus* sp. and *Mus* cf. *musculus*). Augmenting the preliminary analysis of the material (Bazgir et al., 2017), new species were identified, such as *Microtus socialis*, *Microtus irani*, *Microtus guentheri*, *Ellobius fuscocapillus* and *Meriones* cf. *persicus*. We also reconsidered the identification of *Ellobius talpinus*, *Calomyscus* sp. and *Dryomys* cf. *nitedula*, based on modern specimens from museum collections and measurements; this is why they do not appear in the new faunal list of Kaldar Cave.

Given the scarcity of studies in this biogeographical region, we encountered some difficulties in the identification of species, which could slightly affect the palaeoenvironmental and palaeoclimatic interpretations. In order to counter these potential errors, further studies of small mammals in this region are necessary, as well as research on discriminant characters in molars, using reference collections including genetically typed specimens.

The palaeoecological analysis of the rodents from Kaldar Cave revealed lower temperatures and lower precipitation than present-day conditions, and an environment mainly composed of dry steppes with patches of forested areas. The results obtained are supported by palynological, anthracological and large-mammal studies. At a broader geographical scale, colder conditions were also inferred at Dzudzuana Cave. The genera *Microtus*, *Chionomys*, *Cricetulus*, *Mesocricetus*, *Ellobius* and *Allactaga* are present at all the Middle East sites (Aghitu-3, Dzudzuana and Amud) during the Upper Pleistocene, that have yielded small mammals, allowing us to reconstruct the rodent communities of the area.

Considering all the results from Kaldar Cave and other contemporaneous sites, we can conclude that both Neanderthals and AMH lived in dry steppes with patches of forested areas, without major environmental changes occurring between the Middle and the Late Palaeolithic. Climatic shifts during the MIS 4-3 transition were of a magnitude that did not have a major impact on small mammals in the region, suggesting that climate change may not have had the hypothesized effect on the Neanderthal extinction in the Levant.

Acknowledgments: I. Rey-Rodriguez is the beneficiary of a PhD scholarship funded by the Erasmus Mundus Program (IDQP). J.M. López-García was supported by a Ramón y Cajal contract (RYC-2016-19386) with financial sponsorship from the Spanish Ministry of Science, Innovation and Universities. M. Fernández-García is the beneficiary of a PEJ grant (PEJ2018-005222-P) funded by the Spanish National Youth Guarantee System and the European Social Fund. This work was developed within the framework of the projects 2017SGR859, 2017SGR840 and 2017SGR1040 (AGAUR, Generalitat de Catalunya), and 2018PFRURVB291 (Univ. Rovira i Virigli). We thank the head of the Research Institute of Cultural Heritage and Tourism (RICHT) (Dr. B. Omrani) and the head of the Iranian Center for Archaeological Research (ICAR) (Dr. R. Shirazi) for providing us with the necessary support and permissions in studying the materials. We thank the head of the Lorestan Cultural Heritage, Handicraft and Tourism Organization (Mr. A. Ghasemi) for all his support. We also thank the head of International Collaboration and Ties of the RICHT (Mrs. M. Kholghi) for all her cooperation and help. B. Bazgir received his PhD scholarship from the Fundación Atapuerca, for which he is grateful. Laxmi Tumung received her PhD scholarship from the Erasmus Mundus Programme (IDQP). We would like to thank Roberto Portela Miguez, Senior Curator in

Charge of Mammals, for his help with the reference collection in the Natural History Museum of London. We would like to thank Rupert Glasgow for reviewing the English language of the manuscript

References

Abi-Said, M.R., Shehab, A.H., Amr, Z.S., 2014. Diet of the Barn Owl. Jordan Journal of Biological Sciences,Vol. 7, Nº 2, 109–112.

Allué, E., Expósito, I., Tumung, L., Ollé, A., Bazgir, B., 2018. Early evidence of *Prunus* and *Prunus* cf. *amygdalus* from Palaeolithic sites in the Khorramabad Valley, western Iran. Comptes Rendus Palevol 17, 335–345. https://doi.org/10.1016/j.crpv.2018.01.001

Amori, G., Hutterer, R., Kryštufek, B., Yigit, N., Mitsain, G. & Palomo, L.J., 2016. *Apodemus flavicollis*. The IUCN Red List of Threatened Species 2016: e. T1892A115058023. 8235. https://doi.org/http://dx.doi.org/10.2305/IUCN.UK.2016-3.RLTS.T1892A22423256.en

Amori, G. 1999. *Chionomys nivalis*. In: A. J. Mitchell-Jones, G. Amori, W. Bogdanowicz, B. Kryštufek, P. J. H. Reijnders, F. Spitzenberger, M. Stubbe, J. B. M. Thissen, V. Vohralík and J. Zima (eds), *The Atlas of European Mammals*, Academi Press, London, UK

Amr, A., 2015. *Microtus guentheri* , *The IUCN Red List of Threatened Species* 2016: e.T13463A22349143.

Andrews, P., 2006. Taphonomic effects of faunal impoverishment and faunal mixing. Palaeogeography, Palaeoclimatology, Palaeoecology 241, 572–589. https://doi.org/10.1016/j.palaeo.2006.04.012

Andrews, P., 1990. Owls, Caves and Fossils. https://doi.org/10.2307/3889096.

Aşan Baydemir, N., Duman, L., 2009. Molar patterns in *Microtus guentheri* (Danford and Alston, 1880) (Mammalia: Rodentia) from Kirikkale province. Journal of Applied Biological Sciences 3, 47–54.

Bazgir, B., Ollé, A., Tumung, L., Becerra-Valdivia, L., Douka, K., Higham, T., Van Der Made, J., Picin, A., Saladié, P., López-Garciá, J.M., Blain, H.-A., Allué, E., Fernández-Garciá, M., Rey-Rodríguez, I., Arceredillo, D., Bahrololoumi, F., Azimi, M., Otte, M., Carbonell, E., 2017. Understanding the emergence of modern humans and the disappearance of Neanderthals: Insights from Kaldar Cave (Khorramabad Valley, Western Iran). Scientific Reports 7. https://doi.org/10.1038/srep43460

Bazgir, B., Otte, M., Tumung, L., Ollé, A., Deo, S.G., Joglekar, P., López-García, J.M., Picin, A., Davoudi, D., van der Made, J., 2014. Test excavations and initial results at the middle and upper paleolithic sites of Gilvaran, Kaldar, Ghamari caves and Gar Arjene Rockshelter, Khorramabad Valley, western Iran. Comptes Rendus - Palevol 13, 511–525. https://doi.org/10.1016/j.crpv.2014.01.005

Becerra-Valdivia, L., Douka, K., Comeskey, D., Bazgir, B., Conard, N.J., Marean, C.W., Ollé, A., Otte, M., Tumung, L., Zeidi, M., Higham, T.F.G., 2017. Chronometric investigations of the Middle to Upper Paleolithic transition in the Zagros Mountains using AMS radiocarbon dating and Bayesian age modelling. Journal of Human Evolution 109, 57–69. https://doi.org/10.1016/j.jhevol.2017.05.011

Belmaker, M., Bar-Yosef, O., Belfer-Cohen, A., Meshveliani, T., Jakeli, N., 2016. The environment in the Caucasus in the Upper Paleolithic (Late Pleistocene): Evidence from the small mammals from Dzudzuana cave, Georgia. Quaternary International 425, 4–15. https://doi.org/10.1016/j.quaint.2016.06.022

Belmaker, M., Hovers, E., 2011. Ecological change and the extinction of the Levantine Neanderthals: Implications from a diachronic study of micromammals

from Amud Cave, Israel. Quaternary Science Reviews 30, 3196–3209. https://doi.org/10.1016/j.quascirev.2011.08.001

Blain, H.-A., Bailon, S., Cuenca-Bescós, G., 2008. The Early–Middle Pleistocene palaeoenvironmental change based on the squamate reptile and amphibian proxies at the Gran Dolina site, Atapuerca, Spain. Palaeogeography, Palaeoclimatology, Palaeoecology 261, 177–192. https://doi.org/10.1016/j.palaeo.2008.01.015

Bogicevic, K., Nenadic, D., Mihailovic, D., Lazarevic, Z., Milivojevic, J., 2011. Late Pleistocene rodents (Mammalia: Rodentia) from the Baranica cave near Knjaževac (eastern Serbia): Systematics and palaeoecology. Rivista Italiana di Paleontologia e Stratigrafia, Vol. 117, Nº2, 331-346.

Campana, D. V., Crabtree, P., 2019. Evidence for skinning and craft activities from the Middle Paleolithic of Shanidar Cave, Iraq. Journal of Archaeological Science: Reports 25, 7–14. https://doi.org/10.1016/j.jasrep.2019.03.024

Corbet, G.B. and Hill, J.E., 1991. A World List of Mammalian Species. 3rd ed. London, UK: British Museum (Natural History).

Corbet, G.B., 1978. The Mammals of the Palearctic Region: A Taxonomic Review. London, Brit. Mus.(Nat. Hist.). Cornell Univ. Press. 117- 118.

Coşkun, Y., 2016. Review of unique odd chromosome-numbered underground rodent species of the Palearctic region: *Ellobius Lutescens* Thomas 1897 (Rodentia: Cricetidae). Turkish Journal of Zoology 40, 831–841. https://doi.org/10.3906/zoo-1509-53

Coşkun, Y., 1999. Morphological characteristics of *Meriones tristrami* Thomas, 1892 (Rodentia: Gerbillinae) from Diyarbakır, Turkey. Turk. J. Zool 23, 345–355.

Coşkun,Y., 1997. *Ellobius lutescens* Thomas, 1897 (Rodentia: Cricetidae) Turk. J. of Zoology. 21, 349-354.

Darlington, P.J., 1957. Zoogeography: The Geographical Distribution of Animals. New York, NY, USA: John Wiley and Sons.

Darvish, J., 2011. Morphological comparison of fourteen species of the genus *Meriones* Illiger , 1811 (Rodentia : Gerbillinae) from Asia and North Africa. Iranian Journal of Animal Biosystematics 7, 49–74.

Darvish, J., Mohammadi, Z., Mahmoudi, A., Siahsarvie, R., 2014. Faunistic and taxonomic study of Rodents from northwestern Iran. Iranian Journal of Animal Biosystematics (IJAB) 10, 119–136.

Darvish, D., Orth, A., Michaux, J., 2006. *Mus spretus* et *M. musculus* (Rodentia, Mammalia) en zone méditerranéenne: Différenciation biométrique et morphologique: Application à des fossiles marocains pléistocènes. Mammalia 70, 90–97. https://doi.org/10.1515/MAMM.2006.010

Darvish, J., Ghiyasi, R., Khosravi, M., 2000. Recognition of rodents of Robat Sharaf pellets owl by morphological and neontological studies. Journal of Sciences 12.

Denys, C., 2017. Subfamily Deomyinae, Gerbillinae, Leimacomyinae, Lophiomyinae species accounts. Pp. 598-650. in : Wilson, D.E., Lacher, T.E., Jr. & Mittermeier, R.A. eds. Handbook of the Mammals of the World. Vol.7. Rodents II. Lynx Edicions, Barcelona.

Demirel, A., Andrews, P., Yalçinkaya, I., Ersoy, A., 2011. The taphonomy and palaeoenvironmental implications of the small mammals from Karain Cave, Turkey. Journal of Archaeological Science 38, 3048–3059. https://doi.org/10.1016/j.jas.2011.07.003

Dianat, M., Darvish, J., Cornette, R., Aliabadian, M., Nicolas, V., 2017. Evolutionary history of the Persian Jird, *Meriones per-*

sicus, based on genetics, species distribution modelling and morphometric data. Journal of Zoological Systematics and Evolutionary Research 55, 29–45. https://doi.org/10.1111/jzs.12145

Djamali, M., de Beaulieu, J.L., Shah-hosseini, M., Andrieu-Ponel, V., Ponel, P., Amini, A., Akhani, H., Leroy, S.A.G., Stevens, L., Lahijani, H., Brewer, S., 2008. A late Pleistocene long pollen record from Lake Urmia, NW Iran. Quaternary Research 69, 413–420. https://doi.org/10.1016/j.yqres.2008.03.004

Ellerman, J.R, and Morrison-Scott, T.C.S., 1951. Checklist of Palearctic and Indian Mammals, 1780 to 1946. Brit. Mus. Nat. Hist. London, 1-810.

Evans, E.M.N., Van Couvering, J.A.H., Andrews, P., 1981. Palaeoecology of Miocene sites in western Kenya. J. Hum. Evol. 10, 99-116.

Fernández-Jalvo Y., King T., Yepiskoposyan L. & Andrews P. (eds.), 2016a. Azokh Cave and the Transcaucasian Corridor, Vertebrate Paleobiology and Paleoanthropology Series, Springer

Fernández-Jalvo, Y., Andrews, P., Denys, C., Sesé, C., Stoetzel, E., Marin-Monfort, D., Pesquero, D., 2016b. Taphonomy for taxonomists: Implications of predation in small mammal studies. Quaternary Science Reviews 139, 138–157. https://doi.org/10.1016/j.quascirev.2016.03.016

Fiacconi, M., Hunt, C.O., 2015. Pollen taphonomy at Shanidar Cave (Kurdish Iraq): An initial evaluation. Review of Palaeobotany and Palynology 223, 87–93. https://doi.org/10.1016/j.revpalbo.2015.09.003

Firouz, E., 2005. The complete fauna of Iran. Ed. I.B.Tauris & Co Ltd

Frahm, E., 2019. Upper Palaeolithic Settlement and Mobility in the Armenian Highlands : Agent-Based Modeling , Obsidian Sourcing , and Lithic Analysis at Aghitu-3 Cave.

Gerrie, R., Kennerley, R., 2017. *Myomimus personatus*. The IUCN Red List of Threatened Species 2017: e.T14088A22222124 8235. https://doi.org/http://dx.doi.org/10.2305/IUCN.UK.2017- 2.RLTS. T14088A22222124.en

Gharkheloo, M., Kivanç, E., 2003, A study on the morphology, karyology and distribution of *Ellobius* Fischer, 1814 (Mammalia: Rodentia) in Iran. Turkish Journal of Zoology 27(4):281-292

Golenishchev, F.,Malikov, V., Nazari, F., Vaziri, A.,Sablina, O., Polyakov, A., 2002. New species of vole of "*guentheri*" group (Rodentia, Arvicolinae, *Microtus*) from Iran. Russia Journal of Theriology 1 (2), 117-123

Golenishchev, F., Malikov, V., Petrova, T., Bodrov, S., Abramson, N., 2019. Toward assembling a taxonomic puzzle: Case study of Iranian gray voles of the subgenus *Microtus* (Rodentia, Cricetidae). Mammalian Biology 94, 98–105. https://doi.org/10.1016/j.mambio.2018.06.007

Habibi, K. 2004. Mammals of Afghanistan. Zoo Outreach Organisation/USFWS, Coimbatore, India.

Haddadian Shad, H., Darvish, J., Mohammadian, T., Mahmoudi, A., Alaie Kakhki, N., Ghanbarifardi, M., Molavi, F., Barani-Beiranvand, H., 2014. Preliminary study of rodents using pellets of predatory birds in Iran. Iranian Journal of Animal Biosystematics 10, 36–50.

Hassinger, J.D., 1973. A survey of the mammals of Afghanistan: Resulting from the 1965 Street Expedition (Excluding Bats). Fieldiana Zoology, Vol. 60. Chicago, IL, USA: Field Museum of Natural History.

Hernández Fernández, M., Álvarez Sierra, M.Á., Peláez-Campomanes, P., 2007. Bioclimatic analysis of rodent pa-

laeofaunas reveals severe climatic changes in Southwestern Europe during the Plio-Pleistocene. Palaeogeography, Palaeoclimatology, Palaeoecology 251, 500–526. https://doi.org/10.1016/j.palaeo.2007.04.015

Hernandez Fernández, M., Peláez-Campomanes, P., 2003. The bioclimatic model: A method of palaeoclimatic qualitative inference based on mammal associations. Global Ecology and Biogeography 12, 507–517. https://doi.org/10.1046/j.1466-822X.2003.00057.x

Hernández Fernández, M., 2001. Bioclimatic discriminant capacity of terrestrial mammal faunas. Global Ecology and Biogeography 10, 189–204. https://doi.org/10.1046/j.1466-822x.2001.00218.x

Heydari-Guran, S., Ghasidian, E., 2020. Late Pleistocene hominin settlement patterns and population dynamics in the Zagros Mountains : Kermanshah region. Archaeological Research in Asia 21, 100161. https://doi.org/10.1016/j.ara.2019.100161

Hinton, M.A.C., 1926. Monograph of the Voles and Lemmings (Microtinae) Living and Extinct. London: British Museum (Natural History). Vol.1. 488 p.

Jangjoo, M., J.Darvish & J. D. Vign 2011. Application of outline analysis on fossil and modern specimens of *Apodemus*. Iranian J. Anim. Biosystem., 7 (2): 143-155.

Kandel, A.W., Gasparyan, B., Allué, E., Bigga, G., Bruch, A.A., Cullen, V.L., Frahm, E., Ghukasyan, R., Gruwier, B., Jabbour, F., Miller, C.E., Taller, A., Vardazaryan, V., Vasilyan, D., Weissbrod, L., 2017. The earliest evidence for Upper Paleolithic occupation in the Armenian Highlands at Aghitu-3 Cave. Journal of Human Evolution 110, 37–68. https://doi.org/10.1016/j.jhevol.2017.05.010

Karami, M., Hutterer, R., Benda, P., Siahsarvie, R., Kryštufek, B., 2008. Annotated checklist of the mammals of Iran. Lynx (Praha) 39, 63–102.

Kaya, F., Kaymakçı, N., 2018. Systematics and dental microwear of the late Miocene Gliridae (Rodentia, Mammalia) from Hayranlı, Anatolia: Implications for paleoecology and paleobiodiversity. Palaeontologia Electronica 16. https://doi.org/10.26879/385

Kennerley, R., Kryštufek, B., 2019. *Myomimus setzeri*,. The IUCN Red List of Threatened Species 2019: e.T14089A22222049.8235. https://doi.org/http://dx.doi.org/10.2305/IUCN.UK.2019- 1.RLTS.T14089A22222049.en

Knitlová, M., Horáček, I., 2017. Late Pleistocene-Holocene paleobiogeography of the genus *Apodemus* in Central Europe. PLoS ONE 12, 1–23. https://doi.org/10.1371/journal.pone.0173668

Kopij, G., Liven-Schulman, I., 2013. Zoology in the Middle East Diet of the Lesser Kestrel, *Falco naumanni*, in Israel 7140. https://doi.org/10.1080/09397140.2012.10648914

Kretzoi, M., 1969. Skizze einer Arvicoliden Phylogenie -Stand 1969 // Vertebrata Hungarica. Vol.11. No.1–2. P.155–193.

Kryštufek, B., Bukhnikashvili, A., Sozen, M., Isfendiyaroglu, S., 2017. *Cricetulus migratorius*. The IUCN Red List of Threatened Species 2016: e.T5528A1150733908235. https://doi.org/http://dx.doi.org/10.2305/IUCN.UK.2016-3.RLTS.T5528A22391440.en

Krystufek, B., 2017. *Chionomys nivalis* , European Snow Vole. The IUCN Red List of Threatened Species 2016: e.T4659A115069366 8235. https://doi.org/http://dx.doi.org/10.2305/IUCN.UK.2016-3.RLTS.T4659A22379147.en

Kryštufek, B. , Shenbrot, G., 2016. *Ellobius lutescens* , Transcaucasian Mole Vole. The IUCN Red List of Threatened Species

2016: e.T7655A22340006. 8235. https://doi.org/http://dx.doi.org/10.2305/IUCN.UK.2016- 2.RLTS.T7655A22340006.en

Kryštufek, B., Yigit, N., Amori, G., 2015. *Mesocricetus brandti* , Brandt ' s Hamster. The IUCN Red List of Threatened Species 2008: e.T13220A3421550. 8235. https://doi.org/http://dx.doi.org/10.2305/IUCN.UK.2008.RLTS.T13220A3421550.en

Kryštufek, B., Vohralík, V., 2009. Mammals of Turkey and Cyprus, Rodentia II: Cricetinae, Muridae, Spalacidae, Calomyscidae, Capromyidae, Hystricidae, Castoridae. https://doi.org/10.1644/10-MAMM-R-221.1

Kryštufek, B., Kefelioglu, H., 2001. Redescription and species limits of *Microtus irani* Thomas, 1921, and description of a new social vole from Turkey (Mammalia: Arvicolinao).

Lay, D.M., 1967. A Study of the Mammals of Iran, Resulting from the Street Expedition of 1962-63. Fieldiana Zool., 54: 168-171.

López-García, J.M., 2011. Los micromamíferos del Pleistoceno superior de la Península Ibérica: Evolución de la diversidad taxonómica y cambios paleoambientales y paleoclimáticos. Editorial Académica Española

López-García, J.M., Blain, H.-A., Cuenca-Bescós, G., Alonso, C., Alonso, S., Vaquero, M., 2011. Small vertebrates (Amphibia, Squamata, Mammalia) from the late Pleistocene-Holocene of the Valdavara-1 cave (Galicia, northwestern Spain). Geobios 44, 253–269. https://doi.org/10.1016/j.geobios.2010.10.001

Maul, L.C., Bruch, A.A., Smith, K.T., Shenbrot, G., Barkai, R., Gopher, A., 2015a. Palaeoecological and biostratigraphical implications of the microvertebrates of Qesem Cave in Israel. Quaternary International. https://doi.org/10.1016/j.quaint.2015.04.032

Maul, L.C., Smith, K.T., Shenbrot, G., Bruch, A.A., Wegmüller, F., Le Tensorer, J.M., 2015b. Microvertebrates from unit G/ layer 17 of the archaeological site of Hummal (El Kowm, Central Syria): Preliminary results. Anthropologie (France) 119, 676–686. https://doi.org/10.1016/j.anthro.2015.10.010

Miller, G.S., 1896. Genera and subgenera of voles and lemmings// North American Fauna. Vol.12. P.1–85.

Molur, S. & Sozen, M., 2016. *Meriones persicus*, Persian Jird. The IUCN Red List of Threatened Species 2016: e.T13166A22433231. 8235. https://doi.org/http://dx.doi.org/10.2305/IUCN.UK.2016-2.RLTS.T13166A22433231.en

Moradi Gharkheloo, M., 2003. A Study on the Morphology , Karyology and Distribution of *Ellobius* Fischer , 1814 (Mammalia : Rodentia) in Iran. Turkish Journal of Zoology 27, 281–292.

Neumann, K., Yiğit, N., Fritzsche, P., Çolak, E., Feoktistova, N., Surov, A., Michaux, J., 2017. Genetic structure of the Turkish hamster (*Mesocricetus brandti*). Mammalian Biology 86, 84–91. https://doi.org/10.1016/j.mambio.2017.06.004

Nishiaki, Y., Akazawa, T., 2018. The Middle and Upper Paleolithic Archeology of the Levant and Beyond. Replacement of Neanderthals by Modern Humans Series 35–47. https://doi.org/10.1007/978-981-10-6826-3_3

Nowak, R.M., 1999. Walker's Mammals of the World. 6th ed. Baltimore, MD, USA: The Johns Hopkins University Press.

Obuch, J., Khaleghizadeh, A., 2012. Spatial Variation in the Diet of the Barn Owl Tyto alba in Iran 6, 103–116.

Osborn, D.J., 1962. Rodents of subfamily Microtinae from Turkey. J. Mammalia, 43: 515-529.

Rey-Rodríguez, I., Stoetzel, E., López-García,

J.M., Denys, C., 2019. Implications of modern Barn owls pellets analysis for archaeological studies in the Middle East. Journal of Archaeological Science 111, 105029. https://doi.org/10.1016/J.JAS.2019.105029

Roberts, T.J., 1977. The Mammals of Pakistan. London, UK: Ernst Benn Ltd.

Rusin, M., 2017. *Ellobius talpinus* , Northern Mole Vole. The IUCN Red List of Threatened Species 2016: e.T7656A115085720. 8235. https://doi.org/http://dx.doi.org/10.2305/IUCN.UK.2016-3.RLTS.T7656A22339917.en

Sándor, A.D., 2018. Rediscovered after half a century: A new record of the grey dwarf hamster, *Cricetulus migratorius* (Mammalia: Cricetidae), in Romania. Turkish Journal of Zoology 42, 495–498. https://doi.org/10.3906/zoo-1712-15

Shehab, A., Daoud, A., Kock, D., Amr, Z., 2013. Zoology in the Middle East Small mammals recovered from owl pellets from 7140. https://doi.org/10.1080/09397140.2004.10638061

Shenbrot, G., Kryštufek, B., Molur, S., 2016. *Ellobius fuscocapillus* , Southern Mole Vole. The IUCN Red List of Threatened Species 2016: e.T7654A22339730. 8235. https://doi.org/http://dx.doi.org/10.2305/IUCN.UK.2016- 2.RLTS.T7654A22339730.en

Shenbrot, G., 2009. On the conspecifity of *Allactaga hotsoni* Thomas, 1920 and *Allactaga firouzi* Womochel, 1978 (Rodentia: Dipodoidea). Mammalia 73, 231–237. https://doi.org/10.1515/MAMM.2009.043

Shenbrot, G.I. and Krasnov, B.R. 2005. An Atlas of the Geographic Distribution of the Arvicoline Rodents of the World (Rodentia, Muridae: Arvicolinae). Pensoft Publishers, Sofia.

Siahsarvie, R., Darvish, J., 2008. Geometric morphometric analysis of Iranian wood mice of the genus *Apodemus* (Rodentia, Muridae). Mammalia 72, 109–115. https://doi.org/10.1515/MAMM.2008.020

Smith, K.T., Christian, L., Flemming, F., Barkai, R., Gopher, A., 2016. The microvertebrates of Qesem Cave : A comparison of the two concentrations. Quaternary International 1–13. https://doi.org/10.1016/j.quaint.2015.04.047

Souttou K., Manaa A., Stoetzel E., Sekour M., Hamani A. , Doumandji S., Denys C. 2012 Small mammals bone modifications in Black-shouldered Kite *Elanus caeruleus* pellets from Algeria: implications for archaeological sites. J. Taphonomy 10 (1), 1-19.

Stoetzel, E., Cornette, R., Lalis, A., Nicolas, V., Cucchi, T., Denys, C., 2017. Systematics and evolution of the *Meriones shawii/grandis* complex (Rodentia, Gerbillinae) during the Late Quaternary in northwestern Africa: Exploring the role of environmental and anthropogenic changes. Quaternary Science Reviews 164, 199–216. https://doi.org/10.1016/j.quascirev.2017.04.002

Tesakov, A.S., 2016. Early Middle Pleistocene *Ellobius* (Rodentia , Cricetidae , Arvicolinae) from Armenia. Russian J. Theriol. 15 (2): 151–158.

Thomas, O., 1905. *Ellobius woosnami*. Abstr. Proc. Zool. Soc. 23; Proc. Zool. Soc. 526 London.

Tsytsulina, K., Kryštufek, B., Yigit, N., Bukhnikashvili, A., Shenbrot, G., 2017. *Microtus socialis* , Social. The IUCN Red List of Threatened Species 2016: e.T13458A115114745. 8235.https://doi.org/http://dx.doi.org/10.2305/IUCN.UK.2016-3.RLTS.T13458A22348936.en

Walker, E.P., 1964. Mammals of the World. Vol. 2. Baltimore, MD,USA: The Johns Hopkins Press.

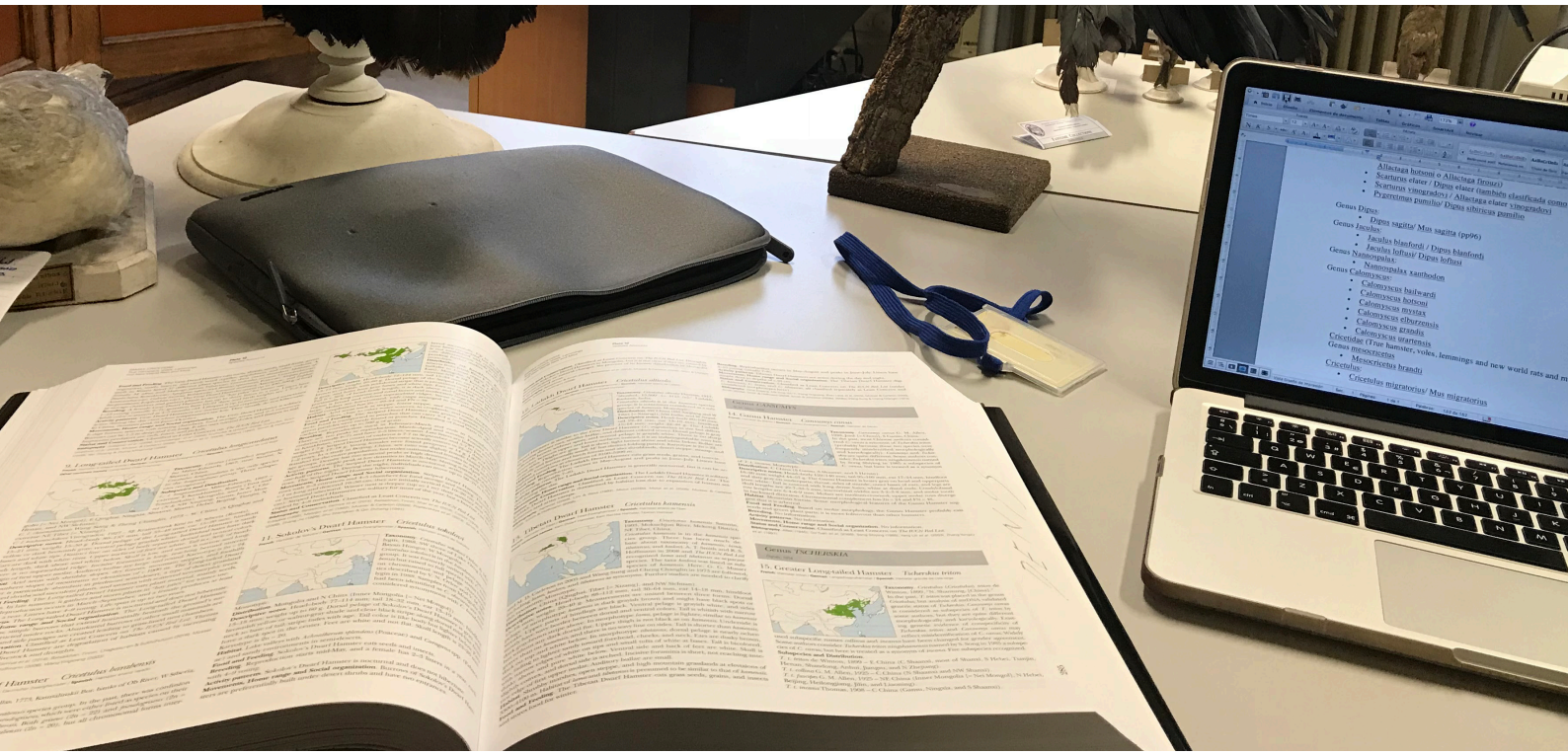
Weissbrod, L., Zaidner, Y., 2014. Taphonomy

and paleoecological implications of fossorial microvertebrates at the Middle Paleolithic open-air site of Nesher Ramla, Israel. Quaternary International 331, 115–127. https://doi.org/10.1016/j.quaint.2013.05.044

Wilson, D.E. and Reeder, D.M., 2005. Mammal Species of the World. Washington, DC, USA: Smithsonian Institution Scholarly Press.

Chapter 7.

General discussion



In the previous chapters we have already included a brief discussion regarding the particular problems for each research question as the correct identification of rodent species, identify the origin of the rodents accumulation and to reconstruct the environmental and climatic conditions of Azokh 1, Kaldar Cave and Birecik.

The aim of this chapter is to summarize and discuss our new data in replacing them in a wider archaeological and climatic regional context. This chapter is divided into two main parts: 1) the identified rodent species, their origin and their current and past distribution will be discussed, with emphasise on the studied archaeological sites; and 2) the main paleoclimatic and palaeoenvironmental inferences will be discussed and compared to the general data available for this region and for the considered chronological period.

7.1. Rodent assemblages

Rodents are one of the most significant tool for the palaeoenvironmental and palaeoclimatic reconstruction (e.g. Rey-Rodríguez et al., 2020) because of their rapid evolution, the limited geographic range of the species and unique niche requirements, as well as their frequent preservation in archaeological and palaeontological sites (Belmaker and Hovers, 2011; Maul and Markova, 2007,among others).

Studies of rodents and other small vertebrates from archaeological sites in the Middle East are increasing during the last years (Bazgir et al., 2017; Belmaker et al., 2016; Belmaker and Hovers, 2011; Demirel et al., 2011; Fernández-Jalvo, 2016a; Kandel et al., 2017; Maul et al., 2015a, 2015b; Rey-Rodríguez et al., 2021, 2020; Weissbrod and Weinstein-Evron, 2020; Weissbrod and Zaidner, 2014, among others). However, most of them mainly propose preliminary faunal lists, and identification are often limited to the genus level, as we commented in the introduction.

During this PhD thesis, we analysed material coming from different localities and chronologies (Figure 7. 1). Two archaeological sites were considered: Azokh 1 Cave, located in Southern Caucasus (Chapter 5), Middle to Late Pleistocene in age (Fernández-Jalvo, 2016a), and Kaldar Cave, situated in the Khorramabad valley (Iran) (Chapter 6), Late Pleistocene in age (Rey-Rodríguez et al., 2020). We also studied owl pellet samples that were collected in 2003 in the region of Birecik in Turkey (Chapter 3) (Rey-Rodríguez et al., 2019).

Quantification of taxonomic frequencies was based on standard measures in zooarchaeological analyses, including the number of identified specimens (NISP) and minimum number of individuals (MNI) (Weissbrod and Zaidner, 2014). This latter was estimated using the most abundant skeletal element present in the assemblage (molars in our case). The Table 7.1 gives the detailed frequency of rodent taxa for the three study sites. A total of 4047 specimens have been identified (NISP), 434 remains belonging to 237 individuals were identified at Azokh 1, 1112 remains belonging to 264 individuals were identified at Kaldar, and 2503 remains belonging to 38 individuals were identified in the pellet samples from Birecik.

The total of the studied assemblage is composed at least by 27 taxa: three cricetinae (*Cricetulus* sp., *Cricetulus migratorius* and *Mesocricetus brandti*), 13 arvicolinae (*Clethrionomys glareolus*, *Arvicola* ex.gr. *persicus, Chionomys nivalis*, *Chionomys gud*, *Microtus* spp., *Microtus socialis, Microtus irani, Microtus guentheri, Microtus* gr. *arvalis-socialis, Microtus (Terricola)* sp., *Ellobius* spp., *Ellobius fuscocapillus* and *Ellobius lutescens*), five gerbillinae (*Meriones* spp., *Meriones tristrami, Meriones* cf. *persicus, Meriones* gr. *dahli-libycus* and *Meriones* gr. *persicus-tristrami),* three

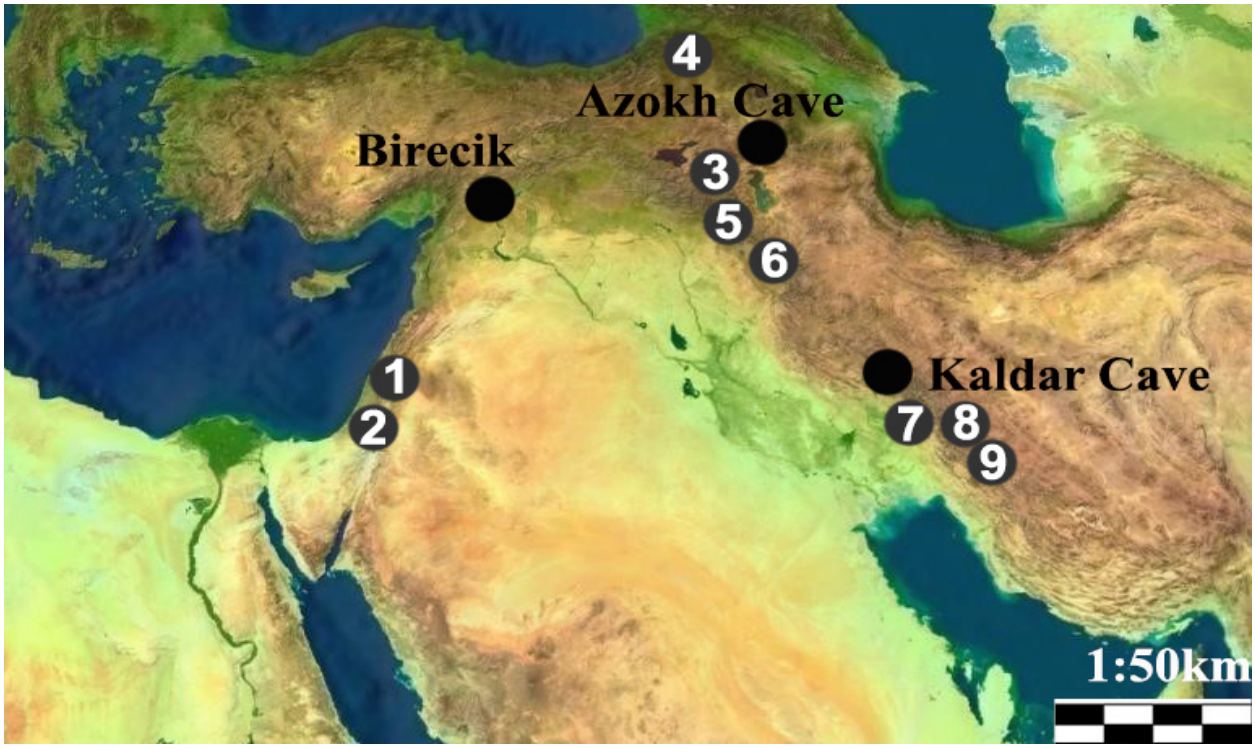


Figure 7.1. Location of the studied sites in this PhD: Azokh Cave (Southern Caucasus), Kaldar Cave (Iran) and Birecik (Turkey); and other sites mentioned in this chapter with small mammals studies: 1) Misliya Cave (Israel, Middle Pleistocene), 2) Qesem Cave (Israel, Middle Pleistocene), 3) Aghitu-3 (Armenia, Late Pleistocene), 4) Dzudzuana (Georgia, Late Pleistocene), 5) Hazar Merd (Iraq, Late Pleistocene), 6) Kani Mikaeli (Iran, Late Pleistocene), 7) Qalaloun (Iran, Late Pleistocene), 8) Yafteh Gar (Iran, Late Pleistocene) and 9) Arjeneh (Iran, Late Pleistocene).

	Azokh 1 Cave									Kaldar Cave									Birecik		
	Unit V			Unit III-IV			Unit II			Layer 5			Layer 4			Layers 1-3					
Taxa	**NISP**	**MNI**	**%**	**NISP**	**MNI**	**%**	**NISP**	**MNI**	**%**	**NISP**	**MNI**	**%**	**NISP**	**MNI**	**%**	**NISP**	**MNI**	**%**	**NISP**	**MNI**	**%**
Indet.										3			11								
Cricetulus sp.	4	4	3.48				6	2	1.74												
Cricetulus migratorius	2	1	0.87				8	2	1.74	5	3	2.27	14	3	2.59	1	1	6.25			
Mesocricetus brandti	6	3	2.61				5	3	2.61	7	4	3.03	3	1	0.86	0	0	0			
Clethrionomys glareolus	-	-	-	-	-	-	4	3	2.61												
Arvicola ex. gr. *persicus*	-	-	-				1	1	0.87												
Chionomys gud	3	2	1.74																		
Chionomys nivalis	-	-	-				4	3	2.61	6	3	2.27	17	12	10.34	2	1	6.25			
Microtus spp.										292	51	52.33	258	31	26.72	4	3	18.75			
Microtus irani										14	9	6.81	0	0	0	1	1	6.25			
Microtus guenteri										0	0	0	16	9	7.76	1	1	6.25			
Microtus socialis										35	20	6.27	36	20	17.24	3	3	18.75			
Microtus gr. *arvalis-socialis*	154	77	66.96	7	5	71.43	135	75	65.22												
Microtus (*Terricola*) spp.	13	7	6.09	1	1	14.29	7	4	3.48												
Ellobius spp.										80	7	5.30	91	8	6.9	2	2	12.5			
Ellobius fuscocapillus										5	4	3.03	5	3	2.59	1	1	6.25			
Ellobius lutescens	13	7	6.09	1	1	14.29	22	12	10.43	10	6	4.44	10	7	6.03	-	-	-			
Meriones spp.	5	3	2.61				4	2	1.74												
Meriones tristami																			2476	32	82.05
Meriones cf. *persicus*										88	18	13.64	65	17	14.66	3	2	12.5			
Meriones gr. dahli-libycus	4	3	2.61				1	1	0.87												
Meriones gr. *persicus-tristrami*	6	3	2.61				2	2	1.74												
Nesokia indica																			4	1	2.56
Mus cf. *musculus*										2	1	0.75	1	1	0.86	0	0	0	21	5	12.82
Apodemus sp.	3	2	1.74				7	4	3.48	5	2	1.52	6	3	2.59	2	1	6.5			
Allactaga sp.	2	2	1.74							1	1	0.75	1	1	0.86	0	0	0			
Allactaga cf. *williamsi*	2	1	0.87				2	1	0.87												
Myomimus sp.										5	3	2.27	0	0	0	0	0	0			
Total	**217**	**115**	100	**9**	**7**	100	**208**	**115**	100	**558**	**132**	100	**534**	**116**	100	**20**	**16**	100	**2501**	**38**	100

Table 7.1.Small mammal taxa representation from the studied archaeological sites (Azokh, Kaldar) and owl pellet samples (Birecik), in terms of number of identified specimens (NISP), minimum number of individuals (MNI) and percentage (%) of the MNI.

murinae (*Nesokia indica*, *Apodemus* sp. and *Mus* cf. *musculus*), two dipodids (*Allactaga* sp. and *Allactaga* cf. *williamsi*) and one glirid (*Myomimus* sp.). The faunal spectrum is much less diversified in the owl pellets (5 taxa) compared to the archaeological sites (13 taxa for Azokh 1, 13 taxa for Kaldar).This could be explained by the formation of archaeological that is produced during a longer period and different seasons and in the pellets study it is a *Tyto alba* nest so taxa represented would be more restricted to the predator and also the season because they were collected in June.

We will now discuss the systematics, ecology and distribution of each of the rodent species found in our assemblages.

Genus *Cricetulus* (Milne-Edwards, 1867) and *Mesocricetus* (Nehring, 1898)

Regarding the Cricetinae subfamily, we identified *Cricetulus* sp., *Cricetulus migratorius* and *Mesocricetus brandti* (Table 7.1). We attributed to *Cricetulus* sp. the broken teeth that could not have been identified at the species level in Azokh 1 Cave, Unit V (Middle Pleistocene) and Unit II (Late Pleistocene). *Cricetulus migratorius* is present in Azokh 1, Unit V (Middle Pleistocene) and Unit II (Late Pleistocene) and also in Kaldar Cave Layer 5 (Late Pleistocene), Layer 4 (Late Pleistocene) and Layer 1-3 (Holocene). *Mesocricetus brandti* has been identified in Azokh 1, in Unit V (Middle Pleistocene) and Unit II (Late Pleistocene) and also in the Late Pleistocene Layers 5 and 4 of Kaldar Cave. Their current distribution (Figure 7.2) indicates that both species (*Cricetulus migratorius* and *Mesocricetus brandti*) are currently present in the areas where our archaeological sites are located.

Also, *Cricetulus migratorius* is present during the Middle Pleistocene at Qesem Cave (Maul et al., 2015a; Smith et al., 2015) and during the Late Pleistocene at Aghitu-3 (Kandel et al., 2017) Aghitu-3 Cave and Dzudzuana (Belmaker et al., 2016); this genus is present during the Middle Pleistocene in Misliya Cave as *Cricetulus* sp. (Weissbrod and Weinstein-Evron, 2020).

Moreover, *Mesocricetus brandti* was also identified in the Late Pleistocene sites of Aghitu-3 (Kandel et al., 2017) and Dzudzuana (Belmaker et al., 2016). *Mesocricetus* sp. was present during the Middle Pleistocene at Misliya Cave (Weissbrod and Weinstein-Evron, 2020) in Israel outside its current distribution; this last one could be another species because the location of the site is not in the current distribution of *Mesocricetus brandti* as we can see in the Figure 7. 2 or it is possible also that the distribution of this species has changed over time .

Genus *Microtus* (Schrank, 1798)

The samples analysed here are dominated by the subfamily Arvicolinae with 13 species. The most abundant genus is *Microtus* (Figure 7.3), represented by several species (Table 7.1).

Microtus is a very diversified genus whose origins probably found in western Asia (Barbosa et al., 2018; Haring et al., 2011) it is also abundant in the archaeological sites. However, the studies carried out in the considered region remain rare, which prevents good identifications. Because of a lack of known discriminant characters, it would be necessary to increase the reference collection and the available fossil data for their correct identification.

In Azokh 1 Cave we identified *Microtus* gr. *arvalis-socialis* (the species included in this group are: *Microtus arvalis*, *Microtus socialis* and *Microtus guentheri*) and *Microtus (Terricola)* spp. (the species included in this group are: *Microtus daghestanicus*, *Microtus nasavori*, *Microtus majori* and *Microtus schidlovskii*), in Unit V (Middle Pleistocene), Unit III-IV (Middle Pleistocene) and Unit II

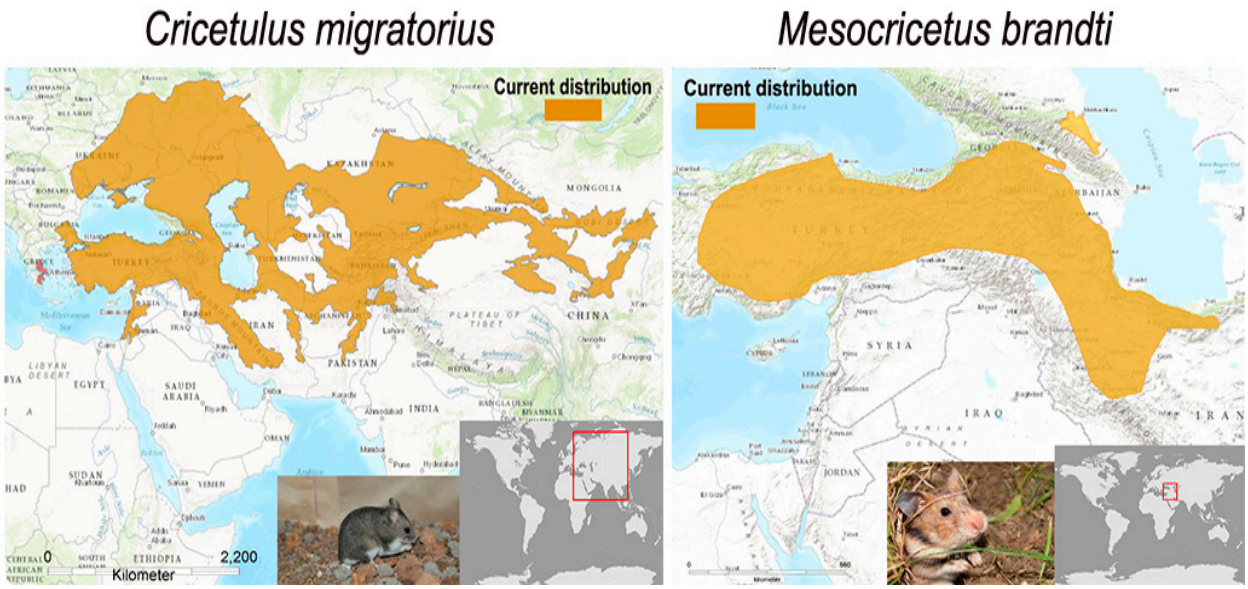


Figure 7.2. *Cricetulus migratorius* and *Mesocricetus brandti* current distribution obtained from IUCN red list (https://www.iucnredlist.org/).

(Late Pleistocene), all of them being present nowadays in the surrounding area. In Kaldar Cave the specimens identified belong to *Microtus* spp., *Microtus irani, Microtus guentheri* and *Microtus socialis. Microtus* spp. refers to all the elements from Layer 5 (Late Pleistocene), Layer 4 (Late Pleistocene) and Layer 1-3 (Holocene), that we cannot attribute to one species or another, in particular because of their poor state of preservation (due to digestion and/or breakage). *Microtus irani*, recorded in Kaldar Cave Layer 5 (Late Pleistocene) and Layer 1-3 (Holocene), and *Microtus socialis*, found out in Layer 5 (Late Pleistocene), Layer 4 (Late Pleistocene) and Layer 1-3 (Holocene), are still present in the surroundings. However, *Microtus guentheri*, present in Layer 4 (Late Pleistocene) and Layer 1-3 (Holocene), is not present nowadays in Iran (https://www.iucnredlist.org/). *Microtus guentheri* is currently present in Israel (Figure 7.3), were it was also recorded in Middle Pleistocene sites such as Qesem Cave (Maul et al., 2015a; Smith et al., 2015) and Misliya Cave (Weissbrod and Weinstein-Evron, 2020). During the Late Pleistocene, *Microtus* spp. was also identified at Aghitu-3 (Kandel et al., 2017) Aghitu-3 Cave permits us to examine the settlement patterns of the Upper Paleolithic (UP and *Microtus* cf. *arvalis* at Dzudzuana (Belmaker et al., 2016). *M. arvalis* is today widespread in the Dzudzuana region (Figure 7. 3).

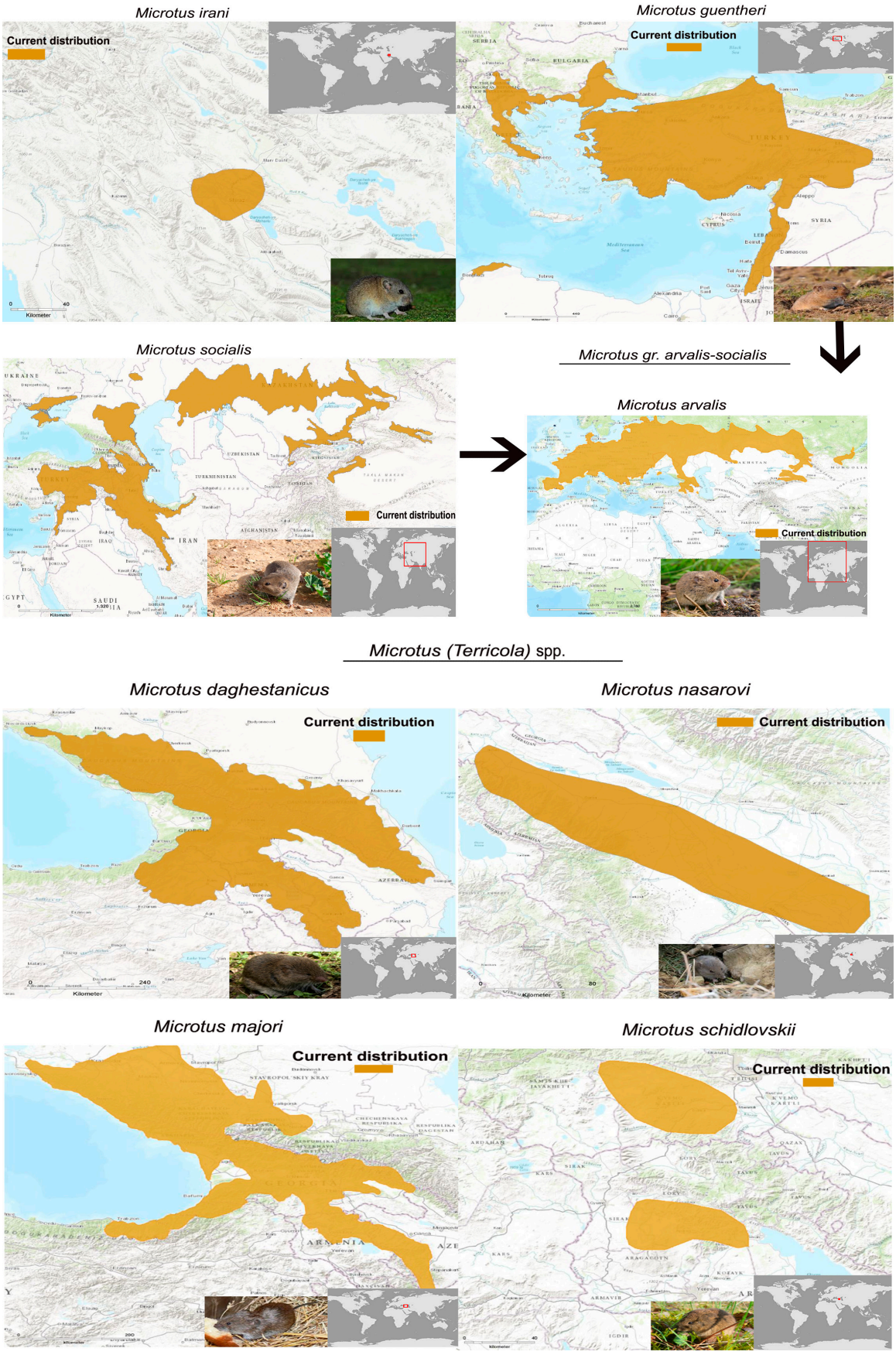


Figure 7.3. Current distribution of *Microtus* species considered in this study, obtained from IUCN red list (https://www.iucnredlist.org/). The arrows indicate that in the *Microtus* gr. *arvalis- socialis* we comment the distribution concerns *Microtus socialis*, *Microtus arvalis* and also *Microtus guentheri*.

Genus *Ellobius* (Fischer, 1814)

Regarding the MNI, the genus *Ellobius* is the second most represented genus in our assemblages after *Microtus* (Table 7.1, Figure 7.4). The genus *Ellobius* occurs today in south-eastern Europe, western and central Asia (Kryštufek and Vohralík, 2009), but its Pleistocene distribution reached North Africa as far as to the Moroccan Atlantic coast (Stoetzel, 2013) and the southern Levant, where it is present at Misliya (Weissbrod and Weinstein-Evron, 2020), while it is absent from these regions today.

In Azokh 1, *Ellobius* is present in Unit V (Middle Pleistocene), Unit III-IV (Middle Pleistocene) and Unit II (Late Pleistocene), only represented by the species *E. lutescens*, which is currently present in the region. In Kaldar Cave, we recognised *Ellobius* spp., *E. fuscocapillus* and *E. lutescens*. We identified as *Ellobius* spp., in Layer 5 (Late Pleistocene), Layer 4 (Late Pleistocene) and Layer 1-3 (Holocene), the m1s that were too broken or digested to be distinguished. *E. lutescens* occurs in Layer 5 (Late Pleistocene) and Layer 4 (Late Pleistocene), and is currently present in the area. *E. fuscocapillus* was documented in Layer 5 (Late Pleistocene), Layer 4 (Late Pleistocene) and Layer 1-3 (Holocene), of Kaldar while it is not present in the area nowadays according to the IUCN red list. The palaeoenvironmental data (obtained with the habitat weighting method) have shown that the landscape was during Pleisto-Holocene mainly composed of steppes in both levels, which are favorable habitats for the *Ellobius* species (Rey-Rodríguez et al., 2020). *Ellobius* genus is present in Misliya Israel (Weissbrod and Weinstein-Evron, 2020) during Middle Pleistocene as *Ellobius* sp., outside its current range (Figure 7.4).

During the Late Pleistocene *E. lutescens* was also found in Iraq (Bate, 1930) at Hazar Merd, in layers dated to 25,000 years ago (Coşkun, 2016). Hashemi et al. (2006) noted that remains of *E. lutescens* have been found in several sites in western and northwestern Iran: Kani Mikaeil (Kordestan), Qalaloun near Kouhdasht, Yafteh Gar, and Arjeneh near Khoramabad (Lorestan). *Ellobius lutescens* has also been documented in Dzudzuana Cave (Georgia, 34.4-6 ka cal BP; Belmaker et al., 2016), and also in Aghitu-3 level VII (Armenia, Upper Palaeolithic, 39-36 ka cal BP; Kandel et al., 2017), where it is present nowadays (Figure 7.4).

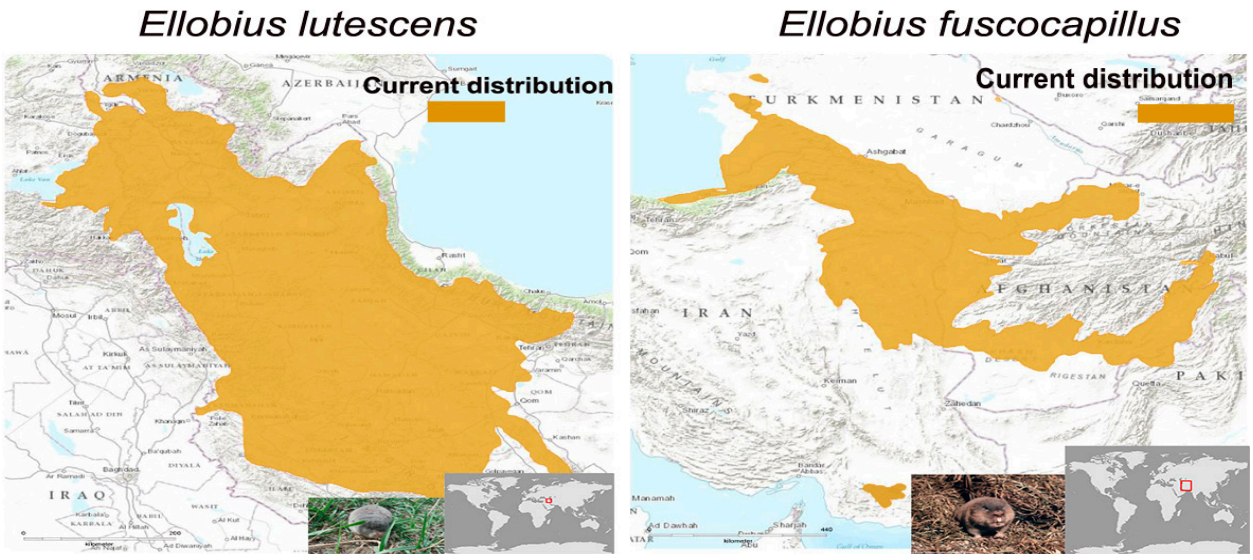


Figure 7.4. Current distribution of *Ellobius lutescens* and *E. fuscocapillus*, obtained from IUCN red list(https://www.iucnredlist.org/).

***Clethrionomys glareolus* (Schreber, 1780)**

The bank vole, *Clethrionomys glareolus*, is today widely distributed in Eurasia and it was present in Azokh 1 (Table 7.1), Unit II (Middle Pleistocene). However, this species is not represented in the region today (Figure 7.5). This species is also present in Dzudzuana (Belmaker et al., 2016) during the Late Pleistocene, outside his current distribution (Figure 7.5). Its presence is an interesting palaeoecological value, suggesting the presence relatively humid conditions supporting scrub and woodland in the archaeological sites.

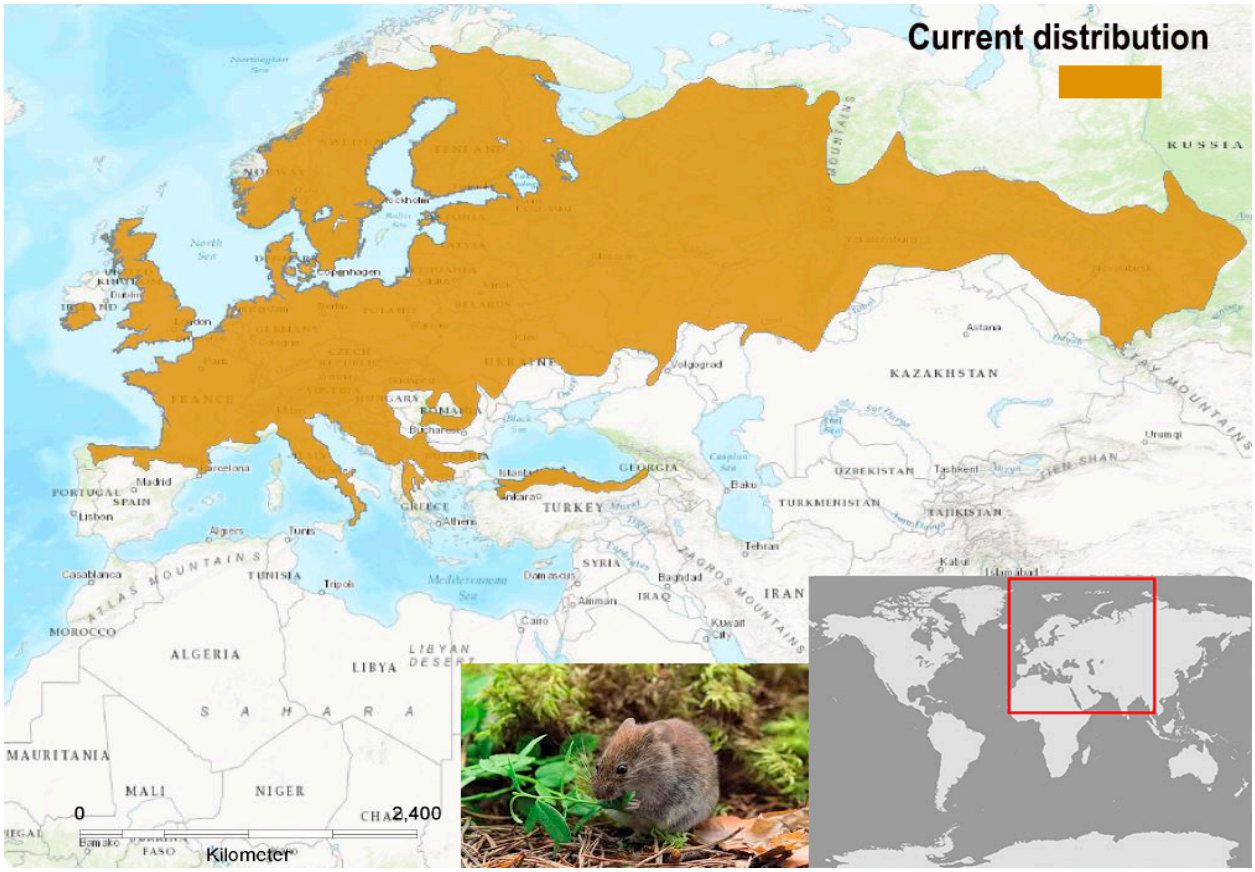


Figure 7.5. Current distribution of *Clethrionomys glareolus* obtained from IUCN red list (https://www.iucnredlist.org/).

***Arvicola* ex. gr. *persicus* (de Filippi , 1865)**

The genus *Arvicola* occupies a vast geographical range, from the Arctic Sea to Lake Baikal in Russia, Tien Shan Mountains in northwest China, through north-western Iran, Iraq, Caucasus, Turkey to northern Israel and throughout Europe (Mahmoudi et al., 2020; Maul et al., 2020). Currently, there are five recognized species: *Arvicola amphibius* (Linnaeus, 1758) for the European and Asian populations; *A. italicus* (Savi, 1838) present in the Italian peninsula; *A. monticola* (de Sélys-Longchamps, 1838) recorded in northern Spain and the nothwestern Alps; *A. sapidus* (Miller, 1908) documented in Spain and France and *A. persicus* (de Filippi, 1865), present in Iran and adjacent regions. The genus *Arvicola* presents a great interest for the biostratigraphy of the Quaternary.

We only recovered one lower m1 ascribed to *Arvicola persicus* at Azokh 1 Unit II, Middle Pleistocene, (Table 7.1)(Chapter 5). This species was not previously identified in this site (Parfitt, 2016). The precise distribution



Figure 7.6. Probably current distribution of *Arvicola persicus* according to Mahmoudi et al. (2020) and Maul et al. (2020).

and ecology of *Arvicola persicus* need to be clarified (Mahmoudi et al., 2020). However, Mahmoudi et al. (2020) and Maul et al. (2020) indicate that the probable distribution area extends from Anatolia to the Caucasus (between the Mediterranean and the Caspian Sea), with lobe-like distribution areas extending eastwards into the northern foothills of the Elbrus mountains (south of the Caspian Sea, Mazandaran Province of Iran) and south-eastwards to the Zagros Mountains (Chaharmahal and Bakhtiari Province of Iran). So, we can suppose that nowadays it is also present in that regions (Figure 7.6). Other representatives of the genus *Arvicola* were found in the Late Pleistocene sites of Aghitu-3 (Kandel et al., 2017) and Dzudzuana, attributed to *Arvicola amphibius* (Belmaker et al., 2016). The presence of *A. persicus* that has a semi-aquatic lifestyle, indicate the existence of water habitats near the cave. *Arvicola* is also an interesting biostratigraphic indicator, applying the SDQ we could correlated with a chronological period, however in our case with just one molar is not possible.

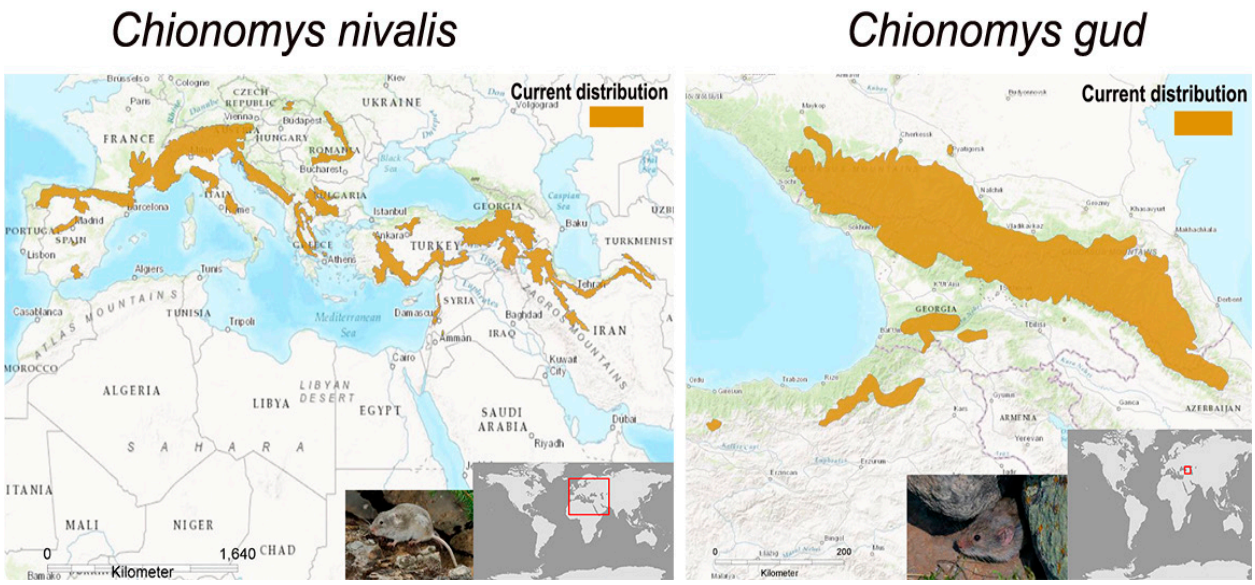


Figure 7.7. Current distribution of *Chionomys nivalis* and *C. gud* obtained from IUCN red list (https://www.iucnredlist.org/).

Genus *Chionomys* (Miller, 1908)

Chionomys is represented in the studied area by *Chionomys nivalis* and *Chionomys gud* (Figure 7.7). *Chionomys nivalis* has a global distribution extending from southwestern Europe and through southeastern Europe to the Caucasus, Turkey, Israel, Lebanon, Syria and Iran. We identified these species at Azokh 1 (Table 7.1), Unit II (Late Pleistocene) and also at Kaldar Cave (Table 7.1), in Layer 5 (Late Pleistocene), Layer 4 (Late Pleistocene) and Layer 1-3 (Holocene). *Chionomys nivalis* occurs today in both regions. *Chionomys gud* was recorded at Azokh 1 Unit V (Middle Pleistocene), while it does not exist anymore in the region today (Kryštufek, 1999; Parfitt, 2016), indicating more mesic conditions than *Chionomys nivalis*. *Chionomys* sp. was identified in the Middle Pleistocene site of Misliya Cave (Weissbrod and Weinstein-Evron, 2020) and *Chionomys nivalis* was identified in the Late Pleistocene sites of Aghitu-3 (Kandel et al., 2017) and Dzudzuana (Belmaker et al., 2016), where is also present today.

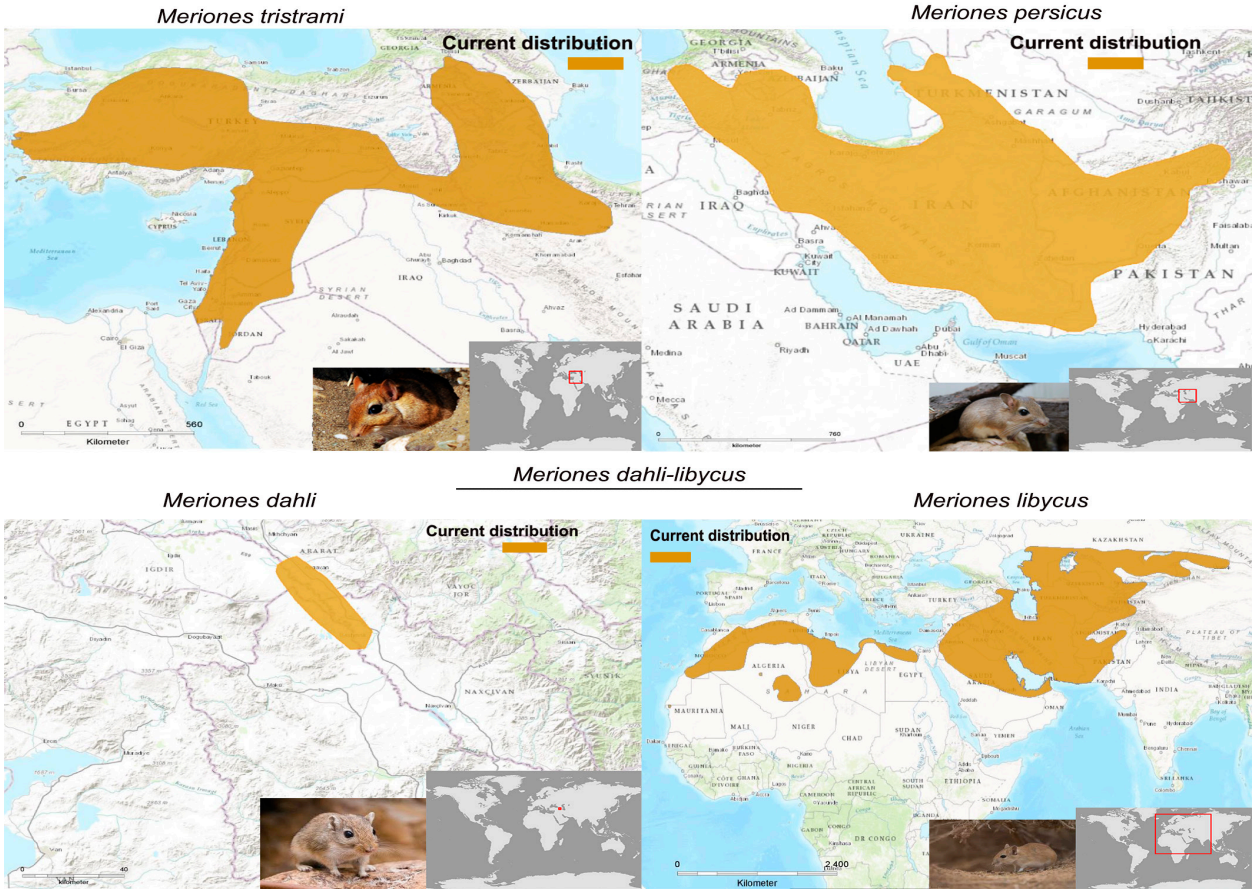


Figure 7.8. Current distribution of *Meriones tristami* and *M. persicus* obtained from IUCN red list (https://www.iucnredlist.org/).

Genus *Meriones* (Illiger, 1811)

The subfamily Gerbillinae, through the genus *Meriones*, represents the third most abundant group recovered in our assemblages (Table 7.1, Figure 7.8). The genus *Meriones* is distributed in North Africa, Central Asia, Transcaucasia, Turkey and Pakistan (Darvish, et al. 2014, Wilson et al. 2017). In Azokh 1, we found *Meriones* spp., *Meriones* gr. *dahli-libycus* and *Meriones* gr. *persicus-tristrami* in Unit V (Middle Pleistocene) and Unit II (Late Pleistocene), and all of them seems to be present in the area nowadays. At Kaldar Cave, we identified *Meriones* cf. *persicus* in Layer 5 (Late Pleistocene), Layer 4 (Late Pleistocene) and Layer 1-3 (Holocene), and this species is present nowadays near the cave. *Meriones tristrami*, present nowadays nowadays in Turkey, was identified also in the Birecik owl pellet sample, representing the most abundant species in the assemblage. During the Middle Pleistocene, Meriones tristrami was also recorded at Qesem Cave (Maul et al., 2015a; Smith et al., 2015) and at Misliya Cave (Weissbrod and Weinstein-Evron, 2020), where it is present today (Figure 7.8).

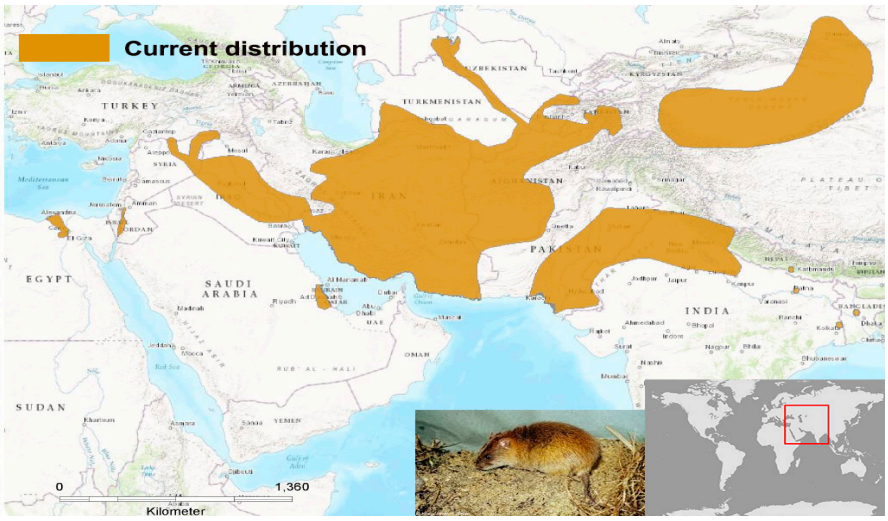


Figure 7.9. *Nesokia* distribution, according to the IUCN red list (https://www.iucnredlist.org/).

Genus *Nesokia* (Gray, 1842)

Nesokia indica is today very widespread in south-western and Central Asia (Boitani and Molur, 2016). We identified this species in the Birecik pellet samples and at Kaldar Cave, in Layer 5 (Late Pleistocene) and Layer 4 (Late Pleistocene). This species is present nowadays in the study regions (Figure 7.9). It was not identified in other Middle to Late Pleistocene sites considered in this chapter.

Genus *Mus* (Linnaeus, 1758)

Mus musculus is a commensal species, well distributed throughout the world: it is present over all the continents except Antarctica (Figure 7.10). We have identified *Mus* remains at Kaldar Cave, in Layer 5 (Late Pleistocene) and Layer 4 (Late Pleistocene), and also in the Birecik pellet samples. *Mus musculus/ macedonicus* was identified in the Middle Pleistocene site of Qesem Cave (Maul et al., 2015a; Smith et al., 2015) and *Mus* sp. in Misliya Cave (Weissbrod and Weinstein-Evron, 2020).

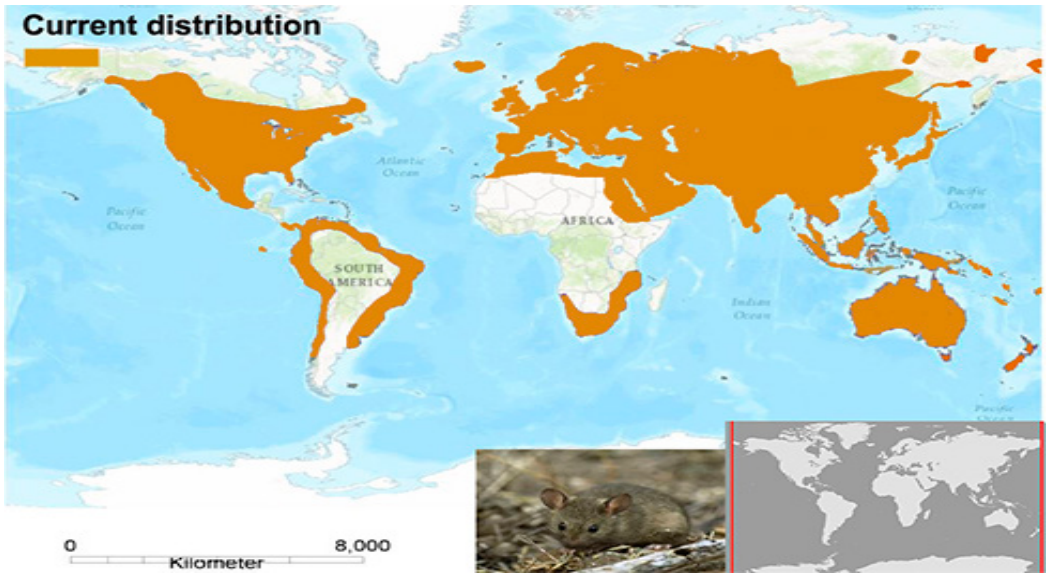


Figure 7.10. *Mus musculus* distribution, according to the IUCN red list (https://www.iucnredlist.org/).

Genus *Apodemus* (Kaup, 1829)

The genus *Apodemus* has a large distribution range (Figure 7.11) extending from Great Britain across much of continental Europe to the Urals. It also extends east through Turkey to western Armenia, the Zagros Mountains of Iran and south to Syria, Lebanon and Israel (Amori et al., 2016). We identified this genus in both archaeological sites (Table 7.1): at Azokh 1, in Unit V (Middle Pleistocene), and Unit II (Late Pleistocene), and at Kaldar Cave, in Layer 5 (Late Pleistocene), Layer 4 (Late Pleistocene) and Layer 1-3 (Holocene) as *Apodemus* sp.

Seven *Apodemus* species are currently recognized in southern Caucasus: *A. hyrcanicus*, *A. flavicollis*, *A. witherbyi, A. ponticus*, *A. agrarius, A. mystacinus* and *A. uralensis*, all belonging to the *Sylvaemus* subgenus (Jangjoo et al., 2011). Five of them are currently recognized in Iran: *A. hyrcanicus*, *A. flavicollis*, *A. witherbyi, A. avicennicus* and *A. uralensis*. At Qesem Cave (Maul et al., 2015a; Smith et al., 2015). *Apodemus* remains were attributed to the *Apodemus flavicollis* group, and at Misliya Cave to *Apodemus flavicollis* and *Apodemus mystacinus* (Weissbrod and Weinstein-Evron, 2020). All of these species are currently distributed near these sites (Figure 7.11). During the Late Pleistocene, *Apodemus* sp. was identified at Dzudzuana, but the precise species is unknown.

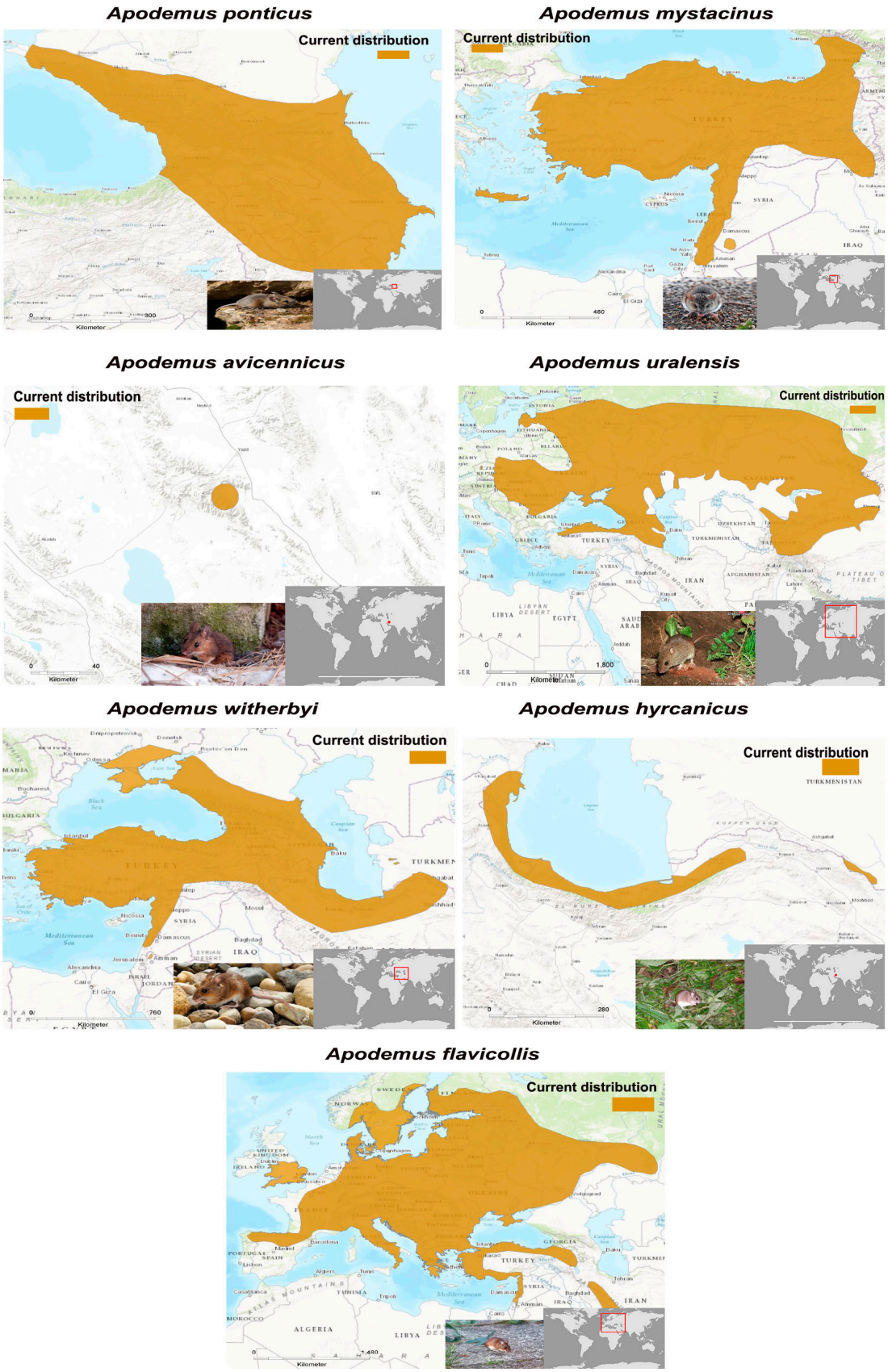


Figure 7.11. Distribution of the *Apodemus* species present in the in southern Caucasus and Iran, according to the IUCN red list (https://www.iucnredlist.org/).

Genus *Allactaga* (Cuvier, 1837)

The *Allactaga* genus is poorly known in the Middle East (Shenbrot, 2009). It is present at Azokh 1, in Unit V (Middle Pleistocene) and Unit II (Late Pleistocene), and at Kaldar Cave, in Layer 5 (Late Pleistocene), Layer 4 (Late Pleistocene) and Layer 1-3 (Holocene) (Table 7.1). The current distribution and ecology of the *Allactaga* species remains poorly known, and this taxon was not identified in the other archaeological sites used for the comparisons. In Kaldar Cave we identify *Allactaga* sp. because Iran four species are currently present: *Allactaga elater*, *Allactaga euphratica*, *Allactaga firouzi* and *Allactaga hotsoni* (Karami et al., 2008). The different species are morphologically very close and remain poorly studied we identify. However in Azokh 1 we probably assign to *Allactaga williamsi* that is distributed in Anatolia (Turkey), the Caucasus (Armenia, Azerbaijan, Iran and Turkey), and northwestern Iran, with an isolated population in central Afghanistan. However is difficult to assign species to this genus pending final molecular analyses.

Genus *Myomimus* (Ognev, 1924)

The species included in this genus are not well known regarding their distribution and ecology (Gerrie & Kennerley, 2017; Kennerley & Kryštufek, 2019). The genus *Myomimus* is currently present in Iran with two species, *Myomimus personatus* and *Myomimus setzeri* (Firouz, 2005; Gerrie & Kennerley, 2017; Karami et al., 2008; Kennerley & Kryštufek, 2019) and both of them can be found in the surrounding area near Kaldar cave (Figure 7. 12).

Myomimus is document at Kaldar Cave (Table 7.1), in Layer 5 (Late Pleistocene). During the Middle Pleistocene, *Myomimus* sp. was identified at Misliya Cave (Weissbrod and Weinstein-Evron, 2020) and at Qesem Cave (Maul et al., 2015a; Smith et al., 2015) as *Myomimus judaicus/setzeri group,* while it seems to be absent of this western Asia today. The presence of *Myomimus* in the archaeological sites would indicate more

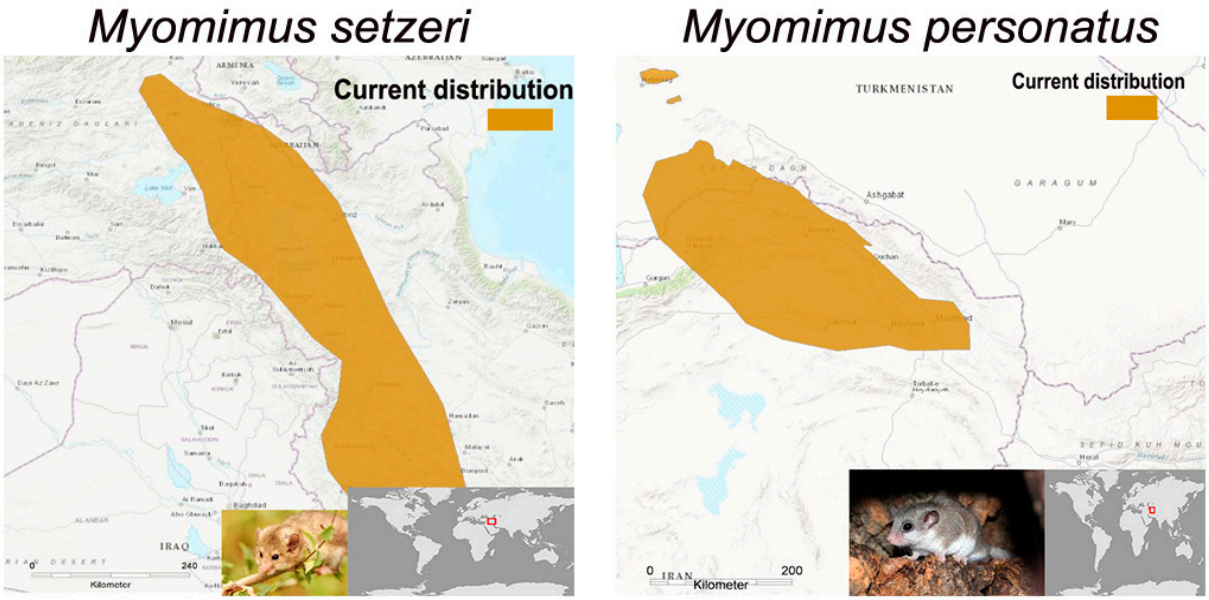


Figure 7.12. Distribution of *Myomimus setzeri* and *M. personatus*, according to the IUCN red list (https://www.iucnredlist.org/).

desertic conditions than present.

Conclusion about the identified rodent species

The studied region represents a crossroads between Africa, Europe and Asia. This influence is observable in the composition of the rodent´s assemblage in the area. The rodent species identified at Azokh Cave, Kaldar Cave and in the Birecik pellet samples can be classified depending on their current distribution and biogeographic affinities (Table 7.2).

The identified species present several biogeographic affinities, but mainly come from Europe and Asia. Qesem Cave and Misliya also recorded the presence of African rodent taxa, such as *Mastomys* and *Arvicanthis* (Maul et al., 2015a; Weissbrod and Weinstein-Evron, 2020). Such species were not found at Azokh or Kaldar, indicating that the Zagros and Caucasus mountains probably acted as a barrier for small mammals coming from Africa. Moreover, most of the species found at Azokh and Kaldar display an Asiatic origin, suggesting the possible importance of the Black and Caspian seas acting as a possible barrier for small mammals coming from Europe, as was previously indicated by Yanina (2014). Both general and specific features of their development under multi-scale and multi-directional changes of climate during the Late Pleistocene were identified. The cold extensive transgressions of the Caspian Sea and the transgressions of the Caspian of the Pontian Basin, not exceeding the present sea level, developed synchronously in the cold (glacial). This tendency was also observed in other Late Pleistocene and early Holocene iranian sites such as Kani Mikaeli,Yafteh or Qalaloun where the african species are not present (Hashemi et al., 2006)

	Origin		
	Europe	**Africa**	**Asia**
Taxa	*Apodemus, Myomimus, Mesocricetus, Cricetulus migratorius, Clethrionomys glareolus, Chionomys nivalis, Microtus guentheri, Microtus socialis*	*Meriones libycus*	*Ellobius fuscocapillus, Ellobius lutescens, Apodemus, Myomimus, Mesocricetus, Cricetulus migratorius, Clethrionomys glareolus, Chionomys gud, Chionomys nivalis, Suncus etruscus, Microtus irani, Microtus socialis, Meriones libycus, Meriones tristrami, Meriones persicus, Meriones dahli, Meriones libycus, Meriones tristrami, Nesokia indica, Allactaga williamsi.*

Table 7.2. Modern biogeographic affinities of the species present in this work

7.2. Synthesis of Taphonomic inferences

As it is exposed in chapter 1, some studies of extant owl pellet assemblages have been performed in the Middle East (Abi-said et al., 2014; Darvish et al., 2000; Haddadian Shad et al., 2014; Kopij and Liven-schulman, 2013; Obuch and Khaleghizadeh, 2012; Rey-Rodríguez et al., 2019; Shehab et al., 2013), providing taxonomic and some taphonomic reference data in Iran, Lebanon, Israel, Turkey and Syria. Preliminary taphonomic studies have been developed in Azokh 1 and Kaldar Cave and attempted to identify the predators responsible of the assemblages accumulations. Predation is the main factor accumulating small mammal remains, both in modern and archaeological sites. Predation can be recognized by the presence and intensity of digestion on the prey teeth and skeleton (Andrews, 1990; Fernández-Jalvo et al., 2016c).

If the diet of nocturnal and diurnal raptors and small carnivores is relatively well studied, their taphonomic impact on prey bones remain poorly known for most of them. The digestion is of different intensity depending on the predator species, and can impact differently the preservation of their prey assemblage. It is important to know the predator at the origin of the accumulations, because it can affect the palaeoecological interpretations depending on the size, diet, ecology, hunting habits, mode of ingestion of the predators (Andrews, 1990; Fernández-Jalvo et al., 2016c). Predation is closely related to ecology for two main reasons that are the density dependence of prey according to population fluctuations and the trophic preferences of the predator. So, the distinction and identification of the predator (s) helps to better identify the nature and origin of the assemblage. It is necessary to take into account these factors for the palaeoecological interpretations based on small mammals studies.

In Azokh 1, a preliminary taphonomic study was performed, with a subsample composed of 100 incisors and 90 rodent molars (mainly murinae and arvicolinae) by unit. The result show different degrees of digestion on molars and incisors between the studied levels: 26.83% in Unit V and 22.22% in Unit II. The grades of digestions in both units are in majority light (14.53% on Unit V and 17.50% on Unit II) and moderate categories (5.77% on Unit V and 8.37% on Unit II). The archaeological samples were, probably, accumulated by a Category 1 predator, such as some barn owl species producing a low degree of digestion (Chapter 5). Barn owls are recognized for being opportunistic hunters giving a good overview of the nocturnal small mammals in their environment.

A preliminary taphonomic study was also performed at Kaldar Cave (Chapter 6), showing a significant number of digested teeth, indicating that predation activity was the origin of a significant part of the accumulation. According to the degrees of digestion observed on the molars (mostly light, moderate, and heavy in a few cases), the predator responsible for this accumulation could be a category 3 predator such as the tawny owl (*Strix aluco*) or the Eurasian eagle owl (*Bubo bubo*). Both of them are present in the area nowadays, have opportunistic hunting habits, and are sedentary, so their prey spectrum is assumed to be a good representation of the ecosystem in which they live (Table 7.3).

In order to enhance the taphonomic referential for Middle Eastern species, and to contribute to a better interpretation of fossil accumulations, we also performed a complete taphonomic study on 40 disintegrated owl pellets coming from Birecik in Turkey (Chapter 3). The taphonomic study focused on bone

representation, fragmentation and digestion of small mammal elements (Andrews, 1990; Fernández-Jalvo et al., 2016c). Following these criteria, our sample corresponds to a Category 1 predator, such as the Barn owl *Tyto alba*. This is an active opportunistic hunter, especially at night. Consequently, nocturnal prey-species are taken more commonly than diurnal ones, which corresponds to what we found in the Birecik pellet assemblage. The diet of *Tyto alba* from our collected pellets fits well with the other studies in Europe and Asia for this owl species. The Barn owls' preys are mainly small vertebrates, including a wide range of rodents and insectivores (Andrews, 1990) (Table 7.3).

Few taphonomic studies were devoted to small mammals in Pleistocene contexts in this region. For example, concerning the comparative sites in Israel, Syria and Iran (Demirel et al., 2011; Maul et al., 2015b; Rey-Rodríguez et al., 2020; Smith et al., 2015), the authors concluded to an origin of the accumulation by predation activity, mainly owls. But most of the time, quantitative data on digestion by predators, or the impact of other taphonomic agents, are not described. Taphonomy is essential for analysing, recognising and understanding the processes and agents involved in the formation of fossil/archaeological records (López et al., 2017). That is why it is important to create and implement a database for the taphonomic studies in this region.

Site	Category
Birecik	**Category 1**: ***Tyto alba***, *Asio flammeus, Asio otus, Bubo lacteus.*
Kaldar Cave	**Category 3**: ***Bubo bubo, Strix aluco, Bubo africanus***, *Athene noctua.*
Azokh 1	Probably a **Category 1**: ***Tyto alba***, *Asio flammeus, Asio otus, Bubo lacteus.*

Table 7.3. Probable agents of accumulation of the archaeological and modern study samples according to Andrews 1990, Demirel et al., 2011 and Fernández-Jalvo 2016c.

7.3. Integration of our data in a broader climatic context

In this part are summarized the various discussions explored in the different chapters of this PhD. Once the identification and the origin of the accumulation are clear, the next step is to compare our paleoenvironmental and paleoclimatic reconstructions with a general climatic context during the Middle and Late Pleistocene in the study region. In Table 7.4 the archaeological and modern studied assemblages are correlated with the geological, cultural climatic and isotopic

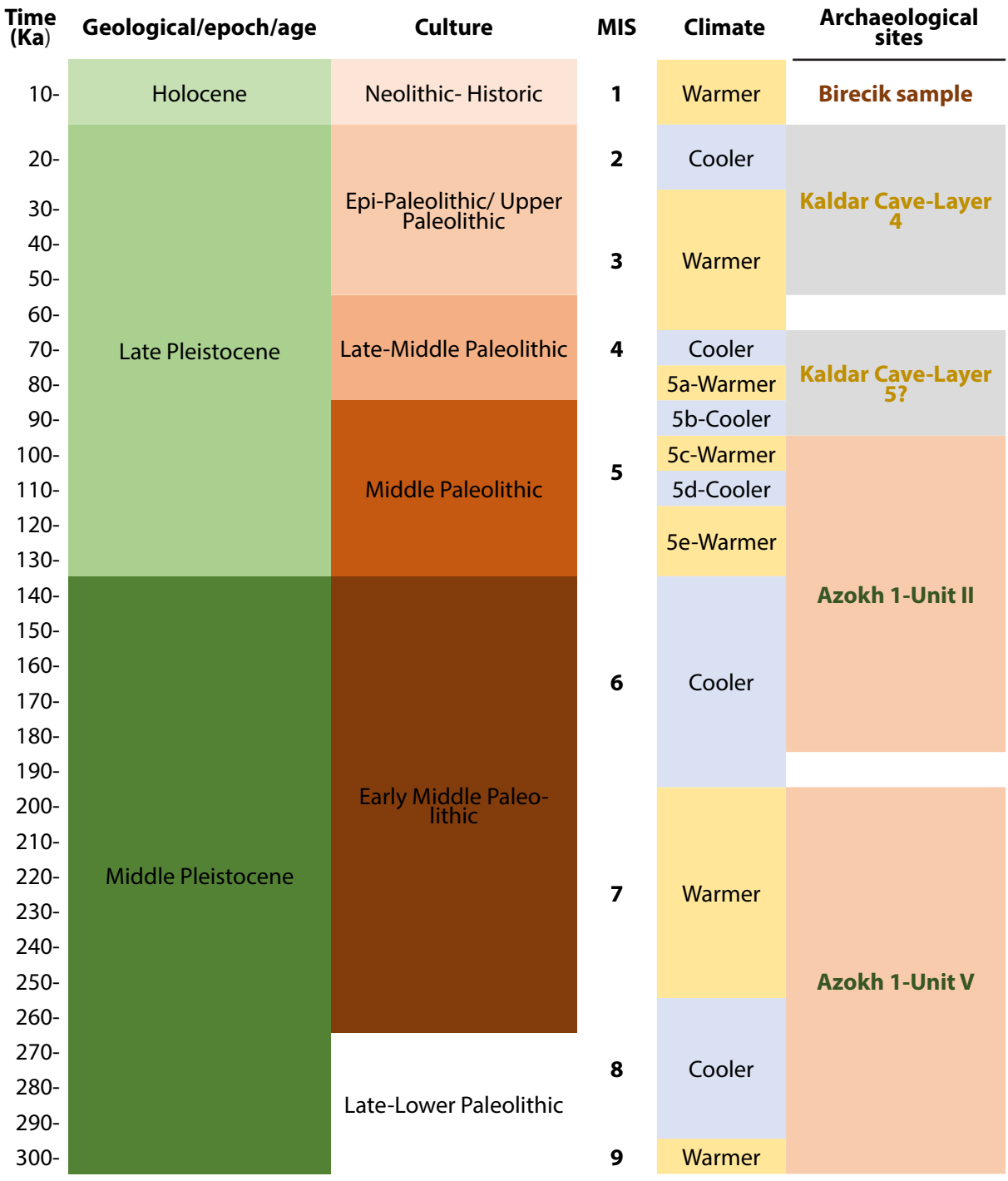


Table 7.4. Time span relation between the major events in human population and the studied sites regarding the published chronological data (modified from Weissbrod et al. 2020 and Hirst 2019). MIS = Marine Isotopic Stage.

	Azokh 1			Kaldar Cave			Birecik	
	Unit V	Unit II	Current Values	Layer 5	Layer 4	Current values		Current values
MAT	11.42ºC	10.86ºC	10.1ºC	10.90 ºC	11.73ºC	16.90 ºC	20.86 °C	18.5ºC
MTW	22.51ºC	22.44ºC	22.9ºC	23.45 ºC	23.10ºC	29.60 ºC	27.61°C	39ºC
MTC	1.43ºC	0.11ºC	-3ºC	-1.69 ºC	0.25ºC	5ºC	11.45°C	2.7ºC
MAP	528.13mm	500.01mm	668mm	258.68mm	104.08mm	488mm	431.98 mm	458.1mm

Table 7.5. Values of mean annual temperatures and precipitations for Azokh 1 Unit V and Unit II, Kaldar Cave Layer 5 and Layer 4 and Birecik samples, obtained with the Bioclimatic Model method. MAT (mean annual temperature); MTC (mean temperature of coldest month); MTW (mean temperature of warmest month); MAP (mean annual precipitation).

chronologies.

Mean annual temperatures and precipitations values obtained through the bioclimatic model applied on the rodent´s assemblages of Azokh 1 (Chapter 5) for the Middle to Late Pleistocene, of Kaldar Cave (Chapter 6) for the Late Pleistocene and of Birecik (Chapter 3) for the current values, have been compared (Table 7.5).

According to the available data and in order to link the palaeoenvironmental and palaeoclimatic conditions with the global isotopic chronology, the different layers of the studied sites were separated in three main groups: the first group ranges from MIS 9 to MIS 7, the second group from MIS 6 to MIS 4, and the third group from MIS 3 to MIS 2.

7.3.1. MIS 9 – MIS 7 (ca. 334-185 ka)

Marine Isotope Stages 9 and 7 are composed of three warm, low ice volume episodes (substages a, c and e) and two intervening cold intervals of greater ice volume (substages b and d) (Litt et al., 2014; Roucoux et al., 2006). MIS 8 is composed of two distinct periods of larger ice volume separated by a period of lower ice volume which contains marine isotope event 8.3; this interval of lower ice volume, between 253 ka and 266 ka is the MIS 8c (Roucoux et al., 2006).

According to Roucoux et al. (2008, 2006) the period comprised between MIS 9 and MIS 7 is characterised by "rapid" fluctuations from cold to warm-temperate climates within the range of the absolute dates for Azokh 1 Unit V, between 293 ± 23 ka (ESR dating) and 200 ka (Uranium series method) (Murray et al., 2016). These climatic shifts are characterized by transition from various steppe landscapes (Groups A, B and C on Figure 7.13) to temperate woodland and heath vegetation (Groups D on Figure 7.13) and finally to temperate woodland with Mediterranean elements (Group E on Figure 7.13).

Regarding the previous studies and the Azokh 1 Unit V chronology (Murray et al., 2016), this unit could be positioned between MIS 9b and MIS 7.

MIS 9b, corresponds to a pronounced tree population collapse with a moderate and brief incursion of sub-polar water offshore and large accumulation of continental ice, indicating dry, cold conditions on land. MIS 9a corresponds to a forest expansion, and *Quercus* is the only Mediterranean taxon present during this period (Roucoux et al., 2006).

For the MIS 8d, the $\delta^{18}O$ values indicate ice volume pointing the occurrence of a Heinrich-type event. It is followed by an interval of warmer conditions (MIS 8c) and then again a return to low temperatures

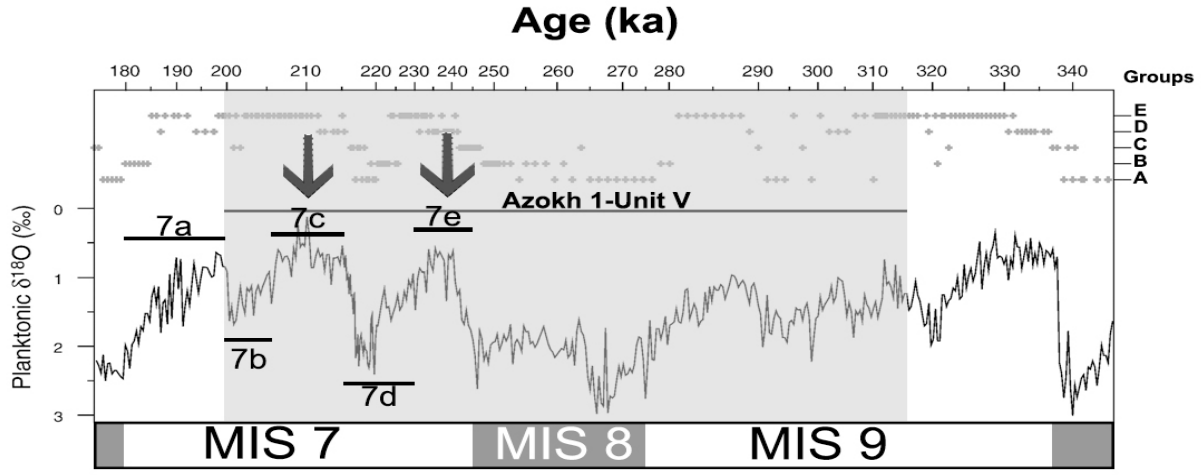


Figure 7.13. Relation of Azokh 1 Unit V with the planktonic δ18O values and vegetation groups (A: Steppe with pioneer vegetation, B: heath with steppe vegetation, C: pioneer with steppe vegetation, D: temperate woodland and heath vegetation and E: temperate woodland with Mediterranean elements) (modified from Blain et al., 2012; Roucoux et al., 2006). The arrows indicate the possible chronological attributions of Azokh 1 Unit V.

before Termination III, with a steppe vegetation and reduced tree populations (Roucoux et al., 2006).

Temperate forest returned with MIS 7e, observed through the δ18O values. The pronounced contraction of the tree populations and expansion of steppe vegetation coincides with MIS 7d, with similar conditions to the early part of MIS 8 (Roucoux et al., 2006). Records from Antarctica and the North Atlantic show MIS 7d as an extremely cold stadial event, with low global temperatures and large ice volume. MIS 7c is the longest forest interval, evidenced by the presence of temperate tree populations. Atlantic sea surfaces temperatures declined only during MIS 7b and sea level estimates indicate only minor accumulation of ice. Of all the stadial events, this has the least polar water influence; steppe elements remained rare, and while temperate tree populations were small, they remained more widespread than during other cold stages recorded here. MIS 7a is represented by a tree population expansion, that is more pronounced than in the previous MIS 7 warm sub-stages, with significant contributions of Mediterranean elements. The decline in tree populations (that marks the end of the forest interval) was followed by a moderate expansion of *Quercus* and accompanied by a pronounced increase in the extent of heathland, especially during the MIS 7/6 transition (Roucoux et al., 2008, 2006).

As we exposed above, the palaeoclimatic results of the Azokh 1 Unit V (Table 7.5) obtained with the BM indicate that the MAT is 11.4ºC, 1.3ºC higher that the current values (nowadays the MAT is Azokh town is 10.1ºC). These climatic estimations suggest that our studied assemblage was deposited during a warm temperate period. Regarding the archaeobotanical data, it is mainly composed of *Quercus* sp. (a Mediterranean tree taxon), *Prunus* and *Maloideae* (Allué, 2016). Large mammals are mainly composed of interglacial species (Van Der Made et al., 2016). Bats assemblage is characterised by open-ground landscape with steppe vegetation (Sevilla, 2016), and herpetofauna seems to be more consistent with a meadow-

steppe environment (Blain, 2016).

According to the absolute dating and all the available proxies (Allué, 2016; Blain, 2016; Murray et al., 2016; Sevilla, 2016; Van Der Made et al., 2016) the shifts that could correspond to Unit V can possibly be warm periods of MIS 9b, MIS 8b, MIS 7e, 7c and 7a (according to Roucoux et al. 2008, 2006). However, taking into account the estimated temperatures (through the BM), the δ18O values and the environmental data (through the habitat weighting), the rodent´s assemblage is associated to arid environments, mainly steppes and shrubland, while large mammals and charcoal data reflect woodland environments. All these data together suggest that Unit V probably corresponds rather to MIS 7 (e or c). The obtained values are similar to the other sites with similar chronology and smal vertebrate studies, as for example in Valdocarros II (Spain) (Blain et al., 2012) with MAT of 12.1ºC for level 2, 13.8ºC for level 3 and 15.3ºC for level 4, indicating similar climatic conditions, as we have in Azokh 1 Unit V.

7.3.2. MIS 6 - MIS 4 (ca. 185-60 ka)

The period comprised between MIS 6 and MIS 4 is characterised by a high climatic variability, with an alternation of warm and cold periods (López-García et al., 2018; Railsback et al., 2015; Roucoux et al., 2008; Wilson et al., 2021). For Azokh 1 - Unit II, the chronology is 184 ± 13 ka for the bottom and 100 ± 7 ka for the contact between Units II and I (Murray et al., 2016). Regarding the data for Kaldar Cave (table 7.5), Layer 5 was deposited during a colder period but we do not have an absolute chronology for that, however as it is under Layer 4 it is considered older than 54,400 years B.P. (Bazgir et al., 2017). We thus attributed Azokh 1 - Unit II to a period comprised between MIS 6 and MIS 5, and Kaldar Cave - Layer 5 to a period comprised between MIS 5 and MIS 4.

MIS 6 ranges from 185 to 130 ka (Wilson et al., 2021), is characterized by an accumulation and wasting of continental ice masses, and was punctuated by millennial-scale climate variability (Roucoux et al., 2006; Wilson et al., 2021). MIS 6 can be divided in substages 6e, 6d, 6c, 6b and 6a (Railsback et al., 2015; Wegwerth et al., 2019). It is globally considered as a cold period, characterized by cold and dry conditions (Roucoux et al., 2006) specially during the substages 6a, 6b and 6e (Railsback et al., 2015).

MIS 5 indicates the beginning of the Late Pleistocene, which was starting with the warm period of the MIS 5e (Eemian), the most recent warm period in Earth´s climate history prior to the Holocene (ca 12-0 ka to nowadays) characterized by reduced terrestrial ice volume and higher-than-modern global sea level (Újvári et al., 2019). Substages 5c and 5a also correspond to warm episodes, but not as warm as 5e. Climate of the MIS 5 was punctuated by several millennial scale cold intervals, in particular two cold periods that are 5b and 5d (Yanina, 2014). While all the forested intervals of MIS 5 (5e, c, a) were characterized by mild climate, the last interglacial (MIS 5e) was the most temperate period, as shown by pollen records and Coleoptera assemblages, and the MIS 5c and 5a intervals had more continental climate regimes (Újvári et al., 2019).

MIS 4 is a stage of short duration, lasting about 14 ka, between 71 and 57 ka (López-García et al., 2018). It began with a cold-dry episode, at the transition MIS 5/4, which however was not as cold as MIS 6 (Yanina, 2014). Minimum summer isolation in the North Hemisphere produced a maximum extension of the polar ice caps during the Late Pleistocene, sea level was a hundred meters above the current one, and the ocean temperatures were 10ºC lower than at

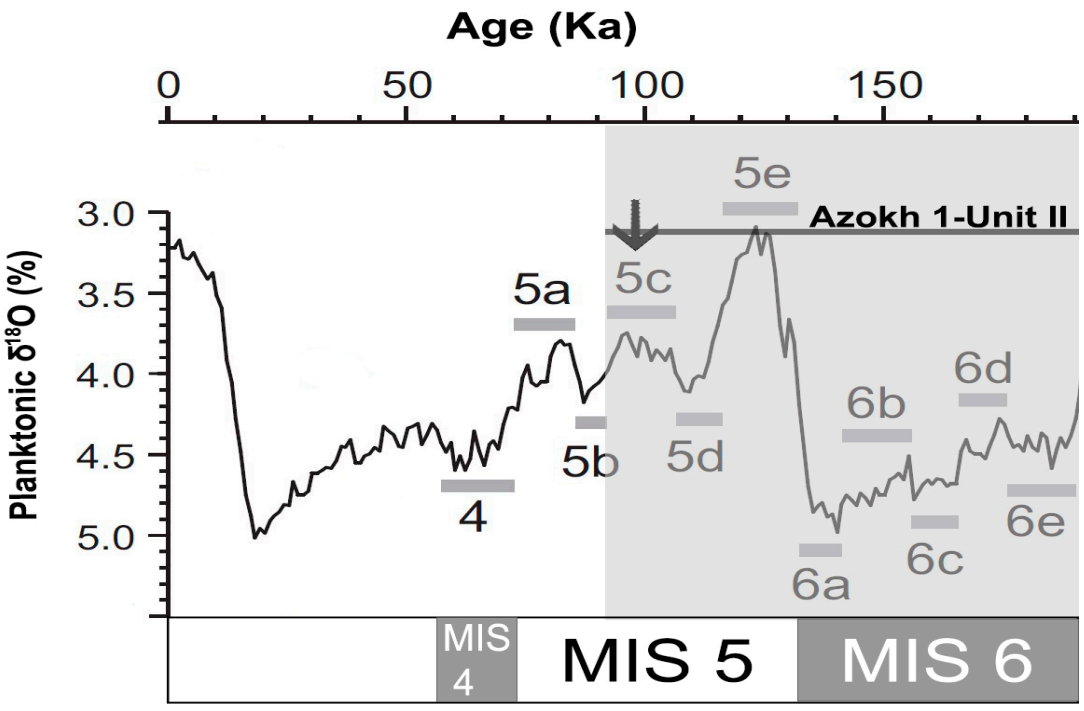


Figure 7.14. Correlation of Azokh 1-Unit II with the δ18O values (modified from Railsback et al., 2015). The arrow indicates the possible chronological attribution of Azokh 1 - Unit II.

present (López-García et al., 2018). Although it is considered a cold isotopic stage, at least one interstadial period has been detected, characterized by a warming of the sea surface, but this is not reflected in an increase in temperatures on the continent.

We can excluded the MIS 6 for the chronological attribution of the studied levels, because this period was much colder and drier than in Azokh 1 - Unit II. Indeed, the BM has shown a warm temperate period, with temperatures similar to the current ones. Within the considered chronological range, the MIS 5e is a warm period, but the temperatures would be around 2ºC higher that the current ones (Újvári et al., 2019). Consequently, the palaeoenvironmental conditions reflected by the Azokh 1 - Unit II indicate a landscape mainly composed of steppe and shrubland with an important proportion of forest formations, notably through the presence of *Clethrionomys glareolus* and *Apodemus* (*Sylvaemus*) sp. Large mammals and charcoal data reflect woodland environments, while small vertebrates and coprolites mainly depict arid environments (steppes and shrubland). All the available data, together with the chronology established, suggest that the Unit II could corresponds rather to the MIS 5c (Figure 7.14).

On the other hand, BM based on the small mammals from Kaldar Cave suggests lower temperatures and lower precipitations than at present in Layer 5 (Table 7.5). The MAT is around 6ºC lower, and there is a higher temperature amplitude between maximum and minimum mean temperatures with a landscape mainly composed of steppes and deserts, notably through the presence of *Myomimus* sp. (Rey-Rodríguez et al., 2020). Charcoal analyses (Allué et al., 2018; Bazgir et al., 2017) indicate that there were active water sources or flows, with specific plant communities characteristic of open forest growing in cool and dry conditions (Allué et al., 2018). The presence of forested areas is also supported by the large mammals, with

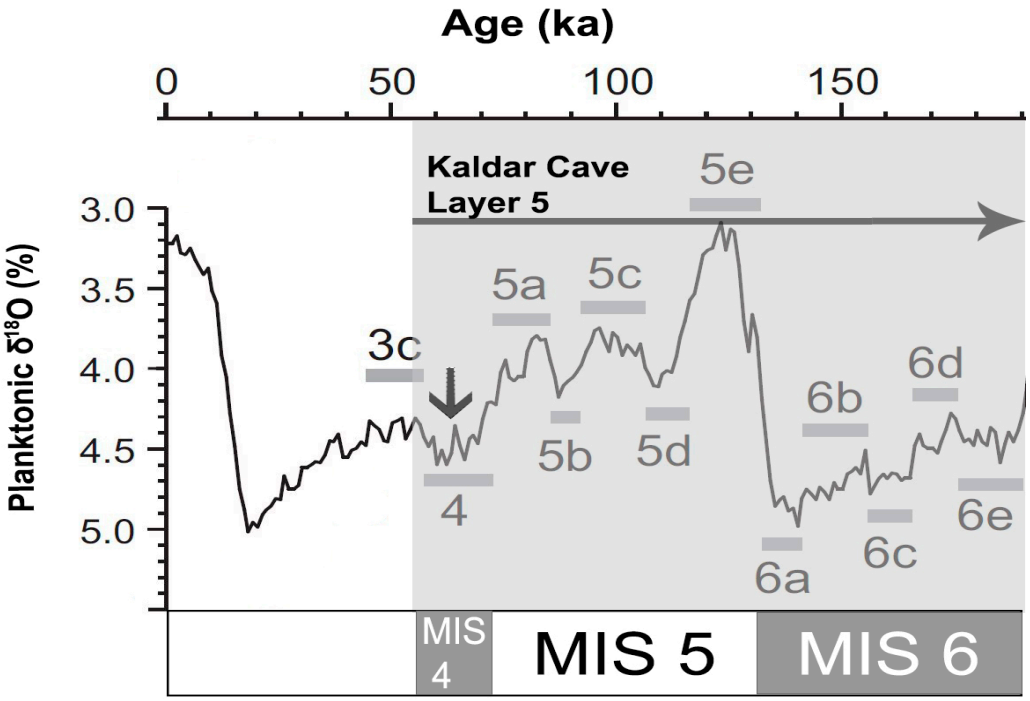


Figure 7.15. Correlation of Kaldar Cave - Layer 5 with the δ18O values (modified from Railsback et al., 2015). The arrow indicates the possible chronological attribution of Kaldar Cave - Layer 5.

the presence of *Sus scrofa*, *Capreolus* sp. and *Cervus elaphus* (Bazgir et al., 2017), thus suggesting a mosaic landscape alternating between dry-steppe areas and wooded patches.

Despite the uncertain chronology, the data suggest a deposition during a cold period for Layer 5, which can possibly be MIS 4, MIS 5b or 5d. In our case, we have 6°C lower than at present, we could rather attribute the Layer 5 to the MIS 4, because during MIS 5b and MIS 5d the temperatures were higher (Újvári et al., 2019). Regarding the lower number of cave sequences that coud be attributed to MIS 4, De Nadale Cave (López-García et al., 2018) in north-eastern Italy, yielded the unique small mammals study for this period. This study indicates MAT values of 5.4°C lower than the present ones, pointing out a colder climate. According to Svendsen et al. (2014), in the Ural mountains the MIS 4 was also characterized by 6°C lower temperatures than at present (Figure 7.15).

7.3.3. MIS 3 - MIS 2 (60-11.6 ka)

Regarding the data for Kaldar Cave - Layer 4 (table 7.5), it was formed during a cooler period, compared with the current values. The chronology ranges from 54,400 BP at the bottom, to 23,100 ± 3 300 BP at the top (Behrouz Bazgir et al., 2017), locating this Layer 4 between the MIS 3 and the beginning of MIS 2, before the Last Glacial Maximum.

The MIS 3 is complex in terms of climatic oscillations, being one of the most highly unstable phases (Badino et al., 2020). Its chronology is comprised between 60 and 30 ka (Li et al., 2019). MIS 3 was characterized by major rapid climatic changes showing high variability associated by abrupt atmospheric shifts over (Dansgaard-Oeschger [D-O] events) and episodes of massive iceberg discharge into the North Atlantic (Heinrich events [HEs]) enhancing cold and dry conditions at mid-to-

low latitudes (Badino et al., 2020).

During MIS 3, there were detected three Heinrich Events (H): H5, H4 and H3 (Obrochta et al., 2014), characterised by a cool and dry climate. There are several several sites with small-vertebrate assemblages where H were detected, as for example: H5 in Xaragalls Cave, H4 in Cueva del Conde N20b, and H3 in Galls Carboners (López-García et al., 2014). In general, all these sites present cold climatic fluctuations characterized by lower MAT, MTC and MTW than at present. However, here are differences between the different H events: H3 is the least cold, in comparison with the H4 and H5 showing similar fluctuations to the LGM. López-García et al. (2014) compared different sites from the same region, concluding that H5 was MAT -5.7ºC to -5.4ºC lower than the present, indicating as that it was also pointed by Royer et al (2013) the driest and coldest period of the MIS3.

The transition from MIS 3 to MIS 2 has been driven by a significantly colder climate (Svendsen et al., 2014). MIS 2 is considered as a cold period, however the temperatures were higher than during the previous MIS 4 (Svendsen et al., 2014), which was characterized by the most severe ice conditions over the last glaciation (Vasilenko et al., 2019).

The paleoclimatic conditions for Kaldar Cave - Layer 4, obtained through the BM, suggest lower temperatures (MAT -5.2ºC) and lower precipitation (-230mm) than at present (Table 7.5). The landscape was mainly composed of steppes, and grasslands were also well represented, notably through the presence of *Microtus guentheri* (Rey-Rodríguez et al., 2020). As in Layer 5, Charcoal analyses of Layer 4 (Allué et al., 2018; Bazgir et al., 2017) indicate that there were active water sources or flows, with specific plant communities characteristic of open forest growing in cool and dry conditions (Allué et al., 2018). The presence of forested areas is also supported by the large mammals, with the presence of *Sus scrofa*, *Capreolus* sp. and *Cervus elaphus* (Bazgir et al., 2017), thus suggesting a mosaic landscape alternating between dry-steppe areas and wooded patches (Rey-Rodríguez et al., 2020).

According to the absolute dating,

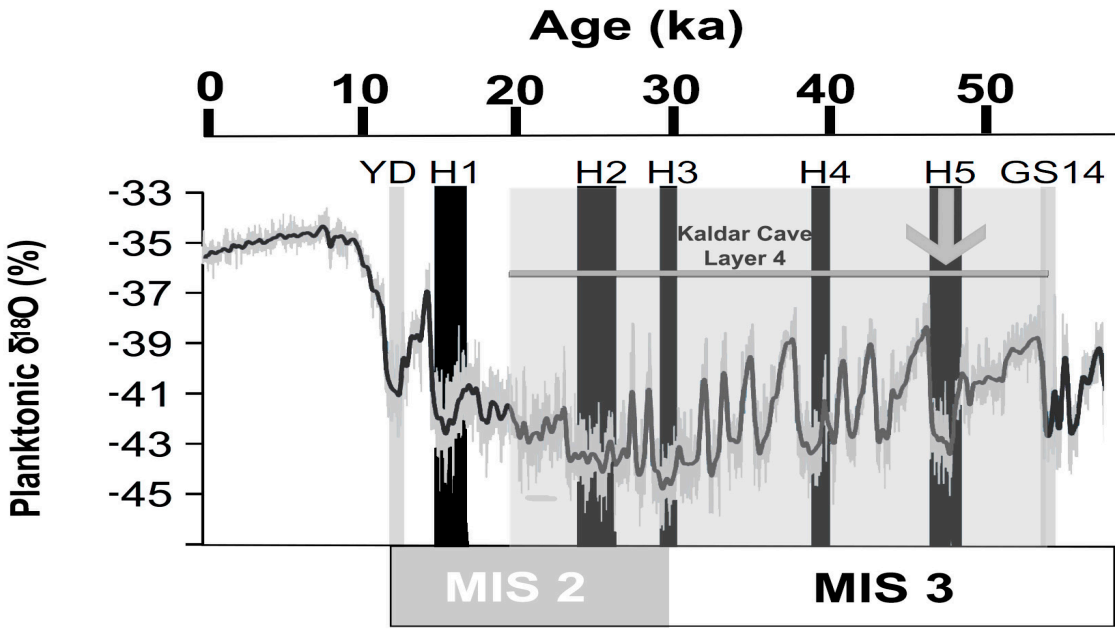


Figure 7.16. Relation of Kaldar Cave - Layer 4 with the δ18O values (modified from Obrochta et al., 2014). The arrow indicates the possible chronological attribution of Kaldar Cave - Layer 4.

situating our sample between the MIS 3 and the beginning of MIS 2, combined with previous studies of other proxies, we can assume that the Layers 4 of Kaldar Cave was deposited during a cold period, probably a Heinrich Event during MIS 3. We can hypothesise that the Layer 4 probably corresponds to the H5 event, because this one was characterized by a MAT between -5.7°C to -5.4°C lower than at present (Royer et al., 2013), and in our case we have a MAT with a value of -5.2°C lower than the current values (Figure 7.16).

Chapter 8.

General conclusions and perspectives



8.1. General conclusions

The aim of this PhD thesis has been to study rodent assemblages in western Asia, focusing on the archaeological sites of Azokh Cave and Kaldar Cave, and also modern pellet samples from Birecik in order to answer the question related with the origin of rodent acumulations. The obtained results allow us to enumerate the following conclusions:

8.1.1. Barn owls pellets analysis

- From the Birecik current pellets sample, we have identified 2501 rodent skeletal elements belonging to *Nesokia indica*, *Mus musculus* and *Meriones tristami.* We also found remains of *Suncus etruscus,* a small shrew of Asiatic origin, recently introduced in the whole Mediterranean area.
- The taphonomic study showed that our assemblage fits well with a predator category of light modification, like the Barn owl. The mean bone relative abundance reached 82%, and the bone fragmentation showed that more than 77% of our sample is intact. The digested elements represent 22% and the low to moderate grades were dominant (83.5%).
- Habitat weighting and Bioclimatic model, have been applied on the Birecik assemblage as a method for the environmental and climatic reconstruction in order to test for the first time the the potential of both methods upon an owl pellet assemblage for environmental and climatic reconstruction and its validity for further archeological studies. The values obtained for the temperatures and precipitations and also the reconstruction of the landscape indicated that they both are valid methods.

8.1.2. Identification of modern and fossil *Ellobius* species using geometric morphometric (GM) methods on molars

- We found potential size and shape differences between *Ellobius* species from southeastern Europe, western and central Asia thanks to GMM analyses. The modern museum specimens (coming from the Natural History Museum of London, the Field Museum of Chicago, and the American Museum of Natural History of New York) allowed to establish a valid referential and then to accurately identify the fossil specimens from Kaldar Cave. Based on the m1 shape, we were able to differentiate two groups: *E. talpinus* on the one hand, and *E. fuscocapillus* and *E. lutescens* on the other. Taking size into account, it was possible to distinguish *E. fuscocapillus* from *E. lutescens.*
- GMM enabled us to obtain good results in fossil species attributions, identify fossil specimens from Kaldar Cave as *E. lutescens* and some as *E. fuscocapillus*, and excluding *E. talpinus.*

8.1.3. Azokh 1 Cave

- Azokh 1 Cave rodent assemblage is composed of 434 identified remains showing at least 13 taxa: seven arvicoline (*Clethrionomys glareolus*, *Microtus* gr. *arvalis-socialis, Microtus* (*Terricola*) spp.*, Arvicola persicus, Chionomys nivalis, Chionomys gud* and *Ellobius lutescens*), two cricetines (*Cricetulus migratorius* and *Mesocricetus brandti*), two gerbillines (*Meriones* gr. *persicus-tristrami, Meriones* gr. *dahli-libycus),* one dipodid (*Allactaga* cf. *williamsi*)

and one murine (*Apodemus* spp.). The same GMM method than that elaborated for Kaldar Cave was applied at Azokh 1 to identify *Ellobius* remains.

- In order to develop a preliminary taphonomic study in Azokh 1, we considered a subsample composed of 380 incisors and rodents molars, mainly muridae and arvicolinae, (100 incisors and 90 molars for each unit). A considerable part of the molars and incisors show evidence of digestion: 26.83% in Unit V and 22.22% in Unit II; the grades are light, suggesting that they were probably accumulated by a category 1 predator. Being the first taphonomic approach for small mammals in the site.
- The palaeoclimatic and paleoenvironmental results obtained from Azokh 1 (Unit V and Unit II) indicate a climate that seems to be relatively warm-temperate and an environment mainly composed of shrubland and steppe, with patches of deciduous forests and desert, similar to the one found nowadays in the area.

8.1.4. Kaldar Cave

- In Kaldar Cave, 1112 rodent remains were identified, belonging to 13 taxa: six arvicoline (*Microtus socialis, Microtus irani, Microtus guentheri, Chionomys nivalis, Ellobius fuscocapillus* and *Ellobius lutescens*), two cricetine (*Cricetulus migratorius* and *Mesocricetus brandti*), one glirid (*Myomimus* sp.), one gerbilline (*Meriones* cf. *persicus),* one dipodid (*Allactaga* sp.) and two murine (*Apodemus* sp. and *Mus* cf. *musculus*).
- A preliminary taphonomic study was performed on the Kaldar Cave micromammal remains. It has shown a significant number of digested teeth indicating that predation activity was the origin of at least part of the accumulation. The different degrees of digestion observed, mostly light and moderate, with some heavy grades in a few cases, indicate that the predator responsible for this accumulation could be a category 3 predator such as the tawny owl (*Strix aluco*) or the Eurasian eagle owl (*Bubo bubo*).
- The first palaeoecological analysis of the rodents from Kaldar Cave revealed lower temperatures and lower precipitation than present-day conditions, and an environment mainly composed of dry steppes with patches of forested areas, in Layer 5 and Layer 4.

In conclusion, the use of various methods of rodents analyses allowed to improve taxonomic identifications, identify the predators at the origins of the assemblages and to recover important paleoenvironemntal and palaeoclimatic information in western Asia, especially in the Zagros mountains of Iran and the Caucasus region.

We also observed that our sample is mainly composed by asiatic species , indicating that the Zagros and Caucasus mountains probably acted as a barrier for small mammals coming from Africa.

8.2. Perspectives

This PhD thesis offered me the opportunity to start with the study of western Asian rodents, however, I am pending to develop some interesting analysis or questions that are not still resolved. I would like to continue my research with the following objectives:

- Extend the GMM study to other modern and fossil *Ellobius* species, increasing the modern reference collection for *E. lutescens* and including the whole geographic range of the genus during the Pleistocene.
- Apply the GMM method to other taxa, such as *Meriones* and *Microtus*, because they are abundant in the archaeological and paleontological sites and a revision of the western and central Asia species are needed, including reference collection, Azokh Cave, Kaldar Cave and other potential sites.
- Perform a complete taphonomic study in Azokh 1 Cave and Kaldar Cave, taking into account post-depositional agents, breakage, bone composition, among others, in order to complete understanding of the formation and pos-depositional processes.
- Try to develop taphonomic experiments with extant reference collections and molars with tartar, and try to see their possible impact in the taphonomic studies. During the study of the barn owl pellets we identified tartar on molars that is the reason because I would like to made some taphonomic experiments and try to see if it is possible to differentiate digested teeth with tartar and non-digested teeth
- Increase the neotaphonomic data based in western and central Asia, collaborating with other Iranian institutions in the pellets studies for the understanding of predation activities and the role of predator in making noise in paleoenvironmental analyses.
- Increase the archaeological samples in space and time lapse and apply the Habitat weighting and the Bioclimatic model for the palaeoenvironmental and palaeoclimatic reconstructions, having more information in this important region for the evolution of the hominines.
- Expand the study to other order small mammals as Eulipothyphla and Chiroptera to obtain more complete view of our potential enviroment and climate.
- To do a regional synthesis on the rodents studies establishing comparisons between the Caucasus, Zagros and the Mediterranean and central Asiatic archaeological and paleontological sites. For the palaeobiogeographic reconstruction.
- Set up a biochronology of the Quaternary rodents in western Asia in order to have an accurate reference dataset of the rodents during this period.
- Try to evidence faunal changes, turnovers or migrations linked to global climatic and environmental changes, expand to the study of other sites for western and central Asia.

References



A

Abi-Said, M.R., Shehab, A.H., Amr, Z.S., 2014. Diet of the barn owl. Jordan J. Biol. Sci. 7 (2), 109e112.

Adams, D.C., Collyer, M.L., Kaliontzopoulou, A., 2020. Geomorph: Software for geometric morphometric analyses. R package version 3.2.1.

Adams, D.C., Rohlf, F.J.,and Slice, D.E. 2009. Geometric morphometrics: Ten years of progress following the revolution. Italian Journal of Zoology, 71 (1): 5-16, https://doi.org/10.1080/11250000409356545

Allué, E., 2016. Charcoal Remains from Azokh 1 Cave: Preliminary Results, in: Fernández-Jalvo, Y., King, T., Yepiskoposyan, L., Andrews, P. (Eds.), Azokh Cave and the Transcaucasian Corridor, Vertebrate Paleobiology and Paleoanthropology. Springer International Publishing, Cham, pp. 297–304. https://doi.org/10.1007/978-3-319-24924-7

Allué, E., Expósito, I., Tumung, L., Ollé, A., Bazgir, B., 2018. Early evidence of Prunus and Prunus cf. amygdalus from Palaeolithic sites in the Khorramabad Valley, western Iran. Comptes Rendus - Palevol 17, 335–345. https://doi.org/10.1016/j.crpv.2018.01.001

Amori, G., Hutterer, R., Kryštufek, B., Yigit, N., Mitsain, G. & Palomo, L.J. 2016. *Apodemus flavicollis* (errata version published in 2017). The IUCN Red List of Threatened Species 2016: e.T1892A115058023. https://dx.doi.org/10.2305/IUCN.UK.2016-3.RLTS.T1892A22423256.en

Amori, G., 1999. *Chionomys nivalis*. In: Mitchell-Jones, A.J., Amori, G., Bogdanowicz, W., Kry_stufek, B., Reijnders, P.J.H., Spitzenberger, F., Stubbe, M., Thissen, J.B.M., Vohralík, V., Zima, J. (Eds.), The Atlas of European Mammals. Academi Press, London, UK

Amr, A., 2015. *Microtus guentheri* , Günther ' s Vole 8235.

Andrews, P., 2018. Seasonal variation in prey composition and digestion in small mammal predator assemblages 1–14. https://doi.org/10.1002/oa.2656

Andrews, P., Hixson A. S., King, T., Fernández-Jalvo, Y., & Nieto-Díaz ,M., 2016. Palaeoecology of Azokh 1, in: Y. Fernández-Jalvo, T. King, L. Yepiskoposyan & P. Andrews (Eds.), Azokh Cave and the Transcaucasian Corridor (pp. 305–320). Dordrecht: Springer.

Andrews, P., 2006. Taphonomic effects of faunal impoverishment and faunal mixing. Palaeogeography, Palaeoclimatology, Palaeoecology 241, 572–589. https://doi.org/10.1016/j.palaeo.2006.04.012

Andrews, P., 1990. Owls, Caves and Fossils. https://doi.org/10.2307/3889096

Aşan Baydemir, N., Duman, L., 2009. Molar patterns in *Microtus guentheri* (Danford and Alston, 1880) (Mammalia: Rodentia) from Kirikkale province. Journal of Applied Biological Sciences 3, 47–54.

Asryan, L., 2015. Azokh Cave lithic assemblages and their contextualization in the Middle and Upper Pleistocene of Southwest Asia (PhD thesis). University Rovira i Virgili, Tarragona.

Asryan, L., Oll, A., Moloney, N., King, T., 2020. Occupying Cave-Sites: A Case Study from Azokh 1 Cave (Southern Caucasus), in: Short-Term OOcupations in Paleolithic Archaeology. pp. 149–181. https://doi.org/10.1007/978-3-030-27403-0

Asryan, L., Ollé, A., Moloney, N., King, T., Murray, J., 2017. Chemical Alteration of Lithic Artefacts: an Experimental Case Study on the effect of Guano on Stone Flakes and Its Contextualization in the Archaeological Assemblage of Azokh Cave (Southern Caucasus). Archaeometry 59, 981–999. https://doi.org/10.1111/arcm.12300

Aulagnier, S., Haffner, P., Mitchell-Jones, T. J., Moutou, F., & Zima, J. ,2014. Mammifères d'Europe, d'Afrique du Nord et du Moyen-Orient. Delachaux et Niestlé

B

Badino, F., Pini, R., Ravazzi, C., Margaritora, D., Arrighi, S., Bortolini, E., Figus, C., Giaccio, B., Lugli, F., Marciani, G., Monegato, G., Moroni, A., Negrino, F., Oxilia, G., Peresani, M., Romandini, M., Ronchitelli, A., Spinapolice, E.E., Zerboni, A., Benaz-

zi, S., 2020. An overview of Alpine and Mediterranean palaeogeography, terrestrial ecosystems and climate history during MIS 3 with focus on the Middle to Upper Palaeolithic transition. Quaternary International 551, 7–28. https://doi.org/10.1016/j.quaint.2019.09.024

Bañuls-Cardona, S., López-García, J.M., Blain, H. a., Lozano-Fernández, I., Cuenca-Bescós, G., 2014. The end of the Last Glacial Maximum in the Iberian Peninsula characterized by the small-mammal assemblages. Journal of Iberian Geology 40, 19–27. https://doi.org/10.5209/rev_JIGE.2014.v40.n1.44085

Barbosa, S., Paupério, J., Pavlova, S. V., Alves, P.C., Searle, J.B., 2018. The Microtus voles: Resolving the phylogeny of one of the most speciose mammalian genera using genomics. Molecular Phylogenetics and Evolution 125, 85–92. https://doi.org/10.1016/j.ympev.2018.03.017

Bate, D.M.A. 1930. Animal remains from the Dark Cave, Hazar Merd. American School of Prehistoric Research Bulletins, 6: 38-41.

Bate, D.M.A. 1937. Palaeontoogy: the fossil fauna of the Wady El-Mughara caves. In Garrod, D.A.E. and Bate, D.M.A. (eds.), Excavations at the Wady El-Mughara. Clarendon Press, Oxford.

Baylac, M., Frieß, M., 2006. Fourier Descriptors, Procrustes Superimposition, and Data Dimensionality: An Example of Cranial Shape Analysis in Modern Human Populations, in: Modern Morphometrics in Physical Anthropology. Kluwer Academic Publishers-Plenum Publishers, New York, pp. 145–165. https://doi.org/10.1007/0-387-27614-9_6

Bazgir, B., Ollé, A., Tumung, L., Becerra-Valdivia, L., Douka, K., Higham, T., Van Der Made, J., Picin, A., Saladié, P., López-Garciá, J.M., Blain, H.-A., Allué, E., Fernández-Garciá, M., Rey-Rodríguez, I., Arceredillo, D., Bahrololoumi, F., Azimi, M., Otte, M., Carbonell, E., 2017. Understanding the emergence of modern humans and the disappearance of Neanderthals: Insights from Kaldar Cave (Khorramabad Valley, Western Iran). Scientific Reports 7. https://doi.org/10.1038/srep43460

Bazgir, B., Otte, M., Tumung, L., Ollé, A., Deo, S.G., Joglekar, P., López-García, J.M., Picin, A., Davoudi, D., van der Made, J., 2014. Test excavations and initial results at the middle and upper paleolithic sites of Gilvaran, Kaldar, Ghamari caves and Gar Arjene Rockshelter, Khorramabad Valley, western Iran. Comptes Rendus - Palevol 13, 511–525. https://doi.org/10.1016/j.crpv.2014.01.005

Becerra-Valdivia, L., Douka, K., Comeskey, D., Bazgir, B., Conard, N.J., Marean, C.W., Ollé, A., Otte, M., Tumung, L., Zeidi, M., Higham, T.F.G., 2017. Chronometric investigations of the Middle to Upper Paleolithic transition in the Zagros Mountains using AMS radiocarbon dating and Bayesian age modelling. Journal of Human Evolution 109, 57–69. https://doi.org/10.1016/j.jhevol.2017.05.011

Beck, H.E., Zimmermann, N.E., Mcvicar, T.R., Vergopolan, N., Berg, A., Wood, E.F., 2018. Data Descriptor : Present and future Köppen-Geiger climate classi fi cation maps at 1 -km resolution. Nature Publishing Group 1–12. https://doi.org/10.1038/sdata.2018.214

Belmaker, M., Bar-Yosef, O., Belfer-Cohen, A., Meshveliani, T., Jakeli, N., 2016. The environment in the Caucasus in the Upper Paleolithic (Late Pleistocene): Evidence from the small mammals from Dzudzuana cave, Georgia. Quaternary International 425, 4–15. https://doi.org/10.1016/j.quaint.2016.06.022

Belmaker, M., Hovers, E., 2011. Ecological change and the extinction of the Levantine Neanderthals: Implications from a diachronic study of micromammals from Amud Cave, Israel. Quaternary Science Reviews 30, 3196–3209. https://doi.org/10.1016/j.quascirev.2011.08.001

Bergl; R.A.; Dunn; A.; Fowler; A.; Imong; I.; Ndeloh; D.; Nicholas; A. & Oates; J.F., 2017. Myodes glareolus. The IUCN Red List of Threatened Species 2016: e. T4973A115070929 8235, 8.

Bermúdez de Castro, J.M., Martinón-Torres, M., 2013. A new model for the evolution of the human Pleistocene populations of Europe. Quaternary International 295, 102–112. https://doi.org/10.1016/j.

quaint.2012.02.036

Berto, C., Krajcarz, M.T., Hoyo, M.M. del, Komar, M., Sinet-Mathiot, V., Zarzecka-Szubińska, K., Krajcarz, M., Szymanek, M., Wertz, K., Marciszak, A., Mętrak, M., Suska-Malawska, M., Wilcke, A., Kot, M., 2021. Environment changes during Middle to Upper Palaeolithic transition in southern Poland (Central Europe). A multiproxy approach for the MIS 3 sequence of Koziarnia Cave (Kraków-Częstochowa Upland). Journal of Archaeological Science: Reports 35. https://doi.org/10.1016/j.jasrep.2020.102723

Blain, H.A., Bisbal-Chinesta, J.F., Martínez-Monzón, A., Panera, J., Rubio-Jara, S., Uribelarrea, D., Yravedra Saínz de los Terreros, J., Pérez-González, A., 2019. The Middle to Late Pleistocene herpetofaunal assemblages from the Jarama and Manzanares valleys (Madrid, central Spain): An ecological synthesis. Quaternary International 520, 49–63. https://doi.org/10.1016/j.quaint.2018.03.004

Blain, H.-A., 2016. Chapter 9: Amphibians and Squamate Reptiles from Azokh 1, in: Fernández-Jalvo, Y., King, T., Yepiskoposyan, L., Andrews, P. (Eds.), Azokh Cave and the Transcaucasian Corridor, Vertebrate Paleobiology and Paleoanthropology. Springer International Publishing, Cham, pp. 211–249. https://doi.org/10.1007/978-3-319-24924-7

Blain, H.-A., Bailon, S., Cuenca-Bescós, G., 2008. The Early–Middle Pleistocene palaeoenvironmental change based on the squamate reptile and amphibian proxies at the Gran Dolina site, Atapuerca, Spain. Palaeogeography, Palaeoclimatology, Palaeoecology 261, 177–192. https://doi.org/10.1016/j.palaeo.2008.01.015

Blasius, W. 1884. Comptes rendus des séances de l´Académie des Sciences. Tome XCVIII. Nos 1 et 2. Paris.

Blyth, E. 1843. The Journal of the Asiatic Society of Bengal. Calcutta: Bishop's College Press,1832-1936

Bogicevic, K., Nenadic, D., Mihailovic, D., Lazarevic, Z., Milivojevic, J., 2011. Late Pleistocene rodents (Mammalia: Rodentia) from the baranica cave near Knja-evac (eastern Serbia): systematics and palaeoecology. Riv. Ital. Paleontol.Stratigr. 117 (2), 331e346.

Boitani, L., Molur, S., 2016. *Nesokia indica* (errata version published in 2017). The IUCN Red List of Threatened Species 2016: e.T14661A115123428. http://dx.doi.org/10.2305/IUCN.UK.2016-3.RLTS.T14661A22410105.en. Downloaded on 23 April 2018.

C

Campana, D. V., Crabtree, P., 2019. Evidence for skinning and craft activities from the Middle Paleolithic of Shanidar Cave, Iraq. Journal of Archaeological Science: Reports 25, 7–14. https://doi.org/10.1016/j.jasrep.2019.03.024

Carleton, M.D. and Musser, G.G. 2005. Order Rodentia, p. 745-752. In Wilson, D.E. and Reeder, D.M. (eds.), Mammal Species of the World, Third Edition. The Johns Hopkins University Press, Baltimore.

Chevret, P., Renaud, S., Helvaci, Z., Ulrich, R.G., Quéré, J.P., Michaux, J.R., 2020. Genetic structure, ecological versatility, and skull shape differentiation in Arvicola water voles (Rodentia, Cricetidae). Journal of Zoological Systematics and Evolutionary Research 58, 1323–1334. https://doi.org/10.1111/jzs.12384

Coil, R., Tappen, M., Ferring, R., Bukhsianidze, M., Nioradze, M., Lordkipanidze, D., 2020. Spatial patterning of the archaeological and paleontological assemblage at Dmanisi, Georgia: An analysis of site formation and carnivore-hominin interaction in Block 2. Journal of Human Evolution 143, 102773. https://doi.org/10.1016/j.jhevol.2020.102773

Corbet, G.B. and Hill, J.E. 1991. A World List of Mammalian Species. 3rd ed. London, UK: British Museum (Natural History).

Corbet, G.B. 1978. The Mammals of the Palearctic Region: A Taxonomic Review. London, Brit. Mus. (Nat. Hist.). Cornell Univ. Press. 117-118.

Cornette, R., Stoetzel, E., Baylac, M., Moulin, S., Hutterer, R., Nespoulet, R., El Hajraoui, M.A., Denys, C., Herrel, A., 2015. Shrews of the genus *Crocidura* from El Harhoura 2 (Témara, Morocco): The contribution of

broken specimens to the understanding of Late Pleistocene-Holocene palaeoenvironments in North Africa. Palaeogeography, Palaeoclimatology, Palaeoecology 436, 1–8. https://doi.org/10.1016/j.palaeo.2015.06.020

Coşkun, Y., 2016. Review of unique odd chromosome-numbered underground rodent species of the Palearctic region: *Ellobius Lutescens* Thomas 1897 (Rodentia: Cricetidae). Turkish Journal of Zoology 40, 831–841. https://doi.org/10.3906/zoo-1509-53

Coşkun, Y. 2001. On distribution, morphology and biology of the mole vole, *Ellobius lutescens* Thomas, 1897 (Mammalia: Rodentia) in eastern Turkey. Zoology in the Middle East, 23:5-12. https://doi.org/10.1080/09397140.2001.10637861

Coşkun, Y., 1999. Morphological characteristics of *Meriones tristrami* Thomas, 1892 (Rodentia: Gerbillinae) from Diyarbakır, Turkey. . Turk. J. Zool 23, 345–355.

Coşkun, Y. 1997. *Ellobius lutescens* Thomas, 1897 (Rodentia: Cricetidae) Turk. Journal of Zoology. 21, 349-354.

Cucchi, T., Mohaseb, A., Peigné, S., Debue, K., Orlando, L., Mashkour, M., 2017. Detecting taxonomic and phylogenetic signals in equid cheek teeth: Towards new palaeontological and archaeological proxies. Royal Society Open Science 4. https://doi.org/10.1098/rsos.160997

Cucchi, T., Barnett, R., Martínková, N., Renaud, S., Renvoisé, E., Evin, A., Sheridan, A., Mainland, I., Wickham-Jones, C., Tougard, C., Quéré, J.P., Pascal, Michel, Pascal, Marine, Heckel, G., O'Higgins, P., Searle, J.B., Dobney, K.M., 2014. The changing pace of insular life: 5000 years of microevolution in the orkney vole (*Microtus arvalis orcadensis*). Evolution 68, 2804–2820. https://doi.org/10.1111/evo.12476

D

Darlington, P.J. 1957. Zoogeography: The Geographical Distribution of Animals. New York, NY, USA, John Wiley and Sons.

Darvish, J., 2011. Morphological comparison of fourteen species of the genus M*eriones* Illiger , 1811 (Rodentia : Gerbillinae) from Asia and North Africa. Iranian Journal of Animal Biosystematics 7, 49–74.

Darvish, J., Mohammadi, Z., Ghorbani, F., Mahmoudi, A., Dubey, S., 2015. Phylogenetic Relationships of *Apodemus* Kaup, 1829 (Rodentia: Muridae) Species in the Eastern Mediterranean Inferred from Mitochondrial DNA, with Emphasis on Iranian Species. Journal of Mammalian Evolution 22, 583–595. https://doi.org/10.1007/s10914-015-9294-9

Darvish, J., Mohammadi, Z., Mahmoudi, A., Siahsarvie, R.., 2014. Faunistic and taxonomic study of Rodents from northwestern Iran. Iranian Journal of Animal Biosystematics (IJAB) 10, 119–136.

Darvish, D., Orth, A., Michaux, J., 2006. *Mus spretus* et *M. musculus* (Rodentia, Mammalia) en zone méditerranéenne: Différenciation biométrique et morphologique: Application à des fossiles marocains plé istocènes. Mammalia 70, 90–97. https://doi.org/10.1515/MAMM.2006.010

Darvish, J., Ghiyasi, R., Khosravi, M., 2000. Recognition of rodents of Robat Sharaf pellets owl by morphological and neontological studies. Journal of Sciences 12.

Dauphin, Y., Denys, C., 1992. Diagenèse différentielle chez les rongeurs fossiles validité des paramètres géochimiques pour les reconstitutions des régimes alimentaires. Palaeogeography, Palaeoclimatology, Palaeoecology 99, 213–223. https://doi.org/10.1016/0031-0182(92)90016-X

Demirel, A., Andrews, P., Yalçinkaya, I., Ersoy, A., 2011. The taphonomy and palaeoenvironmental implications of the small mammals from Karain Cave, Turkey. Journal of Archaeological Science 38, 3048–3059. https://doi.org/10.1016/j.jas.2011.07.003

Denys, C., Stoetzel, E., Andrews, P., Bailon, S., Rihane, A., Huchet, J.B., Fernandez- Jalvo, Y., Laroulandie, V., 2017. Taphonomy of Small Predators multi-taxa accumulations: palaeoecological implications. Hist. Biol. 2963, 1–14. https://doi. org/10.1080/08912963.2017.1347647.

Denys, C., Patou-Mathis, M., 2014. Manuel de Taphonomie, Collection. ed.

Denys, C., Dauphin, Y., Rzebik-Kowalska, B., Kowalski, K., 1996. Taphonomic study of Algerian owl pellet assemblages and differential preservation of some rodents: palaeontological implications. Acta Zoologica Cracoviensia 39, 103–116.

Denys, C., Kowalski, K., Dauphin, Y., 1992. Mechanical and chemical alterations of skeletal tissues in a recent Saharian accumulation of faeces from *Vulpes rueppelli* (Carnivora, Mammalia). Acta Zoologica Cracoviensia 35, 265–283.

Dianat, M., Darvish, J., Aliabadian, M., Siahsarvie, R., Krystufek, B., Nicolas, V., 2020. Systematics and evolution of the libyan jird based on molecular and morphometric data. Journal of Zoological Systematics and Evolutionary Research 58, 439–458. https://doi.org/10.1111/jzs.12335

Dianat, M., Darvish, J., Cornette, R., Aliabadian, M., Nicolas, V., 2017. Evolutionary history of the Persian Jird, *Meriones persicus*, based on genetics, species distribution modelling and morphometric data. Journal of Zoological Systematics and Evolutionary Research 55, 29–45. https://doi.org/10.1111/jzs.12145

Dianat, M., Aliabadian, M., Darvish, J., Akbarirad, S., 2013. Molecular phylogeny of the Iranian Plateau five-toed jerboa, *Allactaga* (Dipodidea: Rodentia), inferred from mtDNA. mammalia 77. https://doi.org/10.1515/mammalia-2012-0011

Djamali, M., de Beaulieu, J.L., Shah-hosseini, M., Andrieu-Ponel, V., Ponel, P., Amini, A., Akhani, H., Leroy, S.A.G., Stevens, L., Lahijani, H., Brewer, S., 2008. A late Pleistocene long pollen record from Lake Urmia, NW Iran. Quaternary Research 69, 413–420. https://doi.org/10.1016/j.yqres.2008.03.004

E

Ellerman, J.R., and Morrison-Scott, T.C.S. 1951. Checklist of Palearctic and Indian Mammals, 1780 to 1946. Brit. Mus. Nat. Hist. London, 1-810.

Eken, G., Bozdogan, M., Molur, S., 2016. *Allactaga williamsi* (errata version published in 2017). The IUCN Red List of Threatened Species 2016: e.T136326A115205783. 8235.

Evans, E.M.N., Van Couvering, J.A.H., Andrews, P., 1981. Palaeoecology of Miocenesites in western Kenya. J. Hum. Evol. 10, 99–116

F

Fernandez-Jalvo, Y., King, T., Yepiskoposyan, L., Andrews, P., 2016a. Azokh Cave and the Transcaucasian Corridor. https://doi.org/10.1007/978-3-319-24924-7

Fernandez-Jalvo, Y., Andrews, P., 2016b. Atlas of Taphonomic Identifications. https://doi.org/10.1007/978-94-017-7432-1

Fernández-Jalvo, Y., Andrews, P., Denys, C., Sesé, C., Stoetzel, E., Marin-Monfort, D., Pesquero, D., 2016c. Taphonomy for taxonomists: Implications of predation in small mammal studies. Quaternary Science Reviews 139, 138–157. https://doi.org/10.1016/j.quascirev.2016.03.016

Fernández-Jalvo, Y., Andrews, P., Sevilla, P., Requejo, V., 2014. Digestion versus abrasion features in rodent bones. Lethaia 47, 323–336. https://doi.org/10.1111/let.12061

Fernández-Jalvo, Y., King, T., Andrews, P., Yepiskoposyan, L., Moloney, N., Murray, J., Domínguez-Alonso, P., Asryan, L., Ditchfield, P., van der Made, J., Torres, T., Sevilla, P., Nieto Díaz, M., Cáceres, I., Allué, E., Marín Monfort, M.D., Sanz Martín, T., 2010. The Azokh Cave complex: Middle Pleistocene to Holocene human occupation in the Caucasus. Journal of Human Evolution 58, 103–109. https://doi.org/10.1016/j.jhevol.2009.07.005

Fiacconi, M., Hunt, C.O., 2015. Pollen taphonomy at Shanidar Cave (Kurdish Iraq): An initial evaluation. Review of Palaeobotany and Palynology 223, 87–93. https://doi.org/10.1016/j.revpalbo.2015.09.003

Fischer von Waldheim, G. 1814. Zoognosia tabulis synopticis illustrata: in usum praelectionum Academiae imperialis medico-chirugicae mosquensis edita. Mosquae: Typis Nicolai S. Vsevolozsky

Firouz, E. (2005). Complete fauna of Iran. IB Tauris.

Freudenthal, M. 1963. Entwicklungsstufen der miozänen Cricetodontinae (Mam. Rod.), Mittelspaniens und ihre stratigraphische Bedeutung. Beaufortia 10:51–157.

Frahm, E., 2019. Upper Palaeolithic Settlement and Mobility in the Armenian Highlands : Agent-Based Modeling , Obsidian Sourcing , and Lithic Analysis at Aghitu-3 Cave.

Fruciano, C. 2016. Measurement error in geometric morphometrics. Development Genes and Evolution, 226:139-158. https://doi.org/10.1007/s00427-016-0537-4

Frumkin, A. and Comay, O. In press. The last glacial cycle of the southern Levant: Paleoenvironment and chronology of modern humans. Journal of Human Evolution 2019, 102609. https://doi.org/10.1016/j.jhevol.2019.04.007

G

Gharkheloo, M.M. 2003. A Study on the Morphology, Karyology and Distribution of *Ellobius* Fischer, 1814 (Mammalia: Rodentia) in Iran. Turkish Journal of Zoology, 27:281-292.

Gerrie, R. & Kennerley, R., 2017. *Myomimus personatus*. The IUCN Red List of Threatened Species 2017: e.T14088A22222124 8235. https://doi.org/http://dx.doi.org/10.2305/IUCN.UK.2017- 2.RLTS. T14088A22222124.en

Golenishchev, F., Malikov, V., Petrova, T., Bodrov, S., & Abramson, N. (2019). Toward assembling a taxonomic puzzle: Case study of Iranian gray voles of the subgenus *Microtus* (Rodentia, Cricetidae). Mammalian Biology, 94 (1), 98-105.

Granjon, L., 2016. *Meriones libycus* (errata version published in 2017). The IUCN Red List of Threatened Species 2016: e. T13164A115110005. 8235.

Gunz, P., Mitteroecker, P., 2013. Semilandmarks: A method for quantifying curves and surfaces. Hystrix 24, 103–109.

H

Habibi, K., 2004. Mammals of Afghanistan. Zoo Outreach Organisation/USFWS, Coimbatore, India

Haddadian Shad, H., Darvish, J., Mohammadian, T., Mahmoudi, A., Alaie Kakhki, N., Ghanbarifardi, M., Molavi, F., Barani-Beiranvand, H., 2014. Preliminary study of rodents using pellets of predatory birds in Iran. Iranian Journal of Animal Biosystematics 10, 36–50.

Haring, E., Sheremetyeva, I.N., Kryukov, A.P., 2011. Phylogeny of Palearctic vole species (genus *Microtus*, Rodentia) based on mitochondrial sequences. Mammalian Biology 76. https://doi.org/10.1016/j.mambio.2010.04.006

Harrison D.L., Bates P.J.J. 1991. The Mammals of Arabia. Sevenoaks: Harrison Zoological Museum Publication.

Hashemi, N., Darvish, J., Mashkour, M., Biglari, F., 2006. Rodents and Lagomorphs remains from late Pleistocene and early Holocene Caves and Rochshelter sites in the Zagros region, Iran. Iranian Journal of Animal Biosystematics (IJAB) 2, 25–33. Hernández Fernández, M., 2001. Bioclimatic discriminant capacity of terrestrial mammal faunas. Global Ecology and Biogeography 10, 189–204. https://doi.org/10.1046/j.1466-822x.2001.00218.

Hassinger, J.D. 1973. A survey of the mammals of Afghanistan: Resulting from the 1965 Street Expedition (Excluding Bats). Fieldiana Zoology, Vol. 60. Chicago, IL, USA, Field Museum of Natural History.

Hernández Fernández, M., Álvarez Sierra, M.Á., Peláez-Campomanes, P., 2007. Bioclimatic analysis of rodent palaeofaunas reveals severe climatic changes in Southwestern Europe during the Plio-Pleistocene. Palaeogeography, Palaeoclimatology, Palaeoecology 251, 500–526. https://doi.org/10.1016/j.palaeo.2007.04.015

Hernández Fernández, M., Peláez-Campomanes, P., 2003. The bioclimatic model: A method of palaeoclimatic qualitative inference based on mammal associations. Glob. Ecol. Biogeogr. 12, 507–517. https://doi.org/10.1046/j.1466-822X.2003.00057.

Hernandez Fernandez, M., 2001. Bioclimatic discriminant capacity of terrestriaL mammal faunas. Global Ecol. Biogeogr. 10, 189e204. https://doi.org/10.1046/

j.1466-822x.2001.00218.x.

Heinrich, W.-D. 1978. Zur biometrischen erfassung eines evolutionstrends bei Arvicola (Rodentia, Mammalia) aus dem pleistozän thüringens.Säugetierkundliche Informationen. 1 (2), 3-21.

Heydari-guran, S., Ghasidian, E., 2020. Late Pleistocene hominin settlement patterns and population dynamics in the Zagros Mountains : Kermanshah region. Archaeological Research in Asia 21, 100161. https://doi.org/10.1016/j.ara.2019.100161

Hinton, M.A.C., 1926. Monograph of the Voles and Lemmings (Microtinae) Living and Extinct, vol. 1. British Museum (Natural History), London, p. 488.

Hulme-Beaman, A., Cucchi, T., Evin, A., Searle, J.B., and Dobney, K. 2018. Exploring R*attus praetor* (Rodentia, Muridae) as a possible species complex using geometric morphometrics on dental morphology. Mammalian Biology, 92:62-67. https://doi.org/10.1016/j.mambio.2018.04.002

J

Jaeger, J.J. 1988. Origine et evolution du genre *Ellobius* (Mammalia, Rodentia) en Afrique Nord-Occidentale. Folia Quaternaria 57:3-50.

Jangjoo, M., Darvish, J., & Vigne, J. D. (2011). Application of outline analysis on fossil and modern specimens of *Apodemus*.

K

Kandel, A.W., Gasparyan, B., Allué, E., Bigga, G., Bruch, A.A., Cullen, V.L., Frahm, E., Ghukasyan, R., Gruwier, B., Jabbour, F., Miller, C.E., Taller, A., Vardazaryan, V., Vasilyan, D., Weissbrod, L., 2017. The earliest evidence for Upper Paleolithic occupation in the Armenian Highlands at Aghitu-3 Cave. Journal of Human Evolution 110, 37–68. https://doi.org/10.1016/j.jhevol.2017.05.010

Karami, M., Hutterer, R., Benda, P., Siahsarvie, R., Kryštufek, B., 2008. Annotated checklist of the mammals of Iran. Lynx (Praha) 39, 63–102.

Kasimova, R. M. (2001). Anthropological research of Azykh Man osseous remains. Human Evolution, 16, 37–44

Kaya, A., Gharakhloo, M.M., Coşkun, Y., 2018. Geographic variation in the skull morphology of *Ellobius lutescens* Thomas, 1897 (Mammalia: Rodentia) by geometric morphometric analyses. Vertebrate Zoology 68, 157–164.

Kaya, F., Kaymakçı, N., 2018. Systematics and dental microwear of the late Miocene Gliridae (Rodentia, Mammalia) from Hayranlı, Anatolia: Implications for paleoecology and paleobiodiversity. Palaeontologia Electronica 16. https://doi.org/10.26879/385

Kefelioglu, H., Yigit, N., Kryštufek, B., 2008. *Meriones dahli*. The IUCN Red List of Threatened Species 2008: e.T13162A3415328.8235.

Kennerley, R. & Kryštufek, B., 2019. *Myomimus setzeri*. The IUCN Red List of Threatened Species 2019: e.T14089A22222049.8235. https://doi.org/http://dx.doi.org/10.2305/IUCN.UK.2019- 1.RLTS.T14089A22222049.en

King, T., Compton, T., Rosas, A., Andrews, P., Yepiskoyan, L., & Asryan, L. (2016). Azokh cave hominin remains, in: Y. Fernández- Jalvo, T. King, L. Yepiskoposyan & P. Andrews (Eds.), Azokh Cave and the Transcaucasian Corridor (pp. 103–116). Dordrecht: Springer

Klenovšek, T., Kryštufek, B., 2013. An ontogenetic perspective on the study of sexual dimorphism, phylogenetic variability, and allometry of the skull of European ground squirrel, *Spermophilus citellus* (Linnaeus, 1766). Zoomorphology 132, 433–445. https://doi.org/10.1007/s00435-013-0196-1

Knitlová, M., Horáček, I., 2017. Late Pleistocene-Holocene paleobiogeography of the genus *Apodemus* in Central Europe. PLoS ONE 12, 1–23. https://doi.org/10.1371/journal.pone.0173668

Kopij, G., Liven-schulman, I., 2013. Zoology in the Middle East Diet of the Lesser Kestrel , *Falco naumanni* , in Israel 7140. https://doi.org/10.1080/09397140.2012.10648914

Kretzoi, M., 1969. Skizze einer Arvicoliden Phylogenie -Stand 1969/. Vertebr. Hung.

11 (1e2), 155e193

Kryštufek, B., Tesakov, A.S., Lebedev, V.S., Bannikova, A.A., Abramson, N.I., Shenbrot, G., 2020. Back to the future: The proper name for red-backed voles is *Clethrionom*ys Tilesius and not *Myodes* Pallas. Mammalia 84, 214–217. https://doi.org/10.1515/mammalia-2019-0067

Kryštufek, B., Bukhnikashvili, A., Sozen, M. & Isfendiyaroglu, S., 2017. *Cricetulus migratorius*. The IUCN Red List of Threatened Species 2016: e.T5528A115073390 8235. https://doi.org/http://dx.doi.org/10.2305/IUCN.UK.2016-3.RLTS.T5528A22391440.en

Krystufek, B., 2017. *Chionomys nivalis* , European Snow Vole. The IUCN Red List of Threatened Species 2016: e. T4659A115069366 8235. https://doi.org/http://dx.doi.org/10.2305/IUCN.UK.2016-3.RLTS.T4659A22379147.en

Kryštufek, B. & Shenbrot, G., 2016. *Ellobius lutescens* , Transcaucasian Mole Vole. The IUCN Red List of Threatened Species 2016: e.T7655A22340006. 8235. https://doi.org/http://dx.doi.org/10.2305/IUCN.UK.2016- 2.RLTS.T7655A22340006.en

Kryštufek, B., Janžekovič, F., Hutterer, R., Klenovšek, T., 2016. Morphological evolution of the skull in closely related bandicoot rats: A comparative study using geometric morphometrics. Hystrix 27, 1–7. https://doi.org/10.4404/hystrix-27.2-11639

Kryštufek, B., Yigit, N. & Amori, G., 2015. *Mesocricetus brandti* , Brandt ' s Hamster. The IUCN Red List of Threatened Species 2008: e.T13220A3421550. 8235. https://doi.org/http://dx.doi.org/10.2305/IUCN.UK.2008.RLTS.T13220A3421550.en

Kryštufek, B., Vohralík, V., 2009. Mammals of Turkey and Cyprus, Rodentia II: Cricetinae, Muridae, Spalacidae, Calomyscidae, Capromyidae, Hystricidae, Castoridae. https://doi.org/10.1644/10-MAMM-R-221.1

Kryštufek B. & Vohralík V., 2005. Mammals of Turkey and Cyprus. Rodentia I: Sciuridae, Dipodidae, Gliridae, Arvicolinae.

Kryštufek, B., Kefelioglu, H., 2001. Redescription and species limits of *Microtus irani* Thomas, 1921, and description of a new social vole from Turkey (Mammalia: Arvicolinao).

Kryštufek,, B., Vohralík, V., 2001. Mammals of Turkey and Cyprus, Introduction, Check-List, Insectivora. Koper.

Kryštufek, B., 1999. Snow voles, genus *Chionomys*, of Turkey. Mammalia 63(3), 323–339.

L

Lay, D.M. 1967. A Study of the Mammals of Iran, Resulting from the Street Expedition of 1962-63. Fieldiana Zool., 54:168-171.

Li, H., Liu, X., Herzschuh, U., Cao, X., Yu, Z., Wang, Y., 2019. Vegetation and climate changes since the middle MIS 3 inferred from a Wulagai Lake pollen record, Inner Mongolia, Northeastern China. Review of Palaeobotany and Palynology 262, 44–51. https://doi.org/10.1016/j.revpalbo.2018.12.006

Litt, T., Pickarski, N., Heumann, G., Stockhecke, M., Tzedakis, P.C., 2014. A 600,000 year long continental pollen record from Lake Van, eastern Anatolia (Turkey). Quaternary Science Reviews 104, 30–41. https://doi.org/10.1016/j.quascirev.2014.03.017

López-García, J.M., Livraghi, A., Romandini, M., Peresani, M., 2018. The De Nadale Cave (Zovencedo, Berici Hills, northeastern Italy): A small-mammal fauna from near the onset of Marine Isotope Stage 4 and its palaeoclimatic implications. Palaeogeography, Palaeoclimatology, Palaeoecology 506, 196–201. https://doi.org/10.1016/j.palaeo.2018.06.033

López-García, J.M., Blain, H.A., Bennàsar, M., Alcover, J.A., Bañuls-Cardona, S., Fernández-García, M., Fontanals, M., Martín, P., Morales, J.I., Muñoz, L., Pedro, M., Vergés, J.M., 2014. Climate and landscape during Heinrich Event 3 in south-western Europe: The small-vertebrate association from Galls Carboners cave (Mont-ral, Tarragona, north-eastern Iberia). Journal of Quaternary Science 29, 130–140. https://doi.org/10.1002/jqs.2687

Lopez-Garcia, J.M., Blain, H. -a., Morales, J.I., Lorenzo, C., Banuls-Cardona, S., Cuenca-Bescos, G., 2013. Small-mammal diversity in Spain during the late Pleistocene to early Holocene: Climate, landscape, and human impact. Geology 41, 267–270. https://doi.org/10.1130/G33744.1

López-García, J.M., Blain, H.-A., Cuenca-Bescós, G., Alonso, C., Alonso, S., Vaquero, M., 2011. Small vertebrates (Amphibia, Squamata, Mammalia) from the late Pleistocene-Holocene of the Valdavara-1 cave (Galicia, northwestern Spain). Geobios 44, 253–269. https://doi.org/10.1016/j.geobios.2010.10.001

López-García, J.M., 2011. Los micromamíferos del Pleistoceno superior de la Península Ibérica: Evolución de la diversidad taxonómica y cambios paleoambientales y pa-leoclimáticos. Editorial Académica Española

López-García, J.M., Blain, H.A., Cuenca-Bescós, G., Ruiz-Zapata, M.B., Dorado-Valiño, M., Gil-García, M.J., Valdeolmillos, A., Ortega, A.I., Carretero, J.M., Arsuaga, J.L., de Castro, J.M.B., Carbonell, E., 2010. Palaeoenvironmental and palaeoclimatic reconstruction of the Latest Pleistocene of El Portalón Site, Sierra de Atapuerca, northwestern Spain. Palaeogeography, Palaeoclimatology, Palaeoecology 292, 453–464. https://doi.org/10.1016/j.palaeo.2010.04.006

López-García, J.M., 2008. Evolución de la diversidad taxonómica de los micromamíferos en la Península Ibérica y cambios Paleoambientales durante el Pleistoceno Superior, Departament d'Història i Història de l'Art.

López-Guerrero, P., García-Paredes, I., Álvarez-Sierra, M.Á., 2013. Revision of *Cricetodon soriae* (Rodentia, Mammalia), new data from the middle Aragonian (middle Miocene) of the Calatayud-Daroca Basin (Zaragoza, Spain). Journal of Vertebrate Paleontology 33, 169–184. https://doi.org/10.1080/02724634.2012.716112

López, J.M., Rosi, M.I., Tabeni, S., Bender, B., Chiavazza, H., 2017. Taphonomic analysis of small mammal bone remains preyed upon by wildcats (Carnivora: Felidae) from the central Monte Desert (Mendoza, Argentina). Boreas 46, 282–293. https://doi.org/10.1111/bor.12211

Lozano-Fernández, I., Agusti, J., Cuenca-Bescós, G., Blain, H.A., López-Garcia, J.M., Vallverdú, J., 2013. Pleistocene evolutionary trends in dental morphology of *Mimomys savin*i (rodentia, mammalia) from iberian peninsula and discussion about the origin of the genus arvicola. Quaternaire 24, 179–190.

Luzi, E., Pazonyi, P., López-García, J.M., 2019. The influence of climate on morphometric traits of fossil populations of *Microtus arvalis* and *M. agrestis* from the Carpathian Basin, northern Hungary. Lethaia 52, 123–132. https://doi.org/10.1111/let.12294

M

Mahmoudi, A., Maul, L.C., Khoshyar, M., Darvish, J., Aliabadian, M., Kryštufek, B., 2020. Evolutionary history of water voles revisited: Confronting a new phylogenetic model from molecular data with the fossil record. Mammalia 1–14. https://doi.org/10.1515/mammalia-2018-0178

Mahmoudi, A., Maul, L.C., Khoshyar, M., Darvish, J., 2019. Evolutionary history of water voles revisited : confronting a new phylogenetic model from molecular data with the fossil record.

Mamkhair, I.H., Samara, F.F., Shehab, A.H., 2007. Morphological characteristics of the libyan jird, *Meriones libycus* lichtenstein, 1823 (rodentia: gerbillinae), in syria. Zoology in the Middle East 42, 37–46. https://doi.org/10.1080/09397140.2007.10638244

Manuk, V.,2010. Atlas of the Nagorno-Karabagh Republic. Stepanakert 2010.

MarÍn-Monfort, M. D., Cáceres, I., Andrews, P., Pinto, A. C. & Fernández-Jalvo, Y. (2016). Taphonomy and Site Formation of Azokh 1, in: Y. Fernández-Jalvo, T. King, L. Yepiskoposyan & P. Andrews (Eds.), Azokh Cave and the Transcaucasian Corridor (pp. 211–249). Dordrecht: Springer

Markova, A., 1992. Fossil rodents (Rodentia, Mammalia) from the Sel'-Ungur Acheulian cave site (Kirghizstan). Acta

Zoologica Cracoviensia 35, 217–239.

Maul, L.C., Rabinovich, R., Biton, R., Maul, L.C., 2020. At the southern fringe : extant and fossil water voles of the genus Arvicola (Rodentia , Cricetidae , Arvicolinae) from Israel , with the description of a new species Cricetidae , Arvicolinae) from Israel , with the description of a new species. Historical Biology 00, 1–21. https://doi.org/10.1080/08912963.2020.1827240

Maul, L.C., Bruch, A.A., Smith, K.T., Shenbrot, G., Barkai, R., Gopher, A., 2015a. Palaeoecological and biostratigraphical implications of the microvertebrates of Qesem Cave in Israel. Quaternary International. https://doi.org/10.1016/j.quaint.2015.04.032

Maul, L.C., Smith, K.T., Shenbrot, G., Bruch, A.A., Wegmüller, F., Le Tensorer, J.M., 2015b. Microvertebrates from unit G/ layer 17 of the archaeological site of Hummal (El Kowm, Central Syria): Preliminary results. Anthropologie (France) 119, 676–686. https://doi.org/10.1016/j.anthro.2015.10.010

Maul, L.C., Markova, A.K., 2007. Similarity and regional differences in Quaternary arvicolid evolution in Central and Eastern Europe. Quaternary International 160, 81–99. https://doi.org/10.1016/j.quaint.2006.09.010

Mikkola, H., 1983. Owls of Europe. T. &; A. D. Poyser, Carlton.

Miller, G.S., 1896. Genera and Subgenera of Voles and Lemmings//North American Fauna, vol. 12, pp. 1e85.

Mitteroecker, P., Windhager, S., Müller, G.B., and Schaefer, K. 2015. The morphometrics of "masculinity" in human faces. PLoS ONE, 10. https://doi.org/10.1371/journal.pone.0118374

Molur, S. & Sozen, M., 2016. *Meriones persicus*, Persian Jird. The IUCN Red List of Threatened Species 2016: e.T13166A22433231.8235. https://doi.org/http://dx.doi.org/10.2305/IUCN.UK.2016-2.RLTS.T13166A22433231.en

Momtazi, F., Darvish, J., Ghassemzadeh, F., Moghimi, A., 2008. Elliptic Fourier analysis on the tympanic bullae in three *Meriones* species (Rodentia, Mammalia): its application in biosystematics. Acta zoologica cracoviensia 51A, 49–58. https://doi.org/10.3409/azc.51a

Murray, J., Lynch, E.P., Dominguez-Alonso, P., Barham, M., 2016. Chapter 2: Stratigraphy and Sedimentology of Azokh Caves, South Caucasus., in: Fernández-Jalvo, Y., King, T., Yepiskoposyan, L., Andrews, P. (Eds.), Azokh Cave and the Transcaucasian Corridor, Vertebrate Paleobiology and Paleoanthropology. Springer International Publishing, Cham, pp. 27–54. https://doi.org/10.1007/978-3-319-24924-7

Murray, J., Domínguez-alonso, P., Fernández-, Y., King, T., Lynch, E.P., Andrews, P., Yepiskoposyan, L., Moloney, N., Cacères, I., Allué, E., Asryan, L., Ditchfield, P., Williams, D.M., Murray, J., Dominguez-alonso, P., Fernandez-jalvo, Y., King, T., Lynch, E.P., Andrews, P., Yepiskoposyan, L., Moloney, N., Caceres, I., Allue, E., Asryan, L., Williams, D.M., 2010. Pleistocenen to Holocene stratigraphy of Azokh 1 Caves, lasser caucasus. Irish Journal of Earth Sciences 28, 75–91. https://doi.org/10.3318/IJES.2010.28.75

Musser, G., Hutterer, R., Kryštufek, B., Yigit, N. & Mitsain, G. 2016. *Mus musculus* (errata version published in 2017). The IUCN Red List of Threatened Species 2016: e.T13972A115117618. https://dx.doi.org/10.2305/IUCN.UK.2016-3.RLTS.T13972A22405706.en.

Musser, G.C., Carleton, M.D., 2005. Superfamily Muroidae, in: Wilson, D.E., Reeder, D.M. (Eds.), Mammal Species of the World. A Taxonomic and Geographic Reference. Baltimore, pp. 894–1531.

N

Nadachowski, A., 1991. Systematics, geographic variation, and evolution of snow voles (*Chionomys*) based on dental characters. Acta Theriologica 36, 1–45.

Naderi, G., Hemami, M.R., Mohammadi, S., 2011. Investigation of habitat preferences of Iranian jerboa (*Allactaga firouzi* Womochel 1978). mammalia 75. https://doi.org/10.1515/mamm.2011.008

Nesin, V., Kovalchuk, O., 2017. A new species of jerboa (Mammalia, Rodentia, *Allacta-*

ga) from the late Miocene of Ukraine. Palaeontologia Electronica 20. https://doi.org/10.26879/751

Nesin, V. and Nadachowski, A. 2001. Late Miocene and Pliocene small mammal faunas (Insectivora, Lagomorpha, Rodentia) of Southeastern Europe. Acta Zoologica Cracoviensia, 44:107-135.

Neumann, K., Yiğit, N., Fritzsche, P., Çolak, E., Feoktistova, N., Surov, A., Michaux, J., 2017. Genetic structure of the Turkish hamster (*Mesocricetus brandti*). Mammalian Biology 86, 84–91. https://doi.org/10.1016/j.mambio.2017.06.004

Nishiaki, Y., Akazawa, T., 2018. The Middle and Upper Paleolithic Archeology of the Levant and Beyond. Replacement of Neanderthals by Modern Humans Series 35–47. https://doi.org/10.1007/978-981-10-6826-3_3

Nowak, R.M. 1999. Walker's Mammals of the World. 6th ed. Baltimore, MD, USA, The Johns Hopkins University Press.

O

Obrochta, S.P., Yokoyama, Y., Morén, J., Crowley, T.J., 2014. Conversion of GISP2-based sediment core age models to the GICC05 extended chronology. Quaternary Geochronology 20, 1–7. https://doi.org/10.1016/j.quageo.2013.09.001

Obuch, J., Khaleghizadeh, A., 2012. Spatial Variation in the Diet of the Barn Owl Tyto alba in Iran 6, 103–116.

Osborn, D.J. 1962. Rodents of subfamily Microtinae from Turkey. Journal of Mammology, 43 (4):515-529. https://doi.org/10.2307/1376914

P

Pallas, P. S. 1770. Spicilegia zoologica quibus novae imprimis et obscurae animalium species iconibus, descriptionibus atque commentariis illustrantur. Fasciculus octavus

Parfitt, S.A., 2016. Chapter 7 Rodents, Lagomorphs and Insectivores from Azokh Cave, in: Fernández-Jalvo, Y., King, T., Yepiskoposyan, L., Andrews, P. (Eds.), Azokh Cave and the Transcaucasian Corridor, Vertebrate Paleobiology and Paleoanthropology. Springer International Publishing, Cham, pp. 163–176. https://doi.org/10.1007/978-3-319-24924-7

Pavlinov, I., 2008. A review of phylogeny and classification of gerbillinae (mammalia:rodentia), Moscow Uni. ed. Moscow.

R

R Core Team, 2020. R: A language and environment for statistical computing. R Foundation for Statistical Computing.

Railsback, L.B., Gibbard, P.L., Head, M.J., Voarintsoa, N.R.G., Toucanne, S., 2015. An optimized scheme of lettered marine isotope substages for the last 1.0 million years, and the climatostratigraphic nature of isotope stages and substages. Quaternary Science Reviews 111, 94–106. https://doi.org/10.1016/j.quascirev.2015.01.012

Redding, W.R., 1978. Rodents and the archaeological palaeoenvironment: Considerations, problems and future. Approaches to faunal analysis in the Middle East. In: Meadow, R.H., Zeder, M.A. (Eds.), Harvard, Peabody Museum of Archaeology and Ethnology, 2. Peabody Museum Bulletin, pp. 63–68

Rey-Rodríguez, I., Arnaud, J., López-García, J.M., Stoetzel, E., Denys, C., Cornette, R., Bazgir, B., 2021. Distinguishing between three modern Ellobius species (Rodentia, Mammalia) and identification of fossil Ellobius from Kaldar Cave (Iran) using geometric morphometric analyses of the first lower molar. Palaeontologia Electronica 24 (1):a01, 1–18. https://doi.org/10.26879/1122

Rey-Rodríguez, I., López-García, J.-M., Blain, H.-A., Stoetzel, E., Denys, C., Fernández-García, M., Tumung, L., Ollé, A., Bazgir, B., 2020. Exploring the landscape and climatic conditions of Neanderthals and anatomically modern humans in the Middle East: the rodent assemblage from the late Pleistocene of Kaldar Cave (Khorramabad Valley, Iran). Quaternary Science Reviews 236, 106278. https://doi.org/10.1016/j.quascirev.2020.106278

Rey-Rodríguez, I., Stoetzel, E., López-García, J.M., Denys, C., 2019. Implications of modern Barn owls pellets analysis for

archaeological studies in the Middle East. Journal of Archaeological Science 111, 105029. https://doi.org/10.1016/J.JAS.2019.105029

Rey-Rodríguez, I., 2015. Reconstrucción paleoambiental y biocronológica del yacimiento del Paleolítico medio- superior de Cova Eirós (Triacastela, Lugo) a partir del análisis de las asociaciones de micromamíferos. Universitat Rovira i Virgili. Master thesis.

Roberts, T.J. 1977. The Mammals of Pakistan. London, UK, Ernst Benn Ltd.

Rohlf, F.J. 2016. tpsDig, Digitize Landmarks and Outlines, Version 2.32. Department of Ecology and Evolution, State University of New York at Stony Brook, New York. http://life.bio.sunysb.edu/morph

Romanenko, S.A., Fedorova, Y.E., Serdyukova, N.A., Zaccaroni, M., Stanyon, R., Graphodatsky, A.S. 2020. Evolutionary rearrangements of X chromosomes in voles (Arvicolinae, Rodentia). Scientific Reports 1–11. https://doi.org/10.1038/s41598-020-70226-4

Romanenko, S.A., Sitnikova, N.A., Serdukova, N.A., Perelman, P.L., Rubtsova, N. V., Bakloushinskaya, I.Y., Lyapunova, E.A., Just, W., Ferguson-Smith, M.A., Yang, F., and Graphodatsky, A.S. 2007. Chromosomal evolution of Arvicolinae (Cricetidae, Rodentia). II. The genome homology of two mole voles (genus *Ellobius*), the field vole and golden hamster revealed by comparative chromosome painting. Chromosome Research, 15:891897. https://doi.org/10.1007/s10577-007-1171-9

Romanenko, S.A., Serdyukova, N.A., Perelman, P.L., Trifonov, V.A., Golenishchev, F.N., Bulatova, N.S., Stanyon, R., and Graphodatsky, A.S. 2018. Multiple intrasyntenic rearrangements and rapid speciation in voles. Scientific Reports 2-10. https://doi.org/10.1038/s41598-018-33300-6

Roucoux, K.H., Tzedakis, P.C., Frogley, M.R., Lawson, I.T., Preece, R.C., 2008. Vegetation history of the marine isotope stage 7 interglacial complex at Ioannina, NW Greece. Quaternary Science Reviews 27, 1378–1395. https://doi.org/10.1016/j.quascirev.2008.04.002

Roucoux, K.H., Tzedakis, P.C., de Abreu, L., Shackleton, N.J., 2006. Climate and vegetation changes 180,000 to 345,000 years ago recorded in a deep-sea core off Portugal. Earth and Planetary Science Letters 249, 307–325. https://doi.org/10.1016/j.epsl.2006.07.005

Royer, A., García, B.A., Laffont, R., Hernández, M., Cnrs, U.M.R., Franche-comté, U.B., Gabriel, B., 2020. New bioclimatic models for the quaternary palaearctic based on insectivore and rodent communities 560.

Royer, A., Lécuyer, C., Montuire, S., Escarguel, G., Fourel, F., Mann, A., Maureille, B., 2013. Late Pleistocene (MIS 3-4) climate inferred from micromammal communities and δ18O of rodents from Les Pradelles, France. Quaternary Research (United States) 80, 113–124. https://doi.org/10.1016/j.yqres.2013.03.007

Rusin, M., 2017. *Ellobius talpinus* , Northern Mole Vole. The IUCN Red List of Threatened Species 2016: e. T7656A115085720. 8235. https://doi.org/http://dx.doi.org/10.2305/IUCN.UK.2016-3.RLTS.T7656A22339917.en

S

Sala, B., Masini, F., Torre, D. 1994. Villanyian arvicolids from Veronese, a karst fissure in the Adige valley, Northeastern Italy. Bolletino Societa Paleontologica Italina, 33:3-11.

Sándor, A.D., 2018. Rediscovered after half a century: A new record of the grey dwarf hamster, *Cricetulus migratorius* (Mammalia: Cricetidae), in Romania. Turkish Journal of Zoology 42, 495–498. https://doi.org/10.3906/zoo-1712-15

Schlager, S., 2017. Morpho and Rvcg Shape Analysis, in: Guoyan Zheng and Shuo Li and Gabor Szekely (Ed.), Statistical Shape and Deformation Analysis. pp. 217–256.

Scott, L., Rossouw, L., Cordova, C., & Risberg, J. (2016). Palaeoenvironmental context of coprolites and plant microfossils from Unit II. Azokh 1. In Fernández-Jalvo, Y.,

King, T., Yepiskoposyan, L., Andrews, P. (Eds.), Azokh Cave and the Transcaucasian Corridor, Vertebrate Paleobiology and Paleoanthropology. Springer International Publishing, Cham, pp. 177–189. https://doi.org/10.1007/978-3-319-24924-7

Sevilla, P., 2016. Chapter 8: Bats from Azokh Cave, in: Fernández-Jalvo, Y., King, T., Yepiskoposyan, L., Andrews, P. (Eds.), Azokh Cave and the Transcaucasian Corridor, Vertebrate Paleobiology and Paleoanthropology. Springer International Publishing, Cham, pp. 177–189. https://doi.org/10.1007/978-3-319-24924-7

Shad, H., Kakhki, A., 2014. Preliminary study of rodents using pellets of predatory birds in Iran. Iranian Journal of Animal Biosystematics 10, 36–50.

Shehab, A., Daoud, A., Kock, D., Amr, Z., 2013. Zoology in the Middle East Small mammals recovered from owl pellets from 7140. https://doi.org/10.1080/09397140.2004.10638061

Shenbrot, G., Kryštufek, B. & Molur, S., 2016. *Ellobius fuscocapillus* , Southern Mole Vole. The IUCN Red List of Threatened Species 2016: e.T7654A22339730. 8235. https://doi.org/http://dx.doi.org/10.2305/IUCN.UK.2016- 2.RLTS.T7654A22339730.en

Shenbrot, G., 2009. On the conspecifity of *Allactaga hotsoni* Thomas, 1920 and *Allactaga firouzi* Womochel, 1978 (Rodentia: Dipodoidea). Mammalia 73, 231–237. https://doi.org/10.1515/MAMM.2009.043

Siahsarvie, R., Darvish, J., 2008. Geometric morphometric analysis of Iranian wood mice of the genus *Apodemus* (Rodentia, Muridae). Mammalia 72, 109–115. https://doi.org/10.1515/MAMM.2008.020

Smith, K.T., Christian, L., Flemming, F., Barkai, R., Gopher, A., 2015. The microvertebrates of Qesem Cave : A comparison of the two concentrations. Quaternary International 1–13. https://doi.org/10.1016/j.quaint.2015.04.047

Souttou K., Manaa A., Stoetzel E., Sekour M., Hamani A. , Doumandji S., Denys C. 2012 Small mammals bone modifications in Black-shouldered Kite *Elanus caeruleus* pellets from Algeria: implications for archaeological sites. J. Taphonomy 10 (1), 1-19.

Sozen, M., Bukhnikashvili, A., Shenbrot, G., Scott, D., Amori, G., Kryštufek, B., Yigit, N., Mitsani, G., 2016. *Meriones tristrami* (errata version published in 2017). The IUCN Red List of Threatened Species 2016: e.T13170A115110701. 8235.

Sözen, M., Özkurt, S.O., , Karataş, A., Çolak, E. and, Matur, F., 2009. On the karyology, morphology and biology of *Chionomys gud* (Satunin, 1909) (Mammalia: Rodentia) in Turkey. North-Western Journal of Zoology 5 (1), 121–129.

Stoetzel, E., Lalis, A., Nicolas,V., Aulagnier, S., Bennazou T., Dauphin, Y. El Hajraoui M. A., El Hassani A., Fahd S., Fekhaoui, M., Geigl, E.M., Lapointe, F.J., Leblois, R., Ohler, A.M., Nespoulet, F., Denys, C. Quaternary terrestrial microvertebrates from northwestern Africa: state-of-the-art focused on recent multidisciplinary studies. Quaternary Science Reviews, 224, 105966. https://doi.org/10.1016/j.quascirev.2019.105966

Stoetzel, E., Cornette, R., Lalis, A., Nicolas, V., Cucchi, T., Denys, C., 2017. Systematics and evolution of the *Meriones shawii/grandis* complex (Rodentia, Gerbillinae) during the Late Quaternary in northwestern Africa: Exploring the role of environmental and anthropogenic changes. Quaternary Science Reviews 164, 199–216. https://doi.org/10.1016/j.quascirev.2017.04.002

Stoetzel, E., 2013. Late cenozoic micromammal biochronology of northwestern africa. Palaeogeography, Palaeoclimatology, Palaeoecology 392, 359–381. https://doi.org/10.1016/j.palaeo.2013.09.026

Stoetzel, E., Marion, L., Nespoulet, R., El Hajraoui, M.A., Denys, C., 2011. Taphonomy and palaeoecology of the late Pleistocene to middle Holocene small mammal succession of El Harhoura 2 cave (Rabat-Témara, Morocco). Journal of Human Evolution 60, 1–33. https://doi.org/10.1016/j.jhevol.2010.07.016

Svendsen, J.I., Krüger, L.C., Mangerud, J., Astakhov, V.I., Paus, A., Nazarov, D., Murray, A., 2014. Glacial and vegetation history of the Polar Ural Mountains in northern

Russia during the Last Ice Age, Marine Isotope Stages 5-2. Quaternary Science Reviews 92, 409–428. https://doi.org/10.1016/j.quascirev.2013.10.008

T

Tabatabaei Yazdi, F., Alhajeri, H., 2018. Sexual dimorphism, allometry, and interspecific variation in the cranial morphology of seven *Meriones* species (Gerbillinae, Rodentia). Hystrix, Italian Journal of Mammalogy 29(2), 162–167. https://doi.org/10.4404/hystrix

Tesakov, A.S. 2016. Early Middle Pleistocene *Ellobius* (Rodentia, Cricetidae, Arvicolinae) from Armenia. Russian Journal of Theriology, 15(2):151-158.

Tesakov, A. S. 1998. Voles of the Tegelen fauna. Mededelingen Nederlands Instituut voor Toegepaste Geowetenschappen TNO, 60, p. 71-134

Tez, C., 2000. Taxonomy and distribution of the white-toothed shrews (*Crocidura*) (Soricidae: Insectivora: Mammalia) of Turkey. Turkish Journal of Zoology 24, 365–374.

Thomas, O.1897.*Ellobius lutescens*. The Annals and Magazine of Natural History, 20: 308. London

Thomas, O. 1905. *Ellobius woosnami.* Abstr. Proc. Zool. Soc. 23; Proceeding of the Zoological Society. 526 London

Topachevsky, V.A. and Rekovets, L.I. 1982. New material to the systematics and evolution of mole voles of the nominative subgenus of the genus *Ellobius* (Rodentia, Cricetidae). Vestnik Zoologii, 5:47-74 (in Russian).

Tores, M., Motro, Y., Motro, U., Yom-Tov, Y., 2006. The barn owl - A selective opportunist predator. Israel Journal of Zoology 51, 349–360. https://doi.org/10.1560/7862-9E5G-RQJJ-15BE

Tsytsulina, K., Kryštufek, B., Yigit, N., Bukhnikashvili, A. & Shenbrot, G., 2017. *Microtus socialis* , Social. The IUCN Red List of Threatened Species 2016: e. T13458A115114745. 8235. https://doi.org/http://dx.doi.org/10.2305/IUCN.UK.2016-3.RLTS.T13458A22348936.en

U

Újvári, G., Kele, S., Bernasconi, S.M., Haszpra, L., Novothny, Á., Bradák, B., 2019. Clumped isotope paleotemperatures from MIS 5 soil carbonates in southern Hungary. Palaeogeography, Palaeoclimatology, Palaeoecology 518, 72–81. https://doi.org/10.1016/j.palaeo.2019.01.002

V

Vagif Atamov, M.A., Gulsefile, A., 2007. Flora of Mezra city (Birecik, SanliurfaTurkey). Asian J. Plant Sci. 6 (2), 225–238.

Van Der Made, J., Torres, T., Ortiz, J.E., Moreno-Pérez, L., Fernández-Jalvo, Y., 2016. Chapter 6: The new material of Large Mammals from Azokh and comments on the older collections. In: Fernández-Jalvo, Y., King, T., Yepiskoposyan, L., Andrews, P. (Eds.), Azokh Cave and the Transcaucasian Corridor, Vertebrate Paleobiology and Paleoanthropology. Springer International Publishing, Cham. https://doi.org/10.1007/978-3-319-24924-7

Vasilenko, Y.P., Gorbarenko, S.A., Bosin, A.A., Artemova, A. V., Yanchenko, E.A., Shi, X.F., Zou, J.J., Liu, Y.G., Toropova, S.I., 2019. Orbital-scale changes of sea ice conditions of Sea of Okhotsk during the last glaciation and the Holocene (MIS 4–MIS 1). Palaeogeography, Palaeoclimatology, Palaeoecology 533, 109284. https://doi.org/10.1016/j.palaeo.2019.109284

Vorontsov, N.N., Lyapunova, E.A., Zakaryan, G.G., and Ivanov, V.G. 1969. The karyology and taxonomy of the genus *Ellobius* (Microtinae, Rodentia). In: The Mammals, Evolution, Karyology, Taxonomy, Fauna. 2nd All-Union Mammalogy Conference, Moscow.

W

Walker, E.P. 1964. Mammals of the World. Vol. 2. Baltimore, MD, USA, The Johns Hopkins Press.

Wegwerth, A., Dellwig, O., Wulf, S., Plessen, B., Kleinhanns, I.C., Nowaczyk, N.R., Jiabo, L., Arz, H.W., 2019. Major hydrological shifts in the Black Sea "Lake" in response to ice sheet collapses during MIS 6 (130–

184 ka BP). Quaternary Science Reviews 219, 126–144. https://doi.org/10.1016/j.quascirev.2019.07.008

Weissbrod, L., Weinstein-Evron, M., 2020. Climate variability in early expansions of *Homo sapiens* in light of the new record of micromammals in Misliya Cave, Israel. Journal of Human Evolution 139, 102741. https://doi.org/10.1016/j.jhevol.2020.102741

Weissbrod, L., Marshall, F.B., Valla, F.R., Khalaily, H., Bar-Oz, G., Auffray, J.-C., Vigne, J.-D., Cucchi, T., 2017. Origins of house mice in ecological niches created by settled hunter-gatherers in the Levant 15,000 y ago. Proceedings of the National Academy of Sciences 114, 4099–4104. https://doi.org/10.1073/pnas.1619137114

Weissbrod, L., Zaidner, Y., 2014. Taphonomy and paleoecological implications of fossorial microvertebrates at the Middle Paleolithic open-air site of Nesher Ramla, Israel. Quaternary International 331, 115–127. https://doi.org/10.1016/j.quaint.2013.05.044

Wilson, G.P., Frogley, M.R., Hughes, P.D., Roucoux, K.H., Margari, V., Jones, T.D., Leng, M.J., Tzedakis, P.C., 2021. Persistent millennial-scale climate variability in Southern Europe during Marine Isotope Stage 6. Quaternary Science Advances 3, 100016. https://doi.org/10.1016/j.qsa.2020.100016

Wilson, D.E., Mittermeier, R.A., and Lacher, T.E. 2017. Handbook of the Mammals of the World. Volume 7. Rodents II. Lynx Edicions, Barcelona, Spain.

Wilson, D.E. and Reeder, D.M. 2005. Mammal Species of the World. Washington, DC, USA: Smithsonian Institution Scholarly Press.

Y

Yicit, N., Çolak, M.S., 1996. Investigations on biology of *Meriones crassus* (Mammalia: Rodentia) in Turkey. Turkish Journal of Zoology 20, 211–215

Yanina, T.A., 2014. The Ponto-Caspian region: Environmental consequences of climate change during the Late Pleistocene. Quaternary International 345, 88–99. https://doi.org/10.1016/j.quaint.2014.01.045

List of tables and figures

Chapter 1. Introduction 27

Table 1.1. Rodent species previously identified in the Middle Eastern archaeo-paleontological studied sites and comparative sites used in this work. 30

Table 1.2. Rodent species composition of the main taphonomic studies based on modern owl pellets. 31

Figure 1.1. Oxygen Isotope ($\delta^{18}O$) data related from the Middle to the Late Pleistocene with the chronology and the palaeomagnetism record. Image modified from http://quaternary.stratigraphy.org/charts/ 32

Figure 1.2. Location of the Caucasus, Zagros Mountains, Mediterranean Sea, Black Sea, Caspian Sea and the sites studied in this PhD thesis (map elaborated by Dr. Ana Fagoaga Moreno). 33

Chapter 2.Material and methods 37

Table 2.1. Modern reference collections that I had the opportunity to consult in different museums: Natural History Museum of London (NHM), American Museum of Natural History of New York (AMNH) and Field Museum of Chicago (FM). 41

Figure 2.1. Sampling on the field. a) buckets with water and sediments from Azokh 1, b) sediments drying from Azokh 1, c) sediments from Azokh 1 prepared for sorting, and d) picking up the sediments at Kaldar Cave 39

Figure 2.2. Pictures from the visited museums during this PhD thesis. 42

Figure 2.3. Photograph equipments used during the museums visits. a) digital camera coupled with a binocular microscope, from the NHM; b) reflex camera (Nikon D300 with and objective of 40mm) in ANHM and c) Dino-Lite microscope (model AM7915MZTL) in the NHM 43

Figure 2.4. Cricetidae nomenclature. *Cricetodon* right first lower molar, m1. a) 1-Anteriosinusid, 2-Anteroconid, 3-Labial anterolophid, 4-Protosinusid, 5-Protoconid,6- Mesolophid, 7-Sinusid, 8-Ectomesolophid, 9-Hypoconid, 10-Posterolophid, 11-Posterosinusid, 12-Entoconid, 13-Metalophulid II, 14-Mesosinusid, 15-Metaconid and 16-Metalophulid I ; b) L- total length and W- total width (modified after Mein and Freudenthal, 1963 and López-Guerrero et al., 2013). 44

Figure 2. 5. Arvicolinae nomenclature. a) Occlusal surface of *Arvicola* right first lower molar m1. T- triangle, BRA- buccal re-entrant angle, LRA- lingual re-entrant angle, AC- anterior cap and PL- posterior lobe, L- total length and W- total width ; b) elements used for the SDQ calculation (According to Van der Meulen, 1972 and modified from Rey-Rodríguez, 2015 and Lozano-Fernández et al., 2013). 44

Figure 2.6. Gerbilinae nomenclature. a) Skull measurements abbreviations. CBL- Condylo-basal length, ZB- Bizygomatic breadth, UTR- Upper tooth row and TBL- tympanic bullae length of Meriones skull; b) L- total length and W- total width, 1- anterolophulide, 2- first lobe, 3-neolophide and 4- second lobe of first right lower molar (m1) of *Meriones*, picture modified from Kryštufek and Vohralík (2009). 45

Figure 2.7. Murinae nomenclature. Upper and lower molars of Apodemus. a) right upper molars. T (1-9)- cusp, t5- protocone, t6- paracone, t8- hypocone, t9- metacone ; b) right lower molars. C- labial accessory cusp, cp- posterior accessory cusp, tma- medium anterior cusp, tF-

principal antero-lingual cusp, tE- principal antero-labial cusp, tD- metaconid, tC- protoconid, tB- entoconid, tA- Hipoconid (according to Michaux 1971 and López-García 2008). 45

Figure 2.8. Dipodida nomenclature. *Allactaga* upper and lower teeth. a) Upper dentition: 1, anterostyle; 2, anteroloph I; 3, anteroloph II; 4, anterocone; 5, anterior arm of the protocone; 6, protocone; 7, protostyle; 8, posterior arm of the protocone; 9, anterior endoloph; 10, mesocone; 11, endosinus; 12, endostyle; 13, posterior endoloph; 14, hypocone; 15, posterior arm of the hypocone; 16, lingual arm of the posteroloph; 17, the metaconule; 18, labial arm of the posteroloph; 19, posterofossette; 20, metaloph II; 21, metaloph I; 22, metacone; 23, mesofossette; 24, mesoloph; 25, mesostyle; 26, protoloph II; 27, protoloph I; 28, paracone; 29, anterofossette; b) Lower dentition: 30, anteroconid; 31, labial arm of the anterolophid; 32, lingual arm of the anterolophid; 33, anterolophulid; 34, anterosinusid; 35, anterior arm of the protoconid; 36, metalophid I; 37, protoconid; 38, posterior arm of the protoconid; 39, metalophid II; 40, ectolophid; 41, mesoconid; 42, ectomesolophid; 43, ectostylid; 44, ectosinusid; 45, anterior arm of the hypoconid; 46, hypoconid; 47, posterior arm of the hypoconid; 48, hypoconulid; 49, labial arm of the posterolophid; 50, posterolophid; 51, posterofossettid; 52, entoconid; 53, anterior arm of the entoconid; 54, mesofossettid; 55, mesolophid; 56, mesostylid; 57, endolophid; 58, metastylid crest; 59, metaconid; 60, anterior arm of the metaconid; 61,anterofossettid; 62, cingulid. Modified from Nesin and Kovalchuk (2017). 46

Figure 2.9. Gliridae nomenclature. *Myomimus* upper and lower teeth. a) Right first upper molar, M1. 1-paracone, 2-anteroloph, 3-protoloph, 4-endoloph, 5-protocone, 6-posterioloph, 7-metaloph, 8-posterior extra ridge, 9-metcanoce, 10-posterior centralloph, 11-anterior centraloph, 12-anterior extra ridge ; b) right first lower molar, m1; 13-metalophid, 14-anterior extra ridge, 15-anterolophid, 16-protoconid, 17-mesolophid, 18-mesoconid, 19-hypoconid, 20-posterior extra ridge, 21-posterolophid, 22-entoconid, 23-endolophid ,24-centrolophid and 25-metaconid. Modified from Kaya and Kaymakçı, (2018). 47

Chapter 3. Implications of modern Barn owls pellets analysis for archaeological studies in the Middle East 51

Table 3.1. MNI: Minimal Number of Individual; %: percentage of relative abundance. 59

Table 3.2. Measurements of the coronoid height of the mandible in mm from Krystufek and Vorhalik (2001) 59

Table 3.3. Comparison between the measurements in the different *Meriones* species found in Syria, Armenia, Iran and Birecik pellets (after this work and Krsytufek & Vorhalik 2009). All measurements are given in millimetres. CBL: Condylo-basal length; ZB: Bizygomatic breadth; UTR: Upper tooth row; TBL: tympanic bullae length. 62

Table 3.4. Anatomical representation of small mammal remains from the Birecik Tyto alba pellets (Ni: Number of elements in our sample; Ei: number of expected element i in the assemblage, Ri: Relative abundance in Percentage). 63

Table 3.5. Proportions of postcrania to crania elements (calculated according Andrews 1990)64

Table 3.6. Number of remains (NR) and percentage of broken postcranial elements of Birecik sample. 64

Table 3.7. Representation (N) and percentage of fragmentation (%) of the cranial elements. 65

Table 3.8. Representation (N) and Percentages of digestion (%) on cranial and post-cranial elements from the Birecik pellets 66

Table 3.9. Distribution of species scores for the Bioclimatic Model of the Birecik assemblage (according to Hernández-Fernández, 2001; Hernández-Fernández et al., 2007). 69

Table 3. 10. Birecik sample Bioclimatic model results. SD (Standard Deviation) 69

Table 3.11. Percentage of the palaeoenvironmental reconstruction for the Birecik sample, Fo (Forest), (Sh) Shrubland, (Gr) Grassland, (De) Desert and (We) Wetlands (Habitat Weighting model). 70

Figure 3.1. Geographic location of the studied area, Birecik (South Anatolia, Turkey). 56

Figure 3.2. Skull measurements abbreviations. CBL: Condylo-basal length; ZB: Bizygomatic breadth; UTR: Upper tooth row; TBL: tympanic bullae length. *Meriones* skull picture modified from Kryštufek and Vohralík (2009) 58

Figure 3.3. 1-Right mandible *Suncus etruscus*, CH (Coronoid height); 2-Right Left Upper M1 molar *Nesokia indica*; 3-*Mus musculus* maxilla; 4-Left lower molar row with m1 and m2 of *Meriones tristami.* *59*

Figure 3.4. PCA graph on skull measurements of *Meriones* spp (Axis 1, horizontal x Axis 2, vertical). Colours indicate the species. Green: *Meriones tristami*; brown: *Meriones vinogradovi*, Red: *Meriones persicus*, Blue: Birecik sample. 61

Figure 3. 5. Profiles of representation percentage of the small mammal skeletal elements for Barn owl pellets from the sample from Birecik. 64

Figure 3.6. SEM pictures of digested rodent elementsfrom the Birecik pellets. 1- Moderate digestion is observable on the trochanter and on the basis of the femoral head and 2- detail of the same femur; 3- Rodent distal femur with strong digestion, 4- Femur head with moderate digestion; 5- Rodent upper incisor with moderate digestion; 6- Incisor with light digestion at the tip 67

Chapter 4. Distinguishing between three modern *Ellobius* species (Rodentia, Mammalia) and identification of fossil *Ellobius* from Kaldar Cave (Iran) using geometric morphometric analyses of the first lower molar 75

Table 4.1. Ranges of month precipitations and mean annual temperatures within the geographic distribution area of various Ellobius species (https://eol.org/). 80

Table 4.2. Modern reference collection for each museum specimen. Natural History Museum of London (NHM), Field Museum of Chicago (FM) and American Museum of Natural History of New York (AMNH). Archaeological specimens from Kaldar Cave, MP = Middle Palaeolithic, UP = Upper Palaeolithic. 85

Table 4.3. Contribution of the first 10th PCs to the total variance (%). PCA: principal component analysis 87

Table 4. 4. Cross-validated classification results in frequencies and %. 89

Figure 4.1. A) Occlusal surface of *Ellobius* right lower m1: triangle (T); buccal re-entrant angle (BRA); lingual re-entrant angle (LRA), anterior cap (AC); posterior lobe (PL); B) Lingual view of

left lower m1. 82

Figure 4.2. *Ellobius* lower m1 (all figured as right ones) from the extant reference collections and Kaldar Cave. 1) *Ellobius fuscocapillus*: 1.A-Kaldar Cave, 2014/4/SL5II/E6/125-130, right lower m1, number 157. 1.B-Kaldar Cave, 2014/4/SL5/E5/109-111, right lower m1, number 520. 1.C-Kaldar Cave, 2014/5/SL7II/E7/170-180, right lower m1, number 104. 1.D- Kaldar Cave, 2014/5/SL7II/F6/135-145, right lower m1, number 547.1.E-modern, NHM86101513, Afghanistan, right lower m1. 1.F-modern, FM111846, Iran, right lower m1. 1.G-modern, NHM86101512, Afghanistan, right lower m1; 2) *Ellobius lutescens***:** 2.A-Kaldar Cave, 2014/5/SL7II/F6/130-140, right lower m1, number 319. 2.B- Kaldar Cave, 2014/4/SL5II/F7/115-118, right lower m1, number 90. 2.C-Kaldar Cave, 2014/4/SL5II/F7/115-118, right lower m1, number 91. 2.D- Kaldar Cave, 2014/5/SL7II/E7/145-150, right lower m1, number 436.2.E-modern, NMH916416, Turkey, right lower m1. 2.F-modern, NMH916414, Turkey, right lower m1. 2.G-modern, NMH916412, Turkey, right lower m1; 3) *Ellobius talpinus***:** 3.A-modern, NHM3421126, Russia, right lower m1. 3.B-modern, FM103163, Afghanistan, right lower m1. 3.C-modern, AMNH59797, Mongolia, right lower m1. Scale equals 1 mm. 84

Figure 4.3. A) Kaldar Cave location. B) Entrance from the south of Kaldar Cave. 85

Figure 4.4. *Ellobius* right lower m1. A) 14 landmarks: Landmarks on the outermost turning point of buccal (2, 4, 6) and lingual (8, 10, 12, 14) salient angles, and on the innermost turning point of buccal (3, 5) and lingual (9, 11, 13) re-entrant angle. B) 60 semi-landmarks on the anterior cap. 86

Figure 4.5. Principal component analysis on the normalized landmarks and sliding semilandmarks and shape configuration at the extreme ends of the PCs. 87

Figure 4.6. A) First two principal components of size and shape including the reference collection and Kaldar Cave material. B) Boxplot of the total length of *Ellobius* from the extant reference collections and Kaldar Cave. 88

Figure 4.7. Morphological differences between *Ellobius fuscocapillus* (left) and *Ellobius lutescens* (right). Arrows depict the displacements between corresponding landmarks in the reference (dots) and E*llobius lutescens* as target specimens. 90

Chapter 5. New palaeoecological inferences using rodent's assemblages for the Middle to the Late Pleistocene site of Azokh 1 Cave (Southern Caucasus) 99

Table 5.1. Scores attributed to each rodent species found at Azokh 1 Cave according to its ecological requirements, used for the habitat weighting method: Forest (Fo), Shrubland (Sh), Grassland (Gr), Desert (De), Wetland (We), Steppe (St) and Rocky (Ro). 111

Table 5.2. Scores attributed to each rodent species found at Azokh 1 Cave for the bioclimatic model (in accordance with Hernández-Fernández, 2001; Hernández-Fernández et al., 2007, updated by Royer et al., 2020). See text for the significance of the Roman numerals corresponding to the climatic groups. 112

Table 5.3. Representation of the Azokh 1 Cave rodent species in terms of number of identified specimens (NISP), minimum number of individuals (MNI) and percentage of the MNI (%). 113

Table 5. 4. Measurements of *Cricetulus migratorius* first lower molar, m1, (in mm): L, total length; W, width. NHM: Natural History Museum of London. NISP: number of identified specim ens 112

Table 5.5. Measurements of *Mesocricetus brandti* and *Mesocricetus raddei* first lower molar, m1, (in mm): L, total length; W, width. NHM: Natural History Museum of London. NISP: number of identified specimens. 115

Table 5. 6. Representation (N) and Percentages of digestion (%) on Isolated incisors and Isolated molars from Azokh 1 Cave, Unit V and Unit II. 123

Table 5.7. Comparison between the new studies carried out in Azokh 1 Cave and Partiff (2016), X: indicate the presence on the sample. 124

Table 5.8. Values of temperatures and precipitations for the Azokh 1 Unit V and Unit II, obtained by the Bioclimatic Model. MAT (mean annual temperature); MTC (mean temperature of coldest month); MTW (mean temperature of warmest month); MAP (mean annual precipitation); Max (maximum of values obtained); Min (minimum of values obtained). The current values where obtained from https://en.climate-data.org/. 125

Table 5.9. Species and elemental interpretations carried our previously in Azokh 1 Cave with different environmental proxies. 127

Table 5.10. Interpretation of environmental conditions and faunal lists of the comparison sites located in Israel. 129

Figure 5.1. Azokh Cave system: a) View of exterior of cave system, showing three main entrance passages (Azokh 1, 2 and 5); b) Plan of Azokh Cave showing the main entrances and internal galleries (Murray et al., 2010); c) Location of Azokh Cave 104

Figure 5.2. Stratigraphy of Azokh 1: a) Cross section through the entrance passage (facing NW) showing the extent of the cave sediments remaining in the chamber. These are physically separated and are labelled Sediment Sequence 1 and 2. The undated Sequence 1 includes Units VI to IX. The archaeological Sequence w (inside the rectangle) includes Units I to V; b) Cross section (orthogonal to the section shown in (a)) of Azokh 1 showing the keyhole shape of the passage; c) Stratigraphy of Sediment Sequence 1; d) Stratigraphy of Sediment Sequence 2 with dating results of archaeological units (photos modified from Murray et al., 2016) 105

Figure 5.3. Some rodents identified at Azokh 1 Cave. 3.1- *Cricetulus migratorius*, Azokh 1 Cave, 2003, Unit V, D45, Z: 224, right M1 and M2, number 221. 3.2- *Mesocricetus brandti*, Azokh 1 Cave, 2014, Unit II, E49, Z: 320-330, left m1 and m2, number 74. 3.3- *Clethrionomys glareolus*, Azokh 1 Cave, 2018, Unit II, G56, Z: 46.48, left m1 occlusal and lingual view, number 703. 3.4- *Arvicola* ex. gr. *persicus*, Azokh 1 Cave, 2014, Unit II, G51, Z: 330-340, left m1, number 536. 3.5-*Chionomys gud*, Azokh 1 Cave, 2003, Unit V, D46, Z: 111, left m1, number 349. 3.6- *Chionomys nivalis*, Azokh 1 Cave, 2014, Unit II, F48, Z: 330-340, left m1,number 529. 3.7- *Microtus* gr. *arvalis-socialis*, Azokh 1 Cave, 2014, Unit II, G53,Z: 330-340, right m1, number 5. 3.8- *Microtus (Terricola)* spp., Azokh 1 Cave, 2005, Unit V, E40, Z: 136, left m1, number 43. 3.9- *Microtus (Terricola)* spp., Azokh 1 Cave, 2005, Unit V, D45, right m1, number 170. 3.10-*Ellobius lutescens*, Azokh 1 Cave, 2015, Unit II, F51, Z: 320-330, left m1 occlusal and lingual view, number 226. 3.11- *Meriones* gr. *persicus- tristrami*, Azokh 1 Cave,2003, Unit V, D45, right m1 occlusal and lingual view, number 169. 3.12- *Meriones* gr. *dahli-libycus*, Azokh 1 Cave,2003, Unit V, D45, Z: 224, left M1, number 222. 3.13- *Apodemus (sylvaemus)* sp., Azokh 1 Cave, 2014, F52, Z: 330-340, left m1, number 80. 3.14- *Allactaga* cf. *williamsi*, Azokh 1 Cave, 2018, H49, G50, right m1, number 635. Scale 1mm. 114

Figure 5.4. a) Principal component analysis on the normalized landmarks and sliding semilandmarks and shape configuration at the extreme ends of the PCs. b) First two principal components of size and shape including the reference collection and Azokh 1 Cave materi al 119

Figure 5.5. Results of the habitat weighting method for Azokh 1 Cave (Unit V and Unit II) 126

Figure 5.6. a) Location of Qesem Cave, Misliya Cave and Azokh 1. b) Climatic map of the studied region, obtained from Zittis (2015) 130

Chapter 6 Exploring the landscape and climatic conditions of Neanderthals and anatomically modern humans in the Middle East : the rodent assemblage from the late Pleistocene of Kaldar Cave (Khorramabad Valley, Iran) 141

Table 6.1. Scores attributed to each rodent species found at Kaldar Cave according to its ecological requirements, used for the habitat weighting method: Forest (Fo), Shrubland (Sh), Grassland (Gr), Desert (De), Wetland (We), Steppe (St) and Rocky (Ro). 148

Table 6.2. Scores attributed to each rodent species found at Kaldar Cave for the bioclimatic model (in accordance with Hernández-Fernández, 2001; Hernández-Fernández et al., 2007). See text for the significance of the Roman numerals corresponding to the climatic groups. 149

Table 6.3. Representation of the Kaldar Cave rodent species in terms of number of identified specimens (NISP), minimum number of individuals (MNI) and percentage of the NISP (%). 151

Table 6.4. Measurements of *Microtus* specimens (in mm): NS, number of specimens; L, length; La, T4 width; Li, T5 width. 152

Table 6.5. Measurements of *Ellobius* specimens (in mm): L, total length; W, width. NHM: Natural History Museum of London. NISP: number of identified specimens. 154

Table 6. 6. Bioclimatic model estimates for Kaldar Cave. SD, standard deviation. Current values obtained from: https://en.climate-data.org/asia/iran/lorestan/khorramabad-764550/. 158

Table 6.7. Comparison between Middle Eastern sites with small-mammal studies 160

Table 6.8. Comparison of the small-mammal lists from several Upper Palaeolithic sites in the Middle East. 161

Table 6.9. Estimates using the bioclimatic method for Aghitu-3 and Dzudzuana Cave. SD, standard deviation. Current values obtained from Kandel et al. (2017) for Aghitu-3 and https://es.climate-data.org/asia/georgia/imereti/jria-414325/?amp=true for Dzudzuana Cave. 162

Figure 6.1. a) Locations of the Late Pleistocene sites with rodent studies in the Middle East, including Kaldar Cave. b) General view of the entrance to Kaldar Cave. c) Stratigraphy of the eastern section of Kaldar Cave, including the location and results of the dated samples, from A. Ollé and B. Bazgir (Bazgir et al., 2017). 146

Figure 6.2. Some rodent species identified at Kaldar Cave in comparison with equivalent (analogue) modern specimens from the NHM of London. 1) *Microtus irani:* 1.1-Kaldar Cave, 2014, Layer 5 (sub-layer 7II), E7, 150-156, right lower m1, number 447. 1.2-modern, NHM205207, Iran (Shiraz), right lower m1; 2) *Microtus guentheri*: 2.1-Kaldar Cave, 2014, Layers 1-3 (sub-layer 4II), F6, 97-107, left lower m1, number 17; 3) *Microtus socialis*: 3.1-Kaldar Cave, 2014, Layer 4 (sub-layer 5II), F7, 115-118, right lower m1, number 106. 3.2-modern, NHM631799, Turkey (Amasya); 4) *Chionomys nivalis*: 4.1-Kaldar Cave, 2014, Layer 4 (sub-layer 5), E6, 94-104, left lower m1, number 542. 4.2-modern, NHM71820, Syria, left lower m1; 5) *Ellobius fuscocapillus*: 5.1-Kaldar Cave, 2014, Layer 4 (sub-layer 5II), E6, 125-130, right lower m1, number 157. 5.2-modern, NHM86101513, Afghanistan, right lower m1; 6) *Ellobius lutescens*: 6.1-Kaldar Cave, 2014, Layer 5 (sub-layer 7II), F6, 130-140, right lower m1, number 319. 6.2-NMH916416, Tur-

key, right lower m1; 7) *Cricetulus migratorius*: 7.1- Kaldar Cave, 2014, Layer 4 (sub-layer 5II), E6, 135-140, left lower m1, number 259. 7.2-modern, NHM773029, Iran, right lower m1; 8) *Mesocricetus brandti*: 8.1-Kaldar Cave, 2014, Layer 5 (sub-layer 7II), F6, 135-145, left upper M1, number 549. 8.2- modern, NHM193461226, Caucasus, left upper M1; 9) *Meriones* cf. *persicus*: 9.1-Kaldar Cave, 2014, Layer 5 (sub-layer 7II), F6, 156-166, left lower m1, number 551. 9.2-modern, NHM510434, Iran, left lower m1; 10) *Allactaga* sp.: 10.1-Kaldar Cave, 2014, Layer 5 (sub-layer 7II), E7, 141-147, right lower m3, number 203; 11) *Myomimus* sp.: 11.1- Kaldar Cave, 2014, Layer 5 (sub-layer 7II), E7, 141-147, left lower m1 and m2. 11.2-modern, *Myomimus personatus*, NHM67623, Turkey, left lower mandible; 12) *Apodemus* sp.: 12.1-Kaldar Cave, 2014, Layer 4 (sub-layer 5), E6, 94-104, right m1 and m2, number 547; 13) *Mus* cf. *musculus*: 13.1-Kaldar Cave, 2014, Layer 5 (sub-layer 7II), 166-174, left lower m1, number 495. Scale 1 mm 150

Figure 6.3. Results of the habitat weighting method for Kaldar Cave (Layer 4 and Layer 5). Forest (Fo), Shrubland (Sh), Grassland (Gr), Desert (De), Wetland (We), Steppe (St) and Rocky (Ro). 159

Figure 6. 4. Results of the habitat weighting method for Aghitu-3 and Dzudzuana Cave. Forest (Fo), Shrubland (Sh), Grassland (Gr), Desert (De), Wetland (We), Steppe (St) and Rocky (Ro) 162

Chapter 7. General discussion 171

Table 7.1.Small mammal taxa representation from the studied archaeological sites (Azokh, Kaldar) and owl pellet samples (Birecik), in terms of number of identified specimens (NISP), minimum number of individuals (MNI) and percentage (%) of the MNI. 175

Table 7.2. Modern biogeographic affinities of the species present in this work 188

Table 7.3. Probable agents of accumulation of the archaeological and modern study samples according to Andrews 1990, Demirel et al., 2011 and Fernández-Jalvo 2016c. 190

Table 7.4. Time span relation between the major events in human population and the studied sites regarding the published chronological data (modified from Weissbrod et al. 2020 and Hirst 2019). MIS = Marine Isotopic Stage. 191

Table 7.5. Values of mean annual temperatures and precipitations for Azokh 1 Unit V and Unit II, Kaldar Cave Layer 5 and Layer 4 and Birecik samples, obtained with the Bioclimatic Model method. MAT (mean annual temperature); MTC (mean temperature of coldest month); MTW (mean temperature of warmest month); MAP (mean annual precipitation). 192

Figure 7.1. Location of the studied sites in this PhD: Azokh Cave (Southern Caucasus), Kaldar Cave (Iran) and Birecik (Turkey); and other sites mentioned in this chapter with small mammals studies: 1) Misliya Cave (Israel, Middle Pleistocene), 2) Qesem Cave (Israel, Middle Pleistocene), 3) Aghitu-3 (Armenia, Late Pleistocene), 4) Dzudzuana (Georgia, Late Pleistocene), 5) Hazar Merd (Iraq, Late Pleistocene), 6) Kani Mikaeli (Iran, Late Pleistocene), 7) Qalaloun (Iran, Late Pleistocene), 8) Yafteh Gar (Iran, Late Pleistocene) and 9) Arjeneh (Iran, Late Pleistocene). 174

Figure 7.2. *Cricetulus migratorius* and *Mesocricetus brandti* current distribution obtained from IUCN red list (https://www.iucnredlist.org/). 177

Figure 7.3. Current distribution of *Microtus* species considered in this study, obtained from IUCN red list (https://www.iucnredlist.org/). The arrows indicate that in the *Microtus* gr. *arvalis-socialis* we comment the distribution concerns *Microtus socialis*, *Microtus arvalis* and also

Microtus guentheri. 178

Figure 7.4. Current distribution of *Ellobius lutescens* and *E. fuscocapillus*, obtained from IUCN red list(https://www.iucnredlist.org/). 179

Figure 7.5. Current distribution of *Clethrionomys glareolus* obtained from IUCN red list (https://www.iucnredlist.org/). 180

Figure 7.6. Probably current distribution of *Arvicola persicus* according to Mahmoudi et al. (2020) and Maul et al. (2020). 181

Figure 7.7. Current distribution of *Chionomys nivalis* and *C. gud* obtained from IUCN red list (https://www.iucnredlist.org/). 182

Figure 7.8. Current distribution of *Meriones tristami* and *M. persicus* obtained from IUCN red list (https://www.iucnredlist.org/). 183

Figure 7.9. *Nesokia* distribution, according to the IUCN red list (https://www.iucnredlist.org/). 184

Figure 7.10. *Mus musculus* distribution, according to the IUCN red list (https://www.iucnredlist.org/). 184

Figure 7.11. Distribution of the *Apodemus* species present in the in southern Caucasus and Iran, according to the IUCN red list (https://www.iucnredlist.org/). 186

Figure 7.12. Distribution of *Myomimus setzeri* and *M. personatus*, according to the IUCN red list (https://www.iucnredlist.org/). 187

Figure 7.13. Relation of Azokh 1 Unit V with the planktonic δ18O values and vegetation groups (A: Steppe with pioneer vegetation, B: heath with steppe vegetation, C: pioneer with steppe vegetation, D: temperate woodland and heath vegetation and E: temperate woodland with Mediterranean elements) (modified from Blain et al., 2012; Roucoux et al., 2006). The arrows indicate the possible chronological attributions of Azokh 1 Unit V. 193

Figure 7.14. Correlation of Azokh 1-Unit II with the δ18O values (modified from Railsback et al., 2015). The arrow indicates the possible chronological attribution of Azokh 1 - Unit II. 195

Figure 7.15. Correlation of Kaldar Cave - Layer 5 with the δ18O values (modified from Railsback et al., 2015). The arrow indicates the possible chronological attribution of Kaldar Cave - Layer 5. 196

Figure 7.16. Relation of Kaldar Cave - Layer 4 with the δ18O values (modified from Obrochta et al., 2014). The arrow indicates the possible chronological attribution of Kaldar Cave - Layer 4. 197

Appendix 1

Climatic Parameters	b	aII	aII/III	aIII	aIV	aV	aVI	aVII	aVIII	aIX	SE
Mean annual temperature in °C (MAT)	26.686	0.024	-0.029	-0.024	-0.074	-0.12	-0.135	-0.217	-0.404	-0.386	3.637
Mean temperature of the warmest month in °C (MTW)	26.219	0.07	0.021	0.02	0.031	-0.212	-0.113	-0.037	-0.121	-0.287	4.754
Mean temperature of the coldest month in °C (MTC)	27.538	-0.033	-0.096	-0.08	-0.175	-0.032	-0.141	-0.418	-0.71	-0.465	5.081
Mean annual precipitation in mm (MAP)	2978.195	-21.237	-27.563	-33.05	-32.648	-6.678	-5.076	-28.4	-33.109	-25.98	470.615

b: intercept

aIV-aIX: slopes of the different bioclimatic components

SE: standard error of estimate

Modified from Hernández-Fernández (2001b) and Hernández-Fernández and Peláez-Campomanes (2005)

Appendix 2

Journal of Archaeological Science 111 (2019) 105029

Contents lists available at ScienceDirect

Journal of Archaeological Science

journal homepage: http://www.elsevier.com/locate/jas

Implications of modern Barn owls pellets analysis for archaeological studies in the Middle East

Iván Rey-Rodríguez [a,b,*], Emmanuelle Stoetzel [a], Juan Manuel López-García [c], Christiane Denys [d]

[a] HNHP UMR 7194, CNRS/Muséum National d'Histoire Naturelle/UPVD/Sorbonne Universités, Paris, France
[b] Sezione di Scienze Preistoriche e Antropologiche, Dipartimento di Studi Umanistici, Università Degli Studi di Ferrara, C.so Ercole I d'Este, 32 - 44121, Ferrara, Italy
[c] Institut Català de Paleoecologia Humana i Evolució Social (IPHES), Zona Educacional, 4, Campus Sescelades URV (Edifici W3), 43007, Tarragona, Spain
[d] ISYEB UMR 7205, CNRS/Muséum National d'Histoire Naturelle/UPMC/EPHE/Sorbonne Universités, Paris, France

ARTICLE INFO

Keywords:
Regurgitation pellets
Tyto alba
Southern Anatolia
Bone modification
Environmental reconstruction

ABSTRACT

Situated at the crossroad between Africa, Asia and Europe, the Middle East is an important region for the knowledge of human and mammal migrations. Among mammals, fossil small mammals are good proxies for palaeoenvironmental reconstructions, and can also play the role of markers of prehistoric movements. In the aim to better characterize the origins and the palaeoecological signal delivered by the small vertebrate assemblages in Middle East archaeological sites, we performed a taxonomic and taphonomic study of the small mammal remains found in pellets from Barn owl (*Tyto alba*) from a poorly known region of South of Turkey at the Syrian border, east of Euphrates River. This will constitute the first available taphonomic referential for this region.

The studied sample constituted by more than 40 disintegrated pellets provided 2503 rodent skeletal elements. The most common preys are *Meriones tristami*, followed by *Mus musculus*. The taphonomic study showed that our assemblage fits well with a predator category of light modification. Regarding the preservation, our mean bone relative abundance reached 82% and the bone fragmentation showed that more than 77% of our sample is intact. The digested elements represented 22% and the low to moderate grades were dominant (83.5%). Implications for environmental and climatic reconstructions based on small mammal communities were also explored using *Bioclimatic Model* and *Habitat Weighting* methods.

1. Introduction

Birds of prey predate small mammals that they usually swallow in the whole and regurgitate bones, teeth and fur as compact pellets (Shad and Kakhki, 2014). The studies of the pellets are really useful because they provide information about small mammal species occurrences in some regions, as well as the extent of bone modifications after the regurgitation process.

Our current understanding of small mammal distribution is based on the specimens found in zoological collections of the museums and most of them result of trapping surveys, or scavenging of road killed individuals. More rarely museums host owl pellet assemblages while they can also provide useful information about the predatory birds diet, as well as rare prey-species abundance or distribution, habitat preferences, cyclic population dynamics, or seasonal changes (Boitani and Molur, 2016; Kryštufek and Vohralík, 2009; Haddadian Shad et al., 2014). Consequently, pellet assemblages are often used as supplementary data for faunistic surveys, and some studies have been performed in the Middle East (Abi-said, Shehab and Amr, 2014; Darvish et al., 2000; Kopij and Liven-schulman, 2013; Obuch and Khaleghizadeh, 2012; Haddadian Shad et al., 2014; Shehab et al., 2013).

For the archaeologists and palaeontologists, owl pellet assemblages are considered as the major source of fossilised accumulations (Andrews, 1990). A taxonomic study of such fossil small mammal assemblages resulting from owl pellets represent an efficient tool for palaeoenvironmental reconstructions, but needs a preliminary taphonomic analysis to ensure that no major bias has altered the palaeoecological signal (e.g., Fernández-Jalvo et al., 2016; Stoetzel et al., 2011). In order to refine these taphonomic analyses and to better identify the origin of the accumulations, we need an exhaustive referential of modern avian predation for the study area (Eurasia, and more precisely Middle East). Indeed, each area has particular characteristics in term of predator and prey species, which may lead to different taphonomic signals.

* Corresponding author. HNHP UMR 7194, CNRS/Muséum National d'Histoire Naturelle/UPVD/Sorbonne Universités, Paris, France.
E-mail address: ivan.rey-rodriguez@edu.mnhn.fr (I. Rey-Rodríguez).

https://doi.org/10.1016/j.jas.2019.105029
Received 19 March 2019; Received in revised form 11 September 2019; Accepted 27 September 2019
0305-4403/Published by Elsevier Ltd.

The Barn owl is one of the major contributors to the fossil bone accumulations, being opportunistic and taking a wide range of prey, including mostly rodents and insectivores (Andrews, 1990). Here we present the first combined taxonomic and taphonomic study of small mammals remains from *Tyto alba* pellets from South Turkey, in order to contribute to a better knowledge of the Middle East small vertebrate predators and their taphonomic impact on prey bones.

2. Material and methods

2.1. Sampling of the studied material

The studied pellets come from the region called Birecik (37°1′N, 37°58′E) in Turkey (Fig. 1). The area is located at the west of Euphrates River, in the Southern Anatolia, close to Syria and Iraq border. Forty pellets have been collected by Jean Francois Noblet in June 2003, in a *Tyto alba* nest behind the breeding station of Northern bald Ibises (*Geronticus seremita)* installed in a valley near the Euphrates riverside, 3 km north of Birecik Şanlıurfa.

The pellets were disintegrated during handling and their contents were sorted by hand under microscope in order to identify and count the skeletal elements.

2.2. Taxonomy

Bones were recovered manually and identified at a specific level when it was possible, following the established available identification keys (Boitani and Molur, 2016; Coşkun, 1999; Darviche et al., 2006; Darvish, 2011; Pavlinov, 2008; Kryštufek and Vohralík, 2009; Mamkhair et al., 2007; Momtazi et al., 2008; Musser and Carleton, 2005; Yicit and Çolak, 1996; Siahsarvie and Darvish, 2008; Tez, 2000). Some measurements were done using Mitutoyo caliper (precision 0.01 mm) on the most complete skull and mandible elements. Regarding the nomenclature and identification keys, for Soricidae we followed Kryštufek & Vohralík (2001), for Gerbillinae we followed Pavlinov (2008) and for Murinae Darviche et al. (2006).

The Minimum Number of Individuals (MNI) has been estimated using the most abundant skeletal element present in the assemblage, including cranial and postcranial elements.

2.3. Taphonomy

The taphonomic study focused upon bone representation, fragmentation and digestion of small mammal elements recovered from the pellets. For this we followed the methodology developed by Andrews (1990), Denys et al. (1996) and Fernández-Jalvo et al. (2016).

2.3.1. Skeletal element proportions

The differing proportions by which the various elements of the prey skeletons are represented in a predator assemblage are frequently used to distinguish different types of predators. The numbers of the skeletal elements are usually expressed to be present for a given number of prey individuals, which is usually the minimum number of individuals (MNI). This proportion is called the relative abundance (Andrews, 1990).

$$\mathbf{R}_i = \mathbf{N}_i/(\mathbf{NMI} \times \mathbf{E}_i)$$

where:

R_i = the relative abundance of the element i
N_i = the number of element i in the sample
MNI = the Minimum Number of Individuals
E_i = the number of element i in the prey skeleton

For example, the number of bones found in the skeleton of an individual of a rodent like a mouse is: 1 skull, 2 maxillae, 2 mandibles, 12 M, 4 incisors, 2 femora, 2 humeri, 2 radii, 2 ulnae, 2 tibiae, 2 scapulae, 2 pelves, 2 astragali, 2 calcanei, 1 sacrum, 20 metapodials, 54 phalangias, 54 vertebrae, 24 ribs (Denys and Patou-Mathis, 2014; Stoetzel et al., 2011).

The calculation is based on the notion that the predator consumes most or all of the body of the prey, and modern samples indicate that predators have characteristic patterns for the proportional abundances of prey elements. As a result, the MNI should approximate to the number of preys eaten.

Three indices have been used to compare the preservation of postcranial and cranial elements. The first compares femora and humeri with the number of mandibles and maxillae ((F + H)/(Md + Max)*100). The second compares the number of all long bones with the major cranial elements and isolated molars ([femora + tibiae + humeri + radii +



Fig. 1. Geographic location of the studied area, Birecik (Southern Anatolia, Turkey).

ulnae]*16/([mandibles + maxillae + molars] *10)*100) and the third is the comparison between tibia and radii, and femora and humeri [(tibia + radii)/(femora + humeri)] (Andrews, 1990; Stoetzel et al., 2011).

2.3.2. Breakage

Breakage can also help to differentiate major groups of predators (Andrews, 1990), notably the breakage of long bones, skulls and mandibles. But in our sample, most of the postcranial material cannot be identified at the species level, so we didn't analyse the breakage by taxa.

We also have to keep in mind that if in modern assemblages bone breakage can help to identify the predator, in archaeological or palaeontological context many post-depositional processes may lead to an over-breakage of the material, and hide the "*predator signal*". Consequently, other taphonomic parameters (notably digestion) have to be taken into account for more reliable interpretations.

2.3.3. Digestion

The corrosive effects of digestion on bones and teeth in the predator's stomach are well distinguishable from other alteration processes (e.g. Fernández-Jalvo et al., 2014). Digestion is the most reliable parameter used to identify the predator type at the origin of a small mammal accumulation. It is based on both the degree of digestion and on the proportion of teeth and bones affected, considering that each type of predator has a different effect of digestion (Andrews, 1990). In our study we have considered light, moderate and strong digestion grades following Andrews (1990) and Fernandez-Jalvo et al. (2016) on molars, incisors, femora and humeri. We precise that we have not found any postpredation modification in our sample.

Patterns of digestion, if they are well visible to the naked eye, are best distinguished using the Scanning Electron Microscope (SEM) (Andrews, 1990; Demirel et al., 2011). In our study we used the SEM Hitachi SU 3500 from the *Service Commun de Microscopie Electronique du Museum National d'Histoire Naturelle* (MNHN-Paris), using secondary electron emission mode at an accelerating voltage of 15 kV.

2.4. Statistical analysis

Size differences have been investigated using Principal Component Analysis (PCA) between our sample and the references provided by the literature using the statistical software XLSTAT 10.0. Skull measurements have been done, taking into account the condylo-basal length, zygomatic breadth, maxillary tooth row and tympanic bullae length (Fig. 2).

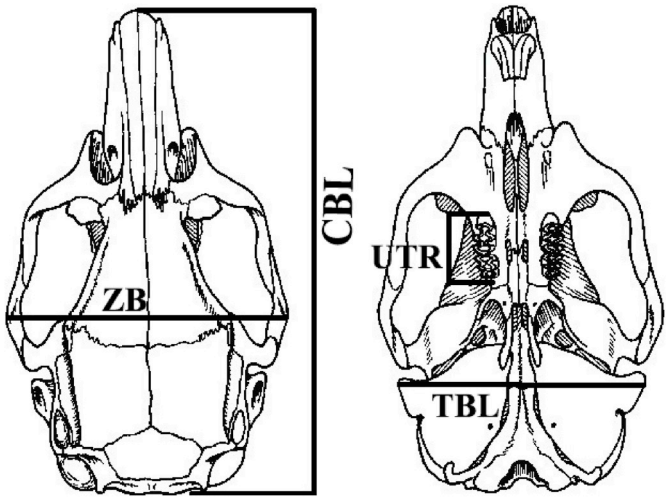


Fig. 2. Skull measurements abbreviations. CBL: Condylo-basal length; ZB: Bizygomatic breadth; UTR: Upper tooth row; TBL: tympanic bullae length. *Meriones* skull picture modified from Kryštufek and Vohralík (2009).

2.5. Climatic reconstruction

Finally, we tried to evaluate the potential of the small mammal associations accumulated by Barn owl to infer environmental and climatic parameters in using methods previously developed for fossil mammal assemblages. The *Bioclimatic Model* (BM) was developed by Hernández-Fernández (2001) in order to reconstruct palaeoclimatic conditions based on faunal spectrum, in assuming that small- and large-mammal species can be ascribed to ten different climates (Hernández-Fernández, 2001; Hernandez Fernández and Peláez-Campomanes, 2003; Hernández-Fernández et al., 2007). We applied this method for the first time on an assemblage from Southern Anatolia. It was first necessary to calculate the Climatic Restriction Index (CRIi = 1/n, where i is the climatic zone where the species appear and n is the number of zones where the species is present) and the Bioclimatic Component (BCi = (Σ CRIi) 100/S, where i is the climatic zone; S is the number of species). From the BC a mathematical model has been developed as a regression that allowed us to calculate climatic parameters (see Appendix 1).

The different climatic groups defined by Hernández-Fernández (2001) and Hernández-Fernández et al. (2007) are: I *Equatorial*; II *Tropical with summer rains*; II/III *Transition tropical semiarid*; IV, *Subtropical* with winter rains and summer droughts; V, *Warm temperate* with not very severe winters but high humidity; VI, *Typical temperate* with cold but not very long winters and cool summers; VII, *Arid-temperate* with large temperature contrasts between winter and summer; VIII, *Cold-temperate* with cool summers and long cold winters (boreal).

By means of the BM we were able to estimate the mean annual temperature (MAT), the mean temperature of the coldest month (MTC), the mean temperature of the warmest month (MTW) and the mean annual precipitation (MAP).

2.6. Environmental reconstruction

The method used for the palaeoenvironmental reconstruction is the *Habitat Weighting* method (Evans et al., 1981; Andrews, 2006; modified by Blain et al., 2008; López-García et al., 2011), which is based on the current distribution of each taxon, in the habitat or habitats where it is possible to find each taxon nowadays. We adapted the method to our studied area, including the following types: Forest (Fo), a long area covered with trees; Shrubland (Sh), where the vegetation is dominated by shrubs; Grassland (Gr), an open area covered with grass; Desert (De), an area with little precipitation and no vegetation cover; Wetlands (We),

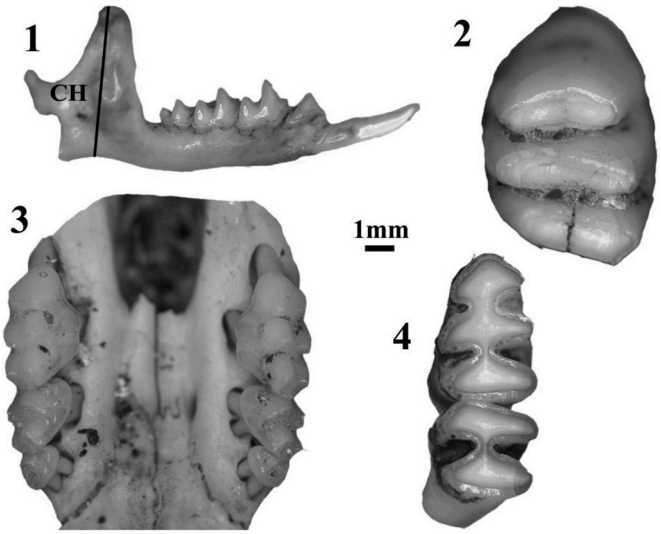


Fig. 3. 1- *Suncus etruscus,* right mandible (CH: Coronoid height); 2- *Nesokia indica,* right left upper M1; 3-*Mus musculus,* maxilla; 4- *Meriones tristami,* left lower molar row with m1 and m2.

which are normally used in agriculture (cereal fields).

3. Results and discussion

3.1. Taxonomic study

In total, 2503 identifiable skeletal elements were recovered from the studied pellets, belonging to only four small mammal taxa (Table 1). Rodents constituted the bulk of *T. alba* Birecik preys with 38 individuals and three genera (*Meriones*, *Nesokia* and *Mus*) followed by Eulipotyphla represented by one species (*Suncus etruscus*) and one individual. We present here some of the cranio-dental characters that allowed taxonomic identifications.

Order Eulipotyphla, Waddell et al., 1999

Family Soricidae, G. Fishcher, 1814

Genus *Suncus*, Ehrenberg, 1832

Suncus etruscus (Savi, 1822)

Material: 2; one right mandible and one left mandible (Fig. 3.1).

Description and discussion: In Turkey four species of white-toothed shrews are documented (Kryštufek & Vohralík, 2001; Tez, 2000): *Crocidura leucodon*, *Crocidura suaveolens*, *Crocidura arispa* and *Suncus etruscus*. *Suncus* differs from *Crocidura* in having four upper unicuspids instead of three. In our material, the absence of maxillary prevents precise identification on this criterion. However, regarding mandibles, we can attribute our samples to *Suncus etruscus*, because of their smaller height of the coronoid process (Table 2).

Habitat and distribution: Found in the Mediterranean region, *Suncus etruscus* prefers abandoned olive groves, vineyards, and other cultivated areas overrun by Mediterranean shrubs, but occurs also in gardens, low maquis, scrub, and open forest of Mediterranean oaks and pines. This species avoids sand dunes, dense forest and intensively cultivated land. It is more active during night than day. *Suncus etruscus* is distributed from Southern Europe, North Africa, parts of the Near East, Arabian Peninsula, Central Asia, South Asia and mainland Southeast Asia, to the island of Borneo in the east. It occurs from sea level to altitudes of 3000 m above sea level (Aulagnier et al., 2017). In Turkey it was found mainly in the western and South Anatolia, especially in anthropogenic habitats up to 1200 m (Krystufek and Vorhalik, 2001).

Order Rodentia Bowdich, 1821

Family Muridae Illiger, 1811

Genus *Nesokia*, Gray 1842

Nesokia indica (Gray, 1830)

Material: 2; one right maxillary fragment with M1 and one isolated upper right M2.

Description and discussion: In our sample (Fig. 3.2), the M1 and the M2 are high-crowned, broad and transversely laminated. There are three simple and isolated laminae on the M1, and only two on the M2. The first laminae of the M1 of Birecik pellets is wide and convex, while in Gerbillinae the first lamina (or prelobe) is small and much narrower; this allows us to distinguish it from *Tatera* and attribute this material to *Nesokia indica*. The relative size of the 2 M also is typical of *Nesokia*, the first molar being the longest and the most complex, and the last molar being the shortest and the most simplified (Kryštufek et al. 2017).

Habitat and distribution: This species has a predominantly Palearctic distribution. It requires firm damp soil to dig in and succulent grass roots or underground bulbs to feed upon. It is found in humid areas in dry steppes, semi-deserts and deserts, but occurs mainly around permanent water bodies (Kryštufek and Vohralík, 2009). *Nesokia indica* is very widespread in south-western and Central Asia (Boitani and Molur, 2016). In South Anatolia, *Nesokia indica* is mainly distributed near cultivated field and it is strictly limited to agricultural activities (Kryštufek and Vohralík, 2009).

Genus *Mus*,Linnée 1758

Mus musculus (Linaeus, 1758)

Material: Skull: one fragmented skull; Mandibles: 10; five complete right mandibles, five complete left mandibles; Maxillae: 4; one complete right maxilla, three complete left maxillae; Isolated Teeth: 4, one right lower m1, one left lower m1; two right upper M2.

Description and discussion: Like in other Murinae, the first upper molar (M1) has three rows of tubercles: the first (t1, t2, t3) and second (t4, t5 and t6) groups situated in the anterior part have three tubercles and the last group (t7 and t9) has two tubercles (Darviche et al., 2006). In Southern Turkey (Kryštufek and Vohralík, 2009) both *Mus musculus* and *Mus macedonicus* may be found.

Our specimens from Birecik *T. alba* pellets fit well with *M. musculus* in the upper M1 morphology (Fig. 3.3): the lingual row of cusps (t1 and t4) is shifted posteriorly; cusp t7 is reduced to an enamel ridge; distal cusps t8 and t9 leave no space for posterior cingulum or postero-labial cusp t12. The second upper molar lacks cusp t3; t7 is suppressed to a mere enamel ridge; t9 is small. The anterior half of m1 has a symmetrical X pattern formed at the anterior portion of the tooth (Siahsarvie and Darvish, 2008). Dental ends of mesial and central cusps on first lower molars fuse early; mesiolabial cusp is small. Upper molars normally have three roots each, one lingual and two labial, lower molars are two rooted, each with an anterior and a posterior root (Kryštufek and Vohralík, 2009). We reported also an incisor with the notch that characterizes *Mus musculus* (Kryštufek and Vohralík, 2009).

Habitat and distribution: This species is well distributed around all over the world, it is present over all continents, except Antarctica. It is found in a wide range of habitats but it not tends to be found in forests and deserts. *Mus musculus* is ecologically highly opportunistic but a weak competitor, it can cope with aridity and can expand also in the desert (Kryštufek and Vohralík, 2009). It is found also on arid habitats along the border with Syria and Iraq, in desert landscape and also near the Euphrates river (Kryštufek and Vohralík, 2009 and Musser et al. 2016).

Genus *Meriones*, Illiger 1811

Meriones tristami (Thomas, 1892)

Material: Skull: 33 fragments; Mandibles: 75; 28 complete right mandibles, 29 complete left mandibles; Maxillae: 57; 27 complete right maxillae, 30 complete left maxillae; Isolated Teeth: 96; nine right lower m1, six left lower m1; 14 right upper M1; 15 left upper M1, 32 M2; 20 M3.

Description and discussion: The genus *Meriones* is one of the most diversified representatives of the Gerbillini tribe in the Palaearctic region, particularly in arid regions of Asia (Darvish 2011; Denys et al., 2017). The current *Meriones* species reported in Turkey according to Kryštufek and Vohralík (2009) are: *Meriones tristami, Meriones vinogradovi*, *Meriones persicus*, *Meriones crassus*, *Meriones dahli* and *Meriones lybicus*. Although regarding their distribution the only one that is today

Table 1
MNI: Minimal Number of Individual; %: percentage of relative abundance.

Species	MNI	%
Suncus etruscus	1	2.56
Nesokia indica	1	2.56
Mus musculus	5	12.82
Meriones tristami	32	82.05
Total	**39**	**100**

Table 2
Measurements (in mm) of the coronoid height of the mandible of several Crocidurinae species; comparative data from Krystufek and Vorhalik (2001).

Specimen	Coronoid Height	Number of specimens	Min-max	Mean
Birecik sample	3.13–3.25	2	3.13–3.25	3.19
Crocidura leucodon	4.3–5.9	63	4.3-5-9	4.92
Crocidura suaveolens	4.0–5.0	230	4.0–5.0	4.52
Crocidura arispa	4.1	2	4.1	4.1
Suncus etruscus	2.8–3.3	43	2.8–3.3	3.06

present in Southern Anatolia is *Meriones tristami* (Kryštufek and Vohralík, 2009 and Sozen et al., 2017).

The Birecik molars attributed to *Meriones* are semi-hypsodont and display the typical morphology of the genus with prismatic triangles of enamel related by a longitudinal crest and no trace of cusps. In our sample we have identified first upper molars (M1) with three roots, so we could infer that it does not belong to *Meriones dalhi*, *Meriones lybicus* or *Meriones vinogradovi,* which present four roots on their M1 (Kryštufek and Vohralík, 2009). Moreover, the dental morphology of *Meriones persicus* and *Meriones tristami* is similar. A PCA was performed on skull measurements, taking into account the condylo-basal length, zygomatic breadth, maxillary tooth row and tympanic bullae length from our specimens compared with the data from Kryštufek and Vohralík (2009) (Fig. 4 and Table 3). The result shows that size is not the main criteria to distinguish between both species.

Axis 1 and 2 explain respectively 81,64% and 8,3% of the total variance. Variables best correlated with Axis 1 are CBL (condylo-basal lenght), UTR (upper tooth row) and ZB (zygomatic Breadth), while TBL (tympanic bullae length) is correlated with Axis 2. The Birecik samples fit well with *Meriones tristrami* specimens but are also close to *Meriones persicus* ones. *Meriones tristrami* has a wide size variability but comparing with Syrian specimens, these latter have relatively long tympanic bullae compared to a small CBL.

We provisionally attribute our specimens to *Meriones tristrami* (Fig. 3.4) pending a revision of the Middle East species of the genus.

Habitat and distribution: the genus *Meriones* is distributed in North Africa, Central Asia, Transcaucasia, Turkey and Pakistan (Darvish et al., 2014;Stoetzel et al., 2017). They mostly live in dry steppes of short or tall grass, open hillside, among rocky outcrops in desolate steppes, or open dry meadows. *Meriones tristrami* habitat is limited to 100 mm of rainfall annually and need well drained soil although it avoids rocky situations. In Turkey it has been mainly found in dry steppes and short or tall grass (Kryštufek and Vohralík, 2009).

3.2. Taphonomic study

3.2.1. Bone representation

On the 2503 skeletal elements recovered in the Birecik *Tyto alba* pellets, a total of 39 individuals (MNI) were counted, following the number of maxillae which were the most abundant elements. We found that all bones are present but in variable proportions. The most represented are maxillae (89%) and mandibles (87%) followed by tibiae

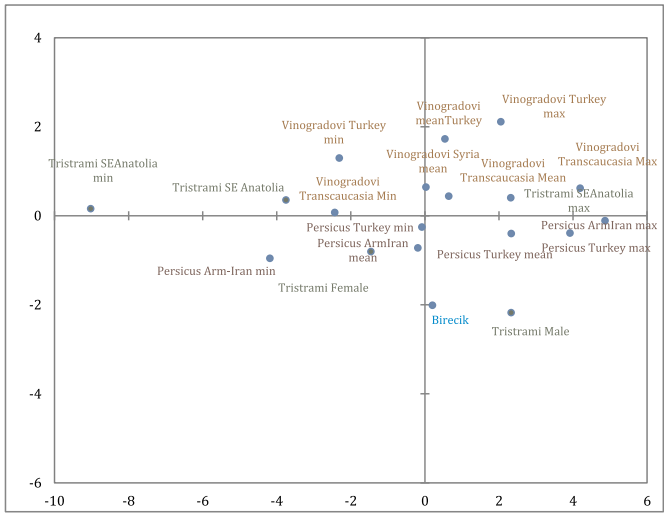


Fig. 4. PCA graph on skull measurements of *Meriones* spp. (Axis 1, horizontal x Axis 2, vertical). Colours indicate the species. Green: *Meriones tristami*; brown: *Meriones vinogradovi*, Red: *Meriones persicus*, Blue: Birecik sample.

Table 3
Comparison between the measurements (in mm) in the different *Meriones* species found in Syria, Armenia, Iran and Birecik pellets (after this work and Krsytufek and Vorhalik 2009). CBL: condylo-basal length; ZB: bizygomatic breadth; UTR: upper tooth row; TBL: tympanic bullae length.

Species	CBL	ZB	UTR	TBL
Birecik sample N = 5				
Mean	38.5	20.5	5.33	11.68
Max-Min	38.5	20.5	5.4–5.26	11.55–11.82
Meriones tristrami N = 22–34				
Male	40.3	21	5.5	13.2
Female	36.3	20.2	5.2	13.2
Meriones persicus Turkey N = 4				
Mean	39.5	22.5	6.5	12.7
Max-Min	37.4–40.8	21.7–23.0	6.1–6.8	11.8–13.6
Armenia, Iran N = 50				
Mean	37.6	21.2	6.3	11.5
Max-Min	34.4–41.4	6.1–6.8	5.9–6.9	10.0–14.4

(82%). On the other hand, the less represented elements (excluding the isolated molars) are the ribs (33%) and the calcanei (34%) (Table 4).

The mean representation percentage is 45.21% for all the taxa present in our assemblage, which is very close to the data provided by Andrews (1990) for Barn owl from Africa (48.91%).

Some rodent bones are anatomically connected: nine femora connected with a tibiae (tibia + fibula) and also with the phalanges, and three humeri linked with radii.

Regarding the taphonomic representation pattern, we can say that all elements are well represented, with small elements like foot bones, isolated teeth and vertebrae lost during collecting.

Most skeletal elements are well preserved and unbroken, as expected from a barn owl assemblage (Fig. 5). There is a preferential loss of some elements, among which the distal parts or the limbs. The average relative abundances (the mean relative abundance for all skeletal elements, except the isolated teeth) vary from 33.01% to 89.06%, which means that between one or two thirds of the prey has been lost from the sample during ingestion and digestion (Andrews, 1990).

Table 5 presents the proportions of postcranial *versus* cranial elements. The ratios (f + h)/(m + max)*100 reaches 108.85%, and 91.06% for the (t + r)/(f + h)+100 ratio. There is a slight long bone overrepresentation compared with mandibles and maxillae.

3.2.2. Fragmentation

Our post-cranial sample presents a low percentage of fragmentation, with more than 77% of complete elements (Table 6). The preservation does not vary too much between the post-cranial bones, but the most broken ones in Birecik pellets are the pelves (67.8%) and the scapulae (48.8%). The best preserved are the femora (98.3%).

In the case of *Suncus etruscus* we only have two complete mandibles. For *Mus musculus* and *Meriones tristami,* most of the maxillae and mandibles are broken. Only 12% of the *Mus* skulls are partially complete, and almost 7% for *Meriones*. For the mandibles, 37% are intact for *Mus* and 24% for *Meriones* (Table 7).

3.2.3. Digestion

In total 22.51% of the studied elements (femora, humeri, molars and incisors) are digested (Table 8 and Fig. 6) and the dominant grade of digestion is the light one (86.6%). The moderate grade was observed on one femur and one humerus, and strong digestion is only present in one femur. We observed also that the isolated molars are more digested than *in situ* ones, because they were more exposed to gastric juces. This value is quite high for *T.alba* but the pellets came from a nest, where digestion by young individuals is slightly higher than for adults (Denys et al., 2018).

For the elements in connexion we found three femora harbouring light digestion upon free epiphysis.

Table 4
Anatomical representation of small mammal remains from the Birecik *Tyto alba* pellets (Ni: Number of elements in our sample; Ei: number of expected element i in the assemblage, Ri: Relative abundance in Percentage).

Prey species	*Suncus etruscus MNI=1*			*Nesokia indica MNI=1*			*Mus musculus MNI=5*			*Meriones tristami MNI=32*		
Anatomical elements	Ni	Ei	Ri%	Ni	Ei	Ri%	NI	Ei	Ri%	Ni	Ei	Ri%
Skull						1						
Maxillae				2	2	100	6	10	60	57	64	89.06
Mandibles	2	2	100				10	10	100	56	64	87.5
Isolated Incisors				1	4	25	1	20	5	39	156	25
Isolated Molars				1	12	8.3	4			96	486	19.75
Femora										63	78	80.77
Tibiae (Tibia + Fibula)										64	78	82.05
Pelves										61	78	78.21
Calcanei (Calcaneum)										26	78	33.33
Tali (Astragalus)										30	78	38.46
Humeri										60	78	76.92
Radii										48	78	61.54
Ulnae										59	78	75.64
Scapulae										53	78	67.95
Ribs										309	936	33.01
Vertebrae										817	2106	38.79
Metapods										340	780	43.59
Phalanges										284	780	36.41
Sacrum										14	39	35.9
Total:	2			4			21			2476	6113	**Mean:** 45.21
MNI	1			1			5			32		

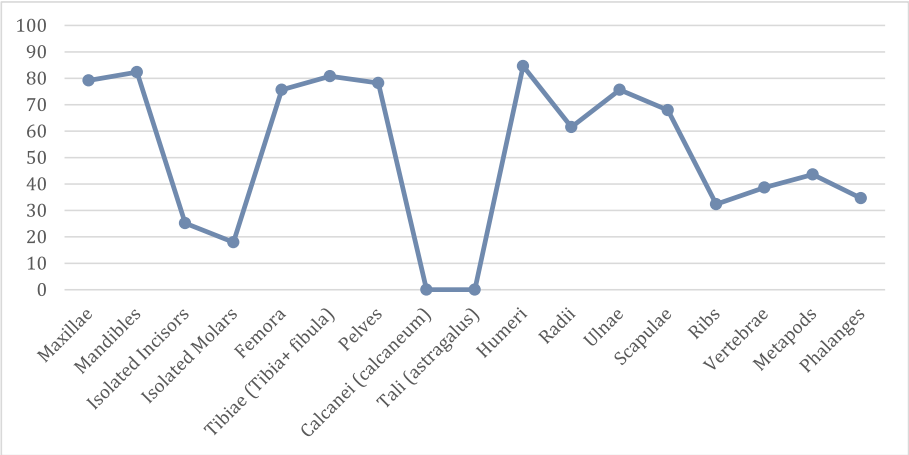


Fig. 5. Profiles of representation percentage of the small mammal skeletal elements for Barn owl pellets from the Birecik sample.

Table 5
Proportions of postcrania to crania elements (calculated according Andrews, 1990).

Ratios	%
(femora + humeri)/(mandibles + maxillae) *100	108.85
(tibia + radii)/(femora + humeri)	91.06
([femora + tibiae + humeri + radii + ulnae]*16/([mandibles + maxillae + molars] *10)*100)	225.08

3.2.4. Taphonomic implications

Tyto alba is an active hunter, especially at night, consequently nocturnal prey-species are taken more commonly than diurnal ones, which corresponds to what we found in the Birecik pellet assemblage. Moreover, the preferred hunting areas of the owl may be over-represented, notably the wetter and more open habitats (Mikkola, 1983). Compared to previous studies performed in the same region, our sample is poorly diversified: we only have four species, mainly rodents (three species) and just one shrew. In other studies, a higher species diversity was found. Shehad et al. (2013) identified 23 species, including chiroptera (five species) and rodents (18 species) (Appendix 2).

In Lebanon, Abi Said et al. (2014) identified six rodents and two shrews. In some assemblages, bats or birds were also identified as preys (Shehab at al., 2013, Maul et al., 2015) but we didn't recover any of

Table 6
Number of remains (NR) and percentage of broken postcranial elements of Birecik sample. Percentage of fragmentation is 22.80%.

Element	Complete	Broken			Total
		Proximal	Distal	Shafts	
Femora	58	1			59
Humeri	61	5			66
Tibiae (Tibia + Fibula)	59	1		3	63
Ulnae	48	9	1	1	59
Radius	47			1	48
Pelves	13	48			61
Scapulae	22	21			43
Total (NR)	**308**	**85**	**1**	**5**	**399**
Relative Percentage	**77.20**	**21.30**	**0.25**	**1.25**	**100.00**

Table 7
Representation (N) and percentage of fragmentation (%) of the cranial elements.

			Suncus etruscus		*Mus musculus*		*Meriones tristami*	
			N	%	N	%	N	%
Skull	Complete				2	12.5	8	6.96
	Broken	Isolated Maxillae with zygomatic				0	1	0.87
		Isolated Maxillae without zygomatic				0		0
		Upper molars loss			1	6.25	28	24.35
		Upper incisors loss			3	18.75	22	19.13
Mandible	Complete		2	100	6	37.5	28	24.35
	Broken	Broken ascendant ramous			1	6.25	3	2.61
		Ascendant ramous missing				0	6	5.22
		Missing and inferior border broken				0	4	3.48
		Fragment				0		0
		Lower molar loss				0	11	9.57
		Lower incisors loss			3	18.75	4	3.48
Total			**2**	**100**	**16**	**100**	**115**	**100**
Percentage of Fragmentation				**100%**		**50%**		**68.7%**

Table 8
Representation (N) and Percentages of digestion (%) on cranial and post-cranial elements from the Birecik pellets.

Elements	Total	Total digested		No digestion		Light digestion		Moderate digestion		Strong digestion		In connexion Not digested		In connexion light digestion	
		N	%	N	%	N	%	N	%	N	%	N	%	N	%
Isolated incisor	39	18	46.15	21	53.85	15	37.46	3	7.69						
In situ incisor	90	34	37.78	56	62.33	34	37.78								
Isolated molars	96	4	4.17	92	95.83	4	4.17								
In situ molars	84	3	3.57	81	96.43	3	3.57								
Femora	62	22	35.48	40	64.52	13	20.97	1	1.61	1	1.61	4	6.45	3	4.84
Humeri	60	16	26.67	44	73.33	12	20	1	1.67			3	5		
Total/Mean %	**431**	**97**	**22.51**	**334**	**74.49**	**81**	**18.79**	**5**	**1.16**	**1**	**0.23**	**7**	**1.62**	**3**	**0.70**

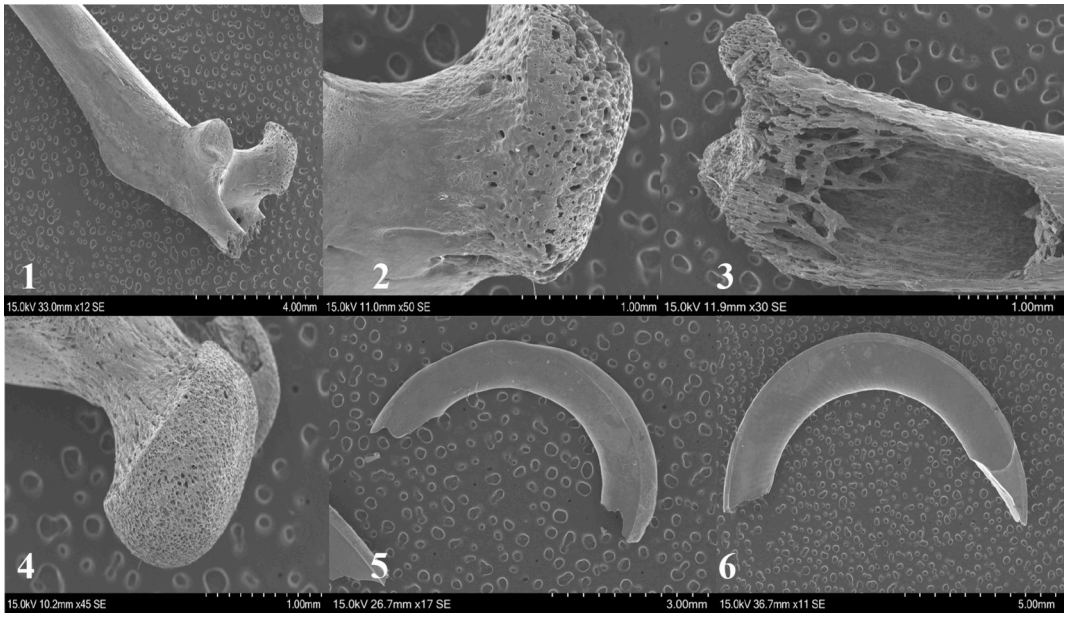


Fig. 6. SEM pictures of digested rodent elements from the Birecik pellets. 1- Moderate digestion is observable on the trochanter and on the basis of the femoral head and 2- detail of the same femur; 3- Rodent distal femur with strong digestion, 4- Femur head with moderate digestion; 5- Rodent upper incisor with moderate digestion; 6- Incisor with light digestion at the tip.

these taxa in our assemblage. *Meriones* may be very abundant locally and represent a high biomass for the owls (Shehab et al., 2013). Considering the opportunistic diet of *Tyto alba* (Andrews, 1990), this may explain why *Meriones* are the most represented species in our material and why the owl did not need to diversify its prey spectrum. Also the predominance of *Meriones* can be explained as a hunting preference of barn owl (Andrews, 2018). Another explanation may result from the low number of pellets analyzed here, or from the season of capture, which both may favor a higher diversity. Indeed, prey composition and digestion can differ from a month to another, but the highest differences occur generally between summer and winter (Andrews, 2018). Our pellets were collected in June 2003, and our values are similar to the ones

Table 9
Distribution of species scores for the Bioclimatic Model of the Birecik assemblage (according to Hernández-Fernández, 2001; Hernández-Fernández et al., 2007).

Species	I	II	II/III	III	IV	V	VI	VII	VIII	IX
Suncus etruscus	0.333	0.333	0	0	0.333	0	0	0	0	0
Nesokia indica	0	0	0.25	0.25	0.25	0	0	0.25	0	0
Mus musculus	0.111	0.111	0.111	0.111	0.111	0.111	0.111	0.111	0.111	0
Meriones tristami	0	0	0	0	1	0	0	0	0	0

Table 10
Birecik sample *Bioclimatic model* (BM) results (SD: Standard Deviation).

	BM	SD	Current values
Mean annual temperature	20.86 °C	3.39	18.5 °C
Maximum mean temperature	27.61 °C	4.77	39 °C
Minimum mean temperature	11.45 °C	4.66	2.7 °C
Mean annual precipitations	431.98 mm	533.24	458.1 mm

Table 11
Values of the habitat frequentation of the species found in the Birecik sample (*Habitat Weighting* model): Fo (Forest), (Sh) Shrubland, (Gr) Grassland, (De) Desert and (We) Wetlands.

	Fo	Sh	Gr	De	We
Meriones tristami		0.5		0.5	
Mus musculus		0.33	0.33		0.33
Nesokia indica	0.33	0.33	0.33		
Suncus etruscus	0.25	0.25	0.25	0.25	
Total	0.6	1.4	0.9	0.8	0.3

displayed by the owls during summer (Andrews, 2018).

The diet of *Tyto alba* from our collected pellets fits well with the other studies in Europe and Asia. The Barn owls' preys are small vertebrates, including a wide range of rodents and insectivores (Andrews, 1990).

Tyto alba is well known because it is widespread around the word and it was identified as one of the major accumulators of small mammal remains in several archaeological sites. Few studies were devoted to taphonomy in Pleistocene archaeological contexts in the Middle East, notably in Iran, Israel and Syria (Bazgir et al., 2017; Demirel et al., 2011; Maul et al., 2015; Smith et al., 2015). Most of the studies concluded that the origin of the accumulation was predation activity, mainly owls, but generally without any study of anatomical representation, bone breakage or digestion.

Regarding the postcranial fragmentation, most of our sample is intact, only 22.8% is fragmented mainly in the proximal part. The best-preserved bone in our Birecik is the femora. These values fit well with other *T. alba* assemblages, where around 80% is intact (Andrews, 1990).

Following the criteria established by Andrews (1990), our sample displays a good proportion of complete elements, corresponding to a category 1 predator, including *Tyto alba*.

Few studies (Dauphin and Denys, 1992; Denys et al., 1996, 1992) have analyzed the differences in the fragmentation in different prey taxa. We were able to analyse it using skulls and mandibles, because most of the post-cranial bones cannot be specifically identified here. Most of the skulls from *Mus musculus* and *Meriones tristami* are complete with a few skulls fragmented. This corresponds well with the data from Denys et al. (1996), which showed a better skull preservation in favor of more robust rodents like *Meriones* spp. and some Dipodidae. The comparison between both species is not well correlated because we only have 16 *Mus* against 115 *Meriones* remains. *Meriones* are medium size rodents, which bones are generally more resistant compared to those of smaller species such as *Mus*. There is no correlation between the size and the preservation, but we have personally seen that *Meriones* skulls are more resistant, as suggested by previous studies (Dauphin and Denys, 1992; Denys et al., 1996, 1992). On the contrary, the fact that we also found small species such as *Suncus etruscus*, indicates that shrews may also display a good resistance to fragmentation.

3.3. Environmental and climatic remarks

3.3.1. Climatic data

Redding (1978) pointed out that small vertebrates are more sensitive to the climatic changes than larger ones and are sources of more detailed and precise paleoenvironmental interpretations. Because predation can bias the faunistic composition of assemblages, it needs to be recognized before any direct paleoecological interpretation of the taxonomic list (Fernández-Jalvo et al., 2016). So, in the archaeological assemblages, the predator responsible for the accumulation should be identified as precisely as possible in order to identify potential bias of faunal and anatomical representation, and get a better picture of past environments and taphonomic history of the site (Demirel et al., 2011).

Barn owls have a restricted hunting area and are opportunistic predators, so their pellets represent a good picture of the relative availability of prey species, and their contents are good indicator for knowing the environment if applied to archaeological assemblages (Demirel et al., 2011).

Birecik is located in the Sanliurfa province, the centre of the Southeastern Anatolia. The altitude of the region is between 300 and 600 m above the sea level and has a semiarid Mediterranean climate. Annual mean temperature is 18.5 °C; the maximum mean temperature is 39 °C and the minimum mean temperature is 2.7 °C. Annual rainfall is about 458.1 mm and the precipitation regime is winter, spring, autumn, and summer. Birecik is characterised by a steppe vegetation (Vagif Atamov and Gulsefile, 2007).

For the climatic reconstruction we applied the *Bioclimatic model* directly based on the faunal list, in order to know if we could obtain the same results as the ones provided by the Vagif Atamov et al. (2007) and validate the methodology for South Anatolia.

Concerning the Birecik rodent assemblage, nine of the different climatic groups defined by Hernández-Fernández (2001) and Hernández-Fernández et al. (2007) are represented (Table 9).

We can observe that there is a relatively good correspondence between the estimated means values of the *Bioclimatic model* and the current temperatures and precipitation, considering the Standard Deviation. We obtain a mean annual temperature of 20.86° ±3.39 with the model against 18.5 °C according to meteorological surveys. Similarly, for the mean annual precipitation we found 432 mm in average, against 458 mm (Table 10).

3.3.2. Environmental data

The *Habitat Weighting* method, based on the habitat frequentation of represented species in the assemblage, where the value of 1 is divided between the habitats where it is possible to find the species at present (Table 11), indicates a steppe-like environment characterised by a vegetation dominated by shrubs and grass with low precipitation, which corresponds well to the environment found in Birecik today.

Mus musculus is highly adaptable and found in all environments, but *Meriones tristrami* is restricted only to habitat IV. *Nesokia indica* is also found in three different zones (II/III, III, IV, VII). Both taxa may be good palaeoenvironmental indicators in archaeological sites.

Nesokia indica and *Suncus etruscus* represent only 5% of the fauna, while*Mus musculus* represents 12,82% and *Meriones tristami* 82%, these two species making up 95% of the preys. *Habitat weighting* does not

consider the proportion of the species, just their presence/absence. Following the percentages obtained with the *Habitat weighting* model, the most represented environment is the Shrubland (vegetation dominated by shrubs) and Grassland (open area covered with grass), followed by desert. On the basis of this result, we can said that the *Habitat weighting* gives a good overview of the landscape in the region today (according to Vagif Atamov et al. 2007).

We have to keep in mind that *Meriones* are the major preys in this faunal assemblage, which indicates a favourable dry open environmental condition for gerbils (steppes). Following the *Bioclimatic model* the results combined with the *Habitat weighting*, support an steppe environment.

We can thus conclude that *Tyto alba* pellets from the region represent good proxies for reconstructing environments, and then it becomes possible to apply these inferences to the archaeological record in the Middle East.

4. Conclusions

This work presents the first combined taxonomic and taphonomic study of *Tyto alba* pellets in the Middle East. Our objective was to increase the modern referential for this predator in that region, to contribute to a better understanding of small vertebrate accumulations in archaeological sites in the Middle East and to test the use of owl pellets faunal lists as proxies for paleoenvironmental reconstructions.

We have identified *Suncus etruscus*, *Nesokia indica*, *Mus musculus* and *Meriones tristami* in our sample. Their current ecology, combined with the *Bioclimatic model* and the *Habitat weighting* methods, confirmed that the values obtained for the climate (temperatures and precipitations) and landscape reconstructions based on owl pellet assemblages are valid and applicable in archaeological context.

Such studies will serve as reference to better identify the origin of some fossil accumulation, before deposition and fossilization. The taphonomic study showed that our assemblage fits well with a predator category of light modification. Most skeletal elements are well preserved and unbroken, the mean bone representation reached 82% and more than 77% of our sample is intact. Around 22% of the total elements are digested, and the light moderate grade is dominant (83.5%). *Tyto alba* represents a major cause of small mammal accumulation in archaeological sites, especially in caves. However, it is not the only predator that can produce such accumulations.

The emphasis of this article has remained on the nature of the modifications, and geographic variation (or lack of it) from one part of the world to another, as we could see, the modifications in this region are the same as we can find in other parts of the world produced by *Tyto alba*. Further studies will allow to define the role and importance of avian predators and mammalian carnivores in the accumulations of small mammals in archaeological sites of the Middle East.

Acknowledgments

I. Rey-Rodriguez is beneficiary of PhD scholarship funded by the Erasmus Mundus Program (IDQP). J.M. López-García was supported by a Ramón y Cajal contract (RYC-2016-19386) with financial sponsor of the Spanish Ministry of Science, Innovation and Universities. SEM pictures have been taken on the *Plateforme de Microscopie Electronique du Muséum national d'Histoire naturelle*, thanks to Geraldine Toutirais for her help. J.F. Noblet must be thanked for providing us the owl pellets material. We also want to thank to the Editor Prof. Marcos Martinón-Torres and the anonymous reviewers for their comments and suggestions that improve the final version of the manuscript.

Appendix A. Supplementary data

Supplementary data to this article can be found online at https://doi.org/10.1016/j.jas.2019.105029.

References

Abi-said, M.R., Shehab, A.H., Amr, Z.S., 2014. Diet of the Barn Owl, pp. 109–112, 7.
Andrews, P., 1990. Owls, Caves and Fossils, Owls, Caves and Fossils. https://doi.org/10.2307/3889096.
Andrews, P., 2006. Taphonomic effects of faunal impoverishment and faunal mixing. Palaeogeogr. Palaeoclimatol. Palaeoecol. 241, 572–589. https://doi.org/10.1016/j.palaeo.2006.04.012.
Andrews, P., 2018. Seasonal Variation in Prey Composition and Digestion in Small Mammal Predator Assemblages 1–14. https://doi.org/10.1002/oa.2656.
Aulagnier, S., Hutterer, R., Jenkins, P., Bukhnikashvili, A., Kryštufek, B., Kock, D., 2017. Suncusetruscus. The IUCN Red List of Threatened Species 2017: e.T90389138A22288134. (Accessed 6 November 2018).
Bazgir, B., Ollé, A., Tumung, L., Becerra-Valdivia, L., Douka, K., Higham, T., Van Der Made, J., Picin, A., Saladié, P., López-Garciá, J.M., Blain, H.A., Allué, E., Fernández-Garciá, M., Rey-Rodríguez, I., Arceredillo, D., Bahrololoumi, F., Azimi, M., Otte, M., Carbonell, E., 2017. Understanding the emergence of modern humans and the disappearance of neanderthals: insights from kaldar cave (Khorramabad valley, western Iran). Sci. Rep. 7, 1–16. https://doi.org/10.1038/srep43460.
Blain, H.-A., Bailon, S., Cuenca-Bescós, G., 2008. The Early–Middle Pleistocene palaeoenvironmental change based on the squamate reptile and amphibian proxies at the Gran Dolina site, Atapuerca, Spain. Palaeogeogr. Palaeoclimatol. Palaeoecol. 261, 177–192. https://doi.org/10.1016/j.palaeo.2008.01.015.
Boitani, L., Molur, S., 2016. Nesokia Indica (Errata Version Published in 2017). The IUCN Red List of Threatened Species 2016: e.T14661A115123428. https://doi.org/10.2305/IUCN.UK.2016-3.RLTS.T14661A22410105.en. Downloaded on 23 April 2018.
Coşkun, Y., 1999. Morphological characteristics of Meriones tristrami Thomas, 1892 (rodentia: gerbillinae) from Diyarbakır, Turkey. Turk. J. Zool. 23, 345–355.
Darviche, D., Orth, A., Michaux, J., 2006. Mus spretus et M. musculus (Rodentia, Mammalia) en zone méditerranéenne: différenciation biométrique et morphologique: application à des fossiles marocains plé istocènes. Mammalia 70, 90–97. https://doi.org/10.1515/MAMM.2006.010.
Darvish, J., 2011. Morphological comparison of fourteen species of the genus Meriones Illiger , 1811 (Rodentia : gerbillinae) from Asia and North Africa. Iran. J. Anim. Biosyst. 7, 49–74.
Darvish, J., Ghiyasi, R., Khosravi, M., 2000. Recognition of rodents of Robat Sharaf pellets owl by morphological and neontological studies. J. Sci. 12.
Darvish, J., Mohammadi, Z., Mahmoudi, A., Siahsarvie, R., 2014. Faunistic and taxonomic study of Rodents from northwestern Iran. Iran. J. Anim. Biosyst. (IJAB) 10, 119–136.
Dauphin, Y., Denys, C., 1992. Diagenèse différentielle chez les rongeurs fossiles — validité des paramètres géochimiques pour les reconstitutions des régimes alimentaires. Palaeogeogr. Palaeoclimatol. Palaeoecol. 99, 213–223. https://doi.org/10.1016/0031-0182(92)90016-X.
Demirel, A., Andrews, P., Yalçinkaya, I., Ersoy, A., 2011. The taphonomy and palaeoenvironmental implications of the small mammals from Karain Cave, Turkey. J. Archaeol. Sci. 38, 3048–3059. https://doi.org/10.1016/j.jas.2011.07.003.
Denys, C., Patou-Mathis, M., 2014. Manuel de Taphonomie, Collection.
Denys, C., Kowalski, K., Dauphin, Y., 1992. Mechanical and chemical alterations of skeletal tissues in a recent Saharian accumulation of faeces from Vulpes rueppelli (Carnivora, Mammalia). Acta Zool. Cracov. 35, 265–283.
Denys, C., Dauphin, Y., Rzebik-Kowalska, B., Kowalski, K., 1996. Taphonomic study of Algerian owl pellet assemblages and differential preservation of some rodents: palaeontological implications. Acta Zool. Cracov. 39, 103–116.
Denys, C., Stoetzel, E., Andrews, P., Bailon, S., Rihane, A., Huchet, J.B., Fernandez-Jalvo, Y., Laroulandie, V., 2017. Taphonomy of Small Predators multi-taxa accumulations: palaeoecological implications. Hist. Biol. 2963, 1–14. https://doi.org/10.1080/08912963.2017.1347647.
Denys, C., Stoetzel, E., Andrews, P., Bailon, S., Rihane, A., Huchet, J.B., Fernandez-Jalvo, Y., Laroulandie, V., 2018. Taphonomy of Small Predators multi-taxa accumulations: palaeoecological implications. Hist. Biol. 30 (6), 868–881. https://doi.org/10.1080/08912963.2017.1347647.
Evans, E.M.N., Van Couvering, J.A.H., Andrews, P., 1981. Palaeoecology of Miocenesites in western Kenya. J. Hum. Evol. 10, 99–116.
Fernández-Jalvo, Y., Andrews, P., Denys, C., Sesé, C., Stoetzel, E., Marin-Monfort, D., Pesquero, D., 2016. Taphonomy for taxonomists: implications of predation in small mammal studies. Quat. Sci. Rev. 139, 138–157. https://doi.org/10.1016/j.quascirev.2016.03.016.
Fernández-Jalvo, Y., Andrews, P., Sevilla, P., Requejo, V., 2014. Digestion versus abrasion features in rodent bones. Lethaia 47, 323–336. https://doi.org/10.1111/let.12061.
Haddadian Shad, H., Darvish, J., Mohammadian, T., Mahmoudi, A., Alaie Kakhki, N., Ghanbarifardi, M., Molavi, F., Barani-Beiranvand, H., 2014. Preliminary study of rodents using pellets of predatory birds in Iran. Iran. J. Anim. Biosyst. 10, 36–50.
Hernández Fernández, M., 2001. Bioclimatic discriminant capacity of terrestrial mammal faunas. Glob. Ecol. Biogeogr. 10, 189–204. https://doi.org/10.1046/j.1466-822x.2001.00218.x.
Hernández Fernández, M., Álvarez Sierra, M.Á., Peláez-Campomanes, P., 2007. Bioclimatic analysis of rodent palaeofaunas reveals severe climatic changes in Southwestern Europe during the Plio-Pleistocene. Palaeogeogr. Palaeoclimatol. Palaeoecol. 251, 500–526. https://doi.org/10.1016/j.palaeo.2007.04.015.
Hernandez Fernández, M., Peláez-Campomanes, P., 2003. The bioclimatic model: A method of palaeoclimatic qualitative inference based on mammal associations. Glob. Ecol. Biogeogr. 12, 507–517. https://doi.org/10.1046/j.1466-822X.2003.00057.x.

Kopij, G., Liven-schulman, I., 2013. Zoology in the Middle East Diet of the Lesser Kestrel , Falco Naumanni , in Israel 7140. https://doi.org/10.1080/09397140.2012.10648914.

Kryštufek, B., Vohralík, V., 2001. Mammals of Turkey and Cyprus, Introduction, Check-List, Insectivora. Koper.

Kryštufek, B., Bukhnikashvili, A., Sozen, M., Isfendiyaroglu, S., 2017. Cricetulus migratorius. The IUCN Red List of Threatened Species 2016: e.T5528A115073390 8235.

Kryštufek, B., Vohralík, V., 2009. Mammals of Turkey and Cyprus, Rodentia II: Cricetinae, Muridae, Spalacidae, Calomyscidae, Capromyidae, Hystricidae, Castoridae. https://doi.org/10.1644/10-MAMM-R-221.1.

López-García, J.M., Blain, H.-A., Cuenca-Bescós, G., Alonso, C., Alonso, S., Vaquero, M., 2011. Small vertebrates (Amphibia, Squamata, Mammalia) from the late pleistocene-holocene of the valdavara-1 cave (Galicia, northwestern Spain). Geobios 44, 253–269. https://doi.org/10.1016/j.geobios.2010.10.001.

Mamkhair, I.H., Samara, F.F., Shehab, A.H., 2007. Morphological characteristics of the libyan jird, meriones libycus lichtenstein, 1823 (rodentia: gerbillinae), in Syria. Zool. Middle East 42, 37–46. https://doi.org/10.1080/09397140.2007.10638244.

Maul, L.C., Smith, K.T., Shenbrot, G., Bruch, A.A., Wegmüller, F., Le Tensorer, J.M., 2015. Microvertebrates from unit G/layer 17 of the archaeological site of Hummal (El Kowm, Central Syria): preliminary results. Anthropologie (France) 119, 676–686. https://doi.org/10.1016/j.anthro.2015.10.010.

Mikkola, H., 1983. Owls of Europe. T. &; A. D. Poyser, Carlton.

Musser, G., Hutterer, R., Kryštufek, B., Yigit, N., Mitsain, G., 2016. Mus musculus (errata version published in 2017). The IUCN Red List of Threatened Species 2016: e. T13972A115117618.

Momtazi, F., Darvish, J., Ghassemzadeh, F., Moghimi, A., 2008. Elliptic Fourier analysis on the tympanic bullae in three Meriones species (Rodentia, Mammalia): its application in biosystematics. Acta Zool. Cracov. 51A, 49–58. https://doi.org/10.3409/azc.51a.

Musser, G.C., Carleton, M.D., 2005. Superfamily muroidae. In: Wilson, D.E., Reeder, D.M. (Eds.), Mammal Species of the World. A Taxonomic and Geographic Reference. Baltimore, pp. 894–1531.

Obuch, J., Khaleghizadeh, A., 2012. Spatial Variation in the Diet of the Barn Owl Tyto alba in Iran, vol. 6, pp. 103–116.

Pavlinov, Igor Ya., 2008. A Review of Phylogeny and Classification of Gerbillinae (Mammalia:rodentia), Moscow Uni (Moscow).

Redding, W.R., 1978. Rodents and the archaeological palaeoenvironment: Considerations, problems and future. Approaches to faunal analysis in the Middle East. In: Meadow, R.H., Zeder, M.A. (Eds.), Harvard, Peabody Museum of Archaeology and Ethnology, 2. Peabody Museum Bulletin, pp. 63–68.

Shad, H., Kakhki, A., 2014. Preliminary study of rodents using pellets of predatory birds in Iran. Iran. J. Anim. Biosyst. 10, 36–50.

Shehab, A., Daoud, A., Kock, D., Amr, Z., 2013. Zoology in the Middle East Small mammals recovered from owl pellets from, p. 7140.

Shehab, A., Daoud, A., Kock, D., Amr, Z., 2013. Zoology in the Middle East Small Mammals Recovered from Owl Pellets from 7140. https://doi.org/10.1080/09397140.2004.10638061.

Siahsarvie, R., Darvish, J., 2008. Geometric morphometric analysis of Iranian wood mice of the genus Apodemus (Rodentia, Muridae). Mammalia 72, 109–115. https://doi.org/10.1515/MAMM.2008.020.

Smith, K.T., Christian, L., Flemming, F., Barkai, R., Gopher, A., 2015. The microvertebrates of Qesem Cave : a comparison of the two concentrations. Quat. Int. 1–13. https://doi.org/10.1016/j.quaint.2015.04.047.

Sozen, M., Bukhnikashvili, A., Shenbrot, G., Scott, D., Amori, G., Kryštufek, B., Yigit, N., Mitsain, G., 2016. Meriones tristrami (errata version published in 2017). The IUCN Red List of Threatened Species 2016: e.T13170A115110701.

Stoetzel, E., Marion, L., Nespoulet, R., El Hajraoui, M.A., Denys, C., 2011. Taphonomy and palaeoecology of the late Pleistocene to middle Holocene small mammal succession of El Harhoura 2 cave (Rabat-Témara, Morocco). J. Hum. Evol. 60, 1–33. https://doi.org/10.1016/j.jhevol.2010.07.016.

Stoetzel, E., Sime, W.B., Pleurdeau, D., Asrat, A., Assefa, Z., Desclaux, E., Denys, C., 2017. Preliminary study of the rodent assemblages of Goda Buticha: new insights on Late Quaternary environmental and cultural changes in southeastern Ethiopia. Quat. Int. https://doi.org/10.1016/j.quaint.2017.08.050.

Tez, C., 2000. Taxonomy and distribution of the white-toothed shrews (Crocidura) (Soricidae: Insectivora: Mammalia) of Turkey. Turk. J. Zool. 24, 365–374.

Vagif Atamov, M.A., Gulsefile, A., 2007. Flora of Mezra city (Birecik, SanliurfaTurkey). Asian J. Plant Sci. 6 (2), 225–238.

Yicit, N., Colak, M.S., 1996. Investigations on biology of Meriones crassus Sundevall, 1842 (Mammalia: Rodentia) in Turkey. Turk. J. Zool. 20, 211–215.

Palaeontologia Electronica
palaeo-electronica.org

Distinguishing between three modern *Ellobius* species (Rodentia, Mammalia) and identification of fossil *Ellobius* from Kaldar Cave (Iran) using geometric morphometric analyses of the first lower molar

Iván Rey-Rodríguez, Julie Arnaud, Juan-Manuel López-García, Emmanuelle Stoetzel, Christiane Denys, Raphaël Cornette, and Behrouz Bazgir

ABSTRACT

Ellobius remains are common and often abundant in southeastern Europe, western and central Asia archaeological sites. A correct identification of species is crucial for our understanding of the evolution of species and communities through time, including biostratigraphic sequences to be established.

This study applies geometric morphometric methods (GMM) to *Ellobius* first lower molars, with the objectives: 1) to discriminate modern species and explore morphological and size differences in reference samples; and 2) to identify fossil specimens recovered in archaeological sites, based on the aforementioned analysis. The reference dataset used in this paper includes specimens belonging to the three species that today occur in the southeastern Europe, western and central Asia: *Ellobius fuscocapillus*, *E. lutescens* and *E. talpinus.* The archaeological material comes from Late Pleistocene Iranian site of Kaldar Cave (Khorramabad valley, Lorestan Province, western Iran).

Our study shows that the shape of the anterior cap and the arrangement of the following triangles allow discriminating the three studied extant *Ellobius* species. The shapes of *E. fuscocapillus* and *E. lutescens* m1 appear rather similar, whereas *Ellobius talpinus* is well separated from these two species. The total length and the anterior cap of m1 in *E. fuscocapillus* is greater than in *Ellobius lutescens.*

The GMM analyses performed on the modern reference dataset allowed us to identify fossil specimens from Kaldar Cave as *Ellobius lutescens* and some as *E. fuscocapillus,* and excluding *E. talpinus*.

Iván Rey-Rodríguez. HNHP UMR 7194, CNRS / Muséum national d'Histoire naturelle / UPVD / Sorbonne

Rey-Rodríguez, Iván, Arnaud, Julie, López-García, Juan-Manuel, Stoetzel, Emmanuelle, Denys, Christiane, Cornette, Raphaël, and Bazgir, Behrouz. 2021. Distinguishing between three modern *Ellobius* species (Rodentia, Mammalia) and identification of fossil *Ellobius* from Kaldar Cave (Iran) using geometric morphometric analyses of the first lower molar. Palaeontologia Electronica, 24(1):a01. https://doi.org/10.26879/1122
palaeo-electronica.org/content/2021/3265-ellobius-and-gmm

Copyright: January 2021 Paleontological Society.
This is an open access article distributed under the terms of Attribution-NonCommercial-ShareAlike 4.0 International (CC BY-NC-SA 4.0), which permits users to copy and redistribute the material in any medium or format, provided it is not used for commercial purposes and the original author and source are credited, with indications if any changes are made.
creativecommons.org/licenses/by-nc-sa/4.0/

Universités, Musée de l'Homme, Palais de Chaillot, 17 place du Trocadéro, 75016 Paris, France. Sezione di Scienze Preistoriche e Antropologiche, Dipartimento di Studi Umanistici, Università degli Studi di Ferrara, C.so Ercole I d'Este, 32 - 44121 Ferrara, Italy. ivanreyrguez@gmail.com
Julie Arnaud. Sezione di Scienze Preistoriche e Antropologiche, Dipartimento di Studi Umanistici, Università degli Studi di Ferrara, C.so Ercole I d'Este, 32 - 44121 Ferrara, Italy. rndjmr@unife.it
Juan-Manuel López-García. Institut Català de Paleoecologia Humana i Evolució Social (IPHES). Zona Educacional 4, Campus Sescelades URV (Edifici W3) 43007 Tarragona, Spain. Área de Prehistòria, Universitat Rovira i Virgili. Facultat de Lletres, Avinguda Catalunya 35, 43002 Tarragona, Spain. jmlopez@iphes.cat
Emmanuelle Stoetzel. HNHP UMR 7194, CNRS / Muséum national d'Histoire naturelle / UPVD / Sorbonne Universités, Musée de l'Homme, Palais de Chaillot, 17 place du Trocadéro, 75016 Paris, France. emmanuelle.stoetzel@mnhn.fr
Christiane Denys. ISYEB UMR 7205, CNRS / Muséum national d'Histoire naturelle / UPMC / UA/ EPHE / Sorbonne Universités, Paris, France. christiane.denys@mnhn.fr
Raphaël Cornette. ISYEB UMR 7205, CNRS / Muséum national d'Histoire naturelle / UPMC / EPHE / Sorbonne Universités, Paris, France. raphael.cornette@mnhn.fr
Behrouz Bazgir. Área de Prehistòria, Universitat Rovira i Virgili. Facultat de Lletres, Avinguda Catalunya 35, 43002 Tarragona, Spain. behrouz.urv@gmail.com

Keywords: Rodentia; Arvicolinae; m1 shape; multivariate analysis; Pleistocene

Submission: 20 August 2020. Acceptance: 28 December 2020.

INTRODUCTION

This study focuses on three species of the vole genus *Ellobius* (Rodentia, Cricetidae, Arvicolinae) nowadays occurring in Iran, and on fossil material from Late Pleistocene Kaldar Cave site in the Zagros mountains. This region is a key area for human evolution and lies at the conjunction of potential migration routes between Africa, Europe and eastern Asia. A well-based characterization of the palaeoenvironmental context is crucial for a good understanding of human occupations (subsistence, cultural adaptations, site occupations, territory, and resource management, dispersal events, etc.). Small mammals may serve as good palaeoenvironmental and palaeoclimatic indicators of the surroundings of an archaeological site. Moreover, voles (arvicolines) in particular are commonly used in Quaternary biostratigraphy because of their rapid evolution and their abundance in the fossil record.

Ellobius is an interesting vole genus since its Pleistocene distribution reached North Africa (Stoetzel, 2013) and the southern Levant (Weissbrod and Weinstein-Evron, 2020), where it is absent now. Nowadays it occurs in southeastern Europe, western and central Asia (e.g., Rey-Rodríguez et al., 2020). It is often abundant in Middle Eastern archaeological sites, and has biostratigraphic potential for this region.

However, the identification of fossil *Ellobius* material is not yet elaborated satisfactory. The identification of most *Ellobius* specimens in museums collections is based on criteria which is usually not applicable to fragmented fossil material. Previous studies on *Ellobius* have mainly focused on chromosomes (Romanenko et al., 2007, 2018, 2020; Coşkun, 2016) and species discrimination based on external characters, not applicable to fossils (Gharkheloo, 2003; Kryštufek and Vohralík, 2009; Tesakov, 2016). In the archaeological literature, taxonomic attributions are often restricted to *Ellobius* sp. (e.g., Maul et al., 2015; Weissbrod and Weinstein-Evron, 2020).

The most common and diagnostic element in fossil vole samples are the teeth, in particular the first lower molars (m1). However, in *Ellobius* m1s morphological differences are hard to find, and there are apparently broad overlaps between the species (Maul et al., 2015; Kandel et al., 2017; Weissbrod et al., 2017).

With the geometric morphometric methods (GMM), fine morphological differences can be detected and variations in shape and size can be quantified, which would have been undetectable by conventional approaches, such as linear measurements or morphotype scores (Adams et al., 2009; Kaya et al., 2018). Previous GMM analyses of various fossil rodent groups (e.g., *Microtus* spp. Cucchi et al., 2014; Luzi et al., 2019; *Meriones* spp.

Stoetzel et al., 2017; and *Rattus* spp. Hulme-Beaman et al., 2018) provided more comprehensive identifications compared to conventional investigations.

The purpose of this study is to investigate morphological and size differences between three species of the genus *Ellobius* from Iran and to apply the results to specimens of the archaeological site of Kaldar Cave. With this article we hope to demonstrate the potential of the GMM approach to the *Ellobius* genus and discuss its use in combination with other morphological criteria.

THE GENUS *ELLOBIUS* FISCHER, 1814

Distribution and Ecological Remarks of the Extant *Ellobius* Species

Nowadays, the genus *Ellobius* Fischer, 1814, occurs in southeast Europe, western and central Asia with five species (Coşkun, 2001, 2016; Wilson et al., 2017, Kaya et al., 2018): *E. talpinus* (Pallas, 1770), *E. tancrei* Blasius, 1884, *E. alaicus* Vorontsov et al., 1969, *E. fuscocapillus* (Blyth, 1843) and *E. lutescens* Thomas, 1897. These fossorial species inhabit steppes, grasslands and semi-deserts, and are highly adapted to subterranean life (Kryštufek and Vohralík, 2009; Coşkun, 2016).

In Iran, where the Kaldar Cave is located and the fossil material under study come from, *Ellobius* is currently represented by *E. lutescens*, *E. fuscocapillus* and *E. talpinus* (Gharkheloo, 2003; Firouz, 2005; Kryštufek and Vohralík, 2009; Kryštufek and Shenbrot, 2016; Rusin, 2017).

Ellobius lutescens (western mole vole) is distributed in northwestern Iran, Iraq, Azerbaijan, Armenia and eastern Anatolia (Thomas, 1905; Ellerman and Morrison-Scott, 1951; Darlington, 1957; Osborn, 1962; Walker, 1964; Lay, 1967; Hassinger, 1973; Roberts, 1977; Corbet, 1978; Corbet and Hill, 1991; Coşkun, 1997; Nowak, 1999; Wilson and Reeder, 2005; Kryštufek and Shenbrot, 2016; Wilson et al., 2017). In Iran, this species is found in mountain grasslands, sandy semi-deserts and steppe areas (Kryštufek and Shenbrot, 2016; Tesakov, 2016).

Ellobius fuscocapillus (southern mole vole) shows a range across northeastern Iran, Turkmenistan, Afghanistan and Pakistan. In Iran it is found in open steppes with loose soil (Gharkheloo, 2003; Shenbrot et al., 2016).

Ellobius talpinus (northern mole vole) is distributed in southeastern Ukraine and Russia, Kazakhstan, Uzbekistan, Turkmenistan and in the small part of northern Iran. Its habitat requirements are similar to that of *Ellobius lutescens* (Rusin, 2017).

The geographical areas occupied by the three species show differences in mean annual temperatures and precipitations (Table 1). *Ellobius talpinus* is found in regions with drier conditions and lower maximum annual temperature than that of the other two species. The geographic ranges of *E. fuscocapillus* and *E. lutescens* display similar temperatures, but *E. fuscocapillus* occurs in wetter environments. All the temperatures and precipitation levels are estimations, consistent with the above-described type of habitat. However, since their subterranean life makes them relatively insensitive to high variations in surface temperatures and precipitations, we can consider that all three species have essentially the same habitat requirements. What can make differences is the resulting vegetation cover, which is of course important for the survival of the animals. But all what we can assume in the current state of knowledge is that the *Ellobius* species provide significant information as indicators for steppe environments. Further studies are needed to evaluate more precisely the potential of the different *Ellobius* species as palaeoenvironmental and palaeoclimatic indicators.

Fossil Record of *Ellobius*

Arvicolines are commonly used in Quaternary biostratigraphy because of their rapid evolution and their abundance in the fossil record. The genus *Ellobius* may represent a crucial biostratigraphic yardstick in the Zagros mountain range, which marks the western limits of its extant distribution range in the western Asia (Weissbrod and Weinstein-Evron, 2020). However, the palaeobiogeographic and stratigraphic range of the genus in this region is still debated.

TABLE 1. Ranges of month precipitations and mean annual temperatures within the geographic distribution area of various *Ellobius* species (https://eol.org/).

	Temperature (Max/Min)	Precipitation (mm per month)
E. fuscocapillus	11.62/ 0.1°C	36.01
E. lutescens	10.79/ 0.1°C	28.17
E. talpinus	4.75 /0.1°C	24.94

Remains of cf. *Ellobius* have been reported in early Pliocene (Ruscinian) sites in Kotovka, Odessa in the Ukraine (Nesin and Nadachowski,

2001), and in two late Pliocene (Late Villanyian) sites, in the west of Ukraine and in Rivoli Veronese, northeastern Italy (Sala et al., 1994). However, Tesakov (1998) believes that the *Ellobius* record from Italy belongs to *Ungaromys dehmi*.

According to several authors (compiled in Topachevsky and Rekovets, 1982; Maul and Markova, 2007; Tesakov, 2016), there was a succession of several *Ellobius* species during the early Pleistocene in Eastern Europe: *E. paleotalpinus, E. melitopoliensis, E. primigenis, E. lakhutensis, E. tauricus, E. kujalnikensis* and *E. tarchancutensis*. The morphology of *E. tarchancutensis* suggests that it could be the ancestor of *E. lutescens* (Topachevsky and Rekovets, 1982; Tesakov, 2016).

In western Asia, *Ellobius* has been recognized in several Middle Pleistocene archaeological sites in Sel'-Ungur in Kyrgyzstan (*Ellobius* ex gr. *tancrei*; Markova, 1992), in Hummal layer G in Syria (*Ellobius* sp.; Maul et al., 2015), Azokh-1 units Vm, Vu, III, II/III, II (*Ellobius* sp.; Fernández-Jalvo, 2016) in Nagorno Karabakh and Krasarin (*Ellobius (Bramus) pomeli;* Tesakov, 2016).

During the Middle Pleistocene, *Ellobius* extended its range westwards to Israel, Tabun C and D (Bate, 1937; Frumkin and Comay, in press), Misliya Cave (Weissbrod and Weinstein-Evron, 2020) and North Africa as far as to the Moroccan Atlantic coast (Jaeger, 1988; Stoetzel, 2013). It probably arrived there from western Asia via the Libyco-Egyptian route during a cooling and aridification of North Africa favouring the development of steppes at the beginning of the Middle Pleistocene (Stoetzel, 2013). The North African species then evolved independently from the Asian ones, through the succession of *E. africanus, E. atlanticus, E. barbarus* and *E. zimae* (Jaeger, 1988). In most studies, it is concluded that *Ellobius*, outside its current range, disappeared at the end of the Middle Pleistocene at the latest (Stoetzel, 2013; Maul et al., 2015; Weissbrod and Weinstein-Evron, 2020).

In the Late Pleistocene, *Ellobius trancrei* has been described from the Mousterian site of Ogzy-Kichik, Tadzhikistan (Markova, 1992). The modern species *E. lutescens* was found in Iraq (Bate, 1930) in the layers of Hazar Merd, dated to 25,000 years ago (Coşkun, 2016). Hashemi et al. (2006) noted that remains of *E. lutescens* have been found in several Late Pleistocene and early Holocene sites in western and northwestern Iran: Kani Mikaeil (Kordestan), Qalaloun near Kouhdasht, Yafteh Gar, and Arjeneh near Khoramabad (Lorestan). *Ellobius lutescens* has also been documented in Upper Palaeolithic and Neolithic units of Dzudzuana Cave (Georgia, 34.4-6 ka cal BP; Belmaker et al., 2016), and also in Aghitu-3 level VII (Armenia, Upper Palaeolithic, 39-36 ka cal BP; Kandel et al., 2017). *Ellobius* sp. has been described in Azokh-1 unit I (157 ± 26 ka BP) and in the Holocene site Azokh-5 (Nagorno Karabakh, Parfitt, 2016).

Description of Tooth Morphology

We restricted our analysis to the first lower molar, the most diagnostic tooth in arvicolines. The *Ellobius* lower m1 is composed of the anterior cap (AC), five triangles (T) with three buccal (BRA) and four lingual (LRA) re-entrant angles, and one posterior lobe (PL) (Figure 1A). *Ellobius* molars are notably characterized by broadly confluent triangles, and the presence of roots that are visible in adult and old individuals (Figure 1B). Moreover, *Ellobius* molars lack cement in the re-entrant angles (Coşkun, 2016).

For modern representatives, the skull morphology (Kaya et al., 2018) and external characters (Kryštufek and Vohralík, 2009) contain the main diagnostic features, whereas fossil samples mostly consist of isolated molars or broken jaws. The occlusal morphology of the lower m1 is rather similar in the various *Ellobius* species (especially the three Iranian species *E. fuscocapillus*, *E. lutescens* and *E. talpinus*). However, some specific morphological characters have been pointed out in previous studies: the AC is broad in *Ellobius lutescens*, narrow in *Ellobius talpinus* and elongated in *Ellobius fuscocapillus* (Maul et al., 2015); the distance between T4 and T5 (W) and the total length (L) differ between the species, *Ellobius fuscocapillus* showing the largest teeth and *Ellobius talpinus* the smallest (Rey-Rodríguez et al., 2020). However, these varying morphological and biometric characters are not always clear nor reliable distinction is possible.

MATERIAL AND METHODS

Modern and Fossil Material Studied

For this study we compared modern reference collections and fossil material of *Ellobius* using dental morphometric markers, because teeth represent the most abundant and diagnostic elements in fossil assemblages (Stoetzel et al., 2017). A total of 111 first lower molars (m1s) were measured. In our analysis, we took into account the individual age of the specimens using the classification of

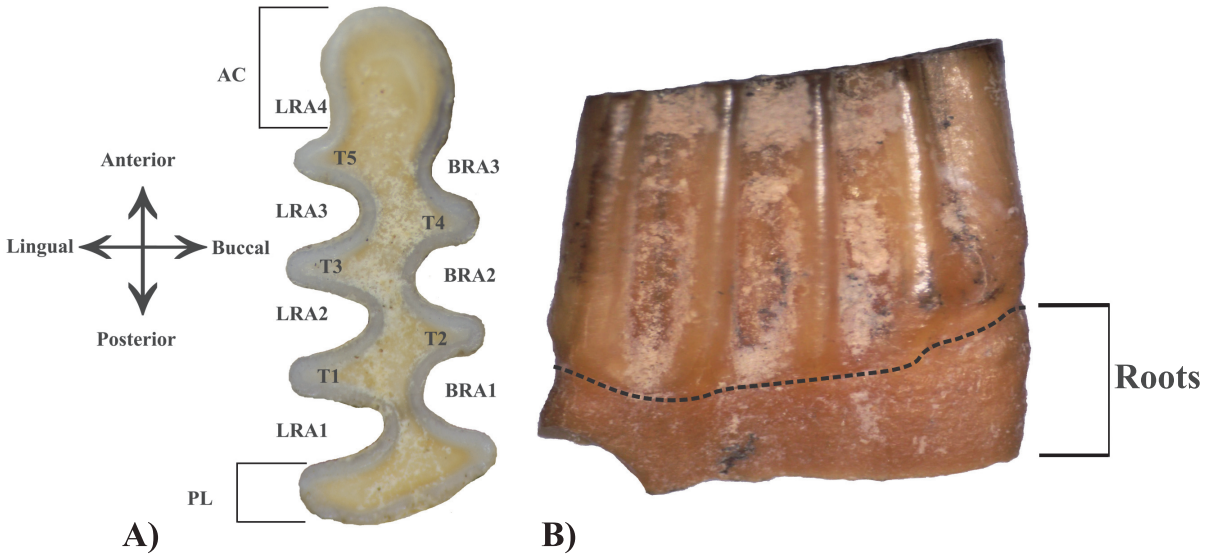


FIGURE 1. A) Occlusal surface of *Ellobius* right lower m1: triangle (T); buccal re-entrant angle (BRA); lingual re-entrant angle (LRA); anterior cap (AC); posterior lobe (PL); **B)** Lingual view of left lower m1.

Coşkun (2016). We observed a striking difference in the occlusal pattern between young and old individuals, so we only used adult individuals, in order to avoid any bias (Stoetzel et al., 2017). Damaged and/or digested molars were not considered. In the reference collections, both males and females were used because no significant sexual dimorphism is known for *Ellobius* (Gharkheloo, 2003). Figure 2 shows the most frequent morphotypes of the three extant and fossil analysed species.

We used specimens from the modern reference collections of the Natural History Museum of London (NHM), the Field Museum of Chicago (FM) and the American Museum of Natural History of New York (AMNH) (Table 2); all the specimens were captured in the field, not bred in captivity.

The archaeological samples come from the Iranian site of Kaldar Cave (Table 2), located in the Zagros Mountains, in the northern part of Khorramabad Valley, Lorestan Province, western Iran (Becerra-Valdivia et al., 2017) (Figure 3). The material is hosted at the Institut Català de Paleoecologia Humana i Evolució Social (IPHES, Tarragona, Spain). More information on the archaeological context and the discoveries from this site can be found in Bazgir et al (2014, 2017) and Rey-Rodríguez et al. (2020).

The study material comes from Layer 5 (attributed to the Middle Palaeolithic) and Layer 4 (attributed to the Upper Palaeolithic) (Bazgir et al., 2014, 2017; Rey-Rodríguez et al., 2020). A total of 264 minimum number of individuals were identified from the small-mammal assemblages of Kaldar Cave. Layers 4 and 5 are dominated by *Microtus* spp. (60 individuals in Layer 4 and 79 in Layer 5), followed by *Ellobius* spp. (18 individuals in Layer 4 and 17 in Layer 5) and *Meriones* cf. *persicus* (17 individuals in Layer 4 and 18 in Layer 5). Other species were found in lesser proportions: *Chionomys nivalis*, *Cricetulus migratorius*, *Mesocricetus brandti*, *Allactaga* sp., *Myomimus* sp. These species indicate that the environment in the area was mainly composed of open dry and steppe areas. However, we also found *Apodemus* sp. which are related rather to a dense vegetation cover (including trees/bush), as well as few remains of *Mus* cf. *musculus* in both Layers 4 and 5. In this cave, there are also other levels, as Layers 1-3, that did not yield enough material to draw palaeoclimatic inferences (MNI < 30). All the species identified at Kaldar Cave still occur in the area today (Rey-Rodríguez et al., 2020).

Small-mammal remains were collected in the field by water screening, using superimposed 5 and 0.5-mm mesh screens. In subsequent years (2018, 2019), the sediment was sorted by hand and under microscope in order to identify and count the small-mammal elements and extract *Ellobius* remains for the present study.

Data Acquisition

The *Ellobius* lower molars were all photographed under constant conditions with a digital camera (Canon EOS 700D) coupled with a binocu-

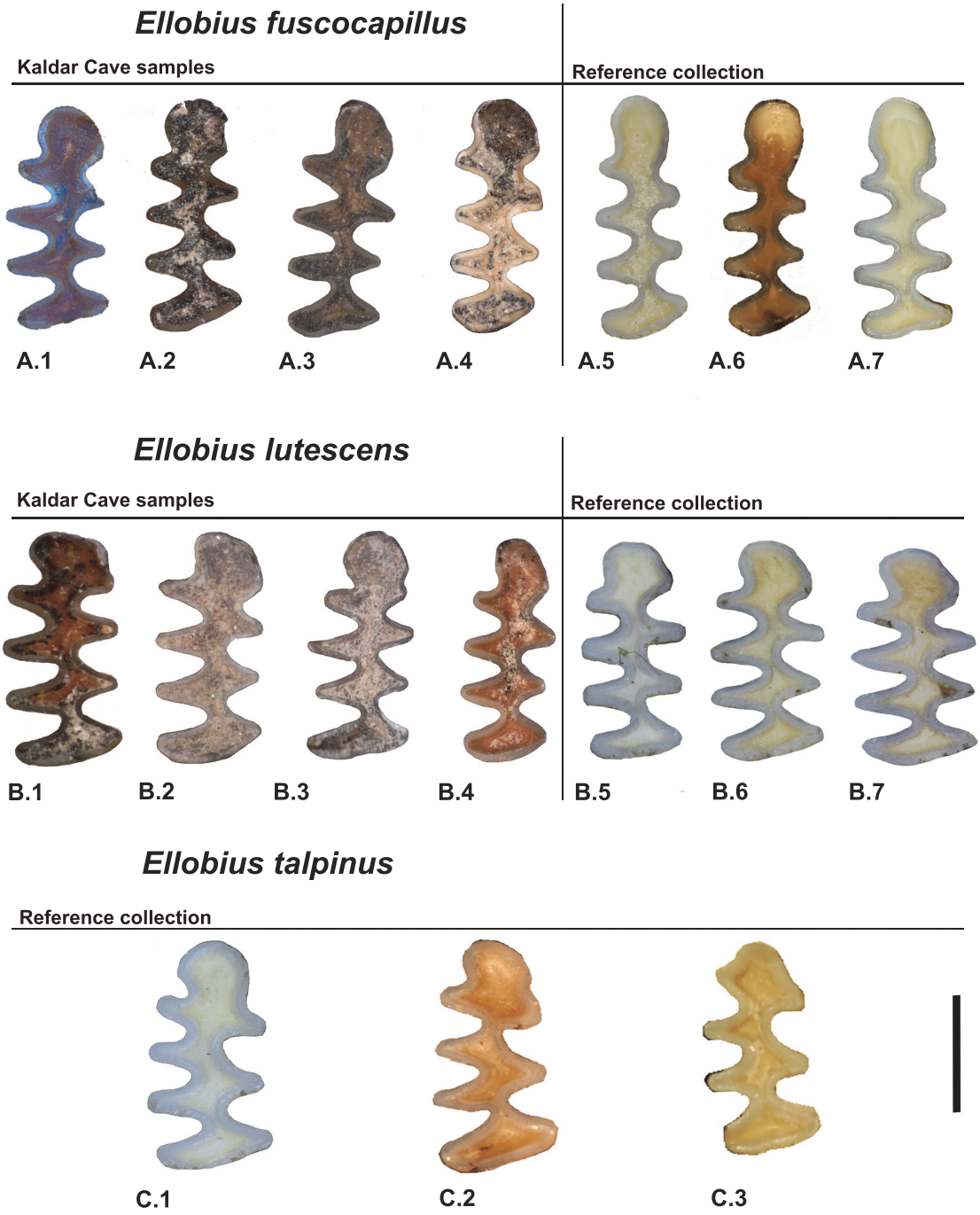


FIGURE 2. *Ellobius* lower m1s (all figured as right ones) from the extant reference collections and Kaldar Cave. **A)** *Ellobius fuscocapillus:* A.1-Kaldar Cave, 2014/4/SL5II/E6/125-130, right lower m1, number 157. A.2-Kaldar Cave, 2014/4/SL5/E5/109-111, right lower m1, number 520. A.3-Kaldar Cave, 2014/5/SL7II/E7/170-180, right lower m1, number 104. A.4- Kaldar Cave, 2014/5/SL7II/F6/135-145, right lower m1, number 547.A.5-modern, NHM86101513, Afghanistan, right lower m1. A.6-modern, FM111846, Iran, right lower m1. A.7-modern, NHM86101512, Afghanistan, right lower m1; **B)** *Ellobius lutescens:* B.1-Kaldar Cave, 2014/5/SL7II/F6/130-140, right lower m1, number 319. B.2-Kaldar Cave, 2014/4/SL5II/F7/115-118, right lower m1, number 90. B.3- Kaldar Cave, 2014/4/SL5II/F7/115-118, right lower m1, number 91. B.4- Kaldar Cave, 2014/5/SL7II/E7/145-150, right lower m1, number 436. B.5-modern, NMH916416, Turkey, right lower m1. B.6-modern, NMH916414, Turkey, right lower m1. B.7-modern, NMH916412, Turkey, right lower m1; **C)** *Ellobius talpinus:* C.1-modern, NHM3421126, Russia, right lower m1. C.2-modern, FM103163, Afghanistan, right lower m1. C.3-modern, AMNH59797, Mongolia, right lower m1. Scale 1 mm.

TABLE 2. Modern reference collection for each museum specimen. Natural History Museum of London (NHM), Field Museum of Chicago (FM) and American Museum of Natural History of New York (AMNH). Archaeological specimens from Kaldar Cave, MP = Middle Palaeolithic, UP = Upper Palaeolithic.

Reference collection				
Right lower m1	**NHM**	**AMNH**	**FM**	**Total**
Ellobius fuscocapillus	6	-	34	40
Ellobius lutescens	6	-	-	6
Ellobius talpinus	7	11	20	38
Total	**19**	**11**	**54**	**84**
Kaldar Cave				
Right lower m1	**Level 5(MP)**		**Level 4(UP)**	**Total**
Ellobius fuscocapillus	1		1	2
Ellobius lutescens	6		2	8
Total	**7**		**3**	**10**
Left lower m1	**Level 5(MP)**		**Level 4(UP)**	**Total**
Ellobius fuscocapillus	4		2	6
Ellobius lutescens	4		7	11

lar microscope (Leica M125). All the pictures of the first lower molars were taken in occlusal view, and right molars were used; when they were not available (only in the fossil material), the left lower molars were used and successively mirrored before the positioning of the landmarks and semi-landmarks. A scale bar was included in all the photographs in order to facilitate the extraction of a scaling factor, which can be used to estimate the centroid size (Tabatabaei Yazdi and Alhajeri, 2018). We took into account the lateral side for the age classification.

To investigate the first lower molar size and shape we combined two-dimensional (2D) landmarks (LM) and semi-landmarks (SLM) on the photographs using TPSdig2 v.2.32 software package (Rohlf, 2016) for 2D geometric morphometric analyses (we include our data on a TPS file, Appendix 1). The methodology was adapted from the previous studies of Klenovšek and Kryštufek (2013), Cucchi et al. (2014, 2017), Cornette et al. (2015), Maul et al. (2015), Kryštufek et al. (2016), Stoetzel et al. (2017) and Dianat et al. (2017, 2020).

Fourteen landmarks were placed at the maximum curvature on the salient and re-entrant lingual and buccal angles, on the posterior lobe and the anterior cap, where the landmarks were positioned on the outline (Figure 4A).

In order to characterize the size and shape of the anterior cap, 60 equidistant semi-landmarks



FIGURE 3. A) Kaldar Cave location. **B)** Entrance from the south of Kaldar Cave.

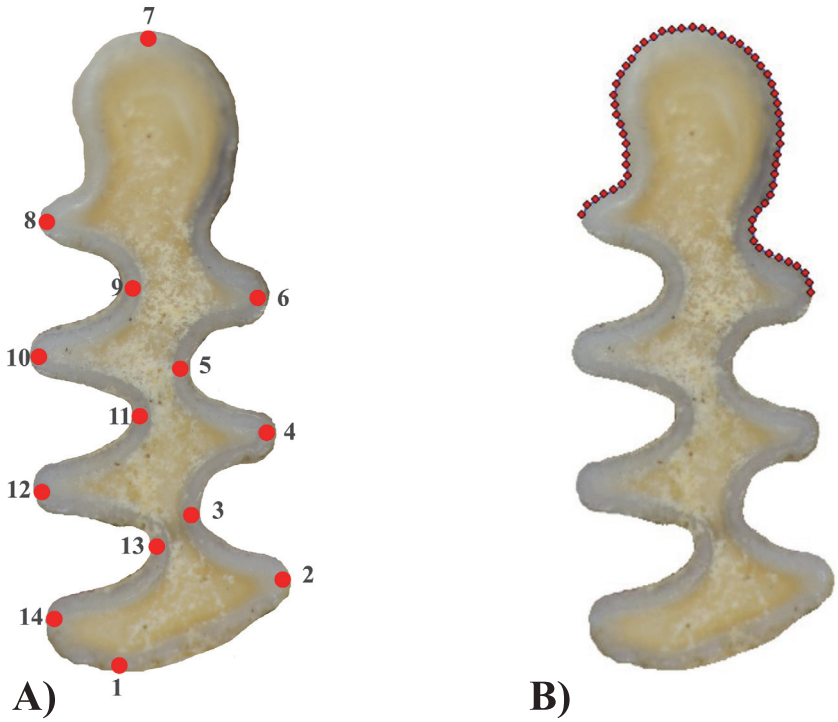


FIGURE 4. *Ellobius* right lower m1. **A)** 14 landmarks: Landmarks on the outermost turning point of buccal (2, 4, 6) and lingual (8, 10, 12, 14) salient angles, and on the innermost turning point of buccal (3, 5) and lingual (9, 11, 13) re-entrant angle. **B)** 60 semi-landmarks on the anterior cap.

were automatically positioned along the curve corresponding to the external outline of the tooth enamel from buccal salient angle 3 to lingual salient angle 4 (Figure 4B).

To test the repeatability of the procedure, we re-digitized the set of landmarks and semi-landmarks 10 times on three randomly selected teeth. We estimate the measurement error on this new set of variables from the Procrustes ANOVA mean squares following the method proposed by Fruciano (2016). The procedure has been retained highly repeatable (R=0.97).

Shape Analyses

All the following analyses were performed with R (R Core Team, 2020) using the Geomorph (Adams et al., 2020) and Morpho (Schlager, 2017) packages.

Before undertaking the statistical analysis, the 2D landmark and semi-landmark coordinates were scaled through a general Procrustes analysis (GPA), allowing the semi-landmarks to slide along the outline (Gunz and Mitteroecker, 2013). A principal component analysis (PCA) was then performed on the new normalized landmark and semi-landmark coordinates of the reference collection. Archaeological specimens were added *a posteriori* as supplementary individuals in the PCA shape space. A canonical variate analysis (CVA) was then performed on the PC scores, keeping 90 % of the overall shape variation (Baylac and Frieß, 2006). To assess the classification accuracy, a cross-validation test was performed on the CVA scores. Finally, the allometric effect was investigated through univariate and multivariate linear regression of the PC scores on the log of the centroid size.

RESULTS

The PCA (Table 3) performed on the normalized landmarks and sliding semi-landmarks of the first lower molar reveals significant differences between the analysed species, the first two principal components (PCs) account for 52.7% of the total variance (Figure 5). Component 3 was also analysed but the variance was too low, and there was no differentiation between the species. We included the complete table with all statistical data in Appendix 2.

The main variation along the PC1 (38.2%) regards the morphology of the Anterior Cap, which is more flattened for the positive values and more

TABLE 3. Contribution of the first 10th PCs to the total variance (%). PCA: principal component analysis.

PC	PC1	PC2	PC3	PC4	PC5	PC6	PC7	PC8	PC9	PC10
%	38.2	14.5	8.1	6.9	4.2	2.8	2.6	2.2	1.6	1.5

rounded for the negatives ones. *Ellobius talpinus* occur on the positive part of the PC1 axis while *E. fuscopapillus* and *E. lutescens* are located on the negatives ones reflecting a broader and more rounded AC. Along the PC2 (14.5%) scores, the positive values show an AC elongated and pronounced on the buccal side, negative values display a more rounded AC with a clear constriction between BRA3 and LRA4. On PC2 there is not a clear differentiation between the three species. However, *E. lutescens* specimens are located principally in the upper half of the *E. fuscocapillus* and *lutescens* cloud, with positive PC2 values.

The shape of *Ellobius talpinus* with narrower AC (Figure 5) is significantly different from that of *E. fuscocapillus* and *lutescens,* which appear morphologically very close one to another. The Kaldar Cave specimens are well distributed in the cloud of *E. lutescens* and *E. fuscocapillus,* with all of them having negative PC1 values. We can conclude that *Ellobius talpinus* is not present in the archaeological sample.

In order to estimate possible allometric effects on the samples, we performed a linear regression of the PCs onto the log of the centroid size (following the approach of Mitteroecker et al., 2015). Only PC1 shows a significant correlation with size (R2 =

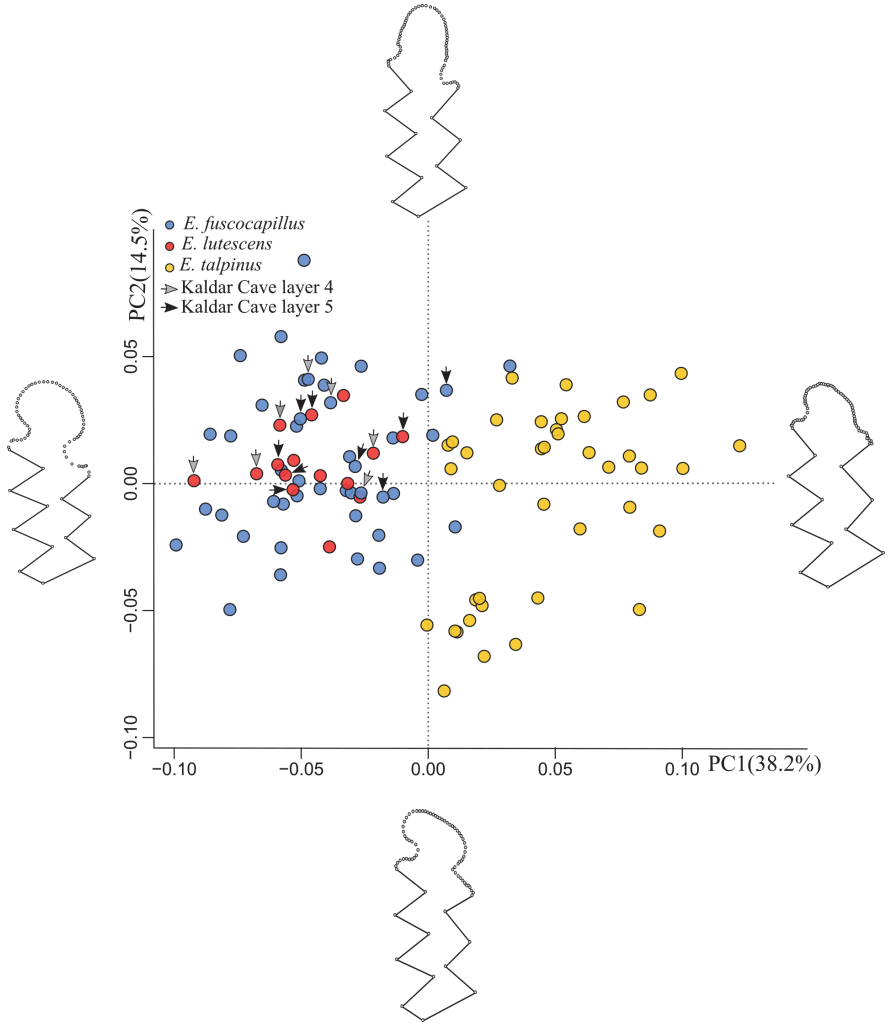


FIGURE 5. Principal component analysis on the normalized landmarks and sliding semilandmarks and shape configuration at the extreme ends of the two first PCs.

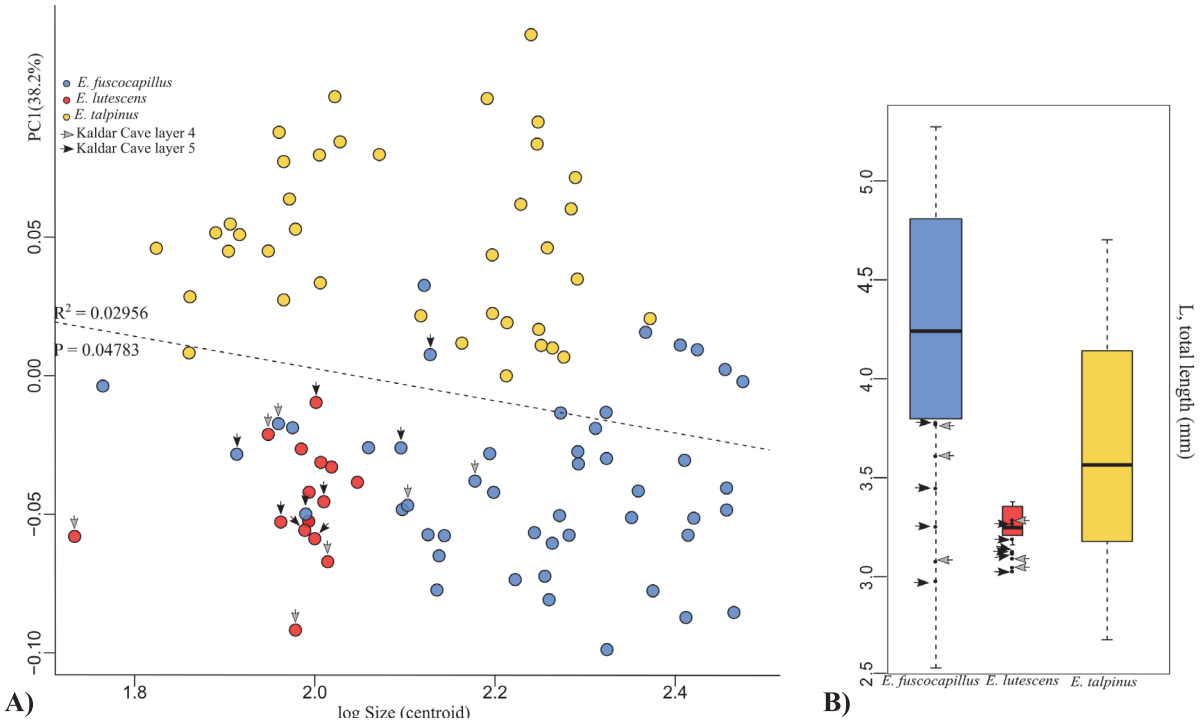


FIGURE 6. A) First two PCs from the Principal component analysis performed on the size and shape including the reference collection and Kaldar Cave material. **B)** Boxplot of the total length of *Ellobius* from the extant reference collections and Kaldar Cave.

0.02956, p=0.04783). In this graph (Figure 6A), it is possible to discriminate *Ellobius lutescens* from *E. fuscocapillus*, the latter showing larger dimensions. *E. talpinus* presents a wide size range overlapping the ranges of the two latter (Figure 6). The archaeological remains are placed again in the cloud of *E. lutescens* and *E. fuscocapillus* but with some ambiguous identifications. We have also evidenced this confusion in the reference dataset with three *E. fuscocapillus* individuals from the Field Museum that were replaced among *E. lutescens* in our analysis, indicating a possible misidentification of the museum specimens. On Figure 6B, Kaldar Cave fossil specimens appear in general smaller than the reference specimens, but inside the standard deviation.

The canonical variate analysis of 90% of the total variation (PCs1 to 16) in the sample and the relative cross-validation procedure give an overall classification accuracy of 86 % (with almost 100% correct classification for *Ellobius talpinus*) (Table 4).

DISCUSSION

Our results indicate that it is possible to accurately identify *Ellobius* species by applying GMM to m1 shape and size. The main differences between species concern the AC shape, the size and the general disposition of the triangles.

One result of the performed GMM is that the shape of *Ellobius fuscocapillus* and *E. lutescens* clusters in one cloud, and *E. talpinus* in another. This is in agreement with the distinction of two clades among the genus *Ellobius*: the subgenus *Bramus* Pomel, 1892 (with *E. fuscocapillus* Blyth, 1843, and *E. lutescens* Thomas, 1897) and the subgenus *Ellobius* Fischer, 1814 (with *E. talpinus*

TABLE 4. Cross-validated classification results in frequencies and %.

	E. fuscocapillus		*E. lutescens*		*E. talpinus*		None	
Taxon	**N**	**%**	**N**	**%**	**N**	**%**	**N**	**%**
E. fuscocapillus	37	78.72	10	21.27	0	-	0	-
E. lutescens	2	13,33	13	86.66	0	-	0	-
E. talpinus	0	-	0	-	36	94.73	2	5.26

Pallas, 1770; *E. tancrei* Blasius, 1884; and *E. alaicus* Vorontsov et al. 1969) (Carleton and Musser, 2005).

The shape differences between *Ellobius fuscocapillus* and *E. lutescens* is grossly in agreement with some earlier considerations based on conventional methods. Previously, Maul et al. (2015) considered the AC shape as a discriminant criteria, being broad in *Ellobius lutescens*, narrow in *Ellobius talpinus* and elongated in *Ellobius fuscocapillus*. Tesakov (2016) found that the size of *E. lutescens* is slightly smaller than *E. fuscocapillus*. Rey-Rodríguez et al. (2020) reported that the confluence between T4 and T5 differs among the species, with T1-T2 and T3-T4 being slightly less pairwise opposed in *E. lutescens*.

Our GMM analyses allowed these previously examined criteria to be assessed all together, in taking into account the size, the morphology of the AC and the general disposition of the triangles. In our fossil samples many teeth are fragmented, and could not have been included in our GMM. However, it could be possible to consider fragments of *Ellobius* m1s in further analyses, for example by focusing only on the shape of the anterior cap.

Sliding Semi-Landmarks and Anatomical Landmarks Compared with Previous Systematic Methods of *Ellobius* Identification

Despite classic methods enable to distinguish between many m1s of some of the species, a throughout discrimination remains unclear. According to Maul et al. (2015), morphological features of the AC (without performing GMM analyses) would be enough to permit species identification, and especially to differentiate *Ellobius talpinus* from *Ellobius lutescens* and *fuscocapillus*, because *Ellobius talpinus* has a less developed and narrower AC than in the other two species. But in the present study, we have seen that there is a morphological overlap between *E. lutescens* and *E. fuscocapillus*. So, while *"classic"* morphological criteria often result in unclear features or overlaps between species, our GMM analysis of *Ellobius* m1 allowed two groups to be accurately differentiated, *Ellobius talpinus* on the one hand and *Ellobius lutescens* and *fuscocapillus* on the other. The distinction between these two latter species is more complex, and indeed no straightforward grouping was observed with the first PCA (Figure 5). However, morphological differences between them could have been detected by comparing the mean shapes of their m1s (Figure 7) and by including the size parameter (Figure 6).

Figure 7 shows the means (dots) and variations (arrows) of the different landmarks and semi-landmarks between *Ellobius fuscocapillus* and *E. lutescens.* Major morphological differences are seen in points 1 (posterior lobe), 3, 4, 5 and 6 (BRAs and BSAs). This means that T1-T2 and T3-T4 are less parallel in *E. lutescens* than in *E. fuscocapillus,* as observed in the buccal part. Rey-Rodríguez et al. (2020) proposed that the width between T4 and T5 (W) and the total length (L) of the two species are different. The configuration of the AC shows that the transition between T4-T5 is narrower in *E. lutescens* than in *E. fuscocapillus,* which generates a smaller and more closed AC in *E. lutescens* than in *E. fuscocapillus*, in accordance with the observations of Maul et al. (2015). Finally, also the previous observation of Tesakov (2016) is confirmed that size is a valid criterion for distinguishing *Ellobius fuscocapillus* (larger) and *Ellobius lutescens* (smaller).

Combining shape and size allowed us identifying the fossil *Ellobius* m1s from Kaldar Cave. The morphology of the AC, the size and the W (width between T4 and T5) are valid criteria in most of the cases, but we have seen that GMM analyses allowed them all to be combined and a number of previous identifications to be re-analysed (Bazgir et al., 2014, 2017; Rey-Rodríguez et al., 2020). The results of the present analysis allowed some *E. lutescens* from the archaeological material to be re-assigned to *E. fuscocapillus* (five *E. fuscocapillus*, three from Layer 4 and two from Layer 5 were re- assigned). These misclassifications were due to the fact that *E. fuscocapillus* and *E. lutescens* are quite similar from a morphological point of view, and because the previous identifications were based on the W, L and the AC, subjected to overlapping problems, which have subsequently been clarified with the GMM.

In this study we have not seen morphological differences between specimens from Layer 4 and 5. As we are working in an archaeological site, the fact that we have two species in the same levels does not mean that they were deposited at the same time. Layer 4 has a chronological range of 54,400–46,050 cal BP at the bottom and 23,100 ± 3,300 to 29,400 ± 2,300 BP at the top, so we have a gap were one species could be replaced by the other one. The same observation can be made for Layer 5, whose chronology is still under review. Moreover, the fact that we have two species in the same levels does not mean that they lived in the exact same place, because the small mammal assemblages from Kaldar Cave were accumulated

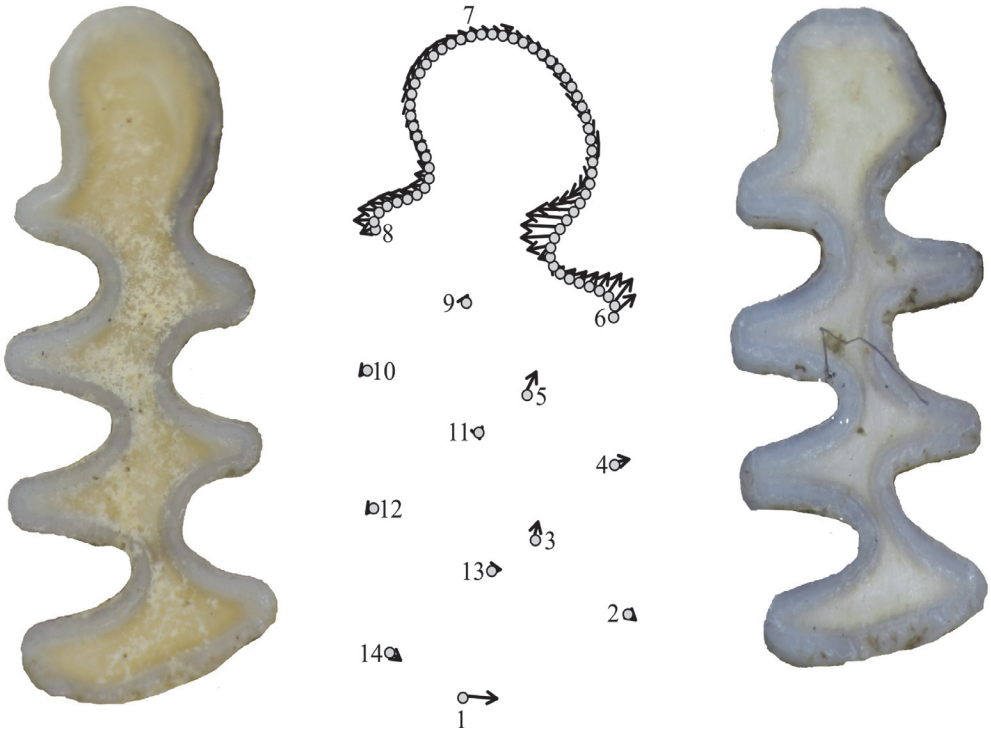


FIGURE 7. Morphological differences between *Ellobius fuscocapillus* (left) and *Ellobius lutescens* (right). Arrows depict the displacements between corresponding landmarks in the reference (dots) and *Ellobius lutescens* as target specimens.

by nocturnal raptors (Rey-Rodríguez et al., 2020), which could hunt in different habitats on a territory of several (tens of) km^2.

Ellobius fuscocapillus is not present in the area nowadays, but it may have lived there in the past. Indeed, at Kaldar Cave, the palaeoenvironmental data (obtained with the *habitat weighting* method) have shown that the landscape was mainly composed of steppes in both levels, which are favorable habitats for the *Ellobius* species (Rey-Rodríguez et al., 2020). The absence of *E. talpinus* in our archaeological sample could be linked to the climatic requirements of the species, but this hypothesis remains to be deepened.

CONCLUSIONS

In the present study, based on modern and fossil specimens of *Ellobius* species, we found potential size and shape differences within the examined material thanks to GMM analyses. On the basis of the m1 shape alone, we were able to differentiate two groups: *E. talpinus* on the one hand, and *E. fuscocapillus* and *E. lutescens* on the other. Taking size into account, moreover, it was possible to distinguish *E. fuscocapillus* from *E. lutescens*. However, we agree that it would be necessary to increase the reference dataset, particularly for *E. lutescens*, which may help us find further discriminative patterns between these three species in future studies.

GMM enabled us to obtain good results in fossil species attributions. Here, only complete teeth were used, i.e. not the whole fossil *Ellobius* sample from Kaldar Cave. We obtained better results in the classifications in including all the teeth landmarks instead of the AC alone. It would thus be really useful to improve the results in order to be able to identify broken or digested molars, albeit with the caveat that when only the anterior cap of the molar is preserved we cannot discriminate between *E. fuscocapillus and E. lutescens*. Accordingly, it would be necessary to combine this method with other techniques and use all the criteria together.

It would be interesting to extend this GMM study to other modern and fossil *Ellobius* species, especially from Middle Pleistocene sites, in order to obtain a more complex overview of their morphological differences and their evolution throughout their current and past geographic range, and to explore the potential and usefulness of this tool in the archaeological sites of southeastern Europe, western and central Asia.

ACKNOWLEDGMENTS

Rey-Rodriguez is the beneficiary of a PhD scholarship funded by the Erasmus Mundus Program (IDQP). J.M. López-García was supported by a Ramón y Cajal contract (RYC-2016-19386) with financial sponsorship from the Spanish Ministry of Science, Innovation and Universities. This work was developed within the framework of projects 2017SGR859, 2017SGR840 and 2017SGR1040 (AGAUR, Generalitat de Catalunya), and 2018PFRURVB291 (Univ. Rovira i Virigli). We thank the head of the Research Institute of Cultural Heritage and Tourism (RICHT) (Dr. B. Omrani) and the head of the Iranian Center for Archaeological Research (ICAR) (Dr. R. Shirazi) for providing us with the necessary support and permissions in studying the materials. We thank the head of the Lorestan Cultural Heritage, Handicraft and Tourism Organization (Mr. A. Ghasemi) for all his support. We also thank the head of International Collaboration and Ties of the RICHT (Mrs. M. Kholghi) for all her cooperation and help. B. Bazgir received his PhD scholarship from the Fundación Atapuerca, for which he is grateful. We would like to thank R. Portela Miguez, Senior Curator in Charge of Mammals, for his help with the reference collection in the Natural History Museum of London; L. Heaney, A. Ferguson and L. Smith of Chicago Field Museum; and M. Surovy, J. Galkin and C. Mehling of the American Museum of Natural History of New York. We thank A. Profico for his precious help.

We would like to thank R. Glasgow for reviewing the English language of the manuscript. We also want to thank to the Editors Dr. D. Nowakowski, Dr. D. Hembree and Dr. C. Haug, as well as the three anonymous reviewers for their comments and suggestions that strongly improved the final version of the manuscript.

REFERENCES

Adams, D.C., Collyer, M.L., and Kaliontzopoulou, A. 2020. Geomorph: software for geometric morphometric analyses. R package version 3.2.1.

Adams, D.C., Rohlf, F.J.,and Slice, D.E. 2009. Geometric morphometrics: ten years of progress following the revolution. Italian Journal of Zoology, 71 (1):5-16. https://doi.org/10.1080/11250000409356545

Bate, D.M.A. 1930. Animal remains from the Dark Cave, Hazar Merd. American School of Prehistoric Research Bulletins, 6:38-41.

Bate, D.M.A. 1937. Palaeontoogy: the fossil fauna of the Wady El-Mughara caves. In Garrod, D.A.E. and Bate, D.M.A. (eds.), Excavations at the Wady El-Mughara. Clarendon Press, Oxford.

Baylac, M. and Frieß, M. 2006. Fourier descriptors, procrustes superimposition, and data dimensionality: an example of cranial shape analysis in modern human populations, p.145-165. In Slice, D.E. (ed.), Modern Morphometrics in Physical Anthropology. Kluwer Academic Publishers-Plenum Publishers, New York. https://doi.org/10.1007/0-387-27614-9_6

Bazgir, B., Otte, M., Tumung, L., Ollé, A., Deo, S.G., Joglekar, P., López-García, J.M., Picin, A., Davoudi, D., and van der Made, J. 2014. Test excavations and initial results at the middle and upper paleolithic sites of Gilvaran, Kaldar, Ghamari caves and Gar Arjene Rockshelter, Khorramabad Valley, western Iran. Comptes Rendus-Palevol, 13:511-525. https://doi.org/10.1016/j.crpv.2014.01.005

Bazgir, B., Ollé, A., Tumung, L., Becerra-Valdivia, L., Douka, K., Higham, T., Van Der Made, J., Picin, A., Saladié, P., López-Garciá, J.M., Blain, H.-A., Allué, E., Fernández-Garciá, M., Rey-Rodríguez, I., Arceredillo, D., Bahrololoumi, F., Azimi, M., Otte, M., and Carbonell, E. 2017. Understanding the emergence of modern humans and the disappearance of Neanderthals: insights from Kaldar Cave (Khorramabad Valley, Western Iran). Scientific Reports 7:43460. https://doi.org/10.1038/srep43460

Becerra-Valdivia, L., Douka, K., Comeskey, D., Bazgir, B., Conard, N.J., Marean, C.W., Ollé, A., Otte, M., Tumung, L., Zeidi, M., and Higham, T.F.G. 2017. Chronometric investigations of the Middle to Upper Paleolithic transition in the Zagros Mountains using AMS radiocarbon dating and Bayesian age modelling. Journal of Human Evolution, 109:57-69. https://doi.org/10.1016/j.jhevol.2017.05.011

Belmaker, M., Bar-Yosef, O., Belfer-Cohen, A., Meshveliani, T., and Jakeli, N. 2016. The environment in the Caucasus in the Upper Paleolithic (Late Pleistocene): evidence from the small mammals from Dzudzuana cave, Georgia. Quaternary International, 425:4-15. https://doi.org/10.1016/j.quaint.2016.06.022

Blasius, W. 1884. Comptes rendus des séances de l´Académie des Sciences. Tome XCVIII. Nos 1 et 2. Paris.

Blyth, E. 1843. The Journal of the Asiatic Society of Bengal. Calcutta: Bishop's College Press,1832-1936.

Carleton, M.D. and Musser, G.G. 2005. Order Rodentia, p. 745-752. In Wilson, D.E. and Reeder, D.M. (eds.), Mammal Species of the World, Third Edition. The Johns Hopkins University Press, Baltimore.

Corbet, G.B. 1978. The Mammals of the Palearctic Region: A Taxonomic Review. British Museum of Natural History, London.

Corbet, G.B. and Hill, J.E. 1991. A World List of Mammalian Species. 3rd ed. British Museum of Natural History, London.

Cornette, R., Stoetzel, E., Baylac, M., Moulin, S., Hutterer, R., Nespoulet, R., El Hajraoui, M.A., Denys, C., and Herrel, A. 2015. Shrews of the genus *Crocidura* from El Harhoura 2 (Témara, Morocco): the contribution of broken specimens to the understanding of Late Pleistocene-Holocene palaeoenvironments in North Africa. Palaeogeography, Palaeoclimatology, Palaeoecology, 436:1-8. https://doi.org/10.1016/j.palaeo.2015.06.020

Coşkun, Y. 1997. *Ellobius lutescens* Thomas, 1897 (Rodentia: Cricetidae) Turkish Journal of Zoology. 21; 349-354.

Coşkun, Y. 2001. On distribution, morphology and biology of the mole vole, *Ellobius lutescens* Thomas, 1897 (Mammalia: Rodentia) in eastern Turkey. Zoology in the Middle East, 23:5-12. https://doi.org/10.1080/09397140.2001.10637861

Coşkun, Y. 2016. Review of unique odd chromosome-numbered underground rodent species of the Palearctic region: *Ellobius Lutescens* Thomas 1897 (Rodentia: Cricetidae). Turkish Journal of Zoology, 40:831-841. https://doi.org/10.3906/zoo-1509-53

Cucchi, T., Barnett, R., Martínková, N., Renaud, S., Renvoisé, E., Evin, A., Sheridan, A., Mainland, I., Wickham-Jones, C., Tougard, C., Quéré, J.P., Pascal, Michel, Pascal, Marine, Heckel, G., O'Higgins, P., Searle, J.B., and Dobney, K.M. 2014. The changing pace of insular life: 5000 years of microevolution in the Orkney vole (*Microtus arvalis orcadensis*). Evolution, 68:2804–2820. https://doi.org/10.1111/evo.12476

Cucchi, T., Mohaseb, A., Peigné, S., Debue, K., Orlando, L., and Mashkour, M. 2017. Detecting taxonomic and phylogenetic signals in equid cheek teeth: towards new palaeontological and archaeological proxies. Royal Society Open Science 4. https://doi.org/10.1098/rsos.160997

Darlington, P.J. 1957. Zoogeography: the Geographical Distribution of Animals. John Wiley and Sons, New York.

Dianat, M., Darvish, J., Aliabadian, M., Siahsarvie, R., Krystufek, B., and Nicolas, V. 2020. Systematics and evolution of the libyan jird based on molecular and morphometric data. Journal of Zoological Systematics and Evolutionary Research, 58:439-458. https://doi.org/10.1111/jzs.12335

Dianat, M., Darvish, J., Cornette, R., Aliabadian, M., and Nicolas, V. 2017. Evolutionary history of the Persian Jird, *Meriones persicus*, based on genetics, species distribution modelling and morphometric data. Journal of Zoological Systematics and Evolutionary Research, 55:29-45. https://doi.org/10.1111/jzs.12145

Ellerman, J.R. and Morrison-Scott, T.C.S. 1951. Checklist of Palearctic and Indian Mammals, 1780 to 1946. British Museum of Natural History, London.

Fischer von Waldheim, G. 1814. Zoognosia tabulis synopticis illustrata: in usum praelectionum Academiae imperialis medico-chirugicae mosquensis edita. Mosquae. Typis Nicolai S. Vsevolozsky.

Fruciano, C. 2016. Measurement error in geometric morphometrics. Development Genes and Evolution, 226:139-158. https://doi.org/10.1007/s00427-016-0537-4

Frumkin, A. and Comay, O. In press. The last glacial cycle of the southern Levant: Paleoenvironment and chronology of modern humans. Journal of Human Evolution 2019:102609. https://doi.org/10.1016/j.jhevol.2019.04.007

Gharkheloo, M.M. 2003. A study on the morphology, karyology and distribution of *Ellobius* Fischer, 1814 (Mammalia: Rodentia) in Iran. Turkish Journal of Zoology, 27:281-292.

Gunz, P. and Mitteroecker, P. 2013. Semilandmarks: a method for quantifying curves and surfaces. Hystrix, 24:103-109.

Hassinger, J.D. 1973. A survey of the mammals of Afghanistan: resulting from the 1965 Street Expedition (Excluding Bats). Fieldiana Zoology, 60. https://doi.org/10.5962/bhl.title.3065

Hashemi, N., Darvish, J., Mashkour, M., and Biglari, F. 2006. Rodents and lagomorphs remains from late Pleistocene and early Holocene Caves and Rochshelter sites in the Zagros region, Iran. Iranian Journal of Animal Biosystematics, 2:25-33.

Hulme-Beaman, A., Cucchi, T., Evin, A., Searle, J.B., and Dobney, K. 2018. Exploring *Rattus praetor* (Rodentia, Muridae) as a possible species complex using geometric morphometrics on dental morphology. Mammalian Biology, 92:62-67. https://doi.org/10.1016/j.mambio.2018.04.002

Jaeger, J.J. 1988. Origine et evolution du genre *Ellobius* (Mammalia, Rodentia) en Afrique Nord-Occidentale. Folia Quaternaria 57:3-50.

Kandel, A.W., Gasparyan, B., Allué, E., Bigga, G., Bruch, A.A., Cullen, V.L., Frahm, E., Ghukasyan, R., Gruwier, B., Jabbour, F., Miller, C.E., Taller, A., Vardazaryan, V., Vasilyan, D., and Weissbrod, L. 2017. The earliest evidence for Upper Paleolithic occupation in the Armenian Highlands at Aghitu-3 Cave. Journal of Human Evolution, 110:37-68. https://doi.org/10.1016/j.jhevol.2017.05.010

Kaya, A., Gharkheloo, M.M., and Coşkun, Y. 2018. Geographic variation in the skull morphology of *Ellobius lutescens* Thomas, 1897 (Mammalia: Rodentia) by geometric morphometric analyses. Vertebrate Zoology, 68:157-164.

Klenovšek, T. and Kryštufek, B. 2013. An ontogenetic perspective on the study of sexual dimorphism, phylogenetic variability, and allometry of the skull of European ground squirrel, *Spermophilus citellus* (Linnaeus, 1766). Zoomorphology, 132:433-445. https://doi.org/10.1007/s00435-013-0196-1

Kryštufek, B. and Shenbrot, G. 2016. *Ellobius lutescens*. The IUCN Red List of Threatened Species 2016: e.T7655A22340006. https://doi.org/10.2305/IUCN.UK.2016-2.RLTS.T7655A22340006.en

Kryštufek, B. and Vohralík, V. 2009. Mammals of Turkey and Cyprus, Rodentia II: Cricetinae, Muridae, Spalacidae, Calomyscidae, Capromyidae, Hystricidae, Castoridae. ZALOŽBA ANNALES, University of Primorska. https://doi.org/10.1644/10-MAMM-R-221.1

Kryštufek, B. and Vohralík, V. 2009. Mammals of Turkey and Cyprus, Rodentia II: Cricetinae, Muridae, Spalacidae, Calomyscidae, Capromyidae, Hystricidae, Castoridae. ZALOŽBA ANNALES, University of Primorska.

Kryštufek, B., Janžekovič, F., Hutterer, R., and Klenovšek, T. 2016. Morphological evolution of the skull in closely related bandicoot rats: a comparative study using geometric morphometrics. Hystrix, 27:1-7. https://doi.org/10.4404/hystrix-27.2-11639

Lay, D.M. 1967. A study of the mammals of Iran, resulting from the street expedition of 1962-63. Fieldiana Zoology, 54:168-171.

Luzi, E., Pazonyi, P., and López-García, J.M. 2019. The influence of climate on morphometric traits of fossil populations of *Microtus arvalis* and *M. agrestis* from the Carpathian Basin, northern Hungary. Lethaia, 52:123132. https://doi.org/10.1111/let.12294

Markova, A. 1992. Fossil rodents (Rodentia, Mammalia) from the Sel'-Ungur Acheulian cave site (Kirghizstan). Acta Zoologica Cracoviensia, 35 (2):217-239.

Maul, L.C. and Markova, A.K. 2007. Similarity and regional differences in Quaternary arvicolid evolution in Central and Eastern Europe. Quaternary International, 160:81-99. https://doi.org/10.1016/j.quaint.2006.09.010

Maul, L.C., Smith, K.T., Shenbrot, G., Bruch, A.A., Wegmüller, F., and Le Tensorer, J.M. 2015. Microvertebrates from unit G/layer 17 of the archaeological site of Hummal (El Kowm, Central Syria): preliminary results. Anthropologie, 119:676-686. https://doi.org/10.1016/j.anthro.2015.10.010

Michaux, J., Reyes, A., and Catzeflis, F. 2001. Evolutionary history of the most speciose mammals: molecular phylogeny of muroid rodents. Molecular Biology and Evolution, 18:2017-2031. https://doi.org/10.1093/oxfordjournals.molbev.a003743

Mitteroecker, P., Windhager, S., Müller, G.B., and Schaefer, K. 2015. The morphometrics of "masculinity" in human faces. PLoS ONE, 10. https://doi.org/10.1371/journal.pone.0118374

Nesin, V. and Nadachowski, A. 2001. Late Miocene and Pliocene small mammal faunas (Insectivora, Lagomorpha, Rodentia) of Southeastern Europe. Acta Zoologica Cracoviensia, 44:107-135.

Nowak, R.M. 1999. Walker's Mammals of the World. The Johns Hopkins University Press, Baltimore.
Osborn, D.J. 1962. Rodents of subfamily Microtinae from Turkey. Journal of Mammology, 43 (4):515-529. https://doi.org/10.2307/1376914
Pallas, P. S. 1770. Spicilegia zoologica quibus novae imprimis et obscurae animalium species iconibus, descriptionibus atque commentariis illustrantur. Fasciculus octavus.
Parfitt, S. A. 2016. Rodents, lagomorphs and insectivores from Azokh Cave, p.163-177. In Fernández-Jalvo, Y., King, T., Yepiskoposyan, L., and Andrews, P. (eds.), Azokh Cave and the Transcaucasian Corridor. Springer, Dordrecht. https://doi.org/10.1007/978-3-319-24924-7
R Core Team, 2020. R: A language and environment for statistical computing. R Foundation for Statistical Computing. http://www.r-project.org/index.html
Rey-Rodríguez, I., Lopez-Garcia, J.M., Blain, H.-A., Stoetzel, E., Denys, C., Bazgir, B., and Ollé, A. 2020. Exploring the landscape and climatic conditions of Neanderthals and anatomically modern humans in the Middle East: the rodent assemblage from the late Pleistocene of Kaldar Cave (Khorramabad Valley, Iran). Quaternary Science Reviews, 236:106278. https://doi.org/10.1016/j.quascirev.2020.106278
Roberts, T.J. 1977. The Mammals of Pakistan. Ernst Benn Ltd., London.
Rohlf, F.J. 2016. tpsDig, Digitize Landmarks and Outlines, Version 2.32. Department of Ecology and Evolution, State University of New York at Stony Brook, New York.
Romanenko, S.A., Fedorova, Y.E., Serdyukova, N.A., Zaccaroni, M., Stanyon, R., and Graphodatsky, A.S. 2020. Evolutionary rearrangements of X chromosomes in voles (Arvicolinae, Rodentia). Scientific Reports, 10:13235. https://doi.org/10.1038/s41598-020-70226-4
Romanenko, S.A., Sitnikova, N.A., Serdukova, N.A., Perelman, P.L., Rubtsova, N. V., Bakloushinskaya, I.Y., Lyapunova, E.A., Just, W., Ferguson-Smith, M.A., Yang, F., and Graphodatsky, A.S. 2007. Chromosomal evolution of Arvicolinae (Cricetidae, Rodentia). II. The genome homology of two mole voles (genus *Ellobius*), the field vole and golden hamster revealed by comparative chromosome painting. Chromosome Research, 15:891897. https://doi.org/10.1007/s10577-007-1171-9
Romanenko, S.A., Serdyukova, N.A., Perelman, P.L., Trifonov, V.A., Golenishchev, F.N., Bulatova, N.S., Stanyon, R., and Graphodatsky, A.S. 2018. Multiple intrasyntenic rearrangements and rapid speciation in voles. Scientific Reports, 8:14980. https://doi.org/10.1038/s41598-018-33300-6
Rusin, M. 2017. *Ellobius talpinus*, Northern Mole Vole. The IUCN Red List of Threatened Species 2016:e.T7656A115085720. https://doi.org/10.2305/IUCN.UK.2016-3.RLTS.T7656A22339917.en
Sala, B., Masini, F., and Torre, D. 1994. Villanyian arvicolids from Veronese, a karst fissure in the Adige valley, Northeastern Italy. Bolletino Societa Paleontologica Italina, 33:3-11.
Schlager, S. 2017. Morpho and Rvcg shape analysis, p. 217-256. In Zheng,G., Li, S., and Szekely, G. (ed.), Statistical Shape and Deformation Analysis. Academic Pres, London.
Shenbrot, G., Kryštufek, B., and Molur, S. 2016. *Ellobius fuscocapillus*, Southern Mole Vole. The IUCN Red List of Threatened Species 2016:e.T7654A22339730. https://doi.org/10.2305/IUCN.UK.2016-2.RLTS.T7654A22339730.en
Stoetzel, E. 2013. Late Cenozoic micromammal biochronology of northwestern Africa. Palaeogeography, Palaeoclimatology, Palaeoecology, 392:359-381. https://doi.org/10.1016/j.palaeo.2013.09.026
Stoetzel, E., Cornette, R., Lalis, A., Nicolas, V., Cucchi, T., and Denys, C. 2017. Systematics and evolution of the *Meriones shawii/grandis* complex (Rodentia, Gerbillinae) during the Late Quaternary in northwestern Africa: exploring the role of environmental and anthropogenic changes. Quaternary Science Reviews, 164:199-216. https://doi.org/10.1016/j.quascirev.2017.04.002
Tabatabaei Yazdi, F. and Alhajeri, H. 2018. Sexual dimorphism, allometry, and interspecific variation in the cranial morphology of seven *Meriones* species (Gerbillinae, Rodentia). Hystrix, Italian Journal of Mammalogy, 29(2):162-167.
Tesakov, A. S. 1998. Voles of the Tegelen fauna. Mededelingen Nederlands Instituut voor Toegepaste Geowetenschappen TNO, 60:71-134.
Tesakov, A.S. 2016. Early Middle Pleistocene *Ellobius* (Rodentia, Cricetidae, Arvicolinae) from Armenia. Russian Journal of Theriology, 15(2):151-158.

Thomas, O. 1897. *Ellobius lutescens*. The Annals and Magazine of Natural History, 20:308.
Thomas, O. 1905. *Ellobius woosnami.* Abstract Proceedings of the Zoological Society, 23:526.
Vorontsov, N.N., Lyapunova, E.A., Zakaryan, G.G., and Ivanov, V.G. 1969. The karyology and taxonomy of the genus Ellobius (Microtinae, Rodentia),p.127-129. In Vorontsov, N.N. (ed.) The Mammals (Evolution, Karyology, Taxonomy, Fauna).Nauka ,Novosibirsk, Moscow (in Russian).Topachevsky, V.A. and Rekovets, L.I. 1982. New material to the systematics and evolution of mole voles of the nominative subgenus of the genus *Ellobius* (Rodentia, Cricetidae). Vestnik Zoologii, 5:47-74 (in Russian).
Vorontsov, N.N., Lyapunova, E.A., Zakaryan, G.G., and Ivanov, V.G. 1969. The karyology and taxonomy of the genus *Ellobius* (Microtinae, Rodentia), p.127-129. In Vorontsov, N.N. (ed.), The Mammals (Evolution, Karyology, Taxonomy, Fauna), Nauka, Novosibirsk, Moscow (in Russian).
Walker, E.P. 1964. Mammals of the World. Vol. 2. The Johns Hopkins Press, Baltimore.
Weissbrod, L., Marshall, F.B., Valla, F.R., Khalaily, H., Bar-Oz, G., Auffray, J.-C., Vigne, J.-D., and Cucchi, T. 2017. Origins of house mice in ecological niches created by settled hunter-gatherers in the Levant 15,000 y ago. Proceedings of the National Academy of Sciences, 114:4099-4104. https://doi.org/10.1073/pnas.1619137114
Weissbrod, L. and Weinstein-Evron, M. 2020. Climate variability in early expansions of *Homo sapiens* in light of the new record of micromammals in Misliya Cave, Israel. Journal of Human Evolution, 139:102741. https://doi.org/10.1016/j.jhevol.2020.102741
Wilson, D.E. and Reeder, D.M. 2005. Mammal Species of the World. Smithsonian Institution Scholarly Press, Washington D.C.
Wilson, D.E., Mittermeier, R.A., and Lacher, T.E. 2017. Handbook of the Mammals of the World. Volume 7. Rodents II. Lynx Edicions, Barcelona, Spain.

APPENDICES

APPENDIX 1.

TPS data. The appendix material is available online as a zipped file at https://palaeo-electronica.org/content/2021/3265-ellobius-and-gmm.

APPENDIX 2.

Complete statistical data for the PCA. The appendix material is available online as a zipped file at https://palaeo-electronica.org/content/2021/3265-ellobius-and-gmm.

Quaternary Science Reviews 236 (2020) 106278

Contents lists available at ScienceDirect

Quaternary Science Reviews

journal homepage: www.elsevier.com/locate/quascirev

Exploring the landscape and climatic conditions of Neanderthals and anatomically modern humans in the Middle East: the rodent assemblage from the late Pleistocene of Kaldar Cave (Khorramabad Valley, Iran)

Iván Rey-Rodríguez [a, b, *], Juan-Manuel López-García [c, d], Hugues-Alexandre Blain [c, d], Emmanuelle Stoetzel [a], Christiane Denys [e], Mónica Fernández-García [b, a], Laxmi Tumung [c, d, a], Andreu Ollé [c, d], Behrouz Bazgir [d]

[a] HNHP UMR 7194, CNRS, Muséum national d'Histoire naturelle, UPVD, Sorbonne Universités, Musée de l'Homme, Palais de Chaillot, 17 place du Trocadéro, 75016, Paris, France
[b] Sezione di Scienze Preistoriche e Antropologiche, Dipartimento di Studi Umanistici, Università degli Studi di Ferrara, C.so Ercole I d'Este, 32 - 44121, Ferrara, Italy
[c] Institut Català de Paleoecologia Humana i Evolució Social (IPHES). Zona Educacional 4, Campus Sescelades URV (Edifici W3), 43007, Tarragona, Spain
[d] Área de Prehistòria, Universitat Rovira i Virgili. Facultat de Lletres, Avinguda Catalunya 35, 43002, Tarragona, Spain
[e] ISYEB UMR 7205, CNRS, Muséum national d'Histoire naturelle, UPMC, EPHE, Sorbonne Universités, Paris, France

ARTICLE INFO

Article history:
Received 23 January 2020
Received in revised form
20 March 2020
Accepted 20 March 2020
Available online xxx

Keywords:
Rodentia
Middle east
Taxonomy
Palaeoecology
Human occupations

ABSTRACT

The Middle East, specially the Zagros region, lies in a strategic position as a crossroads between Africa, Europe and eastern Asia. The landscape of this region that prevailed around the Neanderthal and anatomically modern human occupations is not well known. Only a few sites have been studied in detail in this area, often providing only a faunal list. These reveal that Neanderthals and anatomically modern humans lived in a landscape mainly composed of dry steppes.

Here we extend the data obtained from Kaldar Cave through a systematic study of the rodent assemblage. The site provided evidence of a Pleistocene occupation attested by lithic tools associated with the Middle and Upper Palaeolithic, but it was also occupied during the Holocene, as evidenced by Neolithic artefacts. First excavations have revealed small vertebrates in Layer 4 (sub-layer 5 and 5II), belonging to the Upper Palaeolithic, and Layer 5 (sub-layers 7 and 7II), belonging to the Middle Palaeolithic.

The rodent assemblage of Kaldar Cave is mainly composed of six arvicoline, two cricetine, one glirid, one dipodid, one gerbilline and two murine species.

This assemblage shows that during the Late Pleistocene the environment around the site was mainly composed of open dry steppes, as indicated by the most abundant taxa, *Microtus*, *Ellobius* and *Meriones*. However, murine species indicate the presence of a vegetation cover. The palaeoclimatic conditions are characterized by lower temperatures and also less precipitation than at present.

The results obtained with the rodent assemblages show that there is no major palaeoenvironmental or palaeoclimatic change that would explain the cultural shift between Layer 5 (Middle Palaeolithic) and Layer 4 (Upper Palaeolithic).

Published by Elsevier Ltd.

1. Introduction

Small vertebrates are recognized to be good palaeoecological indicators due to their rapid evolution, the limited geographic range of a species and unique niche requirements, as well as their frequent preservation in archaeological and palaeontological sites.

* Corresponding author. HNHP UMR 7194, CNRS, Muséum national d'Histoire naturelle, UPVD, Sorbonne Universités, Musée de l'Homme, Palais de Chaillot, 17 place du Trocadéro, 75016, Paris, France.
E-mail addresses: ivan.rey-rodriguez@edu.mnhn.fr, ivanreyrguez@gmail.com (I. Rey-Rodríguez).

https://doi.org/10.1016/j.quascirev.2020.106278
0277-3791/Published by Elsevier Ltd.

They might be excellent indicators of palaeovegetation type and provide a high-resolution proxy for palaeoenvironmental changes (e.g. Belmaker and Hovers, 2011). Studies of small vertebrates from archaeological sites in the Middle East are still scarce (Belmaker and Hovers, 2011; Belmaker et al., 2016; Demirel et al., 2011; Fernández-Jalvo, 2016a; Kandel et al., 2017; Maul et al., 2015a, 2015b; Smith et al., 2016; Weissbrod and Zaidner, 2014), and they mainly propose preliminary lists of taxa. On the other hand, some studies of extant owl pellet assemblages have been performed in the Middle East (Abi-said et al., 2014; Darvish et al., 2000; Haddadian Shad et al., 2014; Kopij and Liven-schulman, 2013; Obuch and Khaleghizadeh, 2012; Rey-Rodríguez et al., 2019; Shehab et al., 2013), providing taxonomic and some taphonomic reference data in Iran, Lebanon, Israel, Turkey and Syria.

The main palaeoecological and palaeoclimatic reconstructions based on faunal assemblages relate to the unique niche requirements of a particular species. Belmaker et al. (2011) pointed out that their interpretations, in contrast, are based on analyses of community composition. Analyses of persistence *versus* change over time should take into account species presence-absence, rank abundance and proportional abundance (Belmaker and Hovers, 2011).

The Middle East is a prime location to study Neanderthal and anatomically modern human (AMH) interactions during the Middle to Upper Palaeolithic transition (Belmaker et al., 2016). However, sites yielding evidence of both Neanderthal and AMH occupations in the same sequence are rare, only five sites were well excavated (Bazgir et al., 2014, 2017). In this framework, Kaldar Cave is a key archaeological site for evaluating the influence of environment on cultural changes in both human species because of its location and the faunal and lithic remains. The main objective of this paper is to infer the landscape composition and the climatic conditions in which Neanderthal and AMH populations pursued their activities through the study of small mammals. We identify and describe the rodent fossils recovered from Kaldar Cave in order to establish the main criteria for further identifications in this region and provide a preliminary basis for future systematic studies.

2. Kaldar Cave

Kaldar Cave is located in the northern part of the Khorramabad Valley, Lorestan Province, western Iran (48°17′35″ E, 33°33′25″ N) at 1290 m a.s.l. (Fig. 1a and b). The cave was discovered in 2007, and the first archaeological intervention was undertaken by an Iranian-Spanish team in 2011–2012, revealing the great potential of the cave (Bazgir et al., 2014). A second excavation was performed in 2014–2015. The trench exposed an approximately 2 m-thick section of sedimentary deposits, characterized by 5 main layers, themselves divided into several sub-layers (Fig. 1c).

Layer 5 (including sub-layers 7 and 7II) consists of an extremely cemented reddish-brown sediment with some small angular limestone blocks and Middle Palaeolithic artefacts with Levallois elements. So far, no chronometric data are available for this layer (Bazgir et al., 2017).

Layer 4 (including sub-layers 5, 5II, 6 and 6II) consists of a silty but compact dark-brown sediment with cultural remains attributed to the Upper and early Upper Palaeolithic. In the uppermost parts of this layer, two fireplaces made of clay were recovered and dated through thermoluminescence, yielding ages that ranged from 23,100 ± 3300 to 29,400 ± 2300 BP (Bazgir et al., 2017). The dates obtained show that these fireplaces were made or re-used from existing older sediment from the upper part of this layer in the later stages of the Upper Palaeolithic. AMS radiocarbon dates of 38,650–36,750 cal BP, 44,200–42,350 cal BP, and 54,400–46,050 cal BP have been obtained from charcoal material located below this layer (Bazgir et al., 2017; Becerra-Valdivia et al., 2017).

Layers 1 to 3 (including sub-layers 4 and 4II) consist of ashy sediments of a blackish-green colour containing both thick and thin angular limestone clasts. These layers varied in thickness from 60 to 90 cm and contained many phases dating to the Holocene: Islamic and historical eras, Iron Age, Bronze Age, Chalcolithic and Neolithic. However, due to the presence in these layers of bioturbation mainly by burrowing animals, the phases were recognized only by a preliminary study of the potsherds, metal artefacts and some diagnostic lithic artefacts from the lower layers.

This site provides evidence for the Middle to Upper Palaeolithic transition in the Middle East (Bazgir et al., 2017). Moreover, Kaldar Cave has yielded the oldest evidence of *Prunus* spp. in the area, through the study of thirty charcoal remains (Allué et al., 2018), that helps us to reconstruct the environmental conditions, evidencing a wooded vegetation.

3. Material and methods

The rodent fossil remains used in this study, 1112 molars, come from the archaeological excavation campaigns carried out in Kaldar Cave in 2011–2012 and 2014–2015.

The samples comprise disarticulated bones and isolated teeth that were collected in the field by water screening using superimposed 5 and 0.5 -mm mesh screens.

3.1. Taxonomy

In this article we only focus on rodents, because these are one of the most useful tools for palaeoenvironmental and palaeoclimatic reconstructions of archaeological sites, and the other material, as amphibians, squamates, birds, shrews and bats, will be studied later. The taxonomic identification of the rodent remains is based mainly on molar morphology and measurements of the lower m1, the taxonomically most diagnostic tooth.

The remains were identified at a specific level whenever possible, thanks to comparisons with reference collections from the Natural History Museum of London (NHM) and comparative morphological and biometric data from the literature, notably for *Microtus* (Coşkun, 2016; Kryštufek and Shenbrot, 2016; Kryštufek and Vohralík, 2009; López-García, 2011; Rusin, 2017; Shenbrot et al., 2016; Tesakov, 2016), *Cricetulus* (Bogicevic et al., 2011; Kryštufek et al., 2017; Sándor, 2018), *Mesocricetus* (Kryštufek and Vohralík, 2009), *Meriones* (Coşkun, 1999; Darvish, 2011; Dianat et al., 2017; Kryštufek and Vohralík, 2009; Souttou and Denys, 2012; Stoetzel et al., 2017), *Allactaga* (Karami et al., 2008; Shenbrot, 2009), *Myomimus* (Gerrie and Kennerley, 2017; Karami et al., 2008; Kennerley and Kryštufek, 2019), *Apodemus* (Amori et al., 2016; Bogicevic et al., 2011; Knitlová and Horáček, 2017; Kryštufek and Vohralík, 2009; López-García, 2011) and *Mus* (Darviche et al., 2006; Kryštufek and Vohralík, 2009; Siahsarvie and Darvish, 2008).

Quantification of taxonomic frequencies was based on standard measures in zooarchaeological analyses, including the number of identified specimens (NISP) and minimum number of individuals (MNI) (Weissbrod and Zaidner, 2014). This latter was estimated using the most abundant skeletal element present in the assemblage (molars in our case).

3.2. Taphonomy

A preliminary study was performed on the Kaldar Cave

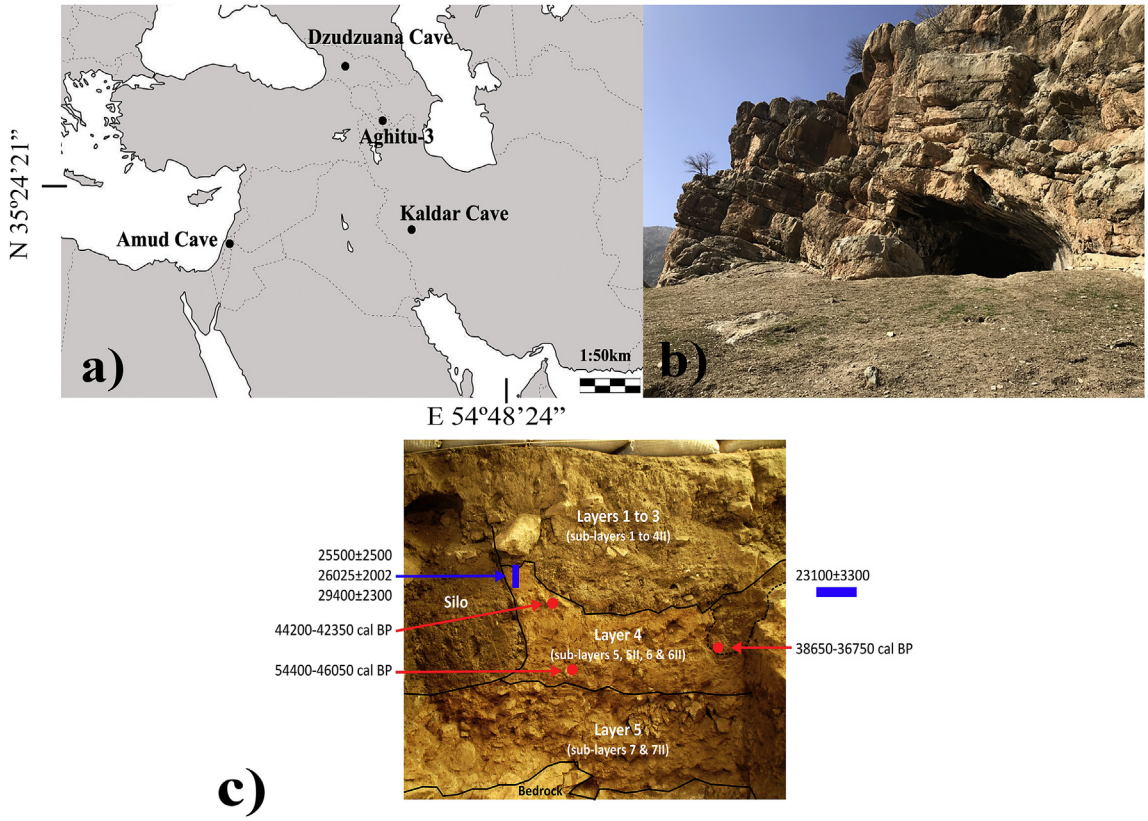


Fig. 1. a) Locations of the Late Pleistocene sites with rodent studies in the Middle East, including Kaldar Cave. b) General view of the entrance to Kaldar Cave. c) Stratigraphy of the eastern section of Kaldar Cave, including the location and results of the dated samples, from A. Ollé and B. Bazgir (Bazgir et al., 2017).

micromammal remains. This was based on the systematic descriptive method that examines the modifications of prey bones induced by predation, focusing on the degree of digestion observed in teeth during the identification (Andrews, 1990; Fernández-Jalvo et al., 2016a,b). This study showed a significant number of digested teeth (Bazgir et al., 2017), indicating that predation activity was the origin of at least part of the accumulation.

3.3. Palaeoenvironmental and palaeoclimatic reconstructions

3.3.1. Habitat weighting method

Palaeoecological interpretations derived from faunal data are based on analyses of community composition (Belmaker and Hovers, 2011). The method used for the palaeoenvironmental reconstruction is the *habitat weighting method*, also named the *taxonomic habitat index* (Evans et al., 1981; Andrews, 2006; modified by Blain et al., 2008; López-García et al., 2011), which is based on the current distribution of each taxon in the habitat(s) where it can be found nowadays. We assume that the Kaldar Cave species had equivalent ecological requirements to their present-day relatives, because the Late Pleistocene species are the same as those today and no extinct fossil species are found in the assemblage. We adapt the method to our studied area, differentiating the following types of habitats: Forest (Fo), a large area covered with trees; Shrubland (Sh), vegetation dominated by shrubs; Grassland (Gr), an open area covered with grass; Desert (De), an area with little precipitation and no vegetation cover; Wetland (We), an area where water covers the soil; Steppe (St), a dry grassy plain; and Rocky (Ro), a rocky or stony substrate. Each species has a score of 1.00, which is divided between the habitats where the species can be found at present (Table 1), all the species ranges were taken from the IUCN Red List of Threatened Species (https://www.iucnredlist.org/resources/spatial-data-download).

Table 1
Scores attributed to each rodent species found at Kaldar Cave according to its ecological requirements, used for the *habitat weighting method*: Forest (Fo), Shrubland (Sh), Grassland (Gr), Desert (De), Wetland (We), Steppe (St) and Rocky (Ro).

Species	Fo	Sh	Gr	De	We	St	Ro
Ellobius lutescens			0.33	0.33		0.33	
Ellobius fuscocapillus						1	
Microtus irani			1				
Microtus guentheri			1				
Microtus socialis		0.5				0.5	
Chionomys nivalis							1
Cricetulus migratorius			0.33	0.33		0.33	
Mesocricetus brandti						1	
Meriones persicus		0.33	0.33				0.33
Allactaga sp.				0.5		0.5	
Apodemus sp.	1						
Mus musculus		0.33	0.33		0.33		
Myomimus sp.				1			

3.3.2. Bioclimatic model

In order to reconstruct the climate at Kaldar Cave, we applied the *bioclimatic model* (*BM*), which was developed by Hernández Fernández (2001) on the basis of the faunal spectrum, assuming that small- and large-mammal species can be ascribed to ten different climates (Hernández Fernández, 2001; Hernández Fernández and Peláez-Campomanes, 2003; Hernández Fernández et al., 2007). It was first necessary to calculate the climatic restriction index ($CRI_i = 1/n$, where i is the climatic zone where the species appear and n is the number of zones where the species is

present) and the bioclimatic component ($BC_i = (\Sigma\ CRI_i)\ 100/S$, where i is the climatic zone and S is the number of species). To BC a mathematical model is applied as a regression that allows us to calculate climatic parameters (see Appendix 1).

The different climatic groups defined by Hernández Fernández (2001) and Hernández Fernández et al. (2007) are: I *equatorial*; II *tropical with summer rains*; II/III *transition tropical semiarid*; III *subtropical arid*; IV, *subtropical* with winter rains and summer droughts; V, *warm temperate* with not very severe winters but high humidity; VI, *typical temperate* with winters that are cold but not very long, but summers that are cool; VII, *arid-temperate* with large temperature contrasts between winter and summer; VIII, *cold-temperate* with cool summers and long cold winters (boreal) and IX, *artic* (Table 2).

By means of the *BM* we were able to estimate the mean annual temperature (MAT), the mean temperature of the coldest month (MTC), the mean temperature of the warmest month (MTW) and the mean annual precipitation (MAP). This method also allowed us to assess whether there were changes in the temperature and precipitation regimes during the Middle to Upper Palaeolithic transition at Kaldar Cave.

4. Results and discussion

4.1. Taxonomic identifications

In total 264 minimum number of individuals (MNI) were identified (Table 3 and Fig. 2). Some differences were found with respect to the preliminary list previously published by Bazgir et al. (2017). We notably found some new specimens and reconsidered the identifications for *Ellobius talpinus*, *Calomyscus* sp. and *Dryomys* cf. *nitedula*.

Order Rodentia Bowdich, 1821

Rodentia indet.

There are 14 teeth (11 in Layer 4 and 3 in Layer 5) that have not been identified to the family or genus level because they were broken.

Family Cricetidae Fisher, 1817

Subfamily Arvicolinae Gray, 1821

Genus *Microtus* Schrank, 1798

***Microtus* spp.**

Material: 554 isolated teeth**. Layer 1**–**3:** four isolated teeth; three left lower m1 and one right lower m1. **Layer 4:** 258 isolated teeth; 81 m^2; 101 m^3, 13 right upper M1, 31 right lower m1; four left upper M1 and 28 left lower m1. **Layer 5:** 292 isolated teeth; 119 m^2; 53 m^3; nine left upper M1, 51 left lower m1; 10 right upper M1; 50 right lower m1.

***Microtus socialis* Pallas, 1773**

Material: 74 isolated teeth. **Layer 1**–**3:** three isolated teeth, three right lower m1. **Layer 4:** 36 isolated teeth; 20 right lower m1 and 16 left lower m1. **Layer 5:** 35 isolated teeth; 20 right lower m1 and 15 left lower m1.

***Microtus irani* Thomas, 1921**

Material: 15 isolated teeth. **Layer 1**–**3:** one isolated tooth, one right lower m1. **Layer 5:** 14 isolated teeth; nine right lower m1 and five left lower m1.

***Microtus guentheri* Danford and Alston, 1880**

Material: 17 isolated teeth. **Layer 1**–**3:** one isolated tooth, one left lower m1. **Layer 4:** 16 isolated teeth; nine right lower m1 and seven left lower m1.

Description and discussion: all the molars are hypsodont and arhizodont with crown cementum in the re-entrant angles. The enamel differentiation is *Microtus*-like. Six extant species of *Microtus* have been identified in Iran: *Microtus arvalis*, *Microtus irani*, *Microtus kermanensis*, *Microtus socialis*, *Microtus transcaspicus* and *Microtus guentheri* (Aşan Baydemir and Duman, 2009; Firouz, 2005; Golenishchev et al., 2002, 2019).

Microtus m1 are characterized by four buccal and five lingual re-entrant angles (Kryštufek and Vohralík, 2009; Tsytsulina et al., 2017) with a posterior lobe (PL), seven triangles (T) and an anterior cap (AC). We identified the Kaldar specimens on the basis of their measurements (Table 4), the arrangement and morphology of the triangles, and the AC (which may or may not be connected with the other elements).

In our sample we identified *Microtus* spp., *Microtus socialis*, *Microtus guentheri* and *Microtus irani.*

In *Microtus socialis*, the triangles from T1-T5 are closed, but T6-T7 are parallel and broadly confluent with the AC. *Microtus guentheri* is distinguishable from *Microtus socialis* by the rounded shape of the AC, which is of an arhombomorph type (Aşan Baydemir and Duman, 2009), and also by T6-T7, which are separated from the AC. In accordance with the measurements given in Aşan Baydemir et al. (2009), the size of *Microtus guentheri* and *Microtus socialis* is similar. In *Microtus irani*, triangles T1-T5 are closed, but T6-T7 are open and not parallel with one another; moreover, *Microtus irani* is clearly larger than the other species considered in our reference collection and also in our sample. Finally, we include in *Microtus* spp. all the elements that we cannot attribute to one species or another, in particular because of their bad state of preservation (due to digestion, breakage).

Habitat and distribution: *Microtus irani* occupies grasslands in Iran, Turkey and the Caucasus (Kryštufek and Kefelioğ;lu, 2001).

Microtus socialis is found in Russia, Ukraine, the Caucasus, Transcaucasia, Turkestan, Iran and Afghanistan (Tsytsulina et al., 2017), although the range is fragmented. It is a highly colonial

Table 2
Scores attributed to each rodent species found at Kaldar Cave for the bioclimatic model (in accordance with Hernández Fernández, 2001; Hernández Fernández et al., 2007). See text for the significance of the Roman numerals corresponding to the climatic groups.

Species	I	II	II/III	III	IV	V	VI	VII	VIII	IX
Ellobius lutescens								1		
Ellobius fuscocapillus				0.33	0.33			0.33		
Microtus irani					1					
Microtus socialis					0.5			0.5		
Chionomys nivalis					0.25		0.25		0.25	0.25
Cricetulus migratorius					0.33		0.33	0.33		
Mesocricetus brandti					1					
Meriones persicus				0.5	0.5					
Allactaga sp.				0.5				0.5		
Apodemus sp.							1			
Mus musculus	0.11	0.11	0.11	0.11	0.11	0.11	0.11	0.11	0.11	

Table 3
Representation of the Kaldar Cave rodent species in terms of number of identified specimens (NISP), minimum number of individuals (MNI) and percentage of the NISP (%).

	Layer 5			Layer 4			Layers 1-3		
Taxon	NISP	MNI	NISP%	NISP	MNI	NISP%	NISP	MNI	NISP%
Indet.	3	–	–	11	–	–	–	–	–
Microtus spp.	292	51	52.33	258	31	48.31	4	3	20
Microtus irani	14	9	2.51	0	0	0.00	1	1	5
Microtus guentheri	0	0	0.00	16	9	3.00	1	1	5
Microtus socialis	35	20	6.27	36	20	6.74	3	3	15
Chionomys nivalis	6	3	1.08	17	12	3.18	2	1	10
Ellobius spp.	80	7	14.34	91	8	17.04	2	2	10
Ellobius fuscocapillus	5	4	0.90	5	3	0.94	1	1	5
Ellobius lutescens	10	6	1.79	10	7	1.87	–	–	–
Cricetulus migratorius	5	3	0.90	14	3	2.62	1	1	5
Mesocricetus brandti	7	4	1.25	3	1	0.56	0	0	0
Meriones cf. *persicus*	88	18	15.77	65	17	12.17	3	2	15
Allactaga sp.	1	1	0.18	1	1	0.19	0	0	0
Myomimus sp.	5	3	0.90	0	0	0.00	0	0	0
Apodemus sp.	5	2	0.90	6	3	1.12	2	1	10
Mus cf. *musculus*	2	1	0.36	1	1	0.19	0	0	0
Total	**558**	**132**	100.00	**534**	**116**	100.00	**20**	**16**	100.00

species, found in steppe habitats and also in agricultural lands, but extending also to bushy scrubs and uncultivated mountain valleys, as well as to open oak forests on dry hillsides (Tsytsulina et al., 2017).

Microtus guentheri occurs from the southeastern Balkans and Turkey through Syria, Lebanon and Israel, with an isolated range segment in northern Libya, Iran and some parts of Europe (Aşan Baydemir and Duman, 2009). This species is present in dry grasslands with sparse vegetation (Amr, 2015).

Genus *Chionomys* Miller, 1908

***Chionomys nivalis* Martins, 1842**

Material: 25 isolated teeth. **Layer 1–3:** two isolated teeth; one left lower m1 and one right lower m1. **Layer 4:** 17 isolated teeth; 12 right lower m1; five left lower m1. **Layer 5:** six isolated teeth; three left lower m1; three right lower m1.

Description and discussion: in our specimens it can be observed that the first lower molars display five triangles and that the morphology of the anteroconid complex (AC) is characteristic of the *nivalis* morphotype, where triangles T6 and T7 are absent and the anterior cap is of an arrowhead or oval shape, inclined towards the labial part. The enamel is of the *Microtus* type with cement (Krystufek, 2017; Kryštufek and Vohralík, 2009; López-García, 2011). These specimens differ from *Microtus* in that they only have five triangles, and the morphology of the AC is the other main characteristic of this species that helps us to differentiate it from *Microtus*.

Habitat and distribution: *Chionomys nivalis* has a global distribution extending from southwestern Europe through southeastern Europe to the Caucasus, Turkey, Israel, Lebanon, Syria and Iran. In Iran it is distributed in the north and also in the west (Shenbrot and Krasnov, 2005; Krystufek, 2017). This is the only *Chionomys* species occurring today in Iran, but two other species (*C. gud, C. roberti*) are represented a little further north (northeastern Turkey, southern Georgia).

Regarding its habitat, it is present in open rocky areas, typically above the tree line and with scarce vegetation cover (Amori, 1999).

Genus *Ellobius* Fischer, 1814

***Ellobius* spp.**

Material: 173 isolated teeth. **Layer 1–3:** two isolated teeth; two left lower m1. **Layer 4:** 91 isolated teeth; seven indet.; eight right lower m1; five left lower m1; 11 upper M1; 43 m^2; 17 m^3. **Layer 5:** 80 isolated teeth; seven left lower m1; three upper M1; 45 m^2; 25 m^3.

***Ellobius fuscocapillus* Blyth, 1843**

Material: 11 isolated teeth. **Layer 1–3:** one isolated tooth; one right lower m1. **Layer 4:** five isolated teeth; two right lower m1; three left lower m1. **Layer 5:** five isolated teeth; four left lower m1 and one right lower m1.

***Ellobius lutescens* Thomas, 1897**

Material: 20 isolated teeth. **Layer 4:** 10 isolated teeth; seven right lower m1 and three left lower m1. **Layer 5:** 10 isolated teeth; four left lower m1 and six right lower m1.

Description and discussion: 204 isolated teeth show the typical traits of the genus *Ellobius* (Miller, 1896; Hinton, 1926; Kretzoi, 1969; Coşkun, 2016; Kryštufek and Shenbrot, 2016; Kryštufek and Vohralík, 2009; Rusin, 2017; Shenbrot et al., 2016; Tesakov, 2016). *Ellobius* molars are notably characterized by the presence of roots that are well visible in adults and old individuals, but not always apparent in young specimens (Coşkun, 2016). Moreover, *Ellobius* molars lack cement in the re-entrant angles. The *Ellobius* m1 is composed of the anterior cap (AC), five triangles (T) with three buccal and four lingual salient angles, and one posterior lobe (PL). Both M3 and m3 are reduced and smaller than the other molars, with three triangles on the labial side and two triangles on the lingual side. M1 has three inner and outer folds, and M2 and M3 have two inner and two outer re-entrant folds. The first and second upper molars have three triangles on the lingual and labial sides. However, the re-entrant angle between the first and the second triangles on the lingual side is more superficial (Gharkheloo and Kıvanç, 2003).

In Iran, the genus *Ellobius* is currently represented by three species: *Ellobius fuscocapillus*, *Ellobius lutescens* and *Ellobius talpinus* (Firouz, 2005; Kryštufek and Shenbrot, 2016; Kryštufek and Vohralík, 2009; Moradi Gharkheloo, 2003; Rusin, 2017; Shenbrot et al., 2016). The m1 is quite similar among these species, but there are some differences that can help us to differentiate them.

The AC is broad in *Ellobius lutescens*, narrow in *Ellobius talpinus* and elongated in *Ellobius fuscocapillus* (Maul et al., 2015b). The distance between T4 and T5 (W) and the total length (L) differ among the species (Table 5). We have observed in modern specimens from the Natural History Museum of London that *Ellobius fuscocapillus* is the largest and *Ellobius talpinus* the smallest.

In our sample we identify as *Ellobius* spp. those m1s that are too broken or digested to distinguish, as well as all the m2, m3, M1, M2 and M3 because of the lack of discriminant characters. The identification of *Ellobius lutescens* and *Ellobius fuscocapillus* in the Kaldar



Fig. 2. Some rodent species identified at Kaldar Cave in comparison with equivalent (analogue) modern specimens from the NHM of London. **1) *Microtus irani***: 1.1-Kaldar Cave, 2014, Layer 5 (sub-layer 7II), E7, 150–156, right lower m1, number 447.1.2-modern, NHM205207, Iran (Shiraz), right lower m1; **2) *Microtus guentheri***: 2.1-Kaldar Cave, 2014, Layers 1–3 (sub-layer 4II), F6, 97–107, left lower m1, number 17; **3) *Microtus socialis***: 3.1-Kaldar Cave, 2014, Layer 4 (sub-layer 5II), F7, 115–118, right lower m1, number 106.3.2-modern, NHM631799, Turkey (Amasya); **4) *Chionomys nivalis***: 4.1-Kaldar Cave, 2014, Layer 4 (sub-layer 5), E6, 94–104, left lower m1, number 542.4.2-modern, NHM71820, Syria, left lower m1; **5) *Ellobius fuscocapillus***: 5.1-Kaldar Cave, 2014, Layer 4 (sub-layer 5II), E6, 125–130, right lower m1, number 157.5.2-modern, NHM86101513, Afghanistan, right lower m1; **6) *Ellobius lutescens***: 6.1-Kaldar Cave, 2014, Layer 5 (sub-layer 7II), F6, 130–140, right lower m1, number 319.6.2-NMH916416, Turkey, right lower m1; **7) *Cricetulus migratorius***: 7.1-Kaldar Cave, 2014, Layer 4 (sub-layer 5II), E6, 135–140, left lower m1, number 259.7.2-modern, NHM773029, Iran, right lower m1; **8) *Mesocricetus brandti***: 8.1-Kaldar Cave, 2014, Layer 5 (sub-layer 7II), F6, 135–145, left upper M1, number 549.8.2- modern, NHM193461226, Caucasus, left upper M1; **9) *Meriones* cf. *persicus***: 9.1-Kaldar Cave, 2014, Layer 5 (sub-layer 7II), F6, 156–166, left lower m1, number 551.9.2-modern, NHM510434, Iran, left lower m1; **10) *Allactaga* sp.**: 10.1-Kaldar Cave, 2014, Layer 5 (sub-layer 7II), E7, 141–147, right lower m3, number 203; **11) *Myomimus* sp.**: 11.1- Kaldar Cave, 2014, Layer 5 (sub-layer 7II), E7, 141–147, left lower m1 and m2. 11.2-modern, ***Myomimus personatus***, NHM67623, Turkey, left lower mandible; **12) *Apodemus* sp.**: 12.1-Kaldar Cave, 2014, Layer 4 (sub-layer 5), E6, 94–104, right m1 and m2, number 547; **13) *Mus* cf. *musculus***: 13.1-Kaldar Cave, 2014, Layer 5 (sub-layer 7II), 166–174, left lower m1, number 495. Scale 1 mm.

material is based on the morphology of the AC and the measurements (L and W). We do not identify *Ellobius talpinus* in our sample, as no specimen displays morphological features characteristic of this species, such as the narrow AC, and because the measured specimens are larger than *E. talpinus*.

Habitat and distribution: *Ellobius* species frequent steppes, grasslands and semi-deserts in eastern Europe and central Asia; these fossorial species are specialised in subterranean life (Coşkun,

Table 4
Measurements of *Microtus* specimens (in mm): NS, number of specimens; L, length; La, T4 width; Li, T5 width.

Species	NS	L (Length)		La (Width T4)		Li (Width T5)		Total Width	
		Mean	Min-Max	Mean	Min-Max	Mean	Min-max	Mean	Max-Min
Reference collection									
Microtus irani	4	3.06	2.98–3.23	0.42	0.40–0.44	0.64	0.62–0.67	1.06	1.03–1.08
Microtus socialis	69	2.78	2.29–3.34	0.42	0.32–0.51	0.6	0.44–0.73	1.02	0.78–1.19
Microtus arvalis	25	2.72	2.45–2.96	0.39	0.32–0.46	0.6	0.50–0.70	1	0.83–1.13
Microtus guentheri	70	2.58	2.2–3						
Kaldar Cave									
Microtus guentheri	17	2.52	2.18–3.01	0.35	0.27–0.43	0.54	0.40–0.68	0.90	0.70–1.10
Microtus irani	15	2.89	2.52–3.39	0.41	0.37–0.50	0.62	0.54–0.70	1.05	0.92–1.18
Microtus socialis	74	2.54	2.06–3.01	0.37	0.28–0.48	0.55	0.40–0.70	0.92	0.70–1.16

Table 5
Measurements of *Ellobius* specimens (in mm): L, total length; W, width. NHM: Natural History Museum of London. NISP: number of identified specimens.

		Ellobius fuscocapillus				*Ellobius lutescens*		*Ellobius talpinus*	
		Layer 5, NISP = 5	Layer 4, NISP = 5	Layer 1–3, NISP = 1	NHM, NISP = 12	Layer 5, NISP = 9	Layer 4, NISP = 10	NHM, NISP = 14	NHM, NISP = 14
L	**Min-Max**	3.29–3.84	3.73–3.74	–	3.06–4.05	3.08–3.32	3.05–3.4	3.07–3.3	2.86–3.35
	Mean	3.45	3.74	–	3.53	3.28	3.29	3.21	3.12
W	**Min-Max**	1.32–1.51	1.40–1.54	–	1.3–1.59	1.20–1.45	1.13–1.48	1.11–1.52	1.09–1.72
	Mean	1.45	1.48	1.5	1.41	1.34	1.32	1.34	1.24

2016; Kryštufek and Vohralík, 2009). *Ellobius lutescens* is a Palaearctic species distributed across Iran, Iraq, Azerbaijan, Armenia, Transcaucasia and East Anatolia (Thomas, 1905; Ellerman and Morrison-Scott, 1951; Darlington, 1957; Osborn, 1962; Walker, 1964; Lay, 1967; Hassinger, 1973; Roberts, 1977; Corbet, 1978; Corbet and Hill, 1991; Wilson and Reeder, 2005; Coşkun, 1997, 2016; Nowak, 1999; Kryštufek and Shenbrot, 2016). In Iran, this species is found in mountain grasslands, sandy semi-deserts and steppe areas (Kryštufek and Shenbrot, 2016; Tesakov, 2016). *Ellobius fuscocapillus* shows a wide range across eastern Iran, Turkmenistan, Afghanistan and Pakistan. In Iran it is found in open steppes with loose soil (Shenbrot et al., 2016).

Subfamily Cricetinae Fischer, 1817

Genus *Cricetulus* Milne-Edwards, 1867

***Cricetulus migratorius* Pallas, 1773**

Material: 19 isolated teeth. **Layer 1–3:** one isolated tooth; one right lower m3. **Layer 4:** 13 isolated teeth; three left lower m1, two left upper M2; three right lower m1, three right upper M1 and two right upper M2. **Layer 5:** five isolated teeth; three left lower m1 and two right lower m1.

Description and discussion: the first molars (m1 and M1) are brachyodont and cuspidate, with two longitudinal series of cusps. Each series of cusps consists of three pairs. The m1 and M1 are the largest and the m3/M3 the smallest. The lower m3 only has two pairs of cusps (Kryštufek and Vohralík, 2009). We identify *Cricetulus migratorius* in all the layers of Kaldar Cave in accordance with the measurements and identification keys for molars based on the morphology and arrangement of the tubercles and cusps provided by Kryštufek and Vohralík (2009). We also draw comparisons with the reference collection from Iran, Afghanistan and Azerbaijan housed in the Natural History Museum of London. The gray hamster, or migratory hamster, is the smallest hamster species (Bogicevic et al., 2011; Sándor, 2018).

Habitat and distribution: *Cricetulus migratorius* extends from eastern Europe through Russia and central Asia to Mongolia and western China (Kryštufek et al., 2017; Kryštufek and Vohralík, 2009). In Iran, this species is found all over the country. The habitats of this species are mostly dry grasslands, steppes and semi-deserts. Arid areas with relatively sparse vegetation are preferred (Kryštufek et al., 2017; Maul et al., 2015a).

Genus *Mesocricetus* Nehring, 1898

***Mesocricetus brandti* Nehring, 1898**

Material: 10 isolated teeth. **Layer 4:** three isolated teeth; one left upper M1, one right lower m1 and one right upper M1. **Layer 5:** seven isolated teeth; four left upper M1, one right upper M2 and two right upper M1.

Description and discussion: the specimens from Kaldar Cave are attributed to *Mesocricetus brandti* on the basis of the size and morphology of the teeth. The molars present a similar morphological pattern to *Cricetulus migratorius*, but are significantly larger in size. The first molars have six tubercles, the second and third molars only four. The largest molars are m1 and M1, whereas m2/M2 and m3/M3 are reduced (Kryštufek and Vohralík, 2009). In Iran we also find *Mesocricetus raddei*, which presents a similar morphology of the teeth to *Mesocricetus brandti*, but compared with the NHM reference collection of the latter, *Mesocricetus raddei* is bigger.

Habitat and distribution: *Mesocricetus brandti* has the largest distributional area of the species belonging to the genus *Mesocricetus*, ranging from Anatolia, Transcaucasia (Armenia, Georgia and Azerbaijan) and southeast Dagestan to northwest Iran (Qazvin in the east, Lorestan in the south; Lay, 1967). This species is found at altitudes from sea level up to 2600 m. However, the primary range is from 1000–2200 m. *Mesocricetus brandti* is found in arid and semi-arid steppe habitats in lowlands and in mountainous areas (Kryštufek et al., 2015; Kryštufek and Vohralík, 2009; Neumann et al., 2017).

Family Muridae Illiger, 1811

Subfamily Gerbillinae Gray, 1825

Genus *Meriones*, Illiger 1811

***Meriones* cf. *persicus* Blanford, 1875**

Material: 157 isolated teeth. **Layer 1–3:** three isolated teeth; two left upper M1 and one right lower m1. **Layer 4:** 65 isolated teeth; 21 m^2; four m3; 17 left lower m1; eight right upper M1, five left upper M1; 10 right lower m1. **Layer 5:** 88 isolated teeth; eight m3; 21 m^2; 18 left lower m1, 10 left upper M1, 16 right upper M1

and 15 right lower m1.

Description and discussion: the genus *Meriones* is one of the most diverse among the tribe Gerbillini in the Palaearctic region, particularly in arid regions of Asia (Darvish et al., 2011; Denys, 2017). The *Meriones* species reported in Iran are: *Meriones crassus*, *Meriones hurrianae, Meriones lybicus, Meriones meridianus, Meriones persicus, Meriones tristrami, Meriones vinogradovi* and *Meriones zarudnyi* (Darvish, 2011; Dianat et al., 2017; Kryštufek and Vohralík, 2009; Souttou and Denys, 2012).

The material from Kaldar Cave attributed to the genus *Meriones* displays the typical morphology of this group, including semi-hypsodont molars with prismatic enamel triangles linked by a longitudinal crest and with no trace of cusps. In our sample, we identify first upper molars (M1) with three roots, which is characteristic of *Meriones persicus* and *Meriones tristrami*. Unfortunately, the dental morphology of *Meriones persicus* and *Meriones tristrami* is very similar; there are three roots in m1, the second molars have two transverse plates and two roots, whereas the third molars are simple and rounded with a single root (Coşkun, 2016; Kryštufek and Vohralík, 2009).

Given its current distribution and the morphological traits observed in the reference collection from Iran, Azerbaijan and Pakistan housed in the Natural History Museum of London, we provisionally attribute our specimens to *Meriones* cf. *persicus,* especially in the light of the number of roots and the morphology of M1 and m1, pending a revision of the Middle Eastern species of the genus.

Habitat and distribution: the genus *Meriones* is distributed across North Africa, Central Asia, Transcaucasia, Turkey and Pakistan (Darvish et al., 2014; Stoetzel et al., 2017). It lives mostly in dry steppes of short or tall grass, on open hillside, among rocky outcrops in desolate steppes, or in open dry meadows. The distribution of *Meriones persicus* ranges from the Caucasus (including the southeastern foothills of the Lesser Caucasus and the Talysh Plateau in Azerbaijan) in the west, through northeastern Iraq and Iran to Turkmenistan, Afghanistan (Habibi, 2004) and Pakistan, where it is widely distributed. It generally occurs in arid, rocky or mountainous regions (Kryštufek and Vohralík, 2009; Molur and Sozen, 2016).

Family Dipodidae Fischer, 1817

Genus *Allactaga* Cuvier, 1837

***Allactaga* sp.**

Material: two isolated teeth. **Layer 4:** one indet. **Layer 5:** one right lower m3.

Description and discussion: this rodent group is poorly known in the Middle East (Shenbrot, 2009) and sometimes there is a size overlap between the species. In our sample, we only found two items attributed to *Allactaga* sp. on the basis of the complete lower m3, which presents a morphology with two inner folds and one outer fold; the other tooth is broken, which prevents any precise identification.

Habitat and distribution: in Iran four species are currently present: *Allactaga elater*, *Allactaga euphratica*, *Allactaga firouzi* and *Allactaga hotsoni* (Karami et al., 2008). The different species are morphologically very close and remain poorly studied. They are mainly found in steppe vegetation and semi-desert areas (Shenbrot, 2009).

Family Gliridae Thomas, 1897

Genus *Myomimus* Ognev, 1924

***Myomimus* sp.**

Material: five isolated teeth, **Layer 5:** five isolated teeth, one right lower m1, three right lower m2 and one left lower m2.

Description and discussion: the genus *Myomimus* is present in Iran with two species, *Myomimus personatus* and *Myomimus setzeri* (Firouz, 2005; Gerrie and Kennerley, 2017; Karami et al., 2008; Kennerley and Kryštufek, 2019). Regarding the remains found at Kaldar, the m1 is of a trapezium-like shape, and its anterior part tends to be narrower than the posterior part. The m1 has three roots, two in the anterior part and one in the posterior part. The m2 is subrectangular, and its occlusal pattern is simpler than in the m1. There are three roots in total, two in the anterior part and one in the posterior part (Kaya and Kaymakçı, 2018; Kryštufek and Vohralík, 2009). The two species are similar to one another and poorly studied. Consequently, we were unable to identify the Kaldar material precisely. Moreover, the reference collection of the Natural History Museum of London only houses *Myomimus personatus* specimens, which could therefore not be compared with *Myomimus setzeri*.

Habitat and distribution: these species are not well known as regards their distribution. They are mainly found in desert areas (Gerrie and Kennerley, 2017; Kennerley and Kryštufek, 2019).

Family Muridae Illiger, 1811

Genus *Apodemus* Kaup, 1829

***Apodemus* sp.**

Material: 13 isolated teeth. **Layer 1**–**3:** two isolated teeth; one left lower m1 and one left lower m2; **Layer 4:** six isolated teeth; three left lower m1, two right lower m1 and one left upper M1. **Layer 5**: five isolated teeth; two left lower m1, one right lower m1, one right upper M1 and one m2.

Description and discussion: the first lower molar (m1) can be seen to present a low occlusal surface with six main cusps. The anterolabial and posterolabial cusps of m1 converge in an X-shape. The posterior cusp of m1 is low, rounded and well developed, with two or three secondary cusps in the labial part, and a mesial tubercle. We attribute the remains found in Kaldar Cave to *Apodemus* sp. because they present the traits characteristic of the genus *Apodemus* (Amori et al., 2016; Bogicevic et al., 2011; Knitlová and Horáček, 2017; Kryštufek and Vohralík, 2009; López-García, 2011).

Habitat and distribution: five *Apodemus* species are currently recognized in Iran: *A. hyrcanicus*, *A. flavicollis*, *A. witherbyi*, *A. avicennicus* and *A. uralensis*, all belonging to the *Sylvaemus* sub-genus (Jangjoo et al., 2011). *Apodemus* has a large distribution range extending from Great Britain across much of continental Europe to the Urals. It also extends east through Turkey to western Armenia, the Zagros Mountains of Iran and south to Syria, Lebanon and Israel. It inhabits a variety of woodland habitats (Amori et al., 2016).

Genus *Mus* Linnaeus, 1758

***Mus* cf. *musculus* Linnaeus, 1758**

Material: three isolated teeth. **Layer 4**: one isolated tooth; one left upper M1. **Layer 5:** two isolated teeth; one indeterminate and one left lower m1.

Description and discussion: as in other murines, the first upper molar (M1) has three rows of tubercles: the first (t1, t2, t3) and second (t4, t5 and t6) groups situated in the anterior part have three tubercles, and the third group (t7 and t9) has two tubercles (Darviche et al., 2006). In Iran (Kryštufek and Vohralík, 2009) both *Mus musculus domesticus* and *Mus macedonicus* may be found.

The specimens from Kaldar Cave fit well with *M. musculus* as regards the upper M1 morphology: the lingual row of cusps (t1 and t4) is shifted posteriorly; cusp t7 is reduced to an enamel ridge; distal cusps t8 and t9 leave no space for a posterior cingulum or posterolabial cusp t12 (Siahsarvie and Darvish, 2008). The dental ends of the mesial and central cusps on m1 fuse early; the mesiolabial cusp is small. Upper molars normally have three roots each, one lingual and two labial, whereas lower molars are two-rooted (one anterior and one posterior) (Kryštufek and Vohralík, 2009).

Despite these observations, bearing in mind the high intra-specific morphological variability, the low quantity of material and the bad state of preservation of some teeth (Fig. 2.13), we only attribute the Kaldar material to *M.* cf. *musculus*.

Habitat and distribution: *Mus musculus* is a commensal species, well distributed throughout the world: it is present over all the continents except Antarctica. It is found in a wide range of habitats but tends not to be found in forest and deserts. *Mus musculus* is ecologically highly opportunistic but a weak competitor; it can cope with aridity and can also expand into the desert (Kryštufek and Vohralík, 2009). It is also found in arid habitats along the border with Syria and Iraq, in desert landscapes and near the Euphrates River (Kryštufek and Vohralík, 2009; Denys, 2017).

4.2. Taphonomic remarks

According to the different degrees of digestion (mostly light, moderate and, heavy in a few cases) observed in the molars previously studied by one of the authors (M. F.-G) and published in Bazgir et al. (2017), the predator responsible for this accumulation could be a category 3 predator such as the tawny owl (*Strix aluco*) or the Eurasian eagle owl (*Bubo bubo*). Both species are currently present in the area, have opportunistic hunting habits, and are sedentary, so their prey spectrum is assumed to be a good representation of the ecosystem in which they live.

4.3. Past landscape and climate at Kaldar Cave

The small-mammal assemblages from Layers 4 and 5 of Kaldar Cave are dominated by the genus *Microtus* (60 individuals in Layer 4 and 79 in Layer 5), followed by *Ellobius* in Layer 4 (17 individuals) and *Meriones* cf. *persicus* (17 individuals in Layer 4 and 18 in Layer 5). These species indicate that the environment in the area was mainly composed of open dry and steppe areas, although we also found *Apodemus* sp. and *Mus* cf. *musculus*, which are related rather to a dense vegetation cover (including trees/bush). All the species identified at Kaldar Cave still occur in the area today.

Layers 1–3 do not yield enough material to draw palaeoclimatic inferences (MNI < 30). For Layers 4 and 5, the *bioclimatic model* shows similar results (Table 6). It should be pointed out that some species are not included in the *BM* data matrix, such as *Myomimus* (present in Layer 4) and *Microtus guentheri* (Layer 5), because their values did not appear in the *BM* and could not be used in the analysis. The *BM* based on the small mammals from Kaldar Cave suggests lower temperatures and lower precipitation than at present in both Layers 4 and 5 (Table 6). The MAT is around 6 °C lower, and there is a higher temperature amplitude between maximum and minimum mean temperatures. This indicates that Layers 4 and 5 of Kaldar Cave were deposited during a colder period, which is not in agreement with the preliminary interpretations of Bazgir et al. (2017) suggesting a temperate "interstadial".

The climate in Khorramabad nowadays is warm and temperate. The mean annual temperature is 16.9 °C, the maximum mean temperature occurs in July with 29.6 °C and the minimum mean temperature is in January with 5 °C (https://en.climate-data.org/asia/iran/lorestan/khorramabad-764550/). This contrast with the climactic conditions inferred form the *BM* on Kaldar Cave with lower temperatures and drier conditions. For layer 5, mean annual temperature is 6 °C lower than nowadays, the maximum mean temperature 6.15 °C lower than the current values and the minimum mean temperature is 6.69 °C lower than the extant temperatures; the mean annual precipitation is 229.32 mm lower than at present. This tendency is also observable on the Layer 4 mean annual temperature is 5.17 °C lower than at present, the maximum mean temperature 6.5 °C lower than nowadays and the minimum mean temperature is 4.75 °C lower than the extant temperatures; the mean annual precipitation is 383.92 mm lower than at present. (Table 6). Comparing both levels Layer 5 is slightly colder than Layer 4, and Layer 4 is drier than Layer 5.

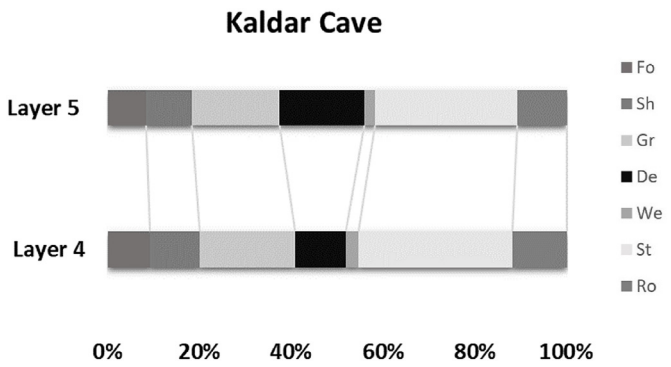


Fig. 3. Results of the *habitat weighting method* for Kaldar Cave (Layer 4 and Layer 5). Forest (Fo), Shrubland (Sh), Grassland (Gr), Desert (De), Wetland (We), Steppe (St) and Rocky (Ro).

Applying the *habitat weighting method*, our data show a palaeoenvironment mainly composed of steppes in both levels. In Layer 4, grasslands are also well represented, notably through the presence of *Microtus guentheri*. In Layer 5, deserts are the second most represented habitat, thanks to the considerable presence of *Myomimus* sp. The proportion of rocky areas is also significant, indicated by the presence of *Chionomys nivalis* and *Meriones* cf. *persicus* (Fig. 3).

There thus seems to be no major palaeoenvironmental or palaeoclimatic change that can explain the cultural shift between Layer 5 (Middle Palaeolithic) and 4 (Upper Palaeolithic). However, as also observed with the climatic parameters, Layer 5 appears slightly colder and drier than Layer 4, with a higher proportion of desert habitats.

We can compare these results with previous studies carried out in Kaldar Cave using other palaeoenvironmental proxies. Charcoal analyses (Allué et al., 2018; Bazgir et al., 2017) indicate that there were active water sources or flows, with specific plant communities characteristic of open forest growing in cool and dry conditions (Allué et al., 2018). The presence of forested areas is also supported by the large mammals, with the presence of *Sus scrofa*, *Capreolus* sp. and *Cervus elaphus* (Bazgir et al., 2017). Several amphibian and squamate species have also been found (Bazgir et al., 2017): a toad

Table 6
Bioclimatic model estimates for Kaldar Cave. SD, standard deviation. Δ (difference between the values obtained by analysing the rodents from Kaldar Cave and current values).Current values obtained from: https://en.climate-data.org/asia/iran/lorestan/khorramabad-764550/.

	Layer 5	SD	Δ	Layer 4	SD	Δ	Current values
Mean annual temperature	10.90 °C	3.39	−6 °C	11.73 °C	3.39	−5.17 °C	16.90 °C
Maximum mean temperature	23.45 °C	4.77	−6.15 °C	23.10 °C	4.77	−6.5 °C	29.60 °C
Minimum mean temperature	−1.69 °C	4.66	−6.69 °C	0.25 °C	4.66	−4.75 °C	5 °C
Mean annual precipitation	258.68 mm	533.24 mm	−229.32 mm	104.08 mm	533.24 mm	−383.92 mm	488 mm

(*Bufo* sp.), an agamid lizard (Agamidae indet.), a gecko (Gekkonidae indet.), a skink (Scincidae indet.), a lacertid (Lacertidae indet.), a glass lizard (*Pseudopus* sp.), a sand boa (*Eryx* sp.), possibly six types of colubrine snakes (Colubrinae indet.), a cobra (Elapidae indet.), and a viper (Viperidae indet.). Most of these taxa (Agamidae, *Eryx* and Elapidae) live in savannahs, steppes and deserts, with a way of life always linked with warm arid areas in rocky or sandy environments. *Pseudopus* lives in dry and bushy environments, sometimes in open woodlands, but avoids dense forest areas (Bazgir et al., 2017).

Our results based on small mammals, combined with previous studies of other proxies, thus suggest a mosaic landscape alternating between dry-steppe areas and wooded patches. Nowadays, the vegetation in the Zagros is a montane grassland-woodland characterized by steppe of grassland and herbs with occasional to fairly common trees. The principal local trees are deciduous oaks and junipers, with maples, walnut, almond and ash at middle elevations, and *Pistacia* and *Olea* in drier areas (Fiacconi and Hunt, 2015). Thus, the landscape during the Middle and Upper Pleistocene at Kaldar Cave was similar to that today, despite a colder climate.

4.4. Kaldar Cave in the Middle Eastern context

Kaldar Cave is situated in the Khorramabad Valley, which played a significant role in human adaptation and dispersal during the Quaternary. Some other caves close to Kaldar, such as Gilvaran, Ghamari and Gar Arjene rock shelter, have yielded Mousterian and Aurignacian occupations (Bazgir et al., 2014). Moreover, surveys in Kermanshah have also documented Middle and Upper Palaeolithic sites (Heydari-Guran and Ghasidian, 2020). None of them has given rise to small-mammal studies. However, Gilvaran Cave has been studied from a palaeoenvironmental point of view through charcoal analyses (Allué et al., 2018), showing a similar pattern to Kaldar, where *Prunus* is also present and indicates the presence of open forest areas. Similarly, other proxies such as pollens and charcoals have been analysed at Shanidar (Campana and Crabtree, 2019; Fiacconi and Hunt, 2015) and Gilvaran (Allué et al., 2018), indicating similar environmental conditions to Kaldar.

Other studies based on small mammals from the Middle East have been performed in Qesem Cave (Maul et al., 2015a; Smith et al., 2016), Hummal (Maul et al., 2015b), Azokh Cave (Fernández-Jalvo, 2016a,b), Aghitu-3 Cave (Frahm, 2019; Kandel et al., 2017; Nishiaki and Akazawa, 2018), Nesher Ramla (Weissbrod and Zaidner, 2014), Amud Cave (Belmaker and Hovers, 2011), Dzudzuana Cave (Belmaker et al., 2016) and Karain Cave (Demirel et al., 2011). These studies did not use *HW* or the *BM* for their palaeoclimatic and palaeoenvironmental reconstructions, and the sites are not always contemporary with Kaldar, except Amud Cave (Belmaker and Hovers, 2011), Aghitu-3 (Djamali et al., 2008; Kandel et al., 2017) and Dzudzuana Cave (Belmaker et al., 2016) (Table 7).

Most of these studies highlight problems in identifying Middle Eastern rodent species, as faced in the present work. There are some studies of present-day taxonomy and systematics in Iran, Turkey, Israel, Jordan, Lebanon and Syria (Abi-said et al., 2014; Darvish et al., 2000; Haddadian Shad et al., 2014; Kopij and Livenschulman, 2013; Obuch and Khaleghizadeh, 2012; Shehab et al., 2013), but these are mostly based on skull morphology and thus not applicable in archaeological or palaeontological contexts where the remains are broken. Very few studies provide descriptions of molars with comparative elements, allowing for the correct identification of fossil specimens. In this context, comparison with modern specimens from museum collections of genetically typed specimens is crucial to establish a correct taxonomic reference.

Palaeoenvironmental inferences have been drawn on the basis of small-mammal studies, as well as palynological and anthracological analyses. During the Upper Pleistocene, small-mammal compositions differ from one site to another (Belmaker et al., 2016; Kandel et al., 2017) (Table 8), probably because the sites are not exactly contemporaneous and are likely to belong to different eco-regions. It is noteworthy that the genera *Microtus*, *Chionomys*, *Cricetulus*, *Mesocricetus*, *Ellobius* and *Allactaga* are represented in all the sites, allowing us to reconstruct the species communities of this region. Kaldar is the most diverse site in terms of small-mammal species.

We applied the *habitat weighting method* at other Middle Eastern sites where small-mammal studies have been performed, namely Aghitu-3 and Dzudzuana Cave, but these are located in other eco-regions (Fig. 1a). Aghitu-3 is located in Armenian Highlands (46°08′22″ E, 39°51′38″ N), at an elevation of 1601 m a.s.l. and the current climate is continental with considerable seasonality in temperature. Dzudzuana Cave is located in Georgian Caucasus foothills (43°06′11″ E, 42°13′27″ N), at an elevation of 560 m a.s.l., and the current climate is warm and temperate. The estimations obtained with the *habitat weighting method* (Fig. 4) show similar environmental conditions between Kaldar Cave and Aghitu-3, where the landscape is dominated by steppe (indicated by the presence of *Ellobius lutescens*, *Mesocricetus brandti*, *Cricetulus migratorius* and *Allactaga*), with a relatively high percentage of grassland and forests.

To ascertain the palaeoclimatic conditions, we calculated and directly compared our results with Aghitu-3 and Dzudzuana Cave using the *bioclimatic method* (Table 9). The results obtained for Aghitu-3 show higher temperatures and precipitation than at present, whereas Dzudzuana Cave shows the same pattern as Kaldar Cave, with drier conditions and lower temperatures than today. For Amud Cave, it was not possible to calculate *HW* and *BM*, but data from the literature (Belmaker and Hovers, 2011) indicate a grassland environment similar to the one that we reconstructed at Dzudzuana Cave.

Table 7
Comparison between Middle Eastern sites with small-mammal studies.

Site/Author	Layer	Human culture	Chronology	Environmental conditions	Rodent
Amud Cave (Belmaker and Hovers, 2011)	B4	Neanderthals	68.5 ± 3.4ka	Grassland vegetation	*Microtus guentheri*
	B2 −B1	Neanderthals	56.5 ± 3.5, 57.6 ± 3.7,respectively	Woodland	*Apodemus* cf. *mystacinus* and *Mus macedonicus*
Dzudzuana Cave (Belmaker et al., 2016)	Unit C	Modern human	27-24ka cal BP	Mild and humid	*Microtus*, *Ellobius*, *Arvicola*, *Apodemus* and *Allactaga*.
Aghitu-3 (Djamali et al., 2008; Kandel et al., 2017)	Level VII-III	Modern human	The oldest layer is VII with a chronology between 39-36,000 cal BP and the most recent is layer III, between 29-24,000 cal BP	This sequence documents that the climate becomes colder	*Microtus* spp., *Chionomys* sp., *Arvicola amphibius* and *Ellobius lutescens*

Table 8
Comparison of the small-mammal lists from several Upper Palaeolithic sites in the Middle East.

Taxon	Kaldar Cave			Aghitu-3				Dzudzuana
	Layers 1-3	Layer 4	Layer 5	VII	VI	V-IV	III	Unit C
Microtus spp.	X	X	X	X	X	X	X	
Microtus cf. *arvalis*								X
Microtus irani	X		X					
Microtus guentheri	X	X						
Microtus socialis	X	X	X					
Chionomys nivalis	–	X	X	X	X	X	X	X
Clethrionomys glareolus								X
Ellobius spp.	X	X	X					
Ellobius fuscocapillus	X	X	X					
Ellobius lutescens	–	X	X	X				X
Cricetus cricetus								X
Cricetulus migratorius	X	X	X	X		X	X	X
Mesocricetus brandti		X	X	X	X	X	X	X
Meriones cf. *persicus*	X	X	X					
Allactaga sp.		X	X	X	X		X	X
Myomimus sp.			X					
Apodemus sp.	X	X	X					X
Mus musculus		X	X					X
Arvicola amphibius				X	X	X	X	X

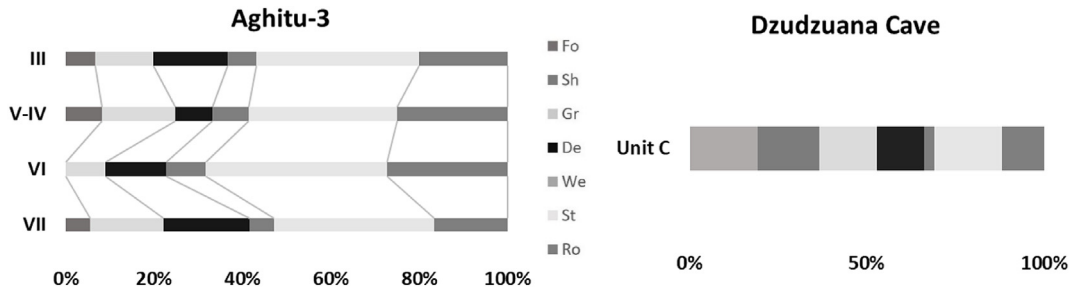


Fig. 4. Results of the *habitat weighting method* for Aghitu-3 and Dzudzuana Cave. Forest (Fo), Shrubland (Sh), Grassland (Gr), Desert (De), Wetland (We), Steppe (St) and Rocky (Ro).

Table 9
Estimates using the *bioclimatic method* for Aghitu-3 and Dzudzuana Cave. SD, standard deviation. Current values obtained from Kandel et al. (2017) for Aghitu-3 and https://es.climate-data.org/asia/georgia/imereti/jria-414325/?amp=true for Dzudzuana Cave.

	Aghitu-3						Dzudzuana Cave		
	VII	VI	V-IV	III	SD	Current Values	Unit C	SD	Current Values
Mean annual Temperature	15.46 °C	19.44 °C	19.21 °C	17.87 °C	3.386	8.5 °C	5.09 °C	3.39	9.7 °C
Maximum mean temperature	23.59 °C	24.44 °C	24.09 °C	24 °C	4.772	20.2 °C	18.55 °C	4.77	20.3 °C
Minimum mean temperature	7.31 °C	14.67 °C	14.72 °C	11.96 °C	4.656	−3.8 °C	−8.26 °C	4.66	−1.6 °C
Mean annual precipitation	1169.04 mm	1729.48 mm	1825.99 mm	1484.60 mm	533.236	532 °C	194.98 mm	533.24	868 mm

5. Conclusions

This work represents the first study of a Late Pleistocene rodent assemblage from the Middle East with palaeoenvironmental and palaeoclimatic reconstructions, using and adapting the *habitat weighting method* and the *bioclimatic model* to this area. We identified 1112 rodent remains, corresponding to a minimum number of 264 individuals. The rodent assemblage is composed of 13 taxa: six arvicoline (*Microtus socialis, Microtus irani, Microtus guentheri, Chionomys nivalis, Ellobius fuscocapillus* and *Ellobius lutescens*), two cricetine (*Cricetulus migratorius* and *Mesocricetus brandti*), one glirid (*Myomimus* sp.), one gerbilline (*Meriones* cf. *persicus),* one dipodid (*Allactaga* sp.) and two murine species (*Apodemus* sp. and *Mus* cf. *musculus*). Augmenting the preliminary analysis of the material (Bazgir et al., 2017), new species were identified, such as *Microtus socialis*, *Microtus irani*, *Microtus guentheri*, *Ellobius fuscocapillus* and *Meriones* cf. *persicus*. We also reconsidered the identification of *Ellobius talpinus*, *Calomyscus* sp. and *Dryomys* cf. *nitedula*, based on modern specimens from museum collections and measurements; this is why they do not appear in the new faunal list of Kaldar Cave.

Given the scarcity of studies in this biogeographical region, we encountered some difficulties in the identification of species, which could slightly affect the palaeoenvironmental and palaeoclimatic interpretations. In order to counter these potential errors, further studies of small mammals in this region are necessary, as well as research on discriminant characters in molars, using reference collections including genetically typed specimens.

The palaeoecological analysis of the rodents from Kaldar Cave revealed lower temperatures and lower precipitation than present-day conditions, and an environment mainly composed of dry steppes with patches of forested areas. The results obtained are supported by palynological, anthracological and large-mammal studies. At a broader geographical scale, colder conditions were

also inferred at Dzudzuana Cave. The genera *Microtus*, *Chionomys*, *Cricetulus*, *Mesocricetus*, *Ellobius* and *Allactaga* are present at all the Middle East sites (Aghitu-3, Dzudzuana and Amud) during the Upper Pleistocene, that have yielded small mammals, allowing us to reconstruct the rodent communities of the area.

Considering all the results from Kaldar Cave and other contemporaneous sites, we can conclude that both Neanderthals and AMH lived in dry steppes with patches of forested areas, without major environmental changes occurring between the Middle and the Late Palaeolithic. Climatic shifts during the MIS 4-3 transition were of a magnitude that did not have a major impact on small mammals in the region, suggesting that climate change may not have had the hypothesized effect on the Neanderthal extinction in the Levant.

Author statement

Regarding the contributions of the authors I.R.R. and J.M.L-G. analysed the rodent assemblage and wrote the article; H.B. analysed amphibian and squamate species, M.F.G performed taphonomic studies; C.D., E.S., L.T, A.O. and B.B. designed the research.

Declaration of competing interest

The authors declare that they have no known competing financial interests or personal relationships that could have appeared to influence the work reported in this paper.

Acknowledgments

I. Rey-Rodriguez is the beneficiary of a PhD scholarship funded by the Erasmus Mundus Program (IDQP). J.M. López-García was supported by a Ramón y Cajal contract (RYC-2016-19386) with financial sponsorship from the Spanish Ministry of Science, Innovation and Universities. M. Fernández-García is the beneficiary of a PEJ gran(PEJ20t 18-005222-P) funded by the Spanish National Youth Guarantee System and the European Social Fund. This work was developed within the framework of the projects 2017SGR859, 2017SGR840 and 2017SGR1040 (AGAUR, Generalitat de Catalunya), and 2018PFRURVB291 (Univ. Rovira i Virigli). We thank the head of the Research Institute of Cultural Heritage and Tourism (RICHT) (Dr. B. Omrani) and the head of the Iranian Center for Archaeological Research (ICAR) (Dr. R. Shirazi) for providing us with the necessary support and permissions in studying the materials. We thank the head of the Lorestan Cultural Heritage, Handicraft and Tourism Organization (Mr. A. Ghasemi) for all his support. We also thank the head of International Collaboration and Ties of the RICHT (Mrs. M. Kholghi) for all her cooperation and help. B. Bazgir received his PhD scholarship from the Fundación Atapuerca, for which he is grateful. Laxmi Tumung received her PhD scholarship from the Erasmus Mundus Programme (IDQP). We would like to thank Roberto Portela Miguez, Senior Curator in Charge of Mammals, for his help with the reference collection in the Natural History Museum of London. We would like to thank Rupert Glasgow for reviewing the English language of the manuscript. We also want to thank to the Editor Prof. José S. Carrión and the two anonymous reviewer for their comments and suggestions that strongly improve the final version of the manuscript.

Appendix 1

Climatic Parameters	b	aII	aII/III	aIII	aIV	aV	aVI	aVII	aVIII	aIX	SE
Mean annual temperature in °C (MAT)	26.686	0.024	−0.029	−0.024	−0.074	−0.12	−0.135	−0.217	−0.404	−0.386	3.637
Mean temperature of the warmest month in °C (MTW)	26.219	0.07	0.021	0.02	0.031	−0.212	−0.113	−0.037	−0.121	−0.287	4.754
Mean temperature of the coldest month in °C (MTC)	27.538	−0.033	−0.096	−0.08	−0.175	−0.032	−0.141	−0.418	−0.71	−0.465	5.081
Mean annual precipitation in mm (MAP)	2978.195	−21.237	−27.563	−33.05	−32.648	−6.678	−5.076	−28.4	−33.109	−25.98	470.615

b: intercept.
aIV-aIX: slopes of the different bioclimatic components.
SE: standard error of estimate.
Modified from Hernández Fernández (2001) and Hernández Fernández and Peláez-Campomanes (2003).

References

Abi-Said, M.R., Shehab, A.H., Amr, Z.S., 2014. Diet of the barn owl. Jordan J. Biol. Sci. 7 (2), 109–112.

Allué, E., Expósito, I., Tumung, L., Ollé, A., Bazgir, B., 2018. Early evidence of *Prunus* and *Prunus* cf. *amygdalus* from palaeolithic sites in the Khorramabad valley, western Iran. Comptes Rendus Palevol 17, 335–345. https://doi.org/10.1016/j.crpv.2018.01.001.

Amori, G., 1999. Chionomys nivalis. In: Mitchell-Jones, A.J., Amori, G., Bogdanowicz, W., Kryštufek, B., Reijnders, P.J.H., Spitzenberger, F., Stubbe, M., Thissen, J.B.M., Vohralík, V., Zima, J. (Eds.), The Atlas of European Mammals. Academi Press, London, UK.

Amori, G., Hutterer, R., Kryštufek, B., Yigit, N., Mitsain, G., Palomo, L.J., 2016. Apodemus flavicollis. The IUCN Red List of Threatened Species 2016. https://doi.org/10.2305/IUCN.UK.2016-3.RLTS.T1892A22423256.en e.T1892A115058023. 8235.

Amr, A., 2015. *Microtus Guentheri*. The IUCN Red List of Threatened Species 2016 e.T13463A22349143.

Andrews, P., 1990. Owls, Caves and Fossils. https://doi.org/10.2307/3889096.

Andrews, P., 2006. Taphonomic effects of faunal impoverishment and faunal mixing. Palaeogeogr. Palaeoclimatol. Palaeoecol. 241, 572–589. https://doi.org/10.1016/j.palaeo.2006.04.012.

Aşan Baydemir, N., Duman, L., 2009. Molar patterns in *Microtus guentheri* (Danford and Alston, 1880) (Mammalia: Rodentia) from Kirikkale province. J. Appl. Biol. Sci. 3, 47–54.

Bazgir, B., Ollé, A., Tumung, L., Becerra-Valdivia, L., Douka, K., Higham, T., Van Der Made, J., Picin, A., Saladié, P., López-Garciá, J.M., Blain, H.-A., Allué, E., Fernández-Garciá, M., Rey-Rodríguez, I., Arceredillo, D., Bahrololoumi, F., Azimi, M., Otte, M., Carbonell, E., 2017. Understanding the emergence of modern humans and the disappearance of Neanderthals: insights from Kaldar cave (Khorramabad valley, western Iran). Sci. Rep. 7 https://doi.org/10.1038/srep43460.

Bazgir, B., Otte, M., Tumung, L., Ollé, A., Deo, S.G., Joglekar, P., López-García, J.M., Picin, A., Davoudi, D., van der Made, J., 2014. Test excavations and initial results at the middle and upper paleolithic sites of Gilvaran, Kaldar, Ghamari caves and Gar Arjene Rockshelter, Khorramabad Valley, western Iran. Comptes Rendus Palevol 13, 511–525. https://doi.org/10.1016/j.crpv.2014.01.005.

Becerra-Valdivia, L., Douka, K., Comeskey, D., Bazgir, B., Conard, N.J., Marean, C.W., Ollé, A., Otte, M., Tumung, L., Zeidi, M., Higham, T.F.G., 2017. Chronometric investigations of the Middle to Upper Paleolithic transition in the Zagros Mountains using AMS radiocarbon dating and Bayesian age modelling. J. Hum. Evol. 109, 57–69. https://doi.org/10.1016/j.jhevol.2017.05.011.

Belmaker, M., Bar-Yosef, O., Belfer-Cohen, A., Meshveliani, T., Jakeli, N., 2016. The environment in the Caucasus in the upper paleolithic (late Pleistocene): evidence from the small mammals from Dzudzuana cave, Georgia. Quat. Int. 425, 4–15. https://doi.org/10.1016/j.quaint.2016.06.022.

Belmaker, M., Hovers, E., 2011. Ecological change and the extinction of the levantine Neanderthals: implications from a diachronic study of micromammals from Amud cave, Israel. Quat. Sci. Rev. 30, 3196–3209. https://doi.org/10.1016/j.quascirev.2011.08.001.

Blain, H.-A., Bailon, S., Cuenca-Bescós, G., 2008. The Early–Middle Pleistocene palaeoenvironmental change based on the squamate reptile and amphibian proxies at the Gran Dolina site, Atapuerca, Spain. Palaeogeogr. Palaeoclimatol. Palaeoecol. 261, 177–192. https://doi.org/10.1016/j.palaeo.2008.01.015.

Bogicevic, K., Nenadic, D., Mihailovic, D., Lazarevic, Z., Milivojevic, J., 2011. Late Pleistocene rodents (Mammalia: Rodentia) from the baranica cave near Knjaževac (eastern Serbia): systematics and palaeoecology. Riv. Ital. Paleontol. Stratigr. 117 (2), 331–346.
Campana, D.V., Crabtree, P., 2019. Evidence for skinning and craft activities from the middle paleolithic of shanidar cave, Iraq. J. Archaeol. Sci.: Report 25, 7–14. https://doi.org/10.1016/j.jasrep.2019.03.024.
Corbet, G.B., 1978. In: The Mammals of the Palearctic Region: A Taxonomic Review. Brit. Mus.(Nat. Hist.). Cornell Univ. Press, London, pp. 117–118.
Corbet, G.B., Hill, J.E., 1991. A World List of Mammalian Species, third ed. British Museum (Natural History), London, UK.
Coşkun, Y., 2016. Review of unique odd chromosome-numbered underground rodent species of the Palearctic region: *Ellobius Lutescens* Thomas 1897 (Rodentia: Cricetidae). Turk. J. Zool. 40, 831–841. https://doi.org/10.3906/zoo-1509-53.
Coşkun, Y., 1999. Morphological characteristics of *Meriones tristrami* Thomas, 1892 (Rodentia: Gerbillinae) from Diyarbakır, Turkey. Turk. J. Zool. 23, 345–355.
Coşkun, Y., 1997. *Ellobius lutescens* Thomas, 1897 (Rodentia: Cricetidae) Turk. J. Zool. 21, 349–354.
Darlington, P.J., 1957. Zoogeography: the Geographical Distribution of Animals. John Wiley and Sons, New York, NY, USA.
Darviche, D., Orth, A., Michaux, J., 2006. *Mus spretus* et *M. musculus* (Rodentia, Mammalia) en zone méditerranéenne: Différenciation biométrique et morphologique: Application à des fossiles marocains pléistocènes. Mammalia 70, 90–97. https://doi.org/10.1515/MAMM.2006.010.
Darvish, J., Mohammadi, Z., Mahmoudi, A., Siahsarvie, R., 2014. Faunistic and taxonomic study of Rodents from northwestern Iran. Iran. J. Anim. Biosyst. 10, 119–136.
Darvish, J., 2011. Morphological comparison of fourteen species of the genus *Meriones* illiger , 1811 (Rodentia : Gerbillinae) from Asia and North Africa. Iran. J. Anim. Biosyst. 7, 49–74.
Darvish, J., Ghiyasi, R., Khosravi, M., 2000. Recognition of rodents of Robat Sharaf pellets owl by morphological and neontological studies. J. Sci. 12.
Denys, C., 2017. Subfamily Deomyinae, Gerbillinae, leimacomyinae, lophiomyinae species accounts. In: Wilson, D.E., Lacher, T.E., Mittermeier, R.A. (Eds.), Handbook of the Mammals of the World, vol. 7. Rodents II. Lynx Edicions, Barcelona, pp. 598–650.
Demirel, A., Andrews, P., Yalçinkaya, I., Ersoy, A., 2011. The taphonomy and palaeoenvironmental implications of the small mammals from Karain Cave, Turkey. J. Archaeol. Sci. 38, 3048–3059. https://doi.org/10.1016/j.jas.2011.07.003.
Dianat, M., Darvish, J., Cornette, R., Aliabadian, M., Nicolas, V., 2017. Evolutionary history of the Persian Jird, *Meriones persicus*, based on genetics, species distribution modelling and morphometric data. J. Zool. Syst. Evol. Res. 55, 29–45. https://doi.org/10.1111/jzs.12145.
Djamali, M., de Beaulieu, J.L., Shah-hosseini, M., Andrieu-Ponel, V., Ponel, P., Amini, A., Akhani, H., Leroy, S.A.G., Stevens, L., Lahijani, H., Brewer, S., 2008. A late Pleistocene long pollen record from Lake Urmia, NW Iran. Quat. Res. 69, 413–420. https://doi.org/10.1016/j.yqres.2008.03.004.
Ellerman, J.R., Morrison-Scott, T.C.S., 1951. Checklist of Palearctic and Indian Mammals, 1780 to 1946. Brit. Mus. Nat. Hist., London, pp. 1–810.
Evans, E.M.N., Van Couvering, J.A.H., Andrews, P., 1981. Palaeoecology of Miocene sites in western Kenya. J. Hum. Evol. 10, 99–116.
Azokh cave and the Transcaucasian Corridor. In: Fernández-Jalvo, Y., King, T., Yepiskoposyan, L., Andrews, P. (Eds.), 2016a. Vertebrate Paleobiology and Paleoanthropology Series. Springer.
Fernández-Jalvo, Y., Andrews, P., Denys, C., Sesé, C., Stoetzel, E., Marin-Monfort, D., Pesquero, D., 2016b. Taphonomy for taxonomists: implications of predation in small mammal studies. Quat. Sci. Rev. 139, 138–157. https://doi.org/10.1016/j.quascirev.2016.03.016.
Fiacconi, M., Hunt, C.O., 2015. Pollen taphonomy at Shanidar Cave (Kurdish Iraq): an initial evaluation. Rev. Palaeobot. Palynol. 223, 87–93. https://doi.org/10.1016/j.revpalbo.2015.09.003.
Firouz, E., 2005. In: Tauris, I.B. (Ed.), The Complete Fauna of Iran. & Co Ltd.
Frahm, E., 2019. Upper Palaeolithic Settlement and Mobility in the Armenian Highlands : Agent-Based Modeling , Obsidian Sourcing , and Lithic Analysis at Aghitu-3 Cave.
Gerrie, R., Kennerley, R., 2017. Myomimus Personatus. The IUCN Red List of Threatened Species 2017. https://doi.org/10.2305/IUCN.UK.2017-2.RLTS.T14088A22222124.en e.T14088A22222124 8235.
Gharkheloo, M., Kivanç, E., 2003. A study on the morphology, karyology and distribution of *Ellobius* Fischer, 1814 (Mammalia: Rodentia) in Iran. Turk. J. Zool. 27 (4), 281–292.
Golenishchev, F., Malikov, V., Nazari, F., Vaziri, A., Sablina, O., Polyakov, A., 2002. New species of vole of "*guentheri* " group (Rodentia, Arvicolinae, *Microtus*) from Iran. Russ. J. Theriol. 1 (2), 117–123.
Golenishchev, F., Malikov, V., Petrova, T., Bodrov, S., Abramson, N., 2019. Toward assembling a taxonomic puzzle: case study of Iranian gray voles of the subgenus *Microtus* (Rodentia, Cricetidae). Mamm. Biol. 94, 98–105. https://doi.org/10.1016/j.mambio.2018.06.007.
Habibi, K., 2004. Mammals of Afghanistan. Zoo Outreach Organisation/USFWS, Coimbatore, India.
Haddadian Shad, H., Darvish, J., Mohammadian, T., Mahmoudi, A., Alaie Kakhki, N., Ghanbarifardi, M., Molavi, F., Barani-Beiranvand, H., 2014. Preliminary study of rodents using pellets of predatory birds in Iran. Iran. J. Anim. Biosyst. 10, 36–50.
Hassinger, J.D., 1973. A survey of the mammals of Afghanistan: resulting from the 1965 street expedition (excluding bats). In: Fieldiana Zoology, vol. 60. Field Museum of Natural History, Chicago, IL, USA.
Hernández Fernández, M., 2001. Bioclimatic discriminant capacity of terrestrial mammal faunas. Global Ecol. Biogeogr. 10, 189–204. https://doi.org/10.1046/j.1466-822x.2001.00218.x.
Hernandez Fernández, M., Peláez-Campomanes, P., 2003. The bioclimatic model: a method of palaeoclimatic qualitative inference based on mammal associations. Global Ecol. Biogeogr. 12, 507–517. https://doi.org/10.1046/j.1466-822X.2003.00057.x.
Hernández Fernández, M., Álvarez Sierra, M.Á., Peláez-Campomanes, P., 2007. Bioclimatic analysis of rodent palaeofaunas reveals severe climatic changes in Southwestern Europe during the Plio-Pleistocene. Palaeogeogr. Palaeoclimatol. Palaeoecol. 251, 500–526. https://doi.org/10.1016/j.palaeo.2007.04.015.
Heydari-Guran, S., Ghasidian, E., 2020. Late Pleistocene hominin settlement patterns and population dynamics in the Zagros Mountains : Kermanshah region. Archaeological Res. Asia 21, 100161. https://doi.org/10.1016/j.ara.2019.100161.
Hinton, M.A.C., 1926. Monograph of the Voles and Lemmings (Microtinae) Living and Extinct, vol. 1. British Museum (Natural History), London, p. 488.
Jangjoo, M., Darvish, J., Vign, J.D., 2011. Application of outline analysis on fossil and modern specimens of *Apodemus*. – Iranian J. Anim. Biosystem. 7 (2), 143–155.
Kandel, A.W., Gasparyan, B., Allué, E., Bigga, G., Bruch, A.A., Cullen, V.L., Frahm, E., Ghukasyan, R., Gruwier, B., Jabbour, F., Miller, C.E., Taller, A., Vardazaryan, V., Vasilyan, D., Weissbrod, L., 2017. The earliest evidence for upper paleolithic occupation in the Armenian Highlands at Aghitu-3 cave. J. Hum. Evol. 110, 37–68. https://doi.org/10.1016/j.jhevol.2017.05.010.
Karami, M., Hutterer, R., Benda, P., Siahsarvie, R., Kryštufek, B., 2008. Annotated check-list of the mammals of Iran. Lynx 39, 63–102.
Kaya, F., Kaymakçı, N., 2018. Systematics and dental microwear of the late Miocene Gliridae (Rodentia, Mammalia) from Hayranlı, Anatolia: implications for paleoecology and paleobiodiversity. Palaeontol. Electron. 16 https://doi.org/10.26879/385.
Kennerley, R., Kryštufek, B., 2019. Myomimus Setzeri. The IUCN Red List of Threatened Species 2019. https://doi.org/10.2305/IUCN.UK.2019-1.RLTS.T14089A22222049.en e.T14089A22222049. 8235.
Knitlová, M., Horáček, I., 2017. Late pleistocene-Holocene paleobiogeography of the genus *Apodemus* in central Europe. PloS One 12, 1–23. https://doi.org/10.1371/journal.pone.0173668.
Kopij, G., Liven-Schulman, I., 2013. Zoology in the Middle East Diet of the lesser Kestrel, Falco naumanni. In: Israel 7140. https://doi.org/10.1080/09397140.2012.10648914.
Kretzoi, M., 1969. Skizze einer Arvicoliden Phylogenie -Stand 1969/. Vertebr. Hung. 11 (1–2), 155–193.
Kryštufek, B., Bukhnikashvili, A., Sozen, M., Isfendiyaroglu, S., 2017. Cricetulus Migratorius. The IUCN Red List of Threatened Species 2016. https://doi.org/10.2305/IUCN.UK.2016-3.RLTS.T5528A22391440.en e.T5528A115073390 8235.
Kryštufek, B., Yigit, N., Amori, G., 2015. Mesocricetus Brandti , Brandt ' S Hamster. The IUCN Red List of Threatened Species 2008. https://doi.org/10.2305/IUCN.UK.2008.RLTS.T13220A3421550.en e.T13220A3421550. 8235.
Kryštufek, B., Shenbrot, G., 2016. Ellobius lutescens , Transcaucasian Mole Vole. The IUCN Red List of Threatened Species 2016. https://doi.org/10.2305/IUCN.UK.2016-2.RLTS.T7655A22340006.en e.T7655A22340006. 8235.
Krystufek, B., 2017. Chionomys Nivalis , European Snow Vole. The IUCN Red List of Threatened Species 2016. https://doi.org/10.2305/IUCN.UK.2016-3.RLTS.T4659A22379147.en e.T4659A115069366 8235.
Kryštufek, B., Kefelioğlu, H., 2001. Redescription and Species Limits of *Microtus Irani* Thomas, 1921, and Description of a New Social Vole from Turkey (Mammalia: Arvicolinae).
Kryštufek, B., Vohralík, V., 2009. Mammals of Turkey and Cyprus, Rodentia II: Cricetinae, Muridae, Spalacidae, Calomyscidae, Capromyidae, Hystricidae, Castoridae. https://doi.org/10.1644/10-MAMM-R-221.1.
Lay, D.M., 1967. A study of the mammals of Iran, resulting from the street expedition of 1962-63. Fieldiana Zool. 54, 168–171.
López-García, J.M., 2011. Los micromamíferos del Pleistoceno superior de la Península Ibérica: Evolución de la diversidad taxonómica y cambios paleoambientales y paleoclimáticos. Editorial Académica Española.
López-García, J.M., Blain, H.-A., Cuenca-Bescós, G., Alonso, C., Alonso, S., Vaquero, M., 2011. Small vertebrates (Amphibia, squamata, Mammalia) from the late pleistocene-Holocene of the Valdavara-1 cave (Galicia, northwestern Spain). Geobios 44, 253–269. https://doi.org/10.1016/j.geobios.2010.10.001.
Maul, L.C., Bruch, A.A., Smith, K.T., Shenbrot, G., Barkai, R., Gopher, A., 2015a. Palaeoecological and biostratigraphical implications of the microvertebrates of Qesem Cave in Israel. Quat. Int. https://doi.org/10.1016/j.quaint.2015.04.032.
Maul, L.C., Smith, K.T., Shenbrot, G., Bruch, A.A., Wegmüller, F., Le Tensorer, J.M., 2015b. Microvertebrates from unit G/layer 17 of the archaeological site of Hummal (El Kowm, Central Syria): preliminary results. Anthropologie (France) 119, 676–686. https://doi.org/10.1016/j.anthro.2015.10.010.
Miller, G.S., 1896. Genera and Subgenera of Voles and Lemmings//North American Fauna, vol. 12, pp. 1–85.
Molur, S., Sozen, M., 2016. Meriones Persicus, Persian Jird. The IUCN Red List of Threatened Species 2016. https://doi.org/10.2305/IUCN.UK.2016-2.RLTS.T13166A22433231.en e.T13166A22433231. 8235.
Moradi Gharkheloo, M., 2003. A study on the morphology , karyology and distribution of *Ellobius* Fischer , 1814 (Mammalia : Rodentia) in Iran. Turk. J. Zool. 27, 281–292.
Neumann, K., Yiğit, N., Fritzsche, P., Çolak, E., Feoktistova, N., Surov, A., Michaux, J., 2017. Genetic structure of the Turkish hamster (*Mesocricetus brandti*). Mamm.

Biol. 86, 84–91. https://doi.org/10.1016/j.mambio.2017.06.004.
Nishiaki, Y., Akazawa, T., 2018. The middle and upper paleolithic Archeology of the levant and beyond. In: Replacement of Neanderthals by Modern Humans Series 35–47. https://doi.org/10.1007/978-981-10-6826-3_3.
Nowak, R.M., 1999. Walker's Mammals of the World, sixth ed. The Johns Hopkins University Press, Baltimore, MD, USA.
Obuch, J., Khaleghizadeh, A., 2012. Spatial Variation in the Diet of the Barn Owl Tyto alba in Iran, vol. 6, pp. 103–116.
Osborn, D.J., 1962. Rodents of subfamily Microtinae from Turkey. J. Mammal. 43, 515–529.
Rey-Rodríguez, I., Stoetzel, E., López-García, J.M., Denys, C., 2019. Implications of modern Barn owls pellets analysis for archaeological studies in the Middle East. J. Archaeol. Sci. 111, 105029. https://doi.org/10.1016/J.JAS.2019.105029.
Roberts, T.J., 1977. The Mammals of Pakistan. Ernst Benn Ltd, London, UK.
Rusin, M., 2017. Ellobius talpinus , Northern Mole Vole. The IUCN Red List of Threatened Species 2016. https://doi.org/10.2305/IUCN.UK.2016-3.RLTS.T7656A22339917.en e.T7656A115085720. 8235.
Sándor, A.D., 2018. Rediscovered after half a century: a new record of the grey dwarf hamster, *Cricetulus migratorius* (Mammalia: Cricetidae), in Romania. Turk. J. Zool. 42, 495–498. https://doi.org/10.3906/zoo-1712-15.
Shehab, A., Daoud, A., Kock, D., Amr, Z., 2013. Zoology in the Middle East Small Mammals Recovered from Owl Pellets from Syria (Mammalia: Chiroptera,Rodentia). https://doi.org/10.1080/09397140.2004.10638061.
Shenbrot, G., Kryštufek, B., Molur, S., 2016. Ellobius fuscocapillus , Southern Mole Vole. The IUCN Red List of Threatened Species 2016. https://doi.org/10.2305/IUCN.UK.2016-2.RLTS.T7654A22339730.en e.T7654A22339730. 8235.
Shenbrot, G., 2009. On the conspecifity of *Allactaga hotsoni* Thomas, 1920 and *Allactaga firouzi* Womochel, 1978 (Rodentia: Dipodoidea). Mammalia 73, 231–237. https://doi.org/10.1515/MAMM.2009.043.
Shenbrot, G.I., Krasnov, B.R., 2005. An Atlas of the Geographic Distribution of the Arvicoline Rodents of the World (Rodentia, Muridae: Arvicolinae). Pensoft Publishers, Sofia.
Siahsarvie, R., Darvish, J., 2008. Geometric morphometric analysis of Iranian wood mice of the genus *Apodemus* (Rodentia, Muridae). Mammalia 72, 109–115. https://doi.org/10.1515/MAMM.2008.020.
Smith, K.T., Christian, L., Flemming, F., Barkai, R., Gopher, A., 2016. The microvertebrates of Qesem Cave : a comparison of the two concentrations. Quat. Int. 1–13. https://doi.org/10.1016/j.quaint.2015.04.047.
Souttou, K., Denys, C., 2012. Small mammal bone modifications in black- shouldered kite *Elanus caeruleus* pellets from Algeria : implications for archaeological sites. J. Taphonomy 10, 1–19.
Stoetzel, E., Cornette, R., Lalis, A., Nicolas, V., Cucchi, T., Denys, C., 2017. Systematics and evolution of the *Meriones shawii/grandis* complex (Rodentia, Gerbillinae) during the Late Quaternary in northwestern Africa: exploring the role of environmental and anthropogenic changes. Quat. Sci. Rev. 164, 199–216. https://doi.org/10.1016/j.quascirev.2017.04.002.
Tesakov, A.S., 2016. Early middle Pleistocene *Ellobius* (Rodentia , Cricetidae , Arvicolinae) from Armenia. Russ. J. Theriol. 15 (2), 151–158.
Thomas, O., 1905. *Ellobius woosnami*. Abstr. Proc. Zool. Soc. 23. Proc. Zool. Soc. 526. London.
Tsytsulina, K., Kryštufek, B., Yigit, N., Bukhnikashvili, A., Shenbrot, G., 2017. Microtus Socialis , Social. The IUCN Red List of Threatened Species 2016. https://doi.org/10.2305/IUCN.UK.2016-3.RLTS.T13458A22348936.en e.T13458A115114745. 8235.
Walker, E.P., 1964. Mammals of the World, vol. 2. The Johns Hopkins Press, Baltimore, MD,USA.
Weissbrod, L., Zaidner, Y., 2014. Taphonomy and paleoecological implications of fossorial microvertebrates at the Middle Paleolithic open-air site of Nesher Ramla, Israel. Quat. Int. 331, 115–127. https://doi.org/10.1016/j.quaint.2013.05.044.
Wilson, D.E., Reeder, D.M., 2005. Mammal Species of the World. Smithsonian Institution Scholarly Press, Washington, DC, USA.